



A University of Sussex DPhil thesis

Available online via Sussex Research Online:

<http://sro.sussex.ac.uk/>

This thesis is protected by copyright which belongs to the author.

This thesis cannot be reproduced or quoted extensively from without first obtaining permission in writing from the Author

The content must not be changed in any way or sold commercially in any format or medium without the formal permission of the Author

When referring to this work, full bibliographic details including the author, title, awarding institution and date of the thesis must be given

Please visit Sussex Research Online for more information and further details

ORGANOOURANIUM COMPLEXES
FOR THE INSERTION AND REDUCTION
OF SMALL MOLECULES

JESSICA ANNE HIGGINS

SUBMITTED FOR THE DEGREE OF DOCTOR OF PHILOSOPHY

UNIVERSITY OF SUSSEX

SEPTEMBER 2014

DECLARATION

All work described in this thesis was carried out at the University of Sussex under the supervision of Professor F. Geoffrey N. Cloke FRS from October 2010 to September 2014. The work is my own unless otherwise stated and has not been submitted in whole or in part to another University for the award of any other degree.

Jessica Anne Higgins (Frey)

September 2014

UNIVERSITY OF SUSSEXPHD CHEMISTRYORGANOOURANIUM COMPLEXES FOR THE INSERTION
AND REDUCTION OF SMALL MOLECULESSUMMARY:

This thesis explores the behaviour of U(III) and U(IV) organometallic complexes towards small molecules, with respect to both their reductive activity and insertion chemistry.

A range of mixed-sandwich U(IV) organyl complexes of the form $U(\eta\text{-C}_8\text{H}_6\{1,4\text{-Si}^i\text{Pr}_3\}_2)(\eta\text{-C}_5\text{Me}_5)(\text{R})$ ($= U(\text{COT}^{\text{TIPS}_2}\text{Cp}^*(\text{R}))$, where $\text{R} = \text{CH}_3, \text{CH}_2\text{Ph}, \text{CH}_2\text{TMS}, \text{CH}\{\text{TMS}\}_2$) have been synthesised and the products of their reactions with CO_2, CO , and H_2 (κ^2 -carboxylates, η^2 -acyls, and a monomeric terminal hydride) have been characterised – all of which are formed under mild conditions (< 1 atm of gas, sub-ambient temperature). The hydride also inserts CO_2 to yield a formate, $U(\text{COT}^{\text{TIPS}_2})\text{Cp}^*(\kappa^2\text{-O}_2\text{CH})$, which is the first example of its kind, and inserts CO to form *cis*-enediolate, $\{U(\text{COT}^{\text{TIPS}_2})\text{Cp}^*\}_2(\mu\text{-}\kappa^1:\kappa^1\text{-OCH=CHO})$. A rare primary amido, $U(\text{COT}^{\text{TIPS}_2})\text{Cp}^*(\text{NH}_2)$, and its CO_2 insertion product, $U(\text{COT}^{\text{TIPS}_2})\text{Cp}^*(\kappa^2\text{-O}_2\text{CNH}_2)$, have also been characterised. The latter is the first crystallographically characterised U(IV) primary carbamate. Deprotonation of the parent amido yield an anionic U(IV) terminal primary imido, $[U(\text{COT}^{\text{TIPS}_2})\text{Cp}^*(\text{NH})][\text{K}(18\text{-crown-6})]$.

U(III) and U(IV) complexes containing a dianionic diamidoamine ligand, $[\text{N}\{\text{SiMe}_3\}(\text{CH}_2\text{CH}_2\text{N}\{\text{SiMe}_3\})_2]^{2-}$ ($= \text{N}'\text{N}'_2$) have been synthesised. It has been found that the migration of a SiMe_3 group along the ligand backbone occurs spontaneously when bound to uranium. Reduction of the U(IV) compound $U(\text{N}'\text{N}'_2)\text{Cp}^*\text{Cl}$ with KC_8 yields either the U(III) product, $U(\text{N}'\text{N}'_2)\text{Cp}^*$, or bridging arene products, $\{U(\text{N}'\text{N}'_2)\}_2(\mu\text{-}\eta^6:\eta^6\text{-C}_6\text{H}_5\text{R})$ (where $\text{R} = \text{H}, \text{Me}$), depending on the reaction stoichiometry. Further reactivity of these diamidoamine complexes with small molecules is also discussed.

ACKNOWLEDGEMENTS

First and foremost I would like to thank my supervisor, Professor Geoff Cloke, for all his support and guidance over the last 5 years. He had me hooked as soon as he told me: “it’s not easy, you know” when I enquired about working for him for my MChem project in May 2009. Thanks also go to the ERC and University of Sussex for their funding. I would also like to make special mention of the Chemistry department at the university as a whole, for inspiring me to continue my chemistry career with their infectious passion for their subjects, which I could sense from day one of my studies when I arrived in October 2006 – thank you for a great 8 years.

My heartfelt thanks go to Drs. Mark Roe and Alistair Frey for their infinite patience and positivity when spending countless hours sifting through poor quality crystal samples to find the gems that have helped me decipher the reactivity of so many of my compounds. I am also indebted to Drs. Ali Abdul-Sada and Iain Day for their support with Mass Spectrometry and NMR Spectroscopy, and to staff at the university workshop and the (now-defunct) glassblowing facility for providing our lab with invaluable specialist equipment – and for speedily repairing my ‘little accidents’. Many thanks to Alex Burns, Barry Jackson and Paul Andrews for keeping both the department and all of us in good working order, and to Mick Henry and Fran Chick in the teaching lab for glassware loans, machinery time and their general endless support.

As always, my love and gratitude goes out to my incredible friends both inside and outside of the Chemistry department, in particular the ‘permanent fixtures’ of Nikki Trathen, Chris Gallop and Laura Nicholls with who I have shared my chemistry journey from the first year of our undergraduate degrees here at Sussex, and to my fellow Cloke group PhDs: Sandy Kilpatrick, Dr. Zoë Button, and Rachel Kahan – I am so proud of you all, we have finally (or almost) made it (Drs!). Thanks also must go to the whole Cloke group, to Markéta Suvova for making me grams of ‘love ligand’ (with love!), to Dr. Joy Farnaby for invaluable chemistry-related help (and non-chemistry related whisky) from my Masters year to the present day, to the wonderful ‘organic office’ for endless coffee and distractions, to Vicki Greenacre for keeping me sane, and to Dr. Ian Crossley and the rest of the Crossley group for cheerfully tolerating my presence as an ‘outsider’ both on their side of the lab and in their office.

Finally, I want to thank the three most important people in my life: my loving parents Karen and Graham, and my best friend and husband Alistair. You have all been inspirations to me in your individual ways and have helped me find the strength to get as far as I have. Thank you from the bottom of my heart – I couldn't have done this without you.

This thesis is dedicated to the memory of two exceptional people, both of who are sorely missed.

Firstly, to my Granddad, Herbert William Kennelly Jackson, who worked for many years at the Atomic Weapons Research Establishment where he was a draftsman, assisting in the design and testing of nuclear weapons – although he always maintained he was making sewing machines.

Secondly, to Dai Evans, the best chemistry teacher I have ever known. Without him I would not have believed that you could succeed doing something you are fascinated by, even if it's not your strong point. Thank you Dai, I never dreamed I would do a PhD in a subject I loved so much, but I think you always knew.

“It is what it is.” – S. M. Roe

“You'll be fine, just don't mess it up.” – A. S. P. Frey

“Chemistry is like a jigsaw puzzle.” – D. Evans

ABBREVIATIONS

°	degrees
18c6	18-crown-6, C ₁₂ H ₂₄ O ₆
Å	angstrom
Ad	adamantyl, C ₁₀ H ₁₅
An	actinide
Ar	generic aryl group
^t BuOMe	<i>tert</i> -butyl methyl ether, C ₅ H ₁₂ O
^x Bu	butyl; x = n, t (<i>tert</i>), i (<i>iso</i>)
COT	cyclooctatetraene, C ₈ H ₈
COT ^{TIPS2}	tri- <i>iso</i> -propylsilyl cyclooctatetraene, 1,4-{Si ⁱ Pr ₃ } ₂ C ₈ H ₆
Cp	cyclopentadienyl, C ₅ H ₅
Cp'	mono-trimethylsilyl cyclopentadienyl, (SiMe ₃)C ₅ H ₄
Cp''	bis-trimethylsilyl cyclopentadienyl, 1,3-(SiMe ₃) ₂ C ₅ H ₃
Cp*	pentamethylcyclopentadienyl, C ₅ Me ₅
Ct	centroid (middle of carbon ring)
<i>d</i> _x	deuterated (x deuterium atoms)
DFT	density functional theory
DME	1,2-dimethoxy ethane, C ₄ H ₁₀ O ₂
dmpe	1,2-bis(dimethylphosphino)ethane, C ₆ H ₁₆ P ₂
DMSB	dimethyl silyl butyl, Me ₂ Si ⁱ Bu
DMSP	dimethyl silyl phenyl, Me ₂ SiPh
Dtbp	di- <i>tert</i> -butyl phenyl, 2,6-(^t Bu) ₂ C ₆ H ₃
DU	depleted uranium
esd	estimated standard deviation
Et	ethyl
Et ₂ O	diethyl ether, C ₄ H ₁₀ O
hpp	1,3,4,6,7,8-hexahydro-2 <i>H</i> -pyrimido[1,2- <i>a</i>]pyrimidinato
ORTEP	Oak Ridge Thermal Ellipsoid Plot
Me	methyl, CH ₃
Mes	mesityl, 2,4,6-Me ₃ -C ₆ H ₂
N''	N(SiMe ₃) ₂
N'N' ₂	diamidoamine, N(SiMe ₃){CH ₂ CH ₂ N(SiMe ₃) ₂ }
Np	neopentyl, C ₄ H ₉

NMR	nuclear magnetic resonance
OTf	triflate, SO_3CF_3
Ph	phenyl
ⁱ Pr	isopropyl
R	alkyl or organyl group
tacn	1,4,7-triazacyclononane
THF	tetrahydrofuran, $\text{C}_4\text{H}_8\text{O}$
TIPS	tri- <i>iso</i> -propyl silyl, $\text{Si}(\text{}^i\text{Pr}_3)_3$
TMS	trimethyl silyl, SiMe_3
Tren ^R	$\text{N}(\text{CH}_2\text{CH}_2\text{N}\{\text{R}\})_3$, R = alkyl, silyl
Ttbp	tri- <i>tert</i> -butyl phenyl, 2,4,6-(^t Bu) ₃ C ₆ H ₂

NMR spectroscopic data abbreviations

{ ¹ H}	proton-decoupled
δ	chemical shift
d	doublet
Hz	hertz
^x J _{yz}	x-bond coupling constant for nuclei y-z
m	multiplet
s	singlet
t	triplet
ppm	parts per million

Mass spectrometric data abbreviations

EI	electron impact
m/z	mass to charge ratio
M ⁺	molecular ion
MS	mass spectrometric

Infrared data abbreviations

br	broad
cm ⁻¹	wavenumber
m	medium
s	strong
w	weak

TABLE OF CONTENTS

CHAPTER 1: INTRODUCTION	1
1.1 Foreword	1
1.2 History of organouranium chemistry	2
1.2.1 Uranium: an overview	2
1.2.2 Development of organouranium chemistry	3
1.3 Ligand systems in organouranium chemistry	4
1.3.1 Metallocene systems	5
1.3.2 Non-metallocene systems: nitrogen-based ligands	9
1.4 Reductive activation and insertion of small molecules.....	12
1.4.1 Carbon monoxide.....	13
1.4.2 Carbon dioxide.....	17
1.4.3 Concluding remarks.....	20
1.5 Sigma-bonded organouranium complexes: U-C and U-H bonds.....	21
1.5.1 Uranium alkyls.....	21
1.5.2 Uranium hydrides	24
1.6 Small molecule insertion and functionalisation by U(IV).....	28
1.6.1 Carbon monoxide.....	29
1.6.2 Carbon dioxide.....	32
1.6.3 Summary and conclusion.....	34
1.7 Scope of thesis	35
1.8 References for Chapter 1	37
CHAPTER 2: SYNTHESIS OF MIXED-SANDWICH U(IV) ALKYL COMPLEXES	46
2.1 Introduction.....	46
2.2 General route to mixed-sandwich alkyls	47
2.3 Synthesis and characterisation of U(COT^{TIPS})Cp*Cl (2.2).....	48
2.4 Synthesis of mixed-sandwich alkyls: R = Me, CH₂Ph, ⁿBu, ^tBu, Np	50
2.4.1 Synthesis and characterisation of benzyl and methyl alkyls.....	50

2.4.2	Attempted syntheses of butyl and neopentyl alkyls.....	54
2.5	Synthesis of mixed-sandwich silyl alkyls: R = CH₂TMS, CH(TMS)₂	55
2.5.1	Syntheses of silyl alkyls.....	55
2.5.2	Attempted synthesis of 2.5 : isolation of side-products.....	59
2.6	Alkyl decomposition: tuck-in complex formation	65
2.6.1	Synthesis and characterisation of the ‘tuck-in’ complex (2.9)	66
2.6.2	‘Tuck-in’ formation from U ^{III} (COT ^{TIPSt})Cp*(THF) (2.1.THF).....	70
2.7	Conclusions and chapter summary	72
2.8	Compound naming for Chapter 2	73
2.9	References for Chapter 2	74

CHAPTER 3: REACTIVITY OF MIXED-SANDWICH U(IV) ALKYLs AND RELATED COMPLEXES WITH SMALL MOLECULES..... 76

3.1	Introduction.....	76
3.2	Reactivity of alkyls with H₂: σ-bond metathesis.....	78
3.2.1	Organouranium hydride complexes.....	78
3.2.2	Synthesis and stability of U(COT ^{TIPSt})Cp*H (3.1)	81
3.2.3	Characterisation of U(COT ^{TIPSt})Cp*H.....	84
3.2.4	Mechanistic investigations: deuterium scrambling.....	88
3.3	Reactivity with CO: insertion reactions.....	90
3.3.1	CO reactivity with 2.3-2.6	90
3.3.2	CO insertion with ‘tuck-in’ (2.9)	99
3.3.3	CO reactivity with U(COT ^{TIPSt})Cp*H.....	104
3.3.4	Reactivity of 2.9 and 3.1 with CO/H ₂ mixture	111
3.3.5	Mechanistic considerations and DFT studies	114
3.4	Reactivity with CO₂: insertion reactions and isomerisation.....	122
3.4.1	CO ₂ reactivity with alkyls: κ ² -carboxylates.....	122
3.4.2	Reactivity with 2.9 : synthesis and characterisation of 3.15	128
3.4.3	Reactivity with 3.1 : synthesis and characterisation of 3.16	130
3.4.4	Further CO ₂ reactivity.....	134
3.5	Conclusions and chapter summary	147

3.6 Compound naming for Chapter 3	149
3.7 References for Chapter 3	150

CHAPTER 4: SYNTHESIS AND REACTIVITY OF A MIXED-SANDWICH

U(IV) PRIMARY AMIDO AND RELATED COMPLEXES	153
4.1 Organouranium amido complexes	153
4.1.1 Introduction and scope of section	153
4.1.2 Synthesis of $U(COT^{TIPS_2})Cp^*(NH_2)$ (4.1)	156
4.1.3 Characterisation of $U(COT^{TIPS_2})Cp^*(NH_2)$	158
4.1.4 Deuterium labelling studies	159
4.1.5 Attempted synthesis of $U(COT^{TIPS_2})Cp^*(N\{TMS\}_2)$ (4.2)	161
4.2 Reactivity of $U(COT^{TIPS_2})Cp^*(NH_2)$ with CO_2 and CO	162
4.2.1 Reactivity with CO_2 – synthesis of $U(COT^{TIPS_2})Cp^*(\kappa^2-O_2CNH_2)$ (4.3)	162
4.2.2 Reactivity with CO	166
4.3 Deprotonation of $U(COT^{TIPS_2})Cp^*(NH_2)$	167
4.3.1 Synthesis and characterisation of $[U(COT^{TIPS_2})Cp^*(NH)][K(18c6)]$ (4.4)	167
4.3.2 Attempted alternative routes to an imido complex	169
4.3.3 Oxidation to a U(V) imido	170
4.3.4 Attempted nitride synthesis	171
4.4 Conclusions and chapter summary	172
4.5 Compound naming for Chapter 4	173
4.6 References for Chapter 5	173

CHAPTER 5: DIAMIDOAMINE U(III) AND U(IV) COMPLEXES: SYNTHESIS AND REACTIVITY

5.1 Introduction	175
5.2 Synthesis and characterisation of diamidoamine chlorides	179
5.2.1 Synthesis of $U(N'N'_2)Cp^*Cl$ (5.1)	179
5.2.2 Silyl group migration	182
5.3 Synthesis of $U^{III}(N'N'_2)Cp^*$ and related compounds	184
5.3.1 Synthesis and characterisation of $U(N'N'_2)Cp^*$ (5.3)	184

5.3.2	Attempted reduction using other methods	187
5.3.3	Attempted synthesis of $U(N'N'_2)Cp^*$ from UI_3	188
5.3.4	Reduction of $\{U(N'NN'')Cp^*Cl\}_2$	189
5.4	Small molecule reactivity	192
5.4.1	Reactivity of $U(N'N'_2)Cp^*$ (5.3) with CO and CO_2	192
5.4.2	Reactivity of $U(N'N'_2)Cp^*Cl$ (5.1) with CO and CO_2	196
5.5	Bridging arene complexes	199
5.5.1	Synthesis and characterisation of $\{U(N'N'_2)\}_2(\mu-\eta^6:\eta^6-C_6H_5R)$ (R = H, Me) .	204
5.5.2	Reactivity of $\{U(N'N'_2)\}_2(\mu-C_7H_8)$ (5.6)	208
5.6	Conclusions and chapter summary	209
5.7	Compound naming for Chapter 5	210
5.8	References for Chapter 5	210
CHAPTER 6: EXPERIMENTAL DETAILS		213
6.1	General procedures and techniques	213
6.2	Instrumentation	214
6.3	Preparation of reagents	216
6.4	Notes on interpreting NMR spectra of paramagnetic organouranium complexes reported in this work.	217
6.5	Experimental details for Chapter 2	219
6.6	Experimental details for Chapter 3	228
6.7	Experimental details for Chapter 4	246
6.8	Experimental details for Chapter 5	255
6.9	References for Chapter 6	267
APPENDIX 1: MISCELLANEOUS DATA		269
A1.1	Summary of relevant bond lengths and angles	269
A1.2	Computational investigations	273
A1.3	References for Appendix 1	275
APPENDIX 2: CRYSTALLOGRAPHIC INFORMATION		276/CD

APPENDIX 3: PUBLICATIONS:

" <i>Synthesis and CO₂ Insertion Chemistry of Uranium(IV) Mixed-Sandwich Alkyl and Hydride Complexes</i> ", J. A. Higgins, S. M. Roe, F. G. N. Cloke, <i>Organometallics</i> , 2013, 32 , 5244-5252	282
" <i>Mixed-sandwich thorium complexes incorporating bis(tri-isopropylsilyl)cyclooctatetraenyl and pentamethylcyclopentadienyl ligands: synthesis, structure and reactivity</i> ", Z. E. Button, J. A. Higgins, M. Suvova, F. G. N. Cloke, S. M. Roe, <i>Dalton Trans.</i> , DOI: 10.1039/C4DT02362E	291
APPENDIX 4: NMR DATA	CD

CHAPTER 1: INTRODUCTION

1.1 Foreword

Discovering new modes of reactivity and effecting new molecular transformations are fundamental goals of organometallic chemistry. Extensive research has been undertaken in the field of organotransition metal chemistry and, to a lesser extent, organolanthanide and organoactinide chemistry, to investigate the possible bonding, behaviour and chemistry of metal-organic systems. Organometallic chemistry has found application in the transformation of biologically or industrially important small molecules, such as H₂, CO, CO₂, O₂, N₂, and NH₃, by catalysing or aiding reactions to afford more complex chemicals.¹ As an example, the potential to utilise CO₂ as a C₁ feedstock has been understood for decades, and with much attention focused on reducing CO₂ emissions globally, research is being developed to make use of this ubiquitous waste product in energy- and molecule-efficient ways.²⁻⁵

Uranium has not been overlooked in organometallic research, and it has proven to be a promising element for new molecular transformations, as recent reviews have detailed.⁶⁻⁹ Whilst using uranium in catalysis may be an unachievable goal due to the demands of rigorously oxygen- and moisture-free environments necessary for its low- and mid-valent chemistry, the study of reactivity patterns and the mechanisms of transformations provides insight into the fundamental nature of bonding and the chemistry of organouranium systems.¹⁰⁻¹⁸ As described herein, its reactivity is uniquely different to lanthanides, transition metals, and even other actinides. Furthermore, many areas of organouranium chemistry are still unexplored or not well understood.

This thesis explores the use of uranium in combination with two ancillary ligand systems, in order to activate small molecules – CO, CO₂, H₂, and NH₃ – by synthesising a variety of reactive precursors, and then characterising the products of subsequent small molecule transformations. A general introduction to organouranium chemistry,

the ligands used, and previous work on small molecule transformations by both U(III) and U(IV) organouranium systems is provided in this chapter.

1.2 History of organouranium chemistry

1.2.1 Uranium: an overview

An early actinide often associated with radioactivity and nuclear fuel, uranium is a naturally occurring element with unique reactivity, first discovered in 1789.¹⁹ Uranium extracted from the earth consists of three isotopes: ^{238}U , ^{235}U , and ^{234}U , with ^{238}U being the most abundant at a weight percentage of 99.2745% and with a half-life of around 4.5 billion years.²⁰ Usage in the nuclear fuel industry requires enrichment of natural uranium to obtain a higher percentage abundance of fissile ^{235}U , producing depleted uranium (DU, containing typically between 0.2-0.4% ^{235}U) as a side product. Current uses for DU include ammunition, airplane counterbalances, radiation shields, and drilling equipment.²¹ ^{238}U is a weak alpha-emitter, and this coupled with its long half-life means that DU can be safely handled in a laboratory environment as long as sufficient care is taken not to ingest or inhale any material.

The chemical behaviour of actinides differs from lanthanides and transition metals, and hence provides potential for use in catalysis, resulting in new forms of reactivity. Actinides possess 5f orbitals that are less shielded by 6s and 6p electrons, in comparison to the greater shielding of the lanthanide 4f orbitals by the 5s and 5p electrons.¹⁰ Whilst bonding models of the f-block elements have mainly been classed as electrostatic, the diffuse nature of the 5f orbitals in the early actinides (Ac to Np) allows some participation in covalent bonding, in comparison to the more ionic bonding of the lanthanides and later actinides. The more radially-extended 5f electrons also mean that π -back bonding is possible, hence multiple bonding is available for the early actinides.²² Also in contrast to transition metals and the lanthanides, the actinides have larger ionic radii, allowing for large coordination numbers, and can access a wider

range of oxidation states. It should be stated that whilst many bonding models for organouranium complexes exist, our understanding of the bonding nature and electronic structure of such systems is not complete. Studying patterns of reactivity is a useful way of building on existing knowledge, helping to expand the global picture of uranium structure and bonding.

Uranium has an electronic configuration of $[\text{Rn}]5f^36d^17s^2$ and can access oxidation states U(II) to U(VI), with U(IV) and U(VI) being the most common. It is a highly electropositive and oxophilic element, and these characteristics along with its large ionic radii and potential for high coordination numbers result in it possessing some unique chemistry. The U(III) oxidation state is highly reducing, and the easily accessible U(III)/U(IV) redox couple (ca -2 V vs $\text{FeCp}_2^{+/0}$)^{23,24} means that U(III) can be used to reduce small molecules such as CO and CO₂ (see section 1.4 for detail); however, the ligand systems installed around the metal centre have a large influence on this redox couple and hence on reactivity.²⁵⁻²⁹ The ability of uranium to form highly polarised bonds between atoms such as C, H, N and O also allows it to facilitate insertion reactions of small molecules into such bonds without a change in oxidation state, demonstrating reactivity that is fundamentally different from the oxidative addition/reductive elimination chemistry observed for transition metals, as detailed in this chapter.

1.2.2 Development of organouranium chemistry

Limited research into the organometallic chemistry of uranium was carried out before the late 1940s, when the Manhattan Project sought to develop volatile uranium complexes for use in isotope separation. Compounds featuring U-C, U-N, U-O and U-S bonds were targeted, to some degrees of success, as later reported by Gilman *et al.* in the mid-1950s.³⁰⁻³⁶ The first π -bound organouranium complexes were reported in 1956 by Reynolds and Wilkinson, where they describe the syntheses of UCp_3 and UCp_3Cl from UCl_3 and UCl_4 respectively.³⁷ The authors note that the reactivity and

spectroscopic properties of UCp_3Cl are consistent with covalent uranium-carbon bonds to the Cp rings and essentially ionic uranium-chloride bonds, in contrast to the purely electrostatic metal-carbon bonds found between $[\text{Cp}]^-$ and lanthanide metal centres in analogous LnCp_3 complexes.³⁸ Their formulation of a π -complex, bonded covalently, was corroborated several years later when the crystal structure of UCp_3Cl was determined.³⁹

Considering the relative size and radial extension of the 5f-orbitals of uranium in comparison to transition metal bonding orbitals, the potential for a uranium analogue of ferrocene featuring two larger 8-membered cyclooctatetraene ligands was postulated by Fischer in 1963.⁴⁰ Its successful synthesis was reported in 1968, and the air-sensitive green compound was dubbed ‘uranocene’, formulated as $\text{U}(\text{C}_8\text{H}_8)_2$ by virtue of its mass spectrum and high thermal stability.⁴¹ Molecular orbital treatments and the later-published X-ray structure provided conclusive evidence that uranocene contained planar, aromatic cyclooctatetraene rings and featured covalent bonding between uranium and carbon, thus representing a new class of sandwich complexes involving 5f-orbitals.^{42,43} This discovery marked the beginning of renewed interest in organouranium chemistry.

1.3 Ligand systems in organouranium chemistry

A crucial goal in the challenge of isolating stable, yet reactive, organouranium complexes is developing ligand systems that enable the metal centre to be sterically and electronically stabilised to some degree. Depending on the synthetic application, complexes may need a reactive ‘pocket’ dictated by ligand steric factors to allow the approach and subsequent reaction of small molecules, or a single ‘U-X’ bond of interest may need to be installed to observe and effect reactivity at that precise position. Electronic stabilisation *via* non-innocent or redox-active ligands may be required to support low oxidation states; also beneficial is the ability to ‘tune’ ligand sets to impart properties such as crystallinity and solubility to compounds. The correct selection of a

ligand system for different purposes is essential to afford the desired reactivity. Uranium is able to bind to a wide range of hard and soft donor ligands, and to aromatic carbocycles, enabling the successful synthesis of many different organouranium complexes. Detailed below are exemplary ligand systems classed either as metallocene, or non-metallocene systems.

1.3.1 Metallocene systems

Ubiquitous in organometallic chemistry is the monoanionic, η^5 -hapticity carbocyclic ligand, cyclopentadienyl (Cp). Its hybridised molecular orbitals efficiently overlap with transition-metal *d*-orbitals,⁴⁰ and are also able to bond to lanthanides³⁸ and actinides; the first π -bound organouranium complexes, UCp₃Cl and UCp₃, feature this ligand.³⁷ Derivatives of Cp, such as the widely-used pentamethylcyclopentadienyl (Cp*), have also been employed in organouranium chemistry. A large class of UCp*₂X₂ (where X = halide, amide, alkyl, alkoxy, hydride) complexes have been characterised over the past 40 years and have shown a remarkable range of reactivity, as well as providing fundamental information about the nature of various ‘U-X’ bonds.^{44–54} Using the Cp* ligand in place of Cp imparts higher solubility, and higher steric and electronic stabilisation, which in turn can prevent unwanted dimerisation of low-coordinate complexes. Additionally, in contrast to UCp₃X complexes, UCp*₃X complexes are resistant to disproportionation to UCp*₂X₂ products due to their increased steric bulk.

In addition to Cp*, many other substituted cyclopentadienyl ligands have been used in combination with uranium, including alkyl-substituted ligands: C₅H₄R (R = Me, ^tBu), 1,3-(^tBu)₂C₅H₃, 1,2,4-(^tBu)₃C₅H₃, C₅Me₄R (R = H, ⁱPr, Et),^{55–62} silyl-substituted ligands: C₅H₄TMS (= Cp', TMS = SiMe₃), 1,3-(TMS)₂C₅H₃ (= Cp''), C₅Me₄(SiMe₂{CH₂CH=CH₂}), C₅Me₄TMS,^{63–66} and ansa-Cp ligands: X(C₅H₄)₂ (X = CH₂, (CH₃)₂Si, ⁿPr), Me₂Si(C₅Me₄)₂.^{67,68} These modifications were carried out to

assist in the design of complexes that can sterically or electronically stabilise a uranium metal centre, further to the more widely-used Cp or Cp* ligands (**Figure 1.1**).

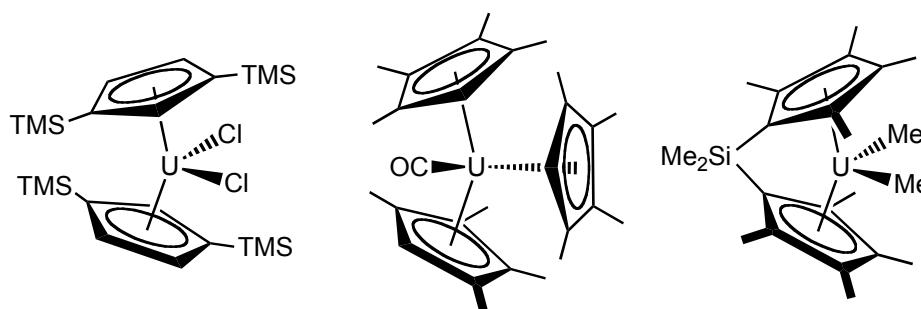


Figure 1.1. Examples of organouranium complexes featuring substituted-Cp ligands, left to right: $U(Cp'')_2Cl_2$, $U(C_5Me_4H)_2(CO)$, $U(SiMe_2\{C_5Me_4\}_2)Me_2$.

The discovery of uranocene, $U(COT)_2$, by Streitwieser and Müller-Westerhoff was a springboard for the synthesis of many complexes involving this larger 10π -aromatic carbocycle.⁴¹ Substitution of the COT ring followed to give mono- or multi-functional ligands, with the 1,1'-monoalkyl COT uranocenes being the most numerous: $U(COT^R)_2$, where R = Me, Et, ⁿBu, Ph, ^tBu, CH=CH₂, Mes, cyclopropyl.^{69–73} These efforts were aimed to afford compounds more soluble than the parent uranocene, and hence ease characterisation by spectroscopic means.^{43,74} Tetra-substituted COT rings enabled the synthesis of $U(C_8H_4R_4)_2$ uranocenes, where R = Me, Ph, and remarkably the latter species proved air-stable for several weeks.^{70,75} Silyl-substitution of COT rings has also been undertaken, and uranocenes featuring (1,4- $\{TMS\}_2C_8H_6$),⁷⁶ (1,4- $\{SiMe_2^tBu\}_2C_8H_6$),⁷⁷ (1,3,5- $\{TMS\}_3C_8H_5$),⁷⁸ and (1,4- $\{SiPh_3\}_2C_8H_6$)⁷⁹ ligands have been synthesised. The silyl groups are advantageous as they impart crystallinity and solubility to the complexes, and also steric saturation, whilst generally being cheaper and easier to synthesise than the alkylated ligands.⁸⁰

Whilst informative with respect to f-element structure and bonding, the uranocenes were largely unreactive and showed little interesting chemistry. Instead, mono-COT ‘half-sandwich’ compounds were developed, which offer some steric protection of the metal centre to avoid decomposition, but which are less coordinatively

saturated than the full sandwiches.⁸¹ There are limited examples of stable mono-COT complexes: Streitwieser *et al.* reported the syntheses of $U(COT)Cl_2(E)_2$ (where $E =$ pyridine (**Figure 1.2, 1A**), THF, PMe_3) and $U(COT)(acac)_2$ ($acac =$ acetylacetonate), however, neither complex would undergo further displacement reactions with metal alkyl or alkoxy reagents.⁸¹ The group suggest that lack of steric saturation precludes the isolation of half-sandwiches, whereas the successful synthesis of $U(COT)(N\{TMS\}_2)_2$ by Sattelberger *et al.* occurs by virtue of the bulky silyl groups and stabilising agostic interactions between uranium and the $SiMe_3$ C-H groups.⁸² Utilising a borohydride ligand in tandem with COT enabled Ephritikhine *et al.* to isolate moderately stable $U(COT)(BH_4)_2$, a precursor for further ligand substitutions, including the ‘mixed-sandwich’ complexes, $U(COT)Cp(BH_4)(L)$ (where $L =$ THF or $OPPh_3$).^{83,84} Later work by Cloke and co-workers used a bulkier, silyl-substituted COT ligand to synthesise the base-free half-sandwich, $U(1,4-\{TMS\}_2C_8H_6)(BH_4)_2$ (**Figure 1.2, 1B**).⁷⁶

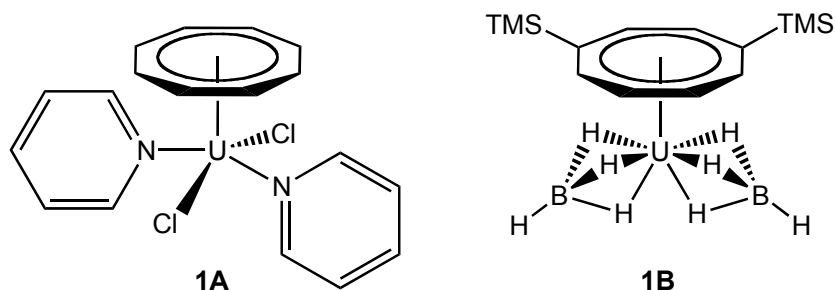


Figure 1.2. ‘Half-sandwich’ organouranium complexes **1A** and **1B**.

The advent of ‘mixed-sandwich’ organouranium complexes enabled the use of sterically stabilising COT rings alongside less bulky Cp rings to ‘fine tune’ the reactivity of the uranium metal centre. With substitution possible for both COT and Cp ligands, a large number of mixed-sandwich combinations exist, each providing different environments for a uranium metal centre. The pseudo bent-metallocene configuration and potential for multiple coordination sites offers an attractive prospect in comparison to single COT-ring or crowded Cp and Cp^* ligand systems. The complexes $U^{IV}(COT)Cp(BH_4)(L)$ (where $L =$ THF, $OPPh_3$) and $U^{III}(COT)Cp^*(THF)$ (**Figure 1.3, 1C**) were the first reported mixed-sandwich species in 1990 and 1993

respectively.^{83,85} The latter complex reacts with Me₂bpy, the product of which was characterised by X-ray crystallographic means and was seen to feature non-parallel rings (Cp*-U-COT angle 138.2 °) angled away from the Me₂bpy ligand (**Figure 1.3**). This ‘pocket’ of reactivity is provided by the bent configuration of the carbocyclic rings, and is large enough to accommodate further bulky ligands.

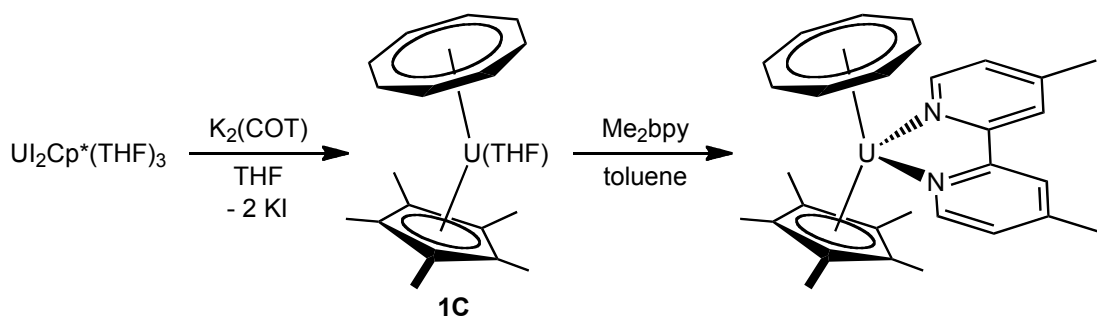


Figure 1.3. Synthesis and reactivity of $U(COT)Cp^*(THF)$ (**1C**).

$U(IV)$ iodide mixed-sandwiches, $U(COT)Cp(I)$ and $U(COT)Cp^*(I)$, were synthesised by Berthet *et al.* in 1994 *via* the reaction of $U(COT)(I)_2(THF)_2$ and $TiCp$ or KCp^* respectively.⁸⁴ X-ray crystallographic studies on $U(COT)Cp^*(I)$ revealed a polymeric structure with bridging iodide ligands, indicating that the mixed-sandwich iodide is sterically unsaturated; the reaction with $LiCH_2TMS$ yielded the monomeric alkyl, $U(COT)Cp^*(CH_2TMS)$. Later work by Evans *et al.* afforded a range of monomeric alkyl and aryl mixed-sandwich complexes.⁸⁶ These complexes also allowed for the study of the insertion of tBuCN and carbodiimides into $U-C$ bonds. A bulkier mixed-sandwich system containing the silyl-substituted COT ring, $(1,4-\{Si^iPr_3\}_2C_8H_6)$ ($= COT^{TIPS2}$), and Cp^* ligands has been used by Cloke *et al.*^{62,87–92}

Other metallocyclic organouranium complexes feature ligands such as indenyl, $[C_9H_7]^-$,^{93–96} and its substituted variants,⁹⁷ pentalene, $[C_8H_6]^{2-}$, and its substituted variants,^{98,99} and cycloheptatrienyl, $[C_7H_7]^{3-}$.^{100–103} Overall, a large range of metallocyclic organouranium complexes have been synthesised, and have helped to elucidate fundamental bonding and structural information.

1.3.2 Non-metallocene systems: nitrogen-based ligands

In addition to carbocyclic ligand systems, a range of nitrogen- and oxygen-based ligand systems have also been utilised. Ligands containing neutral lone pair N-donor or anionic $[N]^-$ atoms have proven popular choices for stabilising uranium metal centers: they are able to π -donate, and can be easily altered in terms of their steric or electronic capacity by changing the amido substituents. In many cases, these ligands have enabled new reactivity with small molecules (see section 1.4). Some multidentate nitrogen-based ligands will be discussed here and compared to the carbocyclic rings discussed earlier.

The N-donor hydrotris(3,5-dimethylpyrazolyl)borate ligand, Tp^* , is widely viewed as an analogous non-carbocyclic ligand to Cp^* , and has been used in organouranium chemistry. Ball *et al.* reported the X-ray crystal structure of $U(Tp^*)Cl_3(THF)$ (**Figure 1.4, 1D**) and demonstrated the tridentate coordination of the three pyrazolyl moieties.¹⁰⁴ They speculated that the coordination of only one THF molecule in comparison to two in the equivalent complex, $UCp^*Cl_3(THF)_2$, indicates the increased steric demands of the Tp^* ligand. Both U(III) and U(IV) can be stabilised by Tp^* ,^{105–111} the alkyl $U^{III}(Tp^*)_2(CH_2Ph)$ (**Figure 1.4, 1E**) can be isolated, whereas the equivalent Cp^* complex, $U^{III}Cp^*_2(CH_2Ph)$ is too unstable to form.^{112–114}

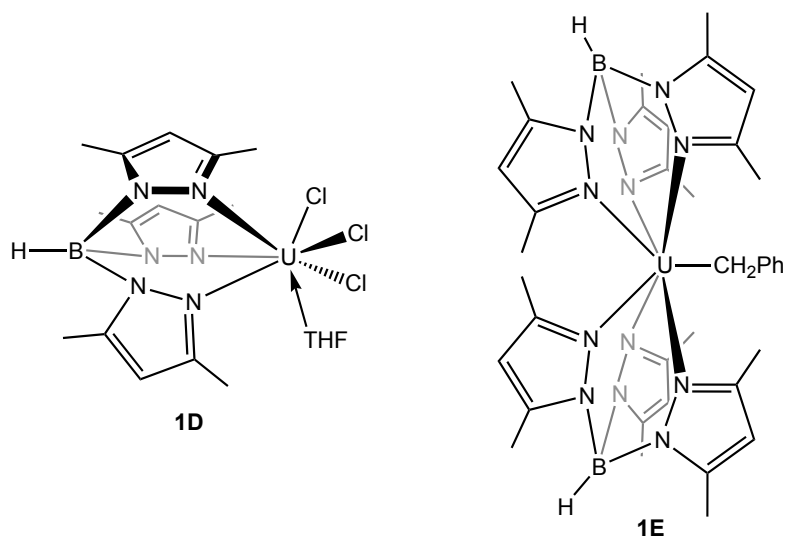


Figure 1.4. Organouranium complexes featuring the Tp^* ligand, **1D** and **1E**.

Scott reported the first triamidoamine complex of uranium in 1994, suggesting that tripodal ligands would be suitable for stabilising the metal centre by the chelate effect, and that their facial coordination would still allow further reactivity to occur.¹¹⁵ The chloride complexes $\{U(N[CH_2CH_2NSiMe_2R]_3)Cl\}_2$ (where R = Me, ^tBu, Ph; Tren^{TMS}, Tren^{DMSB}, Tren^{DMSP}) were reported, and following publications disclosed the ability of the U(Tren^{DMSB}) system to support a mixed-valence U(III)/U(IV) dimeric species (**Figure 1.5, 1F**),¹¹⁶ and to activate dinitrogen.¹¹⁷ Later research conducted by Liddle *et al.* found that U(Tren^{DMSB}) would also homologate CO, forming a ynediolate complex, $\{U(Tren^{DMSB})\}_2(\mu-\eta^1:\eta^1-OCCO)$.¹¹⁸ Further modification of the Tren ligand to feature tri-*iso*-propylsilyl (TIPS) groups in place of the SiMe₂R moiety enabled the isolation of the first uranium-nitride triple bond by design (**Figure 1.5, 1G**), and the first organouranium primary imido complex.^{119,120} This remarkable breadth of chemistry demonstrates the utility of such a tripodal ligand to support reactivity that has not been achieved with the ubiquitous carbocyclic ligand systems.

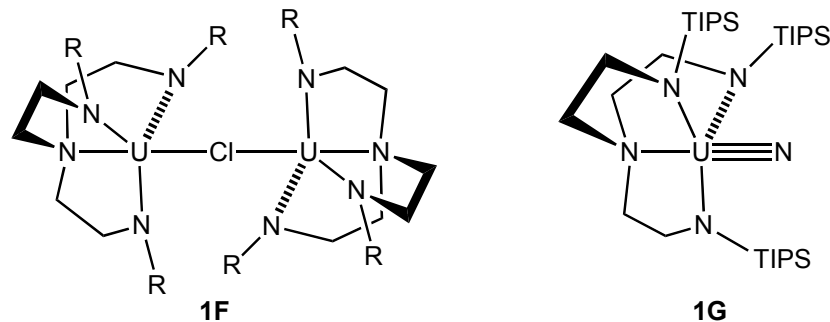


Figure 1.5. Uranium complexes featuring triamidoamine ligands (**1F** and **1G**).



A wide range of dianionic diamido ligands have also been used to support low- and mid-valent organouranium complexes. Wilson *et al.* used the diamidoamine ligand, $[N\{TMS\}(CH_2CH_2N\{TMS\})_2]^{2-}$ (= N^{''}N^{''}₂) – previously installed around transition metal centres^{121–125} – with uranium, and synthesised U^{IV}(N^{''}N^{''}₂)₂ and $\{U^{IV}(N^{\prime\prime}N^{\prime\prime}_2)Cl_2\}_2$ (**Figure 1.6, 1H** and **1I**).¹²⁶ This flexible ligand benefits from a central neutral nitrogen atom, which can participate in bonding through its lone pair if needed to stabilise the metal centre.

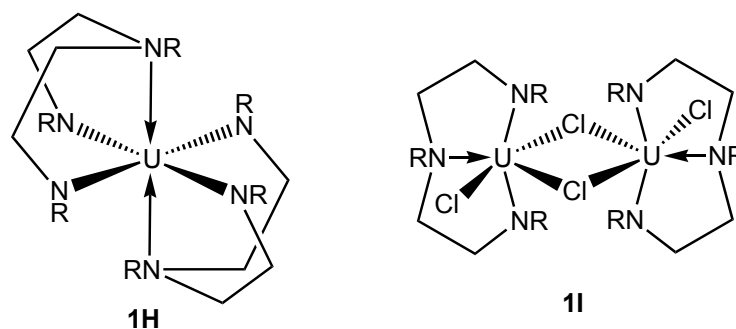


Figure 1.6. Organouranium complexes featuring the N'N'₂ ligand, **1H** and **1I**; R = TMS.

Several diamidoether ligands have been developed by Leznoff and coworkers; a NON-donor ligand framework allows ionic coordination *via* two terminal nitrogen atoms, as well as coordination to the oxophilic metal centre from the central oxygen atom *via* a lone pair interaction. Three NON-donor ligands have been used to support uranium: O(SiMe₂NR)₂ (where R = ^tBu or 2,4,6-Me₃Ph), ^tBuNON and ^{Mes}NON, and O(CH₂CH₂N{2,6-ⁱPr₂Ph})₂, ^{DIPP}NCOCN (**Figure 1.7**).^{127,128} The di-alkyl complexes can be generated from the respective U(IV) di-chloride precursors and alkyl lithium or potassium salts, and both U(^tBuNON)(R)₂ and U(^{DIPP}NCOCN)(R)₂ (where R = CH₂Ph, CH₂TMS) will act as ethylene polymerisation catalysts.¹²⁹ More recently, another NON-donor ligand, XA₂ (**Figure 1.7**), has been used to synthesise U(IV) di-alkyl complexes. The alkyl U(XA₂)(CH₂TMS)₂ will undergo unusual alkyl exchange reactions with NpLi or MeLi to yield U(XA₂)(Np)₂ or [Li(THF)_x][U(XA₂)Me₃], described by the authors as resembling salt metathesis reactions and proceeding *via* a trialkyl intermediate.¹³⁰ Research conducted by Diaconescu *et al.* has shown the utility of diamidoferrocene ligands, fc(NSiMe₂R)₂ (where R = Me, Ph, ^tBu; fc = 1,1'-ferrocenyl, **Figure 1.7**) for supporting a range of U(IV) complexes.^{131,132} The dialkyl complex U(fc{NSiMe₂^tBu})₂(CH₂Ph)₂ will induce reactivity of aromatic N-heterocycles such as ring-opening, alkyl transfer, C-H activation, and C-C coupling,^{133–135} as well as acting as a precatalyst for inter- and intramolecular hydroamination.¹³⁶ This behaviour is attributed to the ability of the diamide ligand to support the electrophilic metal centre to a greater extent than carbocyclic ligands,

allowing further reactivity to occur even when uranium is bound to strongly Lewis basic aromatic heterocycles.¹³³

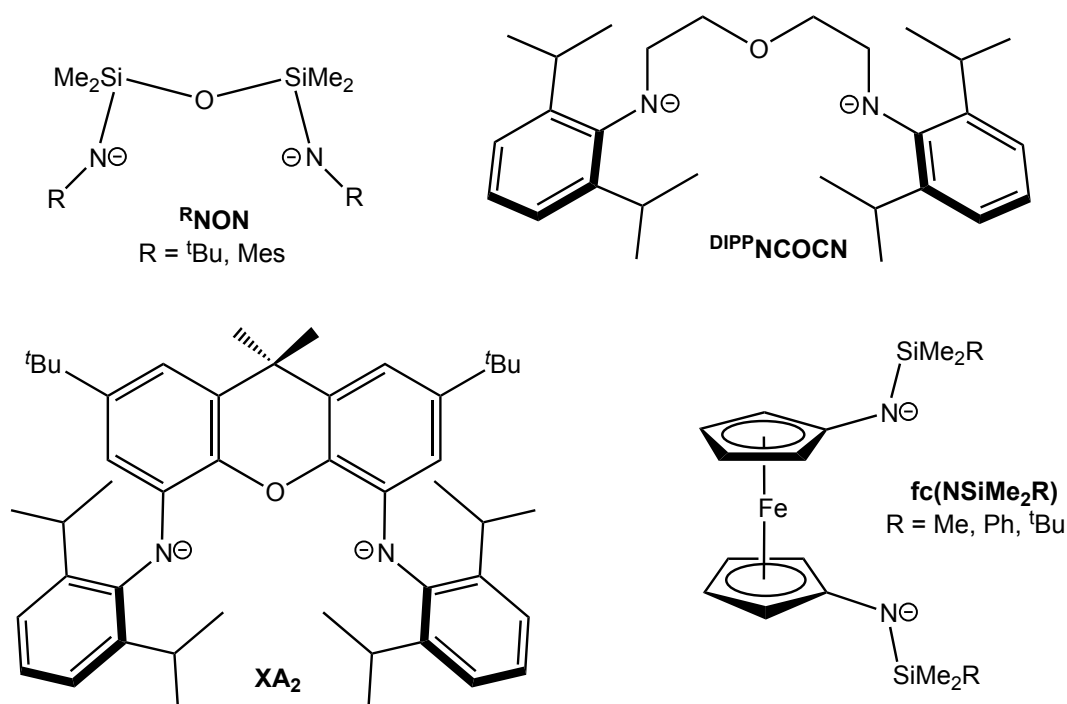


Figure 1.7. Dianionic diamido-based ligands used in organouranium complexes.

Macrocyclic ligands also find application in stabilising reactive uranium metal centres; examples of calixpyrrole,^{137–142} and triazacyclononane^{143–146} ligands bound to low- and mid-valent uranium have been reported. Such complexes have shown magnetic exchange coupling between two U(III) centres,¹⁴⁰ provided the only example of the complete cleavage of dinitrogen by an organouranium complex,¹³⁸ unusual alkane coordination,¹⁴⁵ and rich reductive and insertion chemistry with respect to CO and CO₂.^{147–150}

1.4 Reductive activation and insertion of small molecules

U(III) organometallic complexes have shown the ability to reduce small molecules, by virtue of the easily accessible redox couple between U(III)/U(IV). This, together with the oxophilic nature of uranium and its large ionic radius, which gives it access to large coordination numbers, makes it an ideal candidate for activating small

molecules such as carbon monoxide, and carbon dioxide. Both of these small molecules are of interest due to their potential to act as C₁ feedstocks.

Generally, a reduction process with U(III) involves 2 U(III) molecules gaining 2 electrons in a redox process with a small molecule, such as CO or CO₂, affording two U(IV) centres bound by a reduced bridging moiety – **Equation 1.1** demonstrates the reduction of CO₂ to O²⁻ and CO. Due to the oxophilic nature of uranium, one or more new U-O bonds are typically formed in this process.



Equation 1.1. Reduction of CO₂ by U(III).

Two significant barriers to developing catalytic processes involving U(III) are the difficulty in cycling the resulting U(IV) centres back to U(III), and breaking the strong U-O bonds in order to remove the functionalised product. Nevertheless, some progress has been made towards overcoming these obstacles, and many remarkable reduction and homologation reactions involving U(III) organometallic complexes have been reported; a summary of such reactions reported in the literature is presented here.

1.4.1 Carbon monoxide

Evidence for the binding of CO to uranium was first seen in matrix isolation studies of U(CO)₆ in 1971. Data collected from IR spectroscopic measurements indicated a ν_{CO} band at 1961 cm⁻¹, lowered from free CO in the gas phase (ν_{CO} = 2145 cm⁻¹), supporting the theory that uranium is able to π-donate to carbon monoxide.^{151,152} The first example of a molecular uranium-CO complex, UCp'₃(CO), was reported in 1986, after previous experiments with UCp'₃ and UCp₃ had shown them to be viable π-donors for molecules such as PMe₃, pyridine, THF, and isonitriles.^{64,153} Exposure of UCp'₃ to ¹²CO or ¹³CO elicited a colour change from green to red, and a new IR vibrational band was observed at 1976 or 1935 cm⁻¹ respectively, consistent with the binding of CO. No stable complex could be obtained from the experiment, and

CO was readily lost upon exposure of the red solutions to reduced pressure. Later theoretical work by Bursten and Strittmatter indicated that CO binding as carbonyl rather than isocarbonyl was most stable, according to molecular orbital calculations.¹⁵⁴ An isolable CO complex, $\text{U}(\text{C}_5\text{Me}_4\text{H})_3(\text{CO})$, was synthesised and structurally characterised in 1995 by Carmona *et al.*, showing an almost linear ‘U-CO’ moiety (U-C-O: $175.2(6)^\circ$) and a short U-C bond distance of $2.383(6) \text{ \AA}$, attributed to significant π -backbonding from the uranium centre (see **Figure 1.1** above).¹⁵⁵ These results were complemented by the synthesis of further U-CO metallocene complexes, $\text{U}(\text{C}_5\text{H}_4^t\text{Bu})_3(\text{CO})$ and $\text{UCp}^*\text{}_3(\text{CO})$,¹⁵⁶ which were too unstable to isolate, and the significantly sterically crowded complex, $\text{UCp}^*\text{}_3(\text{CO})$ (**Figure 1.8, 1J**), which was structurally characterised in 2003.¹⁵⁷

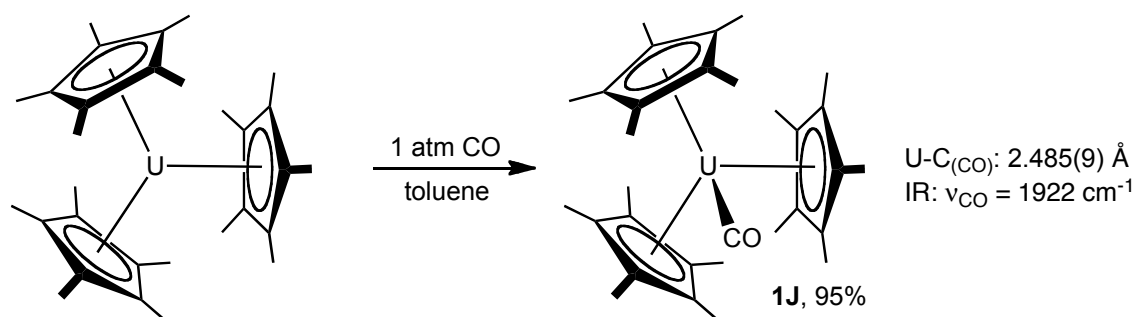
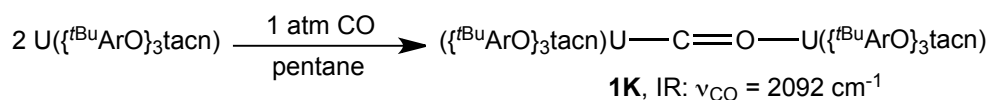


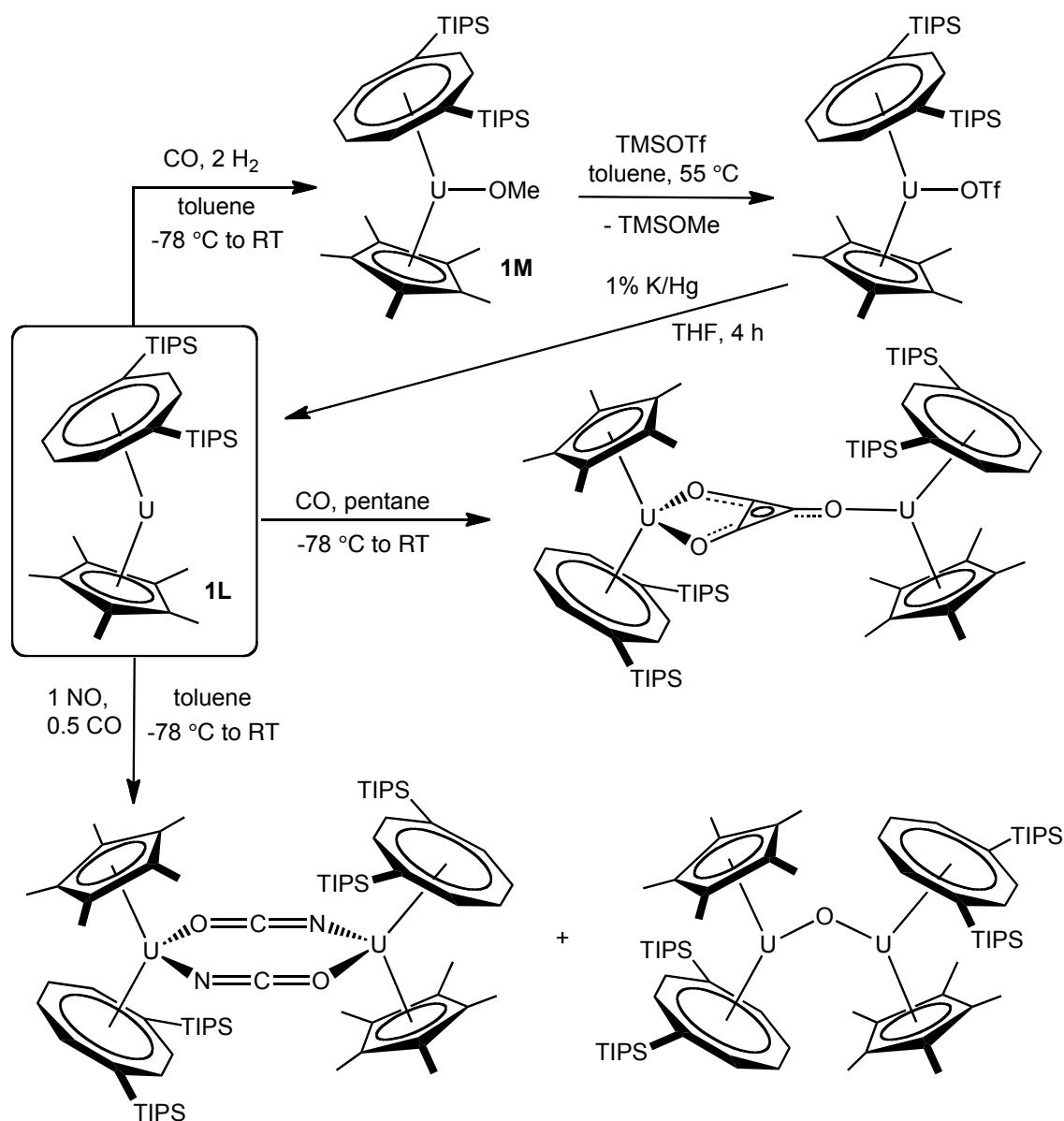
Figure 1.8. Synthesis of $\text{UCp}^*\text{}_3(\text{CO})$ (**1J**).

In contrast to simple coordination complexes of CO with uranium, the reaction of $\text{U}^{\text{III}}(\{\text{}^t\text{BuArO}\}_3\text{tacn})$ affords a dinuclear U(III)/U(IV) complex with a CO bridge, $[\text{U}(\{\text{}^t\text{BuArO}\}_3\text{tacn})]_2(\mu\text{-}\eta^1:\eta^1\text{-CO})$ (**Equation 1.2, 1K**).¹⁴⁷ Castro-Rodriguez and Meyer concluded that the dimer forms *via* attack of ‘ $\text{U}^{\text{IV}}(\{\text{}^t\text{BuArO}\}_3\text{tacn})(\text{CO}\cdot)$ ’, a charge-separated species, on another molecule of $\text{U}^{\text{III}}(\{\text{}^t\text{BuArO}\}_3\text{tacn})$, resulting in a unique $\mu\text{-}\eta^1:\eta^1\text{-CO}$ binding mode. Due to the CO moiety lying on a crystallographic inversion centre, no reliable bond metrics could be obtained from the structure, so no information on the extent of CO activation from bond distances could be inferred.



Equation 1.2. Formation of a U(IV) linear-bound CO complex.

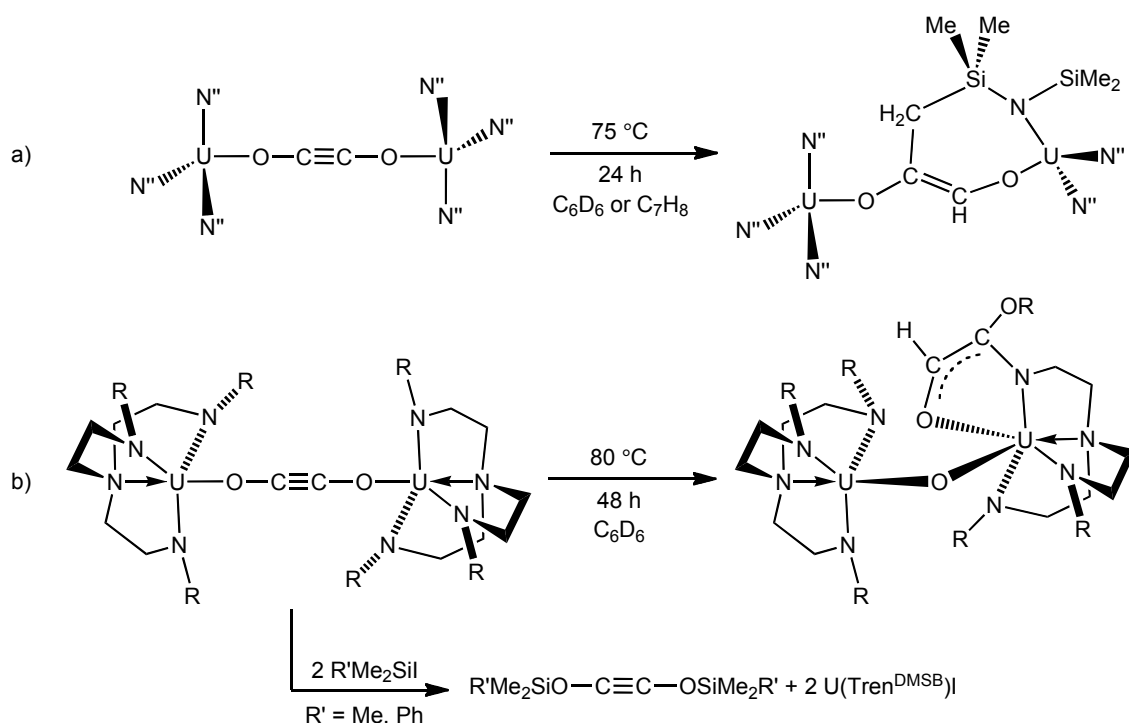
The first examples of CO homologation with an organouranium system were reported by Cloke and coworkers using a mixed-sandwich system, $\text{U}(\text{COT}^{\text{TIPS}2})(\text{C}_5\text{Me}_4\text{R})$ (where $\text{COT}^{\text{TIPS}2} = 1,4\text{-}\{\text{Si}^i\text{Pr}_3\}_2\text{C}_8\text{H}_6$, $\text{R} = \text{Me}, \text{H}$), which will form dimers bound to either a deltate ($\text{R} = \text{Me}$) or squarate ($\text{R} = \text{H}$) oxocarbon upon exposure to 1 bar of CO (**Scheme 1.1**).^{61,87} Coupling of just two molecules of CO was achieved from the reaction of $\text{U}(\text{COT}^{\text{TIPS}2})\text{Cp}^*$ with 0.95 equivalents of CO, but the addition of further CO after ynediolate formation did not yield higher oxocarbons. Altering the steric environment around the metal centre *via* modification of the ligands also enables selective ynediolate formation: $\text{U}(1,4\text{-}\{\text{TMS}\}_2\text{C}_8\text{H}_6)(\text{C}_5\text{Me}_4\text{TMS})$ exposed to 1 bar of CO forms solely the ‘O-C≡C-O’ product.⁶² Experimental and theoretical studies gave insight into the mechanism of the oxocarbon formation, theorised to occur *via* a ‘zig-zag’ intermediate.^{158,159} Identification of this intermediate encouraged experiments involving CO and a co-reactant, and it was demonstrated that $\text{U}(\text{COT}^{\text{TIPS}2})\text{Cp}^*$ (**1L**) will form cyanate derivatives with CO and NO, or a methoxide complex (**1M**) with CO and H_2 (**Scheme 1.1**).^{89,90} The latter reaction is a rare example of CO reduction and functionalisation at a uranium centre – hydrogenation of reduced CO has not been observed in any other organouranium system, and is discussed in further detail in section 1.7. The methoxide **1M** can be liberated from the metal centre by heating it to 55 °C in the presence of TMSOTf (OTf = $\text{O}\{\text{SO}_2\text{CF}_3\}$), yielding TMSOMe and $\text{U}(\text{COT}^{\text{TIPS}2})\text{Cp}^*(\text{OTf})$, which can be reduced back to **1L** with K amalgam.



Scheme 1.1. Reactivity of $\text{U}(\text{COT}^{\text{TIPS}_2})\text{Cp}^*$ with CO , CO/NO , and CO/H_2 .

Although Andersen *et al.* reported in 1979 that the tris-amide uranium system, $\text{U}(\text{N}\{\text{TMS}\}_3)$ ($=\text{UN}^3$), did not react with CO , work by Arnold and coworkers in 2011 proved to the contrary. Exposure of a hydrocarbon solution of UN^3 to 1 bar of CO afforded $\text{N}^3\text{U-O-C}\equiv\text{C-O-UN}^3$ in an 82% yield; the same result occurs with CO and the $\text{U}(\text{III})$ tris(aryloxide) complexes, $\text{U}(\text{OAr})_3$ (where $\text{Ar} = 2,6\text{-}\{\text{tBu}\}_2\text{Ph}$, $2,4,6\text{-}\{\text{tBu}\}_3\text{Ph}$), forming the associated ynediolates in 61 and 57% yields respectively.^{160,161} Another example of this reductive homologation occurs with the $\text{Tren}^{\text{DMSB}}$ derivative and an excess of CO , forming $\{\text{U}(\text{Tren}^{\text{DMSB}})\}_2(\mu\text{-}\kappa^1:\kappa^1\text{-C}_2\text{O}_2)$ in a 62% isolated yield.¹¹⁸

Heating either $(UN''_3)_2(\mu-\kappa^1:\kappa^1-C_2O_2)$ or $\{U(\text{Tren}^{\text{DMSB}})\}_2(\mu-\kappa^1:\kappa^1-C_2O_2)$ results in ligand activation, indicating that the triply-bonded ynediolate fragment is not entirely inert with respect to further functionalisation (**Scheme 1.2**). Accordingly, treating $\{U(\text{Tren}^{\text{DMSB}})\}_2(\mu-\kappa^1:\kappa^1-C_2O_2)$ with Me_3SiI or Me_2PhSiI yields $U(\text{Tren}^{\text{DMSB}})\text{I}$ and the silyl-substituted ynediolates, $\text{RMe}_2\text{Si-O-C}\equiv\text{C-O-SiMe}_2\text{R}$ ($\text{R} = \text{Me}, \text{Ph}$) respectively (**Scheme 1.2b**).



Scheme 1.2. Functionalisation of ynediolate complexes. $\text{R} = \text{SiMe}_2^t\text{Bu}$.

1.4.2 Carbon dioxide

Several examples of CO_2 activation and reduction by U(III) organometallic complexes have been reported, yielding products such as mono-bridged oxo dimers, and bridging carbonates. Initial experiments by Berthet *et al.* with UCp'_3 and excess CO_2 led to the isolation of $(\text{UCp}'_3)_2(\mu\text{-O})$, characterised by X-ray crystallographic means. The mechanism was speculated to involve the initial formation of a ' $\mu\text{-CO}_2$ ' complex with the subsequent extrusion of CO ; related studies on the reaction of the same U(III) system with CS_2 and the isolation of $(\text{UCp}'_3)_2(\mu\text{-CS}_2)$ supported this claim.¹⁶²

Meyer and coworkers have undertaken extensive studies on the activation of CO₂, utilising U(III) supported by tripodal O-chelating ligand frameworks (**Figure 1.9**) and they have demonstrated that subtle steric changes to a ligand environment can significantly alter the outcome of CO₂ reduction. Exposure of excess CO₂ to U({^tBuArO}₃tacn) forms the oxo-bridged species [U({^tBuArO}₃tacn)]₂(μ-O), and releases CO; the bulkier ligand variant, U({^{Ad}ArO}₃tacn) binds CO₂ in an linear, end-on fashion as a charge-separated species, formed from a 1e⁻ reduction.^{147,163}

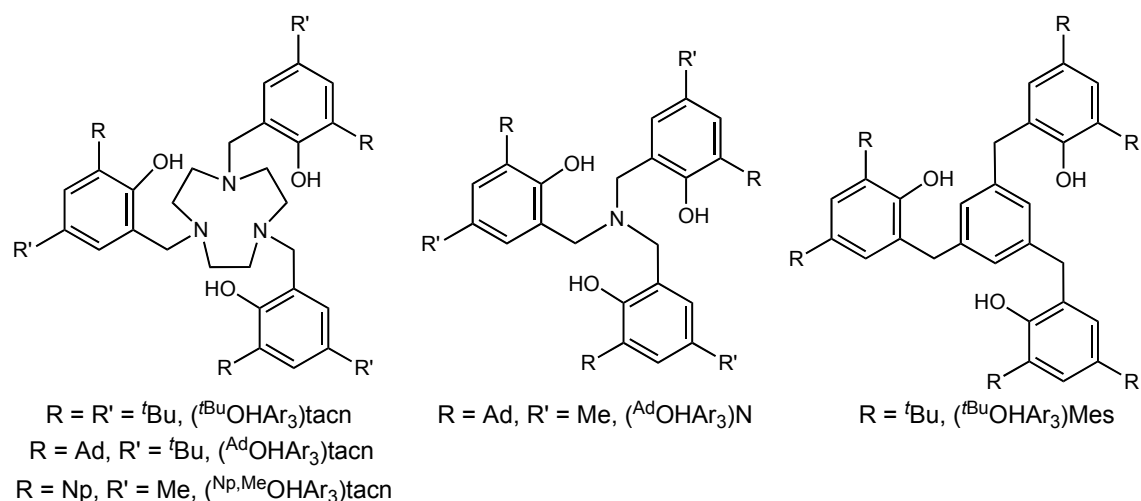
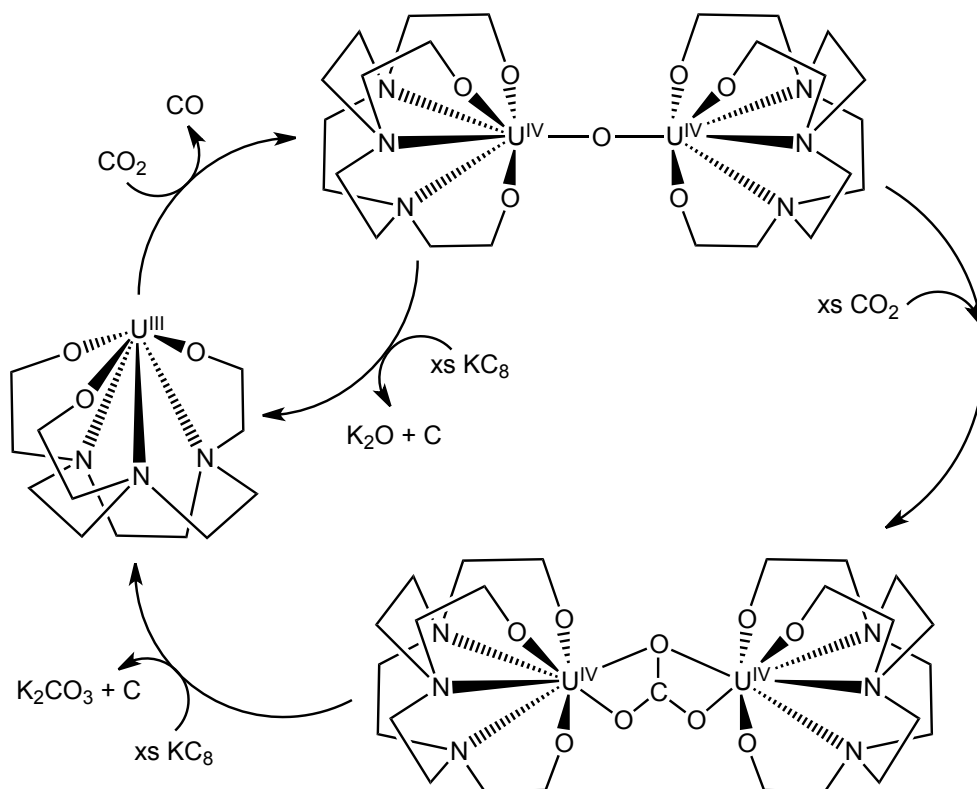


Figure 1.9. Ligand systems employed by the Meyer group.

A pseudo-catalytic process can be achieved using U({^{Np,Me}ArO}₃tacn) and CO₂, forming a bridging carbonate moiety which can be liberated with KC₈, forming K₂CO₃, and leaving the U(III) species available for further reductive activity (**Scheme 1.3**).¹⁵⁰ Precipitation of an insoluble uranium-potassium carbonate cluster terminates the cycle after several turnovers. Altering the tacn-framework to an N- or mesitylene-based ligand to give U({^{Ad}ArO}₃N) or U({^tBuArO}₃Mes) yields complexes that allow the formation of a bridging carbonate moiety when exposed to an excess of CO₂, showing the impact of the varying steric demands of the three ligand systems. Two different carbonate coordination modes are seen in each case, μ-η¹:κ²(O,O')-CO₃ and μ-κ²(O,O'):κ²(O,O'')-CO₃ respectively.¹⁶⁴ Mechanistic studies were carried out to investigate the carbonate formation, and the results showed that a bridging oxo

complex, $\{U(L)\}_2(\mu-O)$ (where L = ligand), is formed initially and then reacts with a further equivalent of CO_2 , extruding free CO.^{165,166}

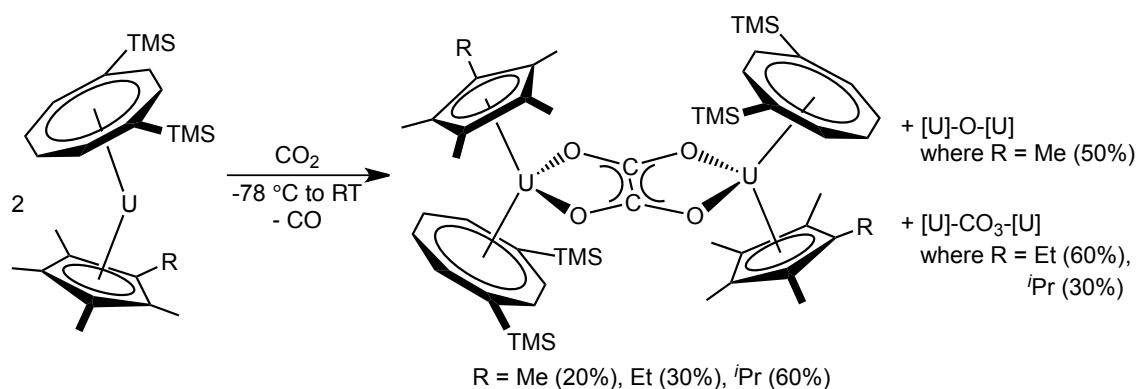


Scheme 1.3. Synthetic cycle of $U(\{^{Np,Me}ArO\}_3tacn)$ with CO_2 and KC_8 ; figurative representation of the ligand framework showing coordinating N and O atoms.

Both $U(COT^{TIPS2})(C_5Me_4H)$ and $[U(OSi\{O^tBu\}_3)_2(\mu-OSi\{O^tBu\}_3)]_2$ will react with excess CO_2 to form bridging carbonate complexes with the concomitant formation of CO.^{88,167} In the former case, the CO extruded will react further with residual U(III) to yield the known squarate compound. In the latter case, the siloxy complex is first reacted with KC_8 to form the heterobimetallic system, $[U(OSi\{O^tBu\}_3)_4K]$, exposure to CO_2 yields a pentavalent terminal oxo complex and free CO in a rare example of a $2e^-$ U(III)/U(V) redox process. The related ion-pair, $[K(18c6)][U(OSi\{O^tBu\}_3)_4]$ (18c6 = 18-crown-6), reacts with excess CO_2 to form a terminally-bound carbonate, $[U(OSi\{O^tBu\}_3)_4(\mu-\kappa^1:\kappa^2-CO_3)K_2(18C6)]$ and $U^{IV}(OSi\{O^tBu\}_3)_4$.¹⁶⁸ The aryloxide, $U^{III}(OTbp)_3$ (Tbp = 2,4,6- $\{^tBu\}_3Ph$), forms a

bridging oxo complex with CO₂, but also inserts a further equivalent of CO₂ into one uranium-aryloxide bond, yielding U(OTtbp)₂(μ-O₂C-OTtbp)₂(μ-O)U(OTtbp)₂.¹⁶¹

Most recently, the reductive coupling of CO₂ to form a bridging oxalate complex has been reported for the first time at a uranium centre. Oxalate formation has been shown for the lanthanide Cp* complexes – first reported for SmCp*₂(THF)¹⁶⁹ – but has not been observed with uranium. Steric factors and temperature are highly important for the success of this reaction: the reactions of U(COT^{TMS2})(CpMe₄R) (where R = Me, Et, ⁱPr) with CO₂ at -78 °C yield a mixture of bridging oxalate and either carbonate or oxo products (**Scheme 1.4**), while when R = ^tBu, only the carbonate product is formed – as is the case with the U(COT^{TIPS2})Cp* mixed-sandwich complex.^{29,88} The reaction of U(COT^{TMS2})Cp* with CO₂ performed at ambient temperature yielded only the bridging oxo dimer.



Scheme 1.4. Synthesis of oxalate complexes from U(III) mixed-sandwiches; percentages indicate isolated product yields.

1.4.3 Concluding remarks

A variety of oxygen-bound U(IV) products have been isolated from the reactions of U(III) with CO and CO₂, the nature of which are largely reliant on the ligand environment encasing the uranium metal centre. This is exemplified most clearly by the reactions of small molecules with tripodal ‘tacn’, mesityl, or N-based ligands as reported by Meyer *et al.*, wherein changes to substituents on the pendant arene arms

dictate the outcome of small molecule activation.¹⁷⁰ Liberation of the reduced products has been achieved in only a few cases, and involves the use of harsh reagents that yield U(IV) halide or triflates, which then require reduction back to U(III) starting materials if a recyclable process is desired.^{61,90,118} The exception is with U($\{\text{Np,MeArO}\}_3\text{tacn}$) and CO₂, which can be readily converted back from oxo and carbonate U(IV) products to the U(III) starting material with KC₈, along with the elimination of K₂O and K₂CO₃.

1.5 Sigma-bonded organouranium complexes: U-C and U-H bonds

1.5.1 Uranium alkyls

In addition to π -bound carbocyclic ligands, uranium can also form σ -bonds to discrete carbon atoms, forming alkyl complexes. Such compounds are well-known in transition metal chemistry, however, initial attempts to synthesise homoleptic alkyl complexes led researchers to the conclusion that uranium alkyls would be too unstable to isolate.¹⁰ This assumption was proven incorrect, and numerous uranium alkyl complexes have been synthesised over the last 50 years, pertinent examples of which will be discussed here.

The first report of organouranium complexes containing σ -bonds was in 1970 by Brandi *et al.* as part of conference proceedings.¹⁷¹ The authors describe here, and in more detail in their later paper, the synthesis of alkyls UCp₃R (where R = Ph, CH₂Ph, CH₂-*p*-C₆H₄CH₃), and describe their ‘remarkable’ thermal stability in the solid state. Two other research groups simultaneously reported their work on σ -bound uranium alkyl and aryl complexes in the same metallocene framework, extending the series to include organyls R = *p*-C₆H₄CH₃, C \equiv CPh, Me, ^{*n*}Bu, Np, C₆F₅, ^{*i*}Pr,¹⁷²⁻¹⁷⁴ followed by R = allyl, ^{*t*}Bu, *cis*-2-butenyl, *trans*-2-butenyl, and vinyl shortly thereafter.¹⁷⁵ All authors concluded that these highly air-sensitive first examples of organouranium σ -bonded species contained a U-C bond considered ionic due to its susceptibility to alcoholysis and hydrolysis, but were resistant to β -hydrogen elimination even when

subjected to high temperatures. Shortly thereafter, Andersen *et al.* reported the first two alkyluranium species containing more than one U-C σ -bond: anionic $\text{Li}_2[\text{U}(\text{CH}_2\text{TMS})_6](\text{TMEDA})_7$ and $\text{Li}_2[\text{U}(\text{C}_9\text{H}_{12}\text{N})_6](\text{TMEDA})_7$ (where $\text{C}_9\text{H}_{12}\text{N}$ is 2-methylbenzylamine).¹⁷⁶

The syntheses of neutral homoleptic uranium alkyls were revisited following the discovery that σ -bonded alkyluranium species *could* exist, and numerous examples have been reported to date.^{177–180} Of prominent focus for further alkyluranium research were compounds containing either one or two alkyl ligands, in order to elucidate the nature of the bond and its potential reactivity in an otherwise inert environment effected by the ancillary ligand system. The advent of bis-Cp* ligand systems enabled the isolation of di-alkyls and -aryls of the form UCp^*_2R_2 , and mono-alkyls and -aryls of the form $\text{UCp}^*_2(\text{R})\text{Cl}$ (where $\text{R} = \text{Me}, \text{CH}_2\text{TMS}, \text{CH}_2\text{Ph}, \text{Ph}$) allowing for further study of the nature of the U-C σ -bond (**Figure 1.10**).^{44,48} These bis-Cp* alkyluranium species are also thermally stable, and showed reactivity towards dihydrogen and small molecules. Remarkably, U(III) alkyls are also supported by bis-Cp* ligands: the reaction of the chloride precursor, $\{\text{UCp}^*_2(\mu\text{-Cl})\}_3$, with $\text{LiCH}\{\text{TMS}\}_2$ yielded the stable alkyl $\text{UCp}^*_2(\text{CH}\{\text{TMS}\}_2)$ in 41% yield¹⁸¹ – few U(III) alkyls have been reported since.^{113,114}

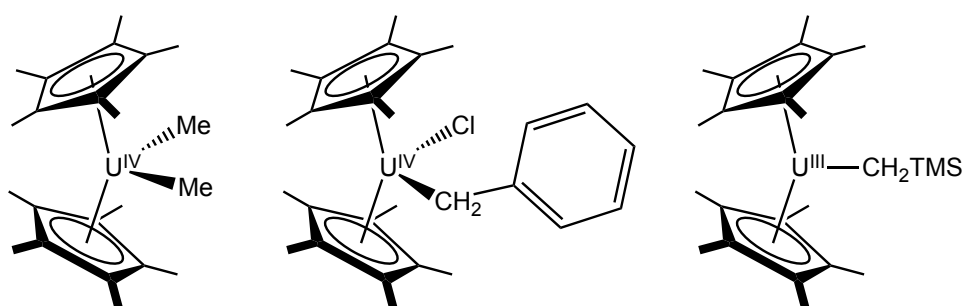
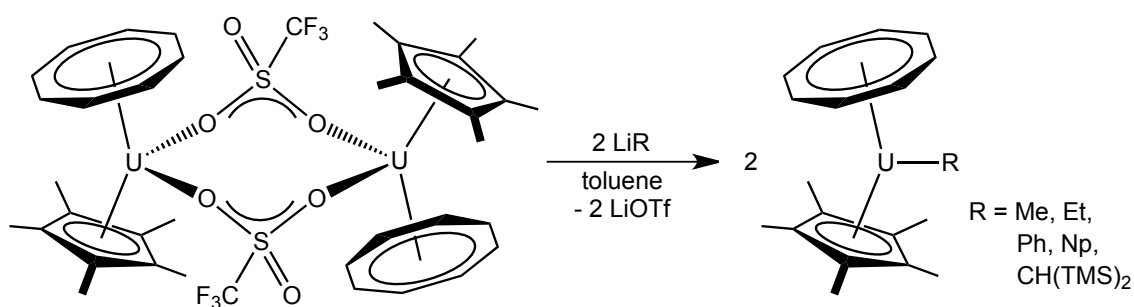


Figure 1.10. Mono- and dialkyl organouranium compounds containing a bis-Cp* ligand framework.

The Tp* ligand, often considered comparable to Cp*, will also support uranium alkyls. U(IV) alkyls of the form $\text{UTp}^*\text{Cl}_{3-x}(\text{R})_x$ ($\text{R} = \text{CH}\{\text{TMS}\}_2$, $x = 2$; $\text{R} = \text{CH}_2\text{TMS}$, $x = 1-3$) were reported in 1994 by Domingos *et al.*^{108,109} Their reactivity towards ketones and aldehydes was explored, yielding tertiary alkoxides or other diketyl

insertion products respectively. This stabilising ligand also demonstrates utility in preventing disproportionation of low-valent uranium species, enabling the synthesis of the U(III) alkyl, $\text{UTp}^*_2(\text{CH}_2\text{Ph})$.¹¹³ Subsequently, the behaviour of a U-C σ -bond of a U(III) – not U(IV) – metal centre could be explored with respect to reactivity with CO_2 , CS_2 , acetone, and organic azides for the first time.^{110,112,114}

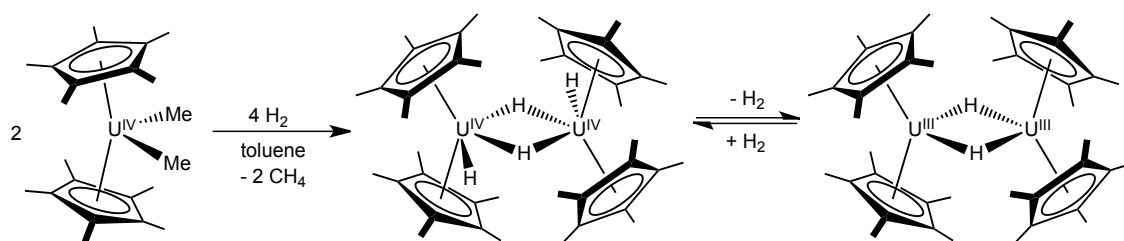
Numerous organouranium mono- and dialkyls have been synthesised in metallocyclic^{49,66,86,182,183} and non-metallocyclic^{128–130,132,184} ligand systems. Many examples of insertion chemistry with small molecules have also been reported, as detailed in section 1.6. Of particular importance to this thesis are previously synthesised mixed-sandwich alkyls featuring COT and Cp rings, which inherently exist as mono-alkyls due to the coordination of the di- and mono-anionic ligands respectively. Gilbert *et al.* have reported the synthesis of $\text{Th}(\text{COT})\text{Cp}(\text{CH}\{\text{TMS}\}_2)$, but no uranium analogues exist.¹⁸⁵ In 2009, Evans and coworkers reported the synthesis of $\text{U}(\text{COT})\text{Cp}^*(\text{R})$ alkyls, targeted with a view to comparing U-C σ -bond reactivity in a ‘ $\text{U}(\text{COT})\text{Cp}^*$ ’ environment to the sterically similar ‘ UCp^*_2 ’ environment.⁸⁶ The organyls $\text{U}(\text{COT})\text{Cp}^*(\text{R})$ where $\text{R} = \text{CH}\{\text{TMS}\}_2$, Ph, Me, Et and Np were obtained from reacting the bridging triflate precursor $\{\text{U}(\text{COT})\text{Cp}^*\}_2(\mu\text{-OTf})_2$ with the appropriate lithium alkyl or aryl reagents (**Scheme 1.5**); only the bulky trimethylsilyl alkyl was structurally characterised and showed no agostic interactions between the TMS groups and uranium metal centre.¹⁸⁶



Scheme 1.5. Synthesis of mixed-sandwich alkyl complexes.

1.5.2 Uranium hydrides

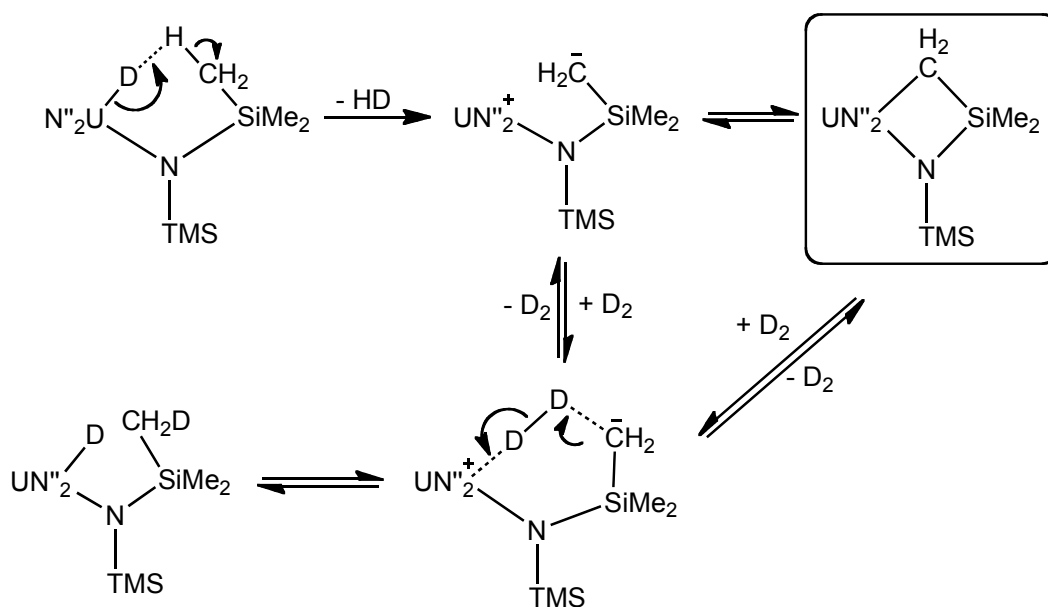
Pioneering work by Marks *et al.* in 1978 led to the synthesis of the first An(IV) hydrides, $\{\text{Cp}^*_2\text{AnH}(\mu\text{-H})\}_2$ (An = Th, U), with the uranium hydride losing 1 equivalent of H_2 at ambient temperature *via* binuclear reductive elimination.⁴⁴ The product of this hydrogen loss was considered to be the U(III) hydride, $\{\text{Cp}^*_2\text{U}(\text{H})\}_2$; the thorium analogue shows no such decomposition due to the difficulties in accessing the Th(III) oxidation state, and addition of H_2 to $\{\text{Cp}^*_2\text{U}(\text{H})\}_2$ re-formed the U(IV) hydride complex (**Scheme 1.6**). Hydrogenolysis of parent alkyl complexes provided access to the hydrides, and the thorium deuteride was formed from the reaction of $\{\text{Cp}^*_2\text{Th}(\text{CH}_3)_2\}_2$ with D_2 in place of H_2 . The uranium deuteride, $\{\text{Cp}^*_2\text{UD}(\mu\text{-D})\}_2$, could not be formed without extensive isotopic scrambling due to rapid exchange between the ligand protons and the U-D bonds. This work was described in greater detail a few years later, and the authors conclude that hydrogenolysis occurs *via* a non-oxidative pathway, with the mechanism involving a four-membered transition state. This occurs at a much faster rate than in analogous group 4 metal systems due to the highly polarised actinide-carbon bonds and relative coordinative unsaturation (a result of the larger ionic radii of the actinides).⁴⁸ They also note the polar nature of actinide-hydride bonds, which they describe as ‘hydridic’ due to the facile reactions of both actinide hydride complexes with ketones and alcohols.



Scheme 1.6. Synthesis and equilibrium of U(IV) and U(III) hydride complexes.

Shortly after, in 1979, Andersen *et al.* reported the first mononuclear non-metallocene uranium mono-hydride, $\text{UN}^{\text{III}}_3\text{H}$ – the first uranium hydride to be characterised by X-ray crystallographic means.^{187,188} Its synthesis was achieved by

reacting $\text{UN}^{\text{III}}\text{Cl}$ with NaN^{III} in refluxing THF (from H-abstraction from the solvent), or with $t\text{BuLi}$ or LiBEt_3H in pentane. The deuteride, $\text{UN}^{\text{III}}\text{D}$, can be prepared by refluxing $\text{UN}^{\text{III}}\text{Cl}$ and NaN^{III} in $d_8\text{-THF}$, or by reacting $\text{UN}^{\text{III}}\text{H}$ with $t\text{BuLi}$ and $\text{CF}_3\text{CO}_2\text{D}$. It was discovered that the hydride would, on repeated exposure to an excess of D_2 , undergo H/D exchange with all of the ligand protons resulting in the formation of $\text{U}(\text{N}\{\text{Si}(\text{CD}_3)_3\}_2)_3(\text{D})$. The reverse reaction also occurs: exposure of the d_{55} -compound to H_2 yields the original hydride.¹⁸⁹ The authors postulate a mechanism involving a four-membered metallocycle, $\text{UN}^{\text{II}}(\kappa^1:\kappa^1\text{-N}\{\text{SiMe}_2\text{CH}_2\}\{\text{TMS}\})$, as an intermediate, which will itself react with either H_2 or D_2 to undergo the same exchange processes and form perdeutero-hydride or deuteride complexes, eventually replacing all ligand protons with deuterium (**Scheme 1.7**).



Scheme 1.7. Mechanism of H-D exchange in $\text{UN}^{\text{III}}\text{H}$.¹⁸⁹

Further work by Marks and coworkers on actinide hydrides and their properties was reported frequently throughout the 1980s. The thorium hydride crystal structure, $\{\text{ThCp}^*_2\text{H}(\mu\text{-H})_2\}$, was determined by neutron diffraction in 1979¹⁹⁰ – the structure of the uranium analogue was not determined until 2007,¹⁹¹ first by X-ray diffraction, then by neutron diffraction in 2012.¹⁹² Monomeric terminal hydrides were synthesised within UCp^*_2X_2 systems by utilising chloride or alkoxide ligands to occupy

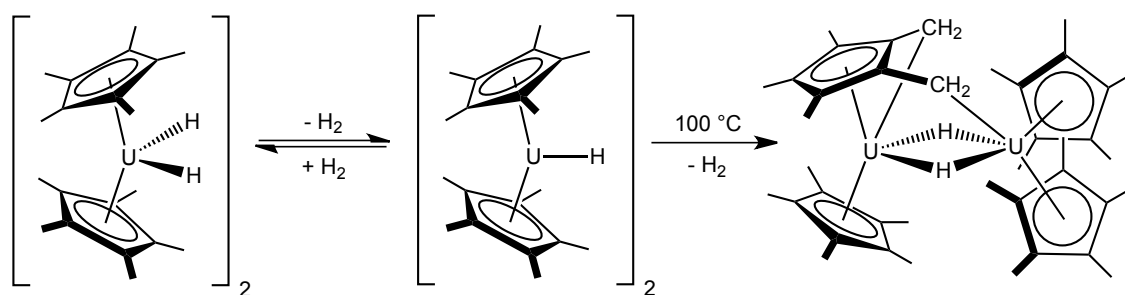
one 'X' position. This led to the collection of IR spectroscopic data that helped to determine typical vibrations of bridging vs terminal hydride ligands, as compounds with the structures $\{\text{UCp}^*_2\text{X}(\mu\text{-H})\}_2$ and UCp^*_2XH were synthesised. Bridging hydrides tend to have IR vibrational bands at ca 1200 cm^{-1} , while terminal hydrides have bands at ca 1400 cm^{-1} – see Chapter 3 for collated data.

A U(III) hydride supported by a diphosphine ligand, $\text{UCp}^*_2(\text{dmpe})\text{H}$ (dmpe = bis(1,2-dimethylphosphino)ethane), was reported and structurally characterised by X-ray diffraction techniques in 1982.¹⁹³ Its synthesis is unusual, as it is formed from the reaction of the U(IV) dialkyl, UCp^*_2R_2 (R = Me, CH_2TMS) and H_2 in the presence of dmpe, generating free alkane and the U(III) hydride.¹⁹³ Precedent for this behaviour is seen when H_2 is added to $\text{U}^{\text{IV}}\text{Cp}^*_2\text{Cl}(\text{R})$ (R = CH_3 , CH_2TMS) which generates $\{\text{U}^{\text{III}}\text{Cp}^*_2\text{Cl}\}_2$ and free alkane. Again, this type of spontaneous reduction from the +4 to +3 oxidation state is not observed for the analogous thorium compound.¹⁸¹

Work by Ephritikhine and coworkers resulted in the synthesis of a series of hydride complexes between 1987 and 1992, notable examples including a non-metallocene bridging hydride, a range of anionic hydrides, and the first stable organouranium(IV) hydride.^{194–199} The U(III) anionic hydride, $[\text{Na}(\text{THF})_2][(\text{UCp}_3)_2(\mu\text{-H})]$, was synthesised from UCp_3 and NaH in THF.¹⁹⁵ The syntheses of $\text{UCp}'_3(\text{H})$ and $\text{U}(\text{C}_5\text{H}_4'\text{Bu})_3(\text{H})$ were achieved from the corresponding U(IV) chloride and KBET_3H . Both complexes are stable with respect to hydrogen loss and can be reduced back to the U(III) metallocenes with sodium amalgam. X-ray diffraction data collected for $\text{U}(\text{C}_5\text{H}_4'\text{Bu})_3(\text{H})$ showed that its geometric parameters were essentially identical to $\text{U}(\text{C}_5\text{H}_4'\text{Bu})_3$ within standard error limits. A tris-phospholyl uranium hydride, $\text{U}(\text{C}_5\text{H}_4\text{P})_3(\text{H})$ was also reported.²⁰⁰ None of these hydrides were synthesised from alkyl precursors and dihydrogen.

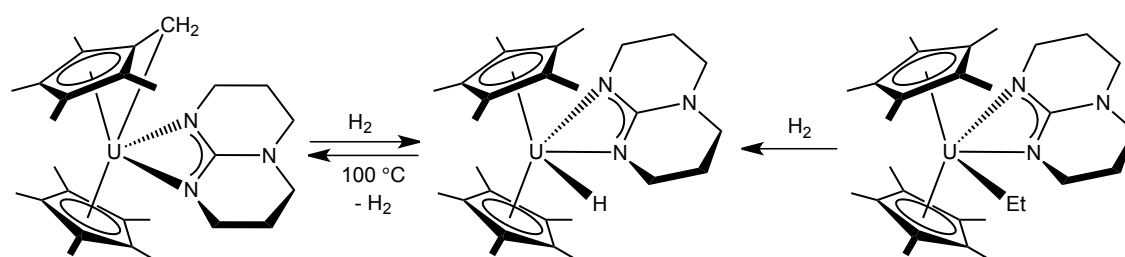
Further studies on the hydrides $\{\text{U}^{\text{III}}\text{Cp}^*_2\text{H}\}_2$ and $\{\text{U}^{\text{IV}}\text{Cp}^*_2\text{H}(\mu\text{-H})\}_2$ by the Evans group elucidated the structure of a 'tuck-in-tuck-over' hydride, formed from

heating the equilibrium mixture of $\{U^{III}Cp^*_2H\}_2$ and $\{U^{IV}Cp^*_2H(\mu-H)\}_2$ to 100 °C (**Scheme 1.8**). IR spectroscopic data showed the presence of a broad band at 1164 cm^{-1} , attributed to the bridging hydride ligands. Synthesis of the deuterio-analogue, containing bridging deuterium ligands that would give a shifted IR vibrational band, was not possible due to H/D exchange between the ligand protons.²⁰¹ This unusual hydride can undergo 4-, 6-, and 8-electron reduction processes, as detailed in later publications.^{192,202}



Scheme 1.8. Synthesis of a ‘tuck-in-tuck-over’ hydride complex.

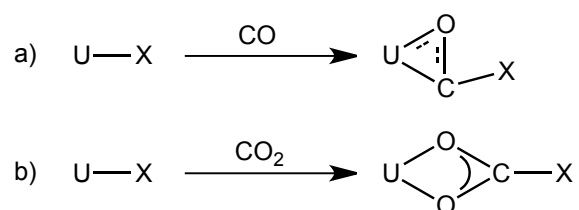
Utilising the Cp* ligand system alongside an ‘hpp’ (1,3,4,6,7,8-hexahydro-2*H*-pyrimido[1,2-*a*]pyrimidinato) ligand enabled the synthesis of a monomeric, U(IV) hydride, $UCp^*_2(hpp)(H)$, synthesised from hydrogenolysis of $UCp^*_2(hpp)(Et)$, or of ‘tucked-in’ $UCp^*(\eta^5:\kappa^1-C_5Me_4CH_2)(hpp)$ (**Scheme 1.9**).^{203,204} The synthesis of $[K(2.2.2-cryptand)][U^{III}Cp^*_3(H)]$ has also been reported, achieved either from the reaction of UCp^*_3 and KH in the presence of 2.2.2-cryptand, or by hydrogenolysis of the remarkable U(II) complex, $[K(2.2.2-cryptand)][UCp^*_3]$.²⁰⁵



Scheme 1.9. Synthesis of $UCp^*_2(hpp)(H)$ from hydrogenolysis of alkyl precursors.

1.6 Small molecule insertion and functionalisation by U(IV)

In contrast to U(III) reductive chemistry, U(IV) complexes do not undergo the same reactions to reduce small molecules – access to the pentavalent oxidation state of uranium is complicated by the typically unstable nature of U(V) complexes, which generally tend to disproportionate.²⁰⁶ However, reactive U-C, U-H and U-N σ -bonds will undergo insertion chemistry with CO and CO₂ – their polar nature, coupled with the oxophilicity of uranium, allows for such behaviour. This insertion of small molecules is accompanied by functionalisation: an alkyl, hydride, or amide group binds to the inserted moiety (**Scheme 1.10**). It should be noted that no insertion of CO into a U-H bond has been reported to date. No oxidation state change occurs upon insertion – the typical oxidative insertion/reductive elimination pathways established in organometallic chemistry featuring non-actinides are not generally found in organouranium chemistry. As a result, the occurrence of β -hydride elimination with organouranium alkyl complexes is uncommon, allowing for the formation and subsequent reactions of alkyls containing a β -hydrogen.



Scheme 1.10. U(IV) insertion reactivity with a) CO, b) CO₂, forming U(IV) products;
X = C, H, N.

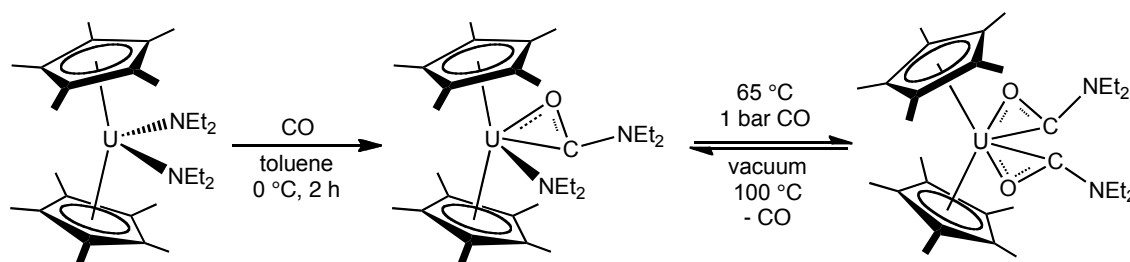
When compared to U(III) reductive processes with CO and CO₂, it can be argued that U(IV) insertion chemistry is a more convenient and practical method of approaching ‘recyclable’ small molecule activation. Functionalisation of reduced small molecules in U(III) reactions is rare (especially without forcing conditions)^{90,118,160} – in contrast, U(IV) insertion reactions functionalise inserted molecules intrinsically. When considering the removal of functionalised groups, the issue of oxidation state change is not a problem – no cycling between U(III) and U(IV) is needed to recycle the starting

material, if the bound moiety can be extruded. However, the barrier of strong, thermodynamically stable U-O bonds is still present in this approach.

Examples of CO and CO₂ insertion into U-C and U-N bonds have been well-documented in the literature, and includes bonds supported by a large variety of ligand frameworks. The patterns of insertion are well-defined, except in the cases of ‘tethered’ uranium-alkyl bonds where more unusual products have been observed, *vide infra*. Insertion of CO and CO₂ into U-H bonds has been less studied, likely due to the instability of many uranium hydride complexes with respect to dihydrogen loss or other decomposition routes. A review of insertion reactions is detailed in this section.

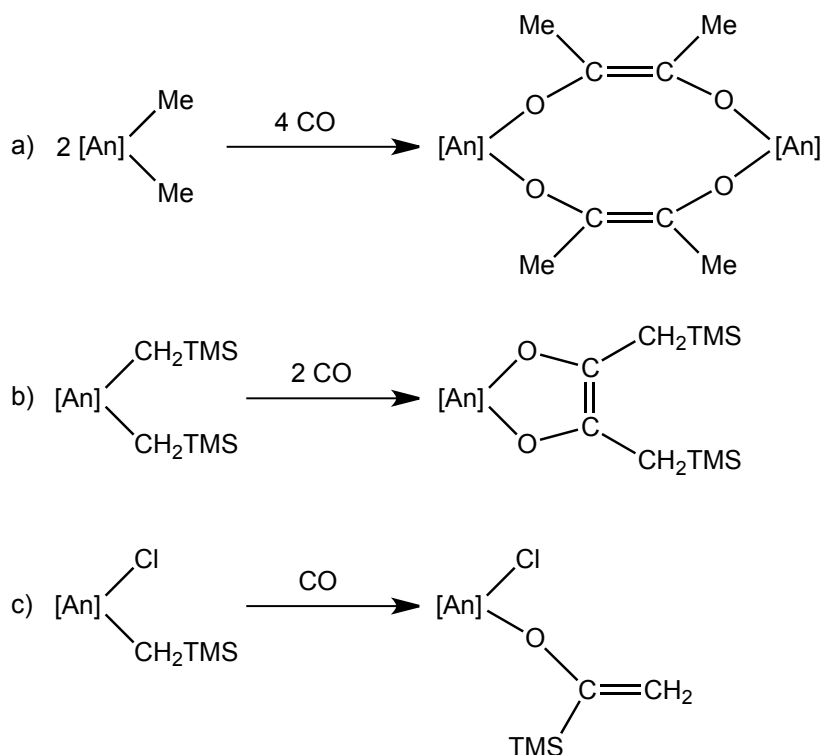
1.6.1 Carbon monoxide

The insertion of CO into U-C and U-N bonds of U(IV) complexes has also been observed. Studies on UCp*₂(NR₂)Cl and UCp*₂(NR₂)₂ (R = Me, Et) systems carried out by Marks *et al.* showed that CO insertion into U-N bonds gave the mono- and bis-carbamoyls, UCp*₂(η²-OCNR₂)Cl and UCp*₂(η²-OCNR₂)₂ respectively. The latter class are unstable with respect to CO loss when subjected to reduced pressure at 100 °C, reverting to the mono-insertion products (**Scheme 1.11**).⁴⁷ Irreversible CO uptake by UCp₃(NEt₂) was observed by Fischer and coworkers during their studies on alkyl and amide complexes, and they proposed the formation of an η²-carbamoyl product, however, this was not verified by X-ray crystallography.²⁰⁷



Scheme 1.11. Insertion of CO into the U-N bonds of UCp*₂(NEt)₂.

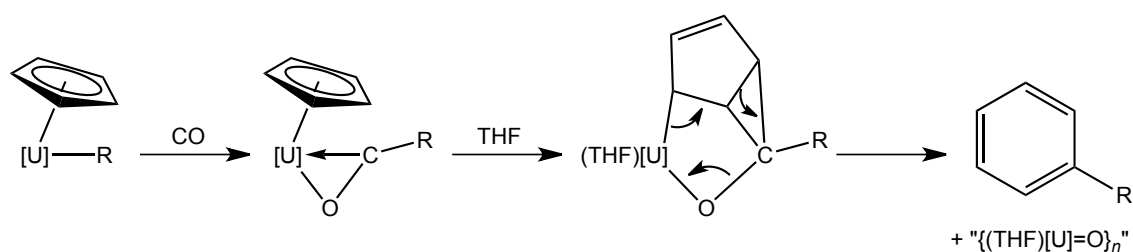
The first examples of CO inserting into a uranium-alkyl bond were reported by Marks in 1978, in a paper detailing the CO migratory insertion products of various uranium and thorium mono- and dialkyl complexes, supported by Cp* ligands.²⁰⁸ The actinide complexes, AnCp*₂Me₂ (where An = Th, U), react with 2 equivalents of CO to produce dimeric enediolate products (**Scheme 1.12a**), while the bulkier alkyl complexes, AnCp*₂(CH₂TMS)₂, form monomeric enediolate products (**Scheme 1.12b**). The related monoalkyl complexes, AnCp*₂Cl(CH₂TMS), form an alkoxide complex wherein the TMS group from the alkyl ligand has migrated to the inserted C atom (**Scheme 1.12c**). The authors suggest a mechanism implicating the initial formation of a carbene-like η²-acyl intermediate, which reacts further to form the resultant products, on the grounds that such dihapto-acyl coordination is known for group IV transition metals.



Scheme 1.12. Products formed from the insertion of CO into An-C bonds as reported by Marks *et al.* [An] = UCp*₂, ThCp*₂.

A later study on the reactivity of tris-Cp U(IV) alkyls with CO concluded that insertion of CO into the U-C alkyl bond resulted in η²-acyl complexes forming for a

wide range of alkyls (Me, Et, ⁱPr, ⁿBu, and ^tBu).²⁰⁷ These acyl complexes gave partial extrusion of CO when heated to 60 °C, but did not show any conversion into other enediolate or rearrangement products even when exposed to an excess of CO. The Me and Et acyls were thought to form dimers from cryoscopic weight measurement evidence, but this was not reflected in ¹H NMR spectroscopic data collected at temperatures between 200 – 300 K. While the structures of these acyls have not been confirmed by X-ray diffraction studies, spectroscopic studies (NMR, IR, MS, NIR/VIS) and protonolysis reactions support the claim of η²-acyl formation. Further investigation of these UCp₃(η²-OCR) complexes by Ephritikhine *et al.* some years later showed that organic products are also formed upon the addition of CO to alkyl complexes. Insertion of the ‘C-R’ moiety into the Cp ring was observed, forming alkylbenzene molecules, upon reacting UCp₃(R) with CO, or when dissolving UCp₃(η²-OCR) in THF (where R = Me, ⁱPr, ⁿBu, ^tBu) (**Scheme 1.13**).²⁰⁹ The irreversible insertion of CO into the tertiary U-C alkyl bond of U(C₅H₄Me)₃(^tBu) has also been observed, forming an acyl complex which decomposes when heated to 90 °C giving an intractable uranium-containing compound (considered to be ‘[UO{C₅H₄Me}₂]_n’) and *m*- and *p*-tertbutyltoluene, formed from the insertion of the ‘C-^tBu’ moiety into a C₅H₄Me ring.⁵⁷



Scheme 1.13. Suggested mechanism of alkylbenzene product formation from η²-acyl complexes, R = Me, ⁱPr, ⁿBu, [U] = Cp₂.

Insertion of CO into ‘tethered’ U-C bonds has also been observed. Simpson and Andersen reported the formation of a five-membered metallocycle upon the addition of CO (18 bar) by insertion initially into a U-C bond, followed by a silyl group migration to form an exocyclic methylene moiety (**Figure 1.11, 1N**).²¹⁰ Similar behaviour was

noted for an N-heterocyclic carbene-supported organouranium complex, which undergoes C-H bond activation upon heating and will subsequently insert CO into the U-C bond (**Figure 1.11, 1O**).²¹¹ A range of ‘tethered’ metallocenes containing ‘U-C-Si-Cp’ linkages will also insert CO into the U-C σ -bonds and undergo silyl-group migration in a similar manner (**Figure 1.11, 1P-R**).^{212,213}

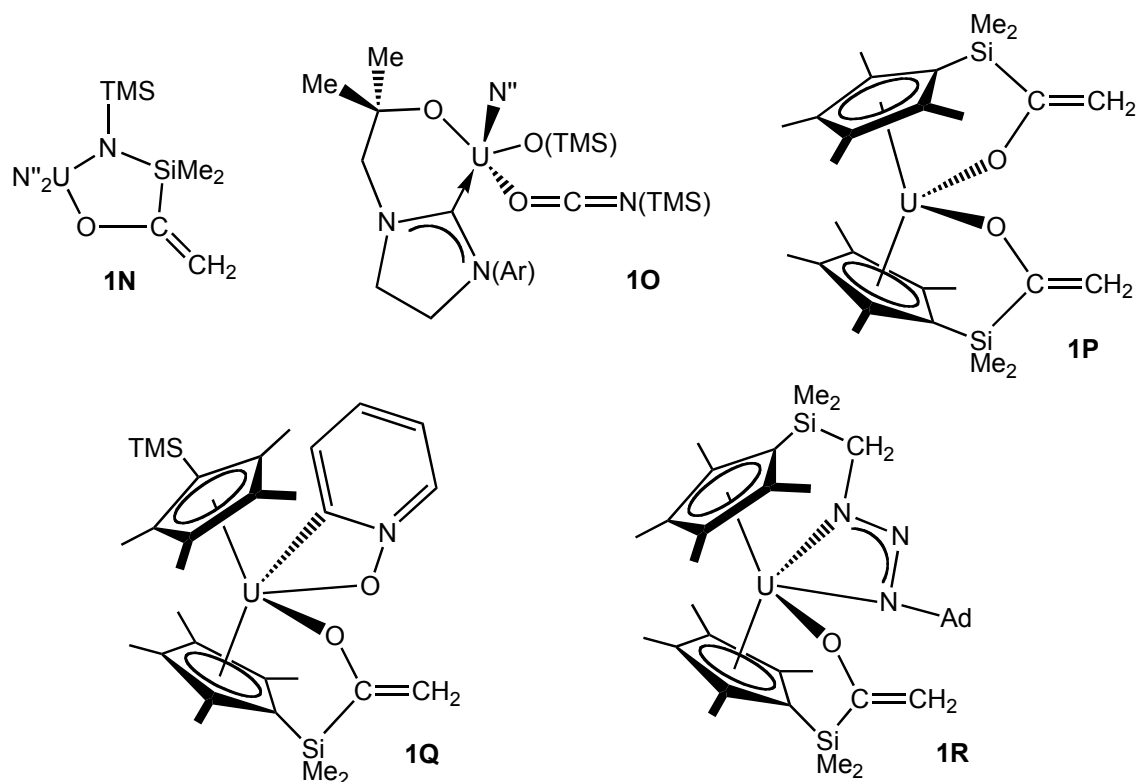


Figure 1.11. CO insertion products of ‘tethered’ U-C bonds, **1N-R**.

1.6.2 Carbon dioxide

Actinide-carbon bonds also undergo insertion reactions with CO₂, as has been documented as far back as the 1980s with the pioneering work of Marks. Complexes of the form AnCp*₂Me₂ (where An = Th, U) are reported to form the corresponding bis-carboxylate complexes, AnCp*(O₂CMe)₂, upon reaction with CO₂ (**Figure 1.12, 1S**); the monoalkyl uranium complex UCp*₂MeCl also produces the expected mono-carboxylate.²¹⁴ The coordination mode of two $\kappa^2(O,O)$ -acetate groups was deduced by IR spectroscopic means, cryoscopic weight measurements, and by

comparison to related structurally characterised complexes. The related ‘bis-tethered’ alkyl, $U(\eta^5:\kappa^1-C_5Me_4SiMe_2CH_2)_2$, will also insert two equivalents of CO_2 to generate a bis-tethered carboxylate, again determined by spectroscopic and comparative means, but not from X-ray crystallographic data (**Figure 1.12, 1T**).²¹² Unusual η^1 -acetate coordination was noted in the amidinate-supported complex, synthesised from the methyl precursor and over 5 atm of CO_2 ; this coordination was structurally verified (**Figure 1.12, 1U**).²¹⁵ Most recently, the insertion of CO_2 into both U-C bonds of a bis- CH_2TMS alkyl supported by a ‘salan’ ligand framework has been observed, with the κ^2 -coordination mode inferred by comparison to the structurally characterised thorium analogue (**Figure 1.12, 1V**).¹⁸⁴

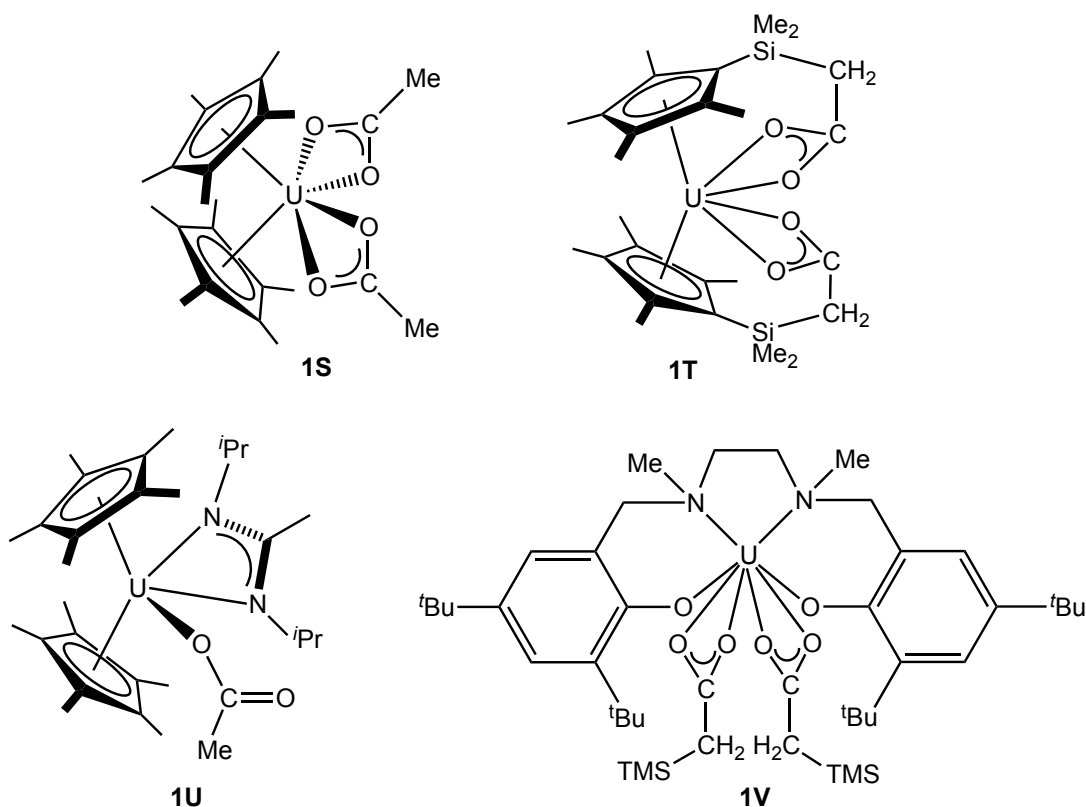


Figure 1.12. Coordination modes of carboxylates formed from alkyls and CO_2 : $UCp^*_2(O_2CR)_2$ (**1S**), bis-‘tethered’ carboxylate (**1T**), η^1 -acetate (**1U**), ‘salan’ bis-carboxylate (**1V**).

Only one example of CO_2 insertion into a U-H bond has been reported in the literature. Berthet and Ephritikhine studied the reaction of UCp^*_3H with CO_2 and deduced from spectroscopic data that a formate complex, $UCp^*_3(OCHO)$, was formed –

no structural determination of the coordination mode was obtained. This complex was shown to react further with the parent hydride to afford a dioxymethylene complex, $(\text{UCp}'_3)_2(\mu\text{-OCH}_2\text{O})$.¹⁹⁹ The paucity of examples of CO_2 insertion into a U-H bond may be due to the few examples of well-defined uranium hydride complexes, and the highly reactive nature of the few that have been characterised.

In a similar manner to U-C bonds, U-N bonds are reactive towards CO_2 , undergoing insertion reactions to form carbamate complexes. The first example of this behaviour was reported by Bagnall and Yanir in 1974, when they probed the reactivity of uranium dialkylamides with CO_2 , CS_2 , CSe_2 , and COS .²¹⁶ Exposing $\text{U}(\text{NR}_2)_4$ ($\text{R} = \text{Me, Et, } ^i\text{Bu}$) to an excess of CO_2 yielded products they characterised as dialkylloxocarbamates, $\text{U}(\text{O}_2\text{CNR}_2)_4$. The reactivity of the *bis*-diethylamide, $\text{UCp}^*_2(\text{NEt}_2)_2$, with CO_2 was reported in 1981, giving the corresponding carbamate product.²¹⁷ The authors conclude that, in the absence of X-ray crystallographic structural information, the coordination mode of the $-\text{O}_2\text{CNEt}_2$ ligand is $\kappa^2(\text{O},\text{O}')$ rather than $\eta^1(\text{O})$, by virtue of IR spectroscopic data. Few recent examples of CO_2 insertion into U-N bonds exist, with the exception of a report by Bart *et al.*: the primary amido complexes $(\{\text{R}^{\text{ArO}}\}_3\text{tacn})\text{U}(\text{NHMe})$ ($\text{R} = ^i\text{Bu, Ad}$) react with CO_2 to form either η^1 ($\text{R} = ^i\text{Bu}$) or κ^2 ($\text{R} = \text{Ad}$) carbamates.¹⁴⁸ The difference in coordination is ascribed to steric factors, with the bulkier Ad-substituted ligand forcing bidentate binding.

1.6.3 Summary and conclusion

Overall, patterns of reactivity of U-C and U-N bonds in organouranium systems have been established; U-H bond insertion reactions remain less well-explored. CO_2 insertion into U-C bonds yields κ^2 -carboxylates – one example of an η^1 -acetate moiety has been reported, while no bridging carboxylates have been characterised from this synthetic route. Products obtained from CO insertion into U-C bonds are more varied, and appear to be dictated by ligand steric pressures. Dialkyls can yield enediolate products, either monomeric or dimeric as dictated by alkyl sterics, and

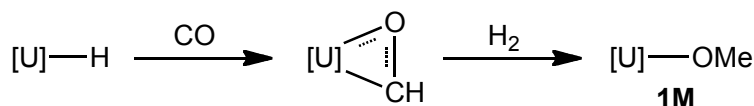
mono-alkyls form η^2 -acyls, or rearrange to form silyl enolates in the presence of a TMS-based parent alkyl ligand. The insertion of CO into Cp ligands has also been observed. U-N bonds insert CO₂ and CO to form κ^2 -carbamates or η^2 -carbonyls, as shown by the few reported examples. No reports of products characterised from the insertion of CO into U-H bonds exist in the literature, and only one example of CO₂ insertion into a U-H bond has been described. This indicates that this is an area requiring exploration to determine whether a stable, well-defined uranium hydride complex can be synthesised for subsequent CO insertion chemistry.

1.7 Scope of thesis

Work within our research group centres around the mixed-sandwich uranium complex, U(COT^{TIPS₂})Cp*, and closely related derivatives thereof. The ligand system has been thoroughly investigated: it is known to allow unusual transformations of small molecules when supporting U(III), and numerous well-defined U(IV) complexes have been synthesised, mainly from small molecule transformations. Substitution of bulky TIPS groups onto the COT ring impart solubility and crystallinity to these mixed-sandwich complexes, which is beneficial for assisting structural characterisation. The combination of the [COT^{TIPS₂}]²⁻ and [Cp*]⁻ ligands leave one remaining site for an anionic ligand around a U(IV) metal centre, ideal for the installation of a single reactive σ -bond, such as U-C, U-N or U-H. As demonstrated in the previous sections, such bonds can be highly reactive and difficult to stabilise, particularly U-H bonds, but can undergo interesting insertion chemistry. It was thought that the mixed-sandwich ligand environment could be stabilising enough to support such bonds, and to allow for the characterisation of the resulting complexes.

Of particular interest in this study is the U(IV) hydride bond, for several reasons. Only fourteen terminal, neutral, U(IV) hydrides exist – of these, three have been structurally characterised, and only one has been examined for reactivity towards small molecules (see Chapter 3).¹⁹⁹ The mixed-sandwich complex may provide a suitable

ligand system for the synthesis and characterisation of ‘U(COT^{TIPS2})Cp*H’, and is likely to force a terminal binding mode of a hydride ligand given the overall steric bulk. Additionally, such a hydride complex and its theoretical CO insertion product, ‘U(COT^{TIPS2})Cp*(OCH)’, have been postulated as intermediates in the formation of the previously-described methoxide complex, U(COT^{TIPS2})Cp*(OMe) (**1M**), synthesised from the reaction of U(COT^{TIPS2})Cp* and a combination of CO and H₂, in the only reported example of reduction and hydrogenation of CO by an organouranium complex.⁹⁰ The synthesis of a hydride complex and its subsequent reactivity with CO to form an η²-formyl, which may potentially react towards H₂ to form **1M**, could corroborate or negate this mechanistic pathway (**Scheme 1.14**).



Scheme 1.14. Possible alternative route to **1M** from a hydride, *via* an η²-formyl,
 [U] = U(COT^{TIPS2})Cp*.

Synthesis of the hydride will be attempted from the reaction of alkyl precursors with dihydrogen; this method has been used previously to obtain hydrides in a straightforward manner, *vide supra*. The insertion chemistry of the alkyls – again, expected to be stabilised by the mixed-sandwich ligand system – will also be investigated, in order to contribute to the relatively limited body of knowledge relating to organouranium alkyls and their reactivity.

The importance of the ligand system around U(III) metal centres in dictating reductive reactivity towards small molecules has been highlighted in the previous sections. As a contrast to the mixed-sandwich metallocene U(COT^{TIPS2})Cp*, the half-sandwich complex U(N'N'₂)Cp* (where N'N'₂ = N(TMS)(CH₂CH₂N{TMS})₂) is targeted as a good candidate for reactivity towards CO; N-donor ligands have been shown to support uranium metal centres capable of coupling carbon monoxide.^{118,160}

U(IV) and U(III) complexes featuring the N'N'₂ ligand will be synthesised and their small molecule reactivity explored.

1.8 References for Chapter 1

1. C. C. Lu and K. Meyer, *Eur. J. Inorg. Chem.*, 2013, **2013**, 3731–3732.
2. M. Aresta, *Activation of Small Molecules: Organometallic and Bioinorganic Perspectives*, Wiley-VCH Verlag GmbH & Co. KGaA, Weinheim, Germany, 2006.
3. W. Leitner, *Coord. Chem. Rev.*, 1996, **153**, 257–284.
4. C. Das Neves Gomes, O. Jacquet, C. Villiers, P. Thuéry, M. Ephritikhine, and T. Cantat, *Angew. Chem. Int. Ed.*, 2012, **51**, 187–90.
5. A. M. Appel, J. E. Bercaw, A. B. Bocarsly, H. Dobbek, D. L. Dubois, M. Dupuis, J. G. Ferry, E. Fujita, R. Hille, P. J. A. Kenis, C. A. Kerfeld, R. H. Morris, C. H. F. Peden, A. R. Portis, S. W. Ragsdale, T. B. Rauchfuss, J. N. H. Reek, L. C. Seefeldt, R. K. Thauer, and G. L. Waldrop, *Chem. Rev.*, 2013, **113**, 6621–6658.
6. M. Ephritikhine, *Dalton Trans.*, 2006, 2501.
7. A. R. Fox, S. C. Bart, K. Meyer, and C. C. Cummins, *Nature*, 2008, **455**, 341–349.
8. B. M. Gardner and S. T. Liddle, *Eur. J. Inorg. Chem.*, 2013, **2013**, 3753–3770.
9. H. S. La Pierre and K. Meyer, in *Progress in Inorganic Chemistry*, vol. 58, ed. K. D. Karlin, Wiley, 2014, vol. 58, pp. 301–413.
10. T. J. Marks, *Science*, 1982, **217**, 989–997.
11. B. E. Bursten, L. F. Rhodes, and R. J. Strittmatter, *J. Am. Chem. Soc.*, 1989, **111**, 2756–2758.
12. A. J. Gaunt, S. D. Reilly, A. E. Enriquez, B. L. Scott, J. A. Ibers, P. Sekar, K. I. M. Ingram, N. Kaltsoyannis, and M. P. Neu, *Inorg. Chem.*, 2008, **47**, 29–41.
13. M. B. Jones, A. J. Gaunt, J. C. Gordon, N. Kaltsoyannis, M. P. Neu, and B. L. Scott, *Chem. Sci.*, 2013, **4**, 1189.
14. T. W. Hayton, *Dalton Trans.*, 2010, **39**, 1145–1158.
15. T. W. Hayton, *Chem. Commun.*, 2013, **49**, 2956–2973.
16. J.-P. Dognon, *Coord. Chem. Rev.*, 2014, **266-267**, 110–122.
17. S. G. Minasian, J. L. Krinsky, and J. Arnold, *Chem.--Eur. J.*, 2011, **17**, 12234–12245.
18. D. D. Schnaars, E. R. Batista, A. J. Gaunt, T. W. Hayton, I. May, S. D. Reilly, B. L. Scott, and G. Wu, *Chem. Commun.*, 2011, **47**, 7647–7649.
19. L. L. Quill, *Chem. Rev.*, 1938, **23**, 87–155.
20. D. R. Lide, Ed., *CRC Handbook of Chemistry and Physics: 86th Edition*, Taylor & Francis, 86th edn., 2005.
21. Department of Health (2007), *Understanding Radiation: Depleted Uranium*, available at: <https://www.gov.uk/depleted-uranium-du-general-information-and-toxicology> (Accessed: April 2014).
22. S. A. Cotton, *Lanthanide and Actinide Chemistry*, John Wiley & Sons, Ltd, Chichester, First Edit., 2006.
23. W. J. Evans and S. A. Kozimor, *Coord. Chem. Rev.*, 2006, **250**, 911–935.

24. K. C. Jantunen, C. J. Burns, I. Castro-Rodriguez, R. E. Da Re, J. T. Golden, D. E. Morris, B. L. Scott, F. L. Taw, and J. L. Kiplinger, *Organometallics*, 2004, **23**, 4682–4692.
25. C. Clappe, D. Leveugle, D. Hauchard, and G. Durand, *J. Electroanal. Chem.*, 1998, **448**, 95–103.
26. T. Cantat, C. R. Graves, K. C. Jantunen, C. J. Burns, B. L. Scott, E. J. Schelter, D. E. Morris, P. J. Hay, and J. L. Kiplinger, *J. Am. Chem. Soc.*, 2008, **130**, 17537–51.
27. T. Cantat, B. L. Scott, D. E. Morris, and J. L. Kiplinger, *Inorg. Chem.*, 2009, **48**, 2114–2127.
28. A. Elkechai, Y. Mani, A. Boucekkine, and M. Ephritikhine, *Inorg. Chem.*, 2012, **51**, 6943–52.
29. N. Tsoureas, L. Castro, A. F. R. Kilpatrick, F. G. N. Cloke, and L. Maron, *Chem. Sci.*, 2014, **5**, 3777–3788.
30. H. Gilman, R. G. Jones, E. Bindschadler, D. Elume, G. Karmas, G. A. Martin Jr., J. F. Nobis, J. R. Thirtle, H. L. Yale, and F. A. Yoeman, *J. Am. Chem. Soc.*, 1956, **78**, 2790–2792.
31. R. G. Jones, G. Karmas, G. A. Martin Jr., and H. Gilman, *J. Am. Chem. Soc.*, 1956, **78**, 4285–4286.
32. R. G. Jones, E. Bindschadler, G. Karmas, F. A. Yoeman, and H. Gilman, *J. Am. Chem. Soc.*, 1956, **78**, 4287–4288.
33. R. G. Jones, E. Bindschadler, G. Karmas, G. A. Martin, J. R. Thirtle, F. A. Yoeman, and H. Gilman, *J. Am. Chem. Soc.*, 1956, **78**, 4289–4290.
34. R. G. Jones, E. Bindschadler, D. Blume, G. Karmas, G. A. Martin, J. R. Thirtle, and H. Gilman, *J. Am. Chem. Soc.*, 1956, **78**, 6027–6030.
35. R. G. Jones, E. Bindschadler, D. Blume, G. Karmas, G. A. Martin, J. R. Thirtle, F. A. Yeoman, and H. Gilman, *J. Am. Chem. Soc.*, 1956, **78**, 6030–6032.
36. R. G. Jones, E. Bindschadler, G. A. Martin, J. R. Thirtle, and H. Gilman, *J. Am. Chem. Soc.*, 1957, **79**, 4921–4922.
37. L. T. Reynolds and G. Wilkinson, *J. Inorg. Nucl. Chem.*, 1956, **2**, 246–253.
38. G. Wilkinson and J. M. Birmingham, *J. Am. Chem. Soc.*, 1954, **76**, 6210–6210.
39. C. H. Wong, T. M. Yen, and T. Y. Lee, *Acta Crystallogr.*, 1965, **18**, 340.
40. R. D. Fischer, *Theor. Chim. Acta*, 1963, **1**, 418–431.
41. A. Streitwieser Jr and U. Müller-Westerhoff, *J. Am. Chem. Soc.*, 1968, **90**, 7364.
42. A. Zalkin and K. N. Raymond, *J. Am. Chem. Soc.*, 1969, **91**, 5667–5668.
43. A. Streitwieser, U. Muller-Westerhoff, G. Sonnichsen, F. Mares, D. G. Morrell, K. O. Hodgson, and C. A. Harmon, *J. Am. Chem. Soc.*, 1973, **95**, 8644–8649.
44. J. M. Manriquez, P. J. Fagan, and T. J. Marks, *J. Am. Chem. Soc.*, 1978, **100**, 3939–3941.
45. R. G. Finke, Y. Hirose, and G. Gaughan, *J. Chem. Soc. Chem. Commun.*, 1981, 232–234.
46. R. G. Bowman, R. Nakamura, P. J. Fagan, R. L. Burwell Jr., and T. J. Marks, *J. Chem. Soc. Chem. Commun.*, 1981, 257–258.
47. P. J. Fagan, J. M. Manriquez, S. H. Vollmer, C. S. Day, V. W. Day, and T. J. Marks, *J. Am. Chem. Soc.*, 1981, **103**, 2206–2220.
48. P. J. Fagan, J. M. Manriquez, E. A. Maatta, A. M. Seyam, and T. J. Marks, *J. Am. Chem. Soc.*, 1981, **103**, 6650–6667.
49. P. J. Fagan, J. M. Manriquez, T. J. Marks, C. S. Day, S. H. Vollmer, and V. W. Day, *Organometallics*, 1982, **1**, 170–180.

50. J. W. Bruno, T. J. Marks, and L. R. Morss, *J. Am. Chem. Soc.*, 1983, **105**, 6824–6832.
51. Z. Lin and T. J. Marks, *J. Am. Chem. Soc.*, 1987, **109**, 7979–7985.
52. R. G. Peters, B. L. Scott, and C. J. Burns, *Acta Crystallogr. Sect. C: Cryst. Struct. Commun.*, 1999, **55**, 1482–1483.
53. W. J. Evans, S. A. Kozimor, J. W. Ziller, and N. Kaltsoyannis, *J. Am. Chem. Soc.*, 2004, **126**, 14533–14547.
54. W. J. Evans, S. A. Kozimor, and J. W. Ziller, *Chem. Commun.*, 2005, 4681–4683.
55. J. G. Brennan and R. A. Andersen, *J. Am. Chem. Soc.*, 1985, **107**, 514–516.
56. S. D. Stults, R. A. Andersen, and A. Zalkin, *Organometallics*, 1990, **9**, 1623–1629.
57. M. Weydert, J. G. Brennan, R. A. Andersen, and R. A. Bergman, *Organometallics*, 1995, **14**, 3942–3951.
58. W. W. Lukens Jr, S. M. Beshouri, L. L. Blosch, and R. A. Andersen, *J. Am. Chem. Soc.*, 1996, **118**, 901–902.
59. W. W. Lukens Jr, S. M. Beshouri, L. L. Blosch, A. L. Stuart, and R. A. Andersen, *Organometallics*, 1999, **18**, 1235–1246.
60. G. Zi, L. L. Blosch, L. Jia, and R. A. Andersen, *Organometallics*, 2005, **24**, 4602–4612.
61. O. T. Summerscales, F. G. N. Cloke, P. B. Hitchcock, J. C. Green, and N. Hazari, *J. Am. Chem. Soc.*, 2006, **128**, 9602–9603.
62. N. Tsoureas, O. T. Summerscales, F. G. N. Cloke, and S. M. Roe, *Organometallics*, 2013, **32**, 1353–1362.
63. P. C. Blake, M. F. Lappert, R. G. Taylor, J. L. Atwood, W. E. Hunter, and H. Zhang, *J. Chem. Soc. Chem. Commun.*, 1986, 1394–1395.
64. J. G. Brennan, R. A. Andersen, and J. L. Robbins, *J. Am. Chem. Soc.*, 1986, **108**, 335–336.
65. P. C. Blake, M. F. Lappert, R. G. Taylor, J. L. Atwood, and H. Zhang, *Inorg. Chim. Acta*, 1987, **139**, 13–20.
66. W. J. Evans, S. A. Kozimor, W. R. Hillman, and J. W. Ziller, *Organometallics*, 2005, **24**, 4676–4683.
67. C. A. Secaur, V. W. Day, R. D. Ernst, W. J. Kennelly, and T. J. Marks, *J. Am. Chem. Soc.*, 1976, **98**, 3713–3715.
68. R. C. Schnabel, B. L. Scott, W. H. Smith, and C. J. Burns, *J. Organomet. Chem.*, 1999, **591**, 14–23.
69. K. O. Hodgson, D. Dempf, and K. N. Raymond, *Chem. Commun.*, 1971, 1592–1593.
70. A. Streitwieser Jr, D. Dempf, G. N. La Mar, D. G. Karraker, and N. M. Edelstein, *J. Am. Chem. Soc.*, 1971, **93**, 7343–7344.
71. C. A. Harmon, D. P. Bauer, S. R. Berryhill, K. Hagiwara, and A. Streitwieser Jr, *Inorg. Chem.*, 1977, **16**, 2143–2147.
72. A. Streitwieser Jr, H. P. G. Burghard, D. G. Morrell, and W. D. Luke, *Inorg. Chem.*, 1980, **19**, 1863–1866.
73. A. Streitwieser, M. H. Lyttle, H. Wang, T. Boussie, A. Weinländer, and J. P. Solar, *J. Organomet. Chem.*, 1995, **501**, 245–249.
74. A. Streitwieser Jr and C. A. Harmon, *Inorg. Chem.*, 1973, **12**, 1102–1104.
75. A. Streitwieser Jr and R. Walker, *J. Organomet. Chem.*, 1975, **97**, C41–C42.
76. N. C. Burton, F. G. N. Cloke, P. B. Hitchcock, H. C. de Lemos, and A. A. Sameh, *J. Chem. Soc. Chem. Commun.*, 1989, 1462–1464.

77. J. Parry, F. G. N. Cloke, S. J. Coles, and M. B. Hursthouse, *J. Am. Chem. Soc.*, 1999, **121**, 6867–6871.
78. U. Kilimann, R. Herbst-Irmer, D. Stalke, and F. T. Edelmann, *Angew. Chem. Int. Ed. Engl.*, 1994, **33**, 1618–1621.
79. V. Lorenz, B. M. Schmiede, C. G. Hrib, J. W. Ziller, A. Edelmann, S. Blaurock, W. J. Evans, and F. T. Edelmann, *J. Am. Chem. Soc.*, 2011, **133**, 1257–1259.
80. P. W. Roesky, *Eur. J. Inorg. Chem.*, 2001, **2001**, 1653–1660.
81. T. R. Boussie, R. M. Moore, A. Streitwieser Jr, A. Zalkin, J. G. Brennan, and K. A. Smith, *Organometallics*, 1990, **9**, 2010–2016.
82. T. M. Gilbert, R. R. Ryan, and A. P. Sattelberger, *Organometallics*, 1988, **7**, 2514–2518.
83. D. Baudry, E. Bulot, M. Ephritikhine, M. Nierlich, M. Lance, and J. Vigner, *J. Organomet. Chem.*, 1990, **388**, 279–287.
84. J.-C. Berthet, J.-F. Le Maréchal, and M. Ephritikhine, *J. Organomet. Chem.*, 1994, **480**, 155–161.
85. A. R. Schake, L. R. Avens, C. J. Burns, D. L. Clark, A. P. Sattelberger, and W. H. Smith, *Organometallics*, 1993, **12**, 1497–1498.
86. W. J. Evans, M. K. Takase, J. W. Ziller, and A. L. Rheingold, *Organometallics*, 2009, **28**, 5802–5808.
87. O. T. Summerscales, F. G. N. Cloke, P. B. Hitchcock, J. C. Green, and N. Hazari, *Science*, 2006, **311**, 829–831.
88. O. T. Summerscales, A. S. P. Frey, F. G. N. Cloke, and P. B. Hitchcock, *Chem. Commun.*, 2009, 198–200.
89. A. S. P. Frey, F. G. N. Cloke, M. P. Coles, and P. B. Hitchcock, *Chem.--Eur. J.*, 2010, **16**, 9446–9448.
90. A. S. P. Frey, F. G. N. Cloke, M. P. Coles, L. Maron, and T. Davin, *Angew. Chem.*, 2011, **123**, 7013–7015.
91. N. Tsoureas, A. F. R. Kilpatrick, O. T. Summerscales, J. F. Nixon, F. G. N. Cloke, and P. B. Hitchcock, *Eur. J. Inorg. Chem.*, 2013, **2013**, 4085–4089.
92. J. A. Higgins, F. G. N. Cloke, and S. M. Roe, *Organometallics*, 2013, **32**, 5244–5252.
93. P. G. Laubereau, L. Ganguly, J. H. Burns, B. M. Benjamin, J. L. Atwood, and J. Selbin, *Inorg. Chem.*, 1971, **10**, 2274–2280.
94. J. H. Burns and P. G. Laubereau, *Inorg. Chem.*, 1971, **10**, 2789–2792.
95. J. Goffart, J. Fuger, B. Gilbert, L. Hocks, and G. Duyckaerts, *Inorg. Nucl. Chem. Lett.*, 1975, **11**, 569–583.
96. J. Goffart, B. Gilbert, and G. Duyckaerts, *Inorg. Nucl. Chem. Lett.*, 1977, **13**, 189–196.
97. W. Beeckman, J. Goffart, J. Rebizant, and M. R. Spirlet, *J. Organomet. Chem.*, 1986, **307**, 23–37.
98. F. G. N. Cloke, J. C. Green, and C. N. Jardine, *Organometallics*, 1999, **18**, 1080–1086.
99. F. G. N. Cloke and P. B. Hitchcock, *J. Am. Chem. Soc.*, 2002, **124**, 9352–3.
100. J. T. Miller and C. W. Dekock, *J. Organomet. Chem.*, 1981, **216**, 39–48.
101. T. Arliguie, M. Lance, M. Nierlich, J. Vigner, and M. Ephritikhine, *J. Chem. Soc. Chem. Commun.*, 1994, 847–848.
102. T. Arliguie, M. Ephritikhine, M. Lance, M. Nierlich, and J. Vigner, *J. Chem. Soc. Chem. Commun.*, 1995, **132**, 183–184.

103. T. Arliguie, M. Lance, and M. Ephritikhine, *J. Chem. Soc. Dalton Trans.*, 1997, 2501–2504.
104. R. G. Ball, F. Edelmann, J. G. Matisons, J. Takats, N. Marques, J. Marcalo, A. Pires De Matos, and K. W. Bagnall, *Inorg. Chim. Acta*, 1987, **132**, 137–143.
105. I. C. Santos, N. Marques, and A. Pires de Matos, *Inorg. Chim. Acta*, 1987, **139**, 89–90.
106. M. Silva, N. Marques, and A. P. De Matos, *J. Organomet. Chem.*, 1995, **493**, 129–132.
107. M. A. Antunes, Â. Domingos, I. C. Santos, N. Marques, and J. Takats, *Polyhedron*, 2005, **24**, 3038–3045.
108. Â. Domingos, N. Marques, A. Pires de Matos, I. C. Santos, and M. Silva, *Organometallics*, 1994, **13**, 654–662.
109. M. P. C. Campello, Â. Domingos, and I. C. Santos, *J. Organomet. Chem.*, 1994, **484**, 37–46.
110. E. M. Matson, M. G. Crestani, P. E. Fanwick, and S. C. Bart, *Dalton Trans.*, 2012, **41**, 7952–7958.
111. M. P. C. Campello, M. Jos, A. Galvao, P. Leal, A. P. De Matos, and I. C. Santos, *J. Organomet. Chem.*, 1997, **538**, 223–239.
112. E. M. Matson, W. P. Forrest, P. E. Fanwick, and S. C. Bart, *Organometallics*, 2013, **32**, 1484–1492.
113. E. M. Matson, W. P. Forrest, P. E. Fanwick, and S. C. Bart, *J. Am. Chem. Soc.*, 2011, **133**, 4948–4954.
114. E. M. Matson, P. E. Fanwick, and S. C. Bart, *Organometallics*, 2011, **30**, 5753–5762.
115. P. Scott and P. B. Hitchcock, *Polyhedron*, 1994, **13**, 1651–1653.
116. P. Roussel, P. B. Hitchcock, N. Tinker, and P. Scott, *Chem. Commun.*, 1996, 2053–2054.
117. P. Roussel and P. Scott, *J. Am. Chem. Soc.*, 1998, **120**, 1070–1071.
118. B. M. Gardner, J. C. Stewart, A. L. Davis, J. McMaster, W. Lewis, A. J. Blake, and S. T. Liddle, *Proc. Natl. Acad. Sci. U. S. A.*, 2012, **109**, 9265–9270.
119. D. M. King, F. Tuna, E. J. L. McInnes, J. McMaster, W. Lewis, A. J. Blake, and S. T. Liddle, *Nat. Chem.*, 2013, **5**, 482–488.
120. D. M. King, J. McMaster, F. Tuna, E. J. L. McInnes, W. Lewis, A. J. Blake, and S. T. Liddle, *J. Am. Chem. Soc.*, 2014, **136**, 5619–5622.
121. F. G. N. Cloke, P. B. Hitchcock, and J. B. Love, *J. Chem. Soc. Dalton Trans.*, 1995, 25–30.
122. H. C. S. Clark, F. G. N. Cloke, P. B. Hitchcock, J. B. Love, and A. P. Wainwright, *J. Organomet. Chem.*, 1995, **501**, 333–340.
123. J. B. Love, H. C. S. Clark, F. G. N. Cloke, J. C. Green, and P. B. Hitchcock, *J. Am. Chem. Soc.*, 1999, **121**, 6843–6849.
124. G. K. B. Clentsmith, V. M. E. Bates, P. B. Hitchcock, and F. G. N. Cloke, *J. Am. Chem. Soc.*, 1999, **121**, 10444–10445.
125. P. E. Collier, S. M. Pugh, H. C. S. Clark, J. B. Love, F. G. N. Cloke, and P. Mountford, *Inorg. Chem.*, 2000, **39**, 2001–5.
126. D. J. Wilson, A. Sebastian, F. G. N. Cloke, A. G. Avent, and P. B. Hitchcock, *Inorg. Chim. Acta*, 2003, **345**, 89–94.
127. K. C. Jantunen, R. J. Batchelor, and D. B. Leznoff, *Organometallics*, 2004, **23**, 2186–2193.
128. K. C. Jantunen, F. Haftbaradaran, M. J. Katz, R. J. Batchelor, G. Schatte, and D. B. Leznoff, *Dalton Trans.*, 2005, 3083–3091.

129. C. E. Hayes and D. B. Leznoff, *Organometallics*, 2010, **29**, 767–774.
130. N. R. Andreychuk, S. Ilango, B. Vidjayacoumar, D. J. H. Emslie, and H. A. Jenkins, *Organometallics*, 2013, **32**, 1466–1474.
131. M. J. Monreal, C. T. Carver, and P. L. Diaconescu, *Inorg. Chem.*, 2007, **46**, 7226–8.
132. M. J. Monreal and P. L. Diaconescu, *Organometallics*, 2008, **27**, 1702–1706.
133. M. J. Monreal, S. I. Khan, and P. L. Diaconescu, *Angew. Chem. Int. Ed.*, 2009, **48**, 8352–8355.
134. S. Duhović, M. J. Monreal, and P. L. Diaconescu, *Inorg. Chem.*, 2010, **49**, 7165–7169.
135. M. J. Monreal and P. L. Diaconescu, *J. Am. Chem. Soc.*, 2010, **132**, 7676–7683.
136. E. M. Broderick, N. P. Gutzwiller, and P. L. Diaconescu, *Organometallics*, 2010, **29**, 3242–3251.
137. I. Korobkov, S. Gambarotta, and G. P. A. Yap, *Organometallics*, 2001, **20**, 2552–2559.
138. I. Korobkov, S. Gambarotta, and G. P. A. Yap, *Angew. Chem.*, 2002, **114**, 3583–3586.
139. P. L. Arnold, N. A. Potter, C. D. Carmichael, A. M. Z. Slawin, P. Roussel, and J. B. Love, *Chem. Commun.*, 2010, **46**, 1833–1835.
140. P. L. Arnold, N. A. Potter, N. Magnani, C. Apostolidis, J.-C. Griveau, E. Colineau, A. Morgenstern, R. Caciuffo, and J. B. Love, *Inorg. Chem.*, 2010, **49**, 5341–3.
141. P. L. Arnold, J. H. Farnaby, R. C. White, N. Kaltsoyannis, M. G. Gardiner, and J. B. Love, *Chem. Sci.*, 2014, **5**, 756–765.
142. P. L. Arnold, C. J. Stevens, J. H. Farnaby, M. G. Gardiner, G. S. Nichol, and J. B. Love, *J. Am. Chem. Soc.*, 2014, **136**, 10218–10221.
143. I. Castro-Rodriguez, K. Olsen, P. Gantzel, and K. Meyer, *Chem. Commun.*, 2002, 2764–2765.
144. I. Castro-Rodriguez, K. Olsen, P. Gantzel, and K. Meyer, *J. Am. Chem. Soc.*, 2003, **125**, 4565–4571.
145. I. Castro-Rodriguez, H. Nakai, P. Gantzel, L. N. Zakharov, A. L. Rheingold, and K. Meyer, *J. Am. Chem. Soc.*, 2003, **125**, 15734–15735.
146. M. A. Antunes, M. Dias, B. Monteiro, Â. Domingos, I. C. Santos, and N. Marques, *Dalton Trans.*, 2006, 3368–3374.
147. I. Castro-Rodriguez and K. Meyer, *J. Am. Chem. Soc.*, 2005, **127**, 11242–3.
148. S. C. Bart, C. Anthon, F. W. Heinemann, E. Bill, N. M. Edelstein, and K. Meyer, *J. Am. Chem. Soc.*, 2008, **130**, 12536–12546.
149. S. J. Zuend, O. P. Lam, F. W. Heinemann, and K. Meyer, *Angew. Chem. Int. Ed.*, 2011, **50**, 10626–10630.
150. A.-C. Schmidt, A. V. Nizovtsev, A. Scheurer, F. W. Heinemann, and K. Meyer, *Chem. Commun.*, 2012, **48**, 8634–8636.
151. J. L. Slater, R. K. Sheline, K. C. Lin, and W. Weltner Jr, *J. Chem. Phys.*, 1971, **55**, 5129–5130.
152. R. K. Sheline and J. L. Slater, *Angew. Chem. Int. Ed. Engl.*, 1975, **14**, 309–313.
153. B. Kanellakopulos, E. O. Fischer, E. Dornberger, and F. Baumgärtner, *J. Organomet. Chem.*, 1970, **24**, 507–514.
154. B. E. Bursten and R. J. Strittmatter, *J. Am. Chem. Soc.*, 1987, **109**, 6606–6608.
155. J. Parry, E. Carmona, S. Coles, and M. Hursthouse, *J. Am. Chem. Soc.*, 1995, **117**, 2649–2650.

156. M. del Mar Conejo, J. S. Parry, E. Carmona, M. Schultz, J. G. Brennan, S. M. Beshouri, R. A. Andersen, R. D. Rogers, S. Coles, and M. B. Hursthouse, *Chem.--Eur. J.*, 1999, **5**, 3000–3009.
157. W. J. Evans, S. A. Kozimor, G. W. Nyce, and J. W. Ziller, *J. Am. Chem. Soc.*, 2003, **125**, 13831–13835.
158. A. S. P. Frey, F. G. N. Cloke, P. B. Hitchcock, I. J. Day, J. C. Green, and G. Aitken, *J. Am. Chem. Soc.*, 2008, **130**, 13816–13817.
159. D. McKay, A. S. P. Frey, J. C. Green, F. G. N. Cloke, and L. Maron, *Chem. Commun.*, 2012, **48**, 4118–4120.
160. P. L. Arnold, Z. R. Turner, R. M. Bellabarba, and R. P. Tooze, *Chem. Sci.*, 2011, **2**, 77–79.
161. S. M. Mansell, N. Kaltsoyannis, and P. L. Arnold, *J. Am. Chem. Soc.*, 2011, **133**, 9036–9051.
162. J.-C. Berthet, J.-F. Le Maréchal, M. Nierlich, M. Lance, J. Vigner, and M. Ephritikhine, *J. Organomet. Chem.*, 1991, **408**, 335–341.
163. I. Castro-Rodriguez, H. Nakai, L. N. Zakharov, A. L. Rheingold, and K. Meyer, *Science*, 2004, **305**, 1757–1759.
164. O. P. Lam, S. C. Bart, H. Kameo, F. W. Heinemann, and K. Meyer, *Chem. Commun.*, 2010, **46**, 3137–3139.
165. L. Castro, O. P. Lam, S. C. Bart, K. Meyer, and L. Maron, *Organometallics*, 2010, **29**, 5504–5510.
166. O. P. Lam and K. Meyer, *Polyhedron*, 2012, **32**, 1–9.
167. V. Mougel, C. Camp, J. Pécaut, C. Copéret, L. Maron, C. E. Kefalidis, and M. Mazzanti, *Angew. Chem. Int. Ed.*, 2012, **51**, 12280–12284.
168. O. Cooper, C. Camp, J. Pécaut, C. E. Kefalidis, L. Maron, S. Gambarelli, and M. Mazzanti, *J. Am. Chem. Soc.*, 2014, **136**, 6716–23.
169. W. J. Evans, C. A. Seibel, and J. W. Ziller, *Inorg. Chem.*, 1998, **37**, 770–776.
170. O. P. Lam, C. Anthon, and K. Meyer, *Dalton Trans.*, 2009, 9677–9691.
171. G. Brandi, M. Brunelli, G. Lugli, A. Mazzei, N. Palladino, U. Pedretti, and T. Salvatori, in *Proceedings of the Third International Symposium*, ed. I. C. A. (Padua), Venice, 1970, paper E10.
172. A. E. Gebala and M. Tsutsui, *Chem. Lett.*, 1972, 775–776.
173. A. E. Gebala and M. Tsutsui, *J. Am. Chem. Soc.*, 1972, **95**, 91–93.
174. T. J. Marks and A. M. Seyam, *J. Am. Chem. Soc.*, 1972, **91**, 6545–6546.
175. T. J. Marks, A. M. Seyam, and J. R. Kolb, *J. Am. Chem. Soc.*, 1973, **95**, 5529–5539.
176. R. A. Andersen, E. Carmona-Guzman, K. Mertis, E. Sigurdon, and G. Wilkinson, *J. Organomet. Chem.*, 1975, **99**, C19–C20.
177. P. G. Edwards, R. A. Andersen, and A. Zalkin, *Organometallics*, 1984, **3**, 293–298.
178. S. Fortier, B. C. Melot, G. Wu, and T. W. Hayton, *J. Am. Chem. Soc.*, 2009, **131**, 15512–15521.
179. S. J. Kraft, P. E. Fanwick, and S. C. Bart, *J. Am. Chem. Soc.*, 2012, **134**, 6160–6168.
180. W. G. Van Der Sluys, C. J. Burns, and A. P. Sattelberger, *Organometallics*, 1989, **8**, 855–857.
181. J. M. Manriquez, P. J. Fagan, T. J. Marks, S. H. Vollmer, C. S. Day, and V. W. Day, *J. Am. Chem. Soc.*, 1979, **101**, 5075–5078.
182. S. Di Bella, G. Lanza, I. L. Fragala, and T. J. Marks, *Organometallics*, 1996, **15**, 205–208.

183. J. L. Kiplinger, K. D. John, D. E. Morris, B. L. Scott, and C. J. Burns, *Organometallics*, 2002, **21**, 4306–4308.
184. E. Mora, L. Maria, B. Biswas, C. Camp, I. C. Santos, J. Pécaut, A. Cruz, J. M. Carretas, J. Marçalo, and M. Mazzanti, *Organometallics*, 2013, **32**, 1409–1422.
185. T. M. Gilbert, R. R. Ryan, and A. P. Sattelberger, *Organometallics*, 1989, **8**, 857–859.
186. M. K. Takase, N. A. Siladke, J. W. Ziller, and W. J. Evans, *Organometallics*, 2011, **30**, 458–465.
187. H. W. Turner, S. J. Simpson, and R. A. Andersen, *J. Am. Chem. Soc.*, 1979, **101**, 2782.
188. R. A. Andersen, A. Zalkin, and D. H. Templeton, *Inorg. Chem.*, 1981, **20**, 622–623.
189. S. J. Simpson, H. W. Turner, and R. A. Andersen, *J. Am. Chem. Soc.*, 1979, **101**, 7728–7729.
190. R. W. Broach, A. J. Schultz, J. M. Williams, G. M. Brown, J. M. Manriquez, P. J. Fagan, and T. J. Marks, *Science*, 1979, **203**, 172–4.
191. W. J. Evans, K. A. Miller, S. A. Kozimor, J. W. Ziller, A. G. Dipasquale, and A. L. Rheingold, *Organometallics*, 2007, **26**, 3568–3576.
192. D. J. Grant, T. J. Stewart, R. Bau, K. A. Miller, S. A. Mason, M. Gutmann, G. J. McIntyre, L. Gagliardi, and W. J. Evans, *Inorg. Chem.*, 2012, **51**, 3613–3624.
193. M. R. Duttera, P. J. Fagan, T. J. Marks, and V. W. Day, *J. Am. Chem. Soc.*, 1982, **104**, 865–867.
194. D. Baudry, P. Charpin, M. Ephritikhine, M. Lance, M. Nierlich, and J. Vigner, *J. Chem. Soc. Chem. Commun.*, 1987, 739–740.
195. J.-F. Le Maréchal, C. Villiers, P. Charpin, M. Lance, M. Nierlich, J. Vigner, and M. Ephritikhine, *J. Chem. Soc. Chem. Commun.*, 1989, 308–310.
196. J.-C. Berthet, C. Villiers, J.-F. Le Maréchal, B. Delavaux-Nicot, M. Lance, M. Nierlich, J. Vigner, and M. Ephritikhine, *J. Organomet. Chem.*, 1992, **440**, 53–65.
197. J.-C. Berthet, J.-F. Le Maréchal, and M. Ephritikhine, *J. Chem. Soc. Chem. Commun.*, 1991, 360–361.
198. J.-C. Berthet, J.-F. Le Maréchal, M. Lance, M. Nierlich, J. Vigner, and M. Ephritikhine, *J. Chem. Soc. Dalton Trans.*, 1992, **1992**, 1573–1577.
199. J.-C. Berthet and M. Ephritikhine, *New J. Chem.*, 1992, **16**, 767–768.
200. P. Gradoz, C. Boisson, D. Baudry, M. Lance, M. Nierlich, J. Vigner, and M. Ephritikhine, *J. Chem. Soc. Chem. Commun.*, 1992, 1720–1721.
201. W. J. Evans, K. A. Miller, A. G. DiPasquale, A. L. Rheingold, T. J. Stewart, and R. Bau, *Angew. Chem. Int. Ed.*, 2008, **47**, 5075–5078.
202. W. J. Evans, E. Montalvo, S. A. Kozimor, and K. A. Miller, *J. Am. Chem. Soc.*, 2008, **130**, 12258–12259.
203. E. Montalvo, J. W. Ziller, A. G. Dipasquale, A. L. Rheingold, and W. J. Evans, *Organometallics*, 2010, **29**, 2104–2110.
204. E. Montalvo, K. A. Miller, J. W. Ziller, and W. J. Evans, *Organometallics*, 2010, **29**, 4159–4170.
205. M. R. MacDonald, M. E. Fieser, J. E. Bates, J. W. Ziller, F. Furche, and W. J. Evans, *J. Am. Chem. Soc.*, 2013, **135**, 13310–3.
206. C. R. Graves and J. L. Kiplinger, *Chem. Commun.*, 2009, **7345**, 3831–53.

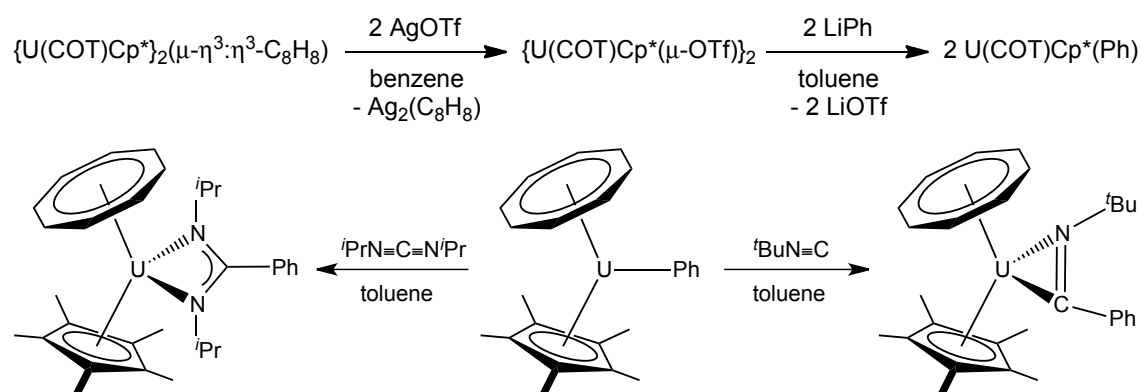
207. G. Paolucci, G. Rossetto, P. Zanella, K. Yünlü, and R. D. Fischer, *J. Organomet. Chem.*, 1984, **272**, 363–383.
208. J. M. Manriquez, P. J. Fagan, T. J. Marks, C. S. Day, and V. W. Day, *J. Am. Chem. Soc.*, 1978, **100**, 7112–7114.
209. C. Villiers, R. Adam, and M. Ephritikhine, *J. Chem. Soc. Chem. Commun.*, 1992, 1555–1556.
210. S. J. Simpson and R. A. Andersen, *J. Am. Chem. Soc.*, 1981, **103**, 4063–4066.
211. P. L. Arnold, Z. R. Turner, A. I. Germeroth, I. J. Casely, G. S. Nichol, R. Bellabarba, and R. P. Tooze, *Dalton Trans.*, 2013, **42**, 1333–7.
212. W. J. Evans, N. A. Siladke, and J. W. Ziller, *Comptes Rendus Chim.*, 2010, **13**, 775–780.
213. N. A. Siladke, J. LeDuc, J. W. Ziller, and W. J. Evans, *Chem.--Eur. J.*, 2012, **18**, 14820–14827.
214. K. G. Moloy and T. J. Marks, *Inorg. Chim. Acta*, 1985, **110**, 127–131.
215. W. J. Evans, J. R. Walensky, and J. W. Ziller, *Inorg. Chem.*, 2010, **49**, 1743–1749.
216. K. W. Bagnall and E. Yanir, *J. Inorg. Nucl. Chem.*, 1974, **36**, 777–779.
217. A. L. Arduini, J. D. Jamerson, and J. Takats, *Inorg. Chem.*, 1981, **20**, 2474–2479.

CHAPTER 2: SYNTHESIS OF MIXED-SANDWICH U(IV) ALKYL COMPLEXES

2.1 Introduction

As reviewed in greater detail in Chapter 1, uranium alkyl complexes have been of interest in organouranium chemistry since the Manhattan Project in the 1940s, where volatile uranium alkyl complexes were targeted as potential aids for isotope separation. Several research groups have synthesised alkyl complexes in a range of ligand frameworks, both carbocyclic¹⁻⁸ and non-carbocyclic,⁹⁻¹⁷ and have explored their stability and reactivity.

Most closely related to the mixed-sandwich alkyls targeted in this work, $U(COT^{TIPS2})Cp^*(R)$ (where R = alkyl, aryl), are alkyls synthesised by Evans *et al.* using an unsubstituted COT ligand in tandem with Cp^* .^{7,18} Five organyls of varying steric bulk were isolated, $U(COT)Cp^*(R)$ (where R = Me, Et, Ph, $CH(TMS)_2$, CH_2^tBu), and several of these were shown to undergo insertion chemistry with the carbodiimide $^iPrN=C=N^iPr$, and with the isocyanide $^tBuN\equiv C$, to give the expected η^2 -bound insertion products. These organyls were synthesised starting from the tetravalent precursor, $[U(COT)Cp^*]_2(\mu-\eta^3:\eta^3-C_8H_8)$, which reacts with $AgOTf$ to form the bridging triflate, $[U(COT)Cp^*(\mu-OTf)]_2$, which provides the desired organyls after further reaction with the appropriate lithium reagents (summarised in **Scheme 2.1**).

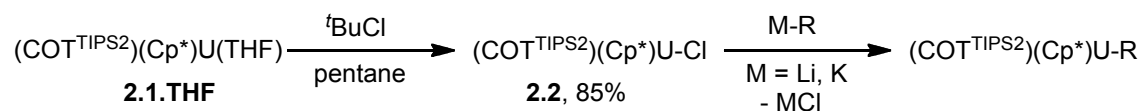


Scheme 2.1. Synthesis and reactivity of a mixed-sandwich alkyl, $U(COT)Cp^*(Ph)$.

In comparison to the COT/Cp* ligand system, it was thought that the bulkier substituted COT^{TIPS2} ligand used in tandem with Cp* in this work may impart greater stability due to steric and electronic effects. It is notable that of the aforementioned mixed-sandwich alkyl complexes, U(COT)Cp*(R), only the R = CH(TMS)₂ variant has been crystallographically characterised;⁷ it was anticipated that the presence of silyl substituents on the COT ring may aid crystallisation of such mixed-sandwich alkyls.

As is typical of paramagnetic U(IV) complexes, NMR spectroscopic data collected from all the complexes described in this work display broadened and shifted resonances from equivalent diamagnetic complexes.¹⁹ A summary of methods used to interpret the paramagnetic NMR spectra collected for mixed-sandwich complexes is provided in Chapter 6, section 6.4.

2.2 General route to mixed-sandwich alkyls

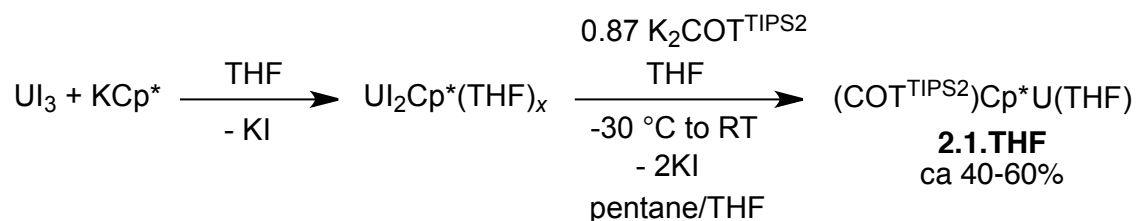


Scheme 2.2. Synthetic route to U(COT^{TIPS2})Cp*(R) where R = alkyl.

The general synthetic route to mixed-sandwich alkyl complexes in this work is shown in **Scheme 2.2**, generating the desired alkyl complexes *via* salt metathesis reactions with potassium or lithium alkyl reagents; the full conditions are described in the following sections. As an extension of initial investigations,²⁰ a range of alkyls were targeted for synthesis: R = Me, CH₂Ph, ⁿBu, ^tBu, Np, CH₂TMS and CH(TMS)₂. The successful syntheses of four alkyls and their characterisation is described in this chapter, along with the attempted syntheses of three other alkyls. Also described are a number of side-products of particular interest or relevance for work detailed in the forthcoming chapters.

2.3 Synthesis and characterisation of $U(COT^{TIPS})Cp^*Cl$ (**2.2**)

Synthesis of the U(III) mixed-sandwich complex, $U(COT^{TIPS_2})Cp^*(THF)$ (**2.1.THF**), was performed following the published procedure but with slight modifications – crystallisation was carried out from a mixture of pentane and THF, instead of pentane alone (**Scheme 2.3**).²¹



Scheme 2.3. Synthesis of **2.1.THF**

The oxidation of **2.1.THF** was carried out in pentane using a slight excess of $tBuCl$ to form the U(IV) chloride complex, $U(COT^{TIPS_2})Cp^*Cl$ (**2.2**). This synthetic route has been employed previously by Finke *et al.* in the reaction of alkyl halides with the bis-cyclopentadienyl U(III) complex, $UCp^*_2Cl(THF)$, wherein the authors report a clean transformation to the U(IV) bis-chloride, $UCp^*_2Cl_2$, when using the bulky alkyl chlorides $tBuCl$ or $PhCH_2Cl$.²² In contrast, when using an alkyl chloride (RCl) where R is less bulky or forms a less stable radical (such as $R = nBu$, cyclopropylmethyl) the alkylated product $UCp^*_2Cl(R)$ is also formed. When employing this route with **2.1.THF** there is no evidence for the formation of the mixed-sandwich alkyl $U(COT^{TIPS_2})Cp^*(tBu)$ in either 1H NMR spectroscopic or mass spectrometric data, and the reaction proceeds cleanly to give **2.2** in isolated yields of 85% or above.

The red-brown powder is not recrystallised before use as it is analytically pure after removal of volatile organic side-products (that are formed from recombination and rearrangement of $tBu\bullet$ radicals), by the sequential addition and removal of pentane and thorough drying under reduced pressure. Recrystallisation of **2.2** from a saturated pentane solution yields small quantities of red crystals suitable for X-ray diffraction

(**Figure 2.1**); whilst the compound has been reported previously, no X-ray crystal structure was determined.²³

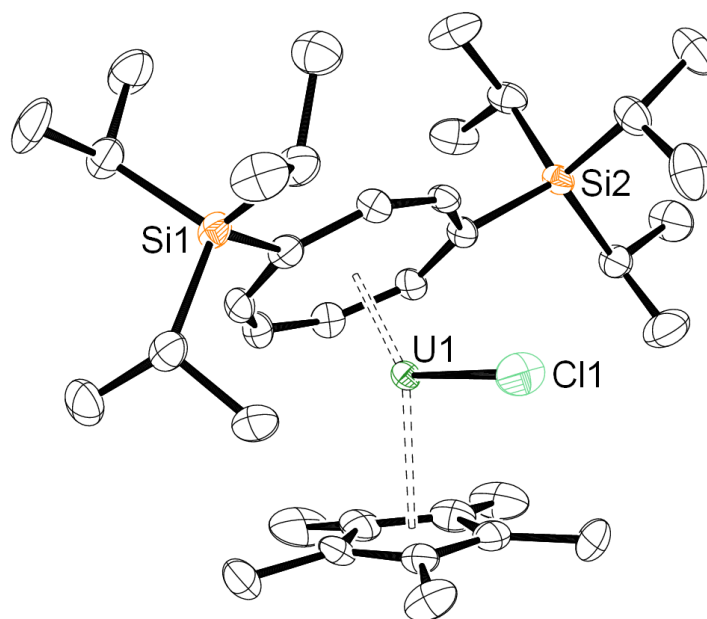


Figure 2.1. Molecular structure of $\text{U}(\text{COT}^{\text{TIPS}2})\text{Cp}^*\text{Cl}$ (**2.2**). ORTEP representation with thermal ellipsoids at the 50% probability level. Hydrogen atoms are omitted for clarity. U1-Cl1: 2.6496(12) Å, U1-Ct1: 1.9142(15) Å, U1-Ct2: 2.465(2) Å, Ct1-U1-Ct2: 139.85(8) °.

The crystal structure of **2.2** is unremarkable; the U1-Cl1 bond distance of 2.6496(12) Å is typical of the U-Cl bond lengths found in other U(IV) terminal mono-chloride complexes containing 5- and/or 8-membered ring ligand frameworks, which lie within the range of 2.570(4) – 3.111(1) Å.²⁴ The most closely related chloride complex reported is the binuclear structure $\text{Cp}^*(\text{COT})\text{ClU}(\mu\text{-Cl})\text{U}(\text{COT})\text{Cp}^*$ (**Figure 2.2, 2A**), featuring both a bridging chloride as well as a terminal chloride ligand.²⁵

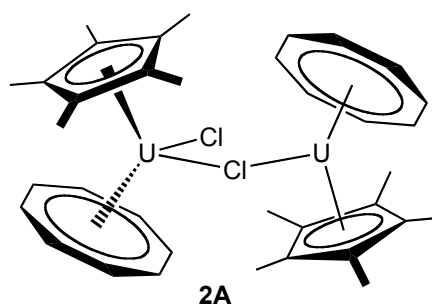


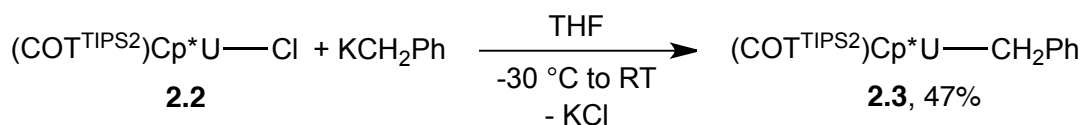
Figure 2.2. $\text{Cp}^*(\text{COT})\text{ClU}(\mu\text{-Cl})\text{U}(\text{COT})\text{Cp}^*$ (**2A**).

The terminal U-Cl bond in **2A** is slightly longer than that found in **2.2** (2.673(4) vs 2.6496(12) Å) presumably due to steric crowding of the uranium metal centre in **2A**: it is bound to a second chloride ligand as well as to the carbocyclic rings, hence possessing a higher coordination number. The U1-Ct1 (COT-ring centroid) and U1-Ct2 (Cp*-ring centroid) distances in **2.2** (1.9142(15) and 2.465(2) Å respectively) are the shortest found in any reported ‘U(COT^{TIPS2})Cp*’ complexes (with free-rotating Cp* rings, see Appendix 1), owing to the small, highly-charged chloride ligand allowing for the close approach of the carbocyclic ligands. The Ct1-U1-Ct2 angle of 139.85(8) ° is consistent with those found in other mixed-sandwich complexes in this work (see Appendix 1).

2.4 Synthesis of mixed-sandwich alkyls: R = Me, CH₂Ph, ⁿBu, ⁱBu, Np

2.4.1 Synthesis and characterisation of benzyl and methyl alkyls

The synthesis of U(COT^{TIPS2})Cp*(CH₂Ph) (**2.3**) was achieved by the dropwise addition of a THF solution of KCH₂Ph to **2.2**, pre-cooled to -30 °C, stirred cold for 1 hour before filtration and workup in pentane (**Equation 2.1**). Red-purple crystals of **2.3** were isolated in a 47% yield, and were characterised as the desired benzyl alkyl by X-ray diffraction, NMR spectroscopy, mass spectrometry, and elemental analysis.



Equation 2.1. Synthesis of U(COT^{TIPS2})Cp*(CH₂Ph) (**2.3**).

The ¹H NMR spectrum collected from a crystalline sample of **2.3** in C₆D₆ exhibited resonances with the correct multiplicity and integral values for the mixed-sandwich ligands, in addition to resonances attributable to a benzyl ligand: a broad singlet of integration 2H at 7.01 ppm corresponding to the CH₂Ph protons, and three resonances corresponding to the phenyl ring protons at 10.47, 7.80 and 1.64 ppm

(t, 2H, *m*-C₆H₅; d, 2H, *o*-C₆H₅; t, 1H, *p*-C₆H₅). ²⁹Si{¹H} NMR spectroscopic analysis of **2.3** showed a single resonance at -96.9 ppm. Mass spectrometric analysis of **2.3** did not show the expected parent ion at 881 m/z, however the 100% ion at 790 m/z corresponds to the U(COT^{TIPS2})Cp* fragment – it is likely that the -CH₂Ph ligand fragments easily from the parent complex and hence the molecular ion is not detected. Elemental analysis of crystalline **2.3** was consistent with the expected composition. Crystalline **2.3** was analysed by X-ray diffraction studies – the structure is shown in **Figure 2.3**.

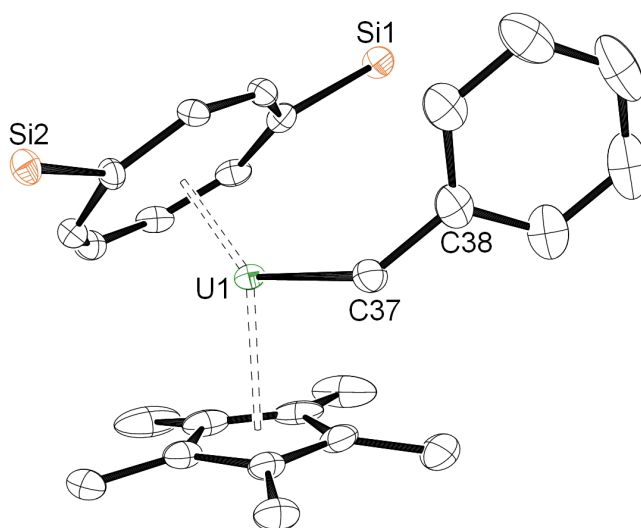


Figure 2.3. Molecular structure of one crystallographically independent molecule of U(COT^{TIPS2})Cp*(CH₂Ph) (**2.3**) in the asymmetric unit.

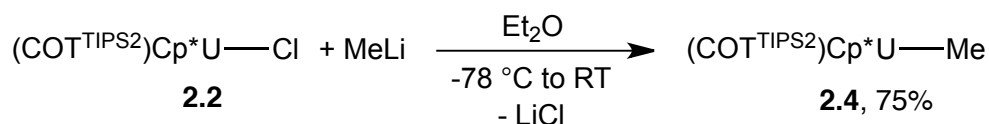
ORTEP representation with thermal ellipsoids at the 50% probability level. One molecule of two present in the asymmetric unit shown. Hydrogen atoms and ⁱPr groups omitted for clarity.

U1-C37: 2.5323(1) Å, U1-C37-C38: 127.8(3) °, U1-Ct1: 1.9297(3) Å, U1-Ct2: 2.4899(3) Å, Ct1-U1-Ct2: 137.217(13) °; from molecule not shown: U51-C87: 2.5433(1) Å, U51-C87-C88: 127.0(3) °, U51-Ct51: 1.9304(3) Å, U51-Ct52: 2.4836(3) Å, Ct51-U51-Ct52: 137.977(13) °.

The molecular structure shows that the benzyl ligand binds to the metal centre in an η¹-fashion with no interaction between the phenyl ring and the central uranium atom, as has been observed in other U(IV) benzyl alkyl complexes.^{13,16,26–28} In comparison to the limited number of U(IV) alkyl complexes containing one or more η¹-benzyl ligands, **2.3** falls outside the typical range of U-C_{alkyl} bond distances

(2.467(5) – 2.508(3) Å), but within the typical range of U-C_{alkyl}-C_{phenyl} angles (98.6(2) – 134.2(4) °). The long U1-C37 bond distance in **2.3** may be due to the bulky benzyl group being close to the COT-ring TIPS groups and forcing a longer U1-C37 bond length to avoid steric interaction; in the solid-state the phenyl ring is orientated away from the Cp*-ring methyl groups, sitting between the two TIPS groups in an asymmetric fashion (Ct3-Si1: 3.829 Å, Ct3-Si2: 6.783 Å; Ct3 is the phenyl ring centroid). The U1-Ct1/U51-Ct51 and U1-Ct2/U51-Ct52 bond distances lie within the typical range for other U(IV) mixed-sandwich complexes in this work, as do the Ct1-U1-Ct2/Ct51-U51-Ct52 angles (see Appendix 1).

The methyl complex, U(COT^{TIPS2})Cp*(Me) (**2.4**) was synthesised in a similar fashion: the reaction of **2.2** and MeLi was performed in Et₂O at -78 °C, allowed to warm to -30 °C and stirred for 1 hour before filtration and workup, yielding a red-orange powder of **2.4** in a 75% yield (Equation 2.2). The reaction of KMe and **2.2** did not provide the desired product in a satisfactory yield.



Equation 2.2. Synthesis of U(COT^{TIPS2})Cp*(Me) (**2.4**).

Red crystals suitable for X-ray diffraction studies were grown from a saturated pentane solution (380 mg in 2 cm³) stored at -35 °C for two weeks. ¹H NMR spectroscopic analysis of **2.4** returned a spectrum containing the expected resonances for the mixed-sandwich ligands, and a resonance of integration 3H at δ_H 52.8 attributable to a methyl group. ²⁹Si{¹H} NMR spectroscopic data collected from this sample showed a single resonance at -99.3 ppm. As with **2.3**, the mass spectrum of **2.4** does not show a parent ion of the expected mass at m/z = 805, only an ion at m/z = 789 indicating that the methyl ligand is labile under EI MS conditions. Elemental analysis of crystalline **2.4** returned values of found %C slightly lower than predicted – this is

suspected to be due to the unstable nature of the complex and its temperature sensitivity, and it is likely that the sample decomposed to a significant extent prior to analysis.

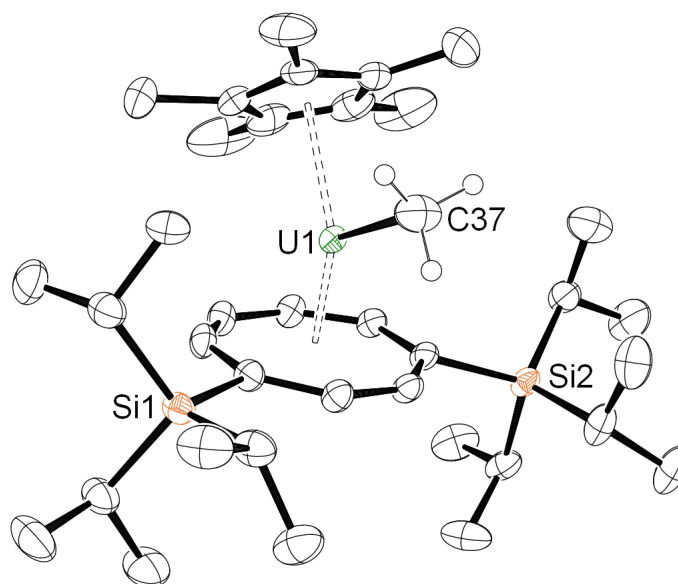


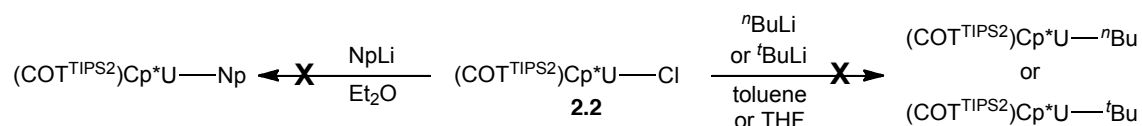
Figure 2.4. Molecular structure of $\text{U}(\text{COT}^{\text{TIPS}_2})\text{Cp}^*(\text{Me})$ (**2.4**).

ORTEP representation with thermal ellipsoids at the 50% probability level. Hydrogen atoms except those on C37 omitted for clarity. U1-C37 2.462(4) Å, U1-Ct1 1.9368(3) Å, U1-Ct2 2.4761(3) Å, Ct1-U1-Ct2 140.664(13) °.

The molecular structure of **2.4** shows the expected methyl complex, with the alkyl ligand bound in an η^1 -fashion, with no indication of any agostic interactions (**Figure 2.4**). The U1-C37 bond distance of 2.462(4) Å lies within the range of U-C_{alkyl} bond distances in comparable U(IV) mono-methyl alkyl complexes (2.400(6) – 2.50(2) Å), collated from the 18 reported in the literature.²⁴ The U1-Ct1 and U1-Ct2 distances of 1.9368(3) and 2.5761(3) Å are comparable to the other mixed-sandwich alkyl complexes reported in this work. The Ct1-U1-Ct2 bond angle of 140.664(13) ° is one of the most obtuse when compared to other mixed-sandwich complexes, as the small size of the bound methyl ligand does not impart any great steric effects on the two carbocyclic rings, not significantly reducing the angle, unlike the bulkier carboxylate ligands (see Appendix 1).

Both **2.3** and **2.4** are temperature-sensitive and prone to decomposition if not stored at temperatures less than -35 °C either in solution or in the solid state. The decomposition product has been characterised and is described in section 2.6.

2.4.2 Attempted syntheses of butyl and neopentyl alkyls



Scheme 2.4. Attempted syntheses of other alkyls.

The reaction of **2.2** and ca 1 equivalent of solid ^tBuLi resulted in a red-brown solution, which contained no new products after 4 hours, as determined by ¹H NMR spectroscopy. Further agitation of the solution and re-examination by ¹H NMR spectroscopy several hours later revealed decomposition into organic ligand fragments. Due to the large steric bulk of *tert*-butyl it was thought that the resulting sterically congested alkyl complex may be highly unstable and might rapidly decompose. A similar result occurred when attempting to synthesise the *n*-butyl complex with ⁿBuLi and **2.2** at -78 °C in THF. After stirring for 1 hour and warming to no more than -30 °C, the solution appeared unchanged; it was stirred for a further hour and allowed to warm to ambient temperature, after which time it became dark brown in colour, indicating formation of the known decomposition product, **2.9**, *vide infra*.

No alkyl product could be isolated from the reaction of **2.2** and NpLi in C₆D₆ – analysis of the reaction mixture by ¹H NMR spectroscopy showed a mixture of decomposition products and unreacted **2.2**. Repetition of the reaction using different reaction conditions (pentane or Et₂O as solvent) yielded an orange-red reaction mixture after 20 minutes of stirring that was analysed by ¹H NMR spectroscopy. Integration of the COT^{TIPS2} signals in the spectrum relative to a prominent signal at δ_H 31.5 indicated that the resonance integrated to 9H, which could correlate to the nine protons present in a Np alkyl ligand. However, the product formed was highly susceptible to

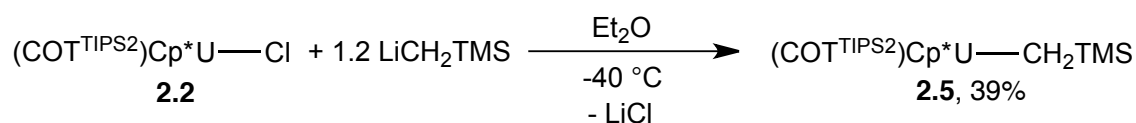
decomposition, and attempts to crystallise the suspected neopentyl alkyl or collection of further characterisation data were not successful.

2.5 Synthesis of mixed-sandwich silyl alkyls: R = CH₂TMS, CH(TMS)₂

Two bulky silyl-alkyls were targeted for synthesis due to their potential for sterically stabilising uranium metal centres, as literature precedent indicates.^{7,11,12,29,30} In contrast to the non-silyl alkyls, **2.3** and **2.4**, the alkyls containing one or two TMS groups were more difficult to synthesise and decomposed more rapidly. The use of alternative reaction conditions when attempting to synthesise **2.5** yielded two unexpected side-products, described in section 2.5.2.

2.5.1 Syntheses of silyl alkyls

The synthesis of U(COT^{TIPS2})Cp*(CH₂TMS) (**2.5**) was achieved by the reaction of **2.2** and 1.2 equivalents of LiCH₂TMS in Et₂O at -40 °C, stirred for 1 hour before filtration and workup. Concentration and storage of the resulting red Et₂O solution at -50 °C afforded red crystals after three days in a 39% yield (**Equation 2.3**).



Equation 2.3. Synthesis of U(COT^{TIPS2})Cp*(CH₂TMS) (**2.5**).

Rapid decomposition of the isolated material complicated the collection of characterising data: elemental analysis of the crystalline sample returned values low for %C, at 54.24% found compared to 54.76% expected. This could be due to decomposition, or to small quantities of side-product co-crystallising with the desired alkyl (see following section for details). ¹H NMR spectroscopic analysis of a freshly-prepared crystalline sample of **2.5** contained more than one set of mixed-sandwich ligand resonances, however, the most intense resonances matched the expected integral values of mixed-sandwich ligand protons and a -CH₂TMS ligand.

$^{29}\text{Si}\{^1\text{H}\}$ NMR spectroscopic data showed two signals at 139.7 and -102.35 ppm, correlating to the TIPS groups and silyl alkyl ligand silicon atoms. EI mass spectrometric analysis returned an ion at $m/z = 833$, corresponding to $\text{M}^+ - \text{CH}_3$, but not the expected parent ion. X-ray diffraction studies determined the structure of **2.5**.

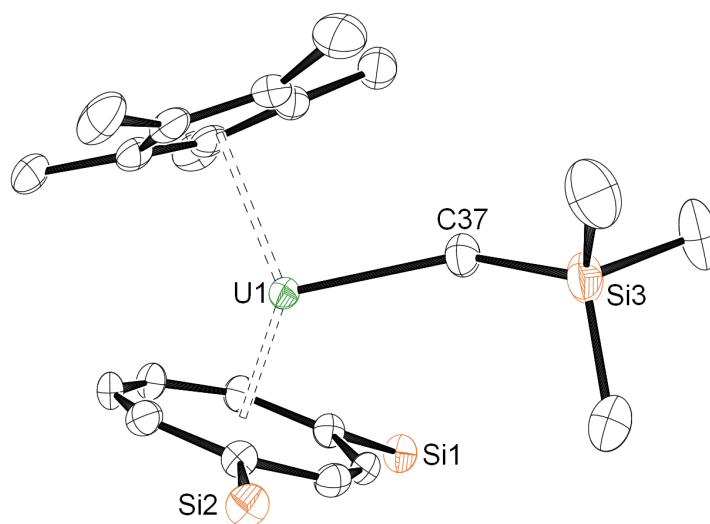


Figure 2.5. Molecular structure of $\text{U}(\text{COT}^{\text{TIPS}_2})\text{Cp}^*(\text{CH}_2\text{TMS})$ (**2.5**).

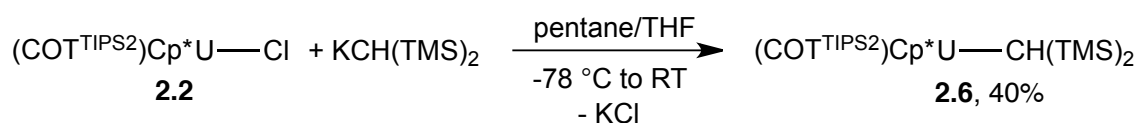
ORTEP representation with thermal ellipsoids at the 50% probability level.

Hydrogen atoms and ^iPr groups omitted for clarity. U1-C37: 2.464(4) Å, U1-Ct1: 1.9361(3) Å, U1-Ct2: 2.4880(3) Å, Ct1-U1-Ct2: 137.171(4)°, U1-C37-Si3: 147.5(2)°.

As seen in **Figure 2.5**, the alkyl ligand is bound in the expected η^1 configuration, and the TMS group is positioned between the two bulky TIPS substituents on the COT ring. The U1-C37 alkyl bond distance of 2.464(4) Å is in agreement with those found in the other crystallographically characterised mixed-sandwich alkyl complexes in this work, and lies within the range of $\text{U}-\text{C}_{\text{alkyl}}$ bond distances in the small number of other U(IV) mono-TMS alkyl complexes reported in the literature (2.40(2) – 2.484(6) Å).²⁴ The U1-C37-Si3 bond angle is 147.5(2)°, and is not acute enough to indicate that any additional agostic interaction between the methyl group protons and the uranium metal centre is present. Of the other reported U(IV) mono-TMS alkyl complexes, only one species is a mono-alkyl: $\text{Cp}^*_2[(\text{Me})\text{NNN}(\text{Ad})-\kappa^2\text{N}^{1,3}]\text{U}(\text{CH}_2\text{TMS})$,³¹ the X-ray diffraction data collected for this structure were only sufficient for determining atom connectivity and not exact geometric parameters. It can, however, be calculated that the

U-C_{alkyl}-Si bond angle is ca 158 °, greater than in **2.5**, presumably due to steric effects of the other ancillary ligands hindering a closer approach. The two other U(IV) mono-TMS alkyl complexes are bis- and tetra-kis alkyls, respectively, and contain more acute U-C_{alkyl}-Si bond angles (125.7(3) – 130.6(3) °), likely due to the lack of steric crowding around the metal centres.^{14,32}

The bulkier bis-TMS alkyl, U(COT^{TIPS2})Cp*(CH{TMS}₂) (**2.6**), was formed from the reaction of **2.2** and KCH{TMS}₂ in a 20:1 mixture of pentane/THF at -78 °C (**Equation 2.4**). Workup after warming to ambient temperature over 12 hours yielded a viscous brown material, that was identified to consist mainly of **2.6**, as determined by ¹H NMR spectroscopy.



Equation 2.4. Synthesis of U(COT^{TIPS2})Cp*(CH{TMS}₂) (**2.6**).

Recrystallisation from (TMS)₂O yielded only red crystals of the known bis-oxo complex, {U(COT^{TIPS2})Cp*}₂(μ-O), formed from either presence of adventitious oxygen or from solvent activation.³³ Crystals of **2.6** suitable for X-ray diffraction studies were obtained from a concentrated pentane solution, stored at -35 °C for three months, along with off-white solids identified as organic ligand decomposition products. The crystalline material was confirmed to be **2.6** (**Figure 2.6**), and matched the ¹H NMR spectroscopic data obtained from the earlier reaction aliquot. ²⁹Si{¹H} NMR spectroscopic studies of the crystals showed two silicon resonances at -60.84 and -119.84 ppm, corresponding to the COT-TIPS and *bis*-TMS alkyl ligand environments. EI mass spectrometry did not show the expected parent ion at m/z = 949, but instead a fragment of m/z = 789 corresponding to ‘UCOT^{TIPS2}Cp*’ without the alkyl ligand. The 100% ion at m/z = 145 is likely to correspond to a fragment of the CH(TMS)₂ ligand. Further attempts to isolate **2.6** found success when using ^tBuOMe to afford microcrystalline brown solids of the alkyl, however the similar solubility of the

organic side-products meant that a sample of **2.6** clean enough for elemental analysis could not be obtained.

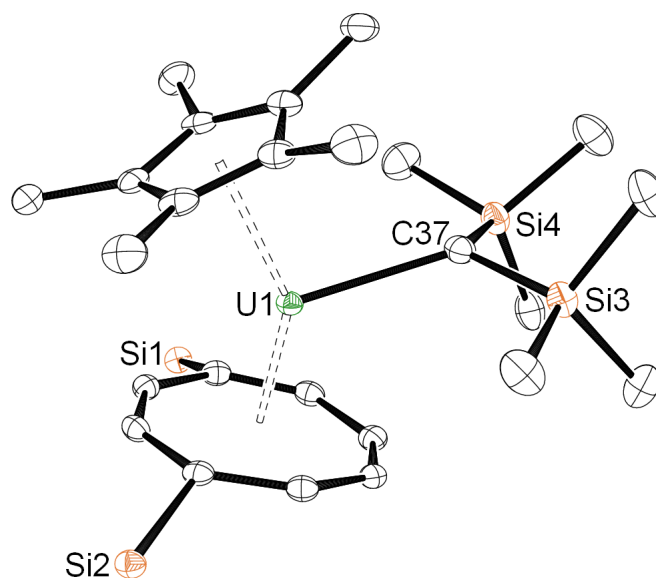


Figure 2.6. Molecular structure of $\text{U}(\text{COT}^{\text{TIPS}_2})\text{Cp}^*(\text{CH}\{\text{TMS}\}_2)$ (**2.6**).

ORTEP representation with thermal ellipsoids at the 50% probability level.

Hydrogen atoms and $i\text{Pr}$ groups omitted for clarity. Selected bond distances and angles presented in **Table 2.1**.

The solid-state structure of **2.6** is distinct in comparison to the three other structurally characterised alkyls, **2.3**, **2.4** and **2.5**, and from any other U(IV) ‘ $\text{U}(\text{COT}^{\text{TIPS}_2})\text{Cp}^*$ ’ mixed-sandwich compound reported in this thesis or in the literature, due to the arrangement of the TIPS groups attached to the COT ring. In contrast to all other molecular structures obtained for U(IV) mixed-sandwich $\text{COT}^{\text{TIPS}_2}/\text{Cp}^*$ systems, the TIPS substituents on the COT ring of **2.6** are orientated away from the alkyl ligand (or other third coordinated ligand) instead of towards it (**Figure 2.7**). This arrangement is most likely due to the steric bulk of the *bis*-TMS ligand interfering with the similarly bulky TIPS groups, forcing the COT ring to rotate and position the TIPS moieties nearer the Cp^* ring methyl groups in a normally unfavoured fashion. In comparison to **2.5**, **2.6** contains longer centroid-U lengths as a result of the steric demands of the *bis*-TMS alkyl ligand; the U1-C37 bond distance is also longer in **2.6** than in **2.5**.

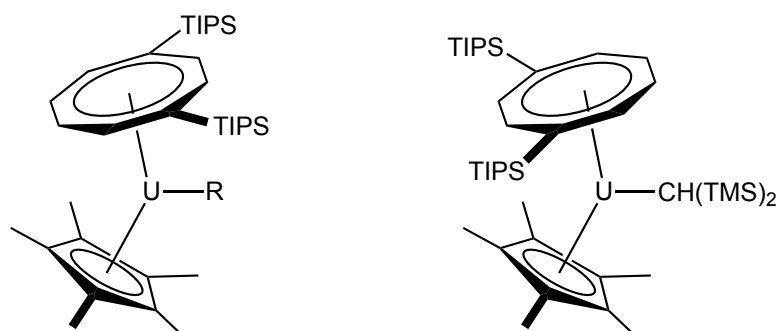


Figure 2.7. Typical orientation of COT ring ^tPr groups (left) and the orientation seen in the molecular structure of **2.6** (right). R = alkyl, chloride, ethoxide, carboxylate, amide.

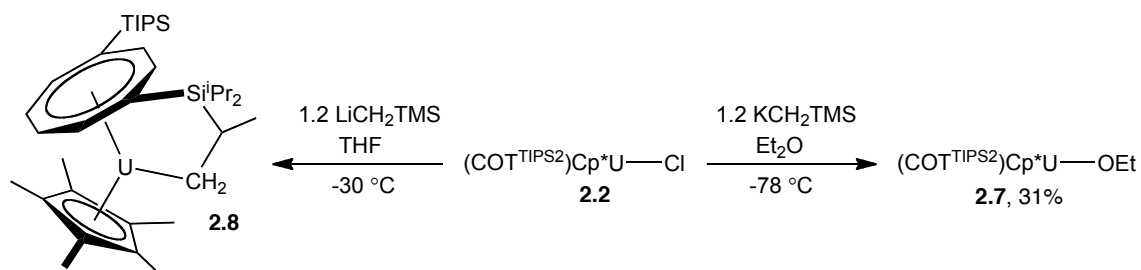
The most closely related complex to **2.6** to consider for structural comparison is the only other crystallographically characterised U(IV) mixed-sandwich alkyl complex outside of this work, U(COT)Cp*(CH{TMS}₂) (**2B**), reported by Evans *et al.* in 2009.⁷ **Table 2.1** contains selected bond lengths and angles from the two structures. The U-C_{alkyl} bond length is longer in **2.6** than in **2B**, presumably due to bulky substituents on the COT ring in **2.6**. In all other respects, the structures are markedly similar. The U-C_{alkyl} bond length of 2.497(3) Å is longer in **2.6** than in alkyls **2.4** and **2.5**, likely due to steric demands of the TMS groups.

Table 2.1. Selected bond distances (Å) and angles (deg) for compounds **2.6** and **2B**. Ct1 is defined as the COT ring centroid, and Ct2 is defined as the Cp* ring centroid.

	2.6	2B
U1-Ct1	1.9774(2)	1.969
U1-Ct2	2.5211(2)	2.499
Ct1-U1-Ct2	141.926(12)	138.2
U-C _{alkyl}	2.497(3)	2.469(3)

2.5.2 Attempted synthesis of **2.5**: isolation of side-products

Initial attempts to synthesise **2.5** used the potassium alkyl reagent, KCH₂TMS, in place of LiCH₂TMS, and a range of reaction solvents with both KCH₂TMS and LiCH₂TMS. Two new U(IV) compounds were unintentionally formed in place of the desired alkyl (**Scheme 2.5**), and are described below.



Scheme 2.5. Side-products **2.7** and **2.8** formed from attempted syntheses of **2.5**.

In a manner similar to that used for synthesising **2.4**, **2.2** and KCH_2TMS were reacted in Et_2O at $-78\text{ }^\circ\text{C}$; an aliquot was obtained from the reaction mixture after 2 hours to monitor the reaction progress and was found to contain only unreacted **2.2**. A further 12 hours of stirring resulted in a dark yellow solution, which afforded orange crystalline material after workup in pentane and storage at $-30\text{ }^\circ\text{C}$ overnight. The ^1H NMR spectrum collected from the crystalline material did not contain a resonance attributable to a $-\text{CH}_2\text{TMS}$ ligand, and the $^{29}\text{Si}\{^1\text{H}\}$ NMR spectrum contained only a single silicon resonance at $\delta_{\text{Si}} -135.9$. Collection of X-ray diffraction data revealed the product to be a U(IV) ethoxide, $\text{U}(\text{COT}^{\text{TIPS}_2})\text{Cp}^*(\text{OEt})$ (**2.7**, **Figure 2.8**), presumably formed *via* activation of the Et_2O solvent used in the metathesis reaction. The synthesis of **2.7** can also be carried out from the reaction of **2.2** and KOEt in THF.

In light of this information, re-examination of the ^1H NMR spectroscopic data confirms the presence of two broad singlets at $\delta_{\text{H}} 142.12$ ppm and 53.58 with integral values of 2H and 3H for the OCH_2CH_3 and OCH_2CH_3 protons respectively. Mass spectrometric analysis shows the molecular ion at $m/z = 834$, and an ion of $m/z = 699$ that corresponds to the fragment ' $\text{U}(\text{COT}^{\text{TIPS}_2})\text{OEt}$ '. Elemental analysis returned results consistent with the molecular formula described above. Abstraction of an 'OEt' fragment from Et_2O would presumably result in the formation of an 'Et radical, which, as in the reaction of 'BuCl with **2.1**, could recombine to form butane. This was not observed in the ^1H NMR spectra collected from reaction aliquots as the

samples undergo removal of volatiles under reduced pressure, therefore any butane formed would be removed before analysis.

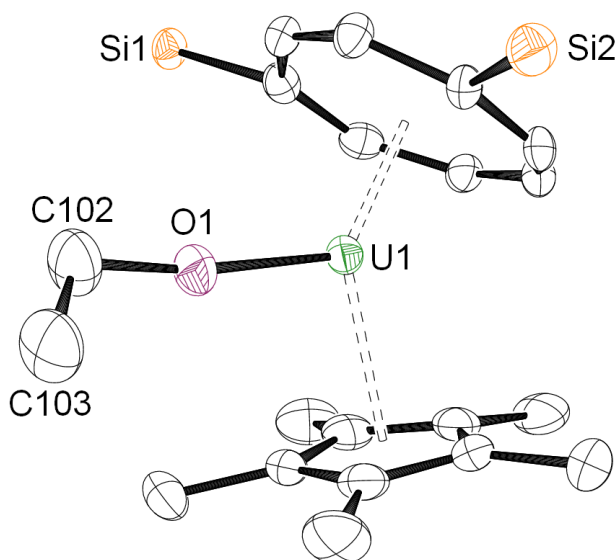


Figure 2.8. Molecular structure of $\text{U}(\text{COT}^{\text{TIPS}_2})\text{Cp}^*(\text{OEt})$ (**2.7**).

ORTEP representation with thermal ellipsoids at the 50% probability level.

Hydrogen atoms and $i\text{Pr}$ groups omitted for clarity. U1-O1: 2.063(4) Å,
U1-Ct1: 1.9592(18) Å, U1-Ct2: 2.497(3) Å, Ct1-U1-Ct2: 135.85(9) °.

Only two other U(IV) mono-ethoxide complexes have been reported in the literature, and both feature supporting Tp^* ligands and either a chloride or iodide bound to the metal centre, $\text{UTp}^*_2(\text{OEt})\text{X}$ (where $\text{X} = \text{Cl}, \text{I}$).³⁴ The $\text{U-O}_{\text{ethoxide}}$ bond distances for these halo-ethoxide complexes are 2.028(9) and 2.027(9) Å respectively, both marginally shorter than the U1-O1 bond distance in **2.7**; this could be an electronic effect due to the coordination of a halide ligand in the other complexes. The structural parameters of **2.7** are essentially identical to the closely related methoxide complex, $\text{U}(\text{COT}^{\text{TIPS}_2})\text{Cp}^*(\text{OMe})$,³⁵ – U-Ct1: 1.95590(2) vs 1.9592(18) Å, U-Ct2 2.4887(2) vs 2.497(3) Å, and Ct1-U1-Ct2: 135.809(9) vs 135.85(9) ° – whilst the U-O bond distance of 2.063(4) found in **2.7** is slightly longer than that found in the methoxide complex (2.058(4) Å).

As an alternative to Et₂O, the reaction of **2.2** and KCH₂TMS was performed in *t*-BuOMe, however ¹H NMR spectra collected from reaction mixture aliquots over a period of 8 days indicated that **2.2** remained mostly unreacted, yet a small number of low-intensity resonances were also present. Closer inspection of the low-intensity resonances revealed that one of the compounds present was the previously reported U(IV) methoxide complex, U(COT^{TIPS2})Cp*(OMe),³⁵ presumably formed from activation of the *t*-BuOMe solvent. It was noted that the δ_H values of the methoxide and ethoxide complexes were very similar, yet still distinguishable from each other, which is unsurprising given the similarity of the two complexes. Another set of the low-intensity resonances also appeared at very similar shifts to the ethoxide and methoxide complexes, and further investigation identified another resonance at δ_H 52.2 with an integral value of 9H (relative to the associated Cp* and TIPS proton environments, assigned on the basis of integration), consistent with the presence of another product that could be the U(IV) *tert*-butoxide, U(COT^{TIPS2})Cp*(O*t*Bu), also formed from solvent activation.

Reacting **2.2** and LiCH₂TMS in THF at -30 °C, *cf.* the formation of **2.3**, resulted in the isolation of a small quantity of orange microcrystalline solids that were determined to be a mixture of **2.6** and an unknown product or products by ¹H NMR spectroscopic analysis. Resonances were present in the ¹H NMR spectrum with the correct character (multiplicity and relative integration values) to be three sets of TIPS doublets in a ratio relative to each other of 1:3:1. The identity of the product responsible for these resonances was discovered at a later date, after the same reaction was performed on similar scale but using Et₂O in place of THF. After recrystallisation from Et₂O a small quantity of orange-red crystals were isolated (23 mg), and examination under a microscope revealed two different crystal morphologies present in the sample (orange plates and orange-red prisms) – this correlated to ¹H NMR spectroscopic data collected from the orange-red crystal sample, which contained the same resonances in a 1:3:1 ratio described above, along with other

paramagnetically-shifted signals. Only one morphology of crystals – the orange-red prisms – were suitable for X-ray diffraction studies, but the sample was twinned and of poor quality hence the data collected could not be fully refined: the R factor is 14.8%, and the maximum shift is 2.224 Å. Regardless, connectivity could be established and the structure of this complex, **2.8**, is shown in **Figure 2.9**.

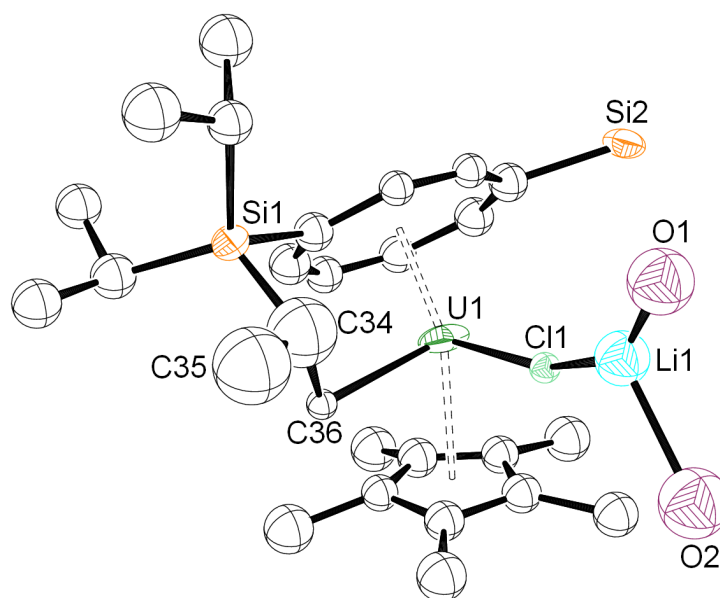


Figure 2.9. Unrefined molecular structure of **2.8**.

ORTEP representation with thermal ellipsoids at the 20% probability level.

Hydrogen atoms, ‘un-tucked’ TIPS group, and disordered OEt_2 groups omitted for clarity.

The twinning and disorder resulted in the appearance of two ‘tucked-in’ TIPS groups, however, this was due to a 50/50 occupancy of ‘tucked-in’ and non ‘tucked-in’ TIPS groups on each side of the molecule: this disorder could not be satisfactorily modelled. Mass spectroscopic data agreed with the presence of only one ‘tucked-in’ TIPS group: data collected from the crystalline material sample containing **2.8** showed ions corresponding to fragments of **2.8**, at $m/z = 824$ (3%, $M^+ - Li(OEt_2)_2$), 788 (55%, $M^+ - Cl.Li(OEt_2)_2$), and 191 (11%, $Cl.Li(OEt_2)_2$). With the structure of one product elucidated, the 1H NMR spectroscopic data were re-examined to identify resonances present due to **2.8**, comparing spectra collected from the two reactions described above. The largest signal present in the spectra is a sharp singlet with an integral value of 15H, which correlates to the Cp* ring of **2.8**. One TIPS group on the COT ring is intact, and

this appears as two doublets of 9H each and a multiplet of 3H. The ‘tucked-in’ TIPS group appears as four doublets of 3H each and two multiplets of 1H each, and as a doublet of integration 6H. Also present are nine broad singlets of integration 1H each at shifts between 59.77 and -101.44 ppm which correlate to the COT-ring protons, and the remaining protons on the ‘tucked-in’ *i*Pr group – this assignment is illustrated in **Figure 2.10**. Broad resonances at 3.27 and 1.08 ppm of integration 8H and 12H respectively are likely to correspond to the two coordinated Et₂O molecules – these resonances are absent in the ¹H NMR spectrum collected from a sample of **2.8** synthesised in THF as a solvent, in place of Et₂O.

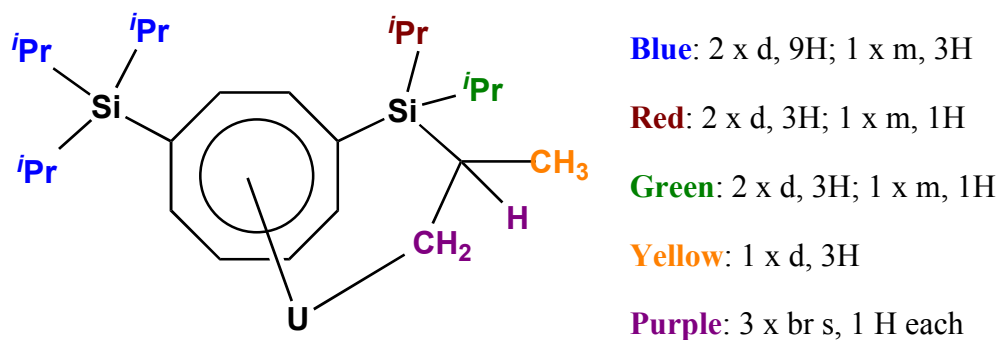
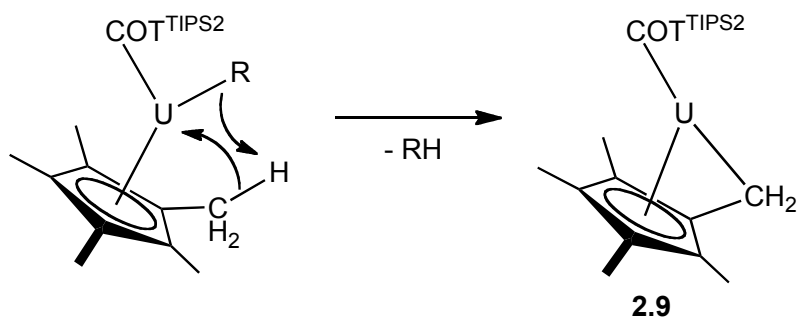


Figure 2.10. Diagram highlighting protons responsible for ¹H NMR spectroscopic shifts corresponding to ‘tucked-in’ TIPS COT ligand in complex **2.8**.

The mechanism for the formation of **2.8** is unclear, however in the crude reaction mixture free SiMe₄ can be detected by ¹H NMR spectroscopy. The latter could arise from hydrogen atom abstraction from the CH₃ group of a TIPS substituent by a -CH₂TMS group, which would afford the ‘tuck-in’ and SiMe₄. A related reaction was reported by Gilbert *et al.* in 1989, as an aside to their work synthesising Th(IV) mixed-sandwich alkyls, wherein (COT)(Cp*)Th(μ-Cl)₂Mg(CH₂^{*t*}Bu)(THF) was formed from the reaction of (COT)(Cp*)Th(Cl)(THF) and MgClCH₂^{*t*}Bu instead of the desired -CH₂^{*t*}Bu alkyl.³⁶ As the side-product **2.8** has only been isolated in small quantities, and as it co-crystallises with several impurities, elemental analysis has not been obtained.

2.6 Alkyl decomposition: tuck-in complex formation

Throughout the experiments conducted to synthesise the alkyl complexes described above, a common decomposition product was observed by ^1H NMR spectroscopy. This product was observed in crude reaction mixtures, and after alkyls had been stored at ambient temperatures over a period of a few days either in solution or in the solid state. Examination of the ^1H NMR spectrum of this material showed the presence of a ‘tucked-in’ complex, $\text{U}(\text{COT}^{\text{TIPS}_2})(\eta^5:\kappa^1\text{-C}_5\text{Me}_4\text{CH}_2)$ (**2.9**, **Scheme 2.6**), characterised initially by its distinctive ^1H NMR spectroscopic resonances: no free-rotating Cp^* ring is present in the structure, so a singlet of integration 15H is not observed in the spectrum, unlike in the spectra of other mixed-sandwich complexes. Instead, two singlets of integration 6H each are observed at δ_{H} 25.4 and 39.8, assigned to the two $\text{Cp}^*\text{-CH}_3$ environments, and a broad singlet of integration 2H assigned to the ‘tucked-in’ -CH_2 proton environment is present at δ_{H} -70.1. Loss of the alkyl ligand as free alkane (CH_3Ph , CH_4 , SiMe_4 , or $\text{CH}_2(\text{TMS})_2$ for alkyls **2.3-2.6** respectively) is also observed by ^1H NMR spectroscopy in samples where volatiles have not been removed.



Scheme 2.6. Formation of a ‘tucked-in’ complex (**2.9**) from activation of a $\text{Cp}^*\text{-Me}$ group.



This behaviour has also been observed in numerous metallocene and non-metallocene ligand system uranium alkyl complexes.^{15,37–40} Most closely related is the example of related mixed-sandwich U(IV) complexes containing an unsubstituted COT ring, $\text{U}(\text{COT})\text{Cp}^*\text{R}$ (where $\text{R} = \text{CH}_3, \text{Et}, \text{Np}, \text{Ph}$), where the ‘tuck-in’ complex $\text{U}(\text{COT})(\eta^5:\kappa^1\text{-C}_5\text{Me}_4\text{CH}_2)$ is formed with concomitant release of free alkane.¹⁸

Evans *et al.* report that more than one organouranium species is observed by ^1H NMR spectroscopy when taking aliquots from reaction mixtures of LiR and $\{\text{U}(\text{COT})\text{Cp}^*(\mu\text{-OTf})\}_2$ (where $\text{R} = \text{Me}, \text{Et}, \text{Np}$). Further investigation deduced that in each reaction mixture an amount of desired alkyl was produced, along with a ‘tuck-in’ species, $\text{U}(\text{COT})(\eta^5\text{-}\kappa^1\text{-C}_5\text{Me}_4\text{CH}_2)$, and free alkane (methane, ethane, or neopentane respectively). The ‘tuck-in’ can also be made from heating $\text{U}(\text{COT})\text{Cp}^*(\text{Ph})$ to $100\text{ }^\circ\text{C}$ for 16 hours. In contrast, it was found that the related *bis*-TMS alkyl, $\text{U}(\text{COT})\text{Cp}^*(\text{CH}\{\text{TMS}\}_2)$, did not form the ‘tuck-in’ species even after heating to $110\text{ }^\circ\text{C}$ for 3 days. This is in contrast to **2.6**, which will ‘tuck-in’ when heated – albeit at a slower rate than the other reported alkyls – assumed to be an effect of the longer (and hence weaker and more reactive) $\text{U-C}_{\text{alkyl}}$ bond in **2.6** than in the unsubstituted COT-ring analogue.

2.6.1 Synthesis and characterisation of the ‘tuck-in’ complex (**2.9**)

The ‘tuck-in’ complex **2.9** can be synthesised from heating any of the alkyl complexes to $70\text{ }^\circ\text{C}$ for 24 hours (for **2.3-2.5**) or for three days (for **2.6**). This transformation can be tracked by ^1H NMR spectroscopy, and it is seen that some decomposition, indicated by diamagnetic resonances attributable to decomposed ligand, is also seen after heating.

Preparative-scale quantities of **2.9** can be isolated by heating a toluene solution of **2.3** (400 mg, 0.345 mmol) to $70\text{ }^\circ\text{C}$ for 24 hours, removing all volatiles under reduced pressure, extracting the solids with Et_2O or pentane, then filtering the resulting brown solution to remove insoluble decomposition material, affording **2.9** as a brown powder in a 70% yield. Whilst the material is contaminated with small amounts of ligand decomposition products, it is clean enough to use in subsequent reactions. Storage of saturated pentane or THF solutions of **2.9** at $-50\text{ }^\circ\text{C}$ yields a small number of brown crystals of the base-free or THF-solvated product suitable for X-ray diffraction studies. The structures of **2.9** and **2.9.THF** are shown in **Figure 2.11** and **Figure 2.12**, with

selected bond metrics in **Table 2.2**. The persistence of ligand degradation material in samples of **2.9** precluded meaningful elemental analysis. Mass spectrometric data showed the expected molecular ion at $m/z = 789$, and a single $^{29}\text{Si}\{^1\text{H}\}$ NMR spectroscopic resonance was observed at -67.0 ppm.

Table 2.2. Selected bond distances (Å) and angles (deg) for structures **2.9** and **2.9.THF**. Ct1 is defined as the COT-ring centroid, Ct2 is defined as the Cp-ring centroid.

	2.9	2.9.THF
U1-Ct1	1.9066(3)	1.9991(4)
U1-Ct2	2.3364(3)	2.4124(4)
U1-ring C(Cp) range	2.437(4)-2.791(4)	2.508(6)-2.840(6)
U1-C14/C33	2.569(4)	2.646(6)
U1-O1	n/a	2.585(4)
Ct1-U1-Ct2	150.724(15)	143.794(17)
U1-C14-C9/ U1-C33-C28	63.3(2)	68.6(3)

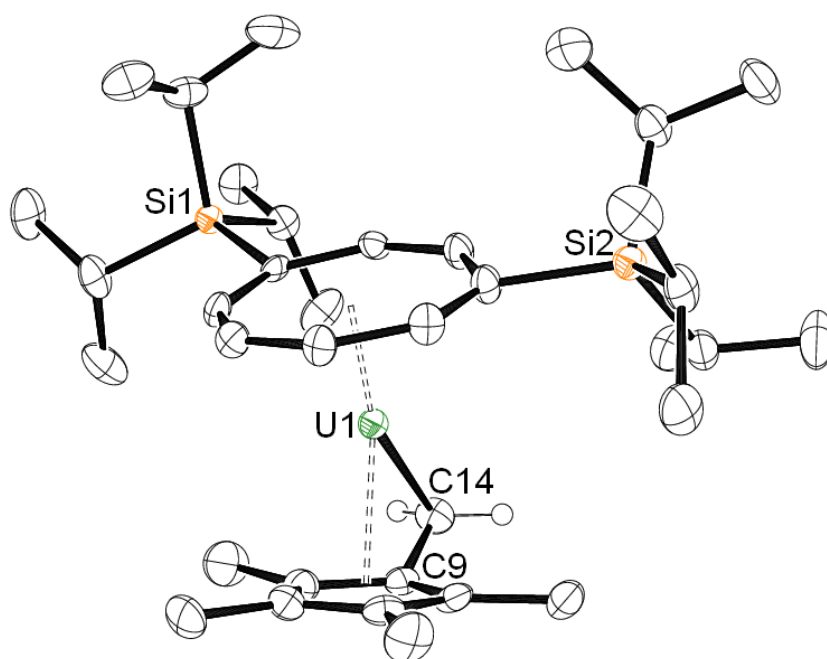


Figure 2.11. Molecular structure of $\text{U}(\text{COT}^{\text{TIPS}_2})(\eta^5:\kappa^1\text{-C}_5\text{Me}_4\text{CH}_2)$ (**2.9**). ORTEP representation with thermal ellipsoids at the 50% probability level.

Hydrogen atoms omitted for clarity.

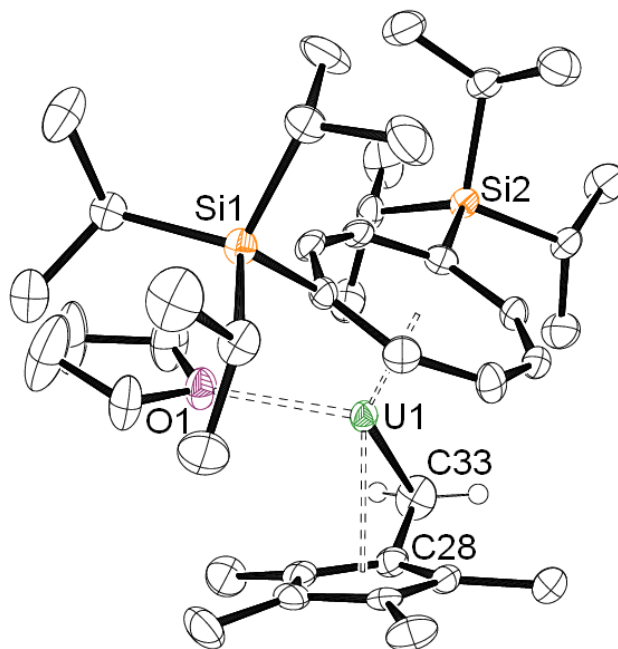


Figure 2.12. Molecular structure of $\text{U}(\text{COT}^{\text{TIPS}_2})(\eta^5:\kappa^1\text{-C}_5\text{Me}_4\text{CH}_2)(\text{THF})$ (**2.9.THF**).

ORTEP representation with thermal ellipsoids at the 50% probability level.

Hydrogen atoms omitted for clarity.

The coordination of THF to the metal centre in **2.9.THF** alters the overall geometry of the molecule in comparison to **2.9**: both uranium-centroid distances increase, as do each of the U1-ring C(Cp) bond lengths. The U1-C14/C33 bond lengthens by ca 0.1 Å, and the Ct1-U1-Ct2 angle decreases as the ‘metallocene wedge’ widens to allow THF binding. In **2.9**, the ‘tucked-in’ -CH₂ moiety lies symmetrically between the TIPS groups attached to the COT ring, whereas in **2.9.THF** the THF molecule occupies this position instead, with the ‘tucked-in’ -CH₂ positioned to one side. In comparison to U-centroid distances in other crystallographically characterised ‘U(COT^{TIPS}₂)Cp*’ complexes (see Appendix 1), the U1-Ct2 distances are the shortest reported: the range for other complexes is 2.449(9) – 2.497(3) Å, compared to the distances of 2.3364(3) and 2.4124(4) Å for **2.9** and **2.9.THF**, which is reasoned to be because of the more highly charged [C₅Me₄CH₂]²⁻ ligand versus [C₅Me₅]⁻, and due to distortion of the ring distances due to the ‘tucked-in’ methylene group. The U1-Ct1 distances for other ‘U(COT^{TIPS}₂)Cp*’ complexes range between 1.9121(13) – 1.9774(2) Å, and again the U1-Ct1 distances for **2.9** (1.9066(3) Å) and

2.9.THF (1.9991(4) Å) lie outside of these values. The COT ring in **2.9** is atypically close to the central metal atom – without the presence of a third separate ligand coordinated to U^{4+} , there is no steric or electronic repulsion forcing the COT ring further away. In contrast, the U1-Ct1 distance in **2.9.THF** is atypically large; this could be due to the central U^{4+} accommodating the dianionic $[C_5Me_4CH_2]^{2-}$ ligand as well as coordinating THF, hence crowding the metal centre and lengthening the average U-C_{COT} bonds; an unusually long U-Ct1 bond distance is also found in the sterically-crowded bis-TMS alkyl complex, **2.6** (1.9774(2) Å). The U1-C14 and U1-C33 bond distances (2.569(4) and 2.646(6) Å), corresponding to the ‘tucked-in’ methylene group, are longer than the ‘untethered’ alkyl bond distances found in complexes **2.3-2.6** (range: 2.462(4) – 2.543(3) Å) as is expected due to the steric constraints of the ‘tucked-in’ Cp* ring, which dictates the position of the tethered methylene group in each case.

Three crystallographically characterised examples of organouranium ‘tucked-in’ species containing a $[\eta^5:\kappa^1-C_5Me_4CH_2]^{2-}$ ligand exist in the literature, and are pictured in **Figure 2.13 (2C-2E)**, and contain U-C_{tuck} bond distances of 2.564(1), 2.567(3), 2.586(7) and 2.596(6) Å respectively – two values are reported for **2E** as two molecules are present in the asymmetric unit.^{8,18,38} These values are very close to the U1-C14 bond distance of 2.569(4) Å in **2.9**, but are shorter than the U1-C33 bond distance of 2.646(6) Å in **2.9.THF**. Closest in structure to **2.9.THF** is **2E**, which features the same $[C_5Me_4CH_2]^{2-}$ and THF ligands, but an unsubstituted COT ring. **2E** possesses slightly shorter U-O_{THF} bond lengths (2.585(4) Å in **2.9.THF** vs 2.519(4) and 2.514(5) Å in **2E**) and U-C_{tuck} bond lengths (2.646(6) Å in **2.9.THF** vs 2.586(7) and 2.596(6) Å in **2E**) due to the lack of bulky substituents on the COT ring allowing closer approach of the coordinated ligands.

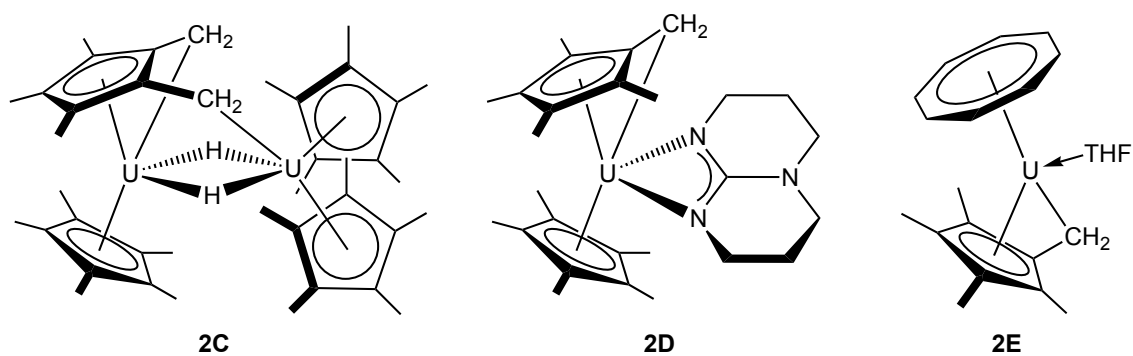


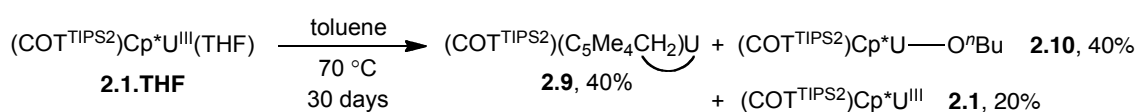
Figure 2.13. Crystallographically characterised organouranium ‘tucked-in’ complexes **2C-2E** containing $[\eta^5:\kappa^1\text{-C}_5\text{Me}_4\text{CH}_2]^{2-}$ ligands.

2.6.2 ‘Tuck-in’ formation from $\text{U}^{\text{III}}(\text{COT}^{\text{TIPS}_2})\text{Cp}^*(\text{THF})$ (**2.1.THF**)

Once **2.9** had been identified as a ‘tuck-in’ complex, its presence was also observed by ^1H NMR spectroscopy in a range of crude reaction mixtures involving uranium mixed-sandwich complexes, including in the mother liquor separated from crystals of the U(III) mixed-sandwich, **2.1.THF**, and from crystalline samples of **2.1.THF** left in solution over an extended period of time or stored as solids at ambient temperature. While not present in large amounts, it was still significant that **2.9** could be formed from a U(III) starting material where no U(IV) alkyl complex had been nominally present.

To probe the mechanism of this reaction, a crystalline sample of **2.1.THF** dissolved in C_7D_8 in a J Young NMR tube was heated to $70\text{ }^\circ\text{C}$ for a period of 30 days, and the reaction progress was tracked by ^1H NMR spectroscopy. It is known that heating the THF-solvated **2.1.THF** at $100\text{-}110\text{ }^\circ\text{C}$ whilst at a pressure of 10^{-6} mbar will form the base-free U(III) complex, $\text{U}(\text{COT}^{\text{TIPS}_2})\text{Cp}^*$ (**2.1**), reportedly without decomposition.⁴¹ After heating **2.1.THF** at $70\text{ }^\circ\text{C}$ for 16 hours, changes can be observed in the ^1H NMR spectrum: low-intensity resonances attributable to the ‘tuck-in’ complex **2.9** appear, resonances attributable to **2.1.THF** decrease in intensity and also shift slightly, and another set of low-intensity resonances appear at positions very similar to $\text{U}(\text{COT}^{\text{TIPS}_2})\text{Cp}^*(\text{OR})$ complexes. Continued heating for a further 32 hours

resulted in the continued shifting and lowering intensity of the **2.1.THF** resonances, and the increasing intensity of the resonances of **2.9** and the suspected alkoxide complex, along with the appearance of free THF. Integration of all signals thought to correspond to the unidentified alkoxide complex indicates that in addition to the $\text{COT}^{\text{TIPS}_2}$ and Cp^* ligand resonances, four additional singlets are present at δ_{H} 141.81, 55.88, 30.70 and 16.88, integrating to 2H, 2H, 2H and 3H respectively. These resonances could correspond to an *n*-butyl alkoxide chain, *i.e.* a U(IV) alkoxide complex, $\text{U}(\text{COT}^{\text{TIPS}_2})\text{Cp}^*(\text{O}^n\text{Bu})$ (**2.10**), *via* activation of THF – an outcome that has been previously observed in other systems (**Scheme 2.7**).⁴²



Scheme 2.7. Proposed activation of THF to form **2.9**, **2.10**, and **2.1**, with spectroscopically determined yields.

After heating the reaction mixture for a total of 20 days, the solution became red-brown in colour and was shown by ^1H NMR spectroscopy to contain a mixture of **2.9**, **2.10** and base-free **2.1** in a ratio of 2:2:1 respectively – this ratio remained constant after the mixture was heated for a further 10 days. Removal of volatiles under reduced pressure, extraction of the red-brown solids in t -BuOMe, and storage of the red solution at -30°C yielded a mixture of crystalline and microcrystalline solids. ^1H NMR spectroscopic analysis of the solids indicated that they were a mixture of the ‘tuck-in’ complex **2.9** and the alkoxide complex **2.10**. Collection of X-ray crystallographic data from the crystalline solids (brown plates of high enough quality to determine connectivity only) revealed the structure to be **2.9** with a molecule of t -BuOMe in the asymmetric unit. Further attempts to separate these two products by sequential crystallisation from other solvents was not possible, hence the structure of **2.10** has not been confirmed and elemental analysis has not been possible. However, the mass spectrum of the isolated solids shows the expected parent ion of **2.10** at 862 m/z (4%) and a fragment corresponding to the loss of the Cp^* ring at

727 m/z (11%, $\text{UCOT}^{\text{TIPS}2}\{\text{OBu}\}$). The $^{29}\text{Si}\{^1\text{H}\}$ NMR spectrum collected from this solid mixture contains two resonances at -67.14 and -135.9 ppm, attributed to **2.9** and **2.10** respectively.

Recently, X-ray diffraction data collected from crystals isolated from the related experiment of heating a 1,4-TMS substituted COT ring U(III) mixed-sandwich complex, $\text{U}(\text{COT}^{\text{TMS}2})\text{Cp}^*(\text{THF})$, revealed that one of the products is $\text{U}(\text{COT}^{\text{TMS}2})\text{Cp}^*(\text{O}^n\text{Bu})$, formed in tandem with a ‘tuck-in’ complex, $\text{U}(\text{COT}^{\text{TMS}2})(\eta^5:\kappa^1\text{-C}_5\text{Me}_4\text{CH}_2)$.⁴² Whilst the mechanism of this reaction is unclear, it is important as it has bearing on the supposed ‘inert’ qualities of the ligand framework, and the potential for low-valent uranium metal centres to activate solvents, reinforcing the importance of selecting correct solvents for any reactions undertaken.

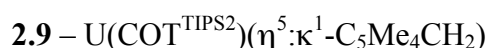
2.7 Conclusions and chapter summary

In summary, four new U(IV) mixed-sandwich alkyl complexes have been synthesised, along with four other U(IV) species as a result of related investigations. The common decomposition product of the alkyls, **2.9**, is formed *via* the activation of a Cp* ring methyl group, releasing free alkane and forming a ‘tucked-in’ species. Three alkoxide complexes have been observed, all reasoned to form from solvent activation, and reinforcing the importance of identifying the correct reaction conditions to successfully synthesise alkyls. Evidence for the activation of a TIPS group has also been seen, indicating the non-innocent behaviour of the $\text{COT}^{\text{TIPS}2}$ ligand system in some cases. The four alkyls should be reactive towards small molecules, such as CO, CO₂ and H₂, providing a starting point for further experiments.

Despite the unexpected nature of its discovery, the ‘tuck-in’ complex **2.9** is still technically an alkyl complex, albeit a ‘tethered’ one, possessing a U-C σ -bonding interaction in addition to the delocalised π -bonding between the metal centre and the other ring-carbon atoms. This means that it too can be probed to determine its reactivity

along with the other ‘non-tethered’ alkyl complexes, and the results can be compared and contrasted. Its presence in almost all alkyl samples presents a challenge in purifying the targeted compounds and ensuring that their observed reactivity with small molecules (as described in later chapters) is due solely to the intended starting alkyl, and not due to interference from **2.9**. However, studying the reactivity between **2.9** and small molecules helps to elucidate what occurs as a result of the behaviour of **2.9**, and what forms as a direct consequence of the behaviour of the intended alkyl.

2.8 Compound naming for Chapter 2



2.9 References for Chapter 2

1. P. J. Fagan, J. M. Manriquez, E. A. Maatta, A. M. Seyam, and T. J. Marks, *J. Am. Chem. Soc.*, 1981, **103**, 6650–6667.
2. M. Weydert, J. G. Brennan, R. A. Andersen, and R. A. Bergman, *Organometallics*, 1995, **14**, 3942–3951.
3. R. C. Schnabel, B. L. Scott, W. H. Smith, and C. J. Burns, *J. Organomet. Chem.*, 1999, **591**, 14–23.
4. J. L. Kiplinger, D. E. Morris, B. L. Scott, and C. J. Burns, *Organometallics*, 2002, **21**, 5978–5982.
5. W. J. Evans, S. A. Kozimor, and J. W. Ziller, *Organometallics*, 2005, **24**, 3407–3412.
6. C. R. Graves, E. J. Schelter, T. Cantat, B. L. Scott, and J. L. Kiplinger, *Organometallics*, 2008, **27**, 5371–5378.
7. W. J. Evans, M. K. Takase, J. W. Ziller, and A. L. Rheingold, *Organometallics*, 2009, **28**, 5802–5808.
8. E. Montalvo, J. W. Ziller, A. G. Dipasquale, A. L. Rheingold, and W. J. Evans, *Organometallics*, 2010, **29**, 2104–2110.
9. R. A. Andersen, E. Carmona-Guzman, K. Mertis, E. Sigurdon, and G. Wilkinson, *J. Organomet. Chem.*, 1975, **99**, C19–C20.
10. S. J. Simpson, H. W. Turner, and R. A. Andersen, *Inorg. Chem.*, 1981, **20**, 2991–2995.
11. W. G. Van Der Sluys, C. J. Burns, and A. P. Sattelberger, *Organometallics*, 1989, **8**, 855–857.
12. Â. Domingos, N. Marques, A. Pires de Matos, I. C. Santos, and M. Silva, *Organometallics*, 1994, **13**, 654–662.
13. M. J. Monreal and P. L. Diaconescu, *Organometallics*, 2008, **27**, 1702–1706.
14. S. Fortier, B. C. Melot, G. Wu, and T. W. Hayton, *J. Am. Chem. Soc.*, 2009, **131**, 15512–15521.
15. C. E. Hayes and D. B. Leznoff, *Organometallics*, 2010, **29**, 767–774.
16. S. Duhović, S. I. Khan, and P. L. Diaconescu, *Chem. Commun.*, 2010, **46**, 3390–3392.
17. N. R. Andreychuk, S. Ilango, B. Vidjayacoumar, D. J. H. Emslie, and H. A. Jenkins, *Organometallics*, 2013, **32**, 1466–1474.
18. M. K. Takase, N. A. Siladke, J. W. Ziller, and W. J. Evans, *Organometallics*, 2011, **30**, 458–465.
19. T. J. Marks, *Organometallics of the f-elements*, D. Reidel Publishing Company, Sogesta, Italy, 1st edn., 1978, vol. 187.
20. J. A. Higgins, MChem Dissertation, University of Sussex, 2010.
21. O. T. Summerscales, F. G. N. Cloke, P. B. Hitchcock, J. C. Green, and N. Hazari, *Science*, 2006, **311**, 829–831.
22. R. G. Finke, Y. Hirose, and G. Gaughan, *J. Chem. Soc. Chem. Commun.*, 1981, 232–234.
23. J. A. Higgins, F. G. N. Cloke, and S. M. Roe, *Organometallics*, 2013, **32**, 5244–5252.
24. *Cambridge Crystal Database Service. Access date March 2014.*, .
25. W. J. Evans, S. A. Kozimor, and J. W. Ziller, *Polyhedron*, 2006, **25**, 484–492.
26. K. C. Jantunen, C. J. Burns, I. Castro-Rodriguez, R. E. Da Re, J. T. Golden, D. E. Morris, B. L. Scott, F. L. Taw, and J. L. Kiplinger, *Organometallics*, 2004, **23**, 4682–4692.

27. E. M. Broderick, N. P. Gutzwiller, and P. L. Diaconescu, *Organometallics*, 2010, **29**, 3242–3251.
28. M. J. Monreal and P. L. Diaconescu, *J. Am. Chem. Soc.*, 2010, **132**, 7676–7683.
29. J. M. Manriquez, P. J. Fagan, T. J. Marks, S. H. Vollmer, C. S. Day, and V. W. Day, *J. Am. Chem. Soc.*, 1979, **101**, 5075–5078.
30. P. B. Hitchcock, M. F. Lappert, A. Singh, R. G. Taylor, and D. Brown, *J. Chem. Soc., Chem. Commun.*, 1983, 561–563.
31. W. J. Evans, J. R. Walensky, and J. W. Ziller, *Organometallics*, 2010, **29**, 101–107.
32. K. C. Jantunen, F. Haftbaradaran, M. J. Katz, R. J. Batchelor, G. Schatte, and D. B. Leznoff, *Dalton Trans.*, 2005, 3083–3091.
33. A. S. P. Frey, F. G. N. Cloke, M. P. Coles, and P. B. Hitchcock, *Chem.--Eur. J.*, 2010, **16**, 9446–9448.
34. M. P. C. Campello, Â. Domingos, and I. C. Santos, *J. Organomet. Chem.*, 1994, **484**, 37–46.
35. A. S. P. Frey, F. G. N. Cloke, M. P. Coles, L. Maron, and T. Davin, *Angew. Chem.*, 2011, **123**, 7013–7015.
36. T. M. Gilbert, R. R. Ryan, and A. P. Sattelberger, *Organometallics*, 1989, **8**, 857–859.
37. S. J. Simpson and R. A. Andersen, *J. Am. Chem. Soc.*, 1981, **103**, 4063–4066.
38. W. J. Evans, K. A. Miller, A. G. DiPasquale, A. L. Rheingold, T. J. Stewart, and R. Bau, *Angew. Chem. Int. Ed.*, 2008, **47**, 5075–5078.
39. N. A. Siladke, J. LeDuc, J. W. Ziller, and W. J. Evans, *Chem.--Eur. J.*, 2012, **18**, 14820–14827.
40. B. M. Gardner, J. McMaster, W. Lewis, A. J. Blake, and S. T. Liddle, *J. Am. Chem. Soc.*, 2009, **131**, 10388–10389.
41. O. T. Summerscales and F. G. N. Cloke, *Organometallic and Coordination Chemistry of the Actinides*, Springer Berlin Heidelberg, Berlin, Heidelberg, 2008, vol. 127.
42. N. Tsoureas, *Unpublished results*, 2013.

CHAPTER 3: REACTIVITY OF MIXED-SANDWICH U(IV) ALKYLs AND RELATED COMPLEXES WITH SMALL MOLECULES

3.1 Introduction

The reactivity of U(IV) alkyl complexes towards small molecules such as H₂, CO, and CO₂ is well known, as described in detail in Chapter 1. With four alkyls synthesised within a mixed-sandwich metallocene framework (**2.3-2.6**), their behaviour with small molecules was examined. Exposure of the alkyls to H₂ resulted in the formation of a hydride complex, U(COT^{TIPS₂})Cp*H (**3.1**) *via* σ -bond metathesis. Insertion reactions with CO or CO₂ formed acyl or carboxylate complexes respectively. Further to this, the reactivity of the ‘tethered’ alkyl, U(COT^{TIPS₂})(η^5 : κ^1 -C₅Me₄CH₂) (**2.9**) was also examined, and was found to undergo insertion reactions with CO and CO₂ to form ‘tethered’ products; exposure of **2.9** to H₂ also resulted in the formation of **3.1**. The reactivity of the hydride **3.1** towards CO and CO₂ was also examined, forming formate and enediolate products, respectively. An overview of the reactivity of complexes **2.3-2.6** is presented overleaf in **Scheme 3.1**. Detailed analysis of their reactivity along with the behaviour of some resulting insertion products with CO₂ is discussed in this chapter, *vide infra*.

Two general procedures were used for the addition of stoichiometric or excess gas to solutions. A Toepler pump equipped with a gas-addition line and attached to a high-vacuum pump was utilised in addition to a mercury manometer to accurately measure out gas volumes. This method was used for adding known quantities of gas, either stoichiometric or accurate excesses, and for adding ¹³C-labelled gas. For the addition of a larger quantity of gas (*i.e.* 1 bar or above), a high-purity H₂, CO, or CO₂ cylinder was employed in tandem with a Schlenk line and either a J Young NMR tube or an ampoule.

3.2 Reactivity of alkyls with H₂: σ -bond metathesis

3.2.1 Organouranium hydride complexes

A small number of organouranium hydride complexes have been synthesised with both metallocene and non-metallocene ligand frameworks. Eleven examples of crystallographically characterised organouranium hydrides have been reported to date, and amongst these only two are neutral, terminal U(IV) hydrides: U(N^{''})₃H and U(C₅H₄[']Bu)₃H.^{1,2} A series of U(IV) hydrides supported by bis-Cp* alkoxy ligand frameworks, UCp*₂(OR)H (OR = OSiMe₂[']Bu, OCH[']Bu₂, O[']Bu, (1*R*,2*S*,5*R*)-menthoxide, (*R*)-2-butoxide, (1*S*)-endo-bornoxide, (1*S*,2*S*,5*R*)-neomenthoxide), have been assigned as either monomeric or terminal by virtue of IR spectroscopic data and cryoscopic weight measurements; terminal U-H vibrations are typically in the region of 1300-1500 cm⁻¹, whilst bridging U-H vibrations occur at < 1200 cm⁻¹.³⁻⁵ Arguably the most thoroughly investigated hydride is the dimeric compound {UCp*₂H(μ -H)}₂, featuring both terminal and bridging hydride ligands. First reported in 1979 by Marks *et al.*, its full structural characterisation (using both X-ray and neutron diffraction methods) and synthetic use as a formal four-electron reductant (after the reductive loss of dihydrogen to form trivalent {UCp*(μ -H)}₂) have been subsequently detailed by Evans and coworkers.^{5,6} No insertion chemistry with CO or CO₂ has been reported for this equilibrium-related pair.

Only one mixed-sandwich actinide hydride complex containing both 5- and 8-membered rings has been reported in the literature. Gilbert *et al.* report the reaction of Th(COT)Cp*(CH{TMS}₂) with H₂, giving what they deduce to be an oligomeric hydride complex, [Th(COT)Cp*H]_x, along with CH₂(TMS)₂.⁷ IR spectroscopic data collected from the hydride and from the corresponding deuteride, [Th(COT)Cp*D]_x, reveal the presence of a broad band at 1147 cm⁻¹ (ν_{U-D} = 843 cm⁻¹), indicating a bridging – rather than terminal – hydride ligand. No hydride resonance was located in

the ^1H NMR spectrum, postulated to be due to exchange of the hydride with deuterium in the deuterated solvent, or to an exchange between monomeric and polymeric forms in solution. Crystalline material could not be isolated from reaction mixtures for structural characterisation due to poor solubility.

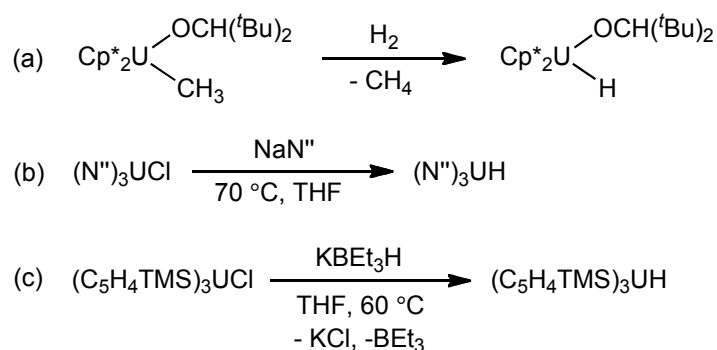
In comparison to the unsubstituted COT ligand used in the synthesis of $[\text{Th}(\text{COT})\text{Cp}^*\text{H}]_x$, the silyl groups on the bulky $\text{COT}^{\text{TIPS}2}$ ligand used as part of the mixed-sandwich system in this work may provide better solubility and crystallinity to a hydride complex of the form $[\text{U}(\text{COT}^{\text{TIPS}2})\text{Cp}^*\text{H}]_x$ (where $x \geq 1$). It was thought that the added stabilising effects of the steric bulk and electronic effects imparted by the silyl groups may also sufficiently stabilise a monomeric, terminal hydride complex, $\text{U}(\text{COT}^{\text{TIPS}2})\text{Cp}^*\text{H}$, and allow for the study of insertion chemistry at a single, terminal, U-H bond. With the exception of one study, the reactivity of CO and CO_2 with such U-H bonds has not been reported in the literature; either the hydrides are too unstable for further experiments to be performed, or they exist as bis-hydrides, or as hydride-bridged dimers. The synthesis of $\text{U}(\text{COT}^{\text{TIPS}2})\text{Cp}^*\text{H}$ described in this section has allowed these studies to be carried out for the first time.

Data utilised for the characterisation of organouranium hydrides in the literature are ^1H NMR spectroscopy, IR spectroscopy, isotopic substitution of a hydride ligand for a deuteride, and X-ray diffraction. A summary of the available spectroscopic data for reported hydrides are presented in **Table 3.1**. The ^1H NMR spectroscopic resonances corresponding to the hydride ligands are extremely shifted, occurring between 265.9 and 333.4 ppm for neutral U(IV) hydrides. Collection of IR spectroscopic data for both 'U-H' and 'U-D' species should show a significant isotopic shift, however, many hydride species are reported to undergo scrambling of deuterium with protons on all ligands. This means that the values reported for 'U-D' complexes below do not necessarily represent effects occurring from the single substitution of 'U-H' for 'U-D', and must be considered with caution.

Table 3.1. Collated data from organouranium hydride complexes, sorted chronologically by year first reported (1979-2014). ^1H NMR chemical shifts of H ligand in ppm (n/a = not located), IR vibrations in cm^{-1} where available (number in brackets represents $\nu_{\text{U-D}}$), X-ray data (XRD) denoted Y if reported, N if not obtained.

Compound	^1H data (ppm)	IR data (cm^{-1})	XRD	Ref.
$\{\text{UCp}^*_2\text{H}(\mu\text{-H})\}_2$	316.8	1335, 1180	Y	6,8
$\text{U}(\text{N}^{\prime\prime})_3\text{H}$	n/a	1430 (1020)	Y	9
$\text{UCp}^*_2(\text{dmpe})\text{H}$	n/a	1219 (870)	Y	10
$\text{UCp}^*_2(\text{OSiMe}_2^t\text{Bu})\text{H}$	n/a	1395 (988)	N	11
$\text{UCp}^*_2(\text{OCH}^t\text{Bu}_2)\text{H}$	276.7		N	12
$\text{UCp}^*_2(\text{O}^t\text{Bu})\text{H}$	267.1	1363	N	12
$(\text{DME})\text{U}(\text{BH}_4)_3\text{H}$	n/a	1195, 1170	Y	13
$[\text{Na}(\text{THF})_2][(\text{Cp}_3\text{U})_2(\mu\text{-H})]$	293.1		Y	14
$\text{Cp}^*_2\text{U}(\{\text{1R,2S,5R}\}\text{-menthoxide})\text{H}$	267.9	1420, 1292	N	3
$\text{Cp}^*_2\text{U}(\{\text{R}\}\text{-2-butoxide})\text{H}$	265.9	1339	N	3
$\text{Cp}^*_2\text{U}[\{(\text{1S-endo})\}\text{-bornoxide}]\text{H}$	269.6	1363	N	3
$\text{Cp}^*_2\text{U}(\{\text{1S,2S,5R}\}\text{-neomenthoxide})\text{H}$	269.2	1370	N	3
$\text{Cp}'_3\text{UH}$	290.5	1395 (1015)	N	15
$(\text{C}_5\text{H}_4^t\text{Bu})_3\text{UH}$	276.1	1410	Y	16
$[\text{Na}(\text{18C6})][\text{Cp}'_3\text{UH}]$	547.1	1405 (1020)	Y	17
$[\text{Na}(\text{18C6})][(\text{C}_5\text{H}_4^t\text{Bu})_3\text{UH}]$	521.3		N	17
$[\text{Na}(\text{THF})_2][\{(\text{C}_5\text{H}_4\text{Me})_3\text{U}\}_2(\mu\text{-H})]$	302.2		N	17
$[\text{Na}(\text{18C6})][(\text{Cp}_3\text{U})_2(\mu\text{-H})]$	293.1		Y	17
$[\text{Na}(\text{18C6})][(\text{Cp}'_3\text{U})_2(\mu\text{-H})]$	319.2		Y	17
$(\text{C}_5\text{Me}_4\text{P})_3\text{UH}$	333.4		N	18
$(\text{C}_5\text{H}_4\text{PPh}_2)_3\text{UH}$	305		N	18,19
$\{\text{UCp}^*(\mu\text{-H})\}_2$	n/a	1163	Y	5,8,20
$\{\text{Cp}^*\text{U}(\mu\text{-}\eta^5\text{:}\eta^1\text{:}\eta^1\text{-C}_5\text{Me}_3(\text{CH}_2)_2)\text{UCp}^*_2(\mu\text{-H})_2$	n/a	1164	Y	21
$\text{Cp}^*_2\text{U}(\text{hpp})\text{H}$	n/a	1380	N	22
$[\text{K}(\text{2.2.2-cryptand})][\text{Cp}'_3\text{UH}]$	560	1362	Y	23

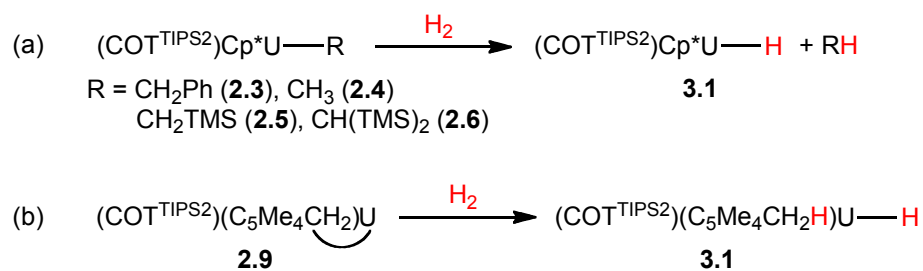
Several synthetic routes have been utilised to form terminal U(IV) hydrides, including: (a) hydrogenolysis of alkyl derivatives, (b), proton abstraction from solvent, or (c) reaction with MH (M = Na, K) or MBEt₂H (M = Li, K) (c); examples of these reactions from the literature are shown in **Equation 3.1(a-c)**. Route (a) is used in the synthesis of the mixed-sandwich hydride, U(COT^{TIPS2})Cp*H.



Equation 3.1. Synthetic routes to hydride complexes.^{1,3,15}

3.2.2 Synthesis and stability of U(COT^{TIPS2})Cp*H (**3.1**)

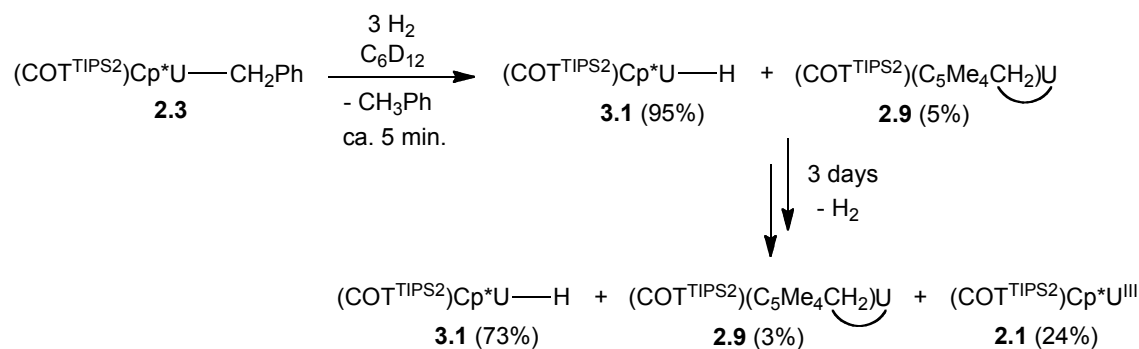
The complexes **2.3-2.6** are precursors for hydrogenolysis reactions: each reacts with H₂ to form a monomeric, terminal hydride complex, U(COT^{TIPS2})Cp*H (**3.1**), via σ -bond metathesis and concomitant release of free alkane (**Equation 3.2a**). The ‘tethered’ alkyl **2.9** also reacts with H₂ to form **3.1**, re-forming a free-rotating Cp*-ring (**Equation 3.2b**); Marks *et al.* have previously reported the same type of interconversion between hydride and ‘tucked-in’ complexes.^{21,22} Characterisation data for **3.1** are presented in section 3.2.3.



Equation 3.2. Synthesis of U(COT^{TIPS2})Cp*H (**3.1**) from **2.3-2.6** (a) or from **2.9** (b).

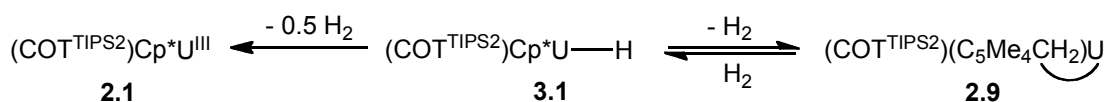
The reactions of **2.3-2.6** with 3 equivalents of H₂ resulted in the complete consumption of the starting material after 12 hours in the cases of **2.3-2.5**, while reaction progress is slower for hydrogenolysis of **2.6**, taking several days. This is reasoned to be due to the steric bulk of the -CH(TMS)₂ ligand that hinders access to the metal centre, as later noted from the lack of reactivity of **2.6** with CO₂, and slow reaction with CO (see section 3.1.6). Examination of ¹H NMR spectra obtained from the reactions of the alkyls and H₂ performed *in situ* in J Young NMR tubes and collected at regular intervals before and after gas addition indicate that the hydrogenolysis reactions are not straightforward due to the inherent instability of **3.1** and its existence in equilibrium with other complexes. Studies to identify what else occurs alongside hydrogenation were carried out using predominantly alkyl **2.3** due to its facile synthesis and isolation in crystalline form.

Hydrogenolysis of **2.3** was performed in C₆D₁₂ (to allow for clear identification of free toluene) in a J Young NMR tube, with 3 equivalents of H₂ added whilst the solution was frozen. Upon thawing, a rapid colour change from dark red-brown to cherry red was observed, indicating the formation of **3.1**. ¹H NMR spectroscopic analysis performed 5 minutes after the solution had thawed showed the presence of **3.1**, free toluene, and a small quantity of **2.9**. Over a period of three days the solution colour became brown, and collection of ¹H NMR spectra at regular intervals during this time indicated that the trivalent mixed-sandwich species, U^{III}(COT^{TIPS2})Cp* (**2.1**) was formed in solution, and the proportion of **3.1** and **2.9** changed, as summarised in **Scheme 3.2** – proportions are reported as percentages relative to ligand integral values. Repetition of the reaction in other solvents (C₇D₈, C₆D₆) afforded the same result.



Scheme 3.2. Results of hydrogenolysis reaction of **2.3** monitored over 3 days.

Further investigations revealed that subjecting a reaction mixture of **3.1** to reduced pressure to remove excess H₂ results in an increase in the proportion of **2.1** and **2.9** relative to **3.1**. Removal of all volatiles from the reaction mixture and thorough drying of the residue results in the complete transformation of **3.1** into a mixture of **2.1** and **2.9**. It is proposed that **3.1** is in equilibrium with **2.9**, and that **3.1** will also lose H₂ irreversibly to form the trivalent species **2.1** when not under a hydrogen headspace (**Scheme 3.3**), in a fashion similar to that reported to {UCp*₂H(μ-H)}₂, which also readily loses H₂ to form the corresponding U(III) hydride, {UCp*₂(μ-H)}₂.²⁰



Scheme 3.3. Proposed equilibrium of **3.1** and **2.9**, and decomposition of **3.1** to **2.1**.

Whilst **3.1** does form from the reaction of an alkyl with stoichiometric H₂, a hydrogen headspace is required to maintain the presence of **3.1**. Experiments conducted by other researchers in the group exploring the chemistry of **2.1** have shown that it does not react with H₂, even under high pressures.^{24,25} This instability with respect to hydrogen loss has complicated the characterisation of **3.1**, and has prevented any meaningful kinetic studies on its equilibrium with **2.9**. However, as the following sections describe, it persists long enough in solution for some characterisation data to be collected, and to study its reactivity with CO and CO₂.

3.2.3 Characterisation of $\text{U}(\text{COT}^{\text{TIPS}_2})\text{Cp}^*\text{H}$

Due to the propensity of **3.1** to decompose into the tuck-in complex **2.9**, and the trivalent mixed-sandwich complex, **2.1**, upon exposure to reduced pressure, isolation of a solid sample of **3.1** for characterisation using standard methods (mass spectrometry, elemental analysis, infrared spectroscopy) has not been possible. Attempts to collect mass spectrometric data and IR spectroscopic data (using NaCl plates for the latter) have returned results consistent with a mixture of **2.1** and **2.9**. ReactIR apparatus has been used to collect *in-situ* IR spectroscopic data over the course of the reaction of **2.3** and excess H_2 , however no new vibrational band corresponding to a hydride ligand (expected to occur at ca 1400 cm^{-1} , see **Table 3.1**) was observed due to strong ligand resonances masking the area of interest. No hydride resonance could be located in the ^1H NMR spectrum across a ± 600 ppm window, as is the case for several other hydrides reported.^{5,8-11,13,20-22} Attempts to crystallise **3.1** from pentane or THF solutions using standard methods (slow-cooled in Schlenk tubes or in glass vials under an Ar headspace) only yielded black crystals of **2.1** or **2.1.THF**.

Despite the tendency of **3.1** to lose H_2 when not under a hydrogen headspace, it was possible to collect X-ray diffraction data from two separate samples of **3.1**: one sample was collected *via* the reaction of **2.3** and 1 bar of H_2 in a minimum amount of pentane (ca 0.5 cm^3), and the second was from the reaction of a solid sample of **2.3** and 1 bar of H_2 . Both reaction mixtures were sealed in gas-tight ampoules in order to maintain a H_2 headspace. In both cases, a small number of red crystals were formed on the vessel walls; rapid extraction of the crystals and subsequent mounting onto a glass fibre under a cryostream allowed for collection of X-ray diffraction data from both samples. Refinement of the data collected provided two structures, both monoclinic, with one in the $P2_1/m$ space group (**3.1A**, **Figure 3.1**) and the other in the space group Cc (**3.1B**, **Figure 3.2**) with two crystallographically distinct molecules in the asymmetric unit; **Table 3.2** details selected bond lengths and angles from the two structures, along with metrics from structurally comparable $\text{U}(\text{COT}^{\text{TIPS}_2})\text{Cp}^*$ (**2.1**).

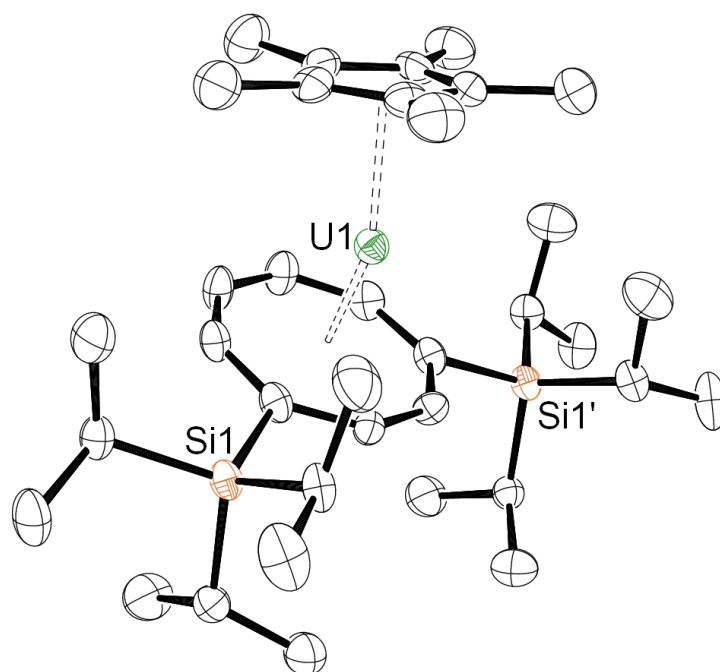


Figure 3.1. Molecular structure of **3.1A**.

ORTEP representation with thermal ellipsoids at the 50% probability level.

Hydrogen atoms omitted for clarity.

'Grown' structure – half of the molecule is present in the asymmetric unit.

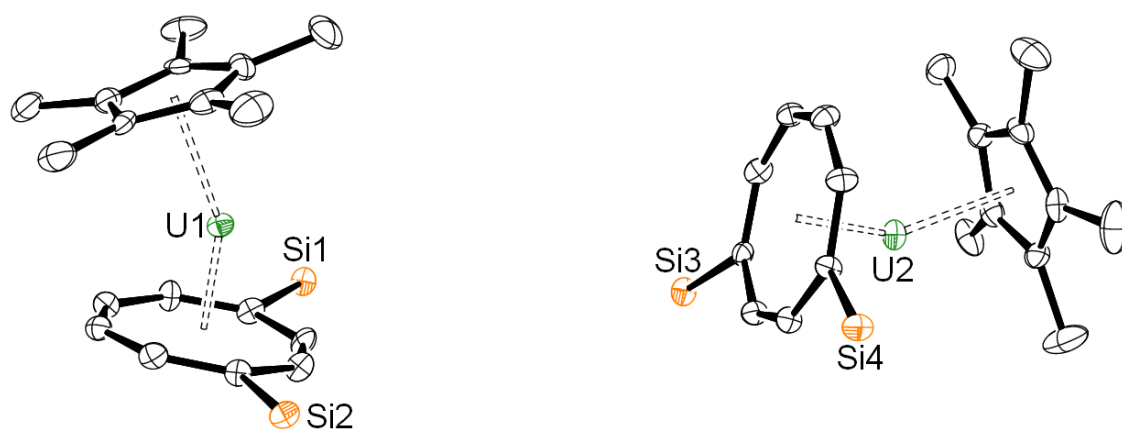


Figure 3.2. Molecular structure of **3.1B**, showing both crystallographically independent molecules in the asymmetric unit. ORTEP representation with thermal ellipsoids at the 50% probability level. Hydrogen atoms and *i*Pr groups omitted for clarity. U1-U2 = 11.167 Å.

Table 3.2. Crystallographic data and selected bond distances (Å) and angles (°) for **3.1A**, **3.1B**, and **2.1**. Ct1 is defined as the COT ring centroid, Ct2 is defined as the Cp* ring centroid.

	3.1A	3.1B	2.1
Space group	<i>P2₁/m</i>	<i>Cc</i>	<i>Cc</i>
Cell lengths	a = 8.4860(2) b = 22.6545(5) c = 9.7819(3)	a = 13.5888(4) b = 36.4517(11) c = 15.9896(4)	a = 13.578(3) b = 36.381(7) c = 16.028(3)
Cell angles	$\alpha = 90$ $\beta = 100.6330(10)$ $\gamma = 90$	$\alpha = 90$ $\beta = 110.568(2)$ $\gamma = 90$	$\alpha = 90$ $\beta = 110.52(3)$ $\gamma = 90$
Cell volume	1848.24	7415.34	7415.16
Z	2	8	4
U1-U2	n/a	11.166 Å	19.713 Å
Ct1-U	1.9182(6) Å	1.917(4), 1.917(2) Å	1.916(4), 1.924(5) Å
Ct2-U	2.4945(6) Å	2.471(4), 2.464(3) Å	2.461(6), 2.471(5) Å
Ct1-U-Ct2	150.20(3) °	152.14(10), 152.4(2) °	154.9(2), 153.1(2) °

In **3.1B**, one of the crystallographically independent molecules contains a Q-peak that persisted during the refinement process, at a distance of 1.04(2) Å from the uranium centre U2 that *could* be assigned as a hydrogen atom (and therefore a hydride ligand), however without corresponding neutron diffraction data this cannot be confirmed.⁶ The structure of **3.1B** negates the possibility that **3.1** is a bridging hydride complex: the U1-U2 distance is too great, and the orientation of each monomer towards others in the crystal lattice is too conformationally unfavourable to indicate the presence of bridging hydride ligand. The crystal packing of **3.1A** also shows that there is no close U-U bond in the lattice that could be bridged by a hydride ligand. These two structures can also be compared to **2.1** – selected crystal data and bond distances and angles (including the distances between U1 and U2 in the asymmetric units of **3.1B** and **2.1**) are also given in **Table 3.2**.²⁵

Comparison of the bond lengths and angles from **3.1A** and **3.1B** reveals that the two structures differ marginally; while the U-Ct1 and U-Ct2 distances are marginally longer in **3.1A**, the Ct1-U-Ct2 angle is 2 ° smaller. Both structures contain U-Ct1 and U-Ct2 distances closely comparable to other U(IV) mixed-sandwich complexes in this work (see Appendix 1); these metrics are consistent with **3.1** being a U(IV) complex, rather than the base-free U(III) complex, U(COT^{TIPS2})Cp* (**2.1**). The Ct1-U-Ct2 angles in both **3.1A** and **3.1B** are more obtuse than other crystallographically characterised ‘U(COT^{TIPS2})Cp*’ complexes, presumably due to the marginal steric bulk of the hydride ligand in comparison to the larger additional ligands – in particular the carboxylates – which force a greater Ct1-U-Ct2 angle. In comparison to the desolvated tuck-in structure of **2.9**, the Ct1-U-Ct2 angle of **3.1A** is almost identical: 150.724(15) ° vs 150.20(3) °.

It can be argued that the unit cell and space group of trivalent **2.1** and tetravalent **3.1** are likely to be very similar – in theory, the only differences between the two structures should be a slightly smaller ionic radius of the central uranium atom (U(IV) being smaller than U(III))²⁶ and the minor structural perturbation of a single hydride ligand occupying space in the open coordination sphere defined by the ‘sandwiching’ COT^{TIPS2} and Cp* rings (and subsequent minor electronic effects). The cell parameters of the structures **3.1B** and **2.1** are only marginally different: the cell volumes are essentially identical, and the cell lengths and angles are only slightly different outside of standard error. The metrical parameters of **2.1** and **3.1B** are most alike: the Ct-U distances are almost identical, however, there is a difference in the Ct1-U-Ct2 angles of around 2 °, and the U1-U2 distances are considerably diverse. Overall, neither **3.1A** nor **3.1B** are similar enough to the structure of **2.1** to conclude that the ‘hydride’ structures are in fact trivalent species formed from the loss of dihydrogen. Whilst the X-ray crystallographic data does not conclusively indicate that **3.1** is a monomeric hydride complex, it does support this theory.

partial decomposition of **3.1-d** to **2.1-d** during this time. These data show that exchange also occurs with the U-D bond and the methyl groups on the COT^{TIPS} ligands; no evidence for a ‘TIPS tuck-in’ species has been observed in ^1H NMR spectra, except in the case of the ‘ate’ complex, **2.8** (see Chapter 2, section 2.5.2), where activation of the TIPS group is irreversible due to the U-Cl bond. Unlike the activation of a $\text{Cp}^*\text{-CH}_3$ group to give complex **2.9**, this TIPS- CH_3 group activation and subsequent reaction with H_2 (or D_2 , or HD) may be too rapid to observe on an NMR timescale.

This scrambling is also seen when following the reaction of **2.3** with D_2 in C_6D_6 , and analysing the ^1H NMR spectra collected during the reaction progress. Ten minutes after D_2 addition, the resonances correlating to proton environments of **3.1-d** and **2.9-d** all became broadened, and their multiplicity was not well defined. This effect is due to partial deuteration of the molecules, altering the environment around the uranium centres, which marginally changes the chemical shift of each ligand resonance. As complexes with differing degrees of deuteration are all present at once, the ligand resonances overlap and appear as broad signals. This effect becomes more pronounced as scrambling continues over a period of several days, along with the gradual reduction in intensity of resonances correlating to ligands that become perdeuterated.

To identify the location of deuterium atoms on the ligands of the mixture of species present in solution in the reaction described above, all volatiles were removed from the reaction mixture, and the solid residue was dissolved in C_6H_6 in order to collect ^2H NMR spectroscopic data. This perturbation of the vessel headspace will alter the relative proportion of the three species (**3.1-d**, **2.9-d** and **2.1-d**) as described previously, however, it was anticipated that some **3.1-d** would still remain intact as the sample was not subjected to sustained high vacuum during solvent removal, and the experiment would still provide information as to the location of deuterium. Resonances observed in the ^2H NMR spectrum correlated to: $\text{Cp}^*\text{-C(H/D)}_3$ and $^i\text{Pr-C(H/D)}_3$ ligands of **3.1-d** and **2.1-d**, and the $\text{Cp}^*\text{-C(H/D)}_3$, $\text{Cp}^*\text{-C(H/D)}_2$, and $^i\text{Pr-C(H/D)}_3$ ligands of **2.9-d** (Figure 3.3; coloured groups indicate partial/full deuteration).

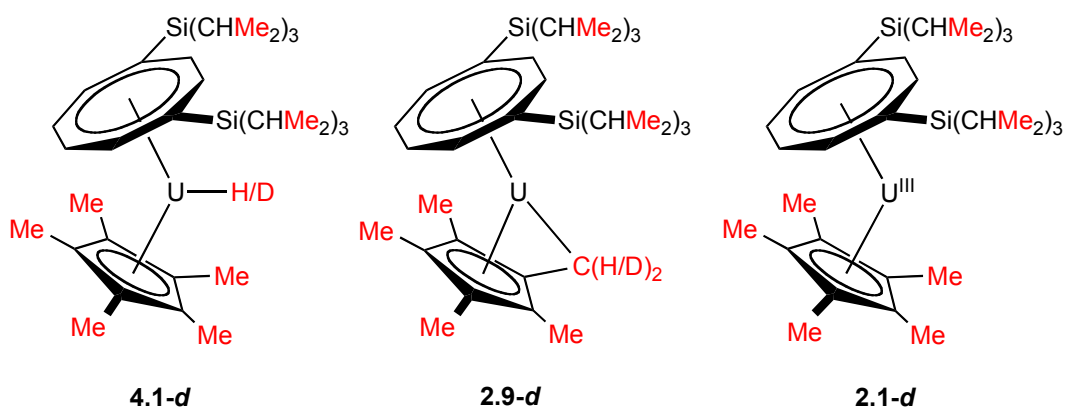


Figure 3.3. Position of deuterium incorporation onto species present in the reaction mixture of **2.3** and D_2 after headspace removal, after 5 days.

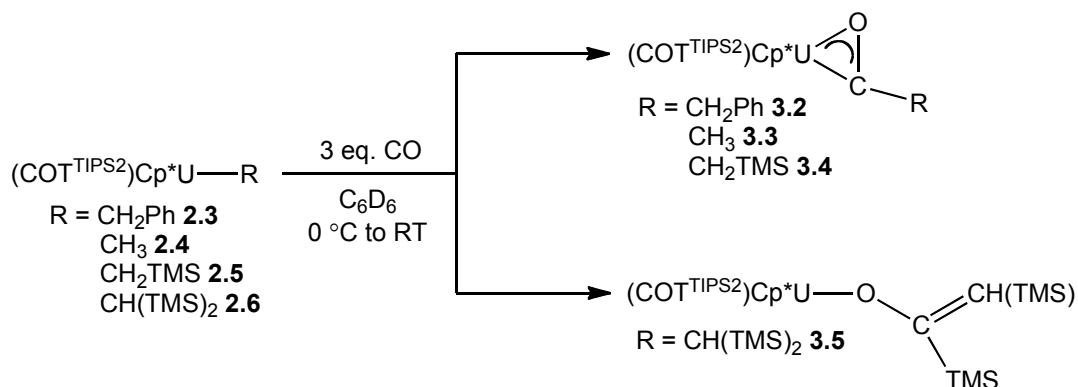
No signal that could be attributed to a ‘deuteride’ ligand was observed in the 2H NMR spectrum, despite collecting spectra over a wide spectral window. Overall, these studies show the extent of perdeuteration when reacting alkyls with D_2 in place of H_2 , but also indicate that a straightforward ‘deuteride’ is not facile to synthesise – a mixture of partially perdeuterated hydride and deuteride complexes is likely to be present in solution at any one time. Attempts to fully deuterate **3.1** by repeatedly adding D_2 to the reaction mixture have not been successful due to decomposition. In order to remove all HD and H_2 from the system, so that only pure **3.1-d₆₄** with a U-D σ -bond is in existence, would involve synthesising the starting alkyl complex with $COT^{TIPS^2-d_{48}}$ and Cp^*-d_{15} ligands, which has not been carried out. This also means that no IR spectra for **3.1-d** can be collected in order for ν_{U-D} to be identified in this case – this has also been noted for other uranium hydrides, where scrambling between D_2 and ligand protons has been observed.^{8,22}

3.3 Reactivity with CO: insertion reactions

3.3.1 CO reactivity with **2.3-2.6**

All four complexes **2.3-2.6** undergo a reaction upon exposure to CO, however, a lack of complete structural data prevents the definitive identification of the CO-insertion products. Literature precedent of the reactions of organoactinide U-C bonds with

CO,²⁷⁻³² along with the data collected from the reactions of **2.3-2.6** with CO, allows the conclusion that CO insertion occurs in each case. For **2.3-2.5**, it is likely that η^2 -acyl products are formed; in the case of **2.6** with CO, a different pattern of reactivity is observed (**Equation 3.3**).



Equation 3.3. Reactivity of **2.3-2.6** with CO.

The following sections outline the data collected during these CO reactivity studies and present evidence for the formation of three η^2 -acyl complexes (**3.2-3.4**) and a silyl enolate (**3.5**). It should be noted that the reactions of **2.3-2.5** with a mixture of CO and H₂ gave the same outcomes as the reactions of the complexes with CO alone – no evidence for H₂ incorporation into the products to form alkoxides was observed.

3.3.1.1 NMR spectroscopic data

The reactions of **2.3-2.6** with ¹³CO were performed in J Young NMR tubes, with the reaction progress monitored by ¹H and ¹³C{¹H} NMR spectroscopy. In each case, an excess of ¹³CO (ca 1-3 equivalents) was added to a frozen solution of the compound, then the reaction mixture was warmed to ambient temperature; none of the solutions displayed noticeable colour changes after warming.

¹H NMR spectra of **3.2-3.5** were collected 5-10 minutes after gas addition, when the solutions had reached ambient temperature. For **3.2-3.4** the spectra each contained a new set paramagnetically-shifted resonances attributed to new ‘U(COT^{TIPS}₂)Cp*’

species, with the $\text{COT}^{\text{TIPS}_2}$ and Cp^* ligand resonances at similar chemical shifts, suggesting the products to be structurally analogous to one another. In each case, one of the normally sharp doublets of integration 18H correlating to a TIPS proton environment is broadened ($\Delta\nu_{1/2} = 33, 44, 49$ Hz for **3.2**, **3.3**, **3.4** respectively) and loses the doublet multiplicity typically observed in other mixed-sandwich complex spectra. Resonances attributable to 'OC-R' moieties are present, at different chemical shifts to the parent complexes; resonances attributable to the protons closest to the uranium centre in compounds **3.2** and **3.4** (CH_2Ph and CH_2TMS respectively) are not observed, likely due to broadening effects. No convincing $^{13}\text{C}\{^1\text{H}\}$ NMR resonances corresponding to a ^{13}C -labelled atom could be found in the spectra of **3.2-3.4** – this is suspected to be due to the close proximity of the ^{13}C atom to the paramagnetic uranium centre, causing substantial broadening and shifting of the signal so that it cannot be observed, even when the spectrum is collected over a large number of scans. As with the $^{13}\text{C}\{^1\text{H}\}$ NMR spectroscopic data, no $^{29}\text{Si}\{^1\text{H}\}$ NMR spectroscopic resonances were observed, even when data were collected over a large number of scans, or using a relaxation delay (d^1) of 10 seconds (due to U^{4+} paramagnetism causing rapid relaxation of other nuclei; this can usually be set to 1-4 seconds for the collection of $^{29}\text{Si}\{^1\text{H}\}$ NMR spectra).

In contrast, the reaction of **2.6** with CO to give **3.5** is relatively slow: the ^1H NMR spectrum showed very little change after 10 minutes, and unreacted starting material was present in the reaction mixture in addition to **3.5** for a further 3 days after CO addition. The chemical shifts and multiplicity of the $\text{COT}^{\text{TIPS}_2}$ and Cp^* ligand resonances differ in the ^1H NMR spectrum of **3.5** in comparison to those of **3.2-3.4**, indicating that the structure of **3.5** may also differ. Two resonances of integration 9H each are seen in the spectrum of **3.5**, consistent with the presence of two chemically inequivalent TMS groups. Another indication that **3.5** differs from the CO-insertion products of **2.3-2.5** is that there is an observable signal in the ^{13}C NMR spectrum when **3.5** is synthesised with ^{13}CO : a broad singlet at 361 ppm.

Other $^{13}\text{C}\{^1\text{H}\}$ NMR resonances seen in this region are from the later-described CO insertion products of **2.9** and **3.1**, which contain ‘O-C(R)=C(R)’ linkages (see sections 3.3.2 and 3.3.3). It is proposed that instead of an η^2 -acyl, a silyl enolate is formed from CO insertion followed by silyl-group migration, as per **Equation 3.3** above; literature precedent supports this proposal.²⁷

3.3.1.2 Mass spectrometric data

A sample of **3.2** analysed by EI^+ mass spectrometry showed the expected parent ion at $m/z = 909$, along with peaks at 789, 773 and 91 m/z corresponding to the fragments ‘ $\text{UCOT}^{\text{TIPS}_2}\text{Cp}^*$ ’, ‘ $\text{UCOT}^{\text{TIPS}_2}\text{OCCH}_2\text{Ph}$ ’, and ‘ CH_2Ph ’ respectively. Similarly, a solid sample of **3.4** showed a molecular ion at $m/z = 905$ in the mass spectrum, along with peaks at $m/z = 770$ (‘ $\text{UCOT}^{\text{TIPS}_2}\text{OCCH}_2\text{TMS}$ ’), 743 (‘ $\text{UCOT}^{\text{TIPS}_2}\text{OTMS}$ ’), and 115 (‘ OCCH_2TMS ’). Mass spectrometric analysis of the methyl acyl **3.3** returned predominantly organic ligand fragments.

3.3.1.3 IR spectroscopic data

IR vibrational bands correlating to η^2 -acyl complexes of U(IV) and Th(IV) are reported to occur in the region of $1437\text{-}1504\text{ cm}^{-1}$.²⁹⁻³¹ IR spectroscopic data were collected of thin films or Nujol mulls between NaCl plates for the acyls **3.2-3.4**, but no obvious bands were observed that could be assigned to an η^2 -acyl vibration. Medium to strong-intensity ligand vibrations at ca 1460 cm^{-1} effectively mask the area in which relevant vibrations would occur.

An alternative approach was taken, using *in-situ* ReactIR methods to collect IR spectra of methylcyclohexane solutions of **2.3-3.5**, which were then exposed to CO. Initial background IR spectra were collected at ambient temperature, then the solutions were cooled to $-60\text{ }^\circ\text{C}$ before addition of an excess of CO. Upon warming to ambient temperature, IR spectra were recorded every 60 seconds in order to identify the

appearance of new vibrational bands attributed to η^2 -acyl formation. Despite collecting spectra for a further 2 hours after gas addition and subsequent warming, no new vibrational bands appeared. Once again, this may be due to masking effects from very intense ligand vibrations in the area of interest.

3.3.1.4 X-ray structures of 3.2 and 3.4

Disorder and twinning issues frustrated numerous attempts to collect X-ray diffraction data of high enough quality to refine to a publishable R-factor for the acyls **3.2** and **3.3**. However, low-resolution data were collected from two separate samples of crystalline **3.4**, which could be sufficiently refined to determine the connectivity of the product (**Figure 3.4**). Data collected from a twinned sample of **3.2** appeared to show the same connectivity, but would not refine sufficiently to confirm this. Repeated attempts to collect X-ray diffraction data for both **3.2** and **3.4** also resulted in the same problems.

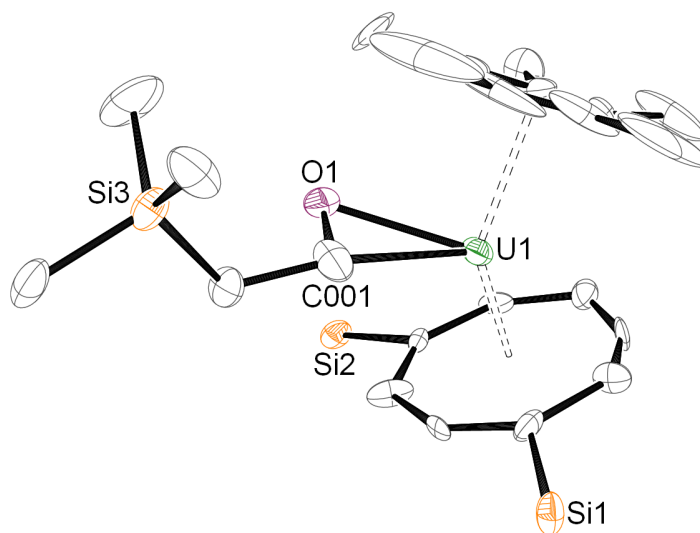
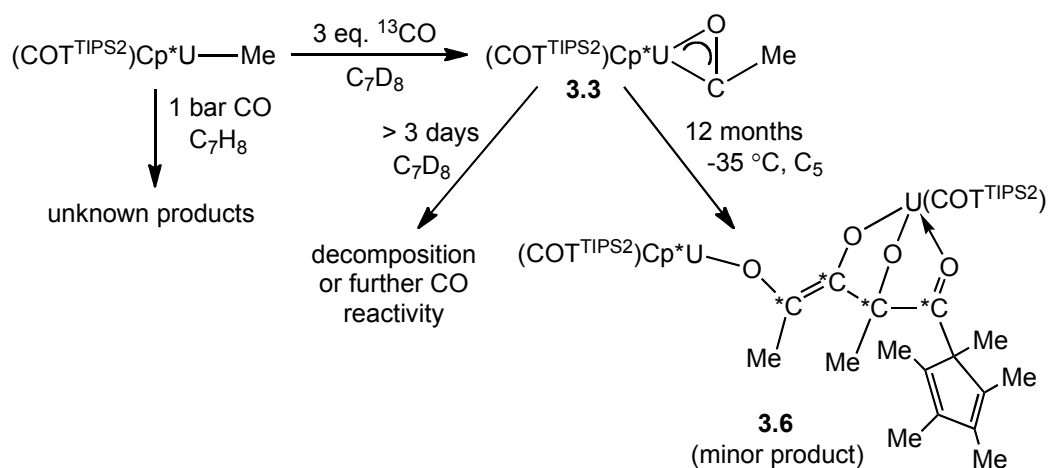


Figure 3.4. Unrefined molecular structure of **3.4**, as determined by low-quality X-ray diffraction data, showing connectivity only. ORTEP representation with thermal ellipsoids at the 20% probability level; ⁱPr groups omitted for clarity.

The X-ray diffraction data reveal an η^2 -acyl connectivity for **3.4**; the structure represents a single CO insertion into the U-C bond, confirming the hypothesis that the acyl product $\text{U}(\text{COT}^{\text{TIPS}_2})\text{Cp}^*(\eta^2\text{-OCCH}_2\text{TMS})$ is formed. Due to the similarities in spectroscopic data collected for **3.2** and **3.3**, it can be inferred that the structures of these products are likely to be the η^2 -acyls $\text{U}(\text{COT}^{\text{TIPS}_2})\text{Cp}^*(\eta^2\text{-OCCH}_2\text{Ph})$ and $\text{U}(\text{COT}^{\text{TIPS}_2})\text{Cp}^*(\eta^2\text{-OCMe})$, analogous to **3.4**.

3.3.1.5 *Crystal structure of product from 2.4 and excess CO*

Monitoring the formation of the methyl CO insertion product by ^1H NMR spectroscopy over a period of several days showed that the assumed acyl product **3.3** is either not stable in solution, or that it reacts further in the presence of excess CO to form a secondary product. The ^1H NMR spectroscopic resonances attributed to **3.3** decrease in intensity relative to the solvent peak over time, and numerous low intensity resonances, which are broad and paramagnetically shifted, begin to form, mainly between -1 and -15 ppm. Adding 1 bar of CO to a solution of **2.4** and analysing the resulting mixture by ^1H NMR spectroscopy shows only a large number of low-intensity resonances, and none of the previously identified acyl product **3.3**. Workup of an NMR-scale reaction of **2.4** with a three-fold excess of CO yielded a small number of red crystals from a saturated pentane solution stored at $-35\text{ }^\circ\text{C}$ over a period of 12 months, indicating that one product is a dimeric complex formed from multiple CO-insertion (**3.6**, **Scheme 3.5**).



Scheme 3.5. Reactivity of **2.4** with excess CO; products indicated where known.

The crystals obtained of **3.6** were not of high enough quality for the collection of complete X-ray diffraction data; it was only possible to collect data to a completeness of 71%, with $I/\sigma = 7.6$, and a maximum resolution of 1 Å. However, connectivity of the structure could be established and is shown in **Figure 3.5**. No material could be recovered from the X-ray sample for ^1H NMR spectroscopic analysis, so it cannot be determined if the structure shown below represents the product which correlates to the numerous low-intensity resonances seen in reaction mixtures of **2.4** and CO. It is possible that over such a long period of time, some of the acyl **3.3** degrades and releases CO, which could then react on with other molecules of **3.3** in the reaction mixture, that **3.6** is the result of slow rearrangement of the original acyl **3.3**, or that **3.6** is initially formed alongside **3.3** when excess CO is present.

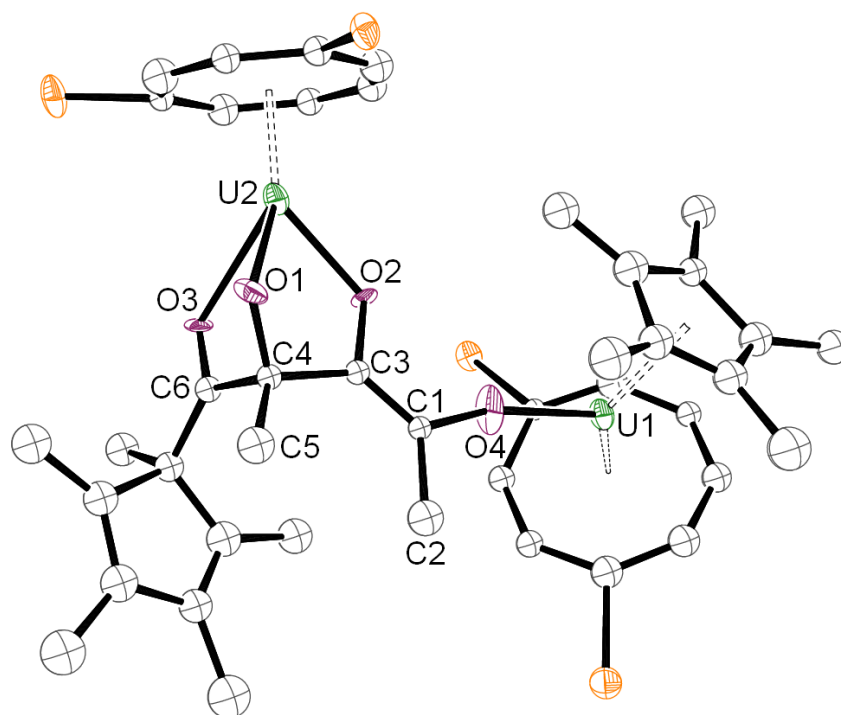
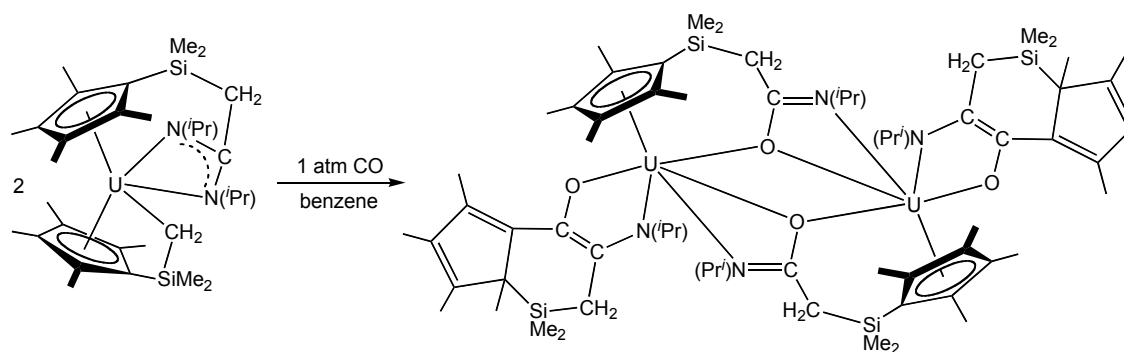


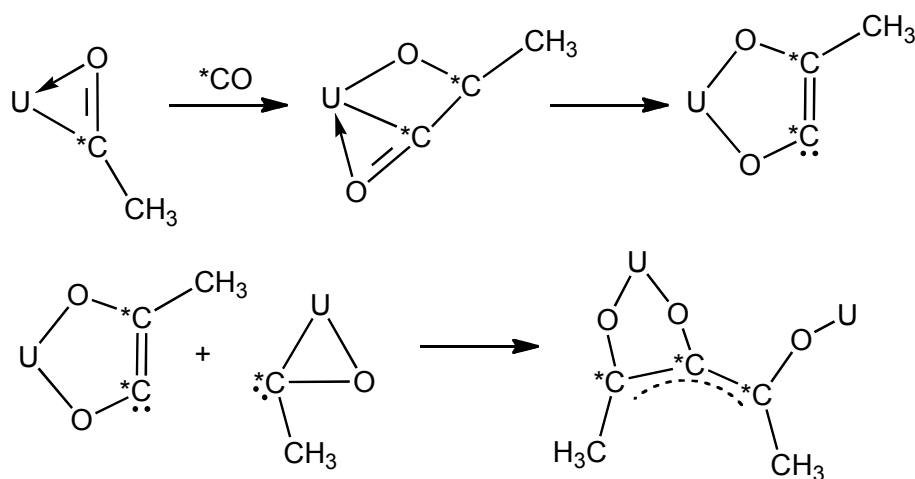
Figure 3.5. Unrefined molecular structure of **3.6**, showing connectivity only. ORTEP representation with thermal ellipsoids at the 50% probability level; carbon atoms are isotropic, ⁱPr groups omitted for clarity.

Overall, two ‘U(COT^{TIPS}₂)Cp*(Me)’ molecules have reacted with four equivalents of ¹³CO, not only inserting into the parent alkyl U-C bonds, but also inserting into a U-C bond between one U centre and its Cp* ring, which could have changed from η⁵ to η¹-coordination due to steric crowding. This type of insertion of CO into what could be considered an η¹-bound Cp ring has been observed previously in the ‘cascade’ reaction between a mixed-tethered metallocene and CO (**Scheme 3.6**).³³



Scheme 3.6. Product of CO insertion into a mixed-tethered metallocene.

If **3.6** is formed during the initial exposure of **2.4** to excess CO, rather than from decomposition, then the following pathway is feasible: after η^2 -acyl formation a U-C interaction is still in existence, hence a second ^{13}CO insertion is possible. A resonance structure wherein two oxygen atoms are bound to the uranium centre, and the secondarily inserted ^{13}C atom is unsaturated and carbenic can be then be considered (**Scheme 3.7**). Reaction with a second acyl molecule is hence possible, forming an asymmetric dimer with three inserted ^{13}CO moieties and two methyl groups. It has been reported that in some particularly sterically congested organolanthanide and organoactinide complexes, Cp* ligands will act as pseudo-alkyl η^1 ligands and undergo insertion reactions with small molecules.³⁴⁻³⁷ As the environment around one of the U centres depicted below becomes sterically crowded, it is possible that the Cp* group changes hapticity from η^5 to η^1 , resulting in a U-C ‘alkyl’ bond that is another potential site for ^{13}CO insertion, forming **3.6** after rearrangement. The driving force for this product could be the three U-O bonds formed around the oxophilic uranium centre in preference to a ‘softer’ η^5 -metallocene interaction. Precedent for speculative mechanisms relating to CO insertion into organoactinide alkyl complexes regularly invoke the ‘carbenic nature’ of inserted C atoms, as implied in the mechanism in **Scheme 3.7**.²⁸



Scheme 3.7. Possible insertion and dimerisation mechanism of **2.4** and CO. *C denotes ^{13}C .

M^+ observed at m/z 1638. Elemental analysis of **3.7** as a mixture of isomers returned a value slightly low in %C found (53.83 vs 54.39 calculated); incomplete combustion is occasionally observed for organouranium complexes.³⁸

Crystalline **3.7** as a mixture of isomers can be obtained from a saturated pentane solution stored at $-35\text{ }^\circ\text{C}$ or from C_6D_6 at ambient temperature. Collection of X-ray diffraction data from a crystalline sample of **3.7** allowed for the determination of the structure of *cis*-**3.7** (Figure 3.6) and *trans*-**3.7** (Figure 3.7) – the crystal morphologies of the two isomers are not distinguishable upon inspection under a microscope, however, the unit cells and volumes are marginally different. The data for *trans*-**3.7** could not be collected to a resolution greater than 0.89 \AA due to low-quality crystals, hence only connectivity could be determined.

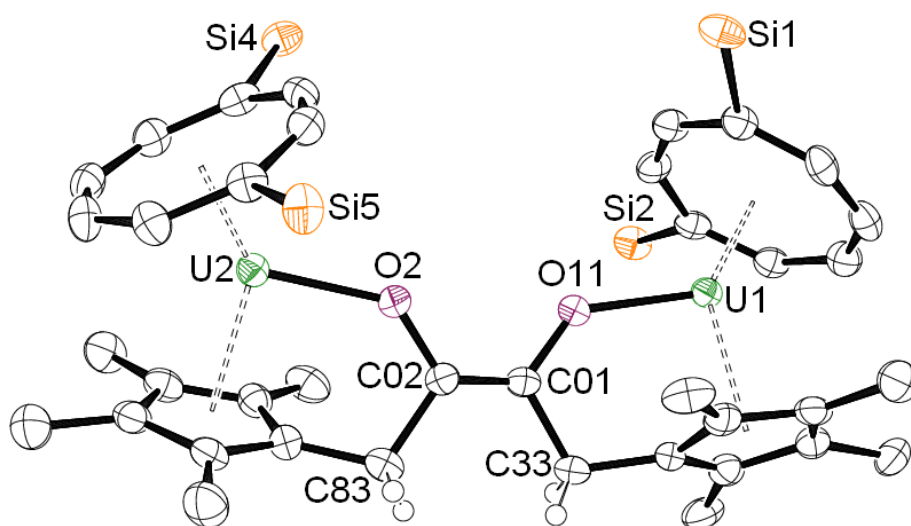


Figure 3.6. Molecular structure of *cis*-**3.7**. ORTEP representation with thermal ellipsoids at the 50% probability level. Hydrogen atoms (except on C33/C83), ^iPr groups and disordered co-crystallised molecule of C_6D_6 omitted for clarity. Selected bond lengths: U1-O1: 2.146(5) Å, U2-O2: 2.143(4) Å, O1-C01: 1.381(8) Å, O2-C02: 1.379(8) Å, C01-C02: 1.313(9) Å.

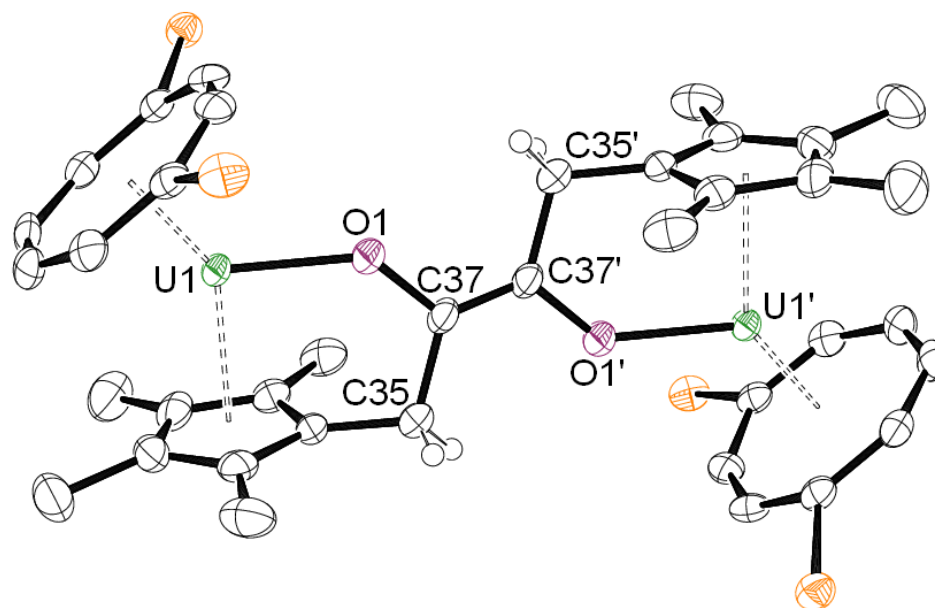


Figure 3.7. Molecular structure of *trans-3.7*.

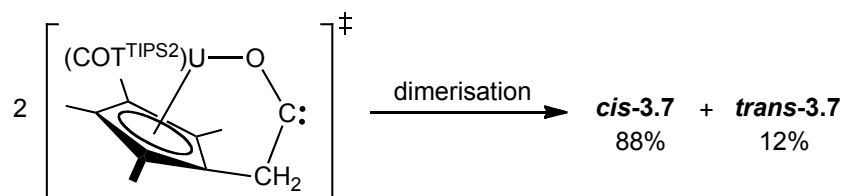
ORTEP representation with thermal ellipsoids at the 50% probability level.

Hydrogen atoms (except on C35) and *i*Pr groups omitted for clarity. Symmetry-related molecule – only one half of the dimer is contained within the asymmetric unit.

No details relating to the geometric parameters of *trans-3.7* are available for discussion due to low resolution data. The C01-C02 bond distance of 1.313(9) Å in *cis-3.7* is indicative of double-bond character, representing the coupling of two molecules of CO upon insertion. The U1-O11 and U2-O2 distances are identical within ESD limits, as are the C01-O11 and C02-O2 distances, showing the symmetrical nature of the U1-O11-C01-C02-O2-U2 moiety. Each half of the dimeric molecule in *cis-3.7* is arranged so that the TIPS groups are staggered, rather than eclipsed, resulting in torsion angles of 8.3(8) and 10.7(8) ° along the U1-O11-C01-C33 and U2-O2-C02-C83 moieties respectively. In comparison to other ‘U(COT^{TIPS2})Cp*’ compounds characterised in this work, the U-Ct1 (COT ring, 1.953(2) and 1.935(2) Å) and U-Ct2 (Cp ring, 2.459(3) and 2.457(3) Å) distances compare favourably to those complexes with free-rotating Cp* rings, as do the Ct1-U-Ct2 angles (139.96(10) and 140.01(10) °).

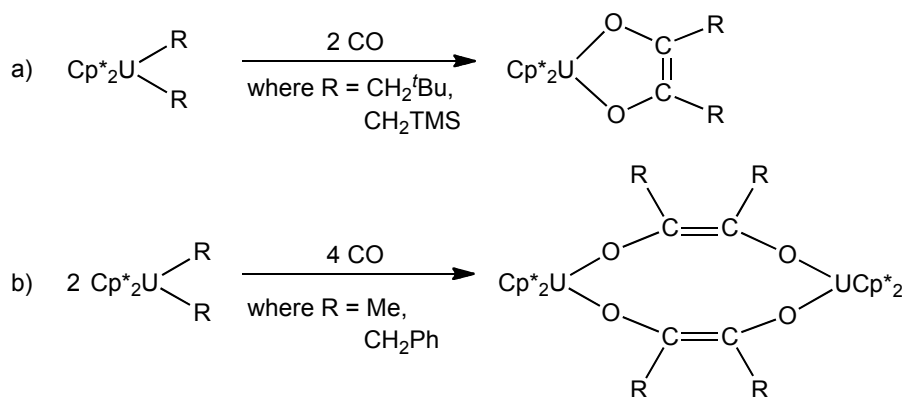
A plausible mechanism for this insertion and subsequent C=C bond forming pathway is as follows: the initial insertion takes place to form a new U-O bond,

however, the attached carbon atom is carbenic in nature and dimerises with another carbenic intermediate, generating the dimeric species with a C=C bond (**Equation 3.5**). This does not necessarily dictate whether the product is *cis* or *trans* in form, hence either other factors must contribute to the preferential formation of *cis*-**3.7**, or another mechanism is responsible.



Equation 3.5. Postulated mechanism for the formation of **3.7**.

Similar reactivity is observed in the reactions of the U(IV) dialkyl species of the form $\text{UCp}^*_2(\text{R})_2$ (where $\text{R} = \text{Me}, \text{CH}_2\text{Ph}, \text{CH}_2\text{CMe}_3, \text{CH}_2\text{TMS}$) reported by Marks *et al.*, where exposure to CO results in double carbonylation to give monomeric (**Scheme 3.8a**) or dimeric (**Scheme 3.8b**) *cis*-enediolate complexes.³⁹ The authors report mechanistic studies that indicate that the mechanism of C=C bond formation proceeds *via* the initial formation of ‘carbene-like’ η^2 -acyl species, which then couple either inter- or intra-molecularly depending on the bulk of the alkyl group. The pattern of reactivity forming **3.7** here is closely related to the above mechanism, and supports the hypothesis that a ‘tethered’ *cis*-enediolate forms as a result of carbenic C-C coupling.



Scheme 3.8. Monomeric and dimeric enediolate structures formed by CO insertion into dialkyl complexes, as reported by Marks *et al.*

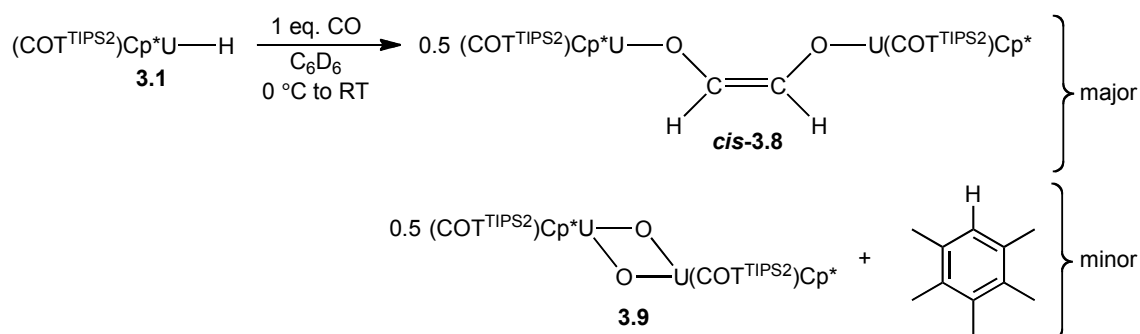
Mechanistic DFT studies were carried out by Maron *et al.* to determine possible mechanisms and likely intermediates.⁴⁰ Calculations suggest a reaction pathway of initial insertion of CO into the ‘tuck-in’ U-C alkyl bond to give a carbenic intermediate, however attempts to locate the C-C coupling transition state were not successful for either the *cis* or *trans* products (see Appendices 1 and 2 for the DFT calculation details). The calculations also indicate that ***trans*-3.7** is slightly thermodynamically favoured (ca 5 kcal mol⁻¹ lower in energy than the *cis* isomer).

Studying the ¹H NMR spectra collected from a number of reactions of **2.9** and CO, it was observed that the ratio of ***cis*-3.7**:***trans*-3.7** remained essentially constant, regardless of reaction conditions. Varying the solvent, reaction temperature, concentration of reagents or quantity of CO added – and combinations thereof – or performing photolysis did not influence the relative ratio of isomers to any significant degree. The *cis* isomer is always the major product in relation to the *trans* isomer, at a ratio of between 8:1 and 7:1 *cis:trans*.

When considering the preference of the system to form *cis* vs *trans* isomers from a purely steric perspective, it would seem unfavourable for the *cis* isomer to form in preference to the *trans* isomer in the initial reaction mixture due to the forced positioning of the bulky TIPS groups on each COT ring. Interconversion between *cis* and *trans* isomers once the initial product is formed would clearly be unfavourable – in order for isomerisation to occur, the C=C double bond would have to be either partially or fully cleaved in order for rotation to occur, forming ***trans*-3.7**. If dimerisation occurs *via* the carbenic C atom from insertion of CO, it would be anticipated that a 50:50 mixture of *cis* and *trans* isomers would be present in the reaction mixture, if no other factors were controlling the linking of the carbenic carbons. However, this is not the case, and either the mechanism is not as described above, or other factors dictate the preference for ***cis*-3.7**. Without further experimental or mechanistic DFT work, the mechanism remains unclear.

3.3.3 CO reactivity with $\text{U}(\text{COT}^{\text{TIPS}_2})\text{Cp}^*\text{H}$

With the successful formation of **3.1**, the insertion of CO into a monomeric U(IV) hydride bond was examined for the first time. The reaction of **3.1** with 1 equivalent of CO resulted in the formation of *cis*-enediolate, $\{\text{U}(\text{COT}^{\text{TIPS}_2})\text{Cp}^*\}_2(\mu\text{-}\kappa^1:\kappa^1\text{-OC(H)=C(H)O})$ (**3.8**), as the major product, along with small quantities of a *bis*-oxo species, $\{\text{U}(\text{COT}^{\text{TIPS}_2})\}_2(\mu\text{-O})_2$ (**3.9**) and pentamethylbenzene ($\text{C}_6\text{Me}_5\text{H}$) (**Equation 3.6**). The side product $\text{C}_6\text{Me}_5\text{H}$ was initially identified by ^1H and ^{13}C NMR spectroscopy from reactions of **3.1** and CO performed in J Young NMR tubes. The dioxo product **3.9** was later isolated in a very low yield (< 2 mg) as a DME adduct from a preparative-scale reaction and characterised by X-ray crystallography, *vide infra* – its ^1H NMR spectrum contains many low-intensity broadened resonances and is not facile to assign or identify in a reaction mixture.



Equation 3.6. Reactivity of **3.1** with CO to form **3.8**, **3.9** and $\text{C}_6\text{Me}_5\text{H}$.

The reaction of a pentane solution of **2.4** and 1 bar of H_2 was followed by stirring the resulting cherry red solution for two hours, then briefly evacuating the vessel headspace before freezing the solution and pressurising the headspace with 2 bar of CO, to afford **3.8** in a crude yield of 32% after filtration and removal of volatiles. Recrystallisation of a 40 mg portion of the crude sample from a saturated pentane solution cooled to -30 °C afforded crystalline **3.8** in a 58% yield (23 mg, **Figure 3.8**). Crystalline material was also obtained from saturated DME, Et_2O , and $t\text{BuOMe}$ solutions. ^1H NMR spectroscopic analysis of the crude and crystalline material showed the presence of a broad singlet of integration 2H (relative to the Cp^* ligand signal of

integration 30H) corresponding to the enediolate protons – this was confirmed from the synthesis of ^{13}C -**3.8** from **2.4**, H_2 , and a 1:1 mixture of $\text{H}_2/^{13}\text{CO}$. The proton-coupled ^{13}C NMR spectrum of ^{13}C -**3.8** contains a broad doublet at 336 ppm ($^1J_{\text{CH}} \approx 190$ Hz), assignable to the ^{13}C -labelled enediolate moiety. Collection of the corresponding ^1H NMR spectrum shows a doublet at δ_{H} 88.3 (also with $^1J_{\text{CH}} = 190$ Hz), which collapses into a singlet of integration 2H when the $^1\text{H}\{^{13}\text{C}\}$ NMR spectrum is obtained, supporting the assignment of this signal to the enediolate protons. Mass spectrometric data showed an ion at $m/z = 1636$ ($\text{M}^+ - 2\text{H}$), and elemental analysis returned the expected values. Infrared spectroscopic data did not show a vibrational band attributable to an enediolate moiety, likely due to masking effects from strong ligand vibrations.

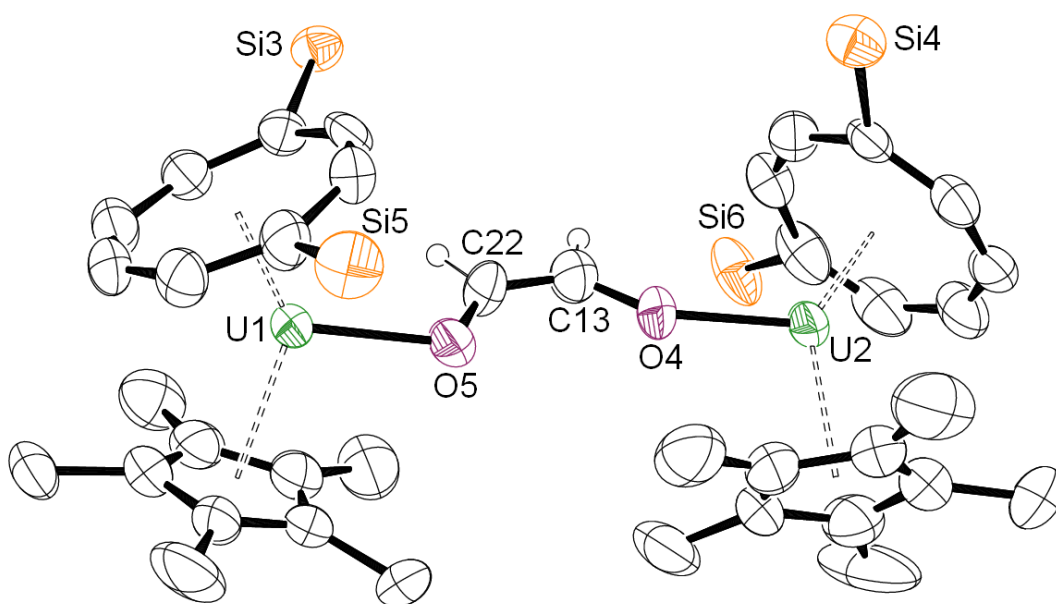


Figure 3.8. Molecular structure of $\{\text{U}(\text{COT}^{\text{TIPS}_2})\text{Cp}^*\}_2(\mu\text{-}\kappa^1:\kappa^1\text{-OCHCHO})$ (**3.8**).

ORTEP representation with thermal ellipsoids at the 50% probability level.

Hydrogen atoms (except on C22/C13) and ^iPr groups omitted for clarity.

Due to disorder in one TIPS group in the crystal structure of **3.8** the final refinement cycle did not converge to a satisfactory level and the carbon atoms contained on the disordered TIPS group were left as isotropic. However, the R factor of the structure is 8.93%, and the metrical parameters relating to the enediolate fragment are

still valid. No other U(IV) enediolate complexes reported in the literature have been structurally characterised, however, three comparable organoactinide and organolanthanide *cis*-enediolates exist (**3A-3C**, **Figure 3.9**). One Th(IV) methyl-substituted enediolate has been structurally characterised, **3A**, formed from the insertion of CO into Th-C bonds.²⁷ Two lanthanide enediolate complexes have been reported from the addition of CO to the corresponding lanthanide hydrides: a Sm(III) triphenylphosphine oxide adduct, *cis*-**3B**,⁴¹ and a Ce(III) product, *cis*-**3C**;⁴² pertinent bond distances and angles of their *cis* isomers are summarised in **Table 3.3**.

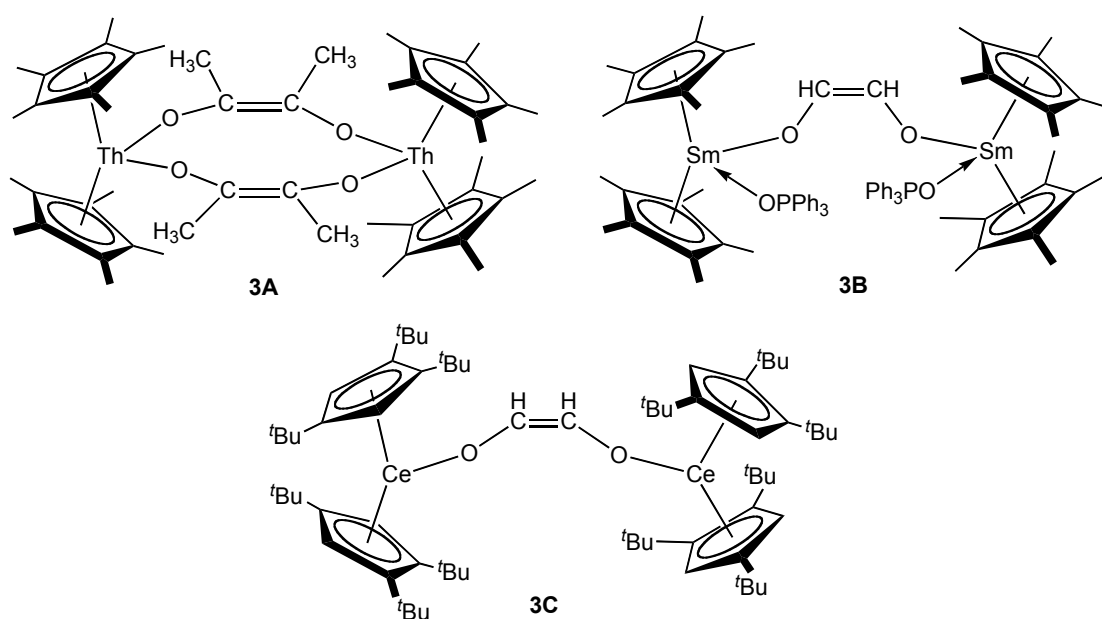


Figure 3.9. Structurally characterised actinide and lanthanide enediolate complexes.

Table 3.3. Selected bond distances (Å) and angles (°) for **3.8**, and **3A-3C**.

	3.8	3A [†]	<i>cis-3B</i>	<i>cis-3C</i>
M-O	2.168(5), 2.113(5)	2.154	2.173(4), 2.170(5)	2.147(10), 2.179(10)
O-C	1.333(10), 1.344(9)	1.37	1.382(8), 1.351(8)	1.319(19), 1.352(18)
C=C	1.302(10)	1.33	1.32(1)	1.324(22)
M-O-C	115.7(4), 148.5(5)	163.6	159.6(4), 160.0(5)	150.7(11), 142.1(11)
O-C=C	128.0(7), 130.5(7)	122	129.1(7), 135.2(7)	132.5(18), 128.4(18)
Torsion angle O-C-C-O	0.1(11)	n/a	7.9(15)	2.9

[†] No ESDs were reported with the data.

The enediolate fragment is not equally bound between the two U centres in **3.8**, with significantly different U-O distances (2.168(5) and 2.113(5) Å), and equally varied U-O-C angles (115.7(4) and 148.5(5) °), however, the geometric parameters associated with the ‘O-CH=CH-O’ moiety are much more regular. The C=C bond distance of 1.302(10) Å is marginally shorter than in **3A-3C**, but still in agreement with typical C=C double bond lengths, and the O-C bond distances in *cis-3.8* are within the range reported (1.319(19) – 1.382(8) Å) but are shorter than typical alcoholic O-C bond distances.⁴³ The O-C=C angles in **3.8** are consistent with angles reported for *cis-3B* and *cis-3C*, greater than for a typical sp² carbon atom. The ‘O-C=C-O’ moiety in **3.8** shows a marginal deviation from planarity with a torsion angle of 0.1(11) °, similar to *cis-3B* and *cis-3C* with torsion angles of 2.9 and 7.9(15) ° respectively. The *cis*-enediolate **3.8** can also be compared to the ‘tethered’ enediolate mixed-sandwich complex, *cis-3.7*. The U-O distances in **3.8** vary by no more than 0.03 Å in comparison to the U-O distances in *cis-3.7*, whilst the O-C distances and the C=C distance are marginally shorter, possibly due to steric constraints in *cis-3.7* imposed by the ‘tethered’ Cp ligand, bound to the substituted enediolate moiety. Overall, the bridging enediolate ligand in **3.8** is

structurally similar to other ‘M-O-C(R)=C(R)-O-M’ linkages in *f*-block organometallic complexes.

Recrystallisation of crude **3.8** from DME yielded two morphologies of crystals: red prisms and orange needles. An exact yield of each product could not be obtained as the orange needles were present in very small quantities. The structure of the red prisms was shown to be **3.8**, while the orange needles are the DME adduct of the bis-bridging oxo complex, **3.9.DME** (**Figure 3.10**). The data collected from the orange needles of **3.9.DME** were not of sufficient quality for full structural refinement - the needles were small and the structure resolution was poor - hence geometric parameters are not discussed here. Higher quality data have been collected from the THF adduct of **3.9**, $\{U(COT^{TIPS_2})THF\}_2(\mu-O)_2$, synthesised and fully characterised by another group member, Kahan, from an unrelated reaction.⁴⁴ In addition to the 1H NMR resonances assigned to **3.8**, several other small, broad, and paramagnetically shifted signals are also observed in the 1H NMR spectrum collected from crude **3.8**, but are too broadened and weak to definitively assign to **3.9**. Mass spectrometric analysis of the crude material returned an ion at $m/z = 686$, correlating to the fragment ‘ $U(COT^{TIPS_2})O_2$ ’.

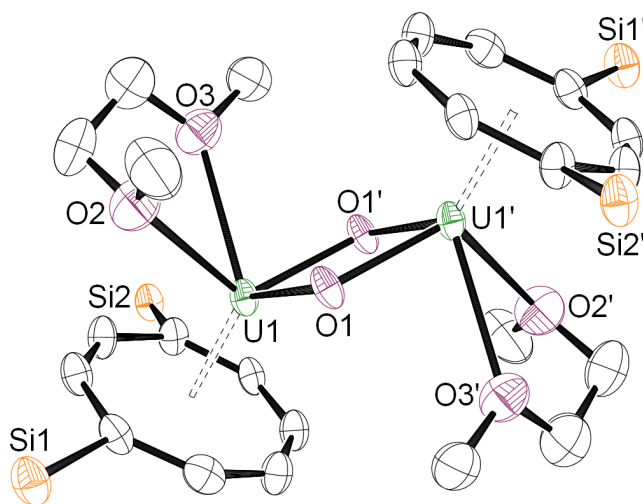


Figure 3.10. Molecular structure of $\{U(COT^{TIPS_2})(DME)\}_2(\mu-O)_2$ (**3.9.DME**).

ORTEP representation with thermal ellipsoids at the 50% probability level. Hydrogen atoms and *i*Pr groups omitted for clarity. One molecule of two present in asymmetric unit shown.

Crucial to understanding why this species is isolated from the reaction of **3.1** and CO was the identification of another organic side-product, pentamethylbenzene, (C_6Me_5H). Variable temperature 1H and $^{13}C\{^1H\}$ NMR spectroscopic analysis was performed on a crude reaction mixture of **3.1** and ^{13}CO to identify resonances corresponding to protons or carbon atoms bound to the paramagnetic uranium metal centre, which shift with varied temperature. Alongside the paramagnetically-shifted resonances were signals corresponding to C_6Me_5H containing one ^{13}C -labelled carbon atom: the 1H NMR spectrum contained signals at δ_H 6.93, 6.55, 2.13, 2.12, 2.04 and 2.01, and the $^{13}C\{^1H\}$ NMR spectrum contained an intense singlet at δ_C 129.6. Collection of the $^1H\{^{13}C\}$ NMR spectrum resulted in the collapse of four of these signals (which are in fact two doublets, δ_H 6.74 and 2.14 with $J_{CH} = 152$ and 5.3 Hz respectively, italicised above) into two singlets, which integrate to a ratio of 1:6 relative to each other. Upon collecting the proton-coupled ^{13}C NMR spectrum, the previously observed singlet became a doublet of septets, with $J_{CH} = 152$ Hz and 5 Hz. These data are consistent with a ^{13}C -labelled atom attached to a single proton, which couple to a further 6 protons in equivalent chemical environments (*i.e.* two CH_3 groups), that are associated with an aromatic system. The assignment of these resonances to ^{13}C - C_6Me_5H is shown in **Figure 3.11**.

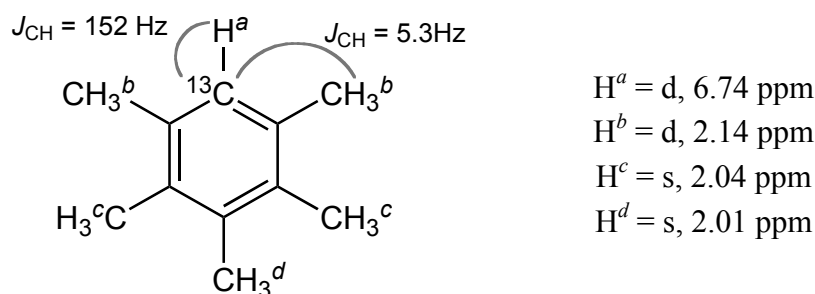
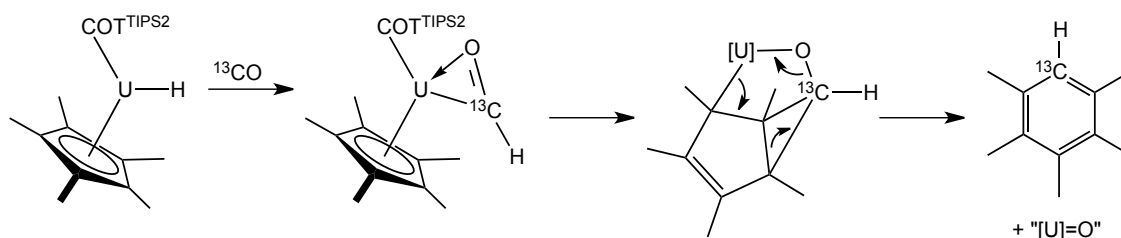


Figure 3.11. 1H NMR spectroscopic assignment of resonances attributable to ^{13}C - C_6Me_5H .

When considering these data with reference to previously reported reactions of U-C σ -bonds with CO in complexes containing 5-membered Cp^R rings (where $R = Me_5, H_5, H_4Me$), which have on occasion yielded substituted benzene species due to activation of the Cp ring, it is feasible that the same mechanism occurs in this

case.^{32,45} Instead of ^{13}CO only inserting into the U-H bond in **3.1**, the ' $^{13}\text{C-H}$ ' moiety may react with the Cp* ring, undergoing ring-expansion to give pentamethylbenzene (**Scheme 3.9**). As this occurs, a ' $\text{U}(\text{COT}^{\text{TIPS}_2})\text{O}$ ' fragment is extruded, providing explanation for the presence of **3.9** alongside $\text{C}_6\text{Me}_5\text{H}$.



Scheme 3.9. Ring-expansion of Cp* in **3.1** to give ^{13}C -labelled pentamethylbenzene;
 $[\text{U}] = \text{U}(\text{COT}^{\text{TIPS}_2})$.

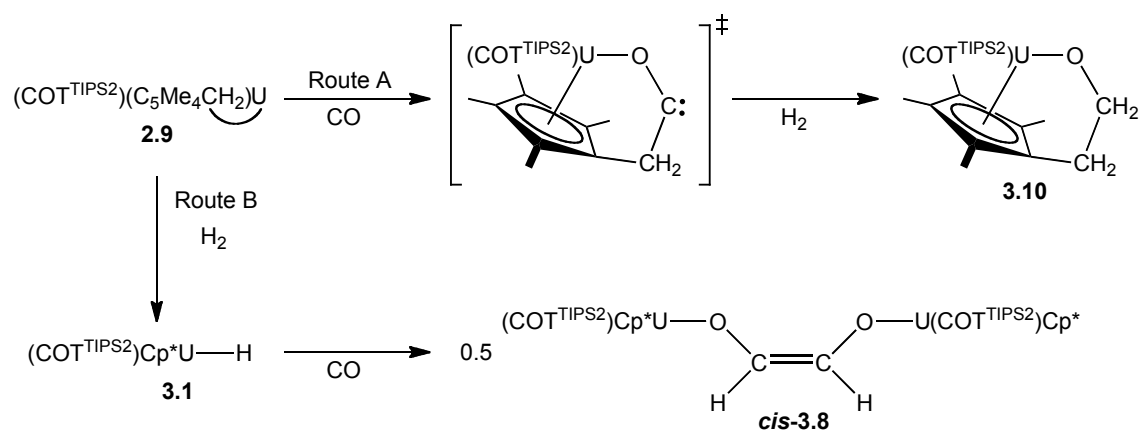
To complement the labelling studies carried out for **3.1**, the addition of D_2 and ^{13}CO to **2.4** was performed so that the position of deuterium atoms in the products – **3.8** and $\text{C}_6\text{Me}_5\text{H}$ – could be located. As discussed previously, scrambling occurs when D_2 is used in place of H_2 to form the hydride/deuteride complex **3.1**. This effect means that there will not necessarily be perdeuteration of the enediolate moiety, as deuterium will exchange with the Cp* and $\text{COT}^{\text{TIPS}_2}$ ligand protons, however, some deuterium may remain bound as a ' U-D ' ligand and hence form a bridging ' O-CD=CD-O ' or ' O-CD=CH-O ' ligand.

The NMR-scale reaction of **2.4**, D_2 , and ^{13}CO in C_7H_8 resulted in a ^2H NMR spectrum containing resonances at δ_{D} 6.84, 6.46, 5.84, 2.00 and 1.91. Only the signal at 5.84 ppm shifted upon performing variable temperature experiments, confirming that the other resonances are attributable to the diamagnetic product, $\text{C}_6\text{Me}_5\text{H-d}$, wherein deuterium is present on both the $\text{C}_6\text{Me}_5\text{D}$ and $\text{C}_6(\text{d-Me})_6\text{H}$ portions of the molecules. The other signal corresponds to partially deuterated Cp*-C(H/D)₃ groups on **3.8**. No signal was observed at ca 88 ppm, where a resonance is expected for ' O-CD=CD-O ', but this could be due to broadening effects. Removal of volatiles and collection of ^1H and $^{13}\text{C}\{^1\text{H}\}$ NMR spectra confirmed the partial deuteration of pentamethylbenzene – a 1:1:1 triplet in the $^{13}\text{C}\{^1\text{H}\}$ NMR spectrum with $^1J_{\text{CD}} = 23$ Hz

is present at 129.1 ppm, arising from the splitting of the resonance attributed to the inserted ^{13}C by attached deuterium.

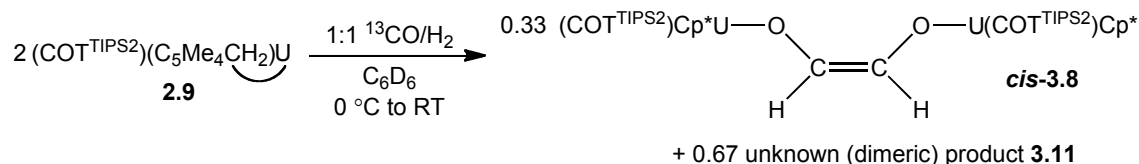
3.3.4 Reactivity of **2.9** and **3.1** with CO/H₂ mixture

In addition to experiments performed with **2.9** and CO, the addition of a 1:1 mixture of CO and H₂ to **2.9** was also studied. This was investigated for three reasons: firstly, the relative rate of reaction between the U-C bond with H₂ or CO in the mixed-sandwich system is of interest; secondly, if a ‘carbene-like’ intermediate is formed upon the reaction of **2.9** and CO, the presence of H₂ may mean that instead of C=C bond-forming, hydrogenation could occur to form a ‘tethered’ alkoxide complex (**3.10**, **Scheme 3.10**); thirdly, this reaction acts as a control experiment for the addition of CO to the hydride **3.1** (under a partial hydrogen headspace) to identify potential side-products in the complex reaction mixture of **3.1** and CO.



Scheme 3.10. Possible reaction pathways for **2.9** with CO/H₂ gas mixture forming a ‘tethered’ alkoxide complex **3.10** (**Route A**, top right) or *cis*-**3.8** (**Route B**, below).

A sample of **2.9** dissolved in C₆D₆ in a J Young NMR tube was exposed to ca 1 equivalent (one ^{13}CO and one H₂ molecule per U atom) of a 1:1 mixture of $^{13}\text{CO}/\text{H}_2$ whilst frozen, and ^1H and $^{13}\text{C}\{^1\text{H}\}$ NMR spectroscopic data were collected 90 minutes after warming to ambient temperature (**Equation 3.7**).



Equation 3.7. Reaction of **2.9** and 1:1 $^{13}\text{CO}/\text{H}_2$.

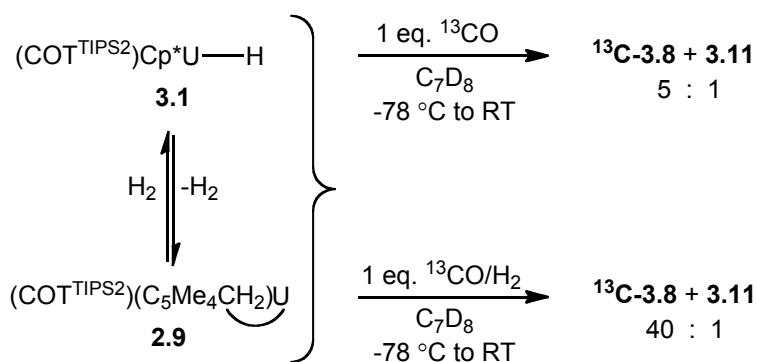
Three sets of TIPS doublets were present in the ^1H NMR spectrum, each of equal integral values – one set correspond to the known enediolate complex **3.8** (**Scheme 3.10 Route B**). The other two sets could either correspond to an asymmetric dimeric species, or two separate species present in a 1:1 ratio (labelled **3.11**). The ^{13}C NMR spectrum contained a doublet at 288 ppm ($J_{\text{CH}} = 92$ Hz), and a broad signal that appears to be a doublet of doublets at 391 ppm, with coupling constants of ca 92 and 74 Hz. A doublet resonance appears in the ^1H NMR spectrum at -59 ppm, also with $J_{\text{CH}} = 92$ Hz, which collapses to a singlet when performing an $^1\text{H}\{^{13}\text{C}\}$ NMR experiment. This is consistent with the insertion of two ^{13}C atoms, one of which is bound to a single proton. More structural information cannot be deduced from these data alone, however, it is clear that the proposed ‘tethered alkoxide’ **3.10** (**Scheme 3.10 Route A**) is *not* a product of this reaction.

Attempts to crystallise the products from a saturated pentane solution resulted in the formation of red microcrystalline material, determined by ^1H NMR spectroscopy to be enediolate, **3.8**. Examination of the residual mother liquor by ^1H NMR spectroscopy showed the presence of a small amount of **3.8**, and the previously observed two sets of TIPS doublets in equal integral values respective to each other. This evidence suggests that **3.11** is a dinuclear species – rather than two separate products in the same ratio – that persists after manipulation of the reaction mixture. Hence, from integral ratios it can be asserted that two products are produced, both dimeric in form, in a ratio of 2:1 (**3.11:3.8**). Repetition of this reaction using stoichiometric or 2 to 3-fold excesses of 1:1 $^{13}\text{CO}/\text{H}_2$ and comparison of ^1H NMR spectroscopic data collected from these reactions allowed for the identification of resonances associated with **3.11**. From integral values and multiplicity, it can be deduced that **3.11** contains only one

free-rotating Cp*-ring. Also present are two inequivalent $\text{COT}^{\text{TIPS}_2}$ ligands, and other moieties represented by numerous low-integral proton resonances, which could not be rationalised by NMR spectroscopic data alone.

A lack of further characterising data precludes identification of **3.11**, however, some qualitative information can be obtained: as the ratio of **3.8:3.11** is 1:2, this indicates that the reaction of **2.9** with H_2 , followed by the insertion of CO and subsequent formation of enediolate, occurs more slowly than the reaction that forms **3.11**. The fact that **3.8** is formed at all demonstrates the difference between **2.9** and the ‘non-tethered’ alkyls **2.3-2.5** – whilst all of these complexes will undergo hydrogenolysis to form **3.1**, exposing them to a mixture of CO and H_2 results in only acyl products, indicative of a faster reaction between the $\text{U-C}_{\text{alkyl}}$ bond and CO than with H_2 . This is not the case for **2.9** and CO/H_2 , as both enediolate (formed *via* **Scheme 3.10, Route B**) and **3.11** are formed, requiring the reaction between the ‘tethered’ U-C bond of **2.9** and H_2 to initially occur.

Following identification of the structurally uncharacterised product **3.11** by ^1H NMR spectroscopy, re-examination of ^1H NMR spectroscopic data collected from the reaction of **3.1** and 1 equivalent of ^{13}CO also identified the presence of a proportion of **3.11** alongside $^{13}\text{C-3.8}$ and the known side-products, **3.9** and $\text{C}_6\text{Me}_5\text{H}$, in a ratio of approximately 5:1 $^{13}\text{C-3.8:3.11}$. The reaction of **3.1** and a stoichiometric quantity of a 1:1 mixture of $^{13}\text{CO/H}_2$ was also performed for comparison: in this case, a 40:1 ratio of $^{13}\text{C-3.8:3.11}$ was formed (**Scheme 3.11**).



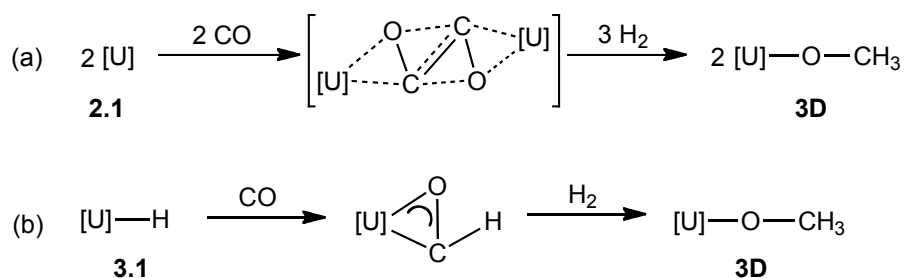
Scheme 3.11. Comparative reactivity of a mixture of **3.1** and **2.9** with ^{13}CO , or $^{13}\text{CO}/\text{H}_2$.

This result can be rationalised by considering that excess H_2 added to the reaction mixture of an alkyl and H_2 , which typically contains 25% of ‘tuck-in’ **2.9**, will result in any **2.9** present reacting on with H_2 to give **3.1**. The higher proportion of hydride present results in the formation of **3.8** almost exclusively. This result is also consistent with **3.11** only forming when hydride is present, and also confirms the theory that the reaction of **2.9** with CO to form the ‘tethered’ enediolates, *cis*- or *trans*-**3.7**, is relatively slow – no **3.7** is observed during this reaction.

3.3.5 Mechanistic considerations and DFT studies

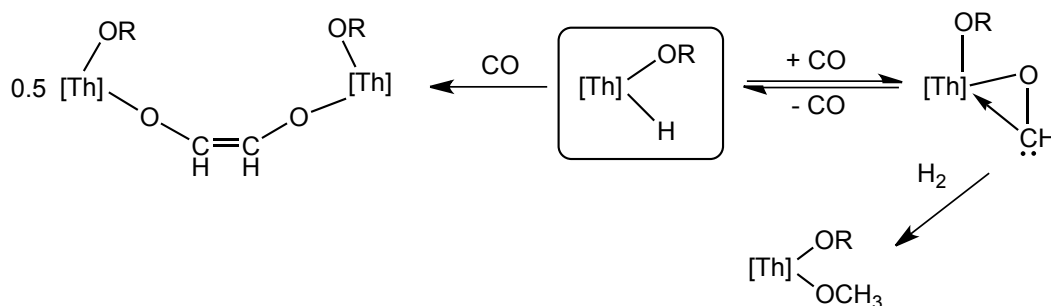
Taking into consideration the precedent of related Th(IV) hydrides with CO , a monomeric ‘formyl’ complex, an enediolate complex, or a product formed *via* multiple CO insertions are all potential products from the reaction of **3.1** with CO .^{29,46,47} No evidence for monomeric ‘formyl’ or multiple- CO insertion products are seen, however, the former could be postulated as an intermediate in the formation of **3.8**. The reaction of trivalent $\text{U}(\text{COT}^{\text{TIPS}2})\text{Cp}^*$ (**2.1**) with a combination of CO and H_2 forms a methoxide complex, $\text{U}(\text{COT}^{\text{TIPS}2})\text{Cp}^*(\text{OMe})$ (**3D**), and previous DFT mechanistic studies have led to the proposal of hydride and formyl complexes as potential intermediates.²⁴ Such species have been previously implicated in the formation mechanisms of two other methoxide complexes, $\text{ZrCp}^*_2(\text{OMe})(\text{H})$,^{48,49} and $\text{Ce}(\text{C}_5\text{H}_2^t\text{Bu}_3)_2(\text{OMe})$,⁴² and so these intermediates were preliminarily considered in this case. It is known that no reaction occurs directly between **2.1** and H_2 , and it was

initially proposed that the short-lived ‘zig-zag’ CO-intermediate reacts with H₂ to form **3D** (**Scheme 3.12a**); later computational investigations into the mechanism by Maron *et al.* suggest that the process is more complex than hydrogenation of the zig-zag intermediate.^{24,50} The following experiments aimed to identify whether an η²-formyl complex forms from the reaction of **3.1** and CO, and whether its subsequent hydrogenation would produce **3D** (**Scheme 3.12b**), which would lend support to the theory that a formyl species is intermediary in the reaction of **2.1** with CO and H₂.



Scheme 3.12. Formation of: a) methoxide (**3D**) from the proposed ‘zig-zag’ intermediate; b) **3D** from an η²-formyl species and H₂. [U] = U(COT^{TIPS})₂Cp*.

Precedent for the formation of η²-formyls and their conversion to methoxides has been established in organoactinide chemistry. Work conducted by Marks *et al.* on the reaction of ThCp*₂(OCH^tBu₂)H with CO and H₂ showed that the addition of CO produces a long-lived (yet reversible) η²-formyl, ThCp*₂(OCH^tBu₂)(η²-OCH), which dimerises to yield a cis-enediolate, {ThCp*₂(OCH^tBu₂)₂(μ-κ¹:κ¹-OCHCHO).⁴⁶ In the presence of excess H₂, the above reaction yields predominantly methoxide, ThCp*₂(OCH^tBu)(OMe), in a 90% yield (**Scheme 3.13**).²⁹



Scheme 3.13. Reactivity of ThCp*₂(OCH^tBu₂)H with CO and H₂; [Th] = ThCp*₂, R = CH^tBu₂.

Whilst an isolable η^2 -formyl complex was not produced from the reaction of **3.1** with CO, it is still possible that a formyl intermediate plays a role in enediolate formation, and could be ‘trapped’ *in situ* with H₂ to form methoxide, **3D**. In order to test this theory, the addition of CO to **3.1** was carried out at low temperature, followed by the immediate addition of H₂; the addition of a combination of CO and H₂ to **3.1** at low temperature was also (separately) performed. The rationale for these methods was that if a short-lived formyl is formed, the presence of H₂ in solution may enable the desired trapping instead of progressing to enediolate formation. If no methoxide is formed, then this result would negate the presence of an η^2 -formyl intermediate in this mechanism, or indicate that the highly reactive and short-lived nature of such an intermediate means that enediolate formation is faster or more favourable than methoxide formation.

Attempts to add a 10-fold excess of H₂ quickly to a cold (-78 °C) reaction mixture of **3.1** and 1 equivalent of ¹³CO in a J Young NMR tube did not yield methoxide – enediolate was produced, along with a smaller quantity of the unidentified product formed from ‘tuck-in’ **2.9** and H₂/CO, **3.11**. A larger-scale reaction was also performed: **2.4** was dissolved in pentane in an ampoule, frozen, the headspace evacuated, and pressurised to 1 bar of H₂ to form **3.1**. Upon warming, a colour change was observed, and the reaction was allowed to stir at ambient temperature for ca 60 minutes. After this time, the ampoule headspace was very briefly evacuated, then the solution was frozen and a thorough headspace evacuation was performed before 1 equivalent of ¹³CO was added *via* Toepler pump; prior to warming to ambient temperature, a further 1.5 bar of H₂ was added to the vessel. Thawing and stirring for ca 12 hours yielded a red solution, which was dissolved in C₇D₈ after all volatiles were removed under reduced pressure, and was shown to contain predominantly **3.8** by ¹H NMR spectroscopic analysis. A number of very low-intensity resonances were also present in the spectrum, including those attributable to the methoxide **3D**, verified by comparison with previously published data.²⁴ Determination of the exact ratio of **3D** to

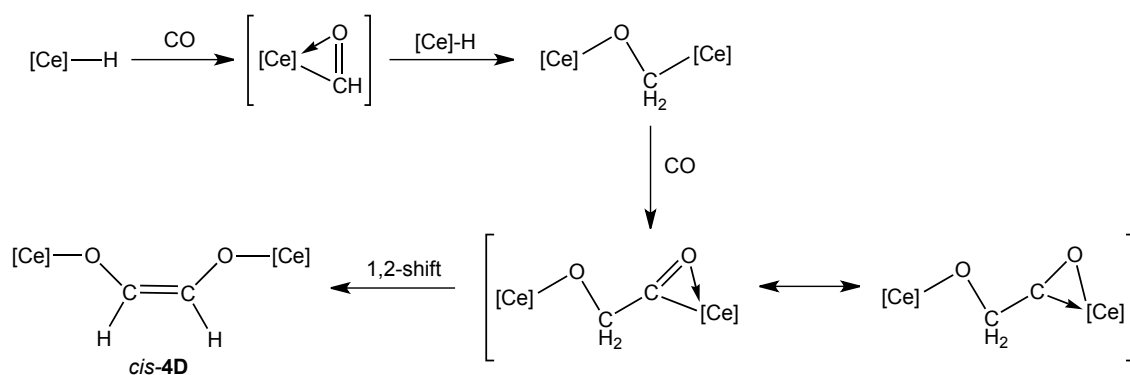
3.8 was precluded by many overlapping paramagnetically-shifted peaks, however, the two products appear to be present in an approximate ratio of 1:8 **3D**:**3.8**. The $^{13}\text{C}\{^1\text{H}\}$ NMR spectrum collected over 20000 scans did not show a resonance at δ_{C} 319 corresponding to **3D**, however, due to the significant amount of decomposition that occurred during the gas addition reactions, the overall concentration of the paramagnetic components of the sample was fairly weak, and it is possible that the resonance was too weak and broad to be observed. Mass spectrometric data collected from the sample did show a low-percentage ion at $m/z = 821$, consistent with the fragment ‘ $\text{U}(\text{COT}^{\text{TIPS}2})\text{Cp}^*(\text{OCH}_3)$ ’.

In conclusion, it does appear that methoxide *can* form in the reaction mixture of an alkyl with H_2 , followed by 1 equivalent of ^{13}CO and 1.5 bar of H_2 . Caution must be exercised with this conclusion, however, when considering that an alternative route to the methoxide is *via* $\text{U}^{\text{III}}(\text{COT}^{\text{TIPS}2})\text{Cp}^*$ (**2.1**). When the hydride **3.1** is formed, it can undergo hydrogen loss to form **2.1**, which could feasibly be present in the reaction mixture described above at some time. If a small quantity of **2.1** exists in solution, it could react with CO and H_2 to give methoxide, as has previously been established.²⁴ It therefore cannot be conclusively stated that methoxide is formed from the exclusive reaction of hydride and CO in the presence of excess H_2 .

The characterisation of enediolate, **3.8**, proves that an η^2 -formyl complex is not the ultimate product of the reaction of **3.1** and CO. Whilst the existence of a short-lived η^2 -formyl complex cannot be entirely ruled out, no evidence has been seen for such a species on an NMR or IR spectroscopic timescale. Mechanistically, it could be considered that **3.8** is a product of a ‘carbenoid’ η^2 -formyl complex which dimerises, forming enediolate. However, if this were the case, it would be anticipated that both *cis*- and *trans*-isomers would be products, which is not the case – no evidence for the existence of a *trans* isomer in any crude reaction mixtures has been observed, unlike for **3.7**. Additionally, it could be postulated that due to steric interactions between the two bulky TIPS groups on the COT rings, the *trans*-configuration of **3.8** would actually be

favourable, given the close approach required for the formyl carbons to undergo dimerisation. In the solid-state structure of *cis*-**3.8**, the two ‘U(COT^{TIPS2})Cp*’ moieties are positioned so that the TIPS groups on each COT ring are staggered, with a Ct1-U1-U2-Ct3 torsion angle of ca 44.5 °, in order to minimise steric interactions. Consideration of steric effects on *cis* vs *trans* preferences has also been briefly discussed by Evans *et al.* when postulating the mechanism of formation of **3B** (**Figure 3.9** above),⁴¹ and by Marks *et al.* in their detailed discussion of Th(IV) formyl complex kinetics.⁴⁷

Other mechanistic pathways are also plausible, one of which involves the initial insertion of CO into the U-H bond, forming an η^2 -formyl, which immediately reacts with a second equivalent of CO, inserting into the U-C_{formyl} bond. Subsequent reaction with another molecule of hydride, **3.1**, could ultimately yield *cis*-enediolate. A similar pathway is suggested by Andersen *et al.* in their studies into the mechanism of formation of **3C** (**Figure 3.9** above), however, they suggest the reaction of an η^2 -formyl complex with another molecule of the parent hydride, generating a oxymethylene intermediate, $\{(C_5H_2^tBu_3)_2Ce\}_2(\mu-OCH_2)$.⁴² This species then inserts another molecule of CO and undergoes a 1,2-hydride shift to give exclusively *cis*-**3C** (**Scheme 3.14**).



Scheme 3.14. Proposed mechanism for the formation of **3C** by Andersen *et al.*⁴²

In both this case, and in the case of the reaction of $ThCp^*_2(OCH^tBu_2)H$ and CO,⁴⁷ the presence of additional H₂ during the course of the reaction will yield methoxide

complexes, $\text{Ce}(\text{C}_5\text{H}_2^t\text{Bu}_3)_2(\text{OCH}_3)$ and $\text{ThCp}^*_2(\text{OCH}^t\text{Bu}_2)(\text{OCH}_3)$ respectively. Both authors conclude that hydrogenation of a ‘ $\text{M}(\text{OCH}_2)$ ’ intermediate is an acceptable explanation for this result. In addition, Andersen *et al.* note that *cis-3C* is formed exclusively upon reaction of the hydride with CO, not *trans-3C*, yet heating *cis-3C* results in the complete and irreversible isomerisation to *trans-3C* as the thermodynamically stable isomer. They attribute the lower barrier to forming *cis-3C* to a favourable arrangement of the ‘ $\text{Ce-O}(\text{CH}_2)\text{CO-Ce}$ ’ moiety that allows for a facile 1,2-hydrogen shift, forming *cis-3C*. It is possible that such an effect dictates the formation of *cis-3.8* in the mixed-sandwich system, however, no isomerism to *trans-3.8* has been seen after heating for prolonged periods of time.

Due to a lack of spectroscopic evidence for any intermediates generated in the course of the reaction of **3.1** and CO, Maron and Kefalidis undertook computational studies to try and determine a potential mechanistic pathway.⁴⁰ Their results are shown in **Figure 3.12**. It is important to note that the calculation results are limited to molecules containing only unsubstituted COT and Cp rings, due to their size, however, this pathway sheds some light on the insertion and rearrangement steps potentially involved. Crucially, it does *not* show the straightforward generation of an η^2 -formyl intermediate, suggesting that there is not a species present during this reaction process which can be easily hydrogenated, forming a methoxide complex, as originally postulated. They find that the *cis*-enediolate is a low-lying energetic product, at an enthalpy of $-94.4 \text{ kcal mol}^{-1}$ in relation to the starting hydride complex. The largest activation energy barrier to be overcome in this pathway is 7 kcal mol^{-1} , for the transition state preceded by C-C bond forming between two inserted CO molecules. Isomerisation results in a ketene intermediate, which reacts with a second molecule of hydride before undergoing a low activation-barrier hydride transfer to generate *cis*-enediolate.

This mechanism is plausible, as it shows an easily accessible kinetic pathway to exclusively the *cis*-product, due to the nature of the hydride transfer. Precedent for a

'ketene' intermediate can also be found in the study of the insertion of CO, isocyanide, and diphenylketene into Th(IV)-carbon bonds by Moloy *et al.*⁵¹ Previous computational work studying uranium reductive mechanisms has also found low-energy ketene-like intermediates.⁵² Further work is needed to confirm the mechanism of this reaction: complementary insertion chemistry of isocyanates may aid elucidation of intermediates.

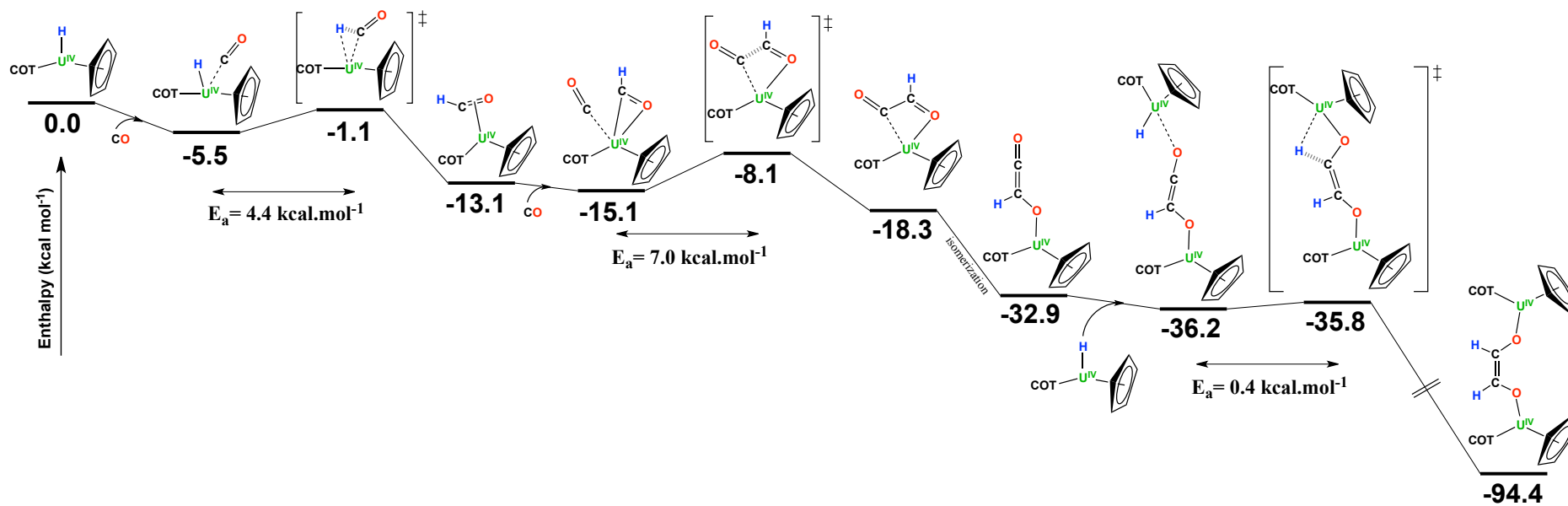


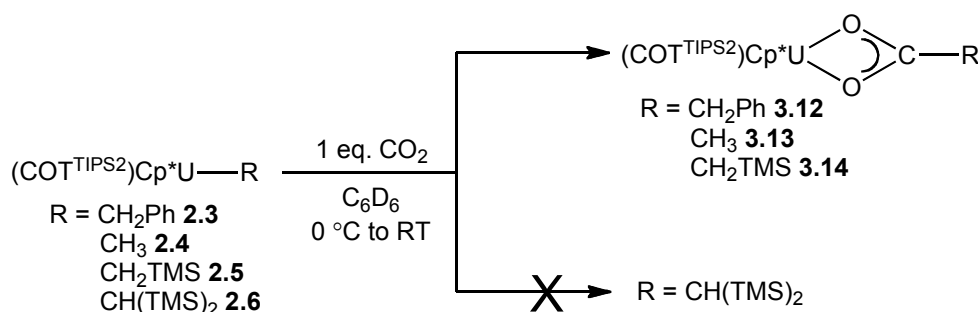
Figure 3.12. Mechanistic pathway computed by Maron and Kefalidis for the formation of enediolate (3.8) from hydride (3.1) *via* the insertion of CO.

Calculation performed for a simplified system (C₅H₅ in place of Cp*, C₈H₈ in place of COT^{TIPS2}). For details, see Appendix 1.

3.4 Reactivity with CO₂: insertion reactions and isomerisation

3.4.1 CO₂ reactivity with alkyls: κ²-carboxylates

The reactions of **2.3-2.5** with ca 1 equivalent of CO₂ yielded cherry-red solutions, determined to be κ²-carboxylates formed by the insertion of CO₂ into the U-C_{alkyl} bonds: U(COT^{TIPS2})Cp*(κ²-O₂CCH₂Ph) (**3.12**), U(COT^{TIPS2})Cp*(κ²-O₂CMe) (**3.13**), and U(COT^{TIPS2})Cp*(κ²-O₂CCH₂TMS) (**3.14**). In contrast to the clean reactions of **2.3-2.5** with CO₂ described above, the bulky *bis*-TMS alkyl **2.6** did not undergo a reaction when exposed to 1 equivalent of CO₂, or to an excess, deduced to be due to the steric bulk of the CH(TMS)₂ ligand (**Equation 3.8**).



Equation 3.8. Reactivity of **2.3-2.6** with CO₂.

The ¹H NMR spectra collected for **3.12-3.14** contained the expected resonances corresponding to the COT^{TIPS2} and Cp* ligands, and in each case the chemical shifts of these ligand resonances are similar. This can be rationalised by considering that the immediate environment around the uranium centres is almost identical in all three cases: all are bound to an 'O₂CR' ligand. Resonances attributed to the expected O₂C-R moieties are observed in each reaction mixture, and occur at chemical shifts closer to those expected in a diamagnetic complex, *i.e.* they are not paramagnetically shifted to the same degree as in the parent alkyls. This is due to the insertion of CO₂ into the U-C bond increasing the distance between the paramagnetic uranium centre and the protons on the alkyl moieties, hence lessening the effects of the Fermi contact and pseudo-contact shift factors and therefore reducing the extent to which the resonances

are shifted. The $^{13}\text{C}\{^1\text{H}\}$ NMR spectra contained a ^{13}C -labelled resonance attributable to each carboxylate ligand at δ_{C} 21.2 (**3.12**), 32.4 (**3.13**) and 57.4 (**3.14**) when the reactions were performed with $^{13}\text{CO}_2$.

3.4.1.1 Characterisation of $U(\text{COT}^{\text{TIPS}2})\text{Cp}^*(\kappa^2\text{-O}_2\text{CCH}_2\text{Ph})$ (**3.12**)

Crystalline **3.12** was isolated from a saturated pentane solution stored at $-35\text{ }^\circ\text{C}$, affording the product in a 46% yield. X-ray diffraction studies confirmed the structure of **3.12** as the carboxylate complex (**Figure 3.13**). The $^{29}\text{Si}\{^1\text{H}\}$ NMR spectrum of crystalline **3.12** contained a single resonance at -88.9 ppm. Mass spectrometric analysis showed the expected parent ion at 924 m/z (12%) and the fragment ‘ $\text{UO}_2\text{CCH}_2\text{Ph}$ ’ at 373 m/z (19%). A Nujol mull of the crystalline solid was prepared and the IR spectrum was collected between NaCl plates, showing an asymmetric ν_{OCO} stretch as a weak band at 1505 cm^{-1} – no symmetric CO stretch was observed due to masking by ligand vibrations.⁵³ Elemental analysis returned a value low in %C (found 56.23, calculated 57.11), and repetition of the analysis did not return a more favourable result; it is assumed that this is due to incomplete combustion occasionally encountered with organouranium complexes.³⁸ **Figure 3.13** shows half of the asymmetric unit of the structure of **3.12**. Two crystallographically independent molecules are present, however their structural metrics are almost identical. The other molecule displays disorder about the Cp^* ring, which has been modeled. No other structurally characterised U(IV) terminal benzyl carboxylate complexes have been reported in the literature. The closest related structure is a U(III) carboxylate, $U(\text{Tp}^*)_2(\kappa^2\text{-O}_2\text{CCH}_2\text{Ph})$ (**3E**), described by Bart *et al.*, which is made *via* the same route as **3.12** – insertion of CO_2 into the U-C bond of the parent alkyl complex⁵⁴ – and its metrics are summarised in **Table 3.1**. The carboxylate ligand in **3E** is structurally near-identical to the carboxylate ligand in **3.12**, the only exception being the O-U-O angle in **3E** of $51.4(3)^\circ$, which is slightly more acute than those in **3.12** ($53.1(2)$ and $53.2(2)^\circ$), owing to the differing ionic radii of U(III) and U(IV).

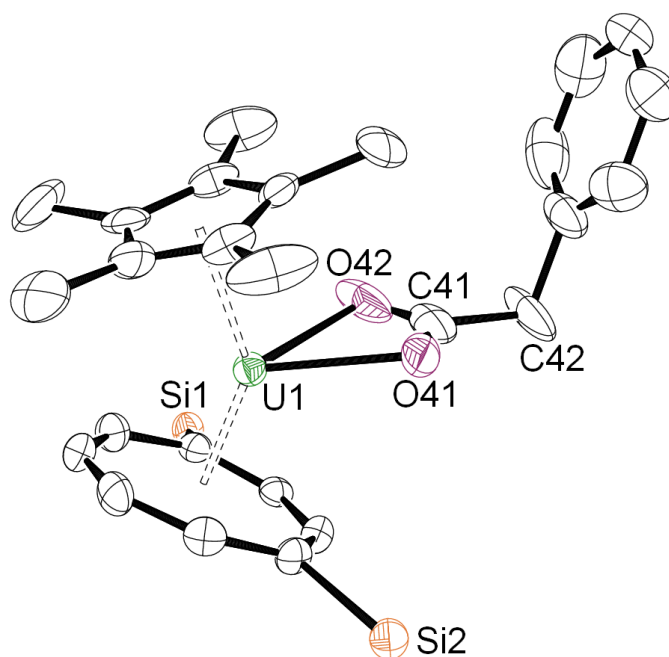


Figure 3.13. Molecular structure of one crystallographically independent molecule of $U(COT^{TIPS_2})Cp^*(\kappa^2-O_2CCH_2Ph)$ (**3.12**) in the asymmetric unit. ORTEP representation with thermal ellipsoids at the 50% probability level. One molecule of two present in the asymmetric unit shown, and hydrogen atoms and tPr groups omitted for clarity.

Table 3.4. Bond distances (Å) and angles (°) from the molecular structure of **3.12**, and from the related U(III) complex, **3E**.

	3.12 (U1 molecule)	3.12 (U2 molecule)	3E
U-O_{carboxylate}	2.405(5), 2.423(5)	2.424(5), 2.419(5)	2.409(7), 2.494(7)
O-C_{carboxylate}	1.260(13), 1.247(13)	1.223(12), 1.273(12)	1.228(12), 1.269(13)
O-U-O	53.1(2)	53.2(2)	51.4(3)
O-C-O	118.7(8)	119.9(8)	119.9(9)

3.4.1.2 Characterisation of $U(COT^{TIPS_2})Cp^*(\kappa^2-O_2CCH_3)$ (**3.13**)

Isolation of crystalline **3.13** in a 66% yield was achieved from a saturated toluene solution stored at -35 °C. X-ray diffraction studies showed the expected κ^2 -acetate structure (**Figure 3.14**), and the $^{29}Si\{^1H\}$ NMR spectrum of **3.13** contained a single

resonance at -111.0 ppm. Mass spectrometric analysis showed the expected parent ion at $m/z = 849$ (7%), the IR spectrum collected as a Nujol mull on NaCl plates contained a wide band at 1501 cm^{-1} attributed to asymmetric ν_{OCO} stretches, and the elemental analysis returned the expected C and H values. **Figure 3.14** shows the molecular structure of the terminal bidentate acetate complex, **3.13**. The U1-O1 and U1-O2 bond distances are identical within standard error ($2.409(5)$ and $2.408(5)\text{ \AA}$), while there is slight asymmetry in the O1-C40 and O2-C40 bond distances ($1.199(7)$ and $1.270(8)\text{ \AA}$) but not to any significant degree, and the U-O1-C40-O2 unit is essentially planar. The O1-U1-O2 angle is more acute than the O1-C40-O2 angle ($52.82(17)^\circ$ vs $120.4(8)^\circ$). The U-Ct1 (COT ring) and U-Ct2 (Cp* ring) bond distances found in complex **3.13** are consistent with those in other structurally characterised ‘U(COT^{TIPS2})Cp*’ complexes – its Ct1-U1-Ct2 angle is essentially identical to that of the chloride, **2.1** (see Appendix 1).

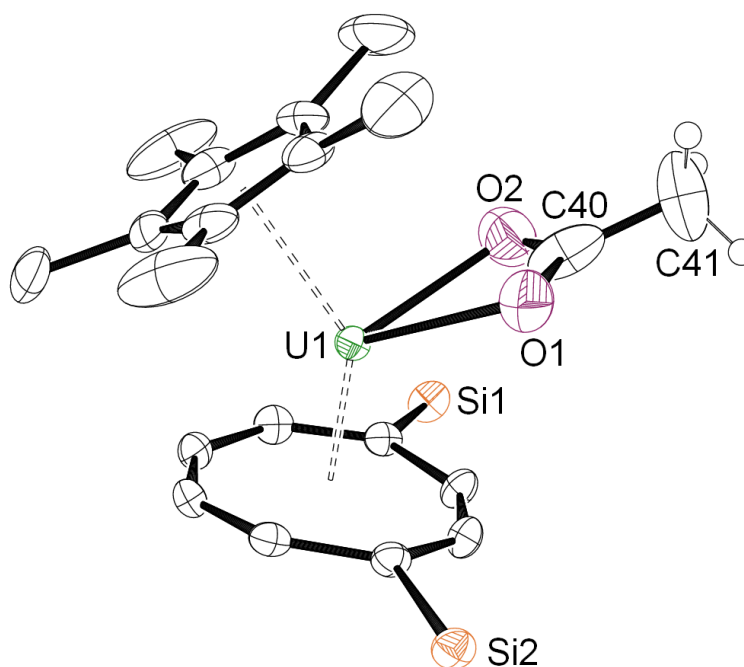


Figure 3.14. Molecular structure of U(COT^{TIPS2})Cp*(κ^2 -O₂CCH₃) (**3.13**).

ORTEP representation with thermal ellipsoids at the 50% probability level. Hydrogen atoms (except for on C41) and ⁱPr groups omitted for clarity. Selected bond lengths and angles: U1-O1: $2.409(5)\text{ \AA}$, U1-O2: $2.408(5)\text{ \AA}$, O1-U1-O2: $52.82(17)^\circ$, O1-C40-O2: $120.4(8)^\circ$.

The only other mononuclear U(IV) organometallic acetate structure described in the literature is U(Tp*)(O₂CMe)₃ (**3E**), a tris-acetato complex reported by Domingos *et al.*, formed by the reaction of the parent trichloride complex with NaO₂CMe.⁵⁵ The six U-O_{acetate} bond lengths in **3E** range between 2.406(12) and 2.439(11) Å, ranging from identical within ESD to slightly greater than in **3.13**, with more acute O-C-O angles (118.2(8) – 120.0(6) °), presumably due to greater steric crowding around the metal center from the three acetate ligands. The two other U(IV) acetate complexes reported in the literature are both tetranuclear and contain Cp ligands, featuring both bridging and terminal acetate ligands; however, in both cases the terminal acetates also interact weakly with another U atom. In the acetate cluster reported by Brianese *et al.* (**3F**), the U-O_{acetate} distances are 2.24(1) and 2.69(1) Å, the differing lengths being an effect of the weak interaction with a second uranium center, with an O-C-O angle of 119(1) °, similar to the angle in **3.13**.⁵⁶ In the tetrakis-Cp uranium acetate dioxide complex described by Rebizant *et al.* (**3G**)⁵⁷ the terminal acetate ligands contain asymmetrical U-O_{acetate} bond lengths of between 2.50(1) and 2.57(1) Å, but smaller O-C-O angles of 116(2) and 117(2)° in comparison to **3.2**, **3E** and **3F**, again likely due to effects of the weak interaction with a second uranium center. The U-O_{acetate} bond distances in **3.13** lie within the range found in structures **3E-3G** (1.17(2) – 1.32(2) Å).

3.4.1.3 Characterisation of U(COT^{TIPS2})Cp*(κ²-O₂CCH₂TMS) (**3.14**)

As detailed previously, the reaction of **2.5** and ¹³CO₂ forms a carboxylate product. This was supported by the ¹³C{¹H} NMR spectrum of **3.14**, which contains a large peak at 57.4 ppm, however, three other signals of considerable size at 18.96, 18.83 and 11.39 ppm were also observed – these resonances have been previously observed in partially-decomposed mixed-sandwich samples. Upon collecting a second ¹H NMR spectrum of **3.14** several hours after its initial synthesis, substantial decomposition into diamagnetic ligand components is observed, indicating that **3.14** is not as stable as **3.12**

or **3.13**, or that some decomposition occurs upon the addition of CO₂ to complex **2.5** (which is extremely unstable during handling) or even immediately after generation of the parent alkyl. The *in situ* generation of **2.5** from the reaction of **2.2** and LiCH₂TMS in pentane/THF, stirred at ambient temperature for 30 minutes, can be followed by filtration, freezing and subsequent CO₂ addition to form **3.14**. This route enabled the isolation of red crystalline **3.14** in a 55% yield, circumventing issues with isolating unstable **2.5**. The ²⁹Si{¹H} NMR spectrum collected from the sample contains two resonances at -10.17 and -92.51 ppm, corresponding to the -CH₂TMS moiety and the SiⁱPr₃ environments. Mass spectrometric analysis showed the expected parent ion at 920 m/z (22%) along with fragments corresponding to M⁺ -Cp* (785 m/z, 83%), M⁺ -COT^{TIPS2} (504 m/z, 12%) and U(O₂CCH₂TMS) (369 m/z, 24%). The IR spectrum contained a weak broad band at 1504 cm⁻¹ attributed to ν_{OCO}. Elemental analysis did not return satisfactory values for %C and H found due to rapid decomposition of the sample once isolated, leading to contamination with decomposed ligand that could not be separated from the bulk product.

Despite repeated attempts to collect X-ray diffraction data for **3.14**, a data set of sufficient quality could not be obtained suitable for full refinement due to low completeness of data (60%). Further recrystallisation of the product from alternative solvents and under different conditions did not yield crystals of high enough quality for X-ray diffraction studies. However, connectivity could still be established from one collected data set, and shows the expected κ²-coordinated carboxylate complex (**Figure 3.15**).

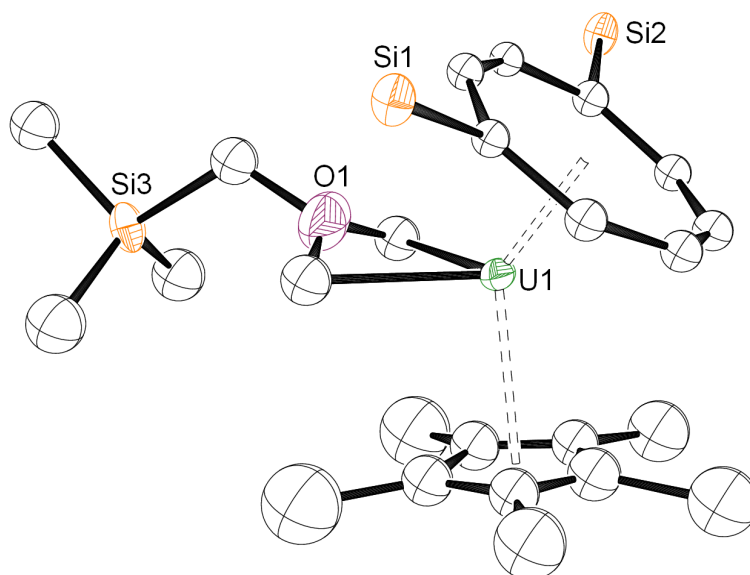
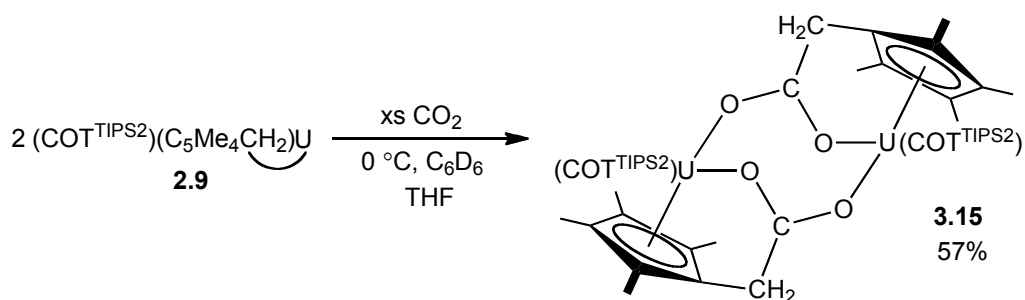


Figure 3.15. Unrefined molecular structure of $\text{U}(\text{COT}^{\text{TIPS}_2})\text{Cp}^*(\kappa^2\text{-O}_2\text{CCH}_2\text{TMS})$ (**3.4**). ORTEP representation with thermal ellipsoids at the 50% probability level showing connectivity only; carbon atoms are isotropic, ^iPr groups omitted for clarity.

3.4.2 Reactivity with **2.9**: synthesis and characterisation of **3.15**

CO_2 will insert into the ‘tethered’ $\text{U-C}_{\text{alkyl}}$ bond of **2.9** to form a dimeric bridging carboxylate, $\{\text{U}(\text{COT}^{\text{TIPS}_2})(\mu\text{-}\eta^5\text{:}\kappa^2(\text{O},\text{O}')\text{-C}_5\text{Me}_4\text{CH}_2\text{O}_2\text{C})\}_2$ (**3.15**, **Equation 3.9**).



Equation 3.9. Reactivity of CO_2 with **2.9**.

Crystalline **3.15** is sparingly soluble in benzene or toluene, but soluble enough in THF for collection of ^1H and $^{13}\text{C}\{^1\text{H}\}$ NMR spectroscopic data: the $^{13}\text{C}\{^1\text{H}\}$ NMR spectrum contained a single weak signal at 60.37 ppm, and the ^1H NMR spectrum contained resonances correctly integrating to environments expected for the structure shown below in **Figure 3.16**. No resonances could be detected in the $^{29}\text{Si}\{^1\text{H}\}$ NMR spectrum of **3.15**, despite collection for a large number of scans. Mass spectrometric

data collected did not show the expected parent ion at $m/z = 1668$, however the 100% ion at $m/z = 834$ corresponds to the half-molecule fragment ‘U(COT^{TIPS2})(C₅Me₄CH₂O₂¹³C)’. IR spectroscopic data collected for **3.15** differed to those collected for the carboxylates **3.12-3.14**, not containing an asymmetric CO vibrational band at ca 1500 cm⁻¹. Instead, the presence of a vibrational band at 1372 cm⁻¹ attributed to the ν_{OCO} frequency reflects the bridging nature of the tethered carboxylate ligands.⁵⁸ Elemental analysis of a crystalline sample of **3.15** returned the expected result. Crystals formed from a benzene solution stored at ambient temperature yielded red crystals suitable for X-ray diffraction studies. Recrystallisation from a saturated THF solution afforded **3.15** in a 57% yield.

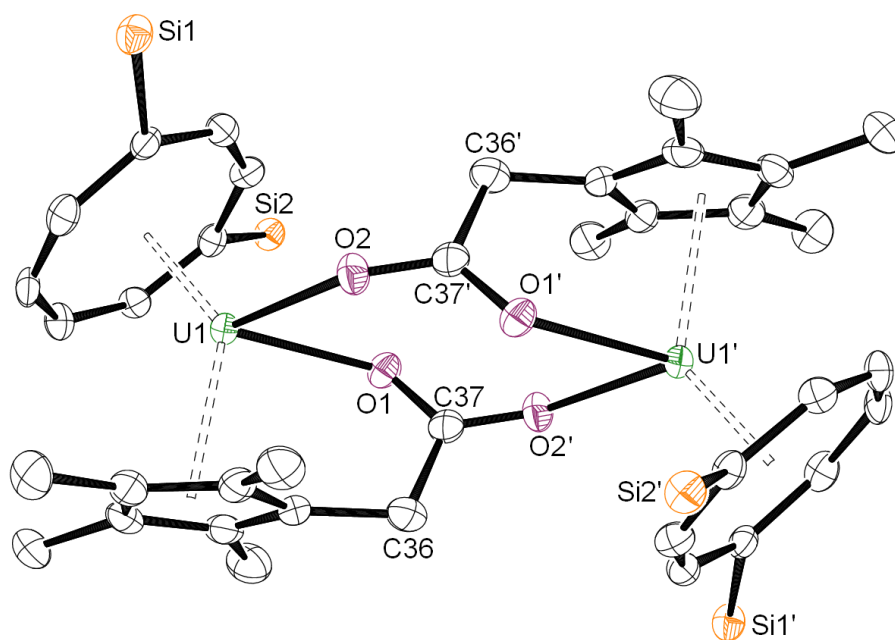


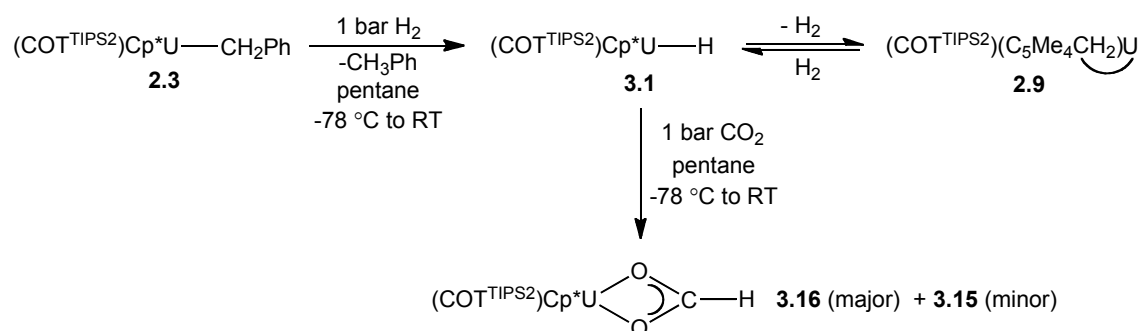
Figure 3.16. Molecular structure of **3.15**. ORTEP representation with thermal ellipsoids at the 50% probability level. Hydrogen atoms, ⁱPr groups and molecule of co-crystallised benzene omitted for clarity. ‘Grown’ asymmetric unit shown; two halves of the molecule are related by symmetry. Selected bond lengths and angles: U1-O1: 2.405(3) Å, U1-O2: 2.404(3) Å, O1-U1-O2: 70.32(12) °, O1-C37-O2: 122.8(5) °.

Whilst **3.15** differs structurally from the other two crystallographically characterised carboxylates **3.12** and **3.13** with its bridging O₂C moiety tethered to the Cp ring, the U1-O1 and U1-O2 bond distances in **3.15** are still similar to the

U-O_{carboxylate} values reported for the two terminal carboxylates. The O-U-O angle of 70.32(12) ° in **3.15** is considerably larger than those in **3.12** and **3.13** (53.1(2)/53.2(2) ° and 52.82(17) ° respectively) due to the less constrained bridging carboxylates versus the terminal carboxylates. In the two structurally comparable U(IV) bridging acetate structures reported by Brianese *et al.*⁵⁶ and Rebizant *et al.*⁵⁷ – **3G** and **3H**, discussed in relation to complex **3.13** in section 3.4.1.2 – the O-C-O bridging acetate angles range from 122(2) to 125(1) ° in **3G**, and from 124(2) to 128(2) ° in the **3H**. The close proximity of the two U centres (enforced by the bridging ‘tethered’ Cp-ligands) in **3.15** means that the O1-C37-O2 angle of 122.8(5) ° is more acute than the other reported O-C-O_{carboxylate} angles for **3G** and **3H**, which exist in molecules without such steric constraints.

3.4.3 Reactivity with **3.1**: synthesis and characterisation of **3.16**

The generation of **3.1** (with some **2.9** also present in solution – see section 3.2.1) *in situ* followed by the addition of CO₂ resulted in the formation of **3.16**, along with a small quantity of the tethered bridging carboxylate complex, **3.15** (Scheme 3.15). The same reaction can be carried out using stoichiometric ¹³CO₂ in C₆D₆ in a J Young NMR tube.



Scheme 3.15. Synthesis of **3.16** from **2.3**, via **3.1** generated *in situ*.

Crystalline **3.16** was obtained in a 33% yield from slow-cooling a pentane solution to -30 °C. Comparison of ¹H NMR spectra collected from **3.16** and ¹³C-**3.16** confirms the assignment of the O₂CH proton on the κ²-formate ligand as a singlet at

8.58 ppm, which splits into a doublet with $^1J_{\text{CH}} = 209$ Hz when $^{13}\text{CO}_2$ is used. The $^{13}\text{C}\{^1\text{H}\}$ and ^{13}C NMR spectra of ^{13}C -**3.16** contain a singlet or a doublet with $J_{\text{CH}} = 210$ Hz respectively, correlating to the inserted $^{13}\text{CO}_2$ carbon atom, attached to a single proton. Also noted was the similar chemical shifts of the $\text{COT}^{\text{TIPS}^2}$ and Cp^* ligand resonances in the ^1H NMR spectrum of **3.16** to those in the spectra of carboxylates **3.12-3.14**, attributed to the similar ligand environments around the uranium centre in all four complexes. The $^{29}\text{Si}\{^1\text{H}\}$ NMR spectrum contained a single resonance at -84.0 ppm, corresponding to the Si^iPr_3 environment. Mass spectrometric analysis showed a parent ion at $m/z = 835$ (56%, M^+) and a 100% ion at $m/z = 700$, corresponding to the fragment ' $\text{UCOT}^{\text{TIPS}^2}\text{O}_2\text{CH}$ '. Elemental analysis returned the expected C and H percentages. Collection and refinement of X-ray diffraction data obtained for **3.16** confirmed the structure as the κ^2 -formate complex, $\text{U}(\text{COT}^{\text{TIPS}^2})\text{Cp}^*(\kappa^2\text{-O}_2\text{CH})$ (**Figure 3.17**). Selected bond lengths and angles are detailed in **Table 3.5**.

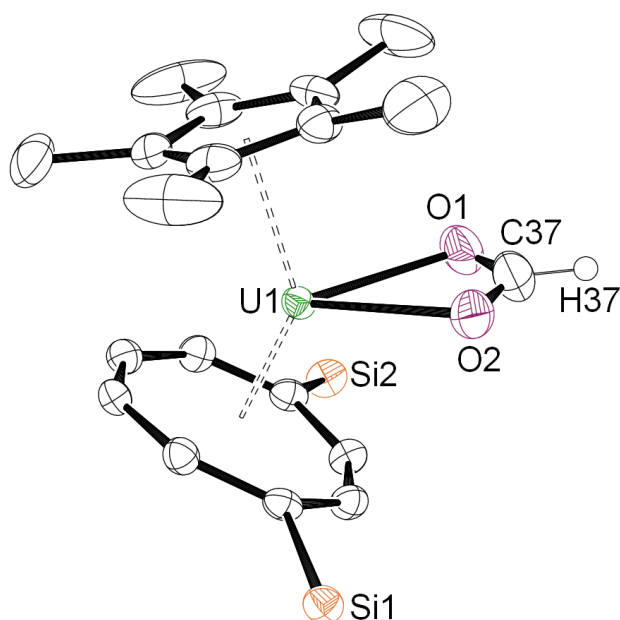


Figure 3.17. Molecular structure of **3.16**. ORTEP representation with thermal ellipsoids at the 50% probability level. Hydrogen atoms (except H37) and $i\text{Pr}$ groups omitted for clarity.

As with the carboxylate complexes, the formate complex is bidentate and monomeric – the first crystallographically characterised example of a U(IV)

mono-formate complex of this particular form. The only other structurally characterised U(IV) formate complexes available for comparison to **3.16** are two hexanuclear formates containing bridging formate ligands, reported by Takao *et al.* in 2009 (no ESDs were reported with the data).⁵⁹ The U-O_{formate} bond distances in the two complexes lie between 2.396 to 2.495 Å, and the equivalent distances in **3.16** fall within this range. The bridging formate O-U-O angles range from 123.16 to 135.86 °, more obtuse than the O-U-O angle of 122.2(5) ° in **3.16**, as expected from the differing hapticity of the bridging vs terminal ligands. In comparison to the crystallographically characterised U(IV) mixed-sandwich carboxylate complexes in this work, U(COT^{TIPS2})Cp*(κ²-O₂CR) (where R = CH₂Ph **3.12**, Me **3.13**), **3.16** contains very similar bond lengths and angles (Table 3.5). The Ct1-U and Ct2-U distances in **3.16** are marginally shorter, due to the small size of the single hydrogen attached to the carboxylate moiety in comparison to the bulkier CH₂Ph and CH₃ groups, allowing closer approach of the COT^{TIPS2} and Cp* rings. The U-O and O1-C37-O2 metrics in **3.16** are slightly greater than in **3.12** and **3.13**, again attributed to the presence of a hydrogen in place of a bulkier and electronically differing alkyl group.

Table 3.5. Selected bond distances (Å) and angles (°) from carboxylates **3.12** and **3.13**, and formate **3.16**. Ct1 is defined as the COT ring centroid, Ct2 is defined as the Cp* ring centroid.

	3.12	3.13	3.16
Ct1-U	1.953(2), 1.956(2)	1.9512(16)	1.9370(14)
Ct2-U	2.472(4), 2.469(7)	2.482(2)	2.4732(19)
U-O	2.405(5), 2.423(5) 2.424(5), 2.419(5)	2.409(5), 2.408(5)	2.451(3), 2.455(3)
Ct1-U-Ct2	140.26(11), 140.29(17)	137.94(8)	138.31(7)
O-C-O	118.7(8), 119.9(8)	120.4(8)	122.2(5)

Infrared spectra were collected from samples of **3.16** made using both ¹²CO₂, and ¹³CO₂, in order to confirm the vibrational band correlating to the carboxylate ligand. ReactIR equipment was used to collect the *in situ* IR spectrum of ¹²C-**3.16** as a solution in methylcyclohexane: a vibrational band was observed at 1588 cm⁻¹ as the reaction

between **3.1** and stoichiometric $^{12}\text{CO}_2$ occurred, alongside the initial appearance and subsequent disappearance of a band at 2339 cm^{-1} corresponding to free $^{12}\text{CO}_2$ (**Figure 3.18**).

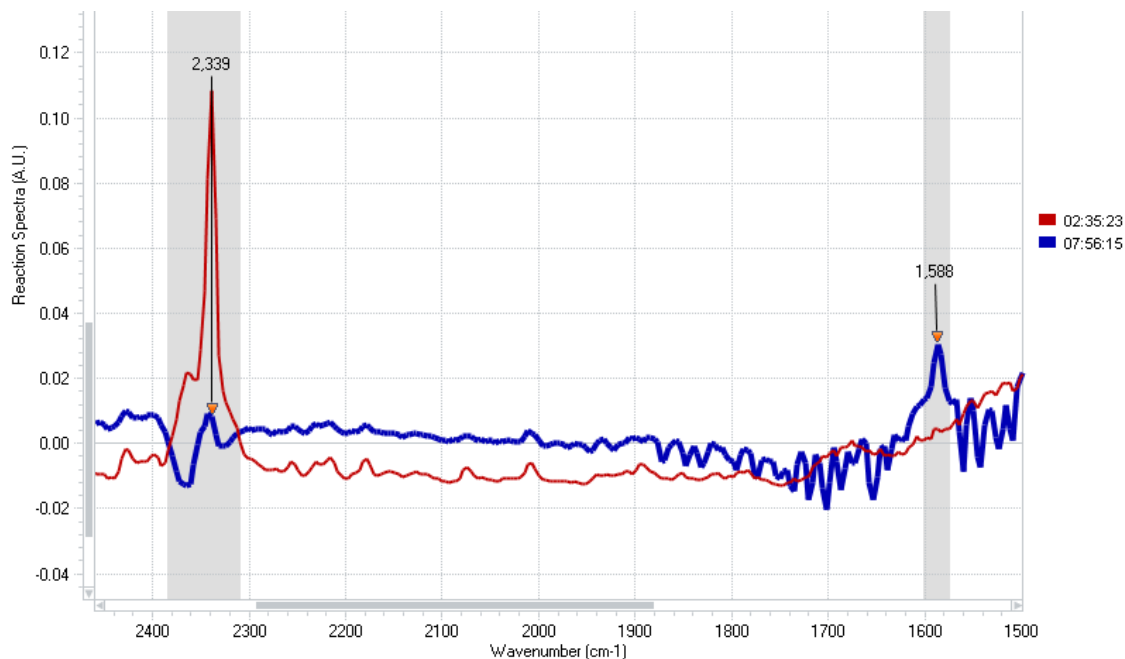


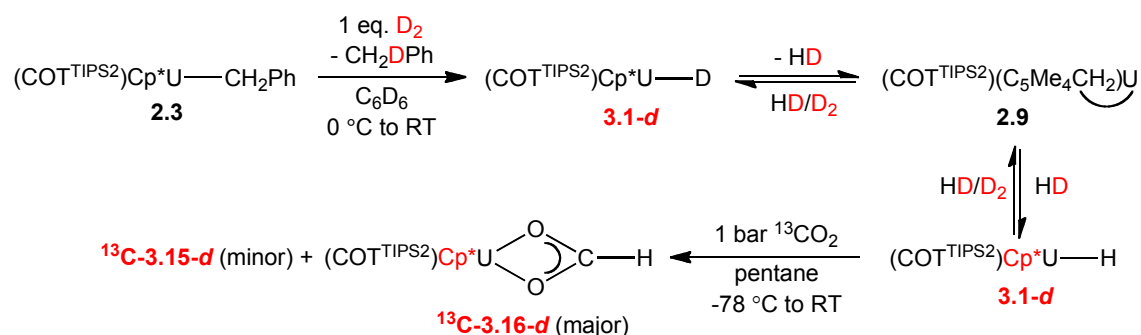
Figure 3.18. ReactIR spectra collected at two time-points during the reaction of **3.1** and $^{12}\text{CO}_2$. Red: immediately after $^{12}\text{CO}_2$ addition; blue: after formation of **3.16**.

The solid-state IR spectrum of **3.16** synthesised from $^{13}\text{CO}_2$ contained a medium-intensity band at 1558 cm^{-1} , corresponding to vibrations of the $-\text{O}_2^{13}\text{CH}$ moiety. The vibration is in the same region as the IR stretches observed for the carboxylates **3.12-3.14** (1506 , 1501 , and 1504 cm^{-1} respectively).

3.4.3.1 Deuterium-labelling studies: **3.1** and D_2

The reaction of **2.3** with D_2 , followed by the addition of $^{13}\text{CO}_2$, was carried out with the intention of observing a signal in the ^2H NMR spectrum of the product at ca 8.6 ppm , and a triplet of intensity 1:1:1 in the $^{13}\text{C}\{^1\text{H}\}$ NMR spectrum at ca -20 ppm , both signals corresponding to a $-\text{O}_2^{13}\text{CD}$ moiety. However, no such signals were observed – the ^2H NMR spectrum contained two resonances at $\delta_{\text{H}} 7.35$ and 4.92 , corresponding to $\text{Cp}^*\text{-C(H/D)}_3$ of $^{13}\text{C-3.16-d}$ and $^{13}\text{C-3.15-d}$ respectively –

an effect of scrambling upon addition of D₂ to **2.3** (Scheme 3.16). No deuterium was present on the TIPS groups of either of these complexes: the addition of ¹³CO₂ was performed within 10 minutes of the D₂ addition, and the rate of scrambling for the TIPS-CH₃ groups is qualitatively slower than for the Cp*-CH₃ groups, so no TIPS-CH₃ scrambling occurs in this time.



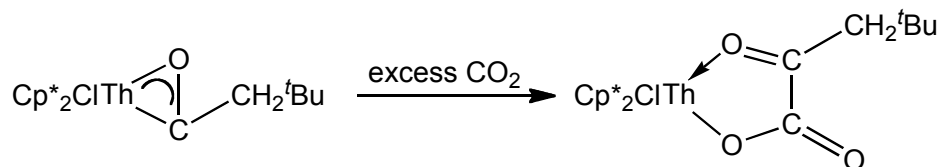
Scheme 3.16. Presence of deuterium (indicated in red) in products formed from the reaction of **2.3** with D₂ and ¹³CO₂.

The ¹³C{¹H} NMR spectrum contained a broad singlet at -20.1 ppm, along with other very low-intensity resonances between δ_C -18.0 and -20.9. Still present in the ¹H NMR spectrum was a doublet at 8.54 ppm, integrating to a value of somewhat less than 1H relative to the other ligand ¹H resonances, assigned to the formate O₂¹³CH proton. As was concluded from the deuterium labelling studies performed with **3.1**, the exclusive formation of the deuteride ‘U(COT^{TIPS}₂)Cp*D’ does not occur, hence the products formed from the reaction of **3.1-d** and ¹³CO₂ will be a mixture of U(COT^{TIPS}₂)Cp*(κ²-O₂¹³CH) molecules with deuterium present on the Cp* ring.

3.4.4 Further CO₂ reactivity

The insertion of CO₂ into a U-C bond occurs for the alkyl complexes, as demonstrated above. In the three η²-acyls, **3.2-3.4**, a U-C bond is still present, and could potentially insert CO₂. The reactivity of f-element acyl complexes with CO₂ is described in only one report: ThCp*₂Cl(η²-OC-CH₂^tBu) reacts with CO₂ to form a “host of products”, as described by the authors.⁶⁰ One proposed product is shown in

Equation 3.10, deduced from IR spectroscopic data (a band at 1653 cm^{-1} correlating to the C=O moiety) and from structural precedent of the reaction of isoelectronic diphenylketene, or CO in the presence of PR_3 (R = organyl), with the η^2 -acyl complex.⁵¹



Equation 3.10. Proposed product from CO_2 insertion into the Th-C bond of an η^2 -acyl complex.

After reviewing the literature, it became apparent that no CO_2 insertion reactions with organouranium η^2 -acyl complexes have been reported, so experiments were carried out to investigate the reactivity of acyls **3.2-3.4** with CO_2 .

In order to lend support to the theory that the η^2 -acyl complexes **3.2-3.4** react with further equivalents of CO_2 due to the presence of a U-C bond, the CO-insertion product of the ‘tuck-in’ complex (**3.7** as a mixture of *cis* and *trans*-isomers) and enediolate (**3.8**) were each exposed to CO_2 . Due to the lack of a U-C bond in these complexes, a reaction was not anticipated. Examination of the reactivity of the ethoxide complex, $\text{U}(\text{COT}^{\text{TIPS}2})\text{Cp}^*(\text{OEt})$ (**2.7**), which contains a U-O bond (as do **3.7** and **3.8**) was also undertaken for comparison of spectroscopic data. Details of these reactions are described below.

3.4.4.1 Reactivity of CO_2 with η^2 -acyls

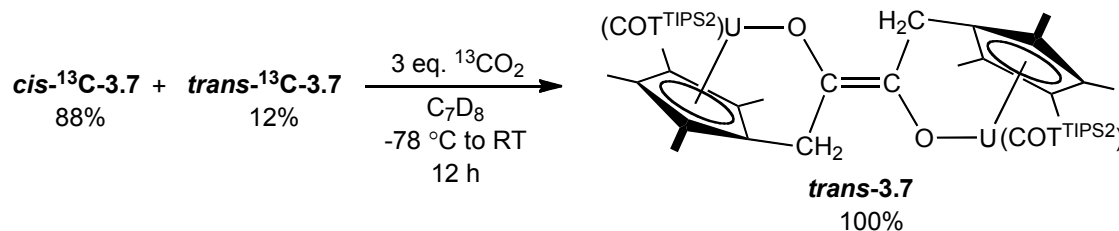
Upon exposure to either stoichiometric or excess CO_2 , each acyl undergoes an immediate reaction as determined by ^1H NMR spectroscopic analysis. No obvious pattern of reactivity is shared for the three acyls, appearing to form dissimilar products, and no detailed conclusions could be drawn from NMR spectra collected. $^{13}\text{C}\{^1\text{H}\}$ NMR spectroscopy was employed in tandem with labelling studies with

combinations of ^{12}C and ^{13}C labelled CO and CO₂ gases, but provided no conclusive results as to the structure or nature of the products formed. The only changes observed in IR spectra collected *in situ* for the reactions of **3.3** and **3.4** with CO₂ were weak vibrational bands at 1653 and 1655 cm⁻¹ respectively, which could be assigned to a ‘carbonyl’-type moiety, however, the intensities of the bands were too low to justify confident assignment. Decomposition of uranium-containing species in all three cases was rapid, and subjecting the reaction mixtures to reduced pressure resulted in the complete disappearance of any organouranium complexes, complicating further analysis.

In conclusion, while it is evident that further reactivity with CO₂ does occur with the acyl complexes, there is not enough data available to determine the outcome of the reactions. However, this does highlight the potential for multiple-insertion chemistry with U-C bonds, homologating or potentially functionalising CO and CO₂ in a series of reactions.

3.4.4.2 Isomerisation of *cis*-**3.7** to *trans*-**3.7**

Exposure of a crystalline sample of ^{13}C -**3.7** (as a mixture of *cis* and *trans* isomers in a ratio of ca 7:1) to an excess (ca 3 eq.) of $^{13}\text{CO}_2$ resulted in a change in the relative ratios of the resonances corresponding to the TIPS groups of the *cis* and *trans* products of ^{13}C -**3.7** from 7:1 to 5:1, as observed in the ^1H NMR spectrum collected 15 minutes after the gas addition. The ^{13}C NMR spectrum also showed an increase in intensity of the *trans*- ^{13}C -**3.7** resonance at 346 ppm relative to the *cis*- ^{13}C -**3.7** resonance at 301 ppm. Three hours later, ^1H NMR spectroscopic analysis showed a further increase in proportion of *trans*- ^{13}C -**3.7** present in the reaction mixture to a *cis:trans* ratio of 0.42:1. After a total of 12 hours, no *cis*- ^{13}C -**3.7** was present in solution, as determined by ^1H and ^{13}C NMR spectroscopy (Equation 3.11).



Equation 3.11. Isomerisation of *cis*-**3.7** to *trans*-**3.7** upon $^{13}\text{CO}_2$ addition.

Although $^{13}\text{CO}_2$ appears to initiate this isomerisation, the relative intensity of the ^{13}C NMR spectroscopic resonance correlating to the added $^{13}\text{CO}_2$ (125 ppm) does not change over the course of the isomerisation reaction, indicating that it is not consumed and could instead be acting as a catalyst. The reaction also does not appear to be reversible: no procedure has been found to re-form the *cis*-isomer after the *trans*-isomer is produced. Labelling studies were carried out to determine whether exchange occurs between the double-bonded carbon in **3.7** and CO_2 , however, no evidence for exchange was observed. Samples of $^{13}\text{C-3.7}$ exposed to $^{12}\text{CO}_2$ showed resonances in the $^{13}\text{C}\{^1\text{H}\}$ NMR spectrum for *trans*- $^{13}\text{C-3.7}$ after the reaction had proceeded, and samples of $^{12}\text{C-3.7}$ exposed to $^{13}\text{CO}_2$ did not show ^{13}C -labelled signals after isomerisation.

The role of CO_2 acting solely as a catalyst in the isomerisation reaction was established by the addition of a sub-stoichiometric quantity of $^{13}\text{CO}_2$ to $^{12}\text{C-3.7}$ (ca 10 mol%), with the reaction progress followed by $^{13}\text{C}\{^1\text{H}\}$ and ^1H NMR spectroscopy. Free $^{13}\text{CO}_2$ was observed immediately after the gas addition, and $^{12}\text{C-3.7}$ was present as both isomers in a *cis:trans* ratio of 7:1. Over a period of 8 days, the isomerisation of *cis*- $^{12}\text{C-3.7}$ to *trans*- $^{12}\text{C-3.7}$ occurred – this rate was noticeably slower than when the addition of stoichiometric or excess CO_2 was performed. No changes were observed in the $^{13}\text{C}\{^1\text{H}\}$ NMR spectrum, indicating that no ^{13}C was incorporated into the *trans* product, and no $^{13}\text{CO}_2$ was consumed. The relative intensities of the TIPS doublets attributable to *cis*- and *trans*- $^{12}\text{C-3.7}$ were recorded relative to an internal standard over the 8 day period, and are plotted in **Figure 3.19**.

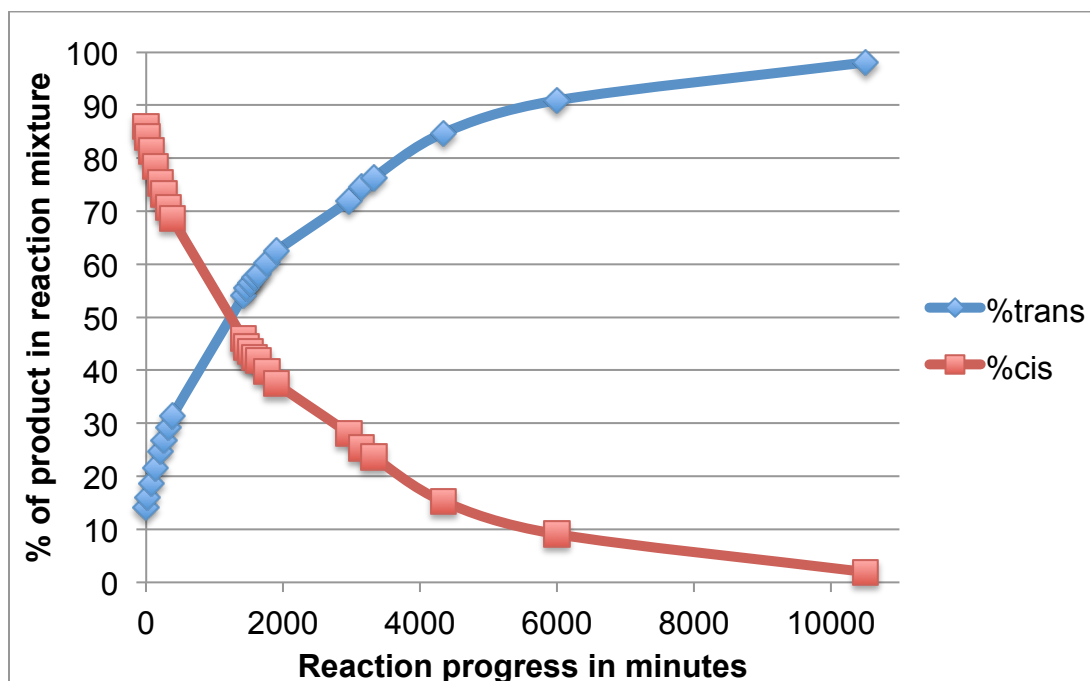
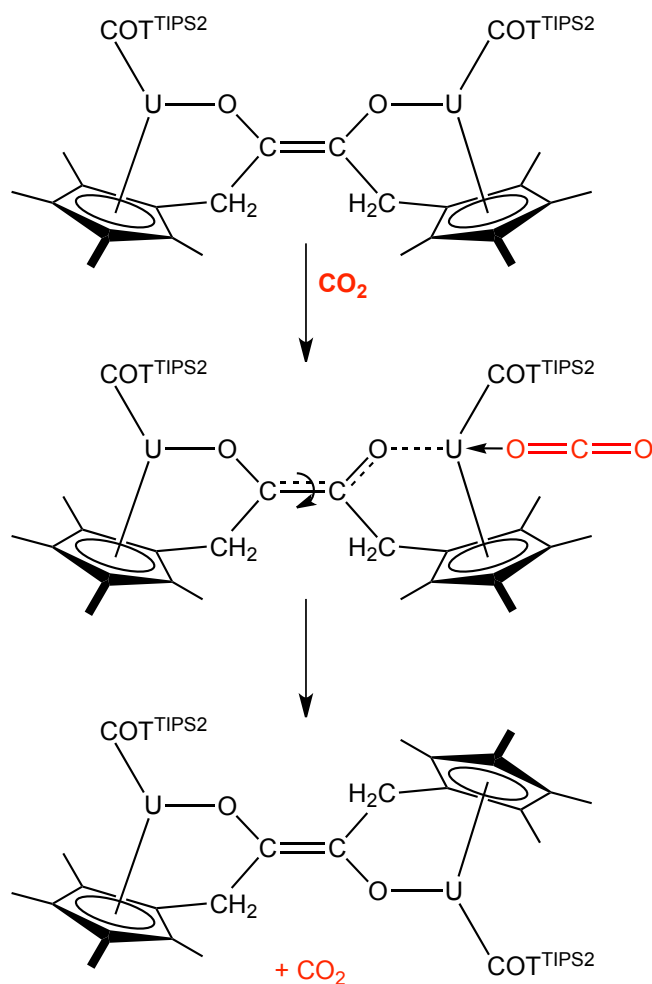


Figure 3.19. Graph showing the relative percentages of *cis*- and *trans*-3.7 present in solution over a period of 8 days, as determined by ^1H NMR spectroscopy.

The mechanism of isomerisation can be considered as one of two pathways: either the C=C bond is broken completely, allowing for the generation of a carbenic monomer and re-combination to form *trans*-3.7, or the C=C bond is distorted due to electron density redistribution in the molecule, allowing a 180° rotation around the bond. It is difficult to postulate a mechanism involving CO_2 wherein the C=C double bond is broken completely; it is possible that CO_2 could weakly coordinate to a uranium centre, altering the bonding between the 'U-O-C=C-O-U' linkage. This could cause the C=C bond to lengthen and become more single-bond-like in character, allowing for rotation to form the *trans*-isomer (**Scheme 3.17**). Since there has been no evidence to suggest that the reverse isomerisation from *trans*- to *cis*-3.7 is also possible, it is thought that the *trans*-isomer is the favoured thermodynamic product, as supported by DFT studies carried out by Maron and Kefalidis (see Appendix 1). The addition of more CO_2 to a solution containing solely *trans*-3.7 elicits no further isomerisation back to *cis*-3.7, even at elevated temperatures or under photolysis conditions.

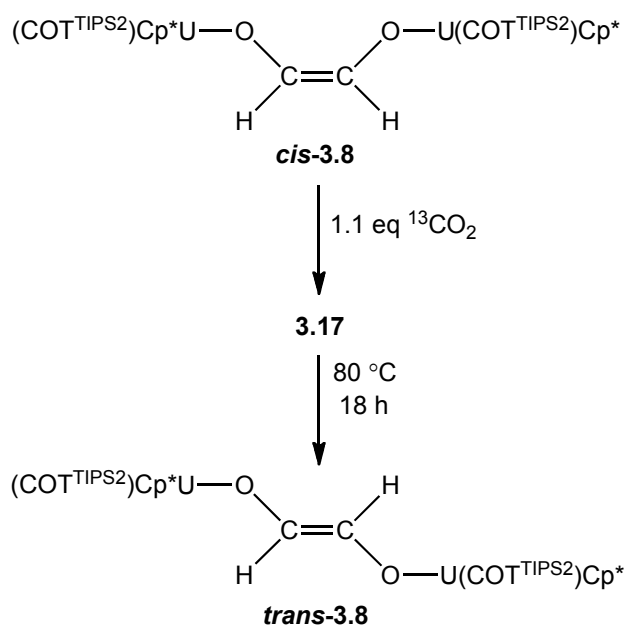


Scheme 3.17. Postulated route to *trans*-3.7 via coordination of CO₂.

To test the idea that the CO₂ may coordinate as an “L-type” ligand to the uranium metal centre, allowing for a change in electronics in the system and freeing the C=C double bond for rotation, other “L-type” ligands were also added to a mixture of *cis*- and *trans*-3.7. Neither THF nor acetonitrile yielded any isomerisation, as confirmed by ¹H NMR spectroscopic studies, and the 7:1 *cis:trans* product ratio was maintained. Further investigation into the mechanism of this unusual isomerisation is warranted, and more extended DFT mechanistic studies could be of great use for elucidating the reaction pathway.

3.4.4.3 Isomerisation of *cis*-3.8 to *trans*-3.8

Following the findings that CO₂ enables the isomerisation of *cis*-3.7 to *trans*-3.7, a sample of *cis*-3.8 was also exposed to CO₂. No evidence is seen to support the existence of a *trans* isomer of 3.8 in crude reaction mixtures, and heating *cis*-3.8 to 90 °C for several days does not induce any change in composition. The addition of 1.1 equivalents of ¹³CO₂ to 3.8 in a J Young NMR tube resulted in a colour change from red to orange, and ¹H NMR spectroscopic analysis showed the complete consumption of 3.8. Resonances consistent with a dimeric species (*i.e.* two sets of ligand resonances, at approximately half the intensity of those seen in 3.8 relative to the solvent signal) were present. ¹³C{¹H} and ¹³C NMR data showed a broad singlet at -55 ppm, along with a peak at 125 ppm corresponding to unreacted ¹³CO₂ (as a slight excess was added) and a very low-intensity peak at 316 ppm. These initial data are consistent with the formation of a new dinuclear species, containing at least one new ¹³C environment, labelled 3.17. Heating 3.17 to 80 °C for 18 hours results in conversion to *trans*-3.8, as confirmed by X-ray diffraction studies, *vide infra* (Equation 3.12). The complete conversion of 3.17 to *trans*-3.8 was also seen after storage of a solid sample of 3.17 at ambient temperature under Ar for a period of 7 months.



Equation 3.12. Isomerisation of *cis*-3.8 to *trans*-3.8 by addition of CO₂.

Unlike the reaction of **3.7** and CO₂, the addition of a substoichiometric amount of CO₂ to **3.8** followed by heating to 80 °C for 21 days does not afford complete conversion of *cis*-**3.8** to *trans*-**3.8**; **3.17** also remains present in solution. Additionally, **3.17** – a persisting and isolable intermediate in the isomerisation – can be observed, and does correlate to a new ¹³C{¹H} NMR spectroscopic resonance. This supports the previously suggested theory that CO₂ binds or loosely coordinates to the uranium centre (or other part of the molecule). It can be rationalised that this coordination is stronger in **3.8** than in **3.7**, or that an equilibrium is established between *cis*-**3.8**, **3.17**, and *trans*-**3.8**, requiring a higher concentration of CO₂ to fully complete the isomerisation.

Conversion of *cis*-**3.8** to *trans*-**3.8** is quantitative by ¹H NMR spectroscopy after addition of CO₂ and subsequent heating; the resonance correlating to the ‘*trans*-OCH’ protons in the enediolate moiety appears at δ_H 153 ppm. Mass spectrometric analysis of *trans*-**3.8** contains an ion at 1636 m/z (M⁺ -2H), giving an essentially identical spectrum to *cis*-**3.8**. X-ray diffraction carried out on *trans*-**3.8** crystallised from DME at -35 °C confirmed the structure as shown in **Figure 3.20**.

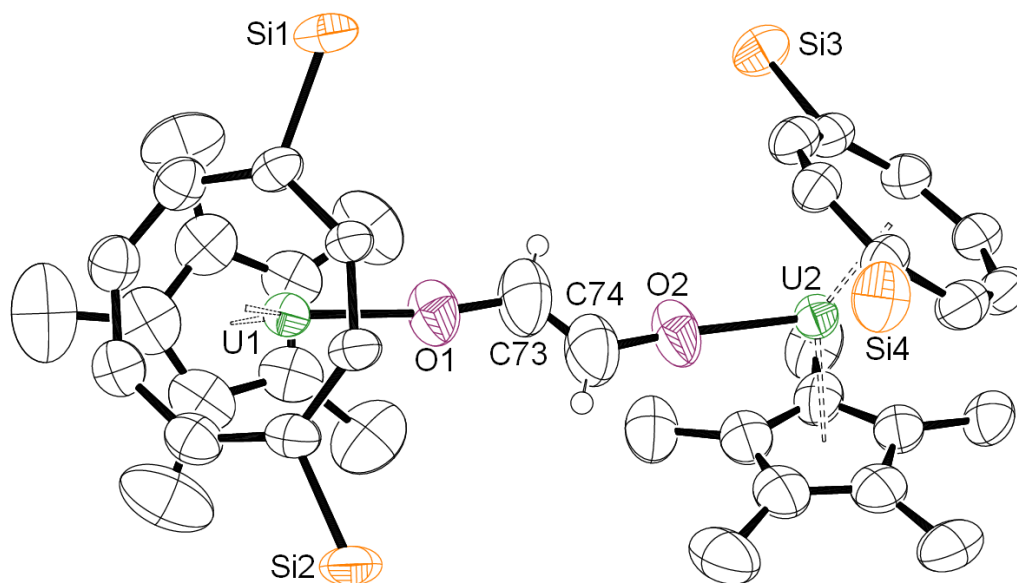


Figure 3.20. Molecular structure of *trans*-**3.8**.

ORTEP representation with thermal ellipsoids at the 50% probability level.

Hydrogen atoms (except on C73/C74) and ^tPr groups omitted for clarity.

Disorder in the TIPS groups that could not be modelled prevented full refinement of the data, and several *i*Pr carbon atoms were left isotropic: satisfactory data convergence was not achieved. Regardless, the R factor is 5.54% and the structure connectivity is clear. As has been reported during refinement of other *trans*-enediolate structures, the C=C bond distance appears to be unrealistically short at 1.24(2) Å, owing to rotational disorder in the enediolate moiety as represented by the thermal ellipsoid shape for C73 and C74.^{41,48} The U1-O1 and U2-O2 distances in *trans*-**3.8** are shorter than those found in *cis*-**3.8** (Table 3.6), as is the case for the M-O distances for *cis* vs *trans* isomers of **3B** and **3C** (see Table 3.3 for comparisons).^{41,42} The U-O distances in *trans*-**3.8** are also identical within ESDs, unlike in *cis*-**3.8** – this is reflected in the equally similar U-O-C angles in *trans*-**3.8** and varying U-O-C angles in *cis*-**3.8**. In comparison to *trans*-**3B** and *trans*-**3C**, the M-O, O-C, and M-O-C metrics of *trans*-**3.8** are reasonably similar; the O-C=C angles in *trans*-**3.8** and *trans*-**3C** are almost identical. Overall, whilst full structural comparisons of the enediolate moiety in *trans*-**3.8** to other f-block enediolates cannot be carried out, it is consistent with previously reported data.

Table 3.6. Selected bond distances (Å) and angles (°) for *cis*-**3.8**, and *trans*-**3.8**, -**3B** and -**3C**.

	<i>cis</i> - 3.8	<i>trans</i> - 3.8	<i>trans</i> - 3B	<i>trans</i> - 3C
M-O	2.168(5), 2.113(5)	2.091(7), 2.098(7)	2.122(8), 2.107(7)	2.118(3)
O-C	1.333(10), 1.344(9)	1.324(15) 1.317(15)	1.334(15), 1.374(17)	1.351(8)
C=C	1.302(10)	1.24(2)	0.964(18) [†]	1.28(1)
M-O-C	115.7(4), 148.5(5)	171.5(9), 170.8(11)	161.9(14), 168.8(10)	165.5(3)
O-C=C	128.0(7), 130.5(7)	120.4(17), 124.1(17)	154.5(20), 158.2(18)	124.9(7)

[†] The authors state that this bond distance is unrealistic due to issues with disorder in the enediolate moiety.

Further data were sought to identify the intermediate **3.17**. No crystalline material suitable for X-ray diffraction studies could be isolated after attempts to crystallise **3.17**

from a range of common solvents. The IR spectrum of **3.17** was collected *in situ* using ReactIR, adding an excess of $^{13}\text{CO}_2$ to **3.8** (synthesised from **3.1** and ^{12}CO) dissolved in methylcyclohexane. During the course of the reaction, the only significant change in the spectrum (aside from the vibrational bands associated with added $^{13}\text{CO}_2$) was a low-intensity vibration at 1329 cm^{-1} . However, the vibrational band is extremely weak in relation to the solvent signals, and its presence does not necessarily indicate that a new species has formed; fluctuations in spectra are often observed upon changes in temperature whilst performing *in situ* IR reactions.

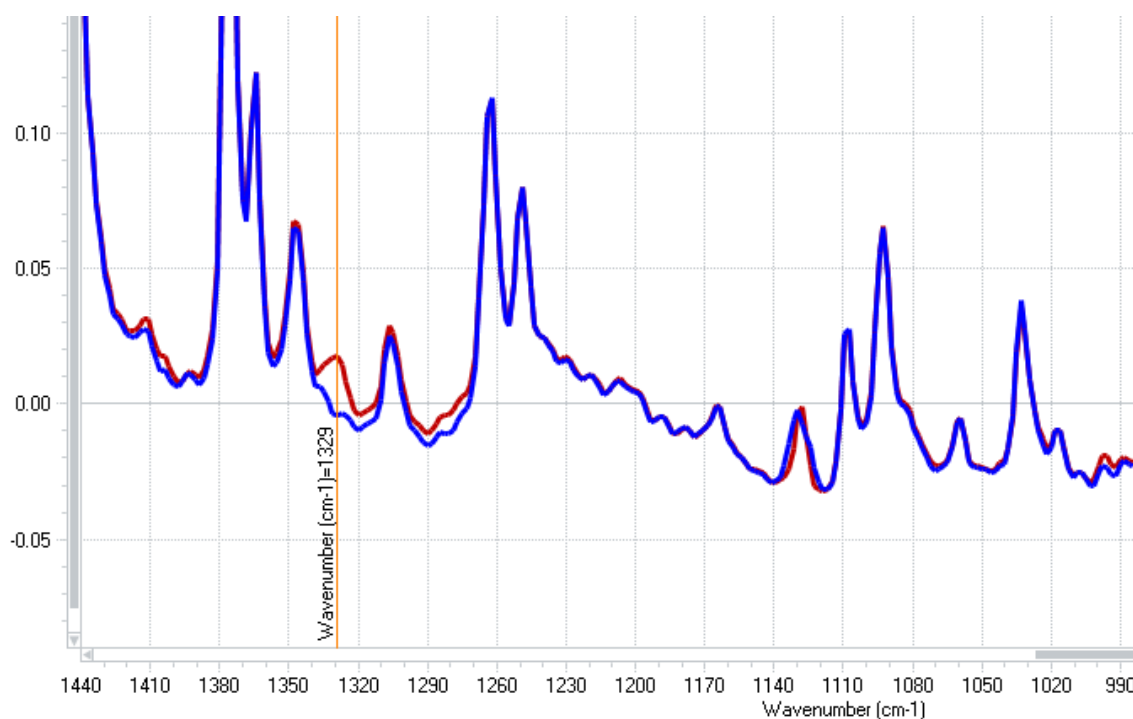


Figure 3.21. ReactIR spectra collected from the reaction mixture of **3.8** + $^{13}\text{CO}_2$ (**3.17**). Spectra obtained before (blue) and after (red) addition of $^{13}\text{CO}_2$.

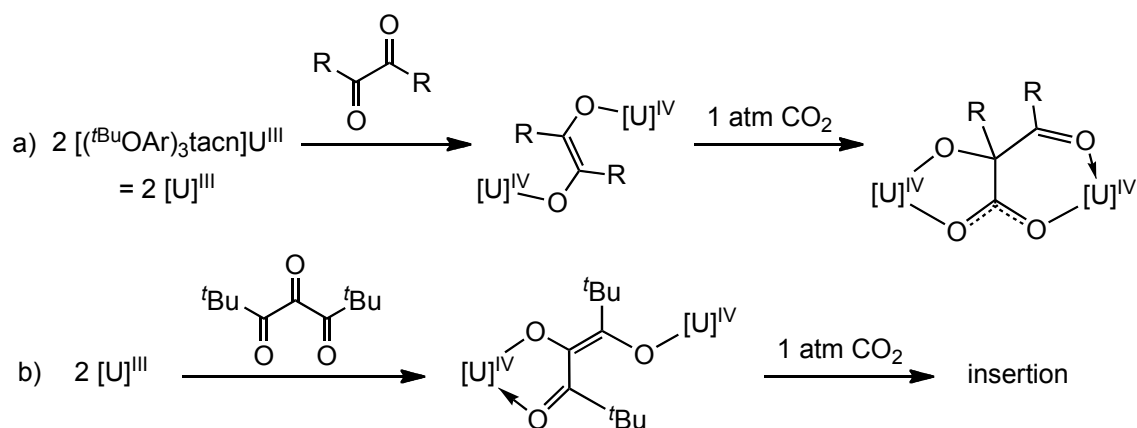
The reaction mixture was retrieved from the ReactIR equipment, and all volatiles removed under reduced pressure to give red solids. Mass spectrometric analysis of these solids returns a spectrum almost identical to that of **3.8**: an ion at m/z 1638 (2%) was the highest value ion observed. It was postulated that, like in the case of ethoxide **2.5** and CO_2 , the product is not stable with respect to loss of CO_2 , and the reaction may be reversible. To trial this, the red solids not used for mass spectrometric analysis were dissolved in C_6D_6 and their ^1H and $^{13}\text{C}\{^1\text{H}\}$ NMR spectrum were obtained. It was

observed that the ^1H NMR spectrum contained approximately a 1:1 mixture of **3.8** and **3.17**; the $^{13}\text{C}\{^1\text{H}\}$ NMR spectrum showed a resonance at -55 ppm correlating to **3.17**. These data indicate that either the reaction of **3.8** with $^{13}\text{CO}_2$ did not go to completion in the ReactIR apparatus, or that the resulting product **3.17** is unstable with respect to CO_2 loss and has partially reverted back to **3.8** while the sample was manipulated. If the latter case is correct, then it is possible that during the process of collecting the mass spectrum, the sample rapidly loses CO_2 in the instrument and hence no parent ion for **3.17** is observed.

It is possible that **3.17** is a substituted carbonate product of the form $\{\text{U}(\text{COT}^{\text{TIPS}2})\text{Cp}^*\}_2(\mu\text{-}\kappa^2:\kappa^2\text{-O}_2\text{CO-CH=CH=OCO}_2)$, which is somewhat unstable with respect to CO_2 loss when subjected to prolonged vacuum, rather than an intermediate that loosely binds CO_2 . This would imply that insertion of CO_2 into a U-O bond occurs, and could also be true of the reaction of the ‘tucked-in’ CO insertion product, *cis*-**3.7**, upon exposure to CO_2 , facilitating subsequent isomerisation by an unknown mechanism.

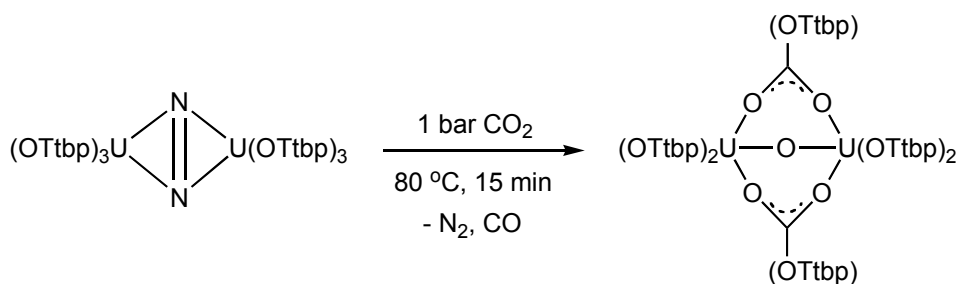
The insertion of CO_2 into U-C σ -bonds is well documented, however, the reaction of CO_2 with a species containing a U-O bond has also been seen, albeit in only a few cases. Meyer *et al.* reported the formation of bridging carbonate species, $\{((^t\text{BuArO})_3\text{Mes})\text{U}\}_2(\mu\text{-}\kappa^2:\kappa^2\text{-CO}_3)$ and $\{((^{\text{Ad}}\text{ArO})_3\text{N})\text{U}\}_2(\mu\text{-}\kappa^1:\kappa^2\text{-CO}_3)$ from the reaction of the parent U(III) species with an excess of CO_2 .⁶¹ In order to investigate the mechanism of this reductive transformation, the corresponding mono-oxo bridged species $[\{((^t\text{BuArO})_3\text{Mes})\text{U}\}_2(\mu\text{-O})]$ and $[\{((^{\text{Ad}}\text{ArO})_3\text{N})\text{U}\}_2(\mu\text{-O})]$ were treated with CO_2 ; this afforded the carbonate compounds, considered to be a result of the insertion of CO_2 into one of the U-O bonds, as also evidenced by computational studies.⁶² This is not insertion into a U-O single bond, but into a longer bridging oxo U-O bond, yet it is still evidence that U-O bonds are not entirely inert to insertion reactions – as would be anticipated given the highly oxophilic nature of uranium. Further to these examples, Meyer *et al.* also reported the reaction of CO_2 with two uranium(IV) enolate complexes,

supported by a macrocyclic ligand framework, $\{({}^t\text{BuArO})_3\text{tacn}\}$ (**Scheme 3.18a**).⁶³ Exposure of the enolates to 1 atm of CO_2 resulted in the addition of CO_2 between the two U centres along with the formation of a new C-C bond. Treatment of the U^{III} precursor, $\{({}^t\text{BuArO})_3\text{tacn}\}\text{U}^{\text{III}}$, with the triketone ${}^t\text{BuCOCOCO}{}^t\text{Bu}$, gives a dinuclear compound that contains asymmetric binding of the tricarbonyl moiety – one U centre is bound to two oxygen atoms, and the other U centre binds to the third oxygen with a U-O bond length of 2.313(4) Å (**Scheme 3.18b**). This complex also reacts with CO_2 , which inserts into the aforementioned U-O bond, however, the authors do not report the product structure due to poor quality X-ray diffraction data.



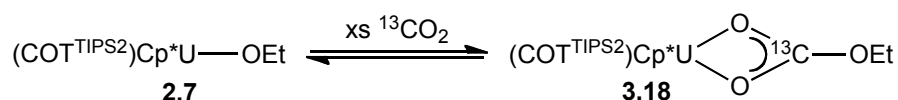
Scheme 3.18. Reaction of $\{({}^t\text{BuOAr})_3\text{tacn}\}\text{U}^{\text{III}}$ with a) 1,2 diketone (where $\text{R} = \text{Ph}$, ${}^t\text{Bu}$) to give enolate products, which will insert CO_2 and b) with di-*tert*-butyl triketone to give a dinuclear product, which will insert CO_2 .

A recent report by Arnold *et al.* has also confirmed that CO_2 will insert into the U-O bond of an aryloxy ligand.⁶⁴ Exposure of $\{\text{U}(\text{OTtbp})_3\}_2(\text{N}_2)$ (where $\text{OTtbp} = \text{OC}_6\text{H}_2-2,4,6-{}^t\text{Bu}_3$), to 1 bar of CO_2 yields a reaction either after 16 hours at ambient temperature, or after 15 minutes at 80°C . Structural characterisation of the green material isolated revealed the insertion of CO_2 into the U-O bond of one of the OTtbp ligands, forming two bridging carbonates (**Scheme 3.19**).



Scheme 3.19. Insertion of CO₂ into the U-O bond of an aryloxide ligand.

An available mixed-sandwich species synthesised in this work containing a single U-O bond is the terminal ethoxide complex, U(COT^{TIPS2})Cp*(OEt) (**2.7**), which can be synthesised rationally from the chloride precursor **2.2** and KOEt, *vide supra*. The U-O bond distance in **2.7** is 2.063(4) Å, marginally shorter than the [{{(AdArO)₃N}U}₂(μ-O)] U-O bond distance of 2.1036(2) Å. To examine the behaviour of a U-O bond in the mixed-sandwich system in isolation, the reaction of ethoxide **2.7** and CO₂ was performed and suggested to reversibly form a substituted carbonate (**Equation 3.13, 3.18**).



Equation 3.13. Proposed reversible insertion of CO₂ into the U-O bond of **2.7**.

Exposure of **2.7** to an excess of ¹³CO₂ resulted in the appearance of some low-intensity resonances in the collected ¹H NMR spectrum after 20 minutes, at chemical shift values similar to those reported for carboxylates **3.12-3.14**. The ¹³C{¹H} NMR spectrum contained resonances at 125 ppm (free ¹³CO₂) and at -49.0 ppm, indicative of a single new ¹³C-labelled species. The NMR spectra are consistent with the formation of a product containing a ligand environment similar to the carboxylates, ‘O₂C-R’, owing to the positions of the COT^{TIPS2} and Cp* ligand proton shifts. Regular collection of ¹H and ¹³C{¹H} NMR spectra over a period of 5 days showed no further conversion of **2.7** into **3.18**, however, the resonances attributed to the new product began to decrease in intensity, and other low-integral paramagnetic signals appeared. After a total of 9 days after ¹³CO₂ addition, the

resonances corresponding to **3.18** had entirely disappeared. In their place were four new TIPS doublets and a range of other low-intensity resonances, which could not be sufficiently interpreted. Attempted workup of the reaction yielded only the starting material, **2.7**. Removal of the headspace from a reaction mixture of **2.7** and CO₂ and subsequent analysis by NMR spectroscopy showed the presence of solely **2.7**, indicating reversibility of the reaction, and rendering full characterisation of the product impossible. ReactIR was used to follow the reaction of **2.7** and CO₂ *in situ*, however, the only change in the spectrum collected after CO₂ addition was a low-intensity vibrational band at 1300 cm⁻¹. This could be attributable to an alkyl carbonato ν_{OCO} stretch, as similar IR vibrations are reported for transition metal and lanthanide alkyl carbonato in the region *ca* 1600-1300 cm⁻¹,⁶⁵⁻⁶⁷ however, the resonance is not of high enough intensity to definitively characterise it as a ν_{OCO} vibration.

In comparison to the intermediate **3.17** formed from the reaction of enediolate **3.8** and CO₂, the spectroscopic data and behaviour of **3.18** are similar: the ¹³C{¹H} NMR spectroscopic resonances appear in the same region (-55 and -49 ppm) as do the associated IR bands (1329 and 1300 cm⁻¹), and neither complex contains a parent ion in their mass spectra. It could be proposed that both **3.17** and **3.18** may share a structural similarity, involving interaction between CO₂ and either the uranium centre or the existing U-O bonds in the parent complexes, which in the case of **3.17** allows for subsequent isomerisation. However, without further investigation, this cannot be confirmed.

3.5 Conclusions and chapter summary

The synthesis of a monomeric hydride complex, U(COT^{TIPS2})Cp*H (**3.1**), can be achieved from the reaction of **2.3-2.6** and H₂. It has been shown that **3.1** is unstable with respect to hydrogen loss: it exists in equilibrium with the common decomposition product ‘tuck-in’ (**2.9**), formed by the activation of a Cp*-CH₃ group and loss of H₂, and will also undergo reductive elimination of H₂ in a bimolecular fashion to yield

trivalent $\text{U}(\text{COT}^{\text{TIPS}_2})\text{Cp}^*$ (**2.1**). Studies carried out using D_2 in place of H_2 to form **3.1-d** have shown the extent of deuterium exchange that occurs and have given insight into this reductive dihydrogen loss. Full characterisation of **3.1** has not been possible due to instability, however, further reactivity with small molecules has provided further evidence for its existence, and the comprehensive study of CO_2 and CO insertion into a monomeric U-H bond in the same ligand system has been carried out for the first time.⁶⁸

The insertion of CO and CO_2 into U-C alkyl bonds has been demonstrated, forming η^2 -acyl or κ^2 -carboxylate complexes in most cases. The ‘tethered’ U-C bond of **2.9** will also undergo insertion reactions with CO and CO_2 , as precedented in the literature; the product of **2.9** and CO (**3.7**) agrees with the previously stated ‘carbenic’ nature of the inserted ‘ CO ’ moiety, enabling the formation of a new C=C bond. However, the nature of the tethered bond in **2.9** is not entirely analogous to alkyls **2.3-2.5**, as it reacts more slowly with CO , allowing for an unidentified product (**3.10**) to form in the presence of H_2 and CO , *via* a currently unknown pathway. This highlights the importance of studying both classical U-C bonds and ‘tethered’ U-C bonds, which show different reactivity, as literature precedent corroborates.^{33,69–73} Studying the insertion chemistry of isonitriles and other small molecules with **2.9**, could give more information about potential intermediates in the reaction pathways that form **3.9** and **3.10**, and should be examined in the future.

Insertion chemistry into the U-H bond of **3.1** has also been studied, and formate and enediolate complexes are formed from reactions with CO_2 and CO respectively. The enediolate complex **3.8** is formed exclusively as the *cis*-isomer, along with side-products identified as pentamethylbenzene – formed from the ring-expansion of Cp^* with a U-bound ‘C-H’ fragment – and a bis- μ -oxo species, $\{\text{U}(\text{COT}^{\text{TIPS}_2})(\mu\text{-O})\}_2$. DFT mechanistic studies performed by Maron and Kefalidis suggest that **3.8** is formed *via* a ketene intermediate, and not by dimerisation of a transient η^2 -formyl. No further reactivity between **3.8** and H_2 to form methoxide, $\text{U}(\text{COT}^{\text{TIPS}_2})\text{Cp}^*(\text{OCH}_3)$ (**3D**), is observed.

Further reactivity is shown between the acyls **3.2-3.4** and CO₂, forming uncharacterised insertion products, and between the enediolate complexes **3.7** and **3.8**, initiating isomerisation reactions from *cis*- to *trans*- isomers. Steric hindrance around the metal centre may be a factor limiting the multiple insertions of CO in metallocene systems such as UCp*₂(η²-OCR)₂ or UCp₃(η²-OCR), in contrast to the more ‘open’ COT^{TIPS2} and Cp* mixed-sandwich system. Whilst the reaction between **3.7** and CO₂ is spontaneous and does not require stoichiometric CO₂, the reaction between **3.8** and CO₂ forms an uncharacterised intermediate **3.17**, which when heated forms *trans*-**3.8**. The identity of **3.17** is unknown, however, it is thought to be similar to the product of the ethoxide (**2.7**) and CO₂, **3.18**, and could be either a substituted carbonate complex or loosely-coordinated to CO₂.

3.6 Compound naming for Chapter 3

- 3.1** – U(COT^{TIPS2})Cp*H
3.2 – U(COT^{TIPS2})Cp*(η²-OCCH₂Ph)
3.3 – U(COT^{TIPS2})Cp*(η²-OCCH₃)
3.4 – U(COT^{TIPS2})Cp*(η²-OCCH₂TMS)
3.5 – U(COT^{TIPS2})Cp*(η¹-OC{TMS}=CH{TMS})
3.6 – U(COT^{TIPS2})Cp*Me with excess CO
3.7 – (η⁵:κ¹-C₅Me₄CH₂OC=COCH₂C₅Me₄){U(COT^{TIPS2})₂}
3.8 – {U(COT^{TIPS2})Cp*}₂(μ-κ¹:κ¹-OCH=CHO)
3.9 – {U(COT^{TIPS2})O}₂
3.10 – Proposed ‘tethered’ alkoxide from **2.9** with 1:1 ¹³CO/H₂
3.11 – Second product of **2.9** with 1:1 ¹³CO/H₂
3.12 – U(COT^{TIPS2})Cp*(κ²-O₂CCH₂Ph)
3.13 – U(COT^{TIPS2})Cp*(κ²-O₂CCH₃)
3.14 – U(COT^{TIPS2})Cp*(κ²-O₂CCH₂TMS)
3.15 – {U(C₈H₆{SiⁱPr₃-1,4})₂}(μ¹:μ¹-κ¹:η⁵-C₅Me₄CH₂OCO)₂
3.16 – U(COT^{TIPS2})Cp*(κ²-O₂CH)
3.17 – {U(COT^{TIPS2})Cp*}₂(μ-η¹:η¹-OCH=CHO) and CO₂ intermediate
3.18 – ‘U(COT^{TIPS2})Cp*(κ²-O₂COEt)’

3.7 References for Chapter 3

1. H. W. Turner, S. J. Simpson, and R. A. Andersen, *J. Am. Chem. Soc.*, 1979, **101**, 2782.
2. J.-C. Berthet and M. Ephritikhine, *New J. Chem.*, 1992, **16**, 767–768.
3. Z. Lin and T. J. Marks, *J. Am. Chem. Soc.*, 1990, **112**, 5515–5525.
4. M. Ephritikhine, *Chem. Rev.*, 1997, **97**, 2193–2242.
5. W. J. Evans, K. A. Miller, S. A. Kozimor, J. W. Ziller, A. G. Dipasquale, and A. L. Rheingold, *Organometallics*, 2007, **26**, 3568–3576.
6. D. J. Grant, T. J. Stewart, R. Bau, K. A. Miller, S. A. Mason, M. Gutmann, G. J. McIntyre, L. Gagliardi, and W. J. Evans, *Inorg. Chem.*, 2012, **51**, 3613–3624.
7. T. M. Gilbert, R. R. Ryan, and A. P. Sattelberger, *Organometallics*, 1989, **8**, 857–859.
8. J. M. Manriquez, P. J. Fagan, and T. J. Marks, *J. Am. Chem. Soc.*, 1978, **100**, 3939–3941.
9. S. J. Simpson, H. W. Turner, and R. A. Andersen, *Inorg. Chem.*, 1981, **20**, 2991–2995.
10. M. R. Duttera, P. J. Fagan, T. J. Marks, and V. W. Day, *J. Am. Chem. Soc.*, 1982, **104**, 865–867.
11. J. W. Bruno, H. A. Stecher, L. R. Morss, D. C. Sonnenberger, and T. J. Marks, *J. Am. Chem. Soc.*, 1986, **108**, 7275–7280.
12. Z. Lin and T. J. Marks, *J. Am. Chem. Soc.*, 1987, **109**, 7979–7985.
13. D. Baudry, P. Charpin, M. Ephritikhine, M. Lance, M. Nierlich, and J. Vigner, *J. Chem. Soc., Chem. Commun.*, 1987, 739–740.
14. J.-F. Le Maréchal, C. Villiers, P. Charpin, M. Lance, M. Nierlich, J. Vigner, and M. Ephritikhine, *J. Chem. Soc., Chem. Commun.*, 1989, 308–310.
15. J.-C. Berthet, J.-F. Le Maréchal, and M. Ephritikhine, *J. Chem. Soc., Chem. Commun.*, 1991, 360–361.
16. J.-C. Berthet, J.-F. Le Maréchal, M. Lance, M. Nierlich, J. Vigner, and M. Ephritikhine, *J. Chem. Soc., Dalton Trans.*, 1992, **1992**, 1573–1577.
17. J.-C. Berthet, C. Villiers, J.-F. Le Maréchal, B. Delavaux-Nicot, M. Lance, M. Nierlich, J. Vigner, and M. Ephritikhine, *J. Organomet. Chem.*, 1992, **440**, 53–65.
18. P. Gradoz, C. Boisson, D. Baudry, M. Lance, M. Nierlich, J. Vigner, and M. Ephritikhine, *J. Chem. Soc., Chem. Commun.*, 1992, 1720–1721.
19. D. Baudry, A. Dormond, and A. Hafid, *New J. Chem.*, 1993, **17**, 465.
20. P. J. Fagan, J. M. Manriquez, E. A. Maatta, A. M. Seyam, and T. J. Marks, *J. Am. Chem. Soc.*, 1981, **103**, 6650–6667.
21. W. J. Evans, K. A. Miller, A. G. DiPasquale, A. L. Rheingold, T. J. Stewart, and R. Bau, *Angew. Chem. Int. Ed.*, 2008, **47**, 5075–5078.
22. E. Montalvo, K. A. Miller, J. W. Ziller, and W. J. Evans, *Organometallics*, 2010, **29**, 4159–4170.
23. M. R. MacDonald, M. E. Fieser, J. E. Bates, J. W. Ziller, F. Furche, and W. J. Evans, *J. Am. Chem. Soc.*, 2013, **135**, 13310–3.
24. A. S. P. Frey, F. G. N. Cloke, M. P. Coles, L. Maron, and T. Davin, *Angew. Chem.*, 2011, **123**, 7013–7015.
25. N. Tsoureas, *Unpublished results*, 2013.
26. D. R. Lide, Ed., *CRC Handbook of Chemistry and Physics: 86th Edition*, Taylor & Francis, 86th edn., 2005.

27. J. M. Manriquez, P. J. Fagan, T. J. Marks, C. S. Day, and V. W. Day, *J. Am. Chem. Soc.*, 1978, **100**, 7112–7114.
28. P. J. Fagan, J. M. Manriquez, T. J. Marks, V. W. Day, S. H. Vollmer, and C. S. Day, *J. Am. Chem. Soc.*, 1980, **102**, 5393–5396.
29. K. G. Moloy and T. J. Marks, *J. Am. Chem. Soc.*, 1984, **106**, 7051–7064.
30. D. C. Sonnenberger, E. A. Mintz, and T. J. Marks, *J. Am. Chem. Soc.*, 1984, **106**, 3484–3491.
31. G. Paolucci, G. Rossetto, P. Zanella, K. Yünlü, and R. D. Fischer, *J. Organomet. Chem.*, 1984, **272**, 363–383.
32. M. Weydert, J. G. Brennan, R. A. Andersen, and R. A. Bergman, *Organometallics*, 1995, **14**, 3942–3951.
33. N. A. Siladke, J. W. Ziller, and W. J. Evans, *J. Am. Chem. Soc.*, 2011, **133**, 3507–3516.
34. W. J. Evans, D. B. Rego, J. W. Ziller, A. G. Dipasquale, and A. L. Rheingold, *Organometallics*, 2007, **26**, 4737–4745.
35. W. J. Evans, K. J. Forrestal, and J. W. Ziller, *J. Am. Chem. Soc.*, 1995, **117**, 12635–12636.
36. W. J. Evans, S. A. Kozimor, G. W. Nyce, and J. W. Ziller, *J. Am. Chem. Soc.*, 2003, **125**, 13831–13835.
37. C. L. Webster, J. E. Bates, M. Fang, J. W. Ziller, F. Furche, and W. J. Evans, *Inorg. Chem.*, 2013, **52**, 3565–3572.
38. N. A. Siladke, J. W. Ziller, and W. J. Evans, *Z. Anorg. Allg. Chem.*, 2010, **636**, 2347–2351.
39. K. Tatsumi, A. Nakamura, P. Hofmann, R. Hoffmann, K. G. Moloy, and T. J. Marks, *J. Am. Chem. Soc.*, 1986, **108**, 4467–4476.
40. C. E. Kefalidis and L. Maron, *Private Communication*, 2014.
41. W. J. Evans, J. W. Grate, and R. J. Doedens, *J. Am. Chem. Soc.*, 1985, **107**, 1671–1679.
42. E. L. Werkema, L. Maron, O. Eisenstein, and R. A. Andersen, *J. Am. Chem. Soc.*, 2007, **129**, 2529–2541.
43. F. H. Allen and A. J. Kirby, *J. Am. Chem. Soc.*, 1984, **106**, 6197–6200.
44. R. J. Kahan, *PhD Second Year Report*, 2013.
45. C. Villiers, R. Adam, and M. Ephritikhine, *J. Chem. Soc., Chem. Commun.*, 1992, 1555–1556.
46. P. J. Fagan, K. G. Moloy, and T. J. Marks, *J. Am. Chem. Soc.*, 1981, **103**, 6959–6962.
47. D. A. Katahira, K. G. Moloy, and T. J. Marks, *Organometallics*, 1982, **1**, 1723–1726.
48. J. M. Manriquez, D. R. McAlister, R. D. Sanner, and J. E. Bercaw, *J. Am. Chem. Soc.*, 1978, **100**, 2716–2724.
49. P. T. Wolczanski, R. S. Threlkel, and J. E. Bercaw, *J. Am. Chem. Soc.*, 1979, **101**, 218–220.
50. L. Maron, *Private Communication*, 2013.
51. K. G. Moloy, P. J. Fagan, J. M. Manriquez, and T. J. Marks, *J. Am. Chem. Soc.*, 1986, **108**, 56–61.
52. D. McKay, A. S. P. Frey, J. C. Green, F. G. N. Cloke, and L. Maron, *Chem. Commun.*, 2012, **48**, 4118–4120.
53. A. L. Arduini and J. Takats, *Inorg. Chem.*, 1981, **20**, 2480–2485.
54. E. M. Matson, W. P. Forrest, P. E. Fanwick, and S. C. Bart, *J. Am. Chem. Soc.*, 2011, **133**, 4948–4954.

55. Â. Domingos, J. Marçalo, N. Marques, and A. Pires de Matos, *Polyhedron*, 1992, **11**, 501–506.
56. N. Brianese, U. Casellato, F. Ossola, M. Porehia, G. Rossetto, P. Zanella, and R. Grazini, *J. Organomet. Chem.*, 1989, **365**, 223–232.
57. J. Rebizant, M. R. Spirlet, C. Apostolidis, and B. Kanellakopoulos, *Acta Crystallogr. Sect. C: Cryst. Struct. Commun.*, 1992, **48**, 452–454.
58. G. B. Deacon, F. Huber, and R. J. Phillips, *Inorg. Chim. Acta*, 1985, **104**, 41–45.
59. S. Takao, K. Takao, W. Kraus, F. Emmerling, A. C. Scheinost, G. Bernhard, and C. Hennig, *Eur. J. Inorg. Chem.*, 2009, **2009**, 4771–4775.
60. K. G. Moloy and T. J. Marks, *Inorg. Chim. Acta*, 1985, **110**, 127–131.
61. O. P. Lam, S. C. Bart, H. Kameo, F. W. Heinemann, and K. Meyer, *Chem. Commun.*, 2010, **46**, 3137–3139.
62. L. Castro, O. P. Lam, S. C. Bart, K. Meyer, and L. Maron, *Organometallics*, 2010, **29**, 5504–5510.
63. S. J. Zuend, O. P. Lam, F. W. Heinemann, and K. Meyer, *Angew. Chem. Int. Ed.*, 2011, **50**, 10626–10630.
64. S. M. Mansell, N. Kaltsoyannis, and P. L. Arnold, *J. Am. Chem. Soc.*, 2011, **133**, 9036–9051.
65. T. V Ashworth and E. Singleton, *J. Chem. Soc., Chem. Commun.*, 1976, 204.
66. T. Ito, K. Hamamoto, S. Kurishima, and K. Osakada, *J. Chem. Soc., Dalton Trans.*, 1990, 1645.
67. L. A. M. Steele, T. J. Boyle, R. A. Kemp, and C. Moore, *Polyhedron*, 2012, **42**, 258–264.
68. J. A. Higgins, F. G. N. Cloke, and S. M. Roe, *Organometallics*, 2013, **32**, 5244–5252.
69. W. J. Evans, E. Montalvo, S. A. Kozimor, and K. A. Miller, *J. Am. Chem. Soc.*, 2008, **130**, 12258–12259.
70. W. J. Evans, N. A. Siladke, and J. W. Ziller, *Chem.--Eur. J.*, 2009, **16**, 796–800.
71. W. J. Evans, N. A. Siladke, and J. W. Ziller, *C. R. Chim.*, 2010, **13**, 775–780.
72. N. A. Siladke, J. LeDuc, J. W. Ziller, and W. J. Evans, *Chem.--Eur. J.*, 2012, **18**, 14820–14827.
73. N. A. Siladke, C. L. Webster, J. R. Walensky, M. K. Takase, J. W. Ziller, D. J. Grant, L. Gagliardi, and W. J. Evans, *Organometallics*, 2013, **32**, 6522–6531.

CHAPTER 4: SYNTHESIS AND REACTIVITY OF A MIXED-SANDWICH U(IV) PRIMARY AMIDO AND RELATED COMPLEXES

4.1 Organouranium amido complexes

4.1.1 Introduction and scope of section

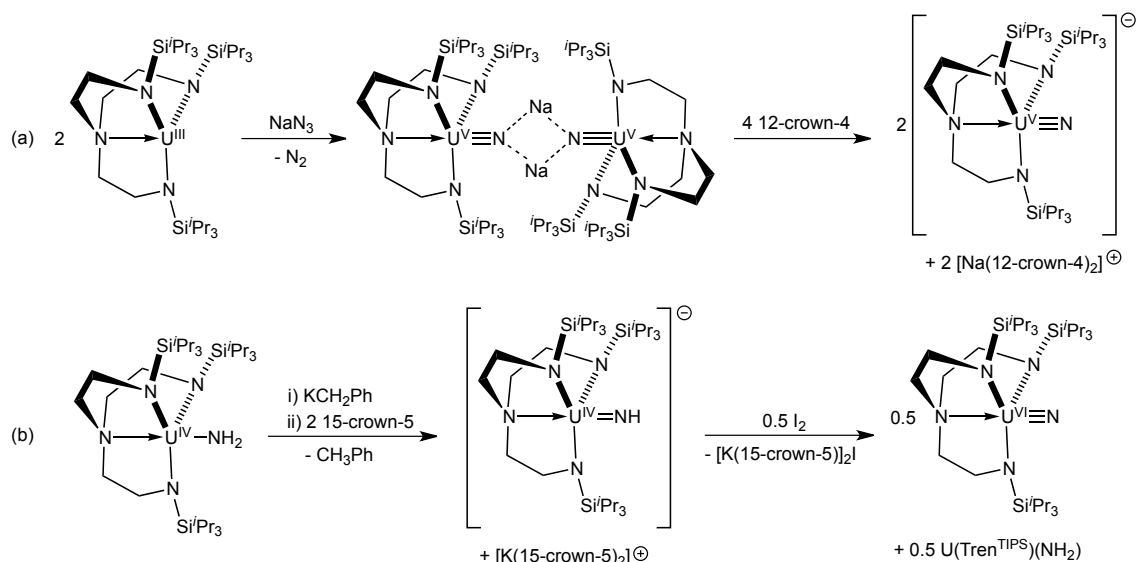
The study of uranium-nitrogen bond reactivity has not been as widely reported in the literature in comparison to uranium-carbon bonds. Whilst U-C bonds have been examined in the context of their insertion reactivity towards small molecules, U-N bonds have been utilised more frequently in ‘inert’ ligand frameworks, supporting U(III) and U(IV) metal centres. In general, U-N bonds are thermodynamically more stable and more kinetically inert than U-C bonds, and as such are more commonly used as spectator ligands to give well-defined metal centres for further reactivity studies.¹ A large number of nitrogen-based ligand frameworks have been designed and used in organouranium chemistry; a summary of these appear in Chapters 1 and 5, with reference to complexes containing U-C σ -bonds and small molecule activation.

Homoleptic amides were investigated as part of the research initiative to synthesise volatile uranium complexes for isotope separation in the 1940s and 50s. The isolation of the first homoleptic U(IV) amido complex, $\text{U}(\text{NEt}_2)_4$, was first described by Gilman *et al.* in 1956.^{2,3} Since then, other homoleptic alkyl- and aryl-amides of the form $\text{U}(\text{NR}_2)_4$ have been reported, where R = Me, ^tBu, Ph (and partially-fluorinated derivatives), ⁿBu, and ⁿPr.⁴⁻⁷ The most ubiquitous amido ligand utilised in organouranium chemistry is the mono-anionic silyl-substituted amide, $[\text{N}^-]$, first reported bound to uranium by Andersen and co-workers in 1979.⁸ Other silyl-substituted variants, either monodentate or multidentate, have been used extensively for both U(III) and U(IV) centres, for their ability to sterically stabilise these reactive species.^{9,10} A limited number of U(IV) terminal

mono- or bis-alkylamido groups exist within cyclopentadienyl or cyclooctatetraenyl ligand frameworks (U-NHPh, -NPh₂, -NMe₂, -NMeEt, -NEt₂, -NHET, -NH(2,6-Me₂Ph), -NH^tBu),¹¹⁻¹⁸ and there are fewer still examples of mono-N^m complexes that also contain cyclopentadienyl moieties and derivatives thereof.^{12,15,19,20} Examples of U(III) amido complexes also exist, both in metallocene and non-metallocene frameworks.^{21,22} Complexes containing primary amido ligands are scarce in U(IV) organometallic systems: the two reported examples in the literature are the bis-amido complex, U(C₅H₂^tBu₃)₂(NH₂)₂,²³ and a mono-amido complex, U(Tren^{TIPS})(NH₂) (Tren^{TIPS} = {N(CH₂CH₂NSi^tPr₂)₃}).²⁴

Uranium imido complexes are known, containing U=NR linkages (where R = alkyl) rather than the primary imido U=NH,²⁵⁻²⁹ in all reported cases except for one particular system.³⁰ Examples of isolable characterised uranium nitrides, U≡N, are extremely scarce. The study of U-N triple bonds is of interest to investigate the extent of 5f and 6d orbital participation in multiple bonding, and for the potential use of [UN]_n materials in ceramic nuclear fuels. Synthetic difficulties in isolating stable, terminal and well-defined U-N triple bonds means that the area is relatively underexplored, and only two examples of terminal nitrides have been reported to date. Addition of NaN₃ to U(Tren^{TIPS}), followed by the addition of 12-crown-4, generates a U(V) anionic uranium nitride (**Scheme 4.1a**).³¹ A U(VI) nitride in the same Tren^{TIPS} ligand framework can be generated by the deprotonation of U(Tren^{TIPS})(NH₂), followed by disproportionation instigated by the addition of I₂, or by the oxidation of [U(Tren^{TIPS})NH][Na(12-crown-4)] (**Scheme 4.1b**).²⁴

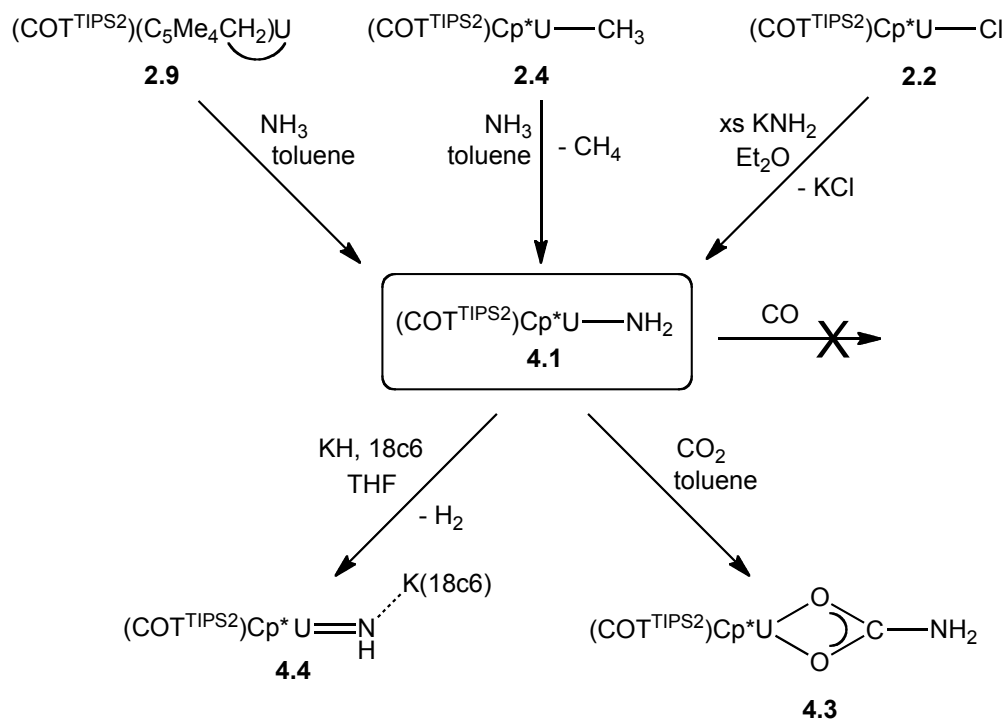
It was thought that the mixed-sandwich system utilised in this work would be successful in supporting a 'U-NH₂' linkage; it has been shown to be sufficient to stabilise highly reactive U-H and U-C bonds. As well as investigating the potential insertion of small molecules into the U-N bond of a primary amido ligand, deprotonation as a route to forming a terminal nitride complex is explored, examples of which are currently of synthetic interest.^{15,24,31}



Scheme 4.1. Routes to uranium nitride complexes for the $\text{U}(\text{Tren}^{\text{TIPS}})$ system:

(a) U(V) nitride; (b) U(VI) nitride.

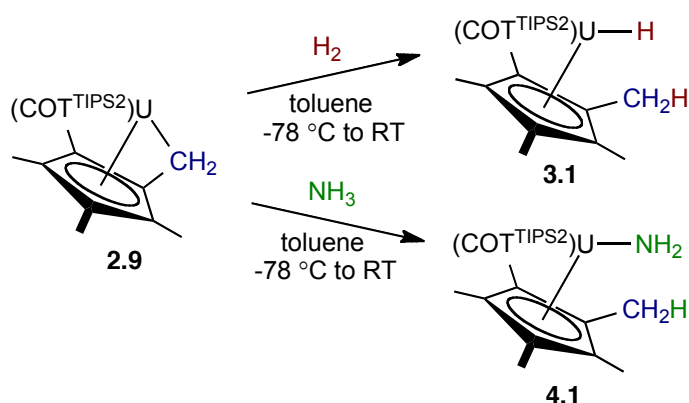
This chapter details the synthesis, insertion chemistry, and deprotonation of the primary amido $\text{U}(\text{COT}^{\text{TIPS}2})\text{Cp}^*(\text{NH}_2)$ (**4.1**), as outlined in **Scheme 4.2** below.



Scheme 4.2. Synthesis and reactivity of **4.1**.

4.1.2 Synthesis of $\text{U}(\text{COT}^{\text{TIPS}2})\text{Cp}^*(\text{NH}_2)$ (**4.1**)4.1.2.1 Synthesis from NH_3

Following the discovery that the ‘tuck-in’ complex **2.9**, which is a ‘tethered’ alkyl complex, will activate H_2 to form the hydride complex, **3.1**, the reactivity of **2.9** with NH_3 was explored. Importantly, forcing conditions (a high pressure of H_2 or raised temperatures) are not required to transform **2.9** into **3.1**. NH_3 can be activated by **2.9** under equally mild reaction conditions, providing a facile and atom-efficient route to a terminal primary amido complex, $\text{U}(\text{COT}^{\text{TIPS}2})\text{Cp}^*(\text{NH}_2)$ (**4.1**, **Scheme 4.3**).



Scheme 4.3. Synthesis of hydride (**3.1**) and primary amido (**4.1**) complexes from the ‘tethered’ alkyl (**2.9**).

The reaction of **2.9** and stoichiometric NH_3 in toluene or benzene yielded an orange-brown powder – after the removal of volatiles under reduced pressure, followed by the addition and subsequent removal of Et_2O portions – characterised as the desired amido product, $\text{U}(\text{COT}^{\text{TIPS}2})\text{Cp}^*(\text{NH}_2)$ (**4.1**), in an 83% yield. ^1H NMR spectroscopic data collected agreed with the formulation of **4.1**, and contained a broad singlet at δ_{H} 202 ppm, correlating to the U-NH₂ protons. This assignment was later confirmed by ^2H NMR spectroscopic studies using ND_3 (see section 4.1.4). Alternatively, **4.1** can be synthesised in an identical manner from the reaction of NH_3 and the alkyl **2.4**; the release of methane can be observed by ^1H NMR spectroscopy.

It was observed that using either stoichiometric or an excess of NH_3 to form **4.1** resulted in ^1H NMR spectra that showed variability in the ligand resonance chemical shifts. Typically, chemical shift values are very sensitive to the coordination environment around the uranium metal centre in paramagnetic mixed-sandwich complexes reported in this work and in the literature. Coordination of THF to $\text{U}(\text{COT}^{\text{TIPS}2})\text{Cp}^*$ (**2.1**) results in the shifting of all ligand resonances in the ^1H NMR spectrum compared to the base-free compound. The removal of THF can be achieved by heating **2.1.THF** to ca 100 °C under high vacuum (10^{-6} mbar). Upon using an excess of NH_3 when synthesising **4.1** an extra resonance at δ_{H} 8.62 is observed – this did not persist upon removal of volatiles from the reaction mixture when obtaining a crude solid product. It is possible that excess NH_3 is acting as a coordinating Lewis base, hence altering the uranium metal centre environment and inducing a change in chemical shift of the ligand proton environments; the extra resonance observed in the ^1H NMR spectrum could be attributed to weakly-bound ammonia, which is easily removed under reduced pressure. However, this interaction does not appear to affect further reactivity with small molecules (*vide infra*).

4.1.2.2 Synthesis from KNH_2 or NaNH_2

The synthesis of **4.1** can also be achieved from the salt metathesis reaction of $\text{U}(\text{COT}^{\text{TIPS}2})\text{Cp}^*\text{Cl}$ (**2.2**) with either KNH_2 or NaNH_2 in Et_2O . Unlike the immediate reaction between **2.9** and NH_3 , stirring must be maintained for 24 hours (KNH_2) or 4 days (NaNH_2), to give **4.1** in yields of 70-75% after filtration and extraction into $t\text{BuOMe}$. For both reactions, an excess of metal amide must be used for the conversion to **4.1** to reach completion. Due to the commercial unavailability of KNH_2 and the large excess needed in the above reaction (2.7 equivalents), the preferred synthetic route to **4.1** is from **2.2** and NaNH_2 , which is commercially available and more soluble in Et_2O , affording a cheaper and more straightforward synthesis, despite the longer reaction time required. The ^1H NMR spectrum of microcrystalline **4.1** isolated from this synthetic

route does not contain a peak at δ_{H} 8.62, further supporting the theory that this previously observed resonance corresponds to bound NH_3 , which is not present in this reaction mixture.

4.1.3 Characterisation of $\text{U}(\text{COT}^{\text{TIPS}_2})\text{Cp}^*(\text{NH}_2)$

Mass spectrometric analysis was carried out on solid samples of **4.1** synthesised from both **2.9** and NH_3 , and from **2.2** and MNH_2 ($\text{M} = \text{K}, \text{Na}$). In each case, the anticipated parent ion at $m/z = 806$ was observed, along with fragments corresponding to $\text{M}^+ - \text{NH}_2$ (789) and $\text{M}^+ - \text{Cp}^*$ (670). The IR spectrum of **4.1** collected as a Nujol mull between NaCl plates showed N-H symmetric and asymmetric vibrational bands at 3582 and 3309 cm^{-1} . The elemental analysis of **4.1.Et₂O**, obtained from a crude sample of **4.1** recrystallised from Et_2O , returned the expected values. It was found that **4.1** will crystallise from a range of solvents, as saturated solutions slow-cooled to $-35\text{ }^\circ\text{C}$: *t*-BuOMe, Et_2O , *iso*-pentane, methylcyclohexane, and SiMe_4 . Red prisms of **4.1.tBuOMe** were examined by X-ray diffraction to determine the molecular structure, as the quality of these crystals were highest and most suited for complete, high-resolution data collection (**Figure 4.1**). Poor-quality crystal data was also collected from crystals of **4.1.Et₂O**, however, only connectivity could be established from the data acquired.

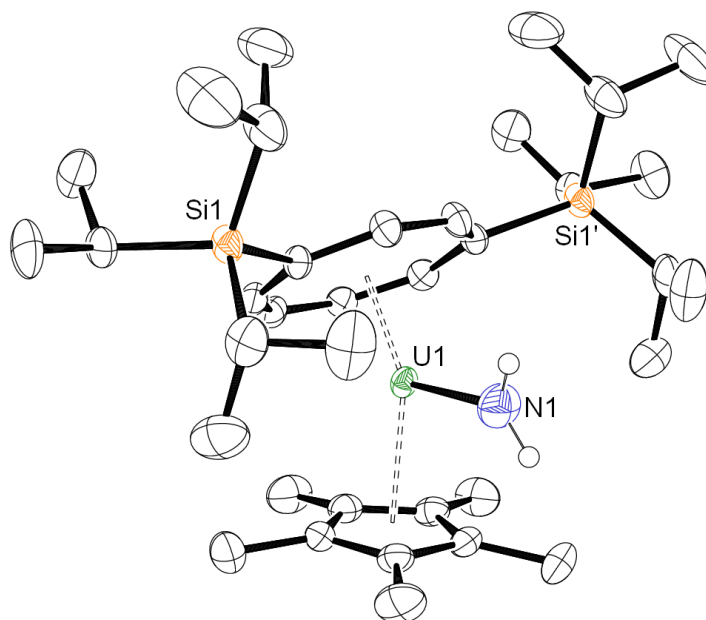


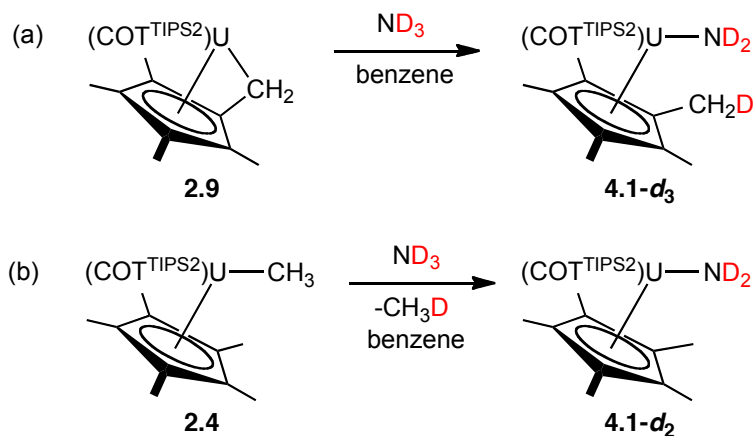
Figure 4.1. Molecular structure of **4.1**.^tBuOMe. ORTEP representation with thermal ellipsoids at the 50% probability level. Hydrogen atoms (except those on N1) and co-crystallising molecule of ^tBuOMe omitted for clarity. U1-N1: 2.217(4) Å, Ct1-U1: 1.9511(17) Å, Ct2-U1: 2.487(2) Å, Ct1-U1-Ct2: 141.88(7) °.

The two other crystallographically-characterised U(IV) primary amido complexes reported in the literature are: U(1,2,4-^tBu₃C₅H₂)₂(NH₂)₂ (**4A**),²³ and U(Tren^{TIPS})(NH₂) (**4B**).²⁴ The U1-N1 bond distance of 2.217(4) Å is essentially identical to the U-N_{amido} bond lengths in complexes **4A** and **4B** (2.228(4) and 2.194(5) Å respectively). The amido protons were not located in the Fourier difference map, but were instead fixed using a riding model; they also appear on a crystallographic symmetry plane positioned along the U1-N1 bond, and are not included in the figure above for this reason. The U1-Ct1, U1-Ct2, and Ct1-U1-Ct2 metrics are all consistent in comparison to other crystallographically characterised monomeric ‘U(COT^{TIPS2})Cp*’ complexes (see Appendix 1).

4.1.4 Deuterium labelling studies

The reaction of **2.9** and NH₃ is assumed to occur *via* a mechanism of N-H bond activation, and subsequent formation of a C-H and a U-N bond to form **4.1**; equally, the

reaction between **2.4** and NH_3 occurs by a similar mechanism, forming **4.1** and CH_4 . Experiments were performed with ND_3 in order to form the partially deuterated primary amides, **4.1- d_x** (where $x = 2$ or 3), and to locate the position of the deuterium atoms incorporated into each product. **Scheme 4.4** outlines the two experiments carried out, and the results of the reactions (as confirmed by ^1H and ^2H NMR spectroscopy): route (a) yields **4.1- d_3** ; route (b) yields **4.1- d_2** and CH_3D .



Scheme 4.4. Routes to **4.1- d_3** and **4.1- d_2** from the reaction of ND_3 with **2.9** (a) or **2.4** (b).

For the reaction of **2.9** and stoichiometric ND_3 (**Scheme 4.4a**), no resonance attributable to the U- NH_2 environment was observed at 202 ppm in the ^1H NMR spectrum, and a resonance at -6.05 ppm was seen in the ^2H NMR spectrum, corresponding to Cp*- CH_2D . A resonance at ca 202 ppm was not seen in the ^2H NMR spectrum as would be expected, corresponding to U- ND_2 , likely due to broadening effects and weak sample concentration. Data collected from the reaction of **2.4** and stoichiometric ND_3 (**Scheme 4.4b**) showed a broad singlet at 0.14 ppm in the ^1H NMR spectrum, corresponding to CH_3D , and no resonance at 202 ppm. The ^2H NMR spectrum contained only a broad singlet at 202 ppm (U- ND_2) – no CH_3D was observed due to removal of volatiles before the spectrum was collected.

In conclusion, the evidence collected from studies with ND_3 confirm that N-D bond activation occurs with both **2.9** and **2.4**, yielding a deuterated primary amido ligand in **4.1- d** . No scrambling occurs during the reaction between **2.9** and ND_3 ,

indicating that there is no intermolecular H/D exchange between the deuterium atoms on the -ND_2 ligand and the protons on the $\text{COT}^{\text{TIPS}_2}/\text{Cp}^*$ ligands, as is observed in the reaction of **2.9** and D_2 (see Chapter 4); this can be rationalised by considering that the U-N bond is stronger than the U-C bond, and hence does not undergo exchange.^{32,33}

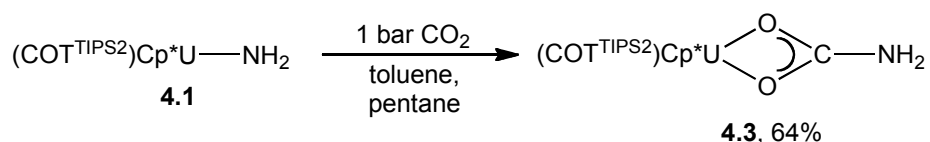
4.1.5 Attempted synthesis of $\text{U}(\text{COT}^{\text{TIPS}_2})\text{Cp}^*(\text{N}\{\text{TMS}\}_2)$ (**4.2**)

Attempts to synthesise the bulky *bis*-TMS amido complex, $\text{U}(\text{COT}^{\text{TIPS}_2})\text{Cp}^*(\text{N}\{\text{TMS}\}_2)$ (**4.2**), were carried out in order to compare its structure and reactivity to the alkyl analogue, $\text{U}(\text{COT}^{\text{TIPS}_2})\text{Cp}^*(\text{CH}\{\text{TMS}\}_2)$ (**2.8**). The unsubstituted COT analogue, $\text{U}(\text{COT})\text{Cp}^*(\text{N}\{\text{TMS}\}_2)$, was reported by Evans *et al.*, and was formed from the reaction of the chloride precursor $[(\text{COT})\text{Cp}^*\text{ClU}(\mu\text{-Cl})\text{U}(\text{COT})\text{Cp}^*]$ and $\text{KN}(\text{TMS})_2$.²⁰ The reaction of **2.2** and $\text{KN}(\text{TMS})_2$ in toluene did not occur at ambient temperature, but a reaction was observed by ^1H NMR spectroscopy once the mixture was heated to 55 °C for 18 hours. A broad resonance ($\Delta\nu_{1/2} = 340$ Hz) present at $\delta_{\text{H}} -12.2$ was tentatively assigned to the 18 $\text{N}(\text{SiMe}_3)$ protons, supported by comparison to ^1H NMR spectroscopic data reported for $\text{U}(\text{COT})\text{Cp}^*(\text{N}\{\text{TMS}\}_2)$ where the $\text{N}(\text{SiMe}_3)$ protons give rise to a very broad singlet ($\Delta\nu_{1/2} = 3000$ Hz) at -12 ppm. Despite repeated attempts, no isolable complex could be obtained from this reaction: the bulk reaction mixture proved extremely sensitive to further manipulations, and decomposed rapidly whilst attempting to prepare the sample for crystallisation. It is feasible that the steric bulk of the $\text{-N}(\text{TMS})_2$ ligand is too great, so **4.2** is susceptible to decomposition *via* unknown routes whilst handling. It should be noted that the common alkyl decomposition product, **2.9**, is *not* observed in these reaction mixtures. In conclusion, whilst it is suspected that the bulky amido complex **4.2** can be synthesised, its instability has prevented characterisation.

4.2 Reactivity of U(COT^{TIPS2})Cp*(NH₂) with CO₂ and CO

4.2.1 Reactivity with CO₂ – synthesis of U(COT^{TIPS2})Cp*(κ²-O₂CNH₂) (4.3)

Exposure of a hydrocarbon solution of **4.1** to CO₂ afforded the κ²-carbamate product, U(COT^{TIPS2})Cp*(κ²-O₂CNH₂) (**4.3**), as red crystalline material in a 64% yield after removal of volatiles under reduced pressure, extraction in pentane and slow-cooling to -35 °C (**Equation 4.1**). The ¹H NMR spectrum contained a singlet at δ_H 15.6 of integration 2H, correlating to the O₂CNH₂ proton environment, later confirmed by deuterium-labelling studies (see section 4.2.1.1). Performing the reaction with ¹³CO₂ resulted in the presence of a broad singlet at δ_C 25.8 in the ¹³C{¹H} NMR spectrum correlating to the ¹³C-labelled carbamate ligand.



Equation 4.1. Synthesis of U(COT^{TIPS2})Cp*(κ²-O₂CNH₂) (**4.3**) from **4.1** and CO₂.

Mass spectrometric analysis of **4.3** showed the expected M⁺ ion at m/z = 850, and for the fragments M⁺ -NH₂, M⁺ -NH₂OC and M⁺ -Cp* at m/z = 833, 806 and 714 respectively. Collection of IR data in situ using ReactIR apparatus (**Figure 4.2**) identified a strong vibrational band at 1611 cm⁻¹, along with further broad absorptions at 1520-1410 cm⁻¹, correlating to ν_{OCN}, in line with previously reported values.^{4,34,35} IR data collected using NaCl plates showed an additional strong vibrational band attributable to ν_{N-H} at 3424 cm⁻¹. Elemental analysis of **4.3** crystallised from Et₂O returned values consistent with **4.3** and one co-crystallising molecule of Et₂O.

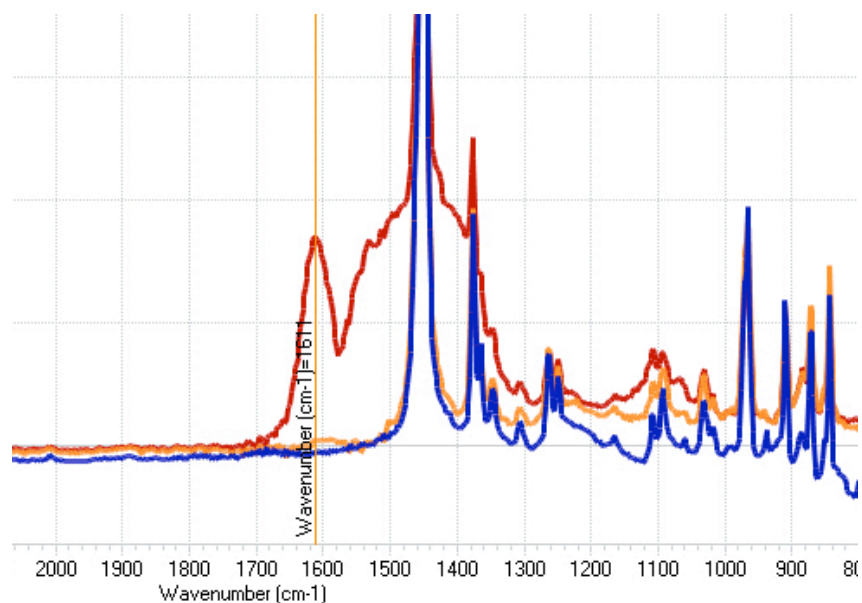


Figure 4.2. ReactIR spectra of the addition of $^{13}\text{CO}_2$ to the primary amido, **4.1**, to form **4.3**.
Blue = **2.9**, yellow = **4.1**, red = **4.3**.

The structure of **4.3** was confirmed by X-ray crystallography, confirming the formation of a primary κ^2 -carbamate ligand (**Figure 4.3**), structurally analogous to the carboxylate complexes (see Chapter 3). Upon reviewing the literature, **4.3** is shown to be the first crystallographically characterised example of a U(IV) organometallic κ^2 -carbamate containing a primary amido moiety. Selected bond distances and angles are reported in **Table 4.1**, alongside relevant metrics from the only two other crystallographically characterised U(IV) κ^2 -carbamate complexes containing terminal bidentate carbamate moieties, $(\{\text{Ad}^{\text{OAr}}\}_3\text{tacn})\text{U}(\text{O}_2\text{CNHMe})$ (**4C**),³⁵ and $\text{U}_4\text{O}_2(\text{O}_2\text{CNEt}_2)_{12}$ (**4D**),³⁶ pictured in **Figure 4.4**. The latter complex is tetrameric and contains terminal bidentate, bridging, and terminal and bridging carbamate ligands: the geometric parameters quoted are only from the terminal bidentate ligands, highlighted in red.

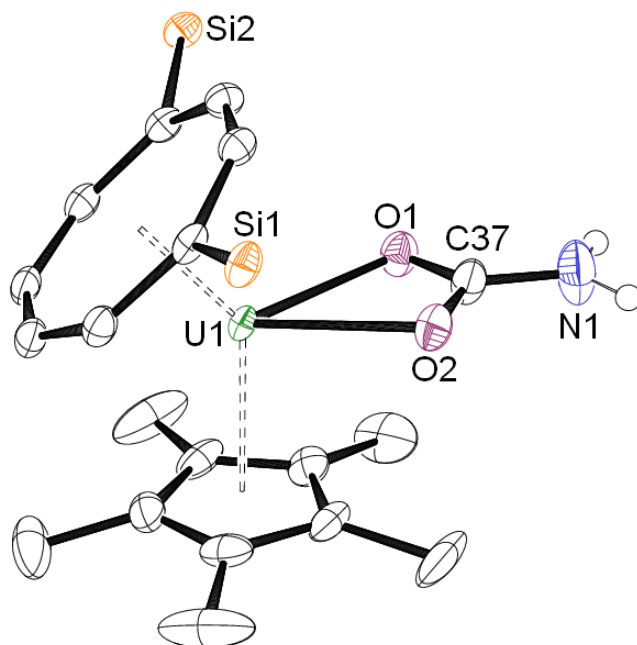


Figure 4.3. Molecular structure of **4.3**. ORTEP representation with thermal ellipsoids at the 50% probability level. Hydrogen atoms (except for on N1) and ⁱPr groups omitted for clarity.

Ct1-U1: 1.9551(3) Å, Ct2-U1: 2.4788(4) Å, Ct1-U1-Ct2: 137.076(12) °.

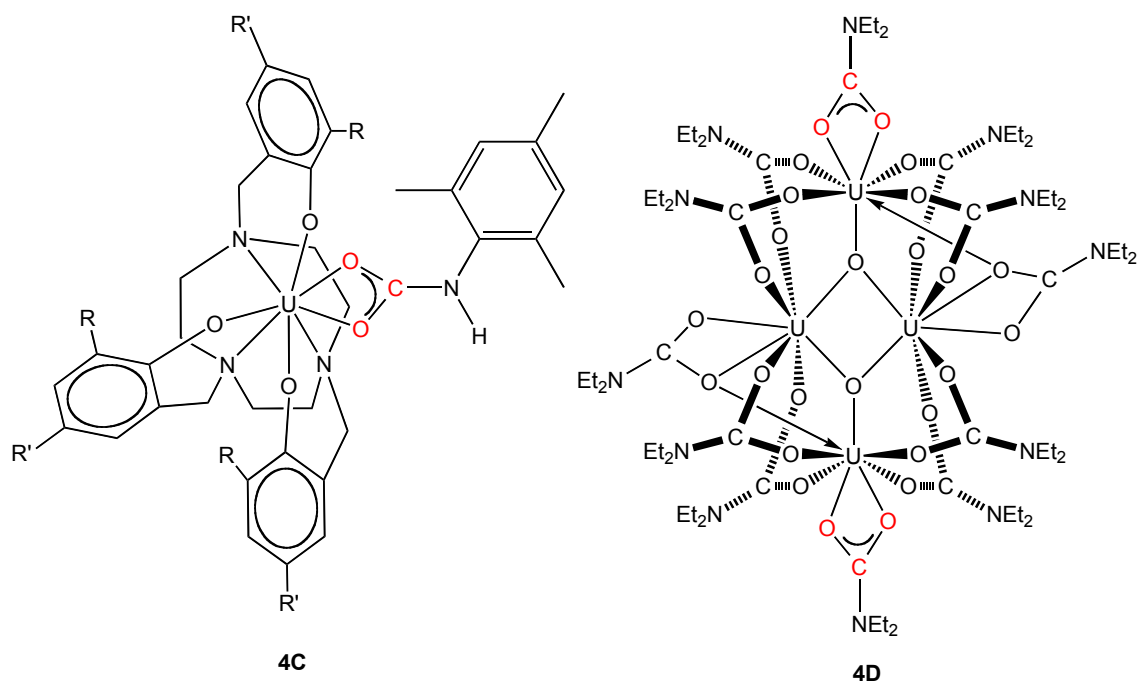


Figure 4.4. **4C** and **4D**, the only two other crystallographically characterised organouranium complexes containing κ^2 -carbamate ligands. R = Ad, R' = ^tBu.

Table 4.1. Selected bond distances (Å) and angles (°) for **4.3**, **4C**, and **4D**.

	4.3	4C	4D
U-O	2.399(2), 2.407(2)	2.434(4), 2.527(4)	2.442(11), 2.419(10)
O-C	1.296(4), 1.269(4)	1.259(7), 1.278(7)	1.205(24), 1.275(23),
C-N	1.335(5)	1.383(7)	1.41(2)
O-U-O	54.72(9)	52.85(12)	51.221(18)
O-C-O	119.0(3)	121.1(5)	121.0(7)

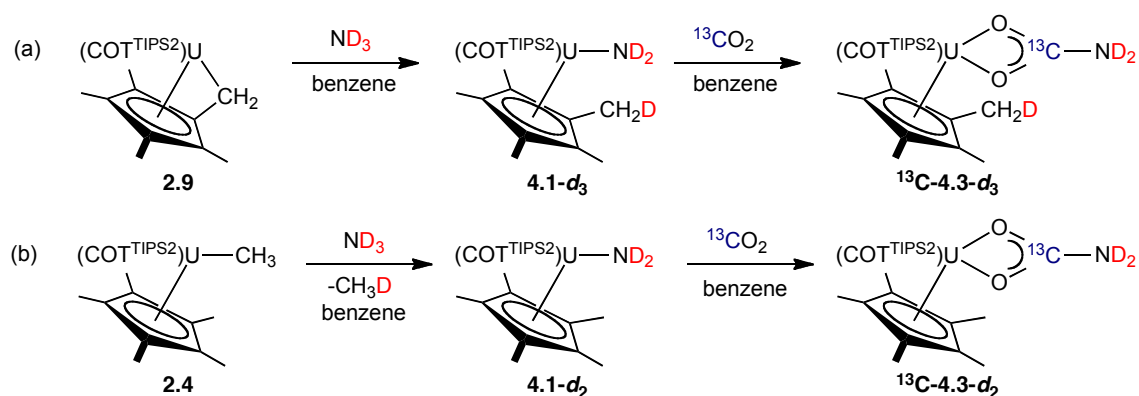
In comparison to **4C** and **4D**, the ‘U-O₂CNR₂’ unit of **4.3** contains a near-symmetric carbamate moiety with almost equal U-O bond distances, in contrast to the asymmetric U-O distances found **4C** and **4D**. All four U-O distances in **4C** and **4D** are longer than in **4.3**, likely due to steric demands of the bulky Ad-substituted tacn ligand in **4C** and the other bridging carbamate units in **4D**, whereas the ‘metallocene wedge’ provided by the carbocyclic rings in **4.3** allows for closer approach of the ligand; this is also reflected in the more obtuse O-U-O angle in **4.3**. There are some variations in the O-C bond distances in **4.3** (0.027 Å), which are also longer than those in **4C** and **4D** – this may well be a compensatory effect due to the shorter U-O bonds. The carbamate unit in **4.3** is essentially planar, with a U1-O1-C37-O2 torsion angle of 1.2(2) °. The bond distances and angles in the ‘U1-O1-C37-O2’ fragment are similar to the related κ^2 -carboxylates, **3.12** and **3.13** (see Appendix 1). In comparison to the primary amido complex **4.1**, the metal-centroid bond distances remain almost unchanged, whilst the Ct1-U1-Ct2 angle is more acute (137.076(12) vs 141.88(7) °) as the carbamate ligand demands greater space in the metallocene coordination sphere.

4.2.1.1 Deuterium-labelling studies

Experiments were performed with both ND₃ and ¹³CO₂ to confirm the location of the carbamate O₂¹³C-NH₂ proton environments, and to confirm the presence of

deuterium solely on the carbamate ligand in ^{13}C -**4.3-*d*₃**. Two pathways were followed to obtain the labelled products, ^{13}C -**4.3-*d*₃** and ^{13}C -**4.3-*d*₂**, starting from either **2.9** or **2.4**, shown as route (a) and (b) respectively in **Scheme 4.5**.

The ^2H NMR spectrum of ^{13}C -**4.3-*d*₃** contained two resonances at δ_{D} 15.6 and 4.50, corresponding to the $\text{O}_2\text{C-ND}_2$ and $\text{Cp}^*\text{-CH}_2\text{D}$ deuterium atoms respectively, while the spectrum of ^{13}C -**4.3-*d*₂** contained a single resonance at δ_{D} 15.6. The ^1H NMR spectra collected for each product each contained a very low-intensity resonance at δ_{H} 15.5, possibly arising from a small amount of NH_3 present in the ND_3 gas source.



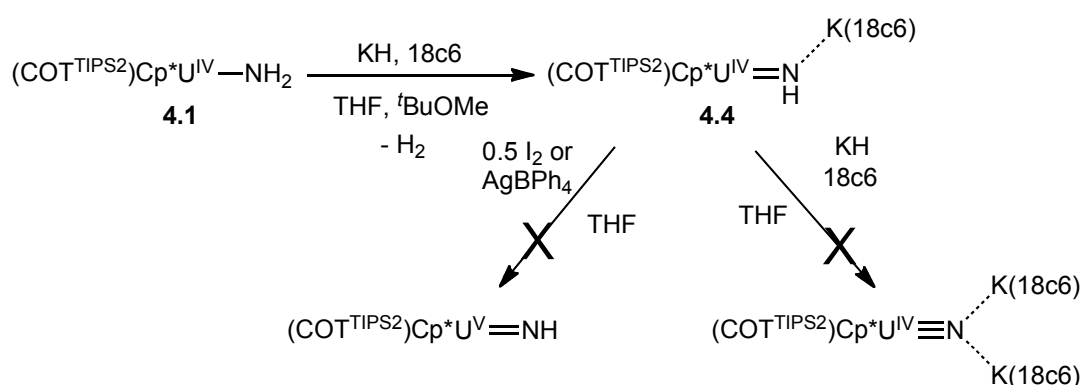
Scheme 4.5. Synthesis of deuterated carbamates: from **2.9** to give ^{13}C -**4.3-*d*₃** (a), or from **2.4** to give ^{13}C -**4.3-*d*₂** (b).

4.2.2 Reactivity with CO

Limited reports of the insertion of CO into U-N bonds in organouranium systems can be found in the literature in comparison to the insertion of CO_2 ,^{33,37} the activation of CO_2 is more facile than CO due to the weaker C-O bonds. Hydrocarbon solutions of **4.1** did not show evidence of reactivity towards either stoichiometric or excess quantities (ca 10 equivalents) of ^{13}CO . Heating a mixture of **4.1** and ^{13}CO to 50 °C for 24 hours also did not elicit a reaction.

4.3 Deprotonation of $\text{U}(\text{COT}^{\text{TIPS}_2})\text{Cp}^*(\text{NH}_2)$

As no known U(IV) primary imido complexes were known when this work commenced, it was thought that deprotonation of **4.1** may yield a novel primary imido. Additionally, deprotonation of such an imido may result in the formation of a terminal nitrido complex; only one example has been reported previously.³⁸ A recent report details the syntheses of a range of alkali metal supported primary imido complexes, also synthesised from deprotonation of a primary amide.³⁰ In the mixed-sandwich system, it was found that the primary imido complex could be synthesised from **4.1**, however, further oxidation or deprotonation did not yield isolable products (**Scheme 4.6**).



Scheme 4.6. Results of experiments aimed to form imido and nitrido complexes from **4.1**.

4.3.1 Synthesis and characterisation of $[\text{U}(\text{COT}^{\text{TIPS}_2})\text{Cp}^*(\text{NH})][\text{K}(\text{18c6})]$ (**4.4**)

The synthetic strategy decided upon was the use of an alkali metal hydride to deprotonate the amido group, in tandem with a sequestering reagent that would chelate to the resulting alkali metal cation. It is desirable to use an alkali metal hydride with a relatively large cation to avoid the formation of “ate” complexes, which are often seen in organouranium chemistry.^{39–42} Employing a chelating agent suitable for complete encapsulation of the alkali metal should result in the removal of the cation from the coordination sphere of the uranium metal centre, potentially allowing access to the ‘U=NH’ linkage for subsequent further deprotonation. It was found that using KH and 18c6 (18-crown-6) was successful for forming $[\text{U}(\text{COT}^{\text{TIPS}_2})\text{Cp}^*(\text{NH})][\text{K}(\text{18c6})]$ (**4.4**), but did not entirely encapsulate the K cation.

The combination of equimolar **4.1**, KH, and 18c6 in THF, pre-cooled to -20 °C, resulted in the formation of a cherry-red solution after stirring for 48 hours. Removal of volatiles and extraction of the tacky solids in toluene afforded microcrystalline solids of unreacted 18c6. The same procedure followed by extraction into Et₂O resulted in the formation of a small number of red needle-like crystals at ambient temperature after approximately 2 minutes; analysis performed on these crystals confirmed the product as **4.4**. A pink powder of **4.4** was also obtained after filtration of the THF solution, removal of volatiles, and addition of ^tBuOMe (or cold Et₂O) in which only **4.1** and 18c6 are readily soluble. Filtration and washing with cold Et₂O or ^tBuOMe yielded **4.4** in a 32% yield.

IR spectroscopic data showed a strong vibrational band at 1112 cm⁻¹, similar to the strong band at 1121 cm⁻¹ seen in the IR spectrum of [U(Tren^{TIPS})(NH)][K(15-crown-5)₂]; no vibration attributable to $\nu_{\text{N-H}}$ is seen (ca 3000 cm⁻¹), nor it is observed for [U(Tren^{TIPS})(NH)][K(15-crown-5)₂].³⁰ Mass spectrometric data did not show the expected parent ion at $m/z = 1108$, and instead contained ions corresponding to COT^{TIPS2} and Cp* ligands at $m/z = 416$ and 374 respectively; it is likely that ion bombardment readily breaks the molecule apart. Elemental analysis of non-crystalline **4.4** returned values consistent with an additional 1 molecule of ^tBuOMe present per molecule of **4.4**. Comparison of ¹H NMR spectra collected at different temperatures (303, 313, and 323 K) allowed for the identification of resonances correlating to protons bound to the paramagnetic uranium metal centre, however, it was not possible to definitively assign all resonances due to broadening effects. Poor solubility of **4.4** in NMR solvents precluded collection of ²⁹Si{¹H} NMR spectroscopic data.

Attempts were made to characterise **4.4** by X-ray crystallography, however satisfactory refinement of the data was not possible due to extensive disorder in the 18c6 moiety and TIPS groups that could not be sufficiently modeled, hence only connectivity was established. As seen in **Figure 4.5**, the structure of **4.4** is confirmed to

be a U(IV) primary imido. It can be seen that full sequestration of the potassium cation was not achieved, as it is still bound to the imido ligand.

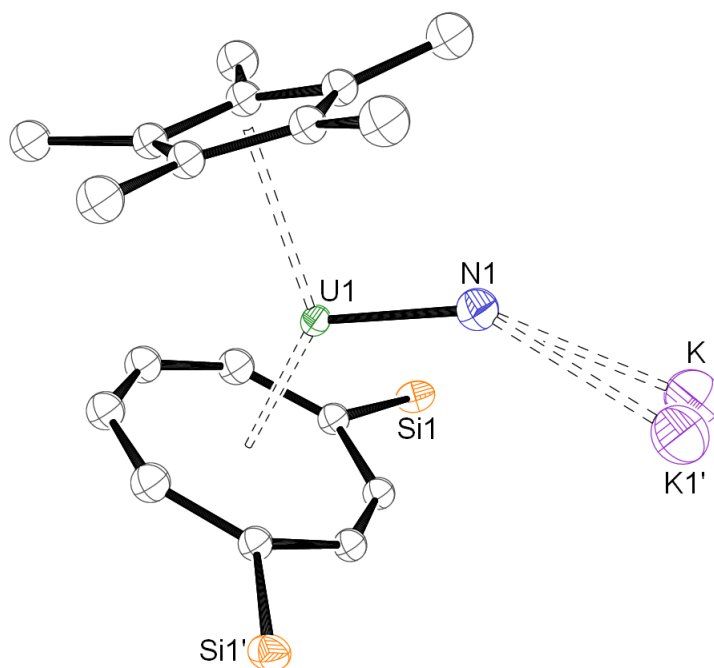


Figure 4.5. Unrefined molecular structure of $[\text{U}(\text{COT}^{\text{TIPS}_2})\text{Cp}^*(\text{NH})][\text{K}(\text{18c6})]$ (4.4).

ORTEP representation with thermal ellipsoids at the 20% probability level. Disordered 18c6 molecules, hydrogen atoms, and ^iPr groups omitted for clarity. Plane of symmetry dissects the imido linkage and K(18c6) moieties and is positioned along the U1-N1 bond.

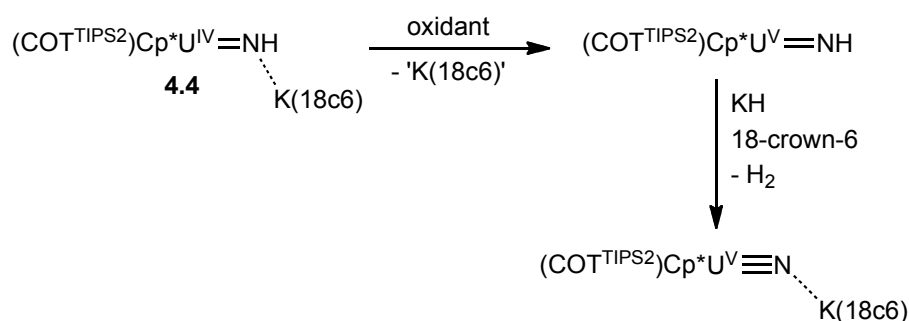
4.3.2 Attempted alternative routes to an imido complex

Other routes to an imido complex were trialled: using 2.2.2-cryptand (= 222-crypt) in place of 18c6 also appeared to form an imido, $[\text{U}(\text{COT}^{\text{TIPS}_2})\text{Cp}^*(\text{NH})][\text{K}(\text{222-crypt})_2]$, as determined by ^1H NMR spectroscopic data. The coordination mode of the 222-crypt appeared to alter after 4 days in solution, potentially indicating instability of the product. Further characterisation was not achieved due to ready decomposition of the material during subsequent manipulations. Variable temperature ^1H NMR spectroscopic studies on a crude sample were consistent with the K cation still being bound to the imido group; resonances attributed to bound 222-crypt shifted with change of temperature, which in a paramagnetic complex

indicates that the proton environments are directly associated with the metal centre. Alternative routes to an imido using NaH, or 12-crown-4 (or combinations thereof with KH, 18c6, or 222-crypt) were unsuccessful.

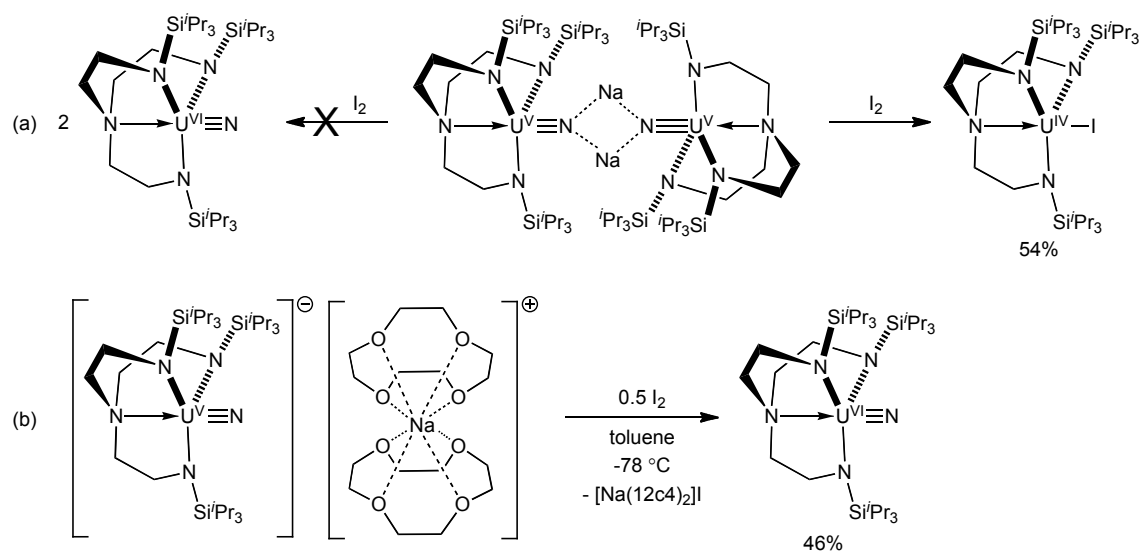
4.3.3 Oxidation to a U(V) imido

The oxidation of **4.4** was attempted with a view to forming the U(V) imido, $\text{U}^{\text{V}}(\text{COT}^{\text{TIPS}_2})\text{Cp}^*(\text{NH})$. Such a complex could potentially be deprotonated in a similar manner to **4.1** to afford a U(V) nitride (**Scheme 4.7**).



Scheme 4.7. Proposed oxidation of **4.4** and subsequent deprotonation.

Attempts to oxidise **4.4** with AgBPh_4 were unsuccessful, yielding only decomposition products. The addition of 0.5 equivalents of I_2 to **4.4** resulted in the formation of several products, as identified by ^1H NMR spectroscopy, including the known iodide, $\text{U}(\text{COT}^{\text{TIPS}_2})\text{Cp}^*\text{I}$,⁴³ but no evidence was seen for the formation of a neutral imide. It was reasoned that $\text{U}(\text{COT}^{\text{TIPS}_2})\text{Cp}^*\text{I}$ may be formed *via* disproportionation of a transitory U(V) complex or by direct reaction with tetravalent **4.4**. Identification of other products formed from the reaction of **4.4** and I_2 was not possible. A similar result was reported for the attempted oxidation of $\{\text{U}(\text{Tren}^{\text{TIPS}})(\mu\text{-N})(\mu\text{-Na})\}_2$ with I_2 , giving $\text{U}(\text{Tren}^{\text{TIPS}})\text{I}$ in a 54% yield, instead of the targeted U(VI) nitride product (**Scheme 4.8a**).



Scheme 4.8. Reported reactivity of $\{U(\text{Tren}^{\text{TIPS}})(\mu\text{-N})(\mu\text{-Na})\}_2$ and $[U(\text{Tren}^{\text{TIPS}})(\text{N})][\text{Na}(12\text{-crown-}4)_2]$ with I_2 .

The authors report the successful formation of the U(VI) nitride by oxidising $[U(\text{Tren}^{\text{TIPS}})(\text{N})][\text{Na}(12\text{-crown-}4)_2]$, and conclude that the success of this second reaction is due to “inner-sphere” versus “outer-sphere” oxidation of the counter ions (**Scheme 4.8b**), as $[U(\text{Tren}^{\text{TIPS}})(\text{N})][\text{Na}(12\text{-crown-}4)_2]$ can be classified as an ion-separated pair.²⁴ The $\text{K}(18\text{c}6)$ counter ion in **4.4** can be considered “inner-sphere” as it is directly bound to the imido group (and **4.4** is not an ion-separated pair), hence the same reasoning can be applied to the failure of the oxidation reaction in this case. It is therefore unknown whether oxidation to a U(V) imido is possible in this mixed-sandwich system, highlighting the importance of the ligand system in determining the stability of ‘U-X’ linkages.

4.3.4 Attempted nitride synthesis

Three approaches were taken in attempts to synthesise a mixed-sandwich nitride complex, none of which were successful. The addition of KH and 18c6 to **4.4** resulted in decomposition, as did the addition of 2 equivalents of KH and 18c6 to **4.1**. In the latter case, the only isolable material from the reaction mixture was $U(\text{COT}^{\text{TIPS}2})_2$, which could be formed as a result of either disproportionation of a transient nitride, or

the removal of both the amido and Cp* ligands from **4.1** by KH, combined with subsequent disproportionation. In case the oxidation of **4.4** with I₂ *does* form a transient U(V) imido complex that decomposes upon isolation attempts (see section 4.3.3), the rapid addition of KH and 18c6 to a crude mixture of **4.4** and 0.5 equivalents of I₂ was performed after filtration and extraction in pentane; only decomposition was observed.

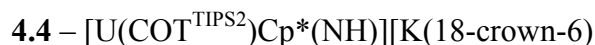
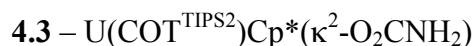
4.4 Conclusions and chapter summary

A rare example of a U(IV) terminal primary amido complex, U(COT^{TIPS₂})Cp*(NH₂) (**4.1**) has been synthesised and fully characterised. The synthesis of another amido complex, U(COT^{TIPS₂})Cp*(N{TMS}₂) (**4.2**), was also attempted, but the product was not fully characterised due to instability, likely due to the substantial steric bulk of the -N{TMS}₂ ligand.

The reactivity of **4.1** towards CO and CO₂ has been examined, and it was found that the carbamate product, U(COT^{TIPS₂})Cp*(κ²-O₂CNH₂) (**4.3**) is formed from the insertion of CO₂, while no reactivity occurs with CO. Deprotonation of **4.1** to form a U(IV) imido complex, [U(COT^{TIPS₂})Cp*(NH)][K(18c6)] (**4.4**) has been achieved. Attempts undertaken to form a mixed-sandwich uranium nitride were not successful.

The utility of the mixed-sandwich ligand system for providing a supporting framework for studying chemistry at a single bond (and in a relatively inert environment) is exemplified by work described in this chapter. Amide complexes are rare, and **4.1** can be synthesised in a unique way – from σ-bond metathesis rather than salt metathesis – although the latter route is also successful. The stability of **4.1** compared to the alkyls can be evaluated: it does not decompose to form **2.9** either at ambient temperature or upon heating, and it does not undergo σ-bond metathesis upon exposure to H₂. It will insert CO₂ to form a κ²-carbamate, but, unlike the alkyls, does not react with CO.

4.5 Compound naming for Chapter 4



4.6 References for Chapter 5

1. T. Schareina and R. Kempe, *Synthetic Methods of Organometallic and Inorganic Chemistry: Catalysis, vol. 10*, Thieme Medical Publishers, Inc., New York, 2002.
2. H. Gilman, R. G. Jones, E. Bindenschadler, D. Elume, G. Karmas, G. A. Martin Jr., J. F. Nobis, J. R. Thirtle, H. L. Yale, and F. A. Yoeman, *J. Am. Chem. Soc.*, 1956, **78**, 2790–2792.
3. R. G. Jones, G. Karmas, G. A. Martin Jr., and H. Gilman, *J. Am. Chem. Soc.*, 1956, **78**, 4285–4286.
4. K. W. Bagnall and E. Yanir, *J. Inorg. Nucl. Chem.*, 1974, **36**, 777–779.
5. J. G. Reynolds, A. Zalkin, D. H. Templeton, and N. M. Edelstein, *Inorg. Chem.*, 1977, **16**, 1090–1096.
6. H. Yin, A. J. Lewis, U. J. Williams, P. J. Carroll, and E. J. Schelter, *Chem. Sci.*, 2013, **4**, 798.
7. J. G. Reynolds and N. M. Edelstein, *Inorg. Chem.*, 1977, **16**, 2822–2825.
8. H. W. Turner, S. J. Simpson, and R. A. Andersen, *J. Am. Chem. Soc.*, 1979, **101**, 2782.
9. J. L. Sessler, P. J. Melfi, and G. D. Pantos, *Coord. Chem. Rev.*, 2006, **250**, 816–843.
10. C. E. Hayes and D. B. Leznoff, *Coord. Chem. Rev.*, 2014, **266-267**, 155–170.
11. B. D. Stubbert, C. L. Stern, and T. J. Marks, *Organometallics*, 2003, **22**, 4836–4838.
12. C. R. Graves, E. J. Schelter, T. Cantat, B. L. Scott, and J. L. Kiplinger, *Organometallics*, 2008, **27**, 5371–5378.
13. C. R. Graves, B. L. Scott, D. E. Morris, and J. L. Kiplinger, *Organometallics*, 2008, **27**, 3335–3337.
14. R. K. Thomson, C. R. Graves, B. L. Scott, and J. L. Kiplinger, *Eur. J. Inorg. Chem.*, 2009, 1451–1455.
15. R. K. Thomson, T. Cantat, B. L. Scott, D. E. Morris, E. R. Batista, and J. L. Kiplinger, *Nat. Chem.*, 2010, **2**, 723–729.
16. E. Montalvo, K. A. Miller, J. W. Ziller, and W. J. Evans, *Organometallics*, 2010, **29**, 4159–4170.
17. T. Straub, W. Frank, G. J. Reiss, and M. S. Eisen, *J. Chem. Soc., Dalton Trans.*, 1996, 2541–2546.
18. R. K. Thomson, B. L. Scott, D. E. Morris, and J. L. Kiplinger, *C. R. Chim.*, 2010, **13**, 790–802.
19. T. M. Gilbert, R. R. Ryan, and A. P. Sattelberger, *Organometallics*, 1988, **7**, 2514–2518.
20. W. J. Evans, S. A. Kozimor, and J. W. Ziller, *Polyhedron*, 2006, **25**, 484–492.

21. L. R. Avens, C. J. Burns, R. J. Butcher, D. L. Clark, J. C. Gordon, A. R. Schake, B. L. Scott, J. G. Watkin, and B. D. Zwick, *Organometallics*, 2000, **19**, 451–457.
22. M. A. Antunes, G. M. Ferrence, Â. Domingos, R. McDonald, C. J. Burns, J. Takats, and N. Marques, *Inorg. Chem.*, 2004, **43**, 6640–6643.
23. G. Zi, L. Jia, E. L. Werkema, M. D. Walter, J. P. Gottfriedsen, and R. A. Andersen, *Organometallics*, 2005, **24**, 4251–4264.
24. D. M. King, F. Tuna, E. J. L. McInnes, J. McMaster, W. Lewis, A. J. Blake, and S. T. Liddle, *Nat. Chem.*, 2013, **5**, 482–488.
25. T. W. Hayton, J. M. Boncella, B. L. Scott, P. D. Palmer, E. R. Batista, and P. J. Hay, *Science*, 2005, **310**, 1941–3.
26. L. P. Spencer, R. L. Gdula, T. W. Hayton, B. L. Scott, and J. M. Boncella, *Chem. Commun.*, 2008, 4986–4988.
27. R. E. Jilek, L. P. Spencer, R. a Lewis, B. L. Scott, T. W. Hayton, and J. M. Boncella, *J. Am. Chem. Soc.*, 2012, **134**, 9876–9878.
28. L. A. Seaman, S. Fortier, G. Wu, and T. W. Hayton, *Inorg. Chem.*, 2011, **50**, 636–646.
29. T. W. Hayton, *Chem. Commun.*, 2013, **49**, 2956–2973.
30. D. M. King, J. McMaster, F. Tuna, E. J. L. McInnes, W. Lewis, A. J. Blake, and S. T. Liddle, *J. Am. Chem. Soc.*, 2014, **136**, 5619–5622.
31. D. M. King, F. Tuna, E. J. L. McInnes, J. McMaster, W. Lewis, A. J. Blake, and S. T. Liddle, *Science*, 2012, **337**, 717–720.
32. J. W. Bruno, T. J. Marks, and L. R. Morss, *J. Am. Chem. Soc.*, 1983, **105**, 6824–6832.
33. P. J. Fagan, J. M. Manriquez, S. H. Vollmer, C. S. Day, V. W. Day, and T. J. Marks, *J. Am. Chem. Soc.*, 1981, **103**, 2206–2220.
34. A. L. Arduini, J. D. Jamerson, and J. Takats, *Inorg. Chem.*, 1981, **20**, 2474–2479.
35. S. C. Bart, C. Anthon, F. W. Heinemann, E. Bill, N. M. Edelstein, and K. Meyer, *J. Am. Chem. Soc.*, 2008, **130**, 12536–12546.
36. F. Calderazzo, G. Dell’Amico, M. Pasquali, and G. Perego, *Inorg. Chem.*, 1978, **17**, 474–479.
37. G. Paolucci, G. Rossetto, P. Zanella, K. Yünlü, and R. D. Fischer, *J. Organomet. Chem.*, 1984, **272**, 363–383.
38. D. M. King, F. Tuna, E. J. L. McInnes, J. McMaster, W. Lewis, A. J. Blake, and S. T. Liddle, *Science*, 2012, **337**, 717–720.
39. R. A. Andersen, E. Carmona-Guzman, K. Mertis, E. Sigurdon, and G. Wilkinson, *J. Organomet. Chem.*, 1975, **99**, C19–C20.
40. P. C. Blake, M. F. Lappert, J. L. Atwood, and H. Zhang, *J. Chem. Soc., Chem. Commun.*, 1988, 1436–1438.
41. P. Roussel, P. B. Hitchcock, N. D. Tinker, and P. Scott, *Inorg. Chem.*, 1997, **36**, 5716–5721.
42. K. C. Jantunen, F. Haftbaradaran, M. J. Katz, R. J. Batchelor, G. Schatte, and D. B. Leznoff, *Dalton Trans.*, 2005, 3083–3091.
43. A. S. P. Frey, *Unpublished results*, University of Sussex, 2014.

CHAPTER 5: DIAMIDOAMINE U(III) AND U(IV) COMPLEXES: SYNTHESIS AND REACTIVITY

5.1 Introduction

Organouranium complexes have been synthesised using a large number of organic ligands, both carbocyclic and non-carbocyclic in nature – a detailed review of these ligands can be found in Chapter 1 – each of which impart different reactivity to the metal centre. As an alternative to the $\text{COT}^{\text{TIPS}2}$ ligand used in the mixed-sandwich compounds described in this work and others,¹⁻⁷ another dianionic ligand was targeted to be installed around a uranium metal centre in tandem with a Cp^* ligand: the diamidoamine ligand, $[\text{N}'\text{N}'_2]^{2-}$ (**Figure 5.1**). The ligand binds to a metal centre *via* the two anionic terminal nitrogen atoms, but can also bind using the central nitrogen atom lone pair to provide further steric and electronic saturation. It can either bind in an κ^2 or κ^3 fashion to one metal centre, or bridge two metals in a $\mu\text{-}\kappa^1:\kappa^1$ fashion, as illustrated in **Figure 5.1**.

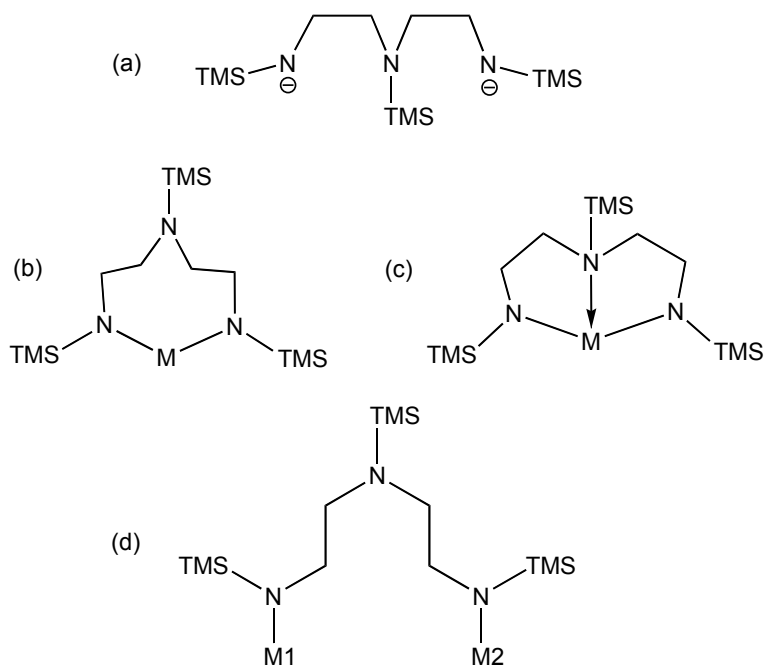
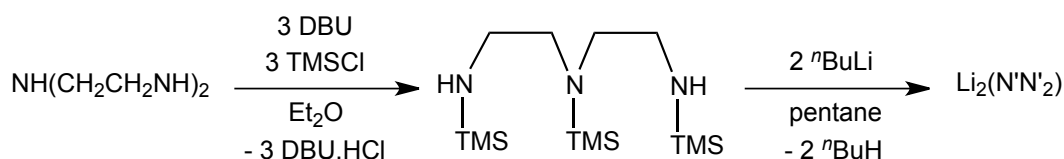


Figure 5.1. Diamidoamine ligand, $\text{N}'\text{N}'_2$, in its dianionic form (a), and in potential binding modes: κ^2 (b), κ^3 (c), and $\mu\text{-}\kappa^1:\kappa^1$ (d). M = metal.

One synthesis used to generate the neutral ligand, $H_2(N'N'_2)$, was reported by Cloke *et al.* in 1995.⁸ It utilised a transilylation reaction between diethylenetriamine and $NH\{TMS\}_2$ in the presence of catalytic H_2SO_4 to form the di-silylated amine, $NH(CH_2CH_2N\{TMS\})_2$, followed by deprotonation of the central nitrogen atom and further silylation using $TMSCl$. Shortly thereafter, an improved synthesis was reported by the same authors: a one-pot reaction of DBU (1,8-diazabicyclo[5.4.0]unde-7-ene) and $TMSCl$, followed by the addition of diethylenetriamine, gave the desired $H_2(N'N'_2)$ product in an 82% yield after distillation.⁹ Double deprotonation of $H_2(N'N'_2)$ using 2 equivalents of $nBuLi$ yields the dilithium salt, $Li_2(N'N'_2)$, which can be used for salt metathesis reactions (**Scheme 5.1**).

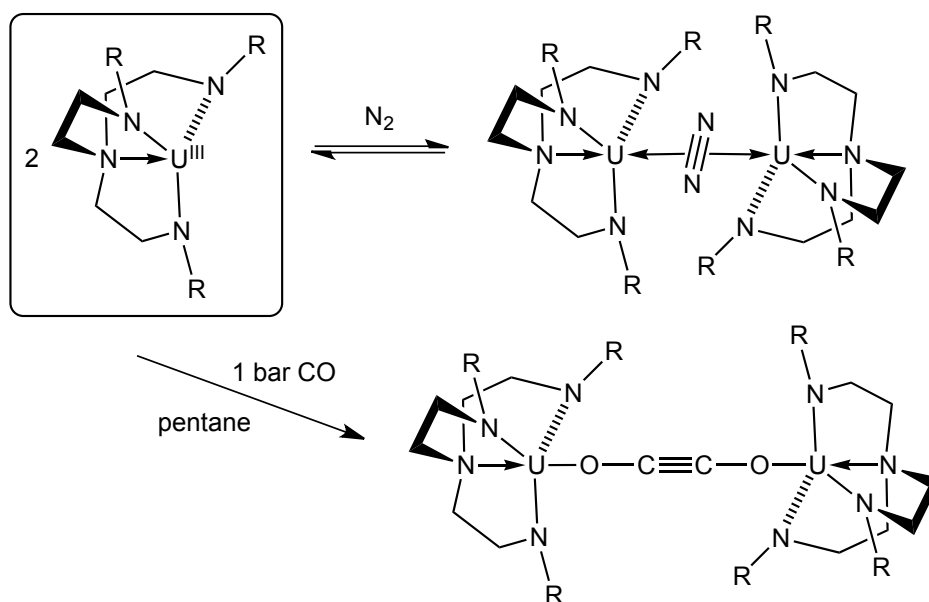


Scheme 5.1. Synthesis of $Li_2(N'N'_2)$.⁹

The diamidoamine ligand has been utilised before in a range of organometallic zirconium,⁸ titanium,^{9–12} aluminium,¹³ scandium,¹⁴ vanadium,^{15–17} thorium and uranium¹⁸ complexes. Most notably, its use with vanadium allows for the reduction of dinitrogen; the reaction of $\{V(N'N'_2)Cl\}_2$ with 1 equivalent of KC_8 under an N_2 atmosphere results in the formation of a nitride dimer, $\{V(N'N'_2)(\mu-N)\}_2$, wherein the $N\equiv N$ bond has been entirely cleaved.¹⁵

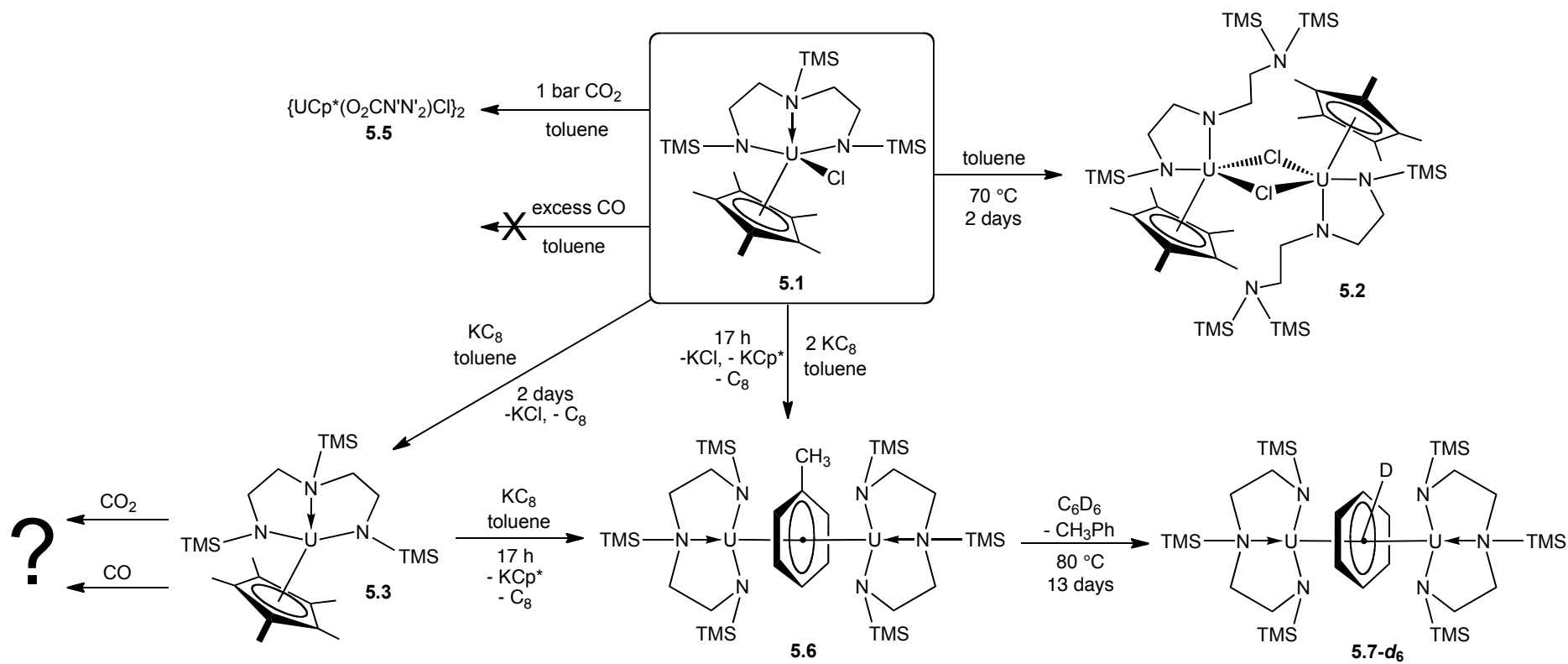
Other organouranium complexes featuring amido-based ligands have shown remarkable reactivity towards dinitrogen and carbon monoxide. The first example of an actinide dinitrogen complex features a triamidoamine ligand, and is formed from the spontaneous reaction of the trivalent precursor, $U(Tren^{DMSB})$, with dinitrogen;¹⁹ this same trivalent species will reductively couple CO to form an ynediolate complex (**Scheme 5.2**).²⁰ The ubiquitous $[N'']^-$ ligand, when used as a homoleptic ligand in trivalent UN''_3 , will also effect the reductive coupling of CO to form an ynediolate complex.²¹ In cooperation with $Mo(N\{Ad\}Ph)_3$, the homoleptic diamido complex

$U(THF)(N\{tBu\}Ar)_3$ will activate dinitrogen under mild conditions, forming a linear $U-N=N=Mo$ moiety, with end-bound N_2 .²²



Scheme 5.2. Reactivity of $U(\text{Tren}^{\text{DMSB}})$ with N_2 and CO, $R = \text{Si}^t\text{BuMe}_2$.

The utility of the $N'_N'_2$ ligand in stabilising low-valent metal centres and providing flexible binding modes was envisaged to be useful for synthesising a U(III) half-sandwich complex, $U(N'_N'_2)\text{Cp}^*$, and investigating its reactivity towards small molecules. Exploring its behaviour with CO and N_2 was hoped to supply new examples of $\mu\text{-N}_2$ or $\mu\text{-CO}$ species, as seen with other amido-based organouranium complexes. It is well-known that ligand systems significantly dictate reactivity around uranium, and it was hoped that the ' $U(N'_N'_2)\text{Cp}^*$ ' system would provide contrast to the more thoroughly-investigated mixed-sandwich ' $U(\text{COT}^{\text{TIPS}_2})\text{Cp}^*$ ' system with respects to its stabilisation, electronics and overall reactivity. This chapter details the synthesis of new U(III) and U(IV) complexes containing the $N'_N'_2$ ligand, and describes the propensity of the $N'_N'_2$ ligand to undergo silyl group migration, hence rendering it unsuitable for use as an inert ligand framework. The syntheses and reactivity detailed in this chapter is summarised in **Scheme 5.3**.



Scheme 5.3. Summary of complexes synthesised in this work containing the N'N'₂ and N'NN'' ligands, and their reactivity.

5.2 Synthesis and characterisation of diamidoamine chlorides

Uranium chloride complexes previously synthesised featuring the diamidoamine ligand, $N'N'_2$, are the bis-chloro complexes, $U(N'N'_2)Cl_2(THF)$ (**5A**) and $\{U(N'N'_2)Cl_2\}_2$ (**5B**),¹⁸ and the mono-chloro complexes, $U(N'N'_2)Cl(N\{TMS\}_2)$ (**5C**) and $U(N'N'_2)Cl(CH\{TMS\}_2)$ (**5D**, **Figure 5.2**).²³ Previous attempts to synthesise $U(N'N'_2)Cp^*Cl$ were not successful.²³

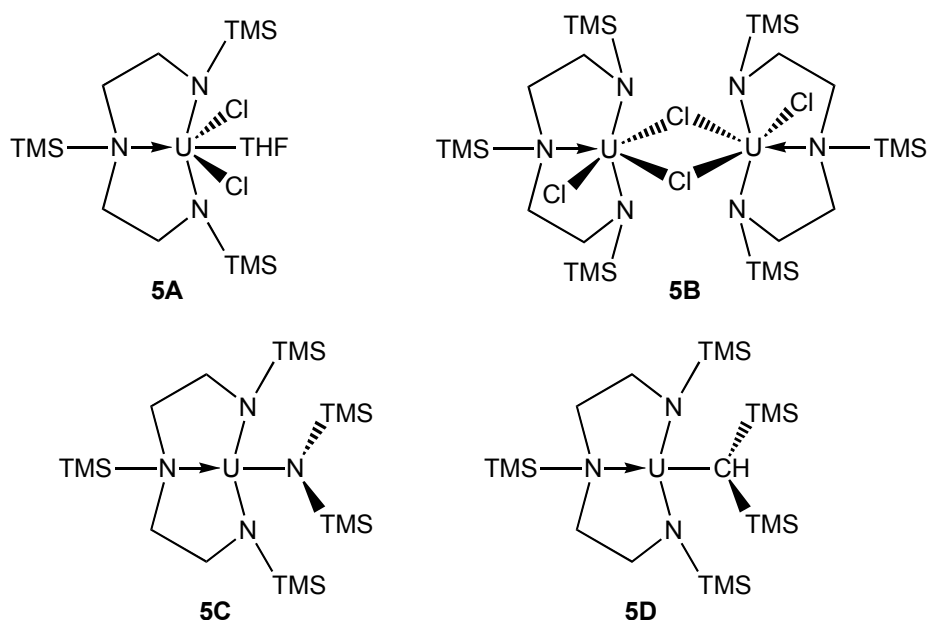
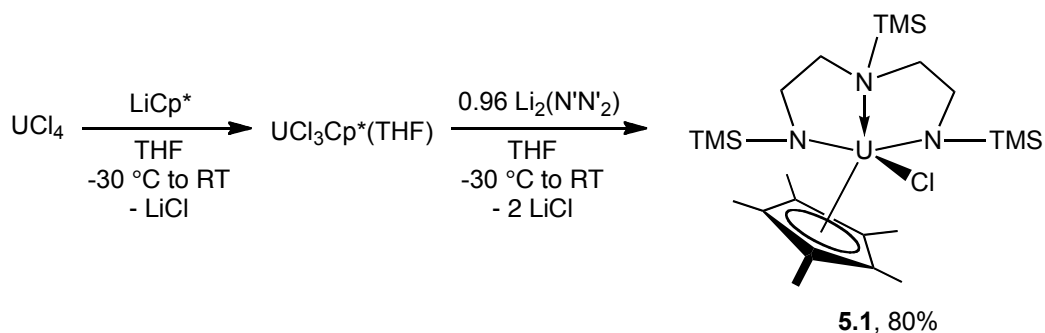


Figure 5.2. Organouranium complexes containing both $N'N'_2$ and Cl ligands.

5.2.1 Synthesis of $U(N'N'_2)Cp^*Cl$ (**5.1**)

The reaction of UCl_4 with 1 equivalent of $LiCp^*$ in THF at $-30\text{ }^\circ\text{C}$, followed by the addition of 0.96 equivalents of $Li_2(N'N'_2)$ as a THF slurry at $-30\text{ }^\circ\text{C}$ resulted in an orange solution containing an off-white precipitate. Removal of volatiles, extraction in toluene and filtration through Celite®, followed by concentration and slow-cooling of the orange toluene solution to $-50\text{ }^\circ\text{C}$, yielded green crystals of $U(N'N'_2)Cp^*Cl$ (**5.1**) in an 80% yield (**Scheme 5.4**). The isolation of $UCl_3Cp^*(THF)$ before the addition of $Li_2(N'N'_2)$ did not improve the yield of **5.1**.



Scheme 5.4. Synthesis of $\text{U}(\text{N}'\text{N}'_2)\text{Cp}^*\text{Cl}$ (**5.1**) from UCl_4 , LiCp^* and $\text{Li}_2(\text{N}'\text{N}'_2)$.

^1H NMR spectroscopic analysis of crystalline **5.1** showed resonances attributable to the Cp^* ligand (δ_{H} 0.16, s, 15H) and the symmetrically-bound $\text{N}'\text{N}'_2$ ligand: the three TMS groups appear as two singlets at δ_{H} 24.8 and -14.2 with integral values of 18H and 9H respectively, and the CH_2CH_2 backbone protons correlate to broad singlets at δ_{H} 29.7, -19.4, -32.7, and -48.4. The $^{29}\text{Si}\{^1\text{H}\}$ NMR spectrum contained two resonances at -45.6 and -50.6 ppm, correlating to the two $\text{N}(\text{SiMe}_3)$ environments (central and terminal). The mass spectrum contained the expected parent ion ($m/z = 727$, 3%) and fragments thereof at $m/z = 691$ ($\text{M}^+ - \text{Cl}$), 591 ($\text{M}^+ - \text{Cp}^*$), 409 ($\text{M}^+ - \text{N}'\text{N}'_2$), 217 ($\text{N}'\text{N}'_2$ fragment, 100%) – the values are +1 amu greater than expected, either due to incorrect instrument calibration or protonation in the beam. Elemental analysis returned the expected values.

X-ray diffraction data were collected from a sample of the green crystalline material, observed under the microscope as gold-coloured rods. The structure is shown below in **Figure 5.3**, and pertinent bond distances from each molecule of **5.1** in the asymmetric unit are detailed in **Table 5.1**. Disorder in the Cp^* ring of each molecule contained within the asymmetric unit has been modeled accordingly.

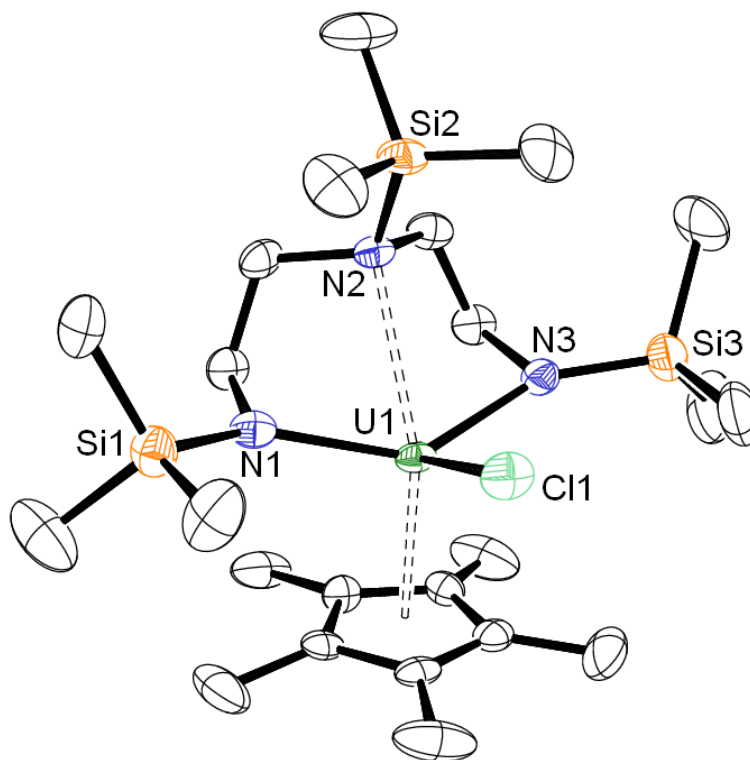


Figure 5.3. Molecular structure of $U(N'N'_2)Cp^*Cl$ (**5.1**). ORTEP representation with thermal ellipsoids at the 50% probability level. One molecule shown of two in the asymmetric unit.

Hydrogen atoms omitted for clarity.

Table 5.1. Selected bond distances (Å) and angles (°) for **5.1**. Values listed for each molecule in the asymmetric unit. Nt and Nc are defined as the terminal and central nitrogen atoms respectively. Ct is defined as the Cp*-ring centroid.

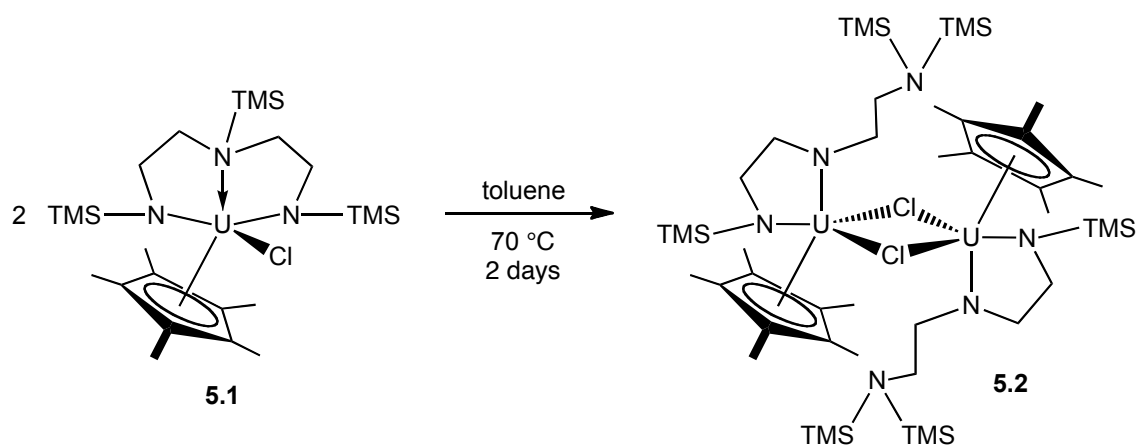
	Molecule 1	Molecule 2
U-Cl	2.6136(17)	2.6159(17)
U-Nt	2.250(7), 2.244(6)	2.246(6), 2.255(6)
U-Nc	2.759(6)	2.755(6)
Nt-U-Nt	140.0(2)	139.8(2)
U-Ct	2.497(4)	2.494(4)

The U1-Cl1 and U2-Cl2 bond distances are in the middle of the range reported for other terminal U(IV)-Cl bond distances found in nitrogen-ligand frameworks (2.511(8) – 2.690(2) Å).²⁴ The central nitrogen atom on the N'N'₂ ligand also binds to the uranium metal centre *via* the nitrogen lone pair; the U-Nc bond distance is

significantly longer than the U-Nt distances owing to the differing bonding interaction (avg. 2.757(6) vs 2.24875(6) Å). In comparison to other crystallographically characterised ‘U(N’N’₂)’ complexes with coordinating Nc atoms, the structure of **5.1** is very similar (see Appendix 1). The U-Nt bond distances are also consistent with those found in other structurally characterised uranium complexes containing the N’N’₂ ligand, and the U-Nc bond distances are closest to that in **5B** (Figure 5.2, 2.647(18) Å) – the longer distances in **5.1** can be attributed to the bulky Cp* ligand occupying significant space in the uranium coordination sphere.

5.2.2 Silyl group migration

The previously reported result of the reaction between UCp*Cl₃(THF) and Li₂(N’N’₂) was not **5.1**, but a related chloride complex wherein the migration of one TMS group along the N’N’₂ ligand backbone had occurred, forming the complex {U(N’NN’’)Cp*Cl₂}₂ (**5.2**, N’NN’’ = N{TMS}CH₂CH₂NCH₂CH₂N{TMS})₂.²³ This migration can be forced by heating a toluene solution of **5.1** to 70 °C for 2 days, and yielded **5.2** after this time in a 26% isolated yield (Equation 5.1); the conversion of **5.1** to **5.2** was essentially quantitative when observed by ¹H NMR spectroscopy.



Equation 5.1. Synthesis of {U(N’NN’’)Cp*Cl₂}₂ (**5.2**) from **5.1**.

The only characterising data for **5.2** previously reported are the crystal structure and the mass spectrum, the latter of which is essentially identical to that obtained for **5.1**, due to the identical empirical formulae and apparent facile fragmentation of the

5.2 dimer. No spectroscopic evidence was consistent with the formation of **5.2** alongside **5.1** in the synthesis described in section 5.2.1, but further data for **5.2** were collected to verify this.

X-ray crystallographic data collected from a red crystalline sample of **5.2** synthesised from **5.1** were identical to the previously reported structure. Mass spectrometric analysis and elemental analysis returned the expected values, and were essentially indistinguishable to those collected for **5.1**. However, the ^1H NMR spectrum of **5.2** is significantly different to that of **5.1**, due to the different ligand environment around the uranium atom in **5.2** resulting in different contact and pseudo-contact shift effects, as is typical in ^1H NMR spectra of paramagnetic U(IV) complexes. The resonance correlating to the Cp* ligand is seen at δ_{H} -2.43, and the N'NN"-SiMe₃ proton environments are present as two singlets of integration 18H and 9H at 0.71 and -4.94 ppm respectively. The CH₂CH₂ backbone protons appear as broad singlets between 102 and -29.4 ppm.

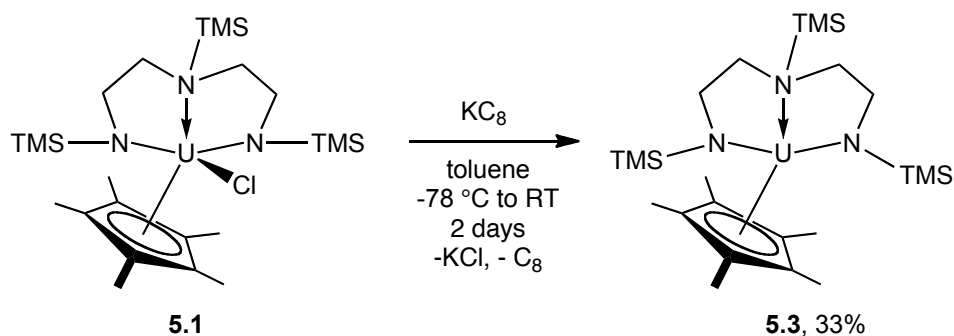
Upon inspection of the experimental details previously reported for the synthesis of **5.2**, the product is described as *green* crystalline material, not red. It is possible that the X-ray diffraction data originally collected were not representative of the bulk sample, and that the intended product, **5.1**, was indeed formed as a major product in the synthesis. It should also be noted that the presence of **5.2** has been observed in other bulk samples of **5.1** that have been left at ambient temperature for periods greater than two weeks, as determined by ^1H NMR spectroscopy, implying that **5.2** is also formed spontaneously, without heating. It is possible that similar silyl-group migrated products of other complexes featuring the N'N'₂ ligand described in the remainder of this chapter may also exist.

5.3 Synthesis of $U^{III}(N'N'_2)Cp^*$ and related compounds

In order to explore the reductive behaviour of a diamidoamine uranium complex with small molecules, such as CO or CO₂, the synthesis of the U(III) complex, $U(N'N'_2)Cp^*$, or a base adduct thereof, must be achieved. The synthesis of **5.1** is clean and high-yielding, providing a U(IV) chloride product that should reduce to the U(III) diamidoamine complex. The results of these reduction attempts are described below.

5.3.1 Synthesis and characterisation of $U(N'N'_2)Cp^*$ (**5.3**)

The reaction of **5.1** with 1 equivalent of KC_8 in toluene was carried out, and afforded a dark brown-green solution after stirring at ambient temperature for 2 days. Filtration, concentration of the toluene solution and slow-cooling to -50 °C initially yielded a small quantity of unreacted **5.1** (5%). After isolation of this material, the removal of volatiles, extraction into Et₂O and then slow-cooling to -50 °C yielded dark green crystals of $U(N'N'_2)Cp^*$ (**5.3**) in a 33% yield (**Equation 5.2**).



Equation 5.2. Synthesis of $U(N'N'_2)Cp^*$ (**5.3**) from **5.1** and KC_8 .

Initial small-scale reactions performed in J Young NMR tubes at ambient temperature showed that **5.3** is not stable in solution once formed. Dark green solutions of **5.3** become brown-black in colour over a period of 48 hours. ¹H NMR spectroscopic analysis of such solutions show the disappearance of resonances attributable to **5.3**, and the appearance of new uninterpretable paramagnetically-shifted signals, and diamagnetic signals thought to correlate to ligand decomposition. Solid samples of **5.3** stored at ambient temperature also show visual signs of decomposition after 24 hours.

To rule out potential dinitrogen activation during reduction under an N₂ atmosphere – which has been reported for a number of trivalent uranium species^{19,22,25–28} – small-scale reactions of **5.1** and KC₈ in J Young NMR tubes were performed under both N₂ and Ar atmospheres. No differences in the ¹H NMR spectra were noted, indicating dinitrogen activation does not occur.

The ¹H NMR spectrum of **5.3** contained the expected resonances attributable to a Cp* ligand (δ_{H} -9.36, 15H) and a symmetrically-bound N'N'₂ ligand (δ_{H} -18.2 and -26.5, 18H and 9H respectively, along with 4 broad singlets for backbone CH₂) at significantly different chemical shift values to those found in **5.1**. Only one resonance was observed in the ²⁹Si{¹H} NMR spectrum – a broad singlet at -130 ppm – presumably due to broadening effects. Mass spectrometric analysis returned a spectrum containing the expected parent ion at *m/z* = 691 (7%), and other reasonable fragments. Satisfactory elemental analysis results for **5.3** could not be obtained due to the inherent instability of the complex; decomposition occurred rapidly after preparing the sample for analysis.

The molecular structure of **5.3** is shown in **Figure 5.4**, with pertinent bond distances and angles quoted in the caption. The structure is monomeric, with the Cp* and N'N'₂ ligands coordinated in η^5 and κ^3 fashions respectively. The central nitrogen atom on the N'N'₂ ligand, N2, is coordinated to the metal centre *via* lone pair interaction, and has a longer U-N bond length than the terminal atoms N1 and N3, as is also seen in **5.1**. The short U1-N1 bond distance of 2.321(5) Å could be indicative of one CH₃ group on the terminal N{TMS} moiety coordinating to the metal centre in a bridging fashion. In comparison to **5.1**, the U-N_t (terminal) bond distances in **5.3** are longer, while the U-N_c (central) bond distance is shorter; the overall geometry of the N'N'₂ ligand is more ‘closed’ above the central metal atom, reflected in the N_t-U-N_t angle of 104.41(17) vs 140.0(2) ° in **5.1**. The N'N'₂ ‘N-CH₂CH₂N{TMS}CH₂CH₂N’ backbone in **5.3** is also not symmetrical in the solid-state – the two ‘CH₂CH₂’ backbone linkages are orthogonal to each other.

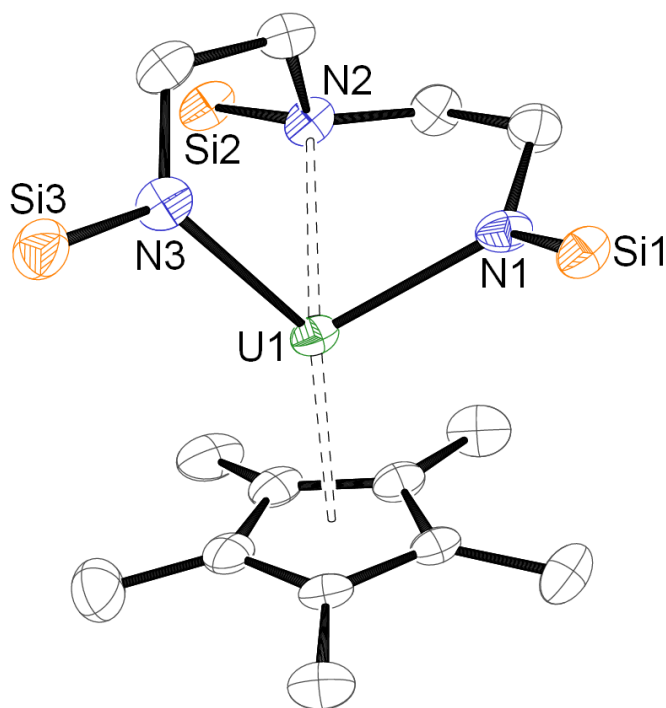


Figure 5.4. Molecular structure of $U(N'N')Cp^*$ (**5.3**). ORTEP representation with thermal ellipsoids at the 50% probability level. Hydrogen atoms and TMS groups omitted for clarity.

U1-Ct: 2.535(3) Å, U1-N1: 2.321(5), U1-N2: 2.667(6) Å, U1-N3: 2.342(5) Å,
N1-U1-N3: 104.41(17) °.

Recrystallisation of **5.3** from a saturated THF solution yielded a small quantity of dark brown crystalline material (ca 15 mg) which was examined by X-ray diffraction techniques, whereby the structure was determined to be the THF adduct of **5.3**, $U(N'N')Cp^*(THF)$ (**5.3.THF**, **Figure 5.5**). In comparison to the structure of **5.3**, **5.3.THF** shows the same κ^3 -coordination mode of the $N'N'_2$ ligand, with the central nitrogen atom N2 binding to the metal centre, with a U1-N2 bond distance of 2.747(6) Å. All U-N and U-Ct bond distances are longer in **5.3.THF** than in **5.3** due to the additionally coordinated THF molecule, which also forces a larger N1-U1-N3 bond angle of 115.6(2) ° compared to that of 104.41(17)° in **5.3**. The U1-O1 bond distance of 2.565(6) Å is similar to that of 2.585(4) Å found in the mixed-sandwich complex, **2.9.THF**.

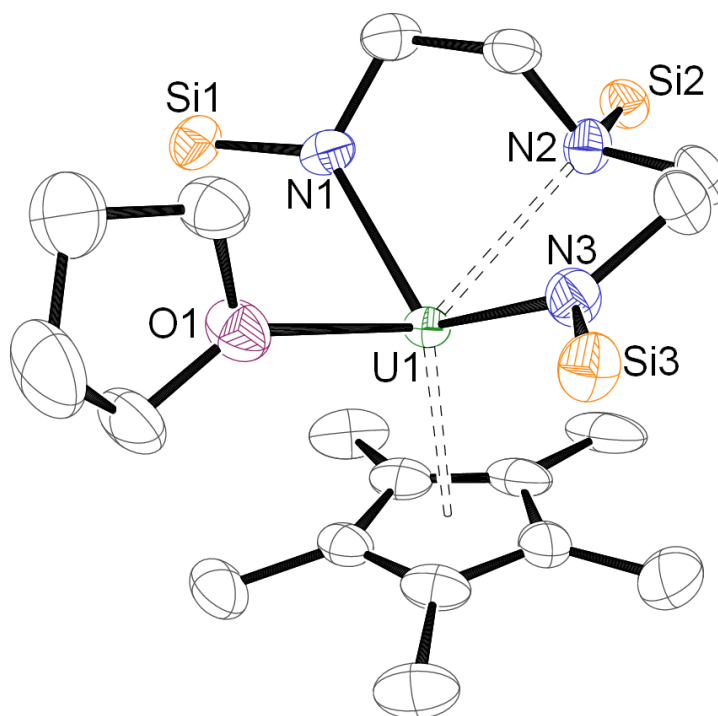


Figure 5.5. Molecular structure of $U(N'N'_2)Cp^*(THF)$ (**5.3.THF**). ORTEP representation with thermal ellipsoids at the 50% probability level. Hydrogen atoms and TMS groups omitted for clarity. U1-Ct: 2.9076(3) Å, U1-N1: 2.377(6), U1-N2: 2.747(6) Å, U1-N3: 2.392(6) Å, N1-U1-N3: 115.6(2) °, U1-O1: 2.565(6) Å.

1H NMR spectroscopic analysis of **5.3.THF** resulted in a spectrum containing three broad singlets at -7.16, -8.56, and -18.7 ppm with relative integral values of 18, 15, and 9H respectively. Due to weak sample concentration and pronounced broadening effects, lower-intensity resonances attributable to the $N'N'_2$ backbone- CH_2 protons and coordinated THF could not be observed. This material also proved unstable – decomposition and a loss of resonances correlating to **5.3.THF** was observed by 1H NMR spectroscopy over the course of 24 hours – precluding further characterisation.

5.3.2 Attempted reduction using other methods

A number of other methods were trialled to reduce **5.1** to **5.3**: solvents other than toluene were used for the KC_8 reduction (THF, Et_2O), and a reduction using mercury amalgam was performed. Some of these reactions produced small quantities of **5.3**, but mainly formed many unidentified products, as determined by

been entirely eliminated in this case. The structure of **5.4** is shown in **Figure 5.6**, however, the small size of the crystal sample examined by X-ray diffraction means that complete data could not be obtained to a sufficient resolution ($I/\sigma = 7.7$), hence only connectivity could be established and geometric parameters cannot be discussed. The disorder in one of the four coordinated THF molecule could not be sufficiently modeled, hence the carbon atoms are omitted for this moiety in the structure.

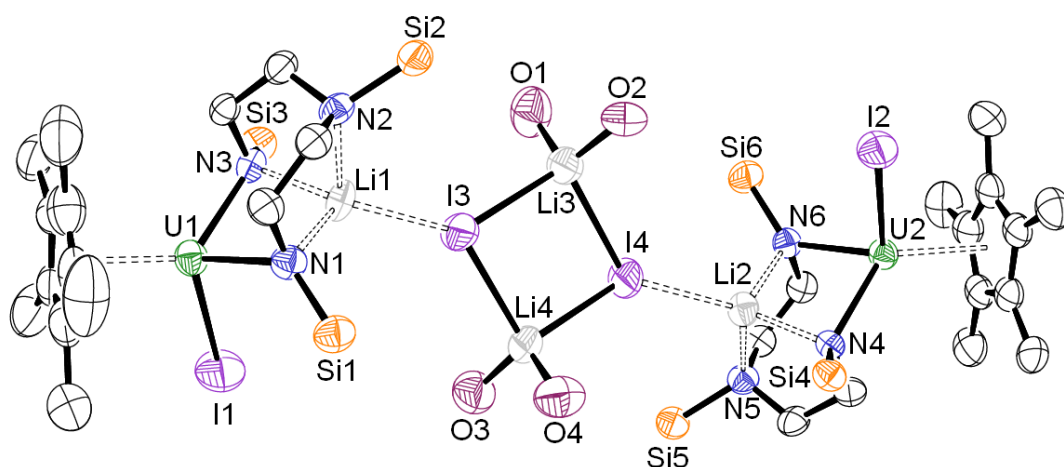


Figure 5.6. Molecular structure of $[U(N'N')_2Cp^*I.Li]_2[Li(THF)_2]_2$ (**5.4**). ORTEP representation with thermal ellipsoids at the 50% probability level.

Hydrogen atoms, TMS groups and THF carbons omitted for clarity.

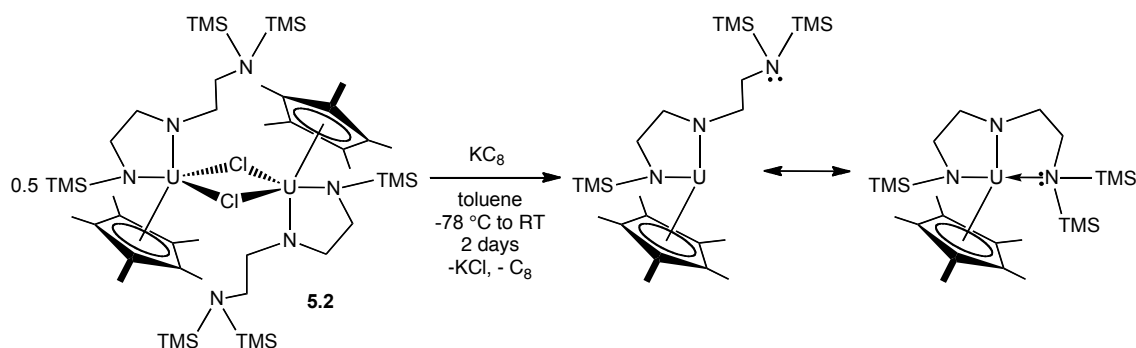
In comparison to the structure of **5.1**, **5.4** displays a different coordination geometry of the $N'N'_2$ ligand, forced by the coordination of all three N atoms to Li. The central nitrogen atoms on the ligand backbones, N2 and N5, do not bind to the uranium metal centre in **5.4**, whereas a U-N interaction exists in the same place in **5.1** – again a consequence of the presence of Li.

Attempts to reduce **5.4** with KC_8 were not successful, and this route was not pursued further.

5.3.4 Reduction of $\{U(N'NN'')Cp^*Cl\}_2$

In an analogous fashion to the reduction of **5.1**, the reduction of the bridging chloride **5.2** was also attempted. It was thought that the free pendant ‘arm’ of the –

$\text{CH}_2\text{CH}_2\text{N}\{\text{TMS}\}_2$ moiety may be able to coordinate *via* the nitrogen lone-pair to the uranium centre, assisting in the stabilisation of a trivalent complex (**Scheme 5.6**). The reduction of **5.2** with 2 equivalents of KC_8 in toluene was also performed, aiming to form the bridging arene, $\{\text{U}(\text{N}'\text{N}'\text{N}'')\}_2(\mu\text{-C}_7\text{H}_8)$ (see section 5.5 for more details on bridging arene complexes).



Scheme 5.6. Postulated route to the trivalent species, $\text{U}(\text{N}'\text{N}'\text{N}'')\text{Cp}^*$.

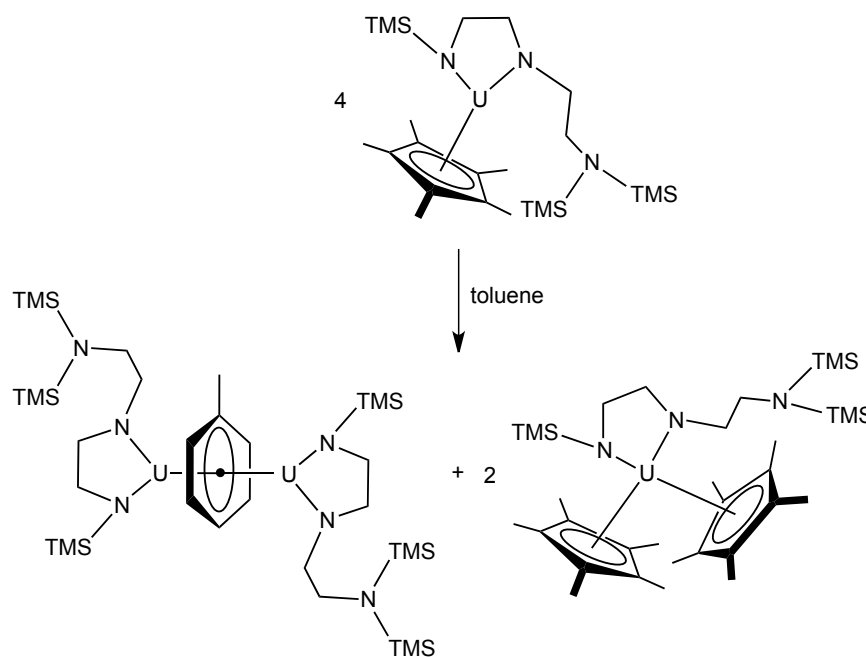
A toluene solution of **5.1** was heated to form **5.2**, which was then reacted with KC_8 at -78°C and allowed to warm to ambient temperature, affording a dark red-brown solution. ^1H NMR spectroscopic analysis of an aliquot showed the complete consumption of **5.2** and many new paramagnetic resonances. Mass spectrometric analysis results are outlined in **Table 5.2**.

Table 5.2. Ions present in the mass spectrum collected from the crude reaction mixture of **5.2** and KC_8 in toluene.

M/z	%	Assignment
825	8	$\text{U}(\text{N}'\text{N}'\text{N}'')\text{Cp}^*_2$
690	18	$\text{U}(\text{N}'\text{N}'\text{N}'')\text{Cp}^*$
651	100	$\text{U}(\text{N}'\text{N}'\text{N}'')(\text{C}_7\text{H}_8)$

Combined analysis of the mass spectrometric and ^1H NMR spectroscopic data indicated the presence of more than one species in solution, one of which could be the bridging arene complex, $\{\text{U}(\text{N}'\text{N}'\text{N}'')\}_2(\mu\text{-C}_7\text{H}_8)$. This would account for resonances present in the ^1H NMR spectrum at 5.58 and -5.45 ppm, in a 2:1 integral ratio – these resonances are also seen in spectra collected for **5.6** (see section 5.5), after

decomposition has occurred, consistent with silyl-group migration after the initial bridging arene has formed. No mass spectrometric evidence for a ‘U(N'NN'')₂’ ion is observed ($m/z = 872$). One possible explanation for the presence of an ion at $m/z = 825$, correlating to a U^{IV} product containing two Cp* rings, is that disproportionation occurs after formation of an unstable trivalent species, U(N'NN'')Cp*, forming tetravalent U(N'NN'')Cp*₂ and a transient ‘U(N'NN'’)’ moiety, which activates the arene solvent to form {U(N'NN'')}₂(μ-C₇H₈) (**Scheme 5.7**). This same behaviour is observed for U^{III} complexes of the form UX₃ (where X = ODtbp, N'') when they are heated in an arene solvent.³⁵ Despite several attempts, the separation and isolation of the proposed products was not possible due to their similar solubilities, and no structural information could be obtained.



Scheme 5.7. Possible disproportionation of transient U(N'NN'')Cp* to give {U(N'NN'')}₂(μ-C₇H₈) and U(N'NN'')Cp*₂.

To identify whether a bridging arene species is formed, **5.2** was combined with 2.2 equivalents of KC₈ in toluene, affording a very dark red solution. ¹H NMR spectroscopic analysis of the mixture showed the presence of resonances at δ_H 5.56 and -5.50, matching the signals observed in the spectrum of **5.2** with 1 eq. KC₈,

along with other resonances correlating to CH_2CH_2 backbone environments: no Cp* ligand resonances could be identified. Signals attributable to a bridging toluene ligand were not observed, due to the reaction occurring in deuterated arene solvent. The mass spectrum collected from the crude reaction mixture contained a 100% ion at $m/z = 651$, correlating to a 'U(N'NN')(C₇D₈)' fragment. Attempts to crystallise the product for X-ray diffraction analysis were not successful, hence the structure of the product cannot be confirmed. However, it can be concluded from the comparison of ¹H NMR spectroscopic and mass spectrometric data to that collected from the reaction of **5.2** with 1 equivalent of KC₈, that the same product – potentially a bridging arene – is produced in both cases.

5.4 Small molecule reactivity

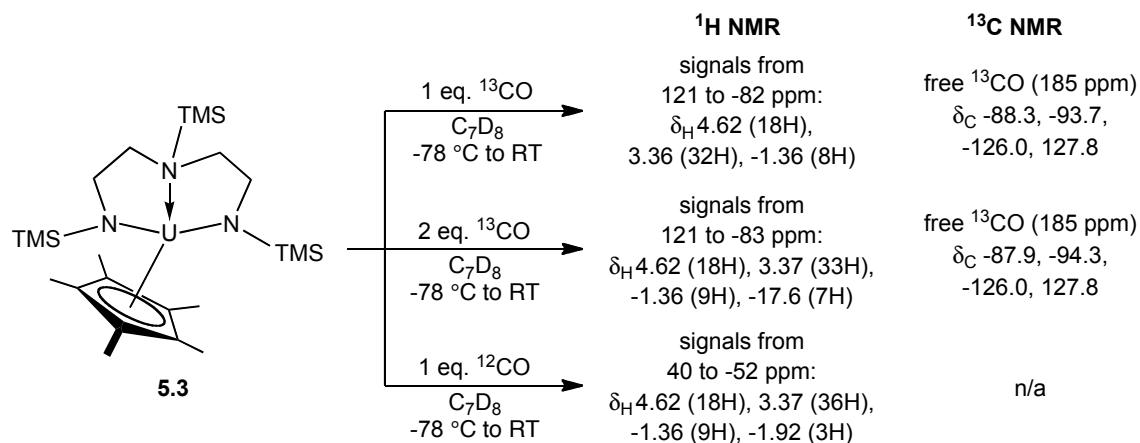
As summarised in detail in Chapter 1, many organometallic U(III) complexes show reactivity towards small molecules, such as CO and CO₂. In addition to this, U(IV) complexes featuring reactive U-X bonds (where X = C, H, N) can also undergo insertion reactions with small molecules. The trivalent complex **5.3** was synthesised with the intention of exploring its reactivity towards CO and CO₂, in analogy to the related mixed-sandwich complex, U(COT^{TIPS}₂)Cp*, which forms ynediolate, deltate, and carbonate products with the aforementioned small molecules.^{1,3,5} The following section details the results of attempted small molecule activation with **5.3**, and also with the tetravalent species, U(N'N'₂)Cp*Cl (**5.1**).

5.4.1 Reactivity of U(N'N'₂)Cp* (**5.3**) with CO and CO₂

5.4.1.1 Reactions of **5.3** with CO

Three experiments were performed using dark green crystalline samples of **5.3**: portions of **5.3** were dissolved in C₇D₈ in J Young NMR tubes, then exposed to either 1 or 2 equivalents of ¹³CO, or 1 equivalent of ¹²CO, *via* Toepler pump apparatus at

-78 °C. In each case, a colour change from dark green to more translucent red-brown was observed upon warming. The results of these reactions are summarised in **Scheme 5.8**.



Scheme 5.8. Summary of results from reactions of **5.3** with CO.

Integration of the most intense common resonances in the ¹H NMR spectra from the three reactions shown above returned values of ca 18, 30, and 9H for three signals at ca 4.62, 3.36, and -1.36 ppm, which *could* correlate to a species of the form ‘U(N’N’₂)Cp*₂’, but this cannot be confirmed. Mass spectrometric analysis of a crude portion of **5.3** and ¹³CO returned a spectrum containing ions correlating to N’N’₂ ligand fragments (m/z = 73 (100%), 116 (65%), 217 (76%)), and uranium-containing fragments at m/z values between 555 and 780, with no sensible assignments apparent. It is clear that no single product, *e.g.* an ynediolate complex, is formed. Removal of the CO headspace from the reaction of **5.3** with 2 eq. ¹³CO did not result in a change in the ¹H NMR spectrum, indicating that none of the products formed are reversible.

ReactIR data were collected *in situ* of the reaction of **5.3** with an excess of ¹³CO, in order to provide further potential identifying information of the number and type of products formed in the reaction mixture. The ¹³CO was delivered to a methylcyclohexane solution of **5.3**, cooled to -60 °C inside a gas-tight vessel containing the IR probe, *via* Toepler pump apparatus. Upon warming to ambient temperature, a colour change was observed from dark green to red-brown, and a very low-intensity

single new IR vibrational band grew just above the baseline at 1946 cm^{-1} (**Figure 5.7**). No other indication of intermediate products or other vibrational bands were observed. Previously reported IR vibrational bands for simple U-CO adducts range between 1880 and 1976 cm^{-1} ,^{36–39} which is consistent with the absorption seen in the ReactIR experiment of **5.3** and ^{13}CO potentially corresponding to a molecular CO complex, $\text{U}(\text{N}'\text{N}'_2)\text{Cp}^*(\text{CO})$, however, the very low intensity nature of this signal precludes a definitive assignment.

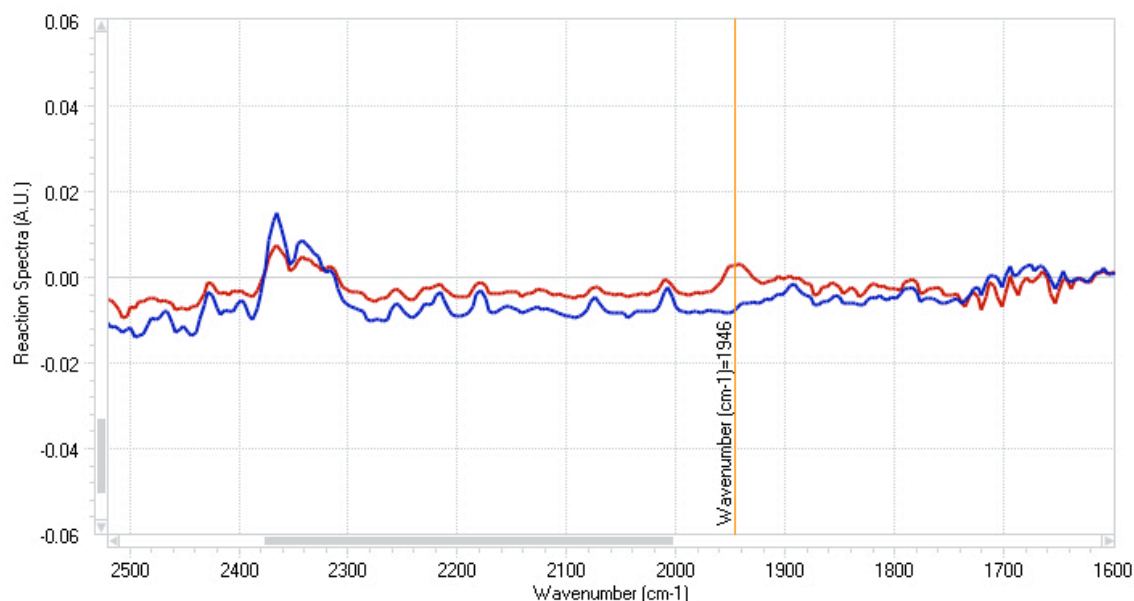


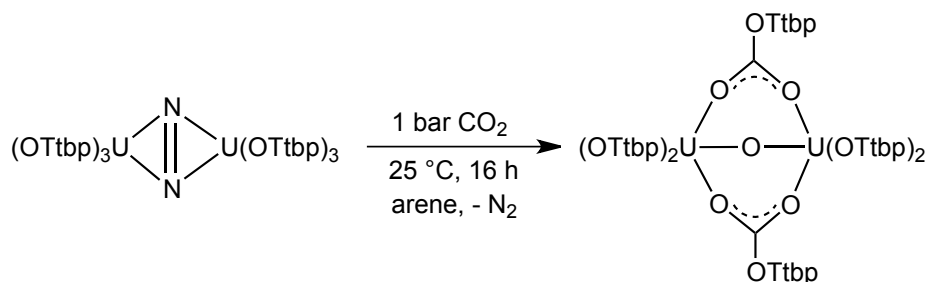
Figure 5.7. ReactIR spectra collected from the reaction of **5.3** and ^{13}CO : blue is the spectrum collected before gas addition; red is the spectrum after gas addition.

Despite repeated attempts to crystallise the product, or multiple products, of the reaction of **5.3** and CO, no X-ray quality crystals were obtained and hence no structural information has been collected. In conclusion, while a reaction between **5.3** and CO does appear to occur, no further data are available to elucidate the identity of the reaction products.

5.4.1.2 Reaction of **5.3** with CO_2

The addition of an excess of $^{13}\text{CO}_2$ to a frozen crystalline sample of **5.3** dissolved in C_6D_6 resulted in a colour change from dark green to yellow-gold upon thawing.

Analysis of the reaction mixture by ^1H NMR spectroscopy after reaching ambient temperature showed the complete consumption of **5.3** and the presence of numerous new paramagnetically-shifted resonances between 13.7 and -15.8 ppm, mostly very broad singlets. Collection of $^{13}\text{C}\{^1\text{H}\}$ NMR spectroscopic data from the sample showed the presence of free $^{13}\text{CO}_2$ (125 ppm) and free ^{13}CO (184 ppm), but no other obvious ^{13}C resonances. This could be due to the formation of an oxo species, and could potentially be accompanied by the insertion of CO_2 into the U-N bonds of the ligand framework – ^{13}C NMR resonances associated with inserted $^{13}\text{CO}_2$ moieties may be very broadened and hence not observed. This type of behaviour has been observed previously in the uranium trisaryloxy system, $\text{U}(\text{OTtbp})_3$, wherein the dinitrogen adduct $\{\text{U}(\text{OTtbp})_3\}_3(\mu\text{-N}_2)$ will react with CO_2 after initial N_2 dissociation, to give a dimeric oxo-bridged species accompanied by CO_2 insertion into two U-O aryloxy bonds (**Equation 5.3**).²⁸



Equation 5.3. Reactivity of $\{\text{U}(\text{OTtbp})_3\}(\mu\text{-N}_2)$ with excess CO_2 .

Also reported by the same authors is the reaction of the tris-amide complex, UN^3 , with an excess of CO_2 , which forms the tetravalent siloxide, $\text{U}(\text{O}\{\text{TMS}\})_4$. This is thought to form *via* the insertion of CO_2 into the three U-N ligand bonds, followed by the elimination of $\text{O}=\text{C}=\text{N}\{\text{TMS}\}$, as supported by IR spectroscopic evidence.²⁸ Again, a similar pattern of reactivity may also occur for the reaction between **5.3** and CO_2 : insertion of CO_2 into one, two, or all of the U-N bonds could give carbamate linkages, potentially followed by further rearrangement or elimination of ligand moieties. Mass spectrometric and IR spectroscopic evidence collected from this reaction did not

provide any further indications as to the reaction products, and all attempts to crystallise a product from the reaction mixture were not successful.

5.4.2 Reactivity of $U(N'N')Cp^*Cl$ (**5.1**) with CO and CO₂

Unlike the relatively inert U-C π -interactions between the U metal centre and carbocyclic 5- and 8-membered rings, U-N σ -bonds – like those in the diamidoamine complexes described in this work – are more susceptible to insertion reactions. To investigate whether the insertion of CO or CO₂ also occurs in addition to any reductive behaviour when trivalent **5.3** is exposed to those small molecules, the tetravalent chloride complex **5.1** was tested for reactivity towards CO and CO₂.

The addition of 3 equivalents of ¹³CO to a C₆D₆ solution of **5.1** did not afford any reaction after 12 hours, or after heating to 70 °C for 14 hours, except for some conversion to **5.2**.

The reactivity of **5.1** with CO₂ was examined: the insertion of CO₂ into the U-N σ -bond in the mixed-sandwich amido complex, $U(COT^{TIPS2})Cp^*(NH_2)$ to give a carbamate, $U(COT^{TIPS2})Cp^*(\kappa^2-O_2CNH_2)$, has already been demonstrated in Chapter 5 and is suspected to occur in the reaction of **5.3** and CO₂. Little useful characterising data were acquired from NMR scale reactions of excess **5.1** and ¹³CO₂, however, the preparative-scale reaction of **5.1** and 1 bar of ¹²CO₂ in toluene afforded the isolation of a small number of brown crystals, identified as a dimeric, bridging carbamate derivative, **5.5** (Figure 6.9), with selected bond distances and angles reported in Table 5.3.

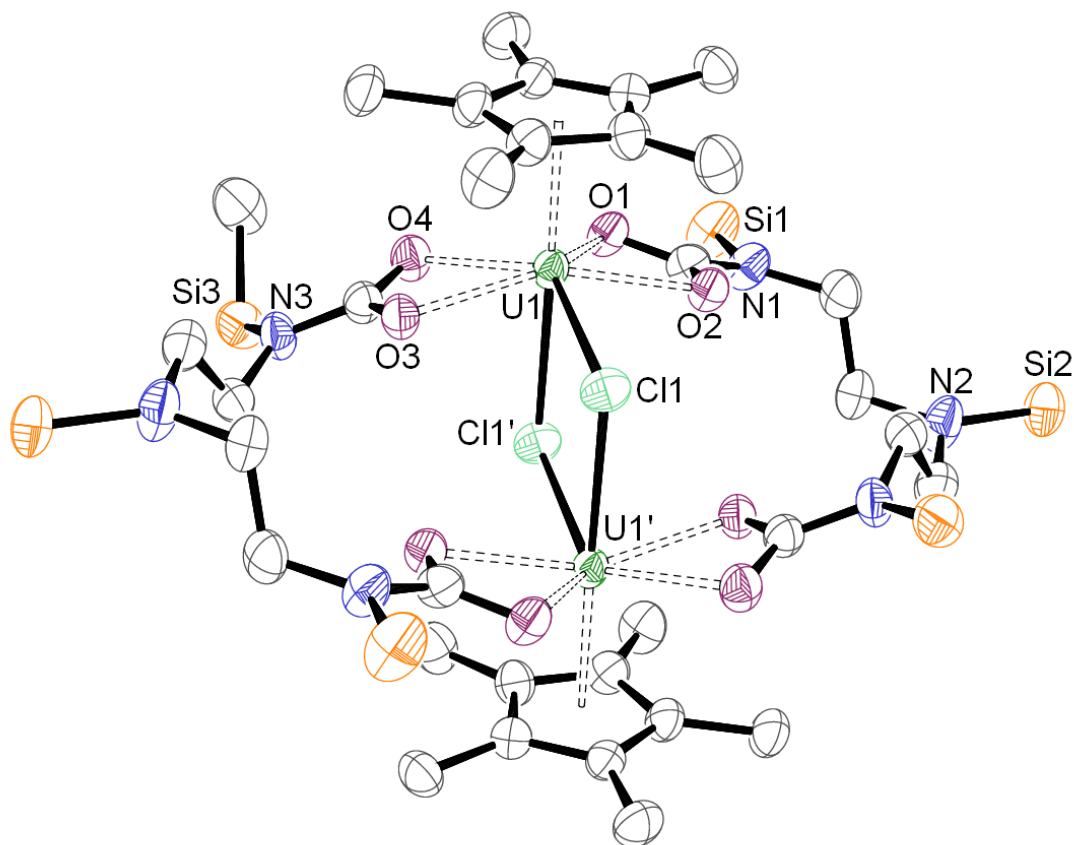


Figure 5.8. Molecular structure of **5.5**.

ORTEP representation with thermal ellipsoids at the 50% probability level. Hydrogen atoms, TMS groups and disordered co-crystallising molecule of toluene omitted for clarity.

Table 5.3. Selected bond distances (Å) and angles (°) for **5.5**. Ct is defined as the Cp*-ring centroid. Half the molecule is contained in the asymmetric unit; both sets of values quoted.

U1-Cl1, U1-Cl1'	2.7858(11), 2.8026(13)
U-O	2.391(3), 2.348(4), 2.367(4), 2.390(4)
O1-U1-O3/O2-U1-O4	133.94(12), 132.38(13)
U-Ct	2.435(2)
U1-Cl1-U1'	101.25(4)
O1-U1-O2/O3-U1-O4	55.28(11), 55.41(12)
O1-C1-O2/O3-C6-O4	117.9(5), 117.8(5)

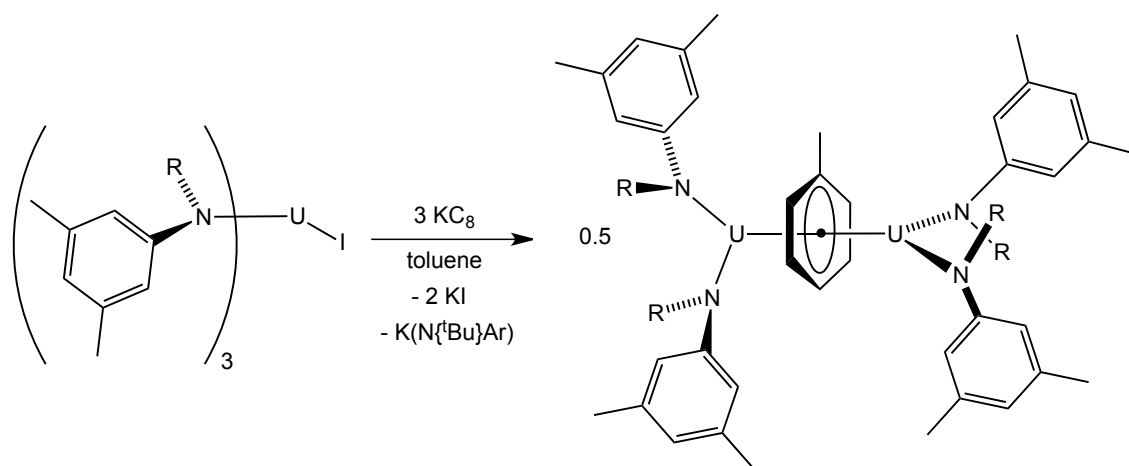
It can be seen that CO₂ insertion has occurred into both U-Nt (terminal) bonds of the original N'N'₂ ligand. The carbamate ligands have forced a dimeric conformation,

with two bridging chloride atoms and two bridging 'O₂C-N'N'₂' ligands, likely due to the steric demands of the bidentate -O₂C moieties. In comparison to the mixed-sandwich uranium carboxylates (**3.1**, **3.2**) and carbamate (**5.3**), the U-O bond distances in **5.5** are shorter and also display asymmetry: one U-O distance in each carbamate moiety is longer than the other, by ca 0.043 and 0.023 Å, whilst those found in **3.1**, **3.2** and **5.3** are essentially identical. As a result of the shorter U-O bonds, the O-U-O angles are greater while the C-O-C angles are more acute in **5.5**, in comparison to **3.1**, **3.2** and **5.3** (range for others: 52.82(17) – 54.72(9) ° and 118.7(8) – 120.4(8) ° respectively). These differences can be rationalised by the significantly different coordination environments around the U(IV) centre in **5.5**. The related bridging chloride dimer featuring an N'N'₂ ligand, {U(N'N'₂)Cl}₂(μ-Cl)₂ (**5B**, **Figure 5.2** above) contains bridging U-Cl bond distances of 2.881(1) and 2.807(1) Å, and a Cl1-U1-Cl1' angle of 158.53(3) °, which are longer and more obtuse than those found in **5.5**. An explanation for these differences can be ascribed to the steric constraints of the bridging N'N'₂ ligands that force a relatively short U-U distance in the dimeric structure of 4.3198(3) Å vs 4.4988(5) Å found in **5B**.

Mass spectrometric analysis revealed that the product readily decomposes in the gas phase; a fragment at $m/z = 1627$ (< 1%) corresponding to M^+ for **5.5**, and another fragment at $m/z = 1491$ (< 1%) corresponding to $M^+ - \text{Cp}^*$ are present in the spectrum at very low intensity values. Elemental analysis of a solid, glass-like sample of **5.5** returned a %C value slightly out of the expected limits: % expected (found): %C 36.87 (37.52). ¹H NMR spectroscopic analysis of the crystalline material and glass-like solids showed numerous broad, uninterpretable resonances that could not be definitively assigned. In conclusion, the tetravalent chloride **5.1** is not inert to CO₂ exposure, which implies that trivalent **5.3** may also undergo CO₂ insertion into the two U-N bonds of the N'N'₂ ligand as well as reducing CO₂, complicating the identification of products from the reaction between **5.3** and CO₂.

5.5 Bridging arene complexes

Several instances of arene complexes bridging two uranium metal centres *via* a $\mu\text{-}\eta^6\text{:}\eta^6$ -coordination mode have been reported in the literature, featuring both a variety of ancillary ligands and uranium oxidation states. The first ‘inverted sandwich’ complex of this type was reported by Cummins *et al.* in 2000: the reduction of $\text{U}(\text{I})(\text{N}[\text{tBu}]\text{Ar})_3$ ($\text{Ar} = 3,5\text{-C}_6\text{H}_3\text{-Me}_2$) with 3 equivalents of KC_8 in toluene resulted in the formation of $\{\text{U}(\text{N}[\text{tBu}]\text{Ar})_3\}_2(\mu\text{-C}_7\text{H}_8)$.⁴⁰ The related benzene-bridged species, and an adamantyl-ligand derivative were also reported (**Scheme 5.9**); corresponding perdeutero-arene bridges were made by reacting the iodide with KC_8 in either C_6D_6 or C_7D_8 .



Scheme 5.9. Formation of bridging-arene ‘inverted sandwich’ complexes reported by Cummins *et al.* R = *t*Bu, Ad.

Structural data was obtained for the adamantyl toluene complex, $\{\text{U}(\text{N}[\text{Ad}]\text{Ar})_3\}_2(\mu\text{-}\eta^6\text{:}\eta^6\text{-C}_7\text{H}_8)$, and it was seen that the bridging toluene molecule undergoes a slight lengthening of C-C bond distances (0.04 Å) in comparison to free toluene. The toluene moiety is very slightly ‘puckered’, with one carbon atom lying outside of the mean plane of the other carbon atoms, potentially perturbing the aromaticity. Discussion about the oxidation state of this and other bridging arene complexes is still ongoing: the U centres could be viewed as two divalent centres with a neutral arene bridge (in which case no diversion from planarity or change in C-C bond

lengths would be observed), two trivalent centres with an [arene]²⁻ ligand, or even two tetravalent centres bound to an [arene]⁴⁻ ligand. Many other examples of organouranium bridging arene complexes are present in the literature, including $\mu\text{-}\eta^6\text{:}\eta^6\text{-toluene}$,^{35,41-48} $\mu\text{-}\eta^6\text{:}\eta^6\text{-benzene}$,^{35,49-51} and other related $\mu\text{-}\eta^6\text{:}\eta^6\text{-arene}$ complexes,^{35,41,45} featuring a variety of ancillary ligands. With some exceptions, most of these reported complexes feature formally U(III)/U(III) centres bridged by a dianionic arene ligand, as concluded by the respective authors. Details of the ¹H NMR spectroscopic shifts of the bridging arene ligands, U-C_{arene} and C-C_{arene} bond distances, and formal charge assignments of the U centres and arene ligands for all reported organouranium $\mu\text{-}\eta^6\text{:}\eta^6\text{-toluene}$ and $\mu\text{-}\eta^6\text{:}\eta^6\text{-benzene}$ complexes are outlined in **Table 5.4** and **Table 5.5**.

Table 5.4. Diuranium $\mu\text{-}\eta^6\text{:}\eta^6\text{-toluene}$ complexes reported in the literature.

Arene complex	$\delta_{\text{H}} \mu\text{-toluene}$ (ppm) 3H (Me), 2H (Ar), 2H (Ar), 1H (Ar)	U-C _{arene} range (Å)	Avg C-C _{arene} (Å)	OS U, arene	Ref.
$\{\text{U}(\text{N}^{\text{tBu}}\text{Ar})_3\}_2(\mu\text{-C}_7\text{H}_8)$ ^a	18.68, -82.98, -88.39, -65.86	n/a	n/a	III/III, arene ²⁻	40
$\{\text{U}(\text{N}[\text{Ad}]\text{Ar})_3\}_2(\mu\text{-C}_7\text{H}_8)$ ^a	19.90, -84.94, -92.20, -61.04	2.503(9) – 2.660(8)	1.438	III/III, arene ²⁻	40
$\{\text{U}(\text{NN}^{\text{fc}})\}_2(\mu\text{-C}_7\text{H}_8)$ ^b	25.09, -84.79, -86.18, -67.52	2.515(8) – 2.662(8)	1.4545(10)	III/III, arene ²⁻	43
$\{\text{U}(\text{BIPM}^{\text{TMS}}\text{H})(\text{I})\}_2(\mu\text{-C}_7\text{H}_8)$ ^c	n/a	2.553(7) – 2.616(7)	1.436(16)	III/III, arene ²⁻	44
$\{\text{U}(\text{ODtbp})_2\}_2(\mu\text{-C}_7\text{H}_8)$ ^d	10.62, -76.23, -83.31, -87.92	2.516(9) – 2.647(9)	1.443(14)	III/III, arene ²⁻	35
$\{\text{U}(\text{N}''')_2(\mu\text{-C}_7\text{H}_8)$	22.10, -81.93, -88.18, -72.01	2.539(9) – 2.600(8)	1.434(12)	III/III, arene ²⁻	35
$\{\text{U}(\text{N}'\text{N}')_2\}_2(\mu\text{-C}_7\text{H}_8)$	43.27, -80.55, -104.20, -64.99	2.566(4) – 2.617(4)	1.447(5)	III/III, arene ²⁻	this work
$[\text{K}_2\text{I}][\text{U}\{\text{NC}'\text{BuMes}\}_3]_2(\mu\text{-C}_7\text{H}_8)$ ^e	34.70, -38.01, -44.63, -43.05	2.620(9) – 2.681(9)	1.45(2)	IV/IV, arene ²⁻	45
$\{\text{U}(\text{OSi}\{\text{O}'\text{Bu}\}_3)_3\}_2(\mu\text{-C}_7\text{H}_8)$	82.94, -112.68, -122.41, -137.88	2.689(3) – 2.694(3)	1.432(3)	IV/IV, arene ²⁻	46
$[\text{K}(\text{DME})][\text{U}\{\text{NC}'\text{BuMes}\}_3]_2(\mu\text{-C}_7\text{H}_8)$ ^e	64.48, -109.52, -113.84, -126.52	2.60140(9) – 2.65564(11)	1.405(15)	IV/V, arene ²⁻	45
$\text{K}_2\{\text{U}(\text{OSi}\{\text{O}'\text{Bu}\}_3)_3\}_2(\mu\text{-C}_7\text{H}_8)$	16.8, -77.1, -77.5, -72.8	2.624(11) – 2.674(13)	1.439(17)	IV/IV, arene ⁴⁻	48
$\text{K}\{\text{U}(\text{OSi}\{\text{O}'\text{Bu}\}_3)_3\}_2(\mu\text{-C}_7\text{H}_8)$	63.2, -80.0, -90.0, -94.3	2.589(4) – 2.621(3)	1.456(8)	IV/V, arene ⁴⁻	48
$(\{\text{U}(\text{Ts}^{\text{Xy}})\}_2(\mu\text{-C}_7\text{H}_8)$ ^f	34.19, -16.71, -32.61, -36.99	2.651(4) – 2.698(4)	1.440(6)	V/V, arene ⁴⁻	42
$\{\text{U}(\text{Ts}^{\text{Tol}})_2\}_2(\mu\text{-C}_7\text{H}_8)$ ^g	32.4, -18.8, -35.0, -21.0	2.535(15) – 2.673(18)	n/a	V/V, arene ⁴⁻	47

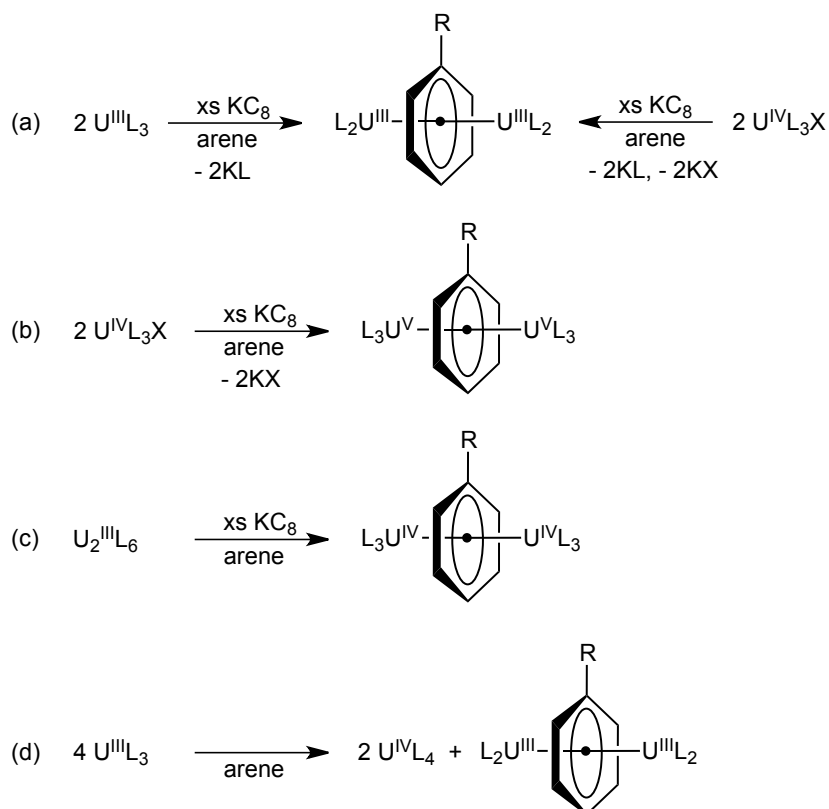
a) Ar = 3,5-C₆H₃-Me₂, b) NN^{fc} = fc{NSi^{tBu}Me₂}₂, c) BIPM^{TMS}H = CH(PPh₂N{TMS})₂, d) Dtbp = 2,6-^tBu₂C₆H₃, e) Mes = (2,4,6-Me₃C₆H₂), f) Ts^{Xy} = CH(SiMe₂NAr')₃; Ar' = 3,5-Me₂C₆H₃, g) Ts^{Tol} = CH(SiMe₂NAr'')₃, Ar'' = 4-MeC₆H₄.

Table 5.5. Diuranium μ - η^6 : η^6 -benzene complexes reported in the literature.

Arene complex	$\delta_{\text{H}} \mu$ -benzene (ppm) (6H, Ar)	U-C _{arene} range (Å)	C-C _{arene} (Å)	OS U, arene	Ref.
{UCp* ₂ } ₂ (μ -C ₆ H ₆)	-98.9	2.509(14) – 2.733(14)	1.42(2) – 1.462(18)	III/III, arene ²⁻	49
{UCp*(N'')} ₂ (μ -C ₆ H ₆)	-84.0	2.559(3) – 2.631(3)	1.449(4) – 1.453(4)	III/III, arene ²⁻	49
{UCp*(OC ₆ H ₂ ^t Bu ₂ -2,6-Me-4)} ₂ (μ -C ₆ H ₆)	-89.27	n/a	n/a	III/III, arene ²⁻	50
{UCp*(CH[TMS] ₂) ₂ } ₂ (μ -C ₆ H ₆)	-79.19	2.5324(15) – 2.6154(15)	1.454(3) – 1.461(3)	III/III, arene ²⁻	50
{UCp*(^t PrNC[Me]N ^t Pr)} ₂ (μ -C ₆ H ₆)	-83.98	n/a	n/a	III/III, arene ²⁻	50
{U(ODtbp) ₂ } ₂ (μ -C ₆ H ₆) ^a	-85.2	2.517(6) – 2.635(6)	1.442(9) – 1.462(9)	III/III, arene ²⁻	35
{U(N'') ₂ } ₂ (μ -C ₆ H ₆)	-82.2	2.568(3) – 2.578(3)	1.447(4) – 1.457(4)	III/III, arene ²⁻	35
{U(ODtbp)N''} ₂ (μ -C ₆ H ₆) ^a	-82.15	2.502(4) – 2.617(4)	1.434(5) – 1.466(5)	III/III, arene ²⁻	35
{U(OTtbp) ₂ } ₂ (μ -C ₆ H ₆) ^b	-85.71	n/a	n/a	III/III, arene ²⁻	35
{U(L ^{Me})I} ₂ (μ -C ₆ H ₆) ^c	-68.59	2.539(8) – 2.587(8)	1.431(13) – 1.464(14)	III/III, arene ²⁻	51
{U(N'N' ₂) ₂ } ₂ (μ -C ₆ H ₆)	-76.37	n/a	n/a	III/III, arene ²⁻	this work
[K(DME)][U{NC ^t BuMes} ₃] ₂ (μ -C ₆ H ₆)	-112.83	n/a	n/a	IV/V, arene ²⁻	45

a) Dtbp = 2,6-^tBu₂C₆H₃, b) Ttbp = 2,4,6-^tBu₃C₆H₂, c) L^{Me} = C{C(Me)NDipp}₂, Dipp = 2,6-ⁱPr₂C₆H₃.

Several methods of forming bridging arenes have been reported and are shown in **Scheme 5.10**: (a) the reaction of a parent U(III) or U(IV) complex and KC_8 in an arene solvent giving a U(III)/U(III) bridging arene; (b) the reaction of a U(IV) complex and KC_8 in an arene solvent giving a U(V)/U(V) bridging arene; (c) the reaction of a dimeric U(III) complex with KC_8 in an arene solvent giving a U(IV)/U(IV) product; (d) the spontaneous reduction of an arene solvent with concomitant disproportionation of a U(III) complex to a bridging arene and a U(IV) complex.



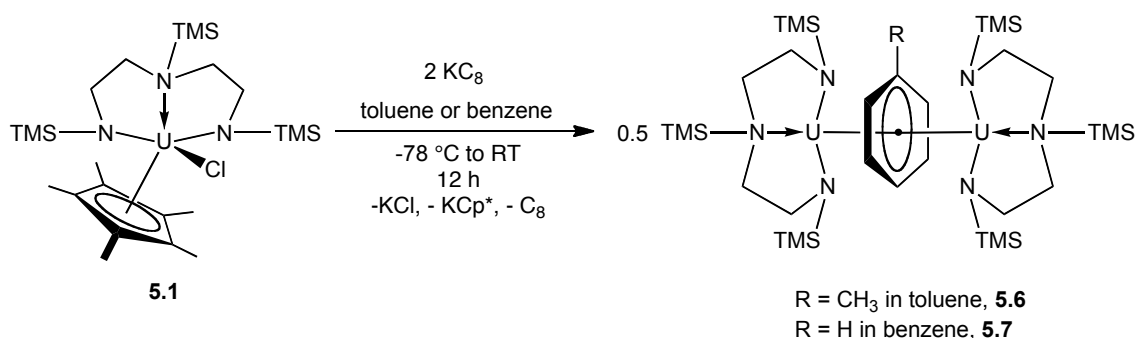
Scheme 5.10. Previously reported routes to uranium bridging arene complexes.

$\text{L} = 1e^-$ donating ligand, $\text{X} = \text{halide}$, $\text{R} = \text{Me}, \text{H}$.

With both the U(IV) chloride, $\text{U}(\text{N}'\text{N}'_2)\text{Cp}^*\text{Cl}$ (**5.1**), and the U(III) complex, $\text{U}(\text{N}'\text{N}'_2)\text{Cp}^*$ (**5.3**), in hand, the reactions of either **5.1** with excess KC_8 (*i.e.* 2 equivalents or greater) in an arene solvent, or **5.3** with stoichiometric KC_8 in an arene solvent would be expected to follow route (a) to form bridging arene complexes; the former reaction could also follow route (b).

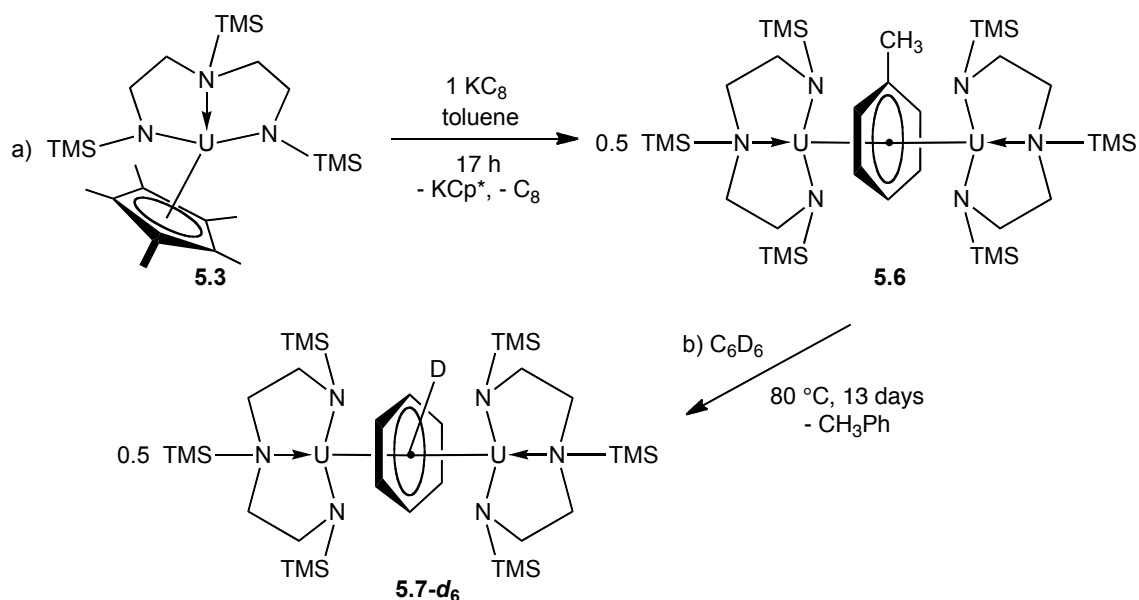
5.5.1 Synthesis and characterisation of $\{U(N'N'_2)\}_2(\mu-\eta^6:\eta^6-C_6H_5R)$ ($R = H, Me$)

The reaction of **5.1** and 2 equivalents of KC_8 in toluene resulted in the formation of a dark brown solution containing off-white precipitate after stirring for 12 hours. Removal of volatiles, extraction into Et_2O and filtration gave a dark brown solution, which yielded very dark brown crystals of $\{U(N'N'_2)\}_2(\mu-\eta^6:\eta^6-C_7H_8)$ (**5.6**, **Scheme 5.11**) in a 20% isolated yield after concentration and slow-cooling to $-50\text{ }^\circ\text{C}$. The same reaction performed in benzene afforded $\{U(N'N'_2)\}_2(\mu-\eta^6:\eta^6-C_6H_6)$ (**5.7**, **Scheme 5.11**), however, crystalline samples of **5.7** could not be obtained.



Scheme 5.11. Synthesis of bridging arene complexes, **5.6** and **5.7**, from **5.1**.

Other synthetic routes to the bridging arene complexes are: the reaction of **5.3** and KC_8 in toluene to yield **5.6** (**Scheme 5.12a**), or the exchange of an arene bridge by heating **5.6** in C_6D_6 to yield **5.7** (**Scheme 5.12b**). The second reaction was quantitative by 1H NMR spectroscopy, but only after heating the sample to $80\text{ }^\circ\text{C}$ for 13 days; the reverse reaction from **5.7** to **5.6** did not occur. This is in line with the findings of Arnold *et al.*, where the authors describe the preferential formation of diuranium benzene-bridged products, $\{U(X_2)\}_2(\mu-\eta^6:\eta^6-C_6H_6)$ ($X = N''$, ODtbp), to anthracene-bridged products, when both benzene and the more easily-reduced dihydroanthracene are present in solution with $U(X_2)_3$. Computational results described in the same report correlate with this observation, finding that the stability of the benzene-bridged product was highest. Heating $\{U(X_2)\}_2(\mu-\eta^6:\eta^6-C_6H_6)$ dissolved in C_6D_6 in the presence of excess dihydroanthracene also does not elicit a reaction.³⁵



Scheme 5.12. Alternative routes to bridging arene complexes.

^1H NMR spectroscopic analysis of both **5.6** and **5.7** showed the presence of two intense resonances, corresponding to the SiMe_3 proton environments of the $\text{N}'\text{N}'_2$ ligands, at δ_{H} -3.16 and -13.6 (**5.6**) and -3.12 and -13.2 (**5.7**). Signals correlating to the CH_2CH_2 backbone environments were also observed, and the bound arene resonances were present at δ_{H} 43.3 (3H, $\text{C}_6\text{H}_5\text{-CH}_3$), -65.0 (1H, *p*-CH), -80.6 (2H, *o/m*-CH) and -104 (2H, *o/m*-CH) for **5.6**, and at δ_{H} -76.2 (6H, C_6H_6) for **5.7**. The latter values are similar to those reported for other μ -toluene and μ -benzene organouranium complexes (see **Table 5.4** and **Table 5.5**). Mass spectrometric analysis showed the expected parent ions for both **5.6** and **5.7**. Elemental analysis of **5.6** returned results consistently high in %N values, with expected %C: 32.93, %H: 6.53, %N: 6.98, and found %C: 32.81, %H: 6.56, %N: 7.69, for reasons that could not be ascertained. Satisfactory elemental analysis results were also not obtained for **5.7**. It was observed that over a period of 48 hours, the sample of **5.7** dissolved in C_7D_8 from which the ^1H NMR spectrum was obtained began change in composition, as determined by ^1H NMR spectroscopy, indicating that the product is not indefinitely stable.

Crystals of **5.6** suitable for X-ray diffraction studies were obtained from slow-cooling a saturated Et_2O solution to -50 °C overnight. Recrystallisation from a

saturated THF solution afforded the THF adduct, **5.6.THF**, but twinning and disorder in the structure did not allow for full data refinement and hence no geometric parameters are quoted, only connectivity is established. The structures of these compounds are shown in **Figure 5.9** and **Figure 5.10**.

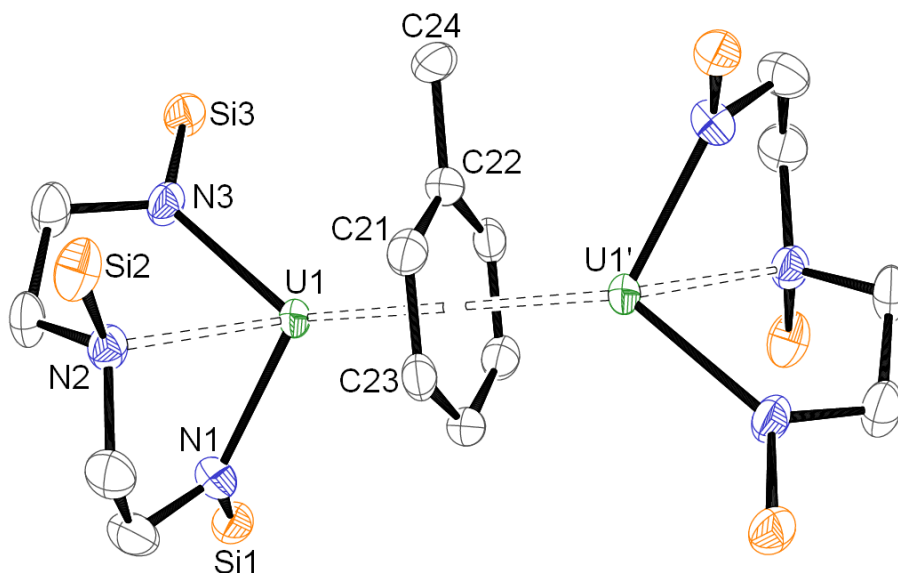


Figure 5.9. Molecular structure of $\{U(N'N')_2\}_2(\mu-C_7H_8)$ (**5.6**). ORTEP representation with thermal ellipsoids at the 50% probability level. Hydrogen atoms and $SiMe_3$ groups omitted for clarity; toluene molecule rests on plane of symmetry – other Me group not shown above.

U1-U2: 4.3132(2) Å, U1-N1: 2.278(3) Å, U1-N2: 2.643(3) Å,
 U1-N3: 2.301(3) Å, N1-U1-N3: 99.91(9), U1-Ct: 2.15661(11) Å,
 U-C_{arene} range: 2.566(3) – 2.618(3) Å, C-C_{arene} range: 1.436(5) – 1.464(5) Å.

In **5.6**, the $N'N'_2$ ligand coordinates in a similar fashion to that seen in **5.3**, with the two CH_2CH_2 backbone moieties orthogonal to each other (unlike the symmetric arrangement seen in **5.1**), and the U1-N2 bond distance of 2.643(3) Å indicates a lone-pair interaction between the middle nitrogen and central uranium atom. The bridging arene ligand is essentially planar, with torsion angles around the ring calculated as 1.0(3) and 1.0(2) °, whilst the bond distances between the arene ring C-C bonds are marginally elongated (ca 0.04-0.07 Å) in comparison to free toluene (1.395(1) Å),⁵² a trend which is observed in many other uranium bridging toluene complexes (see **Table 5.4**). In comparison to other uranium bridging toluene species,

the average U-C_{arene} distance in **5.6** is within the previously reported range (1.434(12) – 1.4545(10) Å), and is closest to the average distance reported for {U(ODtbp)₂}₂(μ-C₇H₈) (1.443(14) vs 1.447(5) Å).

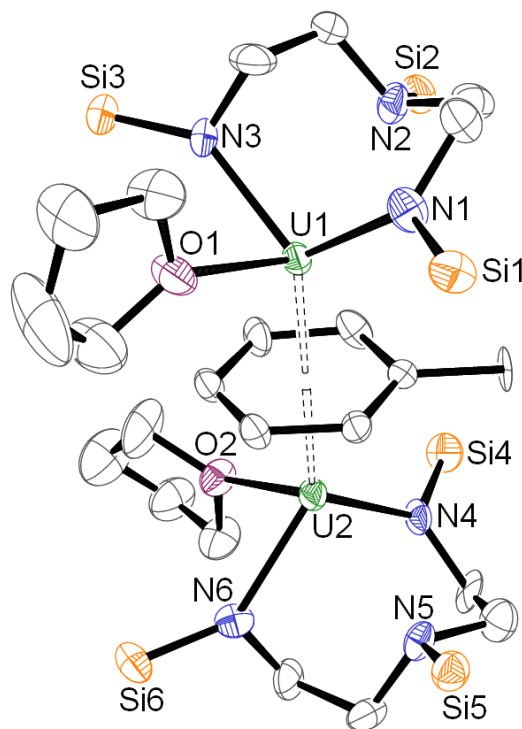


Figure 5.10. Molecular structure of {U(N'N')₂THF}₂(μ-C₇H₈) (**5.6.THF**). ORTEP representation with thermal ellipsoids at the 50% probability level. One molecule of two essentially identical molecules in the asymmetric unit. Data not fully refined so metrical parameters are not reported.

As seen in **Figure 5.10**, the N'N'₂ ligand of **5.6.THF** coordinates in a fashion halfway between the symmetrical coordination seen in **5.1** and the asymmetric orthogonal backbone arrangement observed in base-free **5.6** and **5.3**. The central nitrogen atom does not appear to be coordinated to the uranium centre, and the toluene ligand still appears to be essentially planar, but this cannot be confirmed due to the unrefined nature of the data.

It is proposed that **5.6** contains two U^{III} centres bridged by a toluene²⁻ species, as is most commonly observed for other bridging toluene complexes (see **Table 5.4** and **Table 5.5**). Common structural and spectroscopic features are shared between **5.6** and

other U^{III}/U^{III} , toluene²⁻ species: the U-C_{arene} bond distances in **5.6** fit most closely within the range of those reported for U^{III}/U^{III} , toluene²⁻ species (2.566(4) – 2.617(4) Å vs 2.503(9) – 2.662(8) Å), and the ¹H NMR spectroscopic resonances correlating to the bridging toluene ring protons in **5.6** are closest in similar chemical shift to the others reported (δ_H -64.99, -80.55, and -104.20 compared to a range of δ_H -61.04 – -92.20). For all bridging toluene species, the C-C_{arene} bond distances do not help to elucidate the extent of reduction of the arene ligand, due to the bond distance values in free toluene falling closely within the ESD values of the bound arene distances.

5.5.2 Reactivity of $\{U(N'N'_2)\}_2(\mu-C_7H_8)$ (**5.6**)

Reductive reactivity has been reported for other bridging arene species that contain two U^{III} centres bridged by an arene²⁻ ligand. Both diphenyl disulfide and azobenzene are reduced upon exposure to $\{U(N[R]Ar)_2\}_2(\mu-\eta^6:\eta^6-C_7H_8)$ (where R = Ad, ^tBu), cleaving the S-S and N=N bonds to form U^{IV} dimers.⁴⁰ Quinoxaline will also react with trivalent $\{U(NN^{fc})\}_2(\mu-\eta^6:\eta^6-C_7H_8)$, yielding a tetrameric U^{IV} complex with reduced quinoxaline bridges.⁴³ Reductive cleavage of a Co-Co bond is also possible *via* the reaction of the U^V and arene⁴⁻ complex, $\{U(Ts^{Xy})\}_2(\mu-\eta^6:\eta^6-C_7H_8)$, with $\{Co(CO)_3(PPh_3)\}_2$, resulting in the formation of an unprecedented U-Co bond.⁴²

Novel reactivity is observed when the bridging arene species, $\{U(ODtbp)_2\}_2(\mu-C_6H_6)$ (where Dtbp = 2,6-^tBu₂C₆H₃), is combined with HBBN and heated to 90 °C for 16 hours, resulting in the borylation of the activated benzene bridge and forming $\{U(ODtbp)_2\}_2(\mu-C_6H_5BBN)$. Similar borylation is observed with naphthalene, toluene, and biphenyl, when $U(ODtbp)_3$ is heated in the presence of the respective arene and HBBN, resulting in a new type of C-B bond forming reaction, which is not accessible *via* group 1 metal-based routes.³⁵

In light of the reactions that occur with related species, **5.6** was examined for potential reductive behaviour. Exposure of **5.6** to either stoichiometric or excess azobenzene elicited no reaction, as was the case with CO, which did not result in a reaction even after heating to 100 °C. When an excess of CO₂ was added to a C₇D₈ solution of **5.6** *via* Toepler pump, ¹H NMR spectroscopic data showed the immediate and complete decomposition into uninterpretable diamagnetic products. It was concluded that the bulky nature of the N'N'₂ ligands may inhibit further reactivity of the arene bridge or metal centres on steric grounds.

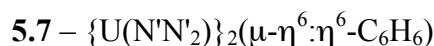
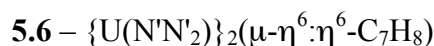
5.6 Conclusions and chapter summary

The aim of installing the N'N'₂ ligand onto uranium, in place of the carbocyclic COT^{TIPS₂} ligand and in tandem with Cp*, was to make a ‘half-sandwich’ complex that could be compared in terms of its reactivity to its mixed-sandwich analogue, U(COT^{TIPS₂})Cp*. However, it has become apparent from work towards synthesising U(N'N'₂)Cp* that the propensity for the N'N'₂ ligand to undergo silyl-group migration means that this trivalent complex is not as robust, and hence not as useful, as its mixed-sandwich counterpart.

Despite many efforts, the isolation of any small molecule reduction products has not been successful, potentially due in part to side-reactions involving silyl-group migrated derivatives of the original precursor or non-inert behaviour of the U-N σ-bonds in the N'N'₂ ligand, hence not affording clean reactions or isolable products.

The syntheses of the bridging arene species, {U(N'N'₂)}₂(μ-η⁶:η⁶-C₆H₅R) (R = Me, **5.6**; R = H, **5.7**), has added to the body of knowledge already collected for organouranium bridging-arenes featuring a variety of ligand systems, and in a range of oxidation states.

5.7 Compound naming for Chapter 5



5.8 References for Chapter 5

1. D. McKay, A. S. P. Frey, J. C. Green, F. G. N. Cloke, and L. Maron, *Chem. Commun.*, 2012, **48**, 4118–4120.
2. A. S. P. Frey, F. G. N. Cloke, P. B. Hitchcock, I. J. Day, J. C. Green, and G. Aitken, *J. Am. Chem. Soc.*, 2008, **130**, 13816–13817.
3. O. T. Summerscales, F. G. N. Cloke, P. B. Hitchcock, J. C. Green, and N. Hazari, *Science*, 2006, **311**, 829–831.
4. J. A. Higgins, F. G. N. Cloke, and S. M. Roe, *Organometallics*, 2013, **32**, 5244–5252.
5. O. T. Summerscales, A. S. P. Frey, F. G. N. Cloke, and P. B. Hitchcock, *Chem. Commun.*, 2009, 198–200.
6. A. S. P. Frey, F. G. N. Cloke, M. P. Coles, L. Maron, and T. Davin, *Angew. Chem.*, 2011, **123**, 7013–7015.
7. A. S. P. Frey, F. G. N. Cloke, M. P. Coles, and P. B. Hitchcock, *Chem.--Eur. J.*, 2010, **16**, 9446–9448.
8. F. G. N. Cloke, P. B. Hitchcock, and J. B. Love, *J. Chem. Soc., Dalton Trans.*, 1995, 25–30.
9. H. C. S. Clark, F. G. N. Cloke, P. B. Hitchcock, J. B. Love, and A. P. Wainwright, *J. Organomet. Chem.*, 1995, **501**, 333–340.
10. J. B. Love, H. C. S. Clark, F. G. N. Cloke, J. C. Green, and P. B. Hitchcock, *J. Am. Chem. Soc.*, 1999, **121**, 6843–6849.
11. P. E. Collier, S. M. Pugh, H. C. S. Clark, J. B. Love, F. G. N. Cloke, and P. Mountford, *Inorg. Chem.*, 2000, **39**, 2001–2005.
12. J. D. Selby, C. D. Manley, A. D. Schwarz, E. Clot, and P. Mountford, *Organometallics*, 2008, **27**, 6479–6494.
13. N. Emig, R. Réau, H. Krautscheid, D. Fenske, and G. Bertrand, *J. Am. Chem. Soc.*, 1996, **118**, 5822–5823.
14. B. D. Ward, S. R. Dubberley, A. Maise-François, L. H. Gade, and P. Mountford, *J. Chem. Soc., Dalton Trans.*, 2002, **2**, 4649–4657.
15. G. K. B. Clentsmith, V. M. E. Bates, P. B. Hitchcock, and F. G. N. Cloke, *J. Am. Chem. Soc.*, 1999, **121**, 10444–10445.
16. G. P. Clancy, H. C. S. Clark, G. K. B. Clentsmith, F. G. N. Cloke, and P. B. Hitchcock, *J. Chem. Soc., Dalton Trans.*, 1999, 3345–3347.

17. K. Feghali, D. J. Harding, D. Reardon, S. Gambarotta, G. Yap, and Q. Wang, *Organometallics*, 2002, **21**, 968–976.
18. D. J. Wilson, A. Sebastian, F. G. N. Cloke, A. G. Avent, and P. B. Hitchcock, *Inorg. Chim. Acta*, 2003, **345**, 89–94.
19. P. Roussel and P. Scott, *J. Am. Chem. Soc.*, 1998, **120**, 1070–1071.
20. B. M. Gardner, J. C. Stewart, A. L. Davis, J. McMaster, W. Lewis, A. J. Blake, and S. T. Liddle, *Proc. Natl. Acad. Sci. U. S. A.*, 2012, **109**, 9265–9270.
21. P. L. Arnold, Z. R. Turner, R. M. Bellabarba, and R. P. Tooze, *Chem. Sci.*, 2011, **2**, 77–79.
22. A. L. Odom, P. L. Arnold, and C. C. Cummins, *J. Am. Chem. Soc.*, 1998, **120**, 5836–5837.
23. C. P. Larch, PhD Thesis, University of Sussex, 2007.
24. *Cambridge Crystal Database Service*. Access date March 2014.
25. I. Korobkov, S. Gambarotta, and G. P. A. Yap, *Angew. Chem.*, 2002, **114**, 3583–3586.
26. F. G. N. Cloke and P. B. Hitchcock, *J. Am. Chem. Soc.*, 2002, **124**, 9352–3.
27. W. J. Evans, S. A. Kozimor, and J. W. Ziller, *J. Am. Chem. Soc.*, 2003, **125**, 14264–14265.
28. S. M. Mansell, N. Kaltsoyannis, and P. L. Arnold, *J. Am. Chem. Soc.*, 2011, **133**, 9036–9051.
29. K. C. Jantunen, F. Haftbaradaran, M. J. Katz, R. J. Batchelor, G. Schatte, and D. B. Leznoff, *Dalton Trans.*, 2005, 3083–3091.
30. D. M. King, W. Lewis, and S. T. Liddle, *Inorg. Chim. Acta*, 2012, **380**, 167–173.
31. I. Korobkov, S. Gambarotta, G. P. A. Yap, L. Thompson, and P. J. Hay, *Organometallics*, 2001, **20**, 5440–5445.
32. P. Roussel, P. B. Hitchcock, N. D. Tinker, and P. Scott, *Inorg. Chem.*, 1997, **36**, 5716–5721.
33. R. A. Andersen, E. Carmona-Guzman, K. Mertis, E. Sigurdson, and G. Wilkinson, *J. Organomet. Chem.*, 1975, **99**, C19–C20.
34. G. M. Jones, P. L. Arnold, and J. B. Love, *Chem.--Eur. J.*, 2013, **19**, 10287–10294.
35. P. L. Arnold, S. M. Mansell, L. Maron, and D. McKay, *Nat. Chem.*, 2012, **4**, 668–674.
36. J. G. Brennan, R. A. Andersen, and J. L. Robbins, *J. Am. Chem. Soc.*, 1986, **108**, 335–336.
37. J. Parry, E. Carmona, S. Coles, and M. Hursthouse, *J. Am. Chem. Soc.*, 1995, **117**, 2649–2650.
38. M. del Mar Conejo, J. S. Parry, E. Carmona, M. Schultz, J. G. Brennan, S. M. Beshouri, R. A. Andersen, R. D. Rogers, S. Coles, and M. B. Hursthouse, *Chem.--Eur. J.*, 1999, **5**, 3000–3009.
39. W. J. Evans, S. A. Kozimor, G. W. Nyce, and J. W. Ziller, *J. Am. Chem. Soc.*, 2003, **125**, 13831–13835.
40. P. L. Diaconescu, P. L. Arnold, T. A. Baker, D. J. Mindiola, and C. C. Cummins, *J. Am. Chem. Soc.*, 2000, **122**, 6108–6109.
41. P. L. Diaconescu and C. C. Cummins, *J. Am. Chem. Soc.*, 2002, **124**, 7660–7661.
42. D. Patel, F. Moro, J. McMaster, W. Lewis, A. J. Blake, and S. T. Liddle, *Angew. Chem. Int. Ed.*, 2011, **50**, 10388–10392.
43. M. J. Monreal, S. I. Khan, J. L. Kiplinger, and P. L. Diaconescu, *Chem. Commun.*, 2011, **47**, 9119–9121.

44. D. P. Mills, F. Moro, J. McMaster, J. Van Slageren, W. Lewis, A. J. Blake, and S. T. Liddle, *Nat. Chem.*, 2011, **3**, 454–460.
45. P. L. Diaconescu and C. C. Cummins, *Inorg. Chem.*, 2012, **51**, 2902–2916.
46. V. Mougél, C. Camp, J. Pécaut, C. Copéret, L. Maron, C. E. Kefalidis, and M. Mazzanti, *Angew. Chem. Int. Ed.*, 2012, **51**, 12280–12284.
47. D. Patel, F. Tuna, E. J. L. McInnes, J. McMaster, W. Lewis, A. J. Blake, and S. T. Liddle, *Dalton Trans.*, 2013, **42**, 5224–5227.
48. C. Camp, V. Mougél, J. Pécaut, L. Maron, and M. Mazzanti, *Chem.--Eur. J.*, 2013, **19**, 17528–40.
49. W. J. Evans, S. A. Kozimor, J. W. Ziller, and N. Kaltsoyannis, *J. Am. Chem. Soc.*, 2004, **126**, 14533–14547.
50. W. J. Evans, C. A. Traina, and J. W. Ziller, *J. Am. Chem. Soc.*, 2009, **131**, 17473–17481.
51. A. J. Wooles, W. Lewis, A. J. Blake, and S. T. Liddle, *Organometallics*, 2013, **32**, 5058–5071.
52. O. Madelung, *Landolt-Börnstein Numerical Data and Functional Relationship in Science and Technology: Structure Data of Free Polyatomic Molecules*, Springer, Berlin, Vol II/15., 1987.

CHAPTER 6: EXPERIMENTAL DETAILS

6.1 General procedures and techniques

Air-sensitive compound manipulations were carried out using standard Schlenk-line techniques under an atmosphere of catalytically dried and deoxygenated argon, or in MBraun glove boxes under catalytically dried and deoxygenated nitrogen or argon atmospheres, with < 1 ppm H_2O and < 1 ppm O_2 . Nitrogen and argon gases were supplied by BOC Gases UK. All glassware was dried by storage in an oven at $120\text{ }^\circ\text{C}$ overnight with subsequent cooling under 10^{-3} mbar vacuum, followed by repeated alternate evacuation and purging with argon. Celite® 545 filter aid was stored in an oven at $200\text{ }^\circ\text{C}$ and flame dried under vacuum before use. Filter cannulae were equipped with Whatman® 25 mm glass microfibre filters dried in an oven at $120\text{ }^\circ\text{C}$ overnight prior to use.

Solvents were pre-dried over sodium wire (with the exception of DCM which was not pre-dried) before heating to reflux over the appropriate drying agent for at least 72 hours before use: pentane, hexane and Et_2O were dried over $\text{NaK}_{2.88}$; THF, $t\text{BuOMe}$, DME and 1,4-dioxane were dried over K; toluene was dried over Na; DCM was dried over CaH_2 . Dried solvents were degassed and stored in potassium-mirrored ampoules after collection, with the exception of THF, DME and DCM, which were stored in ampoules containing flame-dried 4Å molecular sieves. Solvents used in the MBraun glove box were stored in bottles under argon prior to use. Deuterated NMR solvents were purchased from GOSS Scientific Ltd. or Sigma Aldrich, purified by heating at reflux over K before transferring to ampoules *via* freeze-thaw degassing methods, and were stored under nitrogen prior to use.

6.2 Instrumentation

NMR spectroscopic analysis was performed using a Varian VNMRs 400 spectrometer: ^1H NMR was run at 399.5 MHz, ^7Li NMR at 155.3 MHz, ^{13}C NMR at 100.5 MHz, ^{29}Si NMR at 79.4 MHz and ^2H NMR at 61.3 MHz on the VNMR 400. All shifts were internally referenced to residual solvent resonances set using an external SiMe_4 reference, with the exception of ^2H spectra, which were internally referenced to residual deuterio-solvent resonances, ^7Li NMR spectra, which were externally referenced to 1 M LiCl in D_2O , and ^{29}Si spectra, which were referenced to an external SiMe_4 reference. All spectra were recorded at 303 K unless otherwise specified.

Mass spectrometry was carried out by Dr. A. Abdul-Sada at the University of Sussex, using either a VG Autospec Fisons instrument (electron ionisation at 70 eV) or a Kratos MS25 mass spectrometer. Infrared spectroscopy was carried out either using a Perkin Elmer Spectrum ONE machine, with samples prepared as Nujol mulls or thin films between NaCl plates in an argon-filled glovebox before transferal to a gas-tight IR cell, or using *in situ* ReactIR™ equipment with a diamond probe, with samples prepared as methylcyclohexane solutions before transferal into a specially-designed IR cell fitted with gas-tight O-rings and a Rotaflo® stopcock, connected to a high-vacuum/argon line (with an optional Swagelok® connection to a gas line/Toepler pump).

Single crystal X-ray diffraction analysis was performed by Dr. S. M. Roe or by Dr. A. S. P. Frey at the University of Sussex, with data collected either on a Bruker-Nonius rotating anode diffractometer with a sealed-tube source (Mo) or an Agilent Xcalibur diffractometer with a sealed-tube source (Mo or $\text{Cu}/\text{K}\alpha$), both with a Kappa CCD area detector and an Oxford Cryosystems low-temperature device (173 K), operating in ω scanning mode with ψ and ω scans to fill the Ewald sphere. The programs used for control and integration were Collect, Scalepack, and Denzo,¹ or programs associated with CrysAlisPro.² Absorption corrections were based on

equivalent reflections using SADABS. Crystals were mounted on a glass fiber from dried vacuum oil kept over 4 Å sieves in an MBraun glovebox, under argon or nitrogen. All solutions and refinements were performed using the WinGX package and all software packages within,³ or using OLEX2 and software packages within.⁴⁻⁶ Non-hydrogen atoms were refined using anisotropic thermal parameters, and hydrogens were added using a riding model. The exception to these conditions is for the data for U(COT^{TIPS2})Cp*(κ²-O₂CNH₂): the X-ray diffraction analysis was performed by the National Crystallography Service at Southampton, using a Rigaku Saturn724+ diffractometer with a rotating anode Mo/Kα source and graphite monochromator (collection at 100 K), with data collection and reduction controlled by Rigaku CrystalClear-SM Expert 3.1 b10,⁷ and refinement carried out using ShelXL-97.⁶

Elemental analyses were carried out by E. M. Pascher at Mikroanalytisches Labor Pascher, Germany, or by Des Davis at The University of Bristol, UK. Samples were either flame-sealed under vacuum or submitted as triple-sealed vials prepared in an argon-filled glovebox at > 1 atm pressure.

All computational work was carried out by Dr. L. Maron or Dr. C. E. Kefalidis at INSA Toulouse, France. All the structures were fully optimised with the Becke's 3-parameter hybrid functional⁸ combined with the non-local correlation functional provided by Perdew/Wang⁹ (B3PW91). As in all the reactivity there is no change in oxidation state of the uranium center from U(IV) for all the species involved, the 5f-in-large-core ECP (augmented by a f polarisation function, $\alpha = 1.0$) is used as the basis set.¹⁰ For the silicon atoms the quasi-relativistic energy-adjusted *ab-initio* pseudopotential was used, along with its corresponding energy-optimised valence basis set,¹¹ augmented by a d polarisation function.¹² For the remaining atoms, the 6-31G(d,p) basis set was used.¹³⁻¹⁵ In all computations no constraints were imposed on the geometry. All stationary points have been identified as minima (number of imaginary frequencies $N_{\text{imag}} = 0$) or transition states ($N_{\text{imag}} = 1$). Intrinsic Reaction Paths (IRPs)^{16,17} were traced from the various transition structures to make sure that no

further intermediates exist. The vibrational modes and the corresponding frequencies are based on a harmonic force field. Enthalpy energies were obtained at $T = 298.15\text{K}$ within the harmonic approximation. In the case of **2.9**, $\text{U}(\text{COT}^{\text{TIPS}2})(\eta^5\text{-}\kappa^1\text{-C}_5\text{Me}_4\text{CH}_2)$, no p-polarisation functions were used in order to save computational time, due to the consideration of the full size of the ligands. For **3.8**, enediolate, the $i\text{Pr}$ substituents on the experimentally-used $\text{COT}^{\text{TIPS}2}$ ligands were replaced by H; this simplification does not change the results significantly as it has been shown in previous studies in related ligand environment.^{18,19} GAUSSIAN09 program suite was used in all calculations.²⁰

6.3 Preparation of reagents

The following reagents were purchased from Aldrich and used without further purification: potassium metal and TMSCl . The following reagents were purchased from Acros and used without further purification: diethylenetriamine, 1,8-diazabicyclo[5.4.0]undec-7-ene. $\text{KN}(\text{TMS})_2$ was purchased from Fluka and recrystallised from toluene before use. NpLi was purchased from Aldrich as a cyclohexane/toluene solution, filtered, and evaporated to yield a solid. $n\text{BuLi}$ (2.5 M) was purchased from Acros, passed through Celite® and titrated to determine exact molarity. $t\text{BuCl}$ was purchased from Fluka, dried sequentially over sieves and freeze-thaw degassed before use. Isotopically enriched gases (^{13}CO , $^{13}\text{CO}_2$, D_2 , HD and ND_3) were supplied by Cambridge Isotope Laboratories Inc., and used without further purification. Cylinders of ^{12}CO (research grade, 100% purity), $^{12}\text{CO}_2$ (100.000% purity), H_2 (99.999% purity) and NH_3 (anhydrous) were all supplied by BOC gases and used as supplied.

$\text{KCH}(\text{TMS})_2$, KCH_2Ph , $\text{LiCH}_2(\text{TMS})$, $\text{KCH}_2(\text{TMS})$, KH , KOEt , $t\text{BuLi}$, NaH , KC_8 , K/Hg amalgam, NaK_3 , 18-crown-6, 12-crown-4, and MeLi (0.334 M) were kindly supplied by members of Lab 14. U turnings were donated by BNFL and rinsed with nitric acid before use. UI_3 ,²¹ UCl_4 ,²² $\text{K}_2(\text{COT}^{\text{TIPS}2})$,²³ $\text{UCl}_3\text{Cp}^*(\text{THF})$,²² $\text{MgClCp}^*(\text{THF})$,²² KCp^* (made by deprotonating HCp^* with $\text{KN}(\text{TMS})_2$)²⁴ and

$\text{Li}_2(\text{N}'\text{N}'_2)$ (made by deprotonating $\text{H}_2(\text{N}'\text{N}'_2)$ with ${}^t\text{BuLi}$)²⁵ were synthesised according to published procedures.

6.4 Notes on interpreting NMR spectra of paramagnetic organouranium complexes reported in this work.

Due to the effects of paramagnetic U(IV) and U(III) centres, the NMR spectra collected during the course of this work generally contain resonances that are shifted from their typical diamagnetic positions, and are interpreted from signal multiplicity and integration alone (for ${}^1\text{H}$ NMR spectra) or by relative resonance quantities. ${}^1\text{H}$ NMR spectroscopy is the most commonly used technique in this thesis; resonances are extremely sensitive to the overall compound environment, typically appearing at chemical shifts from +150 to -150 ppm. As it is not possible to predict the chemical shifts at which ligand resonances will occur, characterising signals by multiplicity and integration values is relied upon to aid identification of new compounds.

The $\text{COT}^{\text{TIPS}_2}$ ligand gives rise to an easily recognisable set of resonances in ${}^1\text{H}$ NMR spectra: two doublets of integration 18H each, one septet (sometimes seen as a broadened multiplet) of integration 6H – typically at shifts between 0 and -20 ppm – and three broad singlets ($\Delta\nu_{1/2} = \text{ca } 40 \text{ Hz}$) of integration 2H each – typically located between 50 and 100 or -50 and -100 ppm. These resonances are assigned to the protons outlined in Figure 6.1. In addition, the Cp^* ligand appears as a singlet ($\Delta\nu_{1/2} = \text{ca } 5\text{-}10 \text{ Hz}$) of integration 15H, typically between +10 and -10 ppm.

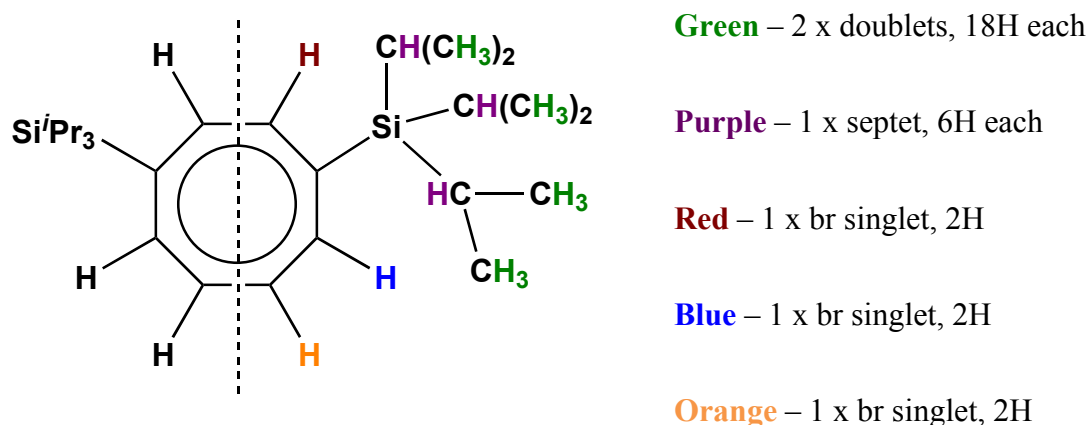


Figure 6.1. Diagram outlining multiplicity and integral values of ^1H NMR spectroscopic resonances corresponding to the COT^{TIPS} ligand in typical U(IV) mixed-sandwich complexes.

The diamidoamine $\text{N}'\text{N}'_2$ ligand also gives rise to distinctive shifts in ^1H NMR spectra, and a change in environment around the uranium metal centre also causes significant changes in chemical shift for each ligand proton resonance. The three TMS groups are seen as two intense singlets, integrating relative to each other in a ratio of 2:1, due to the magnetic equivalence of the two terminal TMS groups. The ligand CH_2CH_2 backbone protons are not always observed due to broadening effects, but often appear as 4 sets of broad singlets with integral values of 2H each, or as 8 singlets with integral values of 1H each.

$^{13}\text{C}\{^1\text{H}\}$ NMR spectra of all the paramagnetic uranium complexes synthesised here display weak, broadened and shifted resonances that are not generally of use in confirming the structure or identity of the complexes, even after collecting decoupled spectra over 10000 scans. As such, they are not routinely reported in the experimental section, unless a ^{13}C -labeled gas has been used during the compound preparation.

$^{29}\text{Si}\{^1\text{H}\}$ NMR spectra are reported for many mixed-sandwich compounds in this work and typically show one resonance (due to the identical $\text{COT}^{\text{TIPS}2}$ ligand Si environments) and appear at chemical shifts between +200/-200 ppm for different complexes, providing a useful handle for elucidating the number and identity of species

present in a reaction mixture. Due to the longer collection time needed for these spectra in comparison to ^1H NMR spectra, complexes that are prone to decomposition in solution cannot always be characterised in this way. For $\text{N}'\text{N}'_2$ and $\text{N}'\text{NN}''$ ligand-containing complexes, two signals correlating to the two inequivalent TMS-group environments are not always seen due to broadening effects. A recent paper that collates $^{29}\text{Si}\{^1\text{H}\}$ NMR spectroscopic data from a large number of reported Si-containing organouranium complexes draws some conclusions relating oxidation state, structure, and ligand environment to $^{29}\text{Si}\{^1\text{H}\}$ NMR spectroscopic shifts.²⁶

By virtue of these distinct resonances and their relative integral values, coupled with their widely varying chemical shifts, it is possible to identify individual species even in complex reaction mixtures. Attempts have been made to assign all paramagnetic ^1H NMR spectra collected, where possible.

6.5 Experimental details for Chapter 2

6.5.1 Synthesis of $\text{U}(\text{COT}^{\text{TIPS}_2})\text{Cp}^*(\text{THF})$ (**2.1.THF**)

This synthesis is a modification of a published procedure:²⁰ an equimolar mixture of KCp^* (0.40 g, 2.30 mmol) and UI_3 (1.42 g, 2.30 mmol) was dissolved in THF (ca 50 cm³) in an ampoule and stirred at ambient temperature for 16 h, during which time the solution changed colour from purple to blue-green. Upon settling, the solution was isolated from residual off-white solids *via* filtration and then cooled to -30 °C. A solution of $\text{K}_2\text{COT}^{\text{TIPS}_2}$ (0.99 g, 2.00 mmol, 0.87 eq.) in THF (ca 20 cm³) was added dropwise *via* cannula to the cold intermediary $\text{UI}_2\text{Cp}^*(\text{THF})_3$ solution over 1 h, before the mixture was stirred for a further 12 h resulting in a dark brown solution containing white precipitate. Removal of volatiles under reduced pressure preceded extraction in pentane (ca 100 cm³), and filtration through Celite® yielded a dark brown solution. Upon reducing the solution volume to 30 cm³ and cooling to -50 °C, black needle-like crystals of **2.1** were obtained.

Yield: 1.13 g (1.31 mmol) 66% w.r.t. $\text{K}_2\text{COT}^{\text{TIPS}2}$.

^1H NMR (C_7D_8 , 399.5 MHz): δ_{H} 48.49 (br s, 2H, COT-*H*), 1.91 (br s, 4H, THF- CH_2), 1.02 (br s, 4H, THF- CH_2), -0.97 (m, br, 6H, ^iPr -*CH*), -4.61 (br s, 18H, ^iPr - CH_3), -8.17 (br s, 18H, ^iPr - CH_3), -15.41 (br s, 15H, Cp^* - CH_3), -83.73 (br s, 2H, COT-*H*), -120.39 (s, br, 2H, COT-*H*). Spectroscopic data matches previously published results.²⁰

6.5.2 Synthesis of $\text{U}(\text{COT}^{\text{TIPS}2})\text{Cp}^*\text{Cl}$ (**2.2**)

To a stirring solution of **2.1.THF** (1.56 g, 1.80 mmol) in pentane (100 cm^3), an excess of $^t\text{BuCl}$ (210 μl , 1.90 mmol) was added *via* microsyringe resulting in an immediate colour change from dark brown to red. After stirring for 2 h, volatiles were removed under reduced pressure to yield sticky red-brown solids. The addition and subsequent removal of small portions of pentane (3 x 10 cm^3) and thorough drying under reduced pressure yielded **2.2** as an analytically pure free-flowing brown powder. Recrystallisation of the powder from a small volume of pentane or THF afforded material suitable for X-ray diffraction studies.

Yield: 1.34 g (1.63 mmol) 90% w.r.t. **2.1**.

^1H NMR (C_6D_6 , 399.5 MHz) δ_{H} 80.28 (br s, 2H, COT-*H*), 10.15 (s, 15H, Cp^* - CH_3), -7.44 (m, 6H, ^iPr -*CH*), -7.73 (d, $^1J_{\text{HH}} = 5.4$ Hz, 18H, ^iPr - CH_3), -8.69 (d, $^1J_{\text{HH}} = 5.4$ Hz, 18H, COT ^iPr - CH_3), -84.70 (br s, 2H, COT-*H*), -103.65 (br s, 2H, COT-*H*).

^1H NMR (C_6D_{12} , 399.5 MHz,) δ_{H} 73.06 (br s, 2H, COT-*H*), 9.45 (s, 15H, Cp^* - CH_3), -7.60 (d, $^1J_{\text{HH}} = 6.7$ Hz, 18H, ^iPr - CH_3), -7.82 (m, 6H, ^iPr -*CH*), -8.82 (d, $^1J_{\text{HH}} = 6.7$ Hz, 18H, ^iPr - CH_3), -77.09 (br s, 2H, COT-*H*), -101.11 (br s, 2H, COT-*H*).

$^{29}\text{Si}\{^1\text{H}\}$ NMR (C_6D_{12} , 79.4 MHz) δ_{Si} -68.4 (br s, Si^iPr_3).

MS (EI)⁺: $m/z = 826$ (M^+ , 11%), 375 (UCp^* , 52%), 157 (Si^iPr_3 , 100%).

Anal. Calcd for C₃₆H₆₃Si₂ClU: C, 52.38; H, 7.69. Found: C, 52.50; H, 7.71.

6.5.3 Synthesis of U(COT^{TIPS2})Cp*(CH₂Ph) (**2.3**)

KCH₂Ph (190 mg, 1.46 mmol, 1.2 eq.) in ca 30 cm³ THF was added dropwise to a stirring THF solution of **2.2** (997 mg, 1.21 mmol) at -30 °C. The mixture was stirred at -30 °C for a further 1 h, during which time it became dark brown in colour. Volatiles were removed under reduced pressure and the resultant brown solids were extracted with 100 cm³ pentane. The brown solution was collected *via* filter cannula, concentrated and cooled to -20 °C to yield red-purple crystals.

Yield: 500 mg (0.57 mmol) 47% w.r.t. **2.2**.

¹H NMR (C₆D₆, 399.5 MHz): δ 17.64 (br, s, 2H, COT-*H*), 10.47 (t, 2H, *m*-C₆H₅), 7.80 (d, 2H, *o*-C₆H₅), 7.01 (v. br, s, 2H, CH₂-Ph), 3.76 (s, 15H, Cp*-CH₃), 1.64 (t, 1H, *p*-C₆H₅), -8.08 (d, 18H, ^{*i*}Pr-CH₃), -9.99 (br, s, 18H, ^{*i*}Pr-CH₃), -11.41 (br, s, 2H, COT-*H*), -11.86 (m, 6H, ^{*i*}Pr-CH), -76.79 (br, s, 2H, COT-*H*).

²⁹Si{¹H} NMR (C₆D₁₂, 79.4 MHz) -96.9 (s, Si^{*i*}Pr).

MS (EI)⁺: m/z 790 (M⁺ -CH₂Ph, 100%), 746 (M⁺ -Cp*, 7%).

Anal. Calcd for C₄₃H₇₀Si₂U: C, 58.60; H, 8.00. Found: C, 58.62; H, 7.94.

6.5.4 Synthesis of U(COT^{TIPS2})Cp*(Me) (**2.4**)

An excess of MeLi solution (0.334 M in Et₂O, 5.5 cm³, 1.82 mmol) was added dropwise to a stirring solution of **2.2** (1000 mg, 1.21 mmol) in ca 40 cm³ of Et₂O pre-cooled to -78 °C. The resultant dark red solution was allowed to warm to -30 °C over 1 h, by which time a colour change to orange had occurred. Et₂O was removed under reduced pressure, the solids extracted with 40 cm³ of pentane and the orange solution was filtered *via* cannula to remove residual solids. Removal of pentane under reduced pressure yields **2.4** as an analytically pure orange-red powder. Recrystallisation from a

saturated pentane or Et₂O solution stored at -35 °C afforded red crystals suitable for X-ray diffraction.

Yield: 729 mg (0.90 mmol) 75% yield w.r.t. **2.2**.

¹H NMR (C₆D₆, 399.5 MHz) δ_H 52.79 (br s, 3H, CH₃), 14.85 (br s, 2H, COT-*H*), 0.93 (s, 15H, Cp*-CH₃), -4.44 (br s, 2H, COT-*H*), -7.46 (d, ¹J_{HH} = 7.4 Hz, 18H, ⁱPr-CH₃), -11.27 (d, ¹J_{HH} = 5.4 Hz, 18H, ⁱPr-CH₃), -12.40 (m, 6H, ⁱPr-CH), -69.11 (br s, 2H, COT-*H*).

²⁹Si {¹H} NMR (C₆D₆, 79.4 MHz) δ_{Si} -99.3 (s, Si^{*i*}Pr).

MS (EI)⁺: m/z = 808 (M⁺ +2 m/z, 6%), 789 (M⁺ -CH₃, 15%), 416 (M⁺ -UCp*CH₃, 41%), 373 (M⁺ -COT^{TIPS2}, 77%), 115 (Si^{*i*}Pr₂, 100%).

Anal. Calcd for C₃₇H₆₆Si₂U: C, 55.19; H, 8.26. Found: C, 54.45; H, 8.24.

6.5.5 Attempted synthesis of U(COT^{TIPS2})Cp*(^{*t*}Bu)

The following reaction was performed in a J Young NMR tube: **2.2** (35 mg, 0.042 mmol) and solid ^{*t*}BuLi (3 mg, ca 0.042 mmol) were combined and C₆D₁₂ was added before the mixture was agitated. ¹H NMR spectroscopic data collected 5 minutes after mixing showed only the presence of **2.2**, and after 4 hours contained resonances attributable to **2.2**, trivalent **2.1**, and the 'tucked-in' complex, **2.9**.

6.5.6 Attempted synthesis of U(COT^{TIPS2})Cp*(^{*n*}Bu)

A THF solution (25 cm³) of **2.2** (83 mg, 0.101 mmol) was cooled to -78 °C and ca 1 cm³ of ^{*n*}BuLi (2.08 M in hexanes, ca 2 eq.) was added *via* syringe. The reaction was stirred for 1 h at -78 °C, then allowed to warm to ambient temperature for 3 hours, after which time it was dark brown in colour and contained off-white solids. Removal of volatiles, extraction into pentane and subsequent filtration *via* filter cannula only yielded a brown solution of **2.9**.

6.5.7 Attempted synthesis of $\text{U}(\text{COT}^{\text{TIPS}_2})\text{Cp}^*(\text{Np})$

Method 1: **2.2** (30 mg, 0.036 mmol) and NpLi (3 mg, 0.044 mmol) were added to a J Young NMR tube and dissolved in C_6D_6 , resulting in a red-brown solution. The ^1H NMR spectrum collected 10 minutes after mixing showed a number of paramagnetically-shifted peaks, attributable to **2.2**, **2.9**, ligand decomposition and other unidentifiable products.

Method 2: Equimolar **2.2** and NpLi (156 mg and 14 mg respectively, 0.019 mmol) were combined in an ampoule before pentane (ca 40 cm^3) pre-cooled to $-78\text{ }^\circ\text{C}$ was added, forming a red-brown slurry. Slow warming to ambient temperature over 2 h yielded a brown solution, determined by ^1H NMR spectroscopy to be predominantly **2.9**.

Method 3: Et_2O (ca 10 cm^3) pre-cooled to $-78\text{ }^\circ\text{C}$ was added to an ampoule containing **2.2** (92 mg, 0.111 mmol) and NpLi (10 mg, 0.124 mmol), and the resulting orange-red mixture was stirred for 20 minutes. Filtration *via* filter cannula to remove off-white precipitate, followed by concentration of the red solution to ca 2 cm^3 and storage at $-20\text{ }^\circ\text{C}$ or $-50\text{ }^\circ\text{C}$ did not afford crystalline material. ^1H NMR spectroscopic analysis of an aliquot showed the presence of **2.2** and other resonances that *could* correlate to $\text{U}(\text{COT}^{\text{TIPS}_2})\text{Cp}^*(\text{Np})$, however, further characterisation was not possible.

6.5.8 Synthesis of $\text{U}(\text{COT}^{\text{TIPS}_2})\text{Cp}^*(\text{CH}_2\text{TMS})$ (**2.5**)

An Et_2O solution (10 cm^3) of LiCH_2TMS (14 mg, 0.149 mmol, 1.2 eq.) was added dropwise *via* cannula to a stirring solution of **2.2** (99 mg, 0.120 mmol) in Et_2O (10 cm^3) at $-40\text{ }^\circ\text{C}$. The resulting red solution was stirred at $-40\text{ }^\circ\text{C}$ for 30 min, then allowed to warm to ambient temperature over a further 30 min before filtration to remove the white precipitate. Reduction of the solvent volume to ca 4 cm^3 and storage at $-50\text{ }^\circ\text{C}$ yielded red crystals of **2.5** suitable for X-ray diffraction studies.

Yield: 41 mg (0.046 mmol) 39% w.r.t. **2.2**.

^1H NMR (C_6D_6 , 399.5 MHz) δ_{H} 66.87 (br s, 2H, CH_2TMS), 11.12 (br s, 2H, COT-*H*), 8.55 (s, 9H, CH_2TMS), 1.82 (s, 15H, Cp*), -4.76 (br s, 2H, COT-*H*), -8.80 (d, $^1J_{\text{HH}} = 6.9$ Hz, 18H, COT $^i\text{Pr-CH}_3$), -9.09 (d, $^1J_{\text{HH}} = 6.9$ Hz, 18H, $^i\text{Pr-CH}_3$), -11.48 (m, 6H, COT $^i\text{Pr-CH}$), -65.99 (br s, 2H, COT-*H*).

$^{29}\text{Si}\{^1\text{H}\}$ NMR (C_6D_6 , 74.9 MHz) δ 139.7, -102.35 assigned to Si^iPr_3 and CH_2SiMe_3 .

MS (EI) $^+$: $m/z = 833$ ($\text{M}^+ - \text{Me}_3$, 13%), 416 ($\text{COT}^{\text{TIPS}2}$, 33%), 373 ($\text{M}^+ - \text{COT}^{\text{TIPS}2}\text{CH}_2\text{TMS}$, 76%), 87 (CH_2TMS , 67%), 59 (SiMe_2 , 100%).

Anal. Calcd for $\text{C}_{43}\text{H}_{70}\text{Si}_2\text{U}_1$: C, 54.76; H, 8.50. Found: C, 54.24; H, 7.91.

6.5.9 Synthesis of $\text{U}(\text{COT}^{\text{TIPS}2})\text{Cp}^*(\text{CH}\{\text{TMS}\}_2)$ (**2.6**)

$\text{KCH}(\text{TMS})_2$ (39 mg, 0.182 mmol) in pentane (30 cm^3) was added dropwise over 30 minutes to a stirred solution of **2.2** (112 mg, 0.121 mmol) in 30 cm^3 pentane and 3 cm^3 THF at -78 °C. The resultant red-brown solution was allowed to warm to ambient temperature over 12 hours, by which time a brown solution with white precipitate had formed. The solution was filtered and all volatiles were removed under reduced pressure. Extraction in pentane (20 cm^3) and re-filtration afforded a brown solution, from which all volatiles were removed before re-extraction in a minimum amount of $^i\text{BuOMe}$. Storage of the $^i\text{BuOMe}$ solution at -50 °C for a week resulted in the formation of brown microcrystalline solids. X-ray diffraction quality crystals of **2.6** were obtained by storing a saturated pentane solution of the microcrystalline solids at -35 °C for three months.

Crude yield: 46 mg (0.048 mmol) 40% w.r.t. **2.2**.

^1H NMR (C_6D_6 , 399.5 MHz) δ_{H} 74.22 (br s, 1H, $\text{CH}\{\text{TMS}\}_2$), 8.17 (br s, 2H, COT-*H*), 6.67 (s, 15H, Cp*- CH_3), -2.18 (d, $^1J_{\text{HH}} = 7.4$ Hz, 18H, $^i\text{Pr-CH}_3$),

-3.45 (d, $^1J_{\text{HH}} = 7.6$ Hz, 18H, $^i\text{Pr-CH}_3$), -5.10 (br s, 2H, COT-*H*), -5.74 (m, 6H, $^i\text{Pr-CH}$), -12.10 (s, 18H, $\text{CH}\{\text{TMS}\}_2$), -52.48 (br s, 2H, COT-*H*).

$^{29}\text{Si}\{^1\text{H}\}$ NMR (C_6D_{12} , 79.4 MHz) δ_{Si} -60.84, -119.84 assigned to Si^iPr and $\text{CH}\{\text{SiMe}_3\}_2$.

MS (EI) $^+$: $m/z = 789$ ($\text{M}^+ - \text{CH}\{\text{TMS}\}_2$, 32%), 373 (UCp^* , 8%), 145 ($\text{CH}\{\text{TMS}\}_2$ fragment, 100%).

Anal. Calcd for $\text{C}_{43}\text{H}_{82}\text{Si}_4\text{U}$: C, 54.39; H, 8.70. Found: C, 54.50; H, 8.60.

6.5.10 Synthesis of $\text{U}(\text{COT}^{\text{TIPS}_2})\text{Cp}^*(\text{OCH}_2\text{CH}_3)$ (**2.7**)

Method 1: A solution of **2.2** (200 mg, 0.240 mmol in 50 cm³ Et₂O) was added dropwise to a stirring solution of KCH_2TMS (36 mg, 0.290 mmol in 100 cm³ Et₂O) at -78 °C. The resultant orange-brown solution was stirred and allowed to warm to ambient temperature over 12 h before volatiles were removed under reduced pressure. Extraction of the orange solids with 10 cm³ of pentane, filtration *via* filter cannula and slow-cooling of the pentane solution to -30 °C afforded orange crystals of **2.7** suitable for X-ray diffraction studies.

Yield: 55 mg (0.09 mmol) 31% w.r.t. **2.2**.

Method 2: **2.2** (218 mg, 0.264 mmol) and an excess of KOEt (47 mg, 0.558 mmol) were combined in an ampoule, to which THF (5 cm³) was added. Stirring the mixture at ambient temperature resulted in an orange solution and off-white precipitate. Removal of volatiles, extraction into pentane and filtration *via* filter cannula gave an orange solution. Concentration of the solution volume to ca 3 cm³ and slow-cooling to -30 °C afforded orange crystals of **2.7** (78 mg). Isolation of the crystals and further concentration and slow-cooling of the mother liquor afforded more crystals (34 mg).

Yield: 112 mg (0.134 mmol) 51% w.r.t. **2.2**.

^1H NMR (C_6D_6 , 399.5 MHz) δ_{H} 142.19 (br s, 2H, OCH_2CH_3), 113.78 (br s, 2H, COT-*H*), 53.58 (s, 3H, OCH_2CH_3), -6.30 (s, 15H, $\text{Cp}^*\text{-CH}_3$), -7.42 (d, $^1J_{\text{HH}} = 7.0$ Hz, 18H, $^i\text{Pr-CH}_3$), -14.45 (d, $^1J_{\text{HH}} = 6.4$ Hz, 18H, $^i\text{Pr-CH}_3$), -17.58 (m, 6H, $^i\text{Pr-CH}$), -39.55 (br s, 2H, COT-*H*), -88.73 (br s, 2H, COT-*H*).

^{29}Si NMR (C_7D_8 , 79.4 MHz) δ_{Si} -136.2 (br s, Si^iPr).

MS (EI) $^+$: $m/z = 834$ (M^+ , 43%), 699 ($\text{M}^+ - \text{Cp}^*$, 96%), 157 (Si^iPr_3 , 100%).

IR (NaCl plate, cm^{-1}): 2959s, 2941s, 2890s, 2863s, 1463m, 1374m, 1259m, 1220w, 1099s, 1067s, 1030s, 1013s, 932w, 909m, 880m, 799m, 764m, 666m, 639m, 582m.

Anal. Calcd for $\text{C}_{38}\text{H}_{68}\text{Si}_2\text{OU}$: C 54.65, H 8.20; found: C 54.99, H 7.99.

6.5.11 Attempted reaction of **2.2** and KCH_2TMS in $^t\text{BuOMe}$

A solution of **2.2** (75 mg) in $^t\text{BuOMe}$ (ca 15 cm^3) was added to a $^t\text{BuOMe}$ slurry of KCH_2TMS , and the mixture was stirred at ambient temperature for 3 days. ^1H NMR spectroscopic analysis after this time showed mostly unreacted **2.2**, and low-intensity resonances attributable to $^t\text{U}(\text{COT}^{\text{TIPS}2})\text{Cp}^*(\text{OMe})$ and $^t\text{U}(\text{COT}^{\text{TIPS}2})\text{Cp}^*(\text{O}^t\text{Bu})$.

6.5.12 Synthesis of $[\text{U}(\eta^8\text{-}\kappa^1(\text{C})\text{-C}_8\text{H}_6\text{Si}^i\text{Pr}_3\{\text{Si}^i\text{Pr}_2\text{CH}(\text{CH}_3)(\text{CH}_2)\})\text{Cp}^*\text{Cl}][\text{Li}(\text{OEt})_2]$ (**2.8**)

A stirred solution of **2.2** (250 mg, 0.303 mmol) was cooled to -30 $^\circ\text{C}$, and to this a Et_2O solution of LiCH_2TMS (34 mg, 0.362 mmol) was added in a dropwise manner over a period of 40 min. The resultant red solution was stirred at -30 $^\circ\text{C}$ for a further hour, then all volatiles were removed under reduced pressure whilst the reaction mixture was kept below 0 $^\circ\text{C}$. Extraction of the red-orange solids with pentane (30 cm^3), filtration *via* filter cannula and subsequent concentration of the solution was followed by storage of the red solution at -50 $^\circ\text{C}$ overnight. Orange microcrystalline solids were isolated, identified as a mixture of **2.8** (predominant species), and small quantities of other products. Separation of these products was not possible.

Combined yield: 23 mg.

^1H NMR (C_7D_8 , 399.5 MHz) δ_{H} 14.09 (d, 2H, $^i\text{Pr-CH}_2$), 5.50 (m, 1H, $^i\text{Pr-CH}$), 5.41 (d, $^1J_{\text{HH}} = 7.4$ Hz, 3H, $^i\text{Pr-CH}_3$), 4.60 (d, $^1J_{\text{HH}} = 7.0$ Hz, 3H, $^i\text{Pr-CH}_3$), 1.95 (s, 15H, $\text{Cp}^*\text{-CH}_3$), -7.09 (s, 9H, $^i\text{Pr-CH}_3$), -8.19 (m, 3H, $^i\text{Pr-CH}$), -10.45 (s, 9H, $^i\text{Pr-CH}_3$), -10.89 (s, 3H, $^i\text{Pr-CH}_3$), -12.30 (s, 3H, $^i\text{Pr-CH}_3$), -14.50 (m, 1H, $^i\text{Pr-CH}$). 7 x br s of integration 2H each at δ_{H} 59.77, 52.54, 20.97, 17.76, -33.41, -91.76, -101.44 assigned to COT-*H* and ‘tucked-in’ $^i\text{Pr-CH}$ protons. Resonances attributable to the 2 CH_2 protons closest to U could not be identified.

MS (EI) $^+$: $m/z = 824$ (3%, $\text{M}^+ - \text{Li}(\text{OEt}_2)_2$), 788 (55%, $\text{M}^+ - \text{Cl.Li}(\text{OEt}_2)_2$), 191 (11%, $\text{Cl.Li}(\text{OEt}_2)_2$).

6.5.13 Synthesis of $\text{U}(\text{COT}^{\text{TIPS}_2})(\eta^5\text{:}\kappa^1\text{-C}_5\text{Me}_4\text{CH}_2)$ (**2.9**)

A solution of **2.3** (400 mg, 0.50 mmol) in 50 cm^3 toluene was heated to 70 $^\circ\text{C}$ for 24 h, during which time the solution changed colour from red-brown to brown. Filtration *via* filter cannula to remove the small amount of white solids produced, removal of volatiles under reduced pressure and the addition and subsequent removal of 3 x 10 cm^3 portions of pentane afforded the product as a free-flowing brown powder, contaminated with some ligand decomposition products inseparable by recrystallisation. Storage of a highly concentrated pentane or THF solution at -50 $^\circ\text{C}$ for 4 weeks yielded a small number of red crystals of **2.9** or **2.9.THF**, respectively, suitable for X-ray diffraction studies. Satisfactory elemental analysis could not be obtained for this compound.

Yield: 274 mg (0.347 mmol) 70% w.r.t. **2.3**.

^1H NMR (C_6D_6 , 399.5 MHz) δ_{H} 57.83 (br s, 2H, COT-*H*), 25.43 (s, 6H, Cp- CH_3), -1.26 (m, 6H, $^i\text{Pr-CH}$), -1.90 (d, $^1J_{\text{HH}} = 7.4$ Hz, 18H, $^i\text{Pr-CH}_3$), -3.88 (d, $^1J_{\text{HH}} = 7.2$ Hz, 18H, $^i\text{Pr-CH}_3$), -39.77 (s, 6H, Cp- CH_3), -70.09 (br s, 2H, Cp- CH_2), -76.41 (br s, 2H, COT-*H*), -85.86 (br s, 2H, COT-*H*).

$^{29}\text{Si}\{^1\text{H}\}$ NMR (C_6D_6 , 79.4 MHz) δ_{Si} -67.0 (br s, Si^iPr_3).

MS (EI)⁺: m/z = 789 (M⁺, 5%), 115 (SiⁱPr₂, 100%).

6.5.14 Thermolysis of **2.1**: **2.9** and U(COT^{TIPS2})Cp*(OⁿBu) (**2.10**)

A solution of **2.1** (39 mg, 0.045 mmol in 1 cm³ C₇D₈) in a J Young tube was heated to 70 °C for 30 days, during which time the solution changed colour from black to dark red. Removal of volatiles, extraction in ^tBuOMe and storage at -35 °C overnight yielded a mixture of red and brown crystals, identified as a mixture of **2.9** and U(COT^{TIPS2})Cp*(OⁿBu) (**2.10**).

Combined isolated yield: 28 mg. Approximate yield of **2.10**: 6 mg, 0.007 mmol, 15%.

By ¹H NMR spectroscopy, yield of **2.9**: 41%; yield of **2.10**: 40%.

¹H NMR (C₆D₆, 399.5 MHz) δ_H 141.81 (br s, 2H, OCH₂CH₂CH₂CH₃),
113.46 (br s, 2H, COT-*H*), 55.88 (s, 2H, OCH₂CH₂CH₂CH₃),
30.70 (s, 2H, OCH₂CH₂CH₂CH₃), 16.88 (s, 3H, OCH₂CH₂CH₂CH₃),
-6.25 (s, 15H, Cp*-CH₃), -7.68 (d, ¹J_{HH} = 4.8 Hz, 18H, ⁱPr-CH₃),
-14.34 (s, 18H, ⁱPr-CH₃), -17.61 (m, 6H, ⁱPr-CH), -39.41 (br s, 2H, COT-*H*),
-88.75 (br s, 2H, COT-*H*).

²⁹Si NMR (C₆D₆, 79.4 MHz) δ_{Si} -135.8 (br s, SiⁱPr).

MS (EI)⁺: m/z = 862 (M⁺, 4%), 727 (M⁺ -Cp*, 11%), 115 (ⁱPr fragment, 100%).

6.6 Experimental details for Chapter 3

6.6.1 Synthesis of U(COT^{TIPS2})Cp*H (**3.1**)

Method 1: A pentane solution (0.5 cm³) of **2.3** (67 mg, 0.076 mmol) in a B10-sidearm ampoule was frozen and then exposed to ca 10 equivalents of H₂ (0.760 mmol) *via* Toepler pump. Upon warming to ambient temperature the solution changed colour from dark brown to red after reaching -30 °C. Removal of volatiles under reduced pressure decomposes the product to give a mixture of **2.9** and **2.1**.

Method 2: An ampoule with a B10-sidearm was charged with a crystalline sample of **2.3** (114 mg, 0.129 mmol) and stirred vigorously to produce a dark brown finely ground powder. The reaction vessel was cooled to $-78\text{ }^{\circ}\text{C}$ before the headspace was evacuated, then pressurised with 1 bar of H_2 . After stirring at $-78\text{ }^{\circ}\text{C}$ for 45 minutes, sticky red-brown solids and a small amount of dark red crystals were observed. No yield was recorded due to instability of the product.

Method 3: A solution of **2.3** was dissolved in C_6D_6 and frozen before being exposed to an excess of H_2 *via* Toepler pump. Upon warming a colour change from dark red-brown to cherry red was observed. ^1H NMR spectroscopic analysis of the mixture shows the presence of **3.1**, and also a small quantity of **2.9**. The reaction can also be performed in C_7D_8 or C_6D_{12} , or using **2.4** or **2.9** in place of **2.3**.

Data for **3.1** synthesised *via* method 3:

^1H NMR (C_6D_6 , 399.5 MHz) δ_{H} 36.97 (br s, 2H, COT-*H*), 2.42 (s, 15H, Cp*- CH_3), -7.66 (d, $^1J_{\text{HH}} = 4.9\text{ Hz}$, 18H, $^i\text{Pr-CH}_3$), -9.73 (br s, 24H, $^i\text{Pr-CH}_3$ and $^i\text{Pr-CH}$ overlapped), -36.08 (br s, 2H, COT-*H*), -83.64 (br s, 2H, COT-*H*).

No resonance attributable to U-*H* is observed.

^1H NMR (C_6D_{12} , 399.5 MHz) δ_{H} 32.53 (br s, 2H, COT-*H*), 2.11 (s, 15H, Cp*- CH_3), -7.35 (d, $^1J_{\text{HH}} = 6.9\text{ Hz}$, 18H, $^i\text{Pr-CH}_3$), -9.88 (d, 18H, $^1J_{\text{HH}} = 6.9\text{ Hz}$, $^i\text{Pr-CH}_3$), -10.03 (m, 6H $^i\text{Pr-CH}$), -31.28 (br s, 2H, COT-*H*), -82.19 (br s, 2H, COT-*H*).

No resonance attributable to U-*H* is observed.

$^{29}\text{Si}\{^1\text{H}\}$ NMR (C_6D_6 , 79.4 MHz) δ_{Si} -82.66 (br s, Si^iPr_3).

6.6.2 Synthesis of $\text{U}(\text{COT}^{\text{TIPS}2})\text{Cp}^*(\eta^2\text{-OC-CH}_2\text{Ph})$ (**3.2**)

An ampoule was charged with crystalline **2.3** (56 mg, 0.064 mmol) and 3 cm^3 toluene, and the resultant dark brown solution was cooled to $-78\text{ }^{\circ}\text{C}$ before the addition of CO (ca 0.634 mmol, 10 eq.) *via* Toepler pump. After warming to ambient temperature

whilst stirring over 2 h a colour change to dark red was observed. Volatiles were removed under reduced pressure before the red solids were extracted in ca 0.5 cm³ Et₂O and slow-cooled to -30 °C affording dark red plate-like crystals, largely unsuitable for X-ray diffraction. Repetition of the reaction with 1 eq. ¹³CO or a 1:1 mixture of H₂/¹³CO in a J Young NMR tube in C₆D₆ or C₆D₁₂ afforded the same result.

Yield: 16 mg (0.0176 mmol) 28% yield w.r.t. **2.3**.

¹H NMR (C₆D₆, 399.5 MHz) δ_H 24.95 (d, ¹J_{HH} = 7.3 Hz, 2H, *o*-C₆H₅), 13.62 (t, ¹J_{HH} = 7.5 Hz, 2H, *m*-C₆H₅), 11.48 (t, ¹J_{HH} = 7.8 Hz, 1H, *p*-C₆H₅), -5.79 (br s, 18H, ⁱPr-CH₃), -5.95 (br s, 15H, Cp*-CH₃), -9.76 (br s, 18H, ⁱPr-CH₃), -13.28 (m, 6H, ⁱPr-CH). Additional resonances attributable to COT-*H* protons not observed.

¹H NMR (C₆D₁₂, 399.5 MHz) δ_H 24.63 (d, ¹J_{HH} = 7.4 Hz, 2H, *o*-C₆H₅), 13.46 (t, ¹J_{HH} = 7.4 Hz, 2H, *m*-C₆H₅), 11.39 (t, ¹J_{HH} = 7.8 Hz, 1H, *p*-C₆H₅), -5.81 (br s, 18H, ⁱPr-CH₃), -5.94 (br s, 15H, Cp*-CH₃), -9.75 (br s, 18H, ⁱPr-CH₃), -13.28 (m, 6H, ⁱPr-CH). Additional resonances attributable to COT-*H* protons not observed.

²⁹Si{¹H} and ¹³C{¹H} NMR did not show any resonances due to broadening effects.

IR (NaCl plates, cm⁻¹, ¹³C-labelled product): 3587w, 3036w, 2942s, 2893m, 2864s, 2721w, 1577w, 1463m, 1381w, 1246m, 1222w, 1173br, 1071w, 1026m, 1013m, 964w, 940w, 883m, 846s, 801w, 752m, 666m, 637m, 580w, 478s.

MS (EI)⁺: m/z = 909 (M⁺, 7%), 789 (M⁺ -OC-CH₂Ph, 52%), 91 ('OCCH₂Ph', 100%).

Anal. Calcd (%) for C₄₅H₇₀Si₂O₂U: C, 58.12; H, 7.76. Found: C, 58.91; H, 8.00.

6.6.3 Synthesis of U(COT^{TIPS2})Cp*(η²-OC-CH₃) (**3.3**)

A J Young NMR tube was charged with crystalline **2.4** (23 mg, 0.029 mmol) and 0.6 cm³ C₆D₆; the resultant red solution was frozen before the addition of CO

(ca 0.043 mmol, 1.5 eq.) *via* Toepler pump. After warming to ambient temperature a colour change to dark red was observed. Volatiles were removed under reduced pressure before the red solids were extracted in ca 0.5 cm³ Et₂O and slow-cooled to -30 °C affording dark red microcrystalline solids. Repetition of the reaction with ¹³C¹⁸O or 1:1 H₂/¹³C¹⁸O afforded the same result. Instability of the product precluded further analysis.

Yield: 8 mg (0.0099 mmol) 35% yield w.r.t. **2.4**.

¹H NMR (C₆D₆, 399.5 MHz) δ_H 31.93 (s, 3H, CH₃), -5.60 (br s, 18H, ⁱPr-CH₃), -6.04 (br s, 15H, Cp*-CH₃), -9.78 (br s, 18H, ⁱPr-CH₃), -13.18 (m, 6H, ⁱPr-CH).

Additional resonances attributable to COT-*H* protons not observed.

²⁹Si{¹H} and ¹³C{¹H} NMR did not show any resonances due to broadening effects.

IR (NaCl plates, cm⁻¹, ¹³C-labelled product): 2944s, 2865s, 2719w, 2363w, 1584w, 1461s, 1382m, 1365m, 1251w, 1229w, 1131w, 1072m, 1016m, 996m, 882s, 853w, 752m, 668s, 647s, 580w, 53w.

MS (EI)⁺: m/z = 159 (100%, SiⁱPr).

6.6.4 Synthesis of U(COT^{TIPS2})Cp*(η²-OC-CH₂TMS) (**3.4**)

A J Young NMR tube was charged with crystalline **2.5** (14 mg, 0.016 mmol) and 0.6 cm³ C₆D₆; the resultant red solution was frozen before 2 eq. (ca 0.032 mmol) of CO was added *via* Toepler pump. After warming to ambient temperature a colour change to dark red was observed. Volatiles were removed under reduced pressure before the red solids were extracted in ca 0.5 cm³ Et₂O and slow-cooled to -30 °C affording dark red microcrystalline solids. Repetition of the reaction with ¹³C¹⁸O afforded the same result.

Yield: 7 mg (0.0077 mmol) 48% yield w.r.t. **2.5**.

^1H NMR (C_6D_6 , 399.5 MHz) δ_{H} 10.17 (s, 9H, CH_2TMS), -6.24 (br s, 18H, $^i\text{Pr}-\text{CH}_3$), -6.39 (br s, 15H, Cp^*-CH_3), -10.29 (br s, 18H, $^i\text{Pr}-\text{CH}_3$), -13.91 (m, 6H, $^i\text{Pr}-\text{CH}$).

Additional resonances attributable to COT-*H* and CH_2TMS protons not observed.

$^{29}\text{Si}\{^1\text{H}\}$ NMR (C_6D_6 , 79.4 MHz) δ_{Si} -16.43 (br s, CH_2SiMe_3). Si^iPr_3 not observed.

IR (NaCl plates, cm^{-1} , ^{13}C -labelled product): 3035w, 2843s, 2864s, 2724w, 1584w, 1544m, 1460s, 1379m, 1246m, 1223w, 1187w, 1142m, 1073w, 1030s, 1018s, 952w, 883s, 842s, 801w, 756m, 668m, 642m.

MS (EI) $^+$: $m/z = 905$ (M^+ , 2%), 743 ($\text{M}^+ - \text{Cp}^*$, $-\text{Me}_2$, 4%), 373 ($^i\text{UCp}^*$, 45%), 73 (TMS, 100%).

6.6.5 Reaction of **2.6** with ^{13}CO (**3.5**)

A C_6D_6 solution of **2.6** (ca 10 mg, 0.0105 mmol) in a J Young NMR tube was frozen and exposed to an excess (ca 3 eq., 0.032 mmol) of ^{13}CO . Reaction progress was monitored by ^1H NMR spectroscopy: after 8 days the reaction proceeded no further. Subsequent addition of 0.86 bar of ^{13}CO did not yield any further reaction. Resonances were attributed to an insertion/rearrangement product, but no structural information could be obtained. Attempts to crystallise **3.5** and separate it from residual **2.6** were not successful.

^1H NMR (C_6D_6 , 399.5 MHz) δ_{H} 13.56 (s, 9H, $\text{Si}-\text{CH}_3$), 11.47 (s, 1H, $\text{OC}=\text{CH}$), 9.43 (s, 9H, $\text{Si}-\text{CH}_3$), -3.55 (s, "19H" overlapped with other resonance, Cp^*-CH_3), -8.06 (d, $^1J_{\text{HH}} = 7.4$ Hz, 18H, $^i\text{Pr}-\text{CH}_3$), -10.16 (d, $^1J_{\text{HH}} = 6.9$ Hz, 18H, $^i\text{Pr}-\text{CH}_3$), -12.48 (m, 6H, $^i\text{Pr}-\text{CH}$). No COT-*H* proton resonances were observed.

6.6.6 Synthesis of $(\eta^5:\eta^1\text{-C}_5\text{Me}_4\text{CH}_2\text{OC}=\text{COCH}_2\text{C}_5\text{Me}_4)\{\text{U}(\text{COT}^{\text{TIPS}2})\}_2$ (*cis*-**3.7**)

Exposure of a frozen C_6D_6 dark brown solution of **2.9** (17 mg, 0.022 mmol) in a J Young NMR tube to an excess of ^{13}CO (0.066 mmol, 3 eq) delivered *via* Toepler pump results in a red solution upon warming; the reaction is complete (as determined by

^1H NMR spectroscopy) after 18 hours, as a mixture of *cis:trans* isomers in a ca 7:1 ratio. Removal of volatiles under reduced pressure and extraction of the red solids in pentane (ca 2 cm³) affords red crystals suitable for X-ray diffraction, as does concentration of the C₆D₆ solution and storage at ambient temperature.

Yield (mix of isomers): 20 mg (0.012 mmol) 56% w.r.t **2.9**.

For *cis*-**3.7**: ^1H NMR (C₇D₈, 399.5 MHz) δ_{H} 92.20 (br, s, 4H, COT-*H*), 62.02 (br, s, 4H, COT-*H*), -4.52 (br s, 36H, ^{*i*}Pr-CH₃), -11.28 (br s, 36H, ^{*i*}Pr-CH₃), -15.18 (m, 12H, ^{*i*}Pr-CH), -33.40 (br s, 4H, Cp*-CH₂), -71.54 (br s, 4H, COT-*H*).

Resonances attributable to CpMe₄ protons not observed.

$^{13}\text{C}\{^1\text{H}\}$ NMR (C₇D₈, 100.5 MHz) δ_{C} 300.8 (CH₂-^{*13*}C=O).

$^{29}\text{Si}\{^1\text{H}\}$ NMR (C₆D₆, 79.4 MHz) δ_{Si} -127.7 (br s, Si^{*i*}Pr₃).

MS (EI)⁺: m/z = 1636 (M⁺, 2%), 1072 (U{COT^{TIPS2}})₂, 100%).

IR (NaCl plates, cm⁻¹): 2944s, 2863s, 2722w, 1581w, 1493w, 1463m, 1382m, 1365m, 1279w, 1251w, 1210m, 1170w, 1109w, 1067w, 1025m, 1018m, 1003m, 961w, 932w, 919w, 882m, 801w, 755m, 668m, 641m, 582m.

Anal. Calcd for C₇₄H₁₂₄Si₄O₂U: C, 54.39; H, 7.65. Found: C, 53.83; H, 7.77.

6.6.7 Synthesis of ($\eta^5:\eta^1$ -C₅Me₄CH₂OC=COCH₂C₅Me₄){U(COT^{TIPS2})}₂ (*trans*-**3.7**)

A C₇D₈ solution of **2.9** (13 mg, 0.0148 mmol) was cooled to -78 °C before exposure to an excess of ¹²CO (ca 1 bar). After allowing the solution to warm to ambient temperature over 18 hours, a colour change to red was observed. Subsequent addition of ¹²CO₂ or ¹³CO₂ (either 1 eq., >1 eq., or an excess) yields the *trans* isomer in a 100% yield, as determined by ^1H NMR spectroscopy. The ¹³C-labelled product, *trans*-**3.7** can be formed from the addition of ¹²CO₂ or ¹³CO₂ to the reaction mixture of **2.9** and an excess of ¹³CO.

Isolated yield: 7 mg, 0.004 mmol, 29% w.r.t. **2.9**.

^1H NMR (C_7D_8 , 399.5 MHz) δ_{H} 96.13 (br, s, 4H, COT-*H*), 88.01 (br, s, 4H, COT-*H*), -1.46 (s, 12H, Cp- CH_3), -1.62 (d, $^1J_{\text{HH}} = 7.0$ Hz, 36H, $^i\text{Pr-CH}_3$), -9.14 (br s, 36H, $^i\text{Pr-CH}_3$), -12.66 (m, 12H, $^i\text{Pr-CH}$), -22.20 (s, 12H, Cp*- CH_3), -30.54 (br s, 4H, Cp*- CH_2), -74.06 (br s, 4H, COT-*H*).

$^{13}\text{C}\{^1\text{H}\}$ NMR (C_7D_8 , 100.5 MHz) δ_{C} 346.5 ($\text{CH}_2\text{-}^{13}\text{CO}$).

$^{29}\text{Si}\{^1\text{H}\}$ NMR (C_7D_8 , 79.4 MHz) δ_{Si} -127.3 (br s, Si^iPr_3).

MS (EI) $^+$: $m/z = 1637$ (M^+ , 98%), 835 ($\text{M}^+ - \text{UCOT}^{\text{TIPS}_2}\text{CpMe}_5\text{CH}_2^{13}\text{C}$, 12%),

IR (NaCl plates, cm^{-1}): 2721w, 1536br, 1463s, 1381m, 1328m, 1132w, 1107w, 1067w, 1030m, 1013m, 993w, 936w, 879s, 748m, 728m, 671m, 642s, 580m, 523w.

6.6.8 Synthesis of $\{\text{U}(\text{COT}^{\text{TIPS}_2})\text{Cp}^*\}_2(\eta^1:\eta^1\text{-OCH=CHO})$ (*cis-3.8*)

Method 1: An ampoule was charged with **2.4** (416 mg, 0.517 mmol) and ca 10 cm^3 of pentane, which was then frozen and degassed before the addition of 1 bar of H_2 . Upon warming to ambient temperature a colour change from orange-red to red-brown was observed. The solution was stirred for 2 h before the headspace was briefly evacuated, the solution frozen, and the ampoule degassed before the addition of 1 bar of CO. No colour change was observed upon warming; some off-white precipitate was formed. The solution was stirred for 16 hours before filtration *via* cannula to remove any solids, and the volatiles were subsequently removed under reduced pressure to give a brown powder of *cis-3.8* in a crude yield of 273 mg (0.333 mmol, 64% yield). Recrystallisation from a saturated pentane solution yields the title compound as analytically pure, X-ray quality crystals.

Yield: 23 mg (from 40 mg in pentane), 58%.

Method 2: A J Young NMR tube was charged with **2.3** (22 mg, 0.025 mmol) dissolved in 0.6 cm^3 C_7D_8 ; the dark brown solution was cooled to -78 $^\circ\text{C}$. A slight excess of H_2 (1.5 eq, 0.037 mmol) was added *via* Toepler pump and the solution was warmed to

ambient temperature over 10 min, during which time a colour change to red occurred. The solution was frozen and the headspace evacuated before the addition of a 1:1 mixture of H₂:¹³CO (1 eq. of ¹³CO, 0.050 mmol). Upon warming to ambient temperature a colour change to dark brown was observed, forming the ¹³C-labelled product *cis*-¹³C-**3.8** in a yield of ca 90%, as determined by ¹H NMR spectroscopy, with reference to solvent peak integral value.

¹H NMR (C₇D₈, 399.5 MHz) δ_H 88.05 (s, 1H, OCH), 79.61 (br s, 2H, COT-H), 5.66 (s, 15H, Cp*-CH₃), -5.12 (d, ¹J_{HH} = 7.4 Hz, 18H ⁱPr-CH₃), -9.23 (d, ¹J_{HH} = 6.9 Hz, 18H, ⁱPr-CH₃), -11.21 (m, 6H, ⁱPr-CH), -44.41 (br s, 2H, COT-H), -48.53 (br s, 2H, COT-H).

²⁹Si{¹H} NMR (C₇D₈, 79.4 MHz) δ_{Si} -116.27 (br s, SiⁱPr₃).

MS (EI)⁺: m/z = 1636 (M⁺ -2H, 12%), 789 ('U(COT^{TIPS2})Cp*', 22%), 699 ('U(COT^{TIPS2})OCO', 22%), 373 ('UCp*', 45%), 157 (SiⁱPr₃, 100%).

IR (NaCl plates, cm⁻¹): 3584w, 2943s, 2890m, 2865s, 2723w, 1463m, 1382w, 1366br, 1258w, 1222w, 1128s, 1070br, 1028m, 1016m, 649w, 935w, 919w, 882s, 822m, 803w, 751m, 670s, 641s.

Anal. Calcd for C₇₄H₁₂₈Si₄O₂U₂: C, 54.25; H, 7.88. Found: C, 54.72; H, 7.99.

¹³C-labelled product (selected data):

¹H NMR (C₇D₈, 399.5 MHz) δ_H 87.99 (d, ¹J_{CH} = 170 Hz, 1H, O¹³CH).

¹H{¹³C} NMR (C₇D₈, 399.5 MHz) δ_H 87.99 (br s, O¹³CH).

¹³C{¹H} NMR (C₆D₆, 100.5 MHz) δ_C 335.84 (br s, O¹³CH).

¹³C NMR (C₇D₈, 100.5 MHz) δ_C 341.40 (d, ¹J_{CH} = 176 Hz, O¹³CH).

6.6.9 Reactivity of **2.9** with H₂/¹³CO (**3.11**)

A C₆D₆ solution of **2.9** (20 mg, 0.025 mmol) was frozen and a 1:1 mixture of H₂/¹³CO (0.025 mmol per gas component) was delivered to the J Young NMR tube *via* Toepler pump. Upon warming, a colour change from dark brown to red was observed. ¹H NMR spectroscopic data collected 90 min after warming showed a complete consumption of **2.9** and the presence of {U(COT^{TIPS2})Cp*}₂(η¹:η¹-OCH=CHO) (*cis*-**3.8**), along with another product, **3.11**. Attempted separation of the products by crystallisation in a range of solvents (pentane, Et₂O, toluene) did not prove possible.

Yield determined by ¹H NMR spectroscopy: 66%.

¹H NMR (C₆D₆, 399.5 MHz): δ_H 1.47 (s, 15H Cp*-CH₃), -2.43 (d, ¹J_{HH} = 6.6 Hz, 18H, ⁱPr-CH₃), -6.25 (d, ¹J_{HH} = 6.8 Hz, 18H, ⁱPr-CH₃), -8.67 (d, ¹J_{HH} = 6.3 Hz, 18H, ⁱPr-CH₃), -9.75 (d, ¹J_{HH} = 6.4 Hz, 18H, ⁱPr-CH₃), -10.77 (m, 6H, ⁱPr-CH), -11.99 (m, 6H, ⁱPr-CH). Other resonances (br s, 1-2H) present at δ_H 94.62, 81.18, 62.59, -32.99, -58.24, and -58.56 attributable to COT-*H* protons or other ligand proton environments.

¹H{¹³C} NMR (C₇D₈, 399.5 MHz, selected data): δ_H -58.2 (br s, 4H).

¹³C{¹H} NMR (C₆D₆, 100.5 MHz): δ_C 390.8 (q, *J* = 92 Hz, 74 Hz), 287.8 (d, *J* = 92 Hz).

6.6.10 Attempted synthesis of U(COT^{TIPS2})Cp*(OMe) (**3D**) from **3.1**, CO, and H₂

A pentane solution of **2.4** (25 mg, 0.031 mmol) in a B10-sidearm ampoule was frozen, the headspace evacuated, and then pressurised with 1 bar of H₂ from a cylinder. The mixture was thawed and allowed to stir for 1 h at ambient temperature, during which time a colour change from dark red to cherry red was observed. A brief evacuation of the headspace to remove excess H₂ preceded re-freezing, completely evacuating the headspace and subsequent addition of 1 eq. of ¹³CO *via* Toepler pump. Without further

evacuation, 1.5 bar of H₂ was delivered to the vessel from a cylinder. The mixture was allowed to thaw and stir for 12 h, during which time it became darker red in colour. Removal of volatiles gave tacky red-brown solids, which were dissolved in C₇D₈ and examined by ¹H NMR spectroscopy. Analysis showed the solution to contain a mixture of **3.8** and several other products, including a small quantity of **3D** (as determined by comparison to literature data)²⁴ in a ratio of approximately 1:8 **3D**:**3.8**. **3D** was not observed by ¹³C{¹H} NMR spectroscopic analysis.

6.6.11 Synthesis of U(COT^{TIPS})₂Cp*(κ²-O₂CCH₂Ph) (**3.12**)

A dark brown solution of **2.3** (49 mg, 0.56 mmol) in pentane (ca 5 cm³) was exposed to 1 bar of CO₂ at ambient temperature resulting in an immediate colour change to red. The solution was stirred overnight to yield a more vivid red solution with some pink solids. Filtration, concentration of the solution and slow cooling to -30 °C yielded cherry red crystals suitable for X-ray diffraction studies. Repetition of the reaction with ¹³CO₂ on a smaller scale in a J Young NMR tube in C₆D₆ afforded the same result.

Yield: 24 mg (0.026 mmol) 46% w.r.t. **2.3**.

¹H NMR (C₆D₆, 399.5 MHz): δ_H 7.01 (t, ¹J_{HH} = 7.0 Hz, 1H, *p*-C₆H₅), 6.73 (d, ¹J_{HH} = 6.7 Hz, 2H, *o*-C₆H₅), 6.04 (s, 15H, Cp*-CH₃), 4.90 (br s, 2H, CH₂-Ph), 0.81 (br s, 2H, COT-H), -4.82 (d, ¹J_{HH} = 7.5 Hz, 18H, ^{*i*}Pr-CH₃), -5.61 (d, ¹J_{HH} = 7.4 Hz, 18H, ^{*i*}Pr-CH₃), -6.93 (m, 6H, ^{*i*}Pr-CH), -24.25 (br s, 2H, COT-H), -54.01 (br s, 2H, COT-H).

Resonance attributable to *m*-C₆H₅ overlapped with solvent residue at 7.1 ppm.

¹³C{¹H} NMR (C₆D₆, 100.5 MHz): δ_C 21.2 (s, bound ¹³CO₂).

²⁹Si{¹H} NMR (C₆D₆, 79.4 MHz): δ_{Si} -88.9 (br s, Si^{*i*}Pr).

MS (EI)⁺: m/z = 924 (M⁺, 12%), 789 (M⁺ -O₂CCH₂Ph, 19%), 373 ('U-O₂CCH₂Ph', 26%), 157 (Si^{*i*}Pr₃, 100%).

IR (Nujol, cm^{-1}) 1506w, 1418w, 1261w, 1020m, 882m, 789w, 757m, 669m, 640m, 581m.

Anal. Calcd for $\text{C}_{44}\text{H}_{70}\text{Si}_2\text{O}_2\text{U}$: C, 57.11; H, 7.63. Found: C, 56.23; H, 7.77.

6.6.12 Synthesis of $\text{U}(\text{COT}^{\text{TIPS}_2})\text{Cp}^*(\kappa^2\text{-O}_2\text{CCH}_3)$ (**3.13**)

A red-orange solution of **2.4** (40 mg, 0.050 mmol) in 4 cm^3 toluene was cooled to $-78\text{ }^\circ\text{C}$ before being exposed to CO_2 (1.5 eq., 0.075 mmol) *via* Toepler pump. Upon warming to ambient temperature whilst stirring a colour change to red was observed. The solution was concentrated to ca 1 cm^3 and slow-cooled to $-30\text{ }^\circ\text{C}$ affording red crystalline material suitable for X-ray diffraction studies. Performing the reaction with $^{13}\text{CO}_2$ affords the same result.

Yield: 28 mg (0.033 mmol) 66 % w.r.t **2.4**.

^1H NMR (C_6D_6 , 399.5 MHz) δ_{H} 5.80 (s, 15H, $\text{Cp}^*\text{-CH}_3$), 4.24 (d, 3H, CH_3), -2.26 (br s, 2H, COT-H), -4.61 (d, $^1J_{\text{HH}} = 7.4\text{ Hz}$, 18H, $^i\text{Pr-CH}_3$), -5.76 (d, $^1J_{\text{HH}} = 5.4\text{ Hz}$, 18H, $^i\text{Pr-CH}_3$), -6.66 (m, 6H, $^i\text{Pr-CH}$), -21.71 (br s, 2H, COT-H), -52.44 (br s, 2H, COT-H).

$^{13}\text{C}\{^1\text{H}\}$ NMR (C_6D_6 , 399.5 MHz) δ_{C} 32.4 (bound $^{13}\text{CO}_2$).

$^{29}\text{Si}\{^1\text{H}\}$ NMR (C_6D_6 , 74.9 MHz) δ_{Si} -111.02 (br s, Si^iPr).

MS (EI) $^+$: $m/z = 849$ (M^+ , 7%), 373 ($^i\text{UCp}^*$, 57%), 157 (Si^iPr_3 , 100%).

IR (Nujol, cm^{-1}) 1501w, 1225m, 1068w, 1028s, 1016s, 993w, 933m, 882s, 767s, 680m, 669s, 637s, 528m.

Anal. Calcd for $\text{C}_{38}\text{H}_{66}\text{Si}_2\text{O}_2\text{U}_1$: C, 53.75; H, 7.83. Found: C, 53.27; H, 7.77.

6.6.13 Synthesis of $U(COT^{TIPS_2})Cp^*(\kappa^2-O_2CCH_2TMS)$ (**3.14**)

A dark orange frozen sample of **2.5** (*ca* 0.126 mmol) in 5 cm³ pentane – prepared immediately before commencing the reaction – was exposed to 1 equivalent of CO₂ *via* Toepler pump. The solution became dark red upon warming to ambient temperature and spontaneously produced red microcrystalline solids after 12 h. Recrystallisation from the slow evaporation of a saturated pentane solution yielded a small number of red crystals suitable for X-ray diffraction studies. Repetition of the reaction with ¹³CO₂ afforded the same result. Elemental analysis was not obtainable for this compound.

Yield: 65 mg (0.07 mmol) 55% w.r.t. **2.5**.

¹H NMR (C₆D₆, 399.5 MHz) δ_H 10.54 (br s, 2H, CH₂SiMe₃), 5.25 (s, 15H, Cp*-CH₃), 0.31 (s, 9H, CH₂SiMe₃), -5.01 (d, J = 7.2 Hz, 18H, ⁱPr-CH₃), -6.09 (d, J = 7.2 Hz, 18H, ⁱPr-CH₃), -7.23 (br s, 2H, COT-H), -7.58 (m, 6H, ⁱPr-CH), -13.01 (br s, 2H, COT-H), -50.83 (br s, 2H, COT-H).

¹³C{¹H} NMR (C₆D₆, 100.5 MHz) δ_C 57.4 (bound ¹³CO₂).

²⁹Si{¹H} NMR (C₆D₆, 79.4 MHz) δ_{Si} -10.2, -92.5 assigned to CH₂SiMe₃ and SiⁱPr.

MS (EI)⁺: m/z = 920 (M⁺, 22%), 785 (M⁺ -Cp*, 83%), 157 (SiⁱPr₃, 100%).

IR (Nujol, cm⁻¹) 1504w, 1234m, 1021m, 920m, 667m, 640m, 540m.

6.6.14 Attempted reaction of **2.6** and ¹³CO₂

A C₆D₆ solution of **2.6** (35 mg, 0.036 mmol) in a J Young NMR tube was frozen before being exposed to 1 equivalent (0.036 mmol) of ¹³CO₂. No reaction was observed by ¹H NMR spectroscopy. Next, 0.86 bar of ¹³CO₂ was added to the vessel – no reaction was observed. Heating the sample to 70 °C for 48 h yielded crystalline **3.15**.

6.6.15 Synthesis of $\{\text{U}(\text{COT}^{\text{TIPS}_2})(\mu\text{-}\eta^5\text{:}\kappa^1\text{-C}_5\text{Me}_4\text{CH}_2\text{-O}_2^{13}\text{C})\}_2$ (**3.15**)

Exposure of a frozen C_6D_6 solution of $\text{U}(\text{COT}^{\text{TIPS}_2})(\eta^5\text{:}\eta^1\text{-C}_5\text{Me}_4\text{CH}_2)$ (20 mg, 0.023 mmol) in a J Young NMR tube to an excess of $^{13}\text{CO}_2$ via Toepler pump afforded an orange solution with red precipitate upon warming. Removal of volatiles under reduced pressure and recrystallisation of the red solids from a saturated THF solution afforded crystals of **3.15**. Crystals suitable for X-ray diffraction were formed from a C_6D_6 solution stored at ambient temperature. The reaction can also be performed in d_8 -THF, C_7D_8 , or C_6D_{12} .

Yield: 22 mg (0.013 mmol) 57% w.r.t. **2.9**.

^1H NMR (d_8 -THF, 399.5 MHz) δ_{H} 4.80 (s, 6H, Cp- CH_3), -0.47 (m, 6H, $^i\text{Pr-CH}$), -0.12 (s, 6H, Cp- CH_3), -0.21 (s, 18H, $^i\text{Pr-CH}_3$), -1.95 (s, 18H, $^i\text{Pr-CH}_3$), -3.49 (s, 18H, $^i\text{Pr-CH}_3$), -4.18 (s, 18H, $^i\text{Pr-CH}_3$), -6.70 (m, 6H, $^i\text{Pr-CH}$), -10.76 (br s, 6H, Cp- CH_3), -11.37 (br s, 6H, Cp- CH_3).

Additional 8 x br s, 2H each, at δ_{H} 49.44, 49.18, 21.61, 15.44, -55.49, -59.51, -76.02, -80.25 assigned to COT- H and Cp- CH_2 protons.

$^{13}\text{C}\{^1\text{H}\}$ NMR (C_7D_8 , 100.5 MHz) δ_{C} 60.37 (bound $^{13}\text{CO}_2$).

$^{29}\text{Si}\{^1\text{H}\}$ NMR data could not be collected due to insolubility of the product.

MS (EI) $^+$: $m/z = 834$ ($\text{M}^+ - \text{U}\{\text{COT}^{\text{TIPS}_2}\}\text{C}_5\text{Me}_4\text{CH}_2\text{O}_2^{13}\text{C}$, 100%).

IR (Nujol, cm^{-1}) 3232w, 2277s, 1611m, 1542s, 1457m, 1372m, 1262w, 1079w, 1014m, 880m, 807w, 673m, 640m, 575w, 490m, 458s.

Anal. Calcd. for $\text{C}_{74}\text{H}_{124}\text{Si}_4\text{O}_4\text{U}_2$: C, 53.34; H, 7.50. Found: C, 52.69; H, 7.26.

6.6.16 Synthesis of $\text{U}(\text{COT}^{\text{TIPS}_2})\text{Cp}^*(\text{O}_2\text{CH})$ (**3.16**)

2.4 (175 mg, 0.217 mmol) was dissolved in ca 3 cm^3 pentane, giving a dark red solution, which was frozen after the headspace was evacuated. The ampoule was pressurised with 1 bar of H_2 from a cylinder and the reaction mixture was warmed to

ambient temperature over 1 h, forming **3.1** *in situ*; no obvious colour change was observed. The dark red solution was cooled to -78 °C and the ampoule headspace was evacuated before being pressurised with 0.8 bar of CO₂ from a cylinder. The dark red solution was stirred and allowed to warm to ambient temperature over 16 h, during which time red crystalline solids formed – these were isolated and washed with 3 x 2 cm³ cold pentane portions. Further crystalline product suitable for X-ray diffraction studies was collected from slow-cooling the mother liquor to -35 °C. Performing the reaction with ¹³CO₂ in a J Young NMR tube in tandem with a Toepler pump yields the labelled product, ¹³C-**3.16**. The partially deuterated product, ¹³C-**3.16-d_x** (where x = 1-64) can be obtained from the reaction of **2.3** with D₂ and ¹³CO₂.

Yield: 60 mg (0.072 mmol) 33% w.r.t. **2.4**.

¹H NMR (C₆D₆, 499.5 MHz) δ_H 13.82 (br s, 2H, COT-*H*), 8.55 (br s, 1H, O₂C-*H*), 7.53 (s, 15H, Cp*-CH₃), -4.61 (d, ¹J_{HH} = 7.3 Hz, 18H ^{*i*}Pr-CH₃), -4.91 (d, ¹J_{HH} = 7.3 Hz, 18H, ^{*i*}Pr-CH₃), -5.67 (m, 6H, ^{*i*}Pr-CH), -40.80 (br s, 2H, COT-*H*), -59.24 (br s, 2H, COT-*H*).

²⁹Si {¹H} NMR (C₆D₆, 79.4 MHz) δ_{Si} -84.00 (br s, Si^{*i*}Pr₃).

MS (EI)⁺: m/z = 835 (M⁺, 56%), 700 (M⁺ -Cp*, 100%).

IR (NaCl, cm⁻¹): 1558m, 1463m, 1382w, 1362w, 1260s, 1089s, 1016s, 881m, 800s, 669s, 641w.

¹³C-labelled product:

¹H NMR (C₆D₆, 399.5 MHz, selected data) δ_H 8.58 (d, J_{CH} = 209 Hz, 1H, O₂¹³C-*H*).

¹³C {¹H} NMR (C₆D₆, 100.5 MHz) δ_C -19.97 (br s, O₂¹³CH).

¹³C NMR (C₆D₆, 100.5 MHz) δ_C -20.05 (d, ¹J_{CH} = 210.4 Hz, O₂¹³CH).

IR (ReactIR in C₇H₁₄, ¹³CO₂, selected data, cm⁻¹): 1588m.

Anal. Calcd for (¹³C)C₃₇H₆₆Si₂O₂U₁: C, 53.27; H, 7.72. Found: C, 54.16; H, 7.77.

6.6.17 Reaction of **3.2** with CO₂

A J Young NMR tube was charged with microcrystalline **3.2** (6 mg, 0.007 mmol) dissolved in C₆D₆; the dark red-brown solution was frozen before exposure to an excess of ¹³CO₂ (0.039 mmol, ca 6 eq.). Upon warming the solution became red in colour. ¹H NMR spectroscopic analysis showed the disappearance of the acyl and the formation of a new product. Over the course of 24 h, the initially-formed product decomposes.

¹H NMR (C₆D₆, 399.5 MHz) δ_H 7.04 (t, ¹J_{HH} = 7.4 Hz, 1H *p*-C₆H₅), 6.49 (br s, 15H, Cp*-CH₃), 6.47 (t, ¹J_{HH} = 7.5 Hz, 2H *m*-C₆H₅), 4.21 (br s, 2H, COT-*H*), 3.38 (d, ¹J_{HH} = 7.1 Hz, 2H, *o*-C₆H₅), -4.16 (m, 36H, 2 x ⁱPr-CH₃ overlapped), -5.55 (m, 6H, ⁱPr-CH), -32.85 (br s, ~1H, CH₂Ph), -54.17 (br s, 2H, COT-*H*).

Additional COT-*H* resonance not observed.

¹³C{¹H} NMR (C₆D₆, 100.5 MHz) δ_C 238.3, 143.85 (d, *J* = 73 Hz), 98.51 (d, *J* = 73.6), 75.16 (d, *J* = 104 Hz).

ReactIR (methylcyclohexane solution): no signal observed.

6.6.18 Reaction of **3.3** with CO₂

A J Young NMR tube was charged with **2.4** (24 mg, 0.030 mmol) and C₇D₈; the orange-red solution was cooled to -78 °C before being exposed to a slight excess of CO (0.036 mmol, 1.2 eq). Upon warming to ambient temperature the solution changed colour to dark red, and ¹H NMR spectroscopic analysis confirmed the formation of the η²-acyl **3.3**. The solution was again cooled to -78 °C before being exposed to a slight excess of ¹³CO₂ (0.0358 mmol, 1.2 eq); upon warming no colour change was observed. The formation of the product was determined by NMR spectroscopic analysis. The reaction can also be performed in C₆D₆. The product decomposes over the course of 48 h in solution, or when subjected to reduced pressure.

¹H NMR (C₆D₆, 399.5 MHz) δ_H 6.15 (s, 15H, Cp*-CH₃), -2.09 (br s, 2H, COT-*H*), -4.20 (d, ¹J_{HH} = 7.2 Hz, 18H, ⁱPr-CH₃), -4.99 (d, ¹J_{HH} = 7.3 Hz, 18H, ⁱPr-CH₃),

-6.11 (m, 6H, ⁱPr-CH), -9.60 (br s, 3H, OC-CH₃), -21.63 (br s, ~1H, COT-H),
-52.95 (br s, 2H, COT-H).

¹³C{¹H} NMR (C₇D₈, 100.5 MHz) δ_C 110.1, 32.4.

ReactIR (methylcyclohexane solution; ¹³CO, ¹³CO₂, selected data, cm⁻¹): 1653m.

6.6.19 Reaction of **3.4** with CO₂

A crystalline sample of **2.5** (12 mg, 0.014 mmol) dissolved in C₆D₆ was placed in a J Young NMR tube; the red solution was frozen before exposure to a slight excess of ¹³CO (0.027 mmol, 2 eq.). Upon warming to ambient temperature there was no obvious colour change and ¹H NMR spectroscopic analysis confirmed the formation of the η²-acyl **3.4**. The solution was frozen again, before being exposed to an excess of ¹²CO₂ (0.082 mmol, 6 eq.). Upon warming to ambient temperature no colour change was observed. A reaction yielding 2 products was confirmed by ¹H NMR spectroscopic analysis; over a period of 1 h resonances attributed to one of the two products disappeared. The same reaction was also performed in C₇D₁₄ in ReactIR equipment, using ¹³CO and ¹³CO₂ – only one product is observed due to time delay in collecting ¹H NMR spectra.

Product synthesised with ¹²CO, ¹³CO₂:

Product A (major; remains present after 1 h): ¹H NMR (C₆D₆, 399.5 MHz, selected data): δ_H 30.13 (s, 2H, COT-H), 30.08 (d, ¹J_{HH} = 8.9 Hz, 2H, CH₂SiMe₃),
1.11 (s, 15H, Cp*-CH₃, overlapped), -3.37 (d, ¹J_{HH} = 6.9 Hz, 18H, ⁱPr-CH₃),
-3.94 (s, 9H, CH₂SiMe₃), -4.64 (d, ¹J_{HH} = 6.4 Hz, 18H, ⁱPr-CH₃),
-6.06 (m, 6H, ⁱPr-CH), -7.96 (br s, 2H, COT-H), -44.33 (br s, 2H, COT-H).

Product B (minor; not present after 1 h): ¹H NMR (C₆D₆, 399.5 MHz, selected data):
δ_H 5.43 (s, 15H, Cp*-CH₃), -1.21 (s, 9H, CH₂SiMe₃),
-4.06 (d, ¹J_{HH} = 6.8 Hz, 18H, ⁱPr-CH₃), -4.11 (d, ¹J_{HH} = 6.8 Hz, 18H, ⁱPr-CH₃),
-5.71(m, 6H, ⁱPr-CH), -6.28 (br s, 2H, CH₂SiMe₃). No COT-H resonances observed.

$^{13}\text{C}\{^1\text{H}\}$ NMR (C_6D_6 , 100.5 MHz) δ_{C} 131.07 (br s).

^{13}C NMR (C_6D_6 , 100.5 MHz) δ_{C} 131.07 (d, $J_{\text{CH}} = 10.4$ Hz).

Product synthesised with ^{13}CO , $^{13}\text{CO}_2$:

Product A: ^1H NMR (C_7D_{14} , 399.5 MHz, selected data): δ_{H} 30.23 (s, 2H, COT-*H*), 29.82 (d, $^1J_{\text{HH}} = 8.9$ Hz, 2H, CH_2SiMe_3), 0.86 (s, 15H, Cp*- CH_3 , overlapped), -3.45 (br s, 18H, $^i\text{Pr-CH}_3$), -4.09 (s, 9H, CH_2SiMe_3), -4.64 (br s, 18H, $^i\text{Pr-CH}_3$, overlapped), -5.87 (m, 6H, $^i\text{Pr-CH}$), -7.77 (br s, 2H, COT-*H*), -44.33 (br d, $J_{\text{CH}} = 118$ Hz, 2H).

^{13}C NMR (C_7D_{14} , 399.5 MHz) δ_{C} 192.5 (d, $J = 73$ Hz), 132.3 (d, $J = 73$ Hz).

ReactIR (methylcyclohexane solution; ^{13}CO , $^{13}\text{CO}_2$, selected data, cm^{-1}): 1655m.

6.6.20 Reaction of *cis-3.8* with CO_2 : **3.17** and isomerisation to *trans-3.8*

A crystalline sample of *cis-3.8* (3.3 mg) dissolved in C_6D_6 in a J Young NMR tube was frozen before exposure to ca 1 eq. of $^{13}\text{CO}_2$. Upon warming, a colour change from red to red-orange was observed. ^1H NMR spectroscopic analysis confirmed the complete consumption of *cis-3.8* and an essentially 100% conversion into **3.17**. Repeating the reaction with substoichiometric $^{13}\text{CO}_2$ does not yield a complete conversion of *cis-3.8* to **3.17**. When performing the reaction with $^{12}\text{CO}_2$, no resonances corresponding to a ^{13}C -atom are present in the $^{13}\text{C}\{^1\text{H}\}$ NMR spectrum. Crystallisation of the product was not successful from pentane, toluene, THF or Et_2O . Heating **3.17** (15 mg) to 80 °C for 18 h yields *trans-3.8* in a 100% yield (as determined by ^1H NMR spectroscopy). Recrystallisation of crude *trans-3.8* yields red-orange crystals suitable for X-ray diffraction studies.

Data for **3.17**:

^1H NMR (C_6D_6 , 399.5 MHz) δ_{H} 58.60 (s, 2H, COT-*H*), 29.90 (s, 1H, OCH), 15.38 (s, 2H, COT-*H*), 10.06 (s, 15H, Cp*- CH_3), -1.74 (s, 15H, Cp*- CH_3),

-3.05 (d, $^1J_{\text{HH}} = 7.0$ Hz, 18H, $^i\text{Pr-CH}_3$), -3.87 (d, $^1J_{\text{HH}} = 7.3$ Hz, 18H, $^i\text{Pr-CH}_3$),
 -4.71 (m, 6H, $^i\text{Pr-CH}$), -6.91 (d, $^1J_{\text{HH}} = 7.1$ Hz, 18H, $^i\text{Pr-CH}_3$),
 -11.89 (br s, 18H, $^i\text{Pr-CH}_3$), -14.35 (m, 6H, $^i\text{Pr-CH}$), -32.82 (br s, 1H, OCH),
 -55.11 (br s, 2H, COT-H), -57.24 (br s, 2H, COT-H). Other COT-H resonances not
 observed (or overlapped with other resonances).

$^{13}\text{C}\{^1\text{H}\}$ NMR (C_6D_6 , 100.5 MHz) δ_{C} -55.4 (br s, ^{13}C).

$^{29}\text{Si}\{^1\text{H}\}$ (C_6D_6 , 79.4 MHz) δ_{Si} -84.3, -115.1 (s, 2 x Si^iPr environments).

MS (EI) $^+$: $m/z = 1638$ (2%).

IR: ReactIR, methylcyclohexane (cm^{-1} , selected data): 1331w.

Data for ***trans*-3.8**:

^1H NMR (C_6D_6 , 399.5 MHz) δ_{H} 153.0 (br s, 2H, OCH), 93.40 (br s, 4H, COT-H), 2.80
 (s, 15H, $\text{Cp}^*\text{-CH}_3$), -3.54 (d, $^1J_{\text{HH}} = 7.0$ Hz, 18H, $^i\text{Pr-CH}_3$), -10.10 (d, $^1J_{\text{HH}} = 6.5$ Hz,
 18H, $^i\text{Pr-CH}_3$), -12.04 (m, 6H, $^i\text{Pr-CH}$), -41.22 (br s, 2H, COT-H), -58.99 (br s, 2H,
 COT-H).

MS (EI) $^+$: $m/z = 1638$ (M^+ , 18%), 789 ($^i\text{UCOT}^{\text{TIPS}2}\text{Cp}^*$, 37%).

6.6.21 Reaction of **2.7** with CO_2 (**3.18**)

Crystalline **2.7** (7 mg) was dissolved in C_6D_6 in a J Young NMR tube; the solution was
 frozen and an excess (ca 3 eq.) of $^{13}\text{CO}_2$ was delivered to the vessel *via* Toepler pump.
 Upon thawing, no obvious colour change was observed. A partial conversion of **2.7** to a
 new product (**3.18**) was observed 20 minutes after gas addition, which persists for
 several days in solution but is no longer seen after the sample is subjected to reduced

pressure. The same reaction can be performed in C₇D₈. Adding further equivalents of ¹³CO₂ does not alter the outcome of the reaction.

¹H NMR (C₆D₆, 399.5 MHz): δ_H 6.28 (s, 15H, Cp*-CH₃), 1.29 (t, ¹J_{HH} = 6.9 Hz, 3H, OCH₂CH₃), -4.68 (d, ¹J_{HH} = 7.4 Hz, 18H, ⁱPr-CH₃), -5.39 (d, ¹J_{HH} = 7.5 Hz, 18H, ⁱPr-CH₃). Broad singlets ca 1-2H each at δ_H 5.27, 2.62, -29.21, -55.96 assigned to 3 x COT-*H* and OCH₂CH₃ proton environments.

¹³C{¹H} NMR (C₆D₆, 100.5 MHz): δ_C -49.26 (br s, ¹³CO₂).

ReactIR (methylcyclohexane solution, selected data, cm⁻¹): 1300m.

6.7 Experimental details for Chapter 4

6.7.1 Synthesis of U(COT^{TIPS2})Cp*(NH₂) (**4.1**)

Method 1: A crystalline sample of **2.3** (210 mg, 0.238 mmol) dissolved in toluene (ca 20 cm³) was heated in an ampoule to 65 °C for 16 h, during which time a colour change from dark red-brown to dark brown was observed, indicating the formation of **2.9**. The solution was cooled to -78 °C, the headspace evacuated and NH₃ (0.238 mmol, 1 eq.) was added *via* Toepler pump. After warming to ambient temperature and stirring overnight a colour change to orange-red was observed; filtration *via* filter cannula and removal of volatiles under reduced pressure, followed by the addition and subsequent removal of small portions of Et₂O (3 x 5 cm³) yielded the product as an orange powder. Slow-cooling a saturated ^tBuOMe solution yields block-shaped red crystals of **4.1**. ^tBuOMe suitable for X-ray diffraction studies. The same reaction can be performed with ND₃ to yield **4.1-d₃**.

Yield: 160 mg (0.199 mmol) 83% w.r.t. **2.3**.

Method 2: A J Young NMR tube was charged with **2.4** (10 mg, 0.012 mmol) dissolved in C₆D₆; the red solution was frozen before exposure to a stoichiometric amount of NH₃

(0.012 mmol). Upon warming no obvious colour change was observed. The same reaction can be performed with ND₃ to yield **4.1-d₂**.

Yield: > 95 % by ¹H NMR.

Method 3: Solid **2.2** (118 mg, 0.143 mmol) and KNH₂ (21 mg, 0.382 mmol, 2.7 eq.) were combined in an ampoule to which ca 20 cm³ of Et₂O was added. The resulting mixture was stirred for 24 h, by which time the solution was orange-red and contained off-white precipitate. Filtration *via* filter cannula and removal of volatiles under reduced pressure, followed by the subsequent addition and removal of small portions of Et₂O (3 x 5 cm³) afforded **4.1** as an orange powder.

Yield: 81 mg (0.100 mmol) 70% w.r.t. **2.2**.

Method 4: An ampoule was charged with NaNH₂ (77 mg, 1.965 mmol) and pre-cooled to -78 °C; to this a solution of **2.2** (1352 mg, 1.638 mmol, 0.83 eq. in 100 cm³ Et₂O) was added over 10 minutes. The resultant red suspension was allowed to warm to ambient temperature and stirred vigorously for 4 days. Filtration of the orange-red solution *via* filter cannula and subsequent removal of volatiles under reduced pressure yielded orange-red solids. Recrystallisation from ca 5 cm³ ^tBuOMe or Et₂O afforded analytically pure red microcrystalline solids after isolation and washing with 3 x 0.5 cm³ cold solvent portions.

Yield: 829 mg (1.029 mmol) 74% w.r.t. **2.2**.

For **4.1**:

¹H NMR (C₆D₆, 399.5 MHz) δ_H 202.28 (br s, ~1H, NH₂), 102.57 (br s, 2H, COT-*H*), -6.08 (d, ¹J_{HH} = 7.2 Hz, 18H, ⁱPr-CH₃), -6.36 (s, 15H, Cp*-CH₃), -13.91 (br s, 18H, ⁱPr-CH₃), -17.59 (m, 6H, ⁱPr-CH), -32.13 (br s, 2H, COT-*H*), -91.11 (br s, 2H, COT-*H*).

²⁹Si NMR (C₆D₆, 79.4 MHz), δ_{Si} -135.26 (Si^{*i*}Pr₃).

MS (EI)⁺: $m/z = 806$ (M^+ , 20%), 789 ($M^+ - \text{NH}_2$, 22%), 670 ($M^+ - \text{Cp}^*$, 26%), 69 (Si^iPr_3 fragment, 100%).

IR (Nujol mull, cm^{-1}): 3582w, 3309w, 3032m, 2721w, 1581w, 1497m, 1257m, 1220m, 1047s, 1032s, 1013s, 934m, 886s, 802m, 755m, 670s, 642s, 581m.

Anal. Calcd (%) for $\text{C}_3\text{H}_6\text{Si}_2\text{NU}(\text{C}_4\text{H}_{10}\text{O})$: C, 54.58; H, 8.59; N, 1.59.

Found: C, 54.50; H, 8.09; N, 1.20.

For **4.1-*d*₃**:

^2H NMR (C_7H_8 , 61.3 MHz) δ_{D} 202.13 (br s, ND_2), -6.17 (br s, $\text{Cp}^*-\text{CH}_2\text{D}$).

For **4.1-*d*₂**:

^2H NMR (C_6H_6 , 61.3 MHz) δ_{D} 201.83 (br s, ND_2).

6.7.2 Attempted synthesis of $\text{U}(\text{COT}^{\text{TIPS}2})\text{Cp}^*(\text{N}\{\text{TMS}\}_2)$ (**4.2**)

A J Young NMR tube was charged with **2.2** (25 mg, 0.030 mmol) and $\text{KN}(\text{TMS})_2$ (7 mg, 0.030 mmol); the solids were dissolved in C_7D_8 . No change was observed after thorough mixing. Heating the solution to 55 °C for 18 h afforded a colour change from red-brown to yellow-brown, and the formation of a new product (**4.2**) was observed by ^1H NMR spectroscopy. Repetition of the reaction on larger scales and subsequent workup did not yield an isolable product or further characterising data – extensive decomposition was observed.

^1H NMR (C_7D_8 , 399.5 MHz): δ_{H} 23.84 (br s, ~1H, COT-*H*), 5.90 (s, 15H, Cp^*-CH_3), -1.22 (s, 18H, $^i\text{Pr}-\text{CH}_3$), -3.72 (d, $^1J_{\text{HH}} = 7.4$ Hz, 18H, $^i\text{Pr}-\text{CH}_3$), -4.31 (m, 6H, $^i\text{Pr}-\text{CH}$), -12.20 (v br s, ca 13H, $\text{N}(\text{SiMe}_3)_2$), -64.32 (br s, 2H, COT-*H*). Other COT-*H* resonance not located.

6.7.3 Synthesis of $U(COT^{TIPS_2})Cp^*(\kappa^2-O_2CNH_2)$ (**4.3**)

Crystalline **4.1** (19mg, 0.022 mmol) was dissolved in C_6D_6 in a J Young NMR tube before being frozen and exposed to CO_2 (0.044 mmol, 2 eq.); a colour change from orange-red to red was observed. Removal of volatiles under reduced pressure and extraction of the red solids with ca 1 cm^3 pentane afforded red crystals suitable for X-ray diffraction. The same reaction can be performed with **4.1- d_x** and $^{13}CO_2$ to yield the perdeuterated products, 13 -**4.3- d_x** (where $x = 2, 3$).

Yield: 12 mg (0.014 mmol) 64% yield w.r.t. **4.1**.

1H NMR (C_6D_6 , 399.5 MHz) δ_H 15.63 (s, 2H, NH_2), 4.63 (s, 15H, Cp^*-CH_3), -4.70 (d, $^1J_{HH} = 7.5$ Hz, 18H, $^iPr-CH_3$), -6.38 (d, $^1J_{HH} = 7.5$ Hz, 18H, $^iPr-CH_3$), -7.44 (m, 6H, ^iPr-CH), -9.65 (br s, 2H, $COT-H$), -10.16 (br s, 2H, $COT-H$), -50.05 (br s, 2H, $COT-H$).

^{29}Si NMR (C_6D_6 , 79.4 MHz), δ_{Si} -94.53 (Si^iPr_3).

MS (EI) $^+$: $m/z = 850$ (M^+ , 1%), 833 ($M^+ - NH_2$, 1%), 806 ($M^+ - NH_2OC$, 4%), 715 ($M^+ - Cp^*$, 8%), 373 (UCp^* , 30%), 115 (Si^iPr fragment, 100%).

IR (NaCl, cm^{-1}): 3423s, 1588s, 1509m, 1456s, 1448s, 1421s, 1375m, 1260m, 1090, 1070m, 1030s, 1016s, 993m, 964m, 924w, 915w, 882s, 766m, 702w, 671m, 640, 582w, 455s.

Anal. Calcd (%) for $C_{37}H_{65}NO_2Si_2U(C_4H_{10}O)$: C, 53.33; H, 8.17; N, 1.51.

Found: C, 53.29; H, 7.67; N, 1.75.

For ^{13}C -**4.3**:

$^{13}C\{^1H\}$ NMR (C_6D_6 , 399.5 MHz) δ_C 25.77 (br s, $O_2^{13}C-NH_2$).

For ^{13}C -**4.3- d_3** :

2H NMR (C_6D_6 , 61.3 MHz) δ_D 15.65 (d, $J_{CD} = 16.7$ Hz, $O_2^{13}C-ND_2$), 4.50 (s, Cp^*-CH_2D).

For ^{13}C -**4.3-*d*₂**:

^2H NMR (C_6D_6 , 61.3 MHz) δ_{D} 15.55 (d, $J_{\text{CD}} = 17.0$ Hz, $\text{O}_2^{13}\text{C-ND}_2$).

6.7.4 Reaction of **4.1** and CO

A sample of **2.9** (19 mg, 0.024 mmol) was dissolved in C_6D_6 in a J Young NMR tube, frozen, and exposed to 1.2 eq (0.029 mmol) of NH_3 . ^1H NMR spectroscopic analysis confirmed the formation of **4.1**. The solution was frozen, the headspace evacuated, and 1.2 eq (0.029 mmol) of ^{13}CO was delivered to the vessel. No reaction was detected by ^1H NMR spectroscopy. Heating the reaction mixture to 50 °C for 24 hours did not afford a change, nor did the addition of an excess of ^{13}CO (0.86 bar). $^{13}\text{C}\{^1\text{H}\}$ NMR spectroscopy showed the presence of free ^{13}CO in solution.

6.7.5 Synthesis of $[\text{U}(\text{COT}^{\text{TIPS}_2})\text{Cp}^*(\text{NH})[\text{K}(18\text{-crown-6})]]$ (**4.4**)

A THF slurry of KH (7.5 mg, 0.186 mmol) and 18-crown-6 (49 mg, 0.186 mmol) was cooled to -30 °C, and to this was added a THF solution of **4.1** (150 mg, 0.186 mmol) pre-cooled to -60 °C (total solvent volume ca 30 cm^3). The resulting orange-brown solution was stirred and allowed to warm to ambient temperature for 2 days, by which time a colour change to dark red had occurred and off-white precipitate was present. Filtration *via* filter cannula and removal of volatiles yielded a red oil. The addition of cold Et_2O (5 cm^3 , -60 °C) resulted in the precipitation of a pink powder and an orange solution, which was filtered away *via* filter cannula – this was repeated until the washings were colourless. The residual pink powder (**4.4**) was dried under reduced pressure, and is sparingly soluble in toluene/benzene with the addition of THF. Red needles of **4.4** were obtained from a saturated Et_2O solution stored at ambient temperature.

Yield: 65 mg (0.059 mmol) 32% w.r.t. **4.1**.

^1H NMR ($\text{C}_7\text{D}_8/d_8\text{-THF}$, 399.5 MHz) δ_{H} -8.90 (br s, 18H, $^i\text{Pr-CH}_3$),

-10.18 (br s, 15H, $\text{Cp}^*\text{-CH}_3$), -17.32 (br s, 18H, $^i\text{Pr-CH}_3$), -21.70 (br s, 6H, $^i\text{Pr-CH}$).

Broad resonance at δ_{H} 7.81 attributed to 18-crown-6; broad, low-integral resonances (ca 1-2H) at δ_{H} 152.01, -79.90, -120.43, and -133.64 *could* be attributed to COT-*H* and U-NH protons.

MS (EI)⁺ only returned values corresponding to ligand fragments ($m/z = 416, 374$).

IR (NaCl, cm^{-1}): 1460s, 1377m, 1351m, 1249w, 1112m, 963m, 836w, 801w, 722w.

Anal. Calcd (%) for $\text{C}_{48}\text{H}_{88}\text{KSi}_2\text{NO}_6\text{U}(\text{C}_5\text{H}_{12}\text{O})$: C, 53.20; H, 8.42; N, 1.17.

Found: C, 52.85; H, 8.39; N, 1.01.

6.7.6 Reaction of **4.1**, KH, and 222-crypt

An ampoule was charged with equimolar quantities of **4.1** (80 mg, 0.100 mmol), KH (4 mg) and 222-crypt (37 mg), followed by 15 cm^3 of THF pre-cooled to $-40\text{ }^\circ\text{C}$. The resulting orange-pink slurry was stirred for 2 days, after which time it was dark red-brown in colour. Filtration *via* filter cannula and removal of volatiles under reduced pressure yielded a red-brown oil. ^1H NMR spectroscopic analysis of an aliquot of crude product showed the conversion of **4.1** into a new product, tentatively characterised as $[\text{U}(\text{COT}^{\text{TIPS}_2})\text{Cp}^*(\text{NH})][\text{K}(222\text{-crypt})_2]$, which appeared to show a change in coordination of 222-crypt after 4 days in solution. Attempts to manipulate the red-brown oil further resulted in decomposition; no isolable product could be obtained.

^1H NMR ($\text{C}_6\text{D}_6/d_8\text{-THF}$, 399.5 MHz, selected data) δ_{H} 17.04 (s, 6H, 222-crypt),

16.85 (s, 6H, 222-crypt), 15.58 (s, 6H, 222-crypt), 12.41 (s, 18H, 222-crypt),

12.21 (s, 18H, 222-crypt), 11.07 (s, 18H, 222-crypt), -4.13 (br s, 18H, $^i\text{Pr-CH}_3$),

-9.27 (br s, 15H, $\text{Cp}^*\text{-CH}_3$), -17.83 (br s, 18H, $^i\text{Pr-CH}_3$), -21.38 (br s, 6H, $^i\text{Pr-CH}$).

Resonances attributable to COT-*H* and U-NH proton environments not observed.

After 4 days in solution:

^1H NMR ($\text{C}_6\text{D}_6/d_8\text{-THF}$, 399.5 MHz, selected data) δ_{H} 11.05 (s, 18H, 222-crypt), 10.91 (s, 18H, 222-crypt), 9.74 (s, 18H, 222-crypt), -4.15 (br s, 18H, $^i\text{Pr-CH}_3$), -9.37 (br s, 15H, $\text{Cp}^*\text{-CH}_3$), -17.91 (br s, 18H, $^i\text{Pr-CH}_3$), -21.43 (br s, 6H, $^i\text{Pr-CH}$). Resonances attributable to COT-*H* and U-NH proton environments not observed.

6.7.7 Reaction of **4.1**, NaH, and 12-crown-4

An equimolar quantity of **4.1** (253 mg, 0.310 mmol) and NaH (7.5 mg) was suspended in THF (15 cm^3) pre-cooled to $-78\text{ }^\circ\text{C}$, and to this was added dropwise an Et_2O solution of 12-crown-4 (0.620 mmol, 0.00109 M) resulting in an orange solution. No discernable colour change was observed after stirring for 5 days; ^1H NMR spectroscopic analysis determined that no reaction had occurred.

6.7.8 Reaction of **4.1**, KH, and 12-crown-4

A THF solution of **4.1** (250 mg, 0.310 mmol) and an excess of 12-crown-4 (2 eq., 0.620 mmol, 0.00109 M solution in Et_2O) cooled to $-30\text{ }^\circ\text{C}$ was added to a THF suspension (5 cm^3) of KH (12.6 mg, 0.314 mmol) and stirred whilst warming to ambient temperature. No obvious colour change was observed after 7 days; ^1H NMR spectroscopic analysis determined that no reaction had occurred.

6.7.9 Reaction of **4.1**, KH, and excess 18c6

An ampoule was charged with **4.1** (87 mg, 0.108 mmol), KH (4 mg, 0.108 mmol) and 18c6 (57 mg, 0.216 mmol, 2 eq.), and to this was added THF (20 cm^3) pre-cooled to $-60\text{ }^\circ\text{C}$. An aliquot collected from the reaction mixture after warming to ambient temperature and stirring for 2 days, and analysed by ^1H NMR spectroscopy showed the presence of resonances corresponding to unreacted **4.1** and a product with similar resonances to **4.4**. Variable temperature ^1H NMR studies determined that the K ion was still bound to the metal centre.

^1H NMR ($\text{C}_7\text{D}_8/d_8\text{-THF}$, 399.5 MHz) δ_{H} -10.13 (br s, 15H, $\text{Cp}^*\text{-CH}_3$), -10.98 (br s, 18H, $^i\text{Pr-CH}_3$), -16.77 (br s, 18H, $^i\text{Pr-CH}_3$), -21.54 (br s, 6H, $^i\text{Pr-CH}$). Broad resonance at δ_{H} 5.46 attributed to 18c6; broad, low-integral resonances (ca 1-2H) at δ_{H} 152.92 and -120.83 *could* be attributed to COT-*H* or U-NH protons.

6.7.10 Attempted oxidation of **4.4** with AgBPh_4

A test reaction was performed: an excess of AgBPh_4 was added to a $\text{C}_7\text{D}_8/d_8\text{-THF}$ solution of **4.4** (containing some **4.1**) and mixed thoroughly. ^1H NMR spectroscopic analysis of the reaction mixture revealed the disappearance of all resonances attributable to **4.4** and no evidence for a new product.

6.7.11 Reaction of **4.4** with 0.5 eq. I_2

Pink **4.4** (29 mg, 0.026 mmol) was dissolved in ca 10 cm^3 THF, and to this was added a freshly-prepared solution of I_2 in THF (0.013 mmol, 120 μl , 0.109 M). The reaction mixture immediately became dark brown from the addition of I_2 . Stirring for 1 h, removal of all volatiles, and extraction into C_7D_8 for ^1H NMR spectroscopic analysis showed the reaction mixture to contain $\text{U}(\text{COT}^{\text{TIPS}_2})\text{Cp}^*\text{I}$ (from comparison to a genuine sample), no residual **4.4**, and a number of other paramagnetically-shifted resonance which could not be assigned.

6.7.12 Attempted syntheses of “ $\text{U}(\text{COT}^{\text{TIPS}_2})\text{Cp}^*(\text{N})$ ”

Method I: A THF solution of **4.4** (92 mg, 0.083 mmol) was pre-cooled to $-20\text{ }^\circ\text{C}$ and added to a THF slurry of KH (6.6 mg, 0.166 mmol) and 18c6 (44 mg, 0.166 mmol). An aliquot was obtained after the reaction mixture was stirred for 12 h, and ^1H NMR spectroscopic analysis showed the presence of resonances very similar in chemical shift and integral values to that of **4.4** and unreacted 18c6. Further workup did not yield an isolable product.

^1H NMR (C_6D_6 , 399.5 MHz) δ_{H} -9.99 (br s, 15H, Cp^*-CH_3), -11.41 (br s, 18H, $^i\text{Pr}-\text{CH}_3$), -16.56 (br s, 18H, $^i\text{Pr}-\text{CH}_3$), -21.40 (br s, 6H, $^i\text{Pr}-\text{CH}$).

Method 2: An ampoule was charged with **4.1** (260 mg, 0.323 mmol), KH (25.9 mg, 0.645 mmol) and 18c6 (170 mg, 0.645 mmol) before ca 30 cm^3 THF was added, which had been pre-cooled to $-78\text{ }^\circ\text{C}$. The resulting dark brown-orange solution was stirred at $-78\text{ }^\circ\text{C}$ for 2 h, then allowed to warm to ambient temperature whilst stirring for 18 h, during which time no obvious colour change was observed. An aliquot obtained for ^1H NMR spectroscopic analysis returned results showing the presence of unreacted **4.1**, and a number of broad, paramagnetically-shifted resonances that could not be assigned. Stirring for a further 12 h, followed by filtration *via* filter cannula, removal of volatiles and the addition of Et_2O (ca 5 cm^3) to the red-brown tacky solids yielded a brown-green solution. Slow-cooling to $-30\text{ }^\circ\text{C}$ yielded red-green crystals of $\text{U}(\text{COT}^{\text{TIPS}2})_2$ and colourless crystals of K(18-crown-6).

Method 3: Pink **4.4** (23 mg, 0.021 mmol) was dissolved in ca 10 cm^3 THF and cooled to $-78\text{ }^\circ\text{C}$; to this was added 0.5 eq. of I_2 (0.011 mmol, 96 μl , 0.109 M in THF) *via* microsyringe. The brown mixture was allowed to warm to ambient temperature whilst stirring for 4 h. Removal of volatiles, extraction of the brown solids in pentane, filtration *via* filter cannula and re-extraction in THF gave a brown solution separated from off-white solids. This was cooled to $-78\text{ }^\circ\text{C}$ and then added to a THF slurry of KH (1 mg, 0.021 mmol) and 18c6 (6 mg, 0.021 mmol) also pre-cooled to $-78\text{ }^\circ\text{C}$, and the resulting mixture was stirred for 2 days. Removal of volatiles from the orange-brown solution, extraction into Et_2O (ca 10 cm^3) followed by filtration *via* filter cannula gave a brown solution. Volatiles were removed under reduced pressure before the remaining orange-brown solids were dissolved in C_7D_8 for ^1H NMR spectroscopic analysis, which showed only the presence of resonances similar in chemical shift to **4.4** alongside organic decomposition resonances. Further workup did not yield isolable material.

^1H NMR (C_7D_8 , 399.5 MHz, selected data) δ_{H} -10.13 (br s, 15H, $\text{Cp}^*\text{-CH}_3$), -11.77 (br s, 18H, $^i\text{Pr-CH}_3$), -16.52 (br s, 18H, $^i\text{Pr-CH}_3$), -21.47 (br s, 6H, $^i\text{Pr-CH}$).

6.8 Experimental details for Chapter 5

6.8.1 Synthesis of $\text{U}(\text{N}'\text{N}'_2)\text{Cp}^*\text{Cl}$ (5.1)

An ampoule was charged with equimolar amounts of UCl_4 (1.524 g, 4.013 mmol) and LiCp^* (0.569 g, 4.013 mmol) before the addition of THF (100 cm^3), pre-cooled to $-30\text{ }^\circ\text{C}$. The resultant mixture was stirred for 16 h, affording a red solution with white solids. After cooling to $-30\text{ }^\circ\text{C}$, $\text{Li}_2(\text{N}'\text{N}'_2)$ (1.264 g, 3.812 mmol, 0.95 eq.) in THF (ca 30 cm^3) was added dropwise to the mixture and stirred for 12 h, giving an orange solution with white precipitate. Extraction in toluene and filtration through Celite® resulted in an orange solution. Storage at $-50\text{ }^\circ\text{C}$ overnight yielded yellow-green crystals of $\text{U}(\text{N}'\text{N}'_2)\text{Cp}^*\text{Cl}$.

Yield: 2.209 g (3.039 mmol) 80% yield w.r.t. $\text{Li}_2(\text{N}'\text{N}'_2)$.

^1H NMR (C_6D_6 , 399.5 MHz) δ_{H} 29.73 (br s, 2H, $\text{N}'\text{N}'_2\text{-CH}_2$ backbone), 24.84 (br s, 18H, terminal $\text{N}\{\text{SiMe}_3\}$), -0.06 (s, 15H, $\text{Cp}^*\text{-CH}_3$), -14.17 (s, 9H, middle $\text{N}\{\text{SiMe}_3\}$), -19.44 (br s, 2H, $\text{N}'\text{N}'_2\text{-CH}_2$ backbone). Resonances at -32.74 and -48.38 (v br s, < 1H) attributed to other $\text{N}'\text{N}'_2\text{-CH}_2$ backbone environments.

$^{29}\text{Si}\{^1\text{H}\}$ (C_6D_6 , 79.4 MHz) δ_{Si} -45.64, -50.60 (middle and terminal SiMe_3).

MS (EI) $^+$: m/z = 725 (M^+ , 3%), 690 ($\text{M}^+ - \text{Cl}$, 2%), 408 ($\text{M}^+ - \{\text{N}'\text{N}'_2\}$, 13 %), 217 ($\text{N}'\text{N}'_2$ fragment, 100%).

Anal. Calcd for $\text{C}_{23}\text{H}_{50}\text{Si}_3\text{N}_3\text{ClU}$: C, 38.03; H, 6.93; N, 5.78.

Found: C, 38.12; H, 6.91; N, 5.86.

6.8.2 Thermolysis of **5.1**: $\{U(N'NN'')Cp^*Cl\}_2$ (**5.2**)

A crystalline sample of **5.1** (75 mg, 0.103 mmol) was dissolved in toluene (ca 5 cm³) and the resulting orange solution was heated at 70 °C for 48 hours, during which time the solution became orange-red in colour. Removal of volatiles under reduced pressure and subsequent slow-cooling of the solids dissolved in ca 2 cm³ toluene yielded red crystalline material of **5.2**.

Yield: 20 mg (0.028 mmol) 26% w.r.t. **5.1**; yield by ¹H NMR spectroscopy: > 90%.

¹H NMR (C₆D₆, 399.5 MHz) δ_H 102.63 (br s, 2H, N'NN''-CH backbone), 49.49 (br s, 2H, N'NN''-CH backbone), 44.61 (br s, 2H, N'NN''-CH backbone), 37.83 (br s, 2H, N'NN''-CH backbone), 37.05 (br s, 2H, N'NN''-CH backbone), 5.37 (br s, 2H, N'NN''-CH backbone), 2.63 (br s, 2H, N'NN''-CH backbone), 0.17 (s, 36H, N{SiMe₃})₂), -2.43 (s, 30H, Cp*-CH₃), -4.94 (s, 18H, N{SiMe₃}), -29.44 (2H, N'NN''-CH backbone). Resonances at δ_H -2.43 (s, 5H) and -3.62 (s, 3H) could not be rationally assigned.

MS (EI)⁺: m/z = 725 (M⁺ - U(N'NN'')Cp*Cl, 3%), 690 (M⁺ - U(N'NN'')Cp*Cl₂, 2%), 590 (U(N'NN'')Cl, 70%), 217 (N'NN'' fragment, 100%).

Anal. Calcd for C₄₆H₁₀₀Cl₂N₆Si₆U₂: C, 38.03; H, 6.94; N, 5.78.

Found: C, 37.89; H, 6.97; N, 5.56.

6.8.3 Synthesis of U(N'N'₂)Cp* (**5.3**)

An ampoule was charged with **5.1** (500 mg, 0.688 mmol) and KC₈ (93 mg, 0.688 mmol) before the addition of 100 cm³ toluene pre-cooled to -78 °C, giving an orange-bronze solution which was allowed to warm to ambient temperature whilst stirring for 24 h. Filtration *via* filter cannula was followed by the reduction of solvent volume under reduced pressure; slow-cooling the dark green solution to -50 °C yielded yellow-green crystals of unreacted **5.1** (26 mg, 5%), which were separated from the reaction mixture. Removal of volatiles and subsequent extraction with Et₂O (ca 5 cm³) followed by

slow-cooling to $-50\text{ }^{\circ}\text{C}$ yielded very dark green crystals of **5.3** suitable for X-ray diffraction studies. Recrystallisation from saturated THF afforded a small number of crystals of **5.3.THF**. The reaction result was the same if an Ar or N_2 atmosphere was used.

Yield: 159 mg (0.230 mmol) 33% w.r.t. **5.1**.

^1H NMR (C_7D_8 , 399.5 MHz) δ_{H} 65.18 (br s, 2H, $\text{N}'\text{N}'_2\text{-CH}_2$ backbone), 37.54 (br s, 2H, $\text{N}'\text{N}'_2\text{-CH}_2$ backbone), 30.30 (br s, 2H, $\text{N}'\text{N}'_2\text{-CH}_2$ backbone), -9.36 (s, 15H, $\text{Cp}^*\text{-CH}_3$), -16.02 (br s, 2H, $\text{N}'\text{N}'_2\text{-CH}_2$ backbone), -18.16 (s, 18H, terminal $\text{N}\{\text{SiMe}_3\}$), -26.45 (s, 9H, middle $\text{N}\{\text{SiMe}_3\}$).

5.3.THF: ^1H NMR (C_7D_8 , 399.5 MHz) δ_{H} -9.03 (s, 15H, $\text{Cp}^*\text{-CH}_3$), -14.99 (s, 18H, terminal $\text{N}\{\text{SiMe}_3\}$), -24.34 (s, 9H, middle $\text{N}\{\text{SiMe}_3\}$). $\text{N}'\text{N}'_2$ ligand backbone CH_2 resonances and bound THF could not be located.

$^{29}\text{Si}\{^1\text{H}\}$ NMR (C_6D_6 , 79.4 MHz) δ_{Si} 130.4 (SiMe_3). Other SiMe_3 resonance was not located due to product instability.

MS (EI) $^+$: $m/z = 691$ (M^+ , 7%), 682 ($\text{M}^+ - 3 \times \text{H}_3$, 30%), 591 ($\text{M}^+ - \text{SiMe}_3$, 47%), 555 ($\text{M}^+ - \text{N}'\text{N}'_2$, 5%), 217 ($\text{N}'\text{N}'_2$ fragment, 50%), 73 (SiMe_3 , 100%).

Elemental analysis could not be obtained for this compound due to instability.

6.8.4 Reaction of **5.1** and KC_8 in THF

An ampoule was charged with **5.1** (494 mg, 0.680 mmol), KC_8 (92 mg, 0.680 mmol), and ca 30 cm^3 THF pre-cooled to $-78\text{ }^{\circ}\text{C}$. The addition of solvent afforded a dark purple solution, which became dark brown-green after stirring at $-78\text{ }^{\circ}\text{C}$ for 2 h. An aliquot was collected at this point for ^1H NMR spectroscopic analysis: no **5.1** was present in solution, and a number of new paramagnetic resonances were observed (detailed below). The solution was stirred further and warmed to ambient temperature before filtration *via* filter cannula and concentration of solvent volume under reduced pressure. Slow-cooling to $-50\text{ }^{\circ}\text{C}$ did not afford any crystalline material. Removal of

volatiles, extraction into Et₂O (5 cm³) and slow-cooling to -30 °C yielded a small number of blue needles, determined to be Cp*U{μ-(N'NN'')₃}U, by X-ray diffraction studies. Decomposition precluded further characterisation.

¹H NMR (C₆D₆, 399.5 MHz, selected data) δ_H 5.58 (s, 18H, N{SiMe₃}), -5.45 (s, 9H, N{SiMe₃}) – this product is suspected to contain the N'NN'' ligand and has been seen in many other reaction mixtures.

¹H NMR (C₆D₆, 399.5 MHz, selected data) δ_H 2.76 (s, 3H), 2.73 (s, 3H), -0.08 (s, 3H), -0.12 (s, 3H), -2.64 (s, 2H), -3.07 (s, 2H) – integrals reported relative to each other and could not be assigned, or rationalised to correspond to the structure determined by X-ray crystallographic studies.

6.8.5 Reaction of **5.1** and KC₈ in Et₂O

An ampoule was charged with **5.1** (176 mg, 0.241 mmol) and KC₈ (33 mg, 0.241 mmol) before the addition of Et₂O (ca 20 cm³) pre-cooled to -78 °C. Stirring for 10 min at -78 °C did not dissolve **5.1**; the slurry was allowed to warm to ambient temperature whilst stirring for 2 h, during which time it became deep emerald green in colour. Further stirring for 16 h yielded a green-brown solution, which was filtered *via* cannula and all volatiles were removed under reduced pressure, yielding dark brown-green tacky solids. Attempts to isolate crystalline material by recrystallisation from various solvents did not yield isolable material.

¹H NMR (C₆D₆, 399.5 MHz, selected data) δ_H 5.58 (s, 18H, N{SiMe₃}), -5.45 (s, 9H, N{SiMe₃}) – as seen in section 6.8.4.

6.8.6 Attempted reduction of **5.1** with K/Hg in toluene

A toluene solution of **5.1** (520 mg, 0.716 mmol in 50 cm³) was stirred in an ampoule before the addition of K/Hg (14 g, 0.2% w/w K/Hg, 0.716 mmol). The resulting mixture was stirred for 12 days, during which time the solution remained orange and the

K/Hg did not change in appearance. THF (30 cm³) was added to the ampoule and stirring was continued for 7 days, after which time a colour change to red-orange was seen. ¹H NMR spectroscopic analysis of an aliquot showed the complete consumption of **5.1**. Filtration and removal of volatiles yielded a dark brown oil, and the addition of 5 cm³ Et₂O afforded an orange precipitate. Removal of the precipitate *via* filter cannula and subsequent extraction of the oil in toluene (10 cm³) and slow-cooling to -50 °C did not yield any crystalline material. Further recrystallisation attempts did not yield an isolable product.

¹H NMR (C₆D₆, 399.5 MHz) δ_H 5.59 (s, 18H), -0.86 (s, 4 H), -5.45 (s, 9H). Assignment of these resonances was not possible – as seen in section 6.8.4

MS (EI)⁺ (crude sample): m/z = 835 (15%), 790 (18%), 417 (28%), 373 (UCp*, 62%), 73 (SiMe₃, 96%), 45 (Me₃, 100%).

MS (EI)⁺ (after recrystallisation attempts): m/z = 217 (N'N'₂ fragment, 38%), 174 (N'N'₂ fragment, 100%).

6.8.7 Synthesis of [U(η²-N'N'₂)Cp*ILi]₂[LiI(THF)₂]₂ (**5.4**)

Equimolar UI₃ (1300 mg, 2.101 mmol) and KCp* (366 mg, 2.101 mmol) were stirred in THF (50 cm³) for 16 h, after which time the mixture was deep green in colour and contained off-white precipitate. Removal of volatiles and extraction of the green-brown solids with toluene preceded filtration *via* filter cannula, affording a dark green solution of UI₂Cp*(THF)_x, which was then cooled to -78 °C. A toluene solution (10 cm³) of Li₂(N'N'₂) (628 mg, 1.927 mmol, 0.9 eq.) was added dropwise to the UI₂Cp*(THF)_x solution over a period of 50 min, during which time no colour change was observed. The dark green mixture was allowed to warm to ambient temperature whilst stirring for 1 h, and became dark purple in colour. Volatiles were removed under reduced pressure giving sticky purple solids, which were extracted into pentane (60 cm³, then 3 x 10 cm³ rinses) and filtered *via* filter cannula to yield a purple solution. Slow-cooling to -20 °C afforded dark purple crystalline and microcrystalline material of **5.4**.

Yield: 739 mg (0.736 mmol) 39% w.r.t. $\text{Li}_2(\text{N}'\text{N}'_2)$.

^1H NMR (C_7D_8 , 399.5 MHz) δ_{H} 9.72 (br s, 1H, $\text{N}'\text{N}'_2$ -CH backbone), 9.32 (s, 9H, middle $\text{N}\{\text{SiMe}_3\}$), 2.56 (br s, 8H, THF- CH_2), 0.27 (br s, 8H, THF- CH_2), -6.41 (br s, 15H, Cp^* - CH_3), -6.73 (br s overlapped, 2H, $\text{N}'\text{N}'_2$ - CH_2 backbone), -8.92 (s, 18H, terminal $\text{N}\{\text{SiMe}_3\}$), -21.24 (br s, 1H, $\text{N}'\text{N}'_2$ -CH backbone), -103.28 (br s, 1-2H, $\text{N}'\text{N}'_2$ - CH_2 backbone). Other resonances attributable to $\text{N}'\text{N}'_2$ -CH backbone environments not observed.

$^{29}\text{Si}\{^1\text{H}\}$ NMR (C_7D_8 , 74.9 MHz) δ_{Si} 28.99, -191.04 (assigned to 2 x SiMe_3).

$^7\text{Li}\{^1\text{H}\}$ NMR (C_7D_8 , 155.3 MHz) δ_{Li} -3.85 (br s) assigned to both Li environments – likely broad, overlapped signals.

MS (EI)⁺: m/z = 687 ('U($\text{N}'\text{N}'_2$)I.Li' -2 H, 4%), 641 ('UI{LiI(THF) $_2$ }', 5%), 552 ('{LiI(THF) $_2$ } $_2$ ', 15%), 217 ($\text{N}'\text{N}'_2$ fragment, 44%), 73 (SiMe_3 , 100%).

6.8.8 Attempted reduction of **5.4** with KC_8

A test reaction was performed in a J Young NMR tube: a C_7D_8 solution of **5.4** (20 mg, 0.020 mmol) and an excess of KC_8 (3 mg, 0.022 mmol, 1.1 eq.) were combined and mixed thoroughly. A colour change from purple to brown was observed over the course of 16 h, with regular mixing maintained for the first 6 h. ^1H NMR spectroscopic analysis returned a spectrum containing a large number of paramagnetically-shifted resonances that could not be sufficiently assigned.

$^7\text{Li}\{^1\text{H}\}$ NMR (C_7D_8 , 155.3 MHz) δ_{Li} 34.65 (br s), 2.36 (br s).

6.8.9 Reaction of **5.2** with 1.2 eq. KC_8 in toluene

A toluene solution of **5.1** (200 mg, 0.275 mmol in 30 cm^3) was heated to 70 °C for 48 h, during which time it changed colour from orange to orange-red. Volatiles were removed under reduced pressure to afford orange-red solids, to which were added a

slight excess of KC_8 (45 mg, 0.330 mmol, 1.2 eq.) and 30 cm³ of toluene, pre-cooled to -78 °C. After stirring at -78 °C for 10 min, the brown-orange slurry was allowed to warm to ambient temperature whilst stirring for 2 h, during which time a colour change to dark red-purple-brown was observed; an aliquot was collected at this point. Stirring was continued for 48 h before the mixture was filtered *via* filter cannula and all volatiles were removed under reduced pressure, affording ca 108 mg of dark red-purple solids. Subsequent attempts to crystallise the material from a range of common solvents were not successful. ¹H NMR spectra collected from the crude reaction mixture could not be sufficiently assigned, but are reported below with integrals relative to suspected bridging arene complex, $\{\text{U}(\text{N}''\text{N}''')\}_2(\mu\text{-C}_7\text{H}_8)$, 5.58 and -5.45 ppm.

¹H NMR (C_6D_6 , 399.5 MHz, aliquot 1): δ_{H} 53.38 (s, 2H), 51.73 (s, 1H), 5.58 (s, 18H, $\text{N}\{\text{SiMe}_3\}_2$), 3.12 (s, 18H), 3.05 (s, 13H), -0.56 (s, 18H), -0.61 (s, 12H), -2.68 (s, 12H), -2.92 (s, 8H), -5.45 (s, 9H, $\text{N}\{\text{SiMe}_3\}$), -55.55 (s, 1H), -67.05 (s, 1H).

¹H NMR (C_6D_6 , 399.5 MHz, crude mixture): δ_{H} 53.37 (s, 1.5H), 51.72 (s, 1H), 5.58 (s, 18H, $\text{N}\{\text{SiMe}_3\}_2$), 3.11 (s, 16H), 3.05 (s, 10H), -0.29 (s, 15H), -0.56 (s, 15H), -0.61 (s, 10H), -2.69 (s, 10H), -2.93 (s, 6H), -5.45 (s, 9H, $\text{N}\{\text{SiMe}_3\}$), -55.55 (s, 1H), -67.04 (s, 1H).

MS (EI)⁺: $m/z = 825$ ($\text{U}(\text{N}''\text{N}''')\text{Cp}^*_2$, 8%), 690 ($\text{U}(\text{N}''\text{N}''')\text{Cp}^*$, 18%), 651 ($\text{U}(\text{N}''\text{N}''')(\text{C}_7\text{H}_8)$, 100%).

6.8.10 Reaction of **5.2** with 2.2 eq. KC_8 in toluene

A test reaction was performed: a J Young NMR tube was charged with **5.1** (28 mg, 0.039 mmol) and C_7D_8 , then heated to 70 °C for 48 h, forming **5.2**. An excess of KC_8 (12 mg, 0.089 mmol, 2.2 eq.) was then added, resulting in a colour change to dark red. ¹H NMR spectroscopic analysis confirmed the consumption of **5.2** and the formation of a new product, suspected to be $\{\text{U}(\text{N}''\text{N}''')\}_2(\mu\text{-C}_7\text{D}_8)$. Preparative-scale

reactions performed in an identical manner with C₇H₈ did not yield clean or isolable material suitable for X-ray crystallographic studies after workup.

¹H NMR (C₇D₈, 399.5 MHz) δ_H 28.74 (s, 2H, N'NN''-CH backbone), 5.56 (s, 36H, N{SiMe₃}₂), -0.22 (s, 3H, N'NN''-CH backbone), -5.50 (s, 18H, N{SiMe₃}), -18.36 (s, 2H, N'NN''-CH backbone), -20.81 (s, 2H, N'NN''-CH backbone), -23.02 (br s, 7H, N'NN''-CH backbone signals overlapped).

MS (EI)⁺: m/z = 826 (6%, U(N'NN'')Cp*₂), 691 (U(N'NN'')Cp*, 30%), 651 (U(N'NN'')(C₇H₈), 100%).

6.8.11 Reactivity of U(N'N'₂)Cp* (**5.3**) with CO

General procedure: Crystalline **5.3** was dissolved in C₇D₈ in a J Young NMR tube, forming a dark green solution, which was promptly cooled to -78 °C. The headspace was evacuated, and a measured quantity of CO added *via* Toepler pump – a colour change to red-brown was observed immediately after gas addition. Then, the vessel was sealed and allowed to warm to ambient temperature. ¹H NMR spectra were collected immediately after warming, and several hours later – many paramagnetic resonances are present, selected resonances only described below. Preparative-scale reactions of **5.3** and 1 bar of ¹²CO did not yield any isolable products.

With 1 eq. ¹³CO: (**5.3** = 15 mg, 0.022 mmol).

¹H NMR (C₇D₈, 399.5 MHz, selected data) δ_H 4.63 (br s, 16H), 3.37 (s, 30H), -1.35 (s, 7H).

¹³C NMR (C₇D₈, 100.5 MHz, selected data) δ_C 184.97 (free ¹³CO), -88.03 (br s), -93.97 (br s), -125.95 (s), -127.79 (s).

MS (EI)⁺: m/z = 780 (U(N'N'₂)Cp* + 3CO, 6%), 640 (6%), 555 (10%), 217 (N'N'₂ fragment, 76%), 116 (N'N'₂ fragment, 65%), 72 (SiMe₃, 100%).

ReactIR (methylcyclohexane solution, cm^{-1} , selected resonances): 1946w.

With 2 eq. ^{13}CO : (**5.3** = 26 mg, 0.038 mmol).

^1H NMR (C_7D_8 , 399.5 MHz, selected data) δ_{H} 4.63 (br s, 18H), 3.37 (s, 33H), -1.35 (s, 8H), -17.62 (s, 7H).

^{13}C NMR (C_7D_8 , 100.5 MHz, selected data) δ_{C} 184.97 (free ^{13}CO), -87.94 (br s), -94.31 (br s), -126.00 (s), -127.83 (s).

With 1 eq. ^{12}CO : (**5.3** = 15 mg, 0.022 mmol).

^1H NMR (C_7D_8 , 399.5 MHz, selected data) δ_{H} 4.63 (br s, 18H), 3.37 (s, 30H), -1.35 (s, 7H), -3.21 (br s, 16H), -18.97 (s, 9H).

6.8.12 Reactivity of **5.3** with CO_2

A test-scale reaction was performed: **5.3** (23 mg, 0.033 mmol) was dissolved in C_6D_6 in a J Young NMR tube before being frozen and the headspace evacuated. An excess (0.071 mmol, 2.2 eq.) of $^{13}\text{CO}_2$ was added *via* Toepler pump, and the solution was thawed after addition, whereby a colour change from dark green to yellow-orange was observed. ^1H NMR spectroscopic analysis showed the complete consumption of **5.3**, and a mixture of new products, the resonances of which could not be assigned.

$^{13}\text{C}\{^1\text{H}\}$ NMR (C_6D_6 , 100.5 MHz) δ_{C} 184.49 (free ^{13}CO), 124.79 (free $^{13}\text{CO}_2$).

MS (EI) $^+$: m/z = 73 (SiMe_3 , 100%), and other ligand fragments – no U-containing fragments.

6.8.13 Reactivity of **5.1** with CO and CO_2

With CO: A sample of **5.1** (20 mg, 0.028 mmol) was dissolved in C_6D_6 in a J Young NMR tube before being frozen and the vessel headspace evacuated. An excess (0.083 mmol, ca 3 eq.) of ^{13}CO was added *via* Toepler pump, and the solution was

allowed to thaw, during which time no colour change from orange was observed. ^1H NMR spectroscopic analysis indicated no reaction had occurred 10 minutes or 24 h after gas addition. Heating the reaction mixture to 70 °C for 24 h only resulted in the partial formation of **5.2**.

^1H NMR showed resonances corresponding to **5.1** and **5.2** only.

$^{13}\text{C}\{^1\text{H}\}$ NMR (C_6D_6 , 100.5 MHz) δ_{C} 184.68 (free ^{13}CO).

With CO₂: A test-scale reaction was performed: **5.1** (10 mg, 0.014 mmol) was dissolved in C_7D_8 in a J Young NMR tube and cooled to -78 °C before the vessel headspace was evacuated, and an excess (0.043 mmol, ca 3 eq.) of $^{13}\text{CO}_2$ added *via* Toepler pump. The reaction mixture was allowed to warm to ambient temperature, during which time no colour change from orange was observed. A preparative-scale reaction of **5.1** (250 mg, 0.344 mmol) and 1 bar of $^{12}\text{CO}_2$ in toluene was performed, yielding similar ^1H NMR spectroscopic resonances; slow-cooling the toluene solution afforded a small quantity of X-ray diffraction quality crystals of **5.5**, and re-crystallisation from toluene gave a dark green-brown glass-like solid on which elemental analysis and mass spectrometric analysis were performed.

Crude yield: 94 mg.

^1H NMR showed many paramagnetically-shifted resonances that could not be interpreted.

$^{13}\text{C}\{^1\text{H}\}$ NMR (C_6D_6 , 100.5 MHz) δ_{C} 125.25 (free $^{13}\text{CO}_2$).

MS (EI)⁺: m/z = 1627 (M^+ , < 1%), 640 (9%), 550 (' U_2Cl_2 ', 5%), 147 ($\text{O}_2\text{CN}\{\text{SiMe}_3\}\text{CH}_2$, 100%).

Anal. Calcd for $\text{C}_{50}\text{H}_{100}\text{Cl}_2\text{N}_6\text{O}_8\text{Si}_6\text{U}_2$: C, 36.87; H, 6.19; N, 5.16.

Found: C, 37.52; H, 6.04; N, 5.51.

6.8.14 Synthesis of $\{U(N'N'_2)\}_2(\mu-\eta^6:\eta^6-C_7H_8)$ (**5.6**)

Method 1: To an ampoule charged with **5.1** (993 mg, 1.367 mmol) and KC_8 (418 mg, 3.094 mmol, 2.2 eq.) was added ca 200 cm³ toluene pre-cooled to -78 °C, giving an orange-bronze solution. Stirring and warming to ambient temperature for 16 h afforded a dark brown solution and off-white precipitate, from which all volatiles were removed under reduced pressure. Extraction of the dark brown solids in Et₂O (ca 40 cm³) and subsequent filtration *via* filter cannula yielded a dark brown solution which, when slow-cooled to -50 °C, yielded black crystals of **5.6**. Recrystallisation from THF yields a small quantity of **5.6.THF**.

Yield: 331 mg (0.275 mmol) 20% w.r.t **5.1**.

Method 2: Crystalline **5.3** (37 mg, 0.054 mmol) and KC_8 (7 mg, 0.054 mmol) were dissolved in toluene (ca 10 cm³) and stirred for 17 h, during which time a colour change from dark green to brown was observed. ¹H NMR spectroscopic analysis of the crude product confirmed the identity of the product as **5.6**.

¹H NMR (C_7D_8 , 399.5 MHz) δ_H 43.27 (s, 3H, $C_6H_5-CH_3$),
33.41 (s, 4H, $N'N'_2-CH_2$ backbone), 32.23 (s, 4H, $N'N'_2-CH_2$ backbone)
0.44 (s, 4H, $N'N'_2-CH_2$ backbone), -3.16 (s, 36H, terminal $SiMe_3$),
-8.93 (s, 4H, $N'N'_2-CH_2$ backbone), -13.59 (s, 18H, middle $SiMe_3$),
-64.95 (s, 1H, *p*- C_6H_5), -80.53 and -104.16 (s, 2H each, *o*- and *m*- C_6H_5).

²⁹Si NMR (C_7D_8 , 79.4 MHz) δ_{Si} -17.48, -84.20 (terminal and middle $N-SiMe_3$).

MS (EI)⁺: m/z = 1203 (M^+ , 12 %), 651 ($M^+ - U(N'N'_2)$, 100 %).

Anal. Calcd (%) for $C_{33}H_{78}N_6Si_6U_2$: C, 32.93; H, 6.53; N, 6.98.

Found: C, 32.81; H, 6.56; N, 7.69.

6.8.15 Synthesis of $\{U(N'N'_2)\}_2(\mu\text{-}\eta^6\text{:}\eta^6\text{-C}_6\text{H}_6)$ (**5.7** and **5.7-d₆**)

Method 1: The benzene-bridged complex was synthesised in a manner identical to **5.6**, but performed in ca 100 cm³ benzene in place of toluene, using **5.1** (204 mg, 0.280 mmol) and 2 eq. KC₈ (76 mg, 0.560 mmol). No crystalline material of **5.7** could be obtained.

Crude yield: 85 mg (0.275 mmol) 26% w.r.t **5.1**.

¹H NMR (*d*₁₄-methylcyclohexane, 399.5 MHz, selected resonances):

δ_{H} 34.62 (br s, 4H, N'N'₂-CH₂ backbone), 34.08 (br s, 4H, N'N'₂-CH₂ backbone), -0.56 (br s, 4H, N'N'₂-CH₂ backbone, overlapped), -2.88 (s, 36H, terminal N{SiMe₃}₂), -8.23 (br s, 4H, N'N'₂-CH₂ backbone), -12.65 (br s, 18H, middle N{SiMe₃}), -76.19 (br s, 6H, bridging C₆H₆).

¹H NMR (C₇D₈, 399.5 MHz, selected resonances):

δ_{H} 33.64 (br s, 8H, N'N'₂-CH₂ backbone), -1.09 (br s, 4H, N'N'₂-CH₂ backbone), -3.16 (s, 36H, terminal N{SiMe₃}₂), -8.93 (br s, 4H, N'N'₂-CH₂ backbone), -13.20 (br s, 18H, middle N{SiMe₃}), -76.37 (br s, 6H, bridging C₆H₆).

Also present after 7 days: δ_{H} 5.55 (s), 4.62 (br s), 3.36 (s), -1.36 (s) and -5.50 (s) – all previously observed in other reaction mixtures.

Method 2 (5.7-d₆): A crystalline sample of **5.6** was dissolved in C₆D₆ in a J Young NMR tube and heated to 80 °C for 13 days, resulting in the complete conversion to the deuterated benzene bridged product, **5.7-d₆**, with the release of free toluene.

¹H NMR (C₆D₆, 399.5 MHz) δ_{H} 33.74 (br s, 4H, N'N'₂-CH₂ backbone), 33.59 (br s, 4H, N'N'₂-CH₂ backbone), 7.13-7.00 (m, Ar-CH₃C₇H₈), 2.12 (s, CH₃Ph), -1.15 (br s, 4H, N'N'₂-CH₂ backbone), -3.12 (s, 36H, terminal N{SiMe₃}₂), -8.97 (br s, 4H, N'N'₂-CH₂ backbone), -13.16 (br s, 18H, middle N{SiMe₃}).

MS (EI)⁺: *m/z* = 1194 (M⁺, 100 %), 555 (M⁺ -C₆D₆-U{N'N'₂}).

Satisfactory elemental analysis results were not obtained.

6.8.16 Reactivity studies of **5.6** with azobenzene, CO, and CO₂

With azobenzene: **5.6** (80 mg, 0.066 mmol) and azobenzene (12 mg, 0.066 mmol) were combined in an ampoule before the addition of pentane (ca 20 cm³) pre-cooled to -78 °C. The reaction mixture was allowed to stir and warm to ambient temperature, and was observed to be a red-brown solution free of solids after reaching ca 20 °C. The mixture was stirred for a total of 7 days, after which time no reaction had occurred, as determined by ¹H NMR spectroscopy. All volatiles were removed under reduced pressure, and a hexane solution of excess of azobenzene (50 mg, 0.274 mmol ca 4 eq.) was added to the residual brown solids. Stirring for a further 10 days did not elicit a reaction, and only unreacted azobenzene could be retrieved from the reaction mixture.

With CO: A crystalline sample of **5.6** (20 mg, 0.017 mmol) was dissolved in C₇D₈, cooled to -78 °C, and exposed to an excess (ca 2 eq.) of ¹³CO. Upon warming to ambient temperature, no reaction was observed by ¹H NMR spectroscopy. The reaction mixture was heated to 100 °C for 1 h; no reaction was observed.

With CO₂: The same sample described above was cooled to -78 °C, thoroughly degassed, and exposed to an excess (ca 6 eq.) of ¹³CO₂. Upon warming, the solution changed colour from dark brown to light brown-yellow, and formed brown precipitate. ¹H NMR spectroscopic analysis did not show the presence of any paramagnetic species.

6.9 References for Chapter 6

1. Z. Otwinowski and W. Minor, *Methods in Enzymology, Vol. 256: Macromolecular Crystallography Part A*, Academic Press, 1997, vol. 276.
2. CrysAlisPRO, Oxford Diffraction/Agilent Technologies UK Ltd., Yarnton, England.
3. L. J. Farrugia, *J. Appl. Crystallogr.*, 2012, **45**, 849–854.
4. O. V. Dolomanov, L. J. Bourhis, R. J. Gildea, J. A. K. Howard, and H. Puschmann, *J. Appl. Crystallogr.*, 2009, **42**, 339–341.
5. L. Palatinus and G. Chapuis, *J. Appl. Crystallogr.*, 2007, **40**, 786–790.
6. G. M. Sheldrick, *Acta Crystallogr., Sect. A: Found. Crystallogr.*, 2008, **64**, 112–22.
7. Rigaku Corporation, 2012.
8. A. D. Becke, *J. Chem. Phys.*, 1993, **98**, 5648–5652.

9. J. P. Perdew and Y. Wang, *Phys. Rev. B*, 1992, **45**, 13244–13249.
10. A. Moritz, X. Y. Cao, and M. Dolg, *Theor. Chem. Acc.*, 2007, 845–854.
11. A. Bergner, M. Dolg, W. Küchle, H. Stoll, and H. Preuß, *Mol. Phys.*, 1993, 1431–1441.
12. A. W. Ehlers, M. Böhme, S. Dapprich, A. Gobbi, A. Höllwarth, V. Jonas, K. F. Köhler, R. Stegmann, A. Veldkamp, and G. Frenking, *Chem. Phys. Lett.*, 1993, 111–114.
13. W. J. Hehre, R. Ditchfield, and J. A. Pople, *J. Chem. Phys.*, 1972, **56**, 2257–2261.
14. P. C. Hariharan and J. A. Pople, *Theor. Chim. Acta*, 1973, **28**, 213–222.
15. J. S. Binkley, J. A. Pople, and W. J. Hehre, *J. Am. Chem. Soc.*, 1980, **102**, 939–947.
16. C. Gonzalez and H. B. Schlegel, *J. Chem. Phys.*, 1989, **90**, 2154–2161.
17. C. Gonzalez and H. B. Schlegel, *J. Phys. Chem.*, 1990, **94**, 5523–5527.
18. D. McKay, A. S. P. Frey, J. C. Green, F. G. N. Cloke, and L. Maron, *Chem. Commun.*, 2012, **48**, 4118–4120.
19. C. E. Kefalidis, A. S. P. Frey, S. M. Roe, F. G. N. Cloke, and L. Maron, *Dalton Trans.*, 2014, **43**, 11202–8.
20. M. J. Frisch, G. W. Trucks, H. B. Schlegel, G. E. Scuseria, M. A. Robb, J. R. Cheeseman, G. Scalmani, V. Barone, B. Mennucci, G. A. Petersson, H. Nakatsujim, M. Caricato, X. Li, H. P. Hratchian, A. F. Izmaylov, J. Blonio, G. Zheng, J. L. Sonnenberg, M. Hada, M. Ehara, K. Toyota, R. Fukuda, J. Hasegawa, M. Ishida, T. Nakajima, Y. Honda, O. Kitao, H. Nakai, T. Vreven, J. A. Montgomery, Jr., J. E. Peralta, F. Ogliaro, M. Bearpark, J. J. Heyd, E. Brothers, K. N. Kudin, V. N. Staroverov, R. Kobayashi, J. Normand, K. Raghavachari, A. Rendell, J. C. Burant, S. S. Iyengar, J. Tomasi, M. Cossi, N. Rega, J. M. Millam, M. Klene, J. E. Knox, J. B. Cross, V. Bakken, C. Adamo, J. Jaramillo, R. Gomperts, R. E. Stratmann, O. Yazyev, A. J. Austin, R. Cammi, C. Pomelli, J. W. Ochterski, R. L. Martin, K. Morokuma, V. G. Zakrzewski, G. A. Voth, P. Salvador, J. J. Dannenberg, S. Dapprich, A. D. Daniels, O. Farkas, J. B. Foresman, J. V. Ortiz, J. Cioslowski, and D. J. Fox, 2009.
21. O. T. Summerscales, "*The Chemistry of Low-Valent Transition Metal and f-Element Complexes Supported by Five- and Eight-Membered Carbocycles*", DPhil Thesis, University of Sussex, 2007.
22. W. A. Hermann and G. Brauer, *Synthetic Methods of Organometallic and Inorganic Chemistry: Lanthanides and Actinides*, George Thieme Verlag, New York, Volume 6., 1997.
23. N. A. Morley-Smith, "*Early Transition Metal Chemistry Incorporating the Disubstituted Dianionic Rings Cyclooctatetraenyl and Pentalenyl*", DPhil Thesis, University of Sussex, 2001.
24. F. X. Kohl and P. Jutzi, *J. Organomet. Chem.*, 1983, **243**, 119–121.
25. F. G. N. Cloke, P. B. Hitchcock, and J. B. Love, *J. Chem. Soc., Dalton Trans.*, 1995, 25–30.
26. C. J. Windorff and W. J. Evans, *Organometallics*, 2014, **33**, 3786–3791.

APPENDIX 1. MISCELLANEOUS DATA

A1.1 Summary of relevant bond lengths and angles

Table A1.1 collates available information from crystallographically characterised uranium(III) and (IV) mixed-sandwich complexes containing the $\text{COT}^{\text{TIPS}_2}$ and Cp^* ligands, featured in this thesis and in the literature. The centroid-uranium distances and angles are listed, as well as uranium-carbon bond distances between the aromatic ring carbons.

Table A1.2 collates available information from crystallographically characterised uranium(III) and (IV) complexes featuring the diamidoamine ligand, $\text{N}'\text{N}'_2$, featured in this thesis, in the literature, and from the thesis of Christopher Larch. Distances between uranium and each nitrogen atom are quoted, as are the angles between each terminal nitrogen atom and uranium, and the distance between the terminal nitrogen atoms (where available) – the latter two providing metrics representing the overall coordination geometry of the $\text{N}'\text{N}'_2$ ligand (**Figure A1.1**).

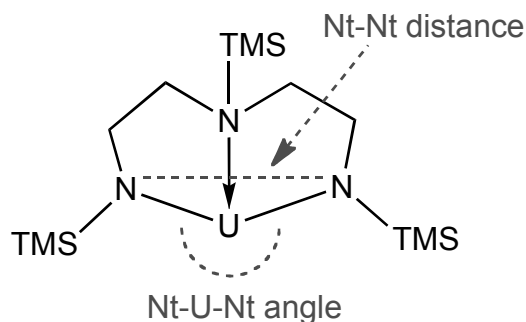


Figure A1.1. Metrics used to aid definition of the coordination geometry of the $\text{N}'\text{N}'_2$ ligand.

Table A1.1. Selected bond distances (Å) and angles (°) of all reported U(III) and U(IV) mixed-sandwich complexes containing COT^{TIPS2} and Cp* ligands (and tucked-in derivatives). Ct1 is defined as the COT-ring centroid, Ct2 is defined as the Cp*-ring centroid.

Compound	U-Ct1	U-C(COT) range	U-Ct2	U-C(Cp*)	Ct1-U-Ct2	Ref.
U(COT ^{TIPS2})Cp*(THF)	1.975(6)	2.674(6)-2.746(6)	2.499(6)	2.763(6)-2.784(6)	144.5(2)	1
U(COT ^{TIPS2})Cp* ^a	1.916(4), 1.924(5)	2.616(12)-2.701(12), 2.618(12)-2.729(12)	2.461(6), 2.471(5)	2.715(12)-2.768(12), 2.744(12)-2.757(12)	154.9(2), 153.1(2)	2
U(COT ^{TIPS2})Cp*Cl	1.9142(15)	2.634(4)-2.686(4)	2.465(2)	2.696(5)-2.752(5)	139.85(8)	3
U(COT ^{TIPS2})Cp*(CH ₂ Ph) ^a	1.9297(3), 1.9304(3)	2.623(4)-2.716(4), 2.628(4)-2.712(4)	2.4899(3), 2.4836(3)	2.739(3)-2.801(4), 2.735(3)-2.810(4)	137.217(13), 137.977(13)	4
U(COT ^{TIPS2})Cp*(CH ₃)	1.9368(3)	2.646(3)-2.697(4)	2.4761(3)	2.719(3)-2.783(6)	140.664(13)	4
U(COT ^{TIPS2})Cp*(CH ₂ TMS)	1.9361(3)	2.635(4)-2.701(4)	2.464(4)	2.728(4)-2.814(4)	137.171(14)	4
U(COT ^{TIPS2})Cp*(CH{TMS} ₂)	1.9774(2)	2.657(3)-2.741(3)	2.497(3)	2.787(3)-2.810(3)	141.926(12)	4
U(COT ^{TIPS2})Cp*(OMe)	1.95590(2)	2.648(5)-2.714(6)	2.4887(2)	2.698(5)-2.884(6)	135.809(9)	5
U(COT ^{TIPS2})Cp*(OEt)	1.9592(18)	2.638(6)-2.712(5)	2.497(3)	2.718(6)-2.884(6)	135.85(9)	3
U(COT ^{TIPS2})(η ⁵ :κ ¹ -C ₅ Me ₄ CH ₂)	1.9066(3)	2.637(3)-2.694(3)	2.3364(3)	2.437(4)-2.719(4)	150.724(15)	4
U(COT ^{TIPS2})(η ⁵ :κ ¹ -C ₅ Me ₄ CH ₂)(THF)	1.9991(4)	2.692(6)-2.797(5)	2.4124(4)	2.508(6)-2.840(6)	143.794(17)	4
U(COT ^{TIPS2})Cp*(κ ² -O ₂ CCH ₂ Ph) ^a	1.953(2), 1.956(2)	2.671(6)-2.739(6), 2.677(7)-2.724(7)	2.472(4), 2.469(7)	2.731(7)-2.766(7), 2.69(2)-2.73(2),	140.26(11), 140.29(17)	4
U(COT ^{TIPS2})Cp*(κ ² -O ₂ CCH ₃)	1.9512(16)	2.650(5)-2.713(5)	2.482(2)	2.725(5)-2.792(5)	137.94(8)	4

$\{\text{U}(\text{COT}^{\text{TIPS}_2})$ $(\mu^1:\mu^1-\kappa^1:\eta^5-\text{C}_5\text{Me}_4\text{CH}_2\text{OCO})\}_2^{\text{b}}$	1.9758(19)	2.668(7)-2.765(6)	2.484(3)	2.665(5)-2.884(7)	136.50(8)	4
$\{\text{U}(\text{COT}^{\text{TIPS}_2})\}_2(\text{C}_5\text{Me}_4\text{CH}_2\text{CO}=\text{OCCH}_2\text{C}_5\text{Me}_4)$ <i>(cis)</i> ^c	1.953(2), 1.935(2)	2.659(7)-2.726(6), 2.650(6)-2.714(6)	2.459(3), 2.457(3)	2.679(6)-2.810(7), 2.661(6)-2.811(7)	140.01(10), 139.96(10)	3
$\text{U}(\text{COT}^{\text{TIPS}_2})\text{Cp}^*(\text{O}\{\text{SO}_2\text{CF}_3\})$	1.92109(3)	2.6220-2.6985	2.46846(4)	2.7201-2.7957	137.3501(10)	6
$\{\text{U}(\text{COT}^{\text{TIPS}_2})\text{Cp}^*\}_2(\mu-\kappa^1:\kappa^1-\text{C}_2\text{O}_2)^{\text{c}}$	1.925(8), 1.923(8)	2.632(8)-2.686(8), 2.631(7)-2.693(8)	2.472(9), 2.449(9)	2.720(9)-2.787(9), 2.684(8)-2.783(9)	140.0(3), 140.4(3)	7
$\{\text{U}(\text{COT}^{\text{TIPS}_2})\text{Cp}^*\}_2(\mu-\kappa^1:\kappa^2-\text{C}_3\text{O}_3)^{\text{c}}$	1.9678(14), 1.9121(13)	2.657(4)-2.753(4), 2.625(4)-2.690(4)	2.503(2), 2.463(2)	2.744(4)-2.807(4), 2.700(4)-2.781(4)	139.8(1). 141.0(1)	1
$\text{U}(\text{COT}^{\text{TIPS}_2})\text{Cp}^*(\text{H})$ (1)	1.9182(6)	2.643(6)-2.649(5)	2.4945(6)	2.730(7)-2.732(5)	150.20(3)	4
$\text{U}(\text{COT}^{\text{TIPS}_2})\text{Cp}^*(\text{H})$ (2) ^a	1.917(4), 1.917(2)	2.615(8)-2.705(4), 2.621(8)-2.703(7)	2.471(4), 2.464(3)	2.709(8)-2.775(8), 2.715(8)-2.76(1)	152.14(10), 152.4(2)	4
$\text{U}(\text{COT}^{\text{TIPS}_2})\text{Cp}^*(\kappa^2-\text{O}_2\text{CH})$	1.9370(14)	2.642(5)-2.707(4)	2.4732(19)	2.724(4)-2.788(5)	138.31(7)	4
$\text{U}(\text{COT}^{\text{TIPS}_2})\text{Cp}^*(\text{NH}_2)$	1.9511(17)	2.665(4)-2.720(3)	2.487(2)	2.740(4)-2.791(5)	141.88(7)	3
$\text{U}(\text{COT}^{\text{TIPS}_2})\text{Cp}^*(\kappa^2-\text{O}_2\text{CNH}_2)$	1.9551(3)	2.653(4)-2.722(3)	2.4788(4)	2.728(3)-2.795(4)	137.076(12)	3

a – Values quoted from both of the two crystallographically independent molecules in the asymmetric unit.

b – Dimeric molecule with half the molecule in the asymmetric unit; only one set of values quoted.

c – Dimeric molecule; two sets of values quoted.

Table A1.2. Selected metrical parameters from all reported crystallographically characterised U(III) and U(IV) complexes containing the N'N'₂ ligand. Nt is defined as the terminal N atom, Nc is defined as in the middle N atom. Ct1 is defined as the Cp*-ring centroid. OS is the complex oxidation state.

Compound	OS	U-Nt (Å)	U-Nc (Å)	U-Ct1 (Å)	Nt-U-Nt (°)	Nt-Nt(Å)	Ref.
U(N'N' ₂)Cp*Cl	4	2.250(7), 2.244(6)	2.759(6)	2.497(4)	140.0(2)	4.228(10)	8
		2.246(6), 2.255(6)	2.755(6)	2.494(4)	139.8(2)	4.225(10)	
{U(N'N' ₂)Cp*(Cl)(Cl/I)} ₂	4	2.962(5), 2.211(19)	2.647(18)	n/a	140.00(7)	n/a	9
{U(N'NN'')Cp*Cl} ₂	4	2.221(7), 2.169(6)	5.645(7)	(avg) 2.457(9)	78.52(3)	n/a	9
U(N'N' ₂)(N{TMS} ₂)Cl	4	2.202(8), 2.215(9)	2.852(8)	n/a	119.60(3)	n/a	9
U(N'N' ₂)(CH{TMS} ₂)Cl	4	2.245(12), 2.144(14)	2.646(13)	n/a	134.96(4)	n/a	9
U(N'N' ₂) ₂	4	2.2690, 2.2611	2.9198	n/a	114.34	3.8065	10
		2.2376, 2.2510	3.9316		100.77	3.4579	
{U(N'N' ₂)Cl ₂ } ₂	4	2.194(3), 2.215(4)	2.567(3)	n/a	142.93(14)	4.1813	10
U(N'N' ₂)Cp*	3	2.321(5), 2.342(5)	2.667(6)	2.535(3)	104.41(17)	3.68559(7)	8
{U(N'N' ₂) ₂ (μ-C ₇ H ₈)}	3	2.278(3), 2.301(3)	2.643(3)	n/a	99.91(9)	3.505(4)	8

A1.2 Computational investigations

Figure A1.2 overleaf shows the results of the computational investigation, performed by Kefalidis and Maron, into the mechanistic pathway involved in the formation of *cis*- and *trans*-**3.7** from the insertion of CO into the U-C bond of the ‘tucked-in’ complex, **2.9**.¹¹ This calculation was carried out using a full system model (*i.e.* the TIPS substituents were included on the COT ring, and the methyl groups were included on the Cp ring) and without polarization with a *p*-function on the hydrogen atoms, due to the lack of direct involvement of protons in the reaction pathway.

Only the first transition state – leading the insertion of CO into the U-C methylene bond to form a ‘tethered’ alkoxide – could be located. The transition state of the C-C coupling reaction to form the *cis* or *trans* products could not be found. Estimations of the energetics of both final products are given, and it is seen that the *trans* isomer of **3.7** is the thermodynamic product by ca. 5 kcal mol⁻¹.

Additional computational details relating to the calculation are provided in Chapter 6.

A1.3 References for Appendix 1.

1. O. T. Summerscales, F. G. N. Cloke, P. B. Hitchcock, J. C. Green, N. Hazari, *Science*, 2006, **311**, 829-831.
2. N. Tsoureas, *Unpublished results*, University of Sussex, 2012-2014.
3. This work.
4. J. A. Higgins, F. G. N. Cloke, S. M. Roe, *Organometallics*, 2013, **32**, 5244-5252; also in this work.
5. A. S. P. Frey, F. G. N. Cloke, M. P. Coles, L. Maron, T. Davin, *Angew. Chem., Int. Ed.*, 2011, **123**, 7013-7015.
6. A. S. P. Frey, *Unpublished results*, University of Sussex, 2012-2014.
7. A. S. Frey, F. G. N. Cloke, P. B. Hitchcock, I. J. Day, J. C. Green, G. Aitken, *J. Am. Chem. Soc.*, 2008, **130**, 13816-13817.
8. This work.
9. C. P. Larch, "Multidentate Amide and Cyclopentadienyl Uranium and Thorium Complexes and Related Studies", PhD Thesis, University of Sussex, 2007.
10. D. J. Wilson, A. Sebastian, F. G. N. Cloke, A. G. Avent, P. B. Hitchcock, *Inorg. Chim. Acta.*, 2003, **345**, 89-94.
11. C. Kefalidis and L. Maron, INSA Toulouse, *Private Communication*, 2014.

APPENDIX 2: CRYSTALLOGRAPHIC INFORMATION

A2.1 Notes

Presented here are tables summarising the crystal data and structure refinement information of all fully refined crystal structures reported in this thesis:

Structure	Table
U(COT ^{TIPS2})Cp*Cl (2.2)	A2.1
U(COT ^{TIPS2})Cp*(CH ₂ Ph) (2.3)	A2.1
U(COT ^{TIPS2})Cp*(Me) (2.4)	A2.1
U(COT ^{TIPS2})Cp*(CH ₂ TMS) (2.5)	A2.1
U(COT ^{TIPS2})Cp*(CH{TMS} ₂) (2.6)	A2.2
U(COT ^{TIPS2})Cp*(OEt) (2.7)	A2.2
U(COT ^{TIPS2})(η ⁵ :κ ¹ -C ₅ Me ₄ CH ₂) (2.9)	A2.2
U(COT ^{TIPS2})(η ⁵ :κ ¹ -C ₅ Me ₄ CH ₂)(THF) (2.9.THF)	A2.2
U(COT ^{TIPS2})Cp*H (3.1A)	A2.3
U(COT ^{TIPS2})Cp*H (3.1B)	A2.3
(η ⁵ :κ ¹ -C ₅ Me ₄ CH ₂ OC=COCH ₂ C ₅ Me ₄){U(COT ^{TIPS2}) ₂ } (cis-3.7)	A2.3
{U(COT ^{TIPS2})Cp*} ₂ (μ-κ ¹ :κ ¹ -OCH=CHO) (cis-3.8)	A2.3
U(COT ^{TIPS2})Cp*(κ ² -O ₂ CCH ₂ Ph) (3.12)	A2.4
U(COT ^{TIPS2})Cp*(κ ² -O ₂ CCH ₃) (3.13)	A2.4
{U(C ₈ H ₆ {Si ⁱ Pr ₃ -1,4}) ₂ (μ ¹ :μ ¹ -κ ¹ :η ⁵ -C ₅ Me ₄ CH ₂ OCO)} ₂ (3.15)	A2.4
U(COT ^{TIPS2})Cp*(κ ² -O ₂ CH) (3.16)	A2.4
U(COT ^{TIPS2})Cp*(NH ₂) (4.1)	A2.5
U(COT ^{TIPS2})Cp*(κ ² -O ₂ CNH ₂) (4.3)	A2.5
U(N'N' ₂)Cp*Cl (5.1)	A2.5
U(N'N' ₂)Cp* (5.3)	A2.5
U(N'N' ₂)Cp*(THF) (5.3.THF)	A2.6
5.1 and CO ₂ (5.5)	A2.6
{U(N'N' ₂) ₂ } ₂ (μ-η ⁶ :η ⁶ -C ₇ H ₈) (5.6)	A2.6

As a supplement to this, cif files, res files, cif checker reports (produced by the ICUR online checkCIF facility) and full crystallographic tables are provided on the CD accompanying this thesis, organised by chapter number.

Also on the CD are data files for unrefined structures mentioned in the preceding chapters, alongside additional refinement notes, for reference, organised by chapter number.

Table A2.1. Crystal data and structure refinement for **2.2-2.5** (Chapter 2). Original file names in brackets.

	2.2 (jah_chloride)	2.3 (jah1053)	2.4 (jah3021)	2.5 (jah5030)
Formula	C ₃₆ H ₆₃ ClSi ₂ U	C ₄₃ H ₇₀ Si ₂ U	C ₃₇ H ₆₆ Si ₂ U	C ₄₀ H ₇₄ Si ₃ U
FW	825.52	881.20	805.11	877.29
Crystal system	Triclinic	Triclinic	Triclinic	Orthorhombic
Space group	P -1	P -1	P -1	P b n n
a/Å	8.60440(10)	12.9743(2)	8.6909(2)	11.53540(1)
b/Å	12.8904(2)	17.3522(3)	12.9149(3)	21.3908(2)
c/Å	17.7078(4)	20.0913(4)	17.6256(4)	34.3625(3)
α/°	91.5750(10)	82.5670(10)	91.3650(10)	90
β/°	96.8350(10)	75.3250(10)	96.4370(10)	90
γ/°	106.682(2)	69.3610(10)	107.0750(10)	90
V/Å ³	1864.08(6)	4090.81(12)	1875.85(7)	8479.00(13)
Z	2	4	2	8
Crystal size/mm ³	0.10 x 0.06 x 0.04	0.08 x 0.06 x 0.04	0.30 x 0.30 x 0.20	0.12 x 0.08 x 0.06
θ range/°	3.42 – 27.12	3.41 – 27.55	1.16 – 27.48	2.24 – 27.48
Completeness to θ _{max}	98.8	98.8	98.5	99.9
Reflections collected, R(int)	23202, 0.0606	59024, 0.0632	28201, 0.0468	125151, 0.1037
Independent reflections	8121	18674	8479	9712
GooF	1.025	0.982	1.219	0.962
Final R indices [I>2σ(I)]	R1 = 0.0358 wR2 = 0.0751	R1 = 0.0339 wR2 = 0.0766	R1 = 0.0243 wR2 = 0.0639	R1 = 0.0329 wR2 = 0.0759
R indices (all data)	R1 = 0.0475 wR2 = 0.797	R1 = 0.0480 wR2 = 0.0824	R1 = 0.0310 wR2 = 0.0773	R1 = 0.0632 wR2 = 0.0882

Table A2.2. Crystal data and structure refinement for **2.6**, **2.7**, **2.9**, **2.9.THF** (Chapter 2). Original file names in brackets.

	2.6 (jah2051)	2.7 (jah2011)	2.9 (jah3009)	2.9.THF (jah3009_THF)
Formula	C ₄₃ H ₈₂ Si ₄ U	C ₃₈ H ₆₈ OSi ₂ U	C ₃₆ H ₆₂ Si ₂ U	C ₄₀ H ₇₀ OSi ₂ U
FW	949.48	835.13	789.07	861.17
Crystal system	Monoclinic	Triclinic	Monoclinic	Monoclinic
Space group	P 21/n	P -1	P 21/n	P 21/n
a/Å	13.4982(2)	9.0212(2)	16.0245(2)	12.0255(2)
b/Å	21.8746(3)	11.9288(4)	8.50720(10)	15.0113(3)
c/Å	16.1720(2)	19.0026(7)	26.9278(3)	22.2071(5)
α/°	90	102.366(2)	90	90
β/°	104.2880(10)	92.598(2)	103.0810(1)	91.1640(10)
γ/°	90	103.358(2)	90	90
V/Å ³	4627.36(11)	1933.73(11)	3575.64(7)	4007.96(14)
Z	4	2	4	4
Crystal size/mm ³	0.15 x 0.10 x 0.04	0.06 x 0.06 x 0.04	0.20 x 0.16 x 0.16	0.10 x 0.04 x 0.04
θ range/°	3.47 – 27.45	3.51 – 27.51	2.85 – 27.88	3.48 – 27.11
Completeness to θ _{max}	98.6	98.7	99.8	99.6
Reflections collected, R(int)	60415, 0.0764	29221 (0.0975)	43315, 0.0565	26878, 0.0721
Independent reflections	10424	8798	8150	8834
GooF	1.025	1.037	0.714	1.015
Final R indices [I>2σ(I)]	R1 = 0.0297 wR2 = 0.0613	R1 = 0.0539 wR2 = 0.0816	R1 = 0.0285 wR2 = 0.0850	R1 = 0.0474 wR2 = 0.0814
R indices (all data)	R1 = 0.0434 wR2 = 0.0652	R1 = 0.0909 wR2 = 0.0923	R1 = 0.0390 wR2 = 0.0959	R1 = 0.0845 wR2 = 0.0906

Table A2.3. Crystal data and structure refinement for **3.1A/B**, *cis-3.7*, and *cis-3.8* (Chapter 3). Original file names in brackets.

	3.1A (jah2040)	3.1B (jah2040b)	<i>cis-3.7</i> (jah2027) [§]	<i>cis-3.8</i> (jah6068)*
Formula	C ₃₆ H ₆₅ Si ₂ U	C ₃₆ H ₆₃ Si ₂ U	C ₇₄ H ₁₂₄ O ₂ Si ₄ U ₂ (C ₆ D ₆)	C ₇₄ H ₁₂₈ O ₂ Si ₄ U ₂
FW	790.07	790.07	1706.22	1638.19
Crystal system	Monoclinic	Monoclinic	Monoclinic	Triclinic
Space group	P 21/m	C c	P 21/c	P -1
a/Å	8.4860(2)	13.5888(4)	12.9685(2)	13.4902(3)
b/Å	22.6545(5)	36.4517(11)	20.9587(2)	15.9128(6)
c/Å	9.7819(3)	15.9896(4)	30.2323(4)	18.8977(7)
α/°	90	90	90	70.479(3)
β/°	100.6330(10)	110.568(2)	100.0710(10)	86.359(2)
γ/°	90	90	90	88.755(2)
V/Å ³	1848.24(8)	7415.3(4)	8090.61(18)	3815.8(2)
Z	2	8	8	2
Crystal size/mm ³	0.06 x 0.04 x 0.02	0.16 x 0.08 x 0.06	0.12 x 0.10 x 0.06	0.20 x 0.20 x 0.05
θ range/°	3.43 – 26.00	2.39 – 27.46	1.19 – 27.47	2.95 – 70.37
Completeness to θ _{max}	99.7	99.0	99.6	97.5
Reflections collected, R(int)	27264, 0.0945	39467, 0.0583	100089, 0.0772	27564, 0.1164
Independent reflections	3724	15160	18434	14221
GooF	1.098	1.047	1.014	1.041
Final R indices [I>2σ(I)]	R1 = 0.0447 wR2 = 0.0743	R1 = 0.0453 wR2 = 0.0857	R1 = 0.0460 wR2 = 0.1191	R1 = 0.0893 wR2 = 0.2298
R indices (all data)	R1 = 0.0613 wR2 = 0.0786	R1 = 0.0602 wR2 = 0.0918	R1 = 0.0770 wR2 = 0.1506	R1 = 0.0938 wR2 = 0.2421

[§] low convergence due to disordered C₆D₆ molecule that could not be resolved with SQUEEZE; * large shift/su_max due to disorder in one TIPS group that could not be satisfactorily modeled – does not affect enediolate geometric parameters quoted

Table A2.4. Crystal data and structure refinement for **3.12**, **3.13**, **3.15** and **3.16** (Chapter 3). Original file names in brackets.

	3.12 (jah1090)	3.13 (jah3005)	3.15 (jah2010)	3.16 (jah2010)
Formula	C ₄₄ H _{62.50} O ₂ Si ₂ U*	C ₃₈ H ₆₆ O ₂ Si ₂ U	C ₈₀ H ₁₃₀ O ₄ Si ₄ U ₂	C ₃₇ H ₆₄ O ₂ Si ₂ U
FW	917.65	849.12	1744.26	835.09
Crystal system	Triclinic	Triclinic	Monoclinic	Triclinic
Space group	P -1	P -1	P 21/a	P -1
a/Å	13.2738(4)	8.9809(2)	11.69590(10)	8.9601(2)
b/Å	15.4834(3)	11.9911(2)	27.3298(3)	11.9408(3)
c/Å	22.6645(5)	19.1345(5)	13.4179(2)	18.1699(6)
α/°	100.0500(10)	101.5340(10)	90	101.4180(10)
β/°	90.1170(10)	93.1190(10)	115.5660(10)	91.9920(10)
γ/°	108.2210(10)	104.471(2)	90	103.723(2)
V/Å ³	4348.64(18)	1943.08(7)	3869.05(8)	1945.82(9)
Z	4	2	2	2
Crystal size/mm ³	0.10 x 0.06 x 0.06	0.06 x 0.06 x 0.02	0.15 x 0.12 x 0.12	0.14 x 0.14 x 0.10
θ range/°	1.62 – 27.54	3.45 – 28.08	3.40 – 27.08	2.35 – 27.49
Completeness to θ _{max}	98.0	91.8	97.1	98.7
Reflections collected, R(int)	55829, 0.1152	29229, 0.0777	29297, 0.0792	33081, 0.0573
Independent reflections	19661	8675	8254	8814
GooF	0.995	1.010	1.030	0.876
Final R indices [I>2σ(I)]	R1 = 0.0545 wR2 = 0.1054	R1 = 0.0432 wR2 = 0.0826	R1 = 0.0407 wR2 = 0.0792	R1 = 0.0332 wR2 = 0.0756
R indices (all data)	R1 = 0.1035 wR2 = 0.1252	R1 = 0.0603 wR2 = 0.0876	R1 = 0.0619 wR2 = 0.0850	R1 = 0.0424 wR2 = 0.0808

* partial hydrogen value due to modeling of disorder in Cp* ring

Table A2.5. Crystal data and structure refinement for **4.1** and **4.3** (Chapter 4) and **5.1** and **5.3** (Chapter 5). Original file names in brackets.

	4.1. BuOMe (jah4028)	4.3 (jah3040)	5.1 (jah5030)	5.3 (jah4027)
Formula	C ₃₆ H ₆₅ NSi ₂ U(C ₅ H ₁₂ O)	C ₃₇ H ₆₅ NO ₂ Si ₂ U	C ₂₃ H ₅₀ ClN ₃ Si ₃ U	C ₂₃ H ₅₀ N ₃ Si ₃ U
FW	894.25	850.11	726.41	690.96
Crystal system	Monoclinic	Triclinic	Triclinic	Triclinic
Space group	P 21/m	P -1	P -1	P -1
a/Å	9.22460(10)	8.8461(2)	11.2079(2)	11.0789(2)
b/Å	20.7046(3)	11.9688(3)	15.0687(2)	11.4137(2)
c/Å	11.5888(2)	19.1218(13)	18.5455(4)	12.4601(3)
α/°	90	101.496(7)	89.976(1)	83.966(1)
β/°	101.0660(10)	93.003(7)	89.994(1)	87.542(1)
γ/°	90	104.307(7)	89.986(1)	77.123(1)
V/Å ³	2127.21(5)	1911.37(15)	3132.12(10)	1527.15(5)
Z	2	2	4	2
Crystal size/mm ³	0.12 x 0.12 x 0.08	0.10 x 0.09 x 0.03	0.18 x 0.06 x 0.06	0.40 x 0.30 x 0.20
θ range/°	2.45 – 27.09	3.06 – 27.48	3.438 – 27.221	3.41 – 27.10
Completeness to θ _{max}	99.6	99.3	98.5	98.2
Reflections collected, R(int)	31233, 0.0674	41797, 0.0434	45052, 0.0659	20021, 0.0495
Independent reflections	4900	8721	13791	6617
GooF	1.025	1.050	1.023	1.027
Final R indices [I>2σ(I)]	R1 = 0.0285 wR2 = 0.0593	R1 = 0.0266 wR2 = 0.0687	R1 = 0.0348 wR2 = 0.0664	R1 = 0.0514 wR2 = 0.1306
R indices (all data)	R1 = 0.0367 wR2 = 0.0617	R1 = 0.0287 wR2 = 0.0699	R1 = 0.0599 wR2 = 0.0733	R1 = 0.0561 wR2 = 0.1344

Table A2.6. Crystal data and structure refinement for **5.3.THF**, **5.5**, **5.6** (Chapter 5). Original file names in brackets.

	5.3.THF (jah4027_THF)	5.5 (jah4055)	5.6 (jah4037)
Formula	C ₂₇ H ₅₀ N ₃ OSi ₃ U	C ₃₂ H ₅₈ ClN ₃ O ₄ Si ₃ U	C ₃₃ H ₇₈ N ₆ Si ₆ U ₂
FW	763.06	906.65	1203.61
Crystal system	Monoclinic	Triclinic	Triclinic
Space group	P 21/a	P -1	P -1
a/Å	18.7655(4)	11.4075(3)	10.4888(3)
b/Å	9.0156(1)	12.2726(3)	10.5825(2)
c/Å	19.9341(5)	16.4659(4)	13.3131(4)
α/°	90	69.949(1)	74.9160(10)
β/°	90.941(1)	70.785(1)	72.7220(10)
γ/°	90	83.216(2)	60.9680(10)
V/Å ³	3372.04(12)	2044.82(9)	1221.76(6)
Z	4	2	1
Crystal size/mm ³	0.12 x 0.04 x 0.04	0.14 x 0.12 x 0.08	0.18 x 0.16 x 0.12
θ range/°	1.022 – 27.443	2.32 – 27.51	2.56 – 27.50
Completeness to θ _{max}	99.9	98.7	98.8
Reflections collected, R(int)	58596, 0.0496	35082, 0.0588	21004, 0.0563
Independent reflections	7696	9287	5550
GooF	1.162	1.060	0.985
Final R indices [I>2σ(I)]	R1 = 0.0507 wR2 = 0.0690	R1 = 0.0392 wR2 = 0.0946	R1 = 0.0243 wR2 = 0.0601
R indices (all data)	R1 = 0.1146 wR2 = 0.1216	R1 = 0.0517 wR2 = 0.1006	R1 = 0.0287 wR2 = 0.0621

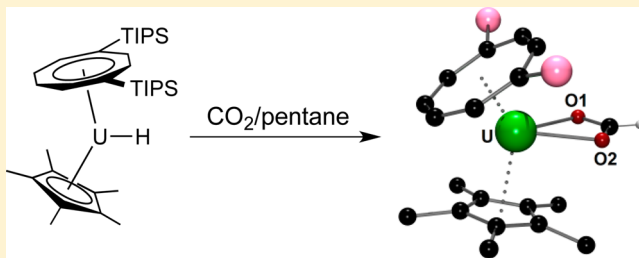
Synthesis and CO₂ Insertion Chemistry of Uranium(IV) Mixed-Sandwich Alkyl and Hydride Complexes

Jessica A. Higgins, F. Geoffrey N. Cloke,* and S. Mark Roe

Department of Chemistry, School of Life Sciences, University of Sussex, Brighton BN1 9QJ, United Kingdom

S Supporting Information

ABSTRACT: A series of U(IV) mixed-sandwich alkyls of the form $[\text{U}(\text{COT}^{\text{TIPS}2})\text{Cp}^*\text{R}]$ ($\text{R} = \text{Me}, \text{CH}_2\text{Ph}, \text{CH}_2\text{TMS}, \text{CH}(\text{TMS})_2$; $\text{COT}^{\text{TIPS}2} = \text{C}_8\text{H}_6(\text{Si}^i\text{Pr}_3\text{-}1,4)_2$; $\text{Cp}^* = \text{C}_5\text{Me}_5$; $\text{TMS} = \text{SiMe}_3$) have been synthesized and structurally characterized, and their reactivity toward H_2 and CO_2 has been investigated. The alkyls $\text{R} = \text{Me}, \text{CH}_2\text{Ph}, \text{CH}_2\text{TMS}$ react at room temperature with a stoichiometric amount of CO_2 to form κ^2 -carboxylate complexes. Reaction of all four alkyls with H_2 yields a monomeric, terminal hydride complex, $[\text{U}(\text{COT}^{\text{TIPS}2})\text{Cp}^*\text{H}]$, which is unstable with respect to hydrogen loss and reacts with CO_2 to give the κ^2 -formate complex $[\text{U}(\text{COT}^{\text{TIPS}2})\text{Cp}^*(\kappa^2\text{-O}_2\text{CH})]$. Additionally, a common decomposition product of the alkyls and hydride complex—activation of a Cp^* methyl group to give a “tucked-in” alkyl—has been isolated and structurally characterized and its insertion chemistry toward CO_2 has been examined.



INTRODUCTION

Studies on the synthesis of uranium alkyl complexes were first reported in the early 1970s^{1–4} and subsequently followed by the pioneering work of Andersen and Marks on organometallic uranium hydrides.^{5,6} Since then, a range of uranium alkyl complexes have been reported featuring a variety of supporting ligand systems, both carbocyclic and noncarbocyclic in nature. Alkyl complexes utilizing the ubiquitous cyclopentadienyl (Cp) ligand and its substituted derivatives,^{7–11} hard-donor ligands,^{12–17} and bis(hydrotris(3,5-dimethylpyrazolyl)borate) ligands^{18,19} have all been described, and the ability of U–C bonds to insert, in particular, CO_2 has been exemplified by the formation of a number of κ^2 -carboxylate complexes.^{16,20–24} Uranium hydride complexes are still rare, and those reported feature substituted Cp ligands,^{25–28} with the exception of Andersen’s bis(trimethylsilyl)amide hydride complex $[\text{UH}(\text{N}\{\text{TMS}\}_2)_3]$.²⁹ Correspondingly, there are very few examples of CO_2 insertion into uranium– or indeed actinide–hydride bonds.^{21,30}

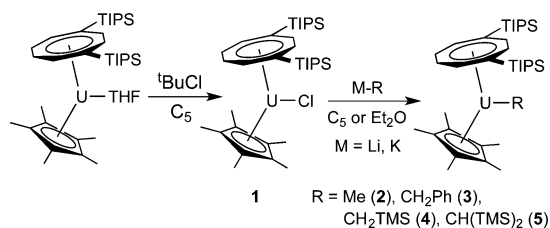
Our recent work in organometallic uranium chemistry has largely focused on the reductive activation of small molecules by U(III) complexes, in particular mixed-sandwich complexes incorporating sterically demanding cyclooctatetraenyl and cyclopentadienyl ligands: e.g., $[\text{U}(\text{COT}^{\text{TIPS}2})\text{Cp}^*]$.^{31,32} We envisaged that this ligand framework might also be suitable to support a U(IV)–alkyl bond and hence a monomeric, reactive hydride via a σ -bond metathesis reaction with hydrogen. Examples of alkyls of the form $[\text{U}(\text{COT})\text{Cp}^*\text{R}]$ (where $\text{R} = \text{CH}(\text{TMS})_2, \text{Ph}, \text{Me}, \text{Et}, \text{CH}_2\text{CMe}_3$) have been reported by Evans et al.,^{11,33} but no such mixed-sandwich hydrides, carboxylates, or formates have been previously reported.

In this paper we describe the synthesis and characterization of four alkyl complexes of the type $[\text{U}(\text{COT}^{\text{TIPS}2})\text{Cp}^*\text{R}]$ (where $\text{R} = \text{Me}, \text{CH}_2\text{Ph}, \text{CH}_2\text{TMS}, \text{CH}(\text{TMS})_2$) and the insertion of CO_2 into the U–C σ bond of three of the aforementioned alkyls to form the κ^2 -carboxylates $[\text{U}(\text{COT}^{\text{TIPS}2})\text{Cp}^*(\kappa^2\text{-O}_2\text{C-R})]$ ($\text{R} = \text{Me}, \text{CH}_2\text{Ph}, \text{CH}_2\text{TMS}$). Hydrogenolysis of the alkyls results in the formation of a monomeric, terminal hydride complex, $[\text{U}(\text{COT}^{\text{TIPS}2})\text{Cp}^*\text{H}]$, which will insert CO_2 into the U–H bond to give the first structurally characterized, organouranium(IV) bidentate formate complex, $[\text{U}(\text{COT}^{\text{TIPS}2})\text{Cp}^*(\kappa^2\text{-O}_2\text{CH})]$.

RESULTS AND DISCUSSION

Synthesis of Alkyl Complexes. The mixed-sandwich chloride complex $[\text{U}(\text{COT}^{\text{TIPS}2})\text{Cp}^*\text{Cl}]$ (**1**) was first prepared in high yield by treatment of $[\text{U}(\text{COT}^{\text{TIPS}2})\text{Cp}^*(\text{THF})]$ with *tert*-butyl chloride in pentane (Scheme 1). This synthetic route has previously been employed by Finke to prepare $[\text{Cp}^*_2\text{UCl}_2]$ from $[\text{Cp}^*_2\text{UCl}(\text{THF})]$ by treatment with alkyl chlorides,

Scheme 1. Synthetic Route to U(IV) Alkyls



Received: July 22, 2013

although the latter reaction proceeds much less cleanly than the formation of **1**, which is the only product observed.³⁴

NMR-scale reactions of **1** with an excess of alkylating agent in *d*₆-benzene resulted in conversion of **1** to the alkyls [U(COT^{TIPS2})Cp**R*] (R = Me (**2**), CH₂Ph (**3**), CH₂TMS(**4**), CH(TMS)₂ (**5**)) in >90% conversion after ca. 1 h, as determined by ¹H NMR spectroscopy (Scheme 1). However, the alkyls did not persist indefinitely in solution and decomposed at room temperature over a few days (vide infra). Scaling up and optimization of the reactions gave alkyls **2–5** in isolated yields ranging from 39 to 75%. All four complexes were structurally characterized by X-ray crystallography, and the structures are shown in Figures 1–4, with

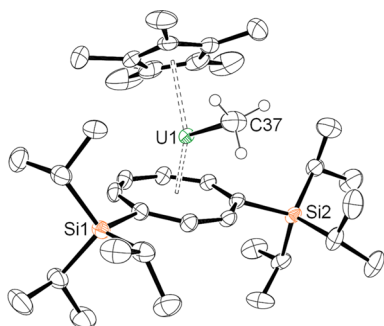


Figure 1. Molecular structure of **2** with thermal ellipsoids at the 50% probability level. Non-alkyl ligand hydrogen atoms are omitted for clarity.

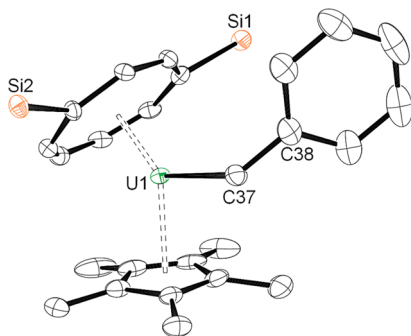


Figure 2. Molecular structure of one crystallographically independent molecule of **3** in the asymmetric unit, with thermal ellipsoids at the 50% probability level. Hydrogen atoms and ^tPr groups are omitted for clarity.

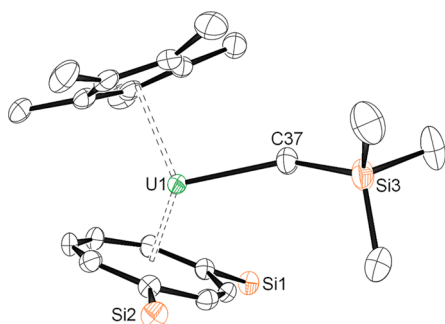


Figure 3. Molecular structure of **4** with thermal ellipsoids at the 50% probability level. Hydrogen atoms and ^tPr groups are omitted for clarity.

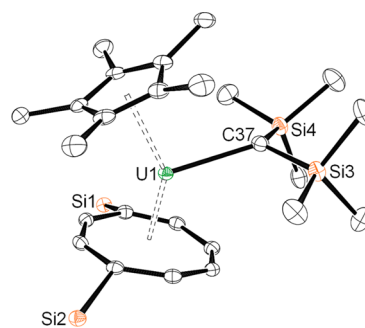


Figure 4. Molecular structure of **5** with thermal ellipsoids at the 50% probability level. Hydrogen atoms and ^tPr groups are omitted for clarity.

selected distances and angles in Table 1. The U–C_{alkyl} distances range between 2.462(4) and 2.543(4) Å; that in the

Table 1. Selected Distances (Å) and Angles (deg) for Compounds **2–5**^a

	2	3 ^b	4	5
U1–Ct1	1.9368(3)	1.9297(3) {1.9304(3)}	1.9361(3)	1.9774(2)
U1–Ct2	2.4761(3)	2.4899(3) {2.4836(3)}	2.4880(3)	2.5211(2)
U1–C37	2.462(4)	2.532(4) {2.543(4)}	2.464(4)	2.497(3)
Ct1–U1–Ct2	140.664(13)	137.217(13) {137.977(13)}	137.171(14)	141.926(12)

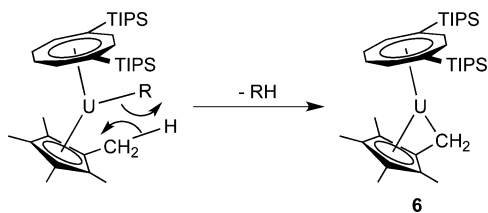
^aCt1 is defined as the COT ring centroid, and Ct2 is defined as the Cp* ring centroid. ^bNumbers in brackets represent values from the second independent molecule in the asymmetric unit.

CH(TMS)₂ derivative **5** (2.497(3) Å) is slightly longer than the previously reported U–C bond length of 2.469(3) Å in the only other related, crystallographically characterized alkyl complex, [U(COT)Cp*CH(TMS)₂],¹¹ presumably due to bulky substituents on the COT ring in **5**. The ring centroid distances in **5** (1.9774(2) and 2.5211(2) Å) are similarly slightly longer than those in [U(COT)Cp*CH(TMS)₂] (1.969 and 2.499 Å), and the ring centroid–U–ring centroid angle is slightly wider (141.926(12) vs 138.2°).

In view of the modest (ca. 40%) isolated yields of the alkyls **4** and **5** in particular, their formation on a preparative scale was monitored by NMR: indeed, ¹H NMR spectroscopic analysis of the crude reaction mixtures showed approximately 50% of the desired alkyl product and another, new paramagnetic complex. Upon close examination of the spectra it was evident that the second product did not contain a freely rotating Cp* ring (a singlet resonance of integration 15H) but instead two resonances at 25.4 and –39.8 ppm, integrating to 6H each, suggesting that a Cp* methyl group had been activated to form a “tuck-in” complex, [U(COT^{TIPS2})(η⁵:η¹-C₅Me₄CH₂)] (**6**; Scheme 2).

This behavior has also been observed in the mixed-sandwich system [U(COT)Cp**R*] (where R = Me, Et, CH₂CMe₃, Ph), where the “tuck-in” complex [U(COT)(η⁵:η¹-C₅Me₄CH₂)] is formed with concomitant release of free alkane.³³ Other metallocene and nonmetallocene ligand system alkyl complexes have also shown a propensity to form “tuck-in” species.^{15,35–38} Indeed we subsequently found that *all* the alkyl complexes **2–5** decompose either in solution or in the solid state to form the

Scheme 2. Formation of “Tuck-in” Complex 6



“tuck-in” complex **6** over a period of a few days with the release of free alkane (CH_4 , CH_3Ph , SiMe_4 , or $\text{CH}_2(\text{TMS})_2$ respectively), **4** and **5** being particularly prone to this reaction. Alternatively, heating any of the alkyl complexes to 70°C for 24 h also resulted in the formation of **6**, together with small amounts of ligand degradation products, which proved impossible to completely separate from **6** despite repeated recrystallizations. However, recrystallization of **6** from saturated pentane or THF solutions did afford a few X-ray-quality crystals of base-free complex or the THF adduct, **6**·THF, respectively. The structures of **6** and **6**·THF are shown in Figure 5, with selected distances and angles in Table 2.

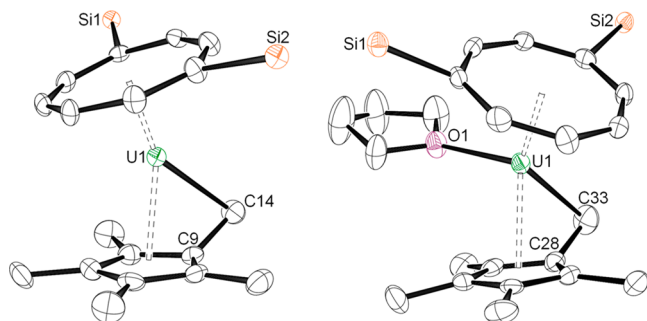


Figure 5. Molecular structures of **6** (left) and **6**·THF (right) with thermal ellipsoids at the 50% probability level. Hydrogen atoms and ⁱPr groups are omitted for clarity.

Table 2. Selected Bond Distances (Å) and Angles (deg) for Structures **6** and **6**·THF^a

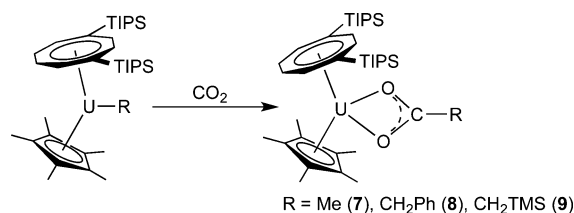
	6	6 ·THF
U1–Ct1	1.9066(3)	1.9991(4)
U1–Ct2	2.3364(3)	2.4124(4)
U1–ring C(Cp*) range	2.437(4)–2.791(4)	2.508(6)–2.840(6)
U1–C14/C33	2.569(4)	2.646(6)
U1–O1	n/a	2.585(4)
Ct1–U1–Ct2	150.724(15)	143.794(17)
U1–C14–C9/U1–C33–C28	63.3(2)	68.6(3)

^aCt1 is defined as the COT ring centroid, and Ct2 is defined as the Cp* ring centroid.

Four other uranium–cyclopentadienyl “tuck-in” species have been crystallographically characterized: a 1,3,4,6,7,8-hexahydro-2H-pyrimido[1,2-*a*]pyrimidinato (hpp) complex, $\text{U}(\text{Cp}^*)(\eta^5:\eta^1\text{-C}_3\text{Me}_4\text{CH}_2)(\text{hpp})$,³⁹ with a $\text{U}\text{-C}_{\text{tuck-in}}$ bond length of 2.566(4) Å, a “tuck-in tuck-over” hydride complex³⁶ with a $\text{C}_{\text{tuck-in}}$ bond length of 2.568(8) Å, a “tuck-in” with an activated SiMe_3 methyl group attached to a parent Cp ring, $\text{U}(\text{Cp}^*)(\eta^5:\eta^1\text{-C}_3\text{Me}_4\text{SiMe}_2\text{CH}_2)\text{Cl}$,⁴⁰ with a $\text{C}_{\text{tuck-in}}$ bond length of 2.416(3) Å, and the double “tuck-in” with the related TMS-substituted Cp ring system, $\text{U}(\eta^5:\eta^1\text{-C}_5\text{Me}_4\text{SiMe}_2\text{CH}_2)_2$,⁴¹ with

both $\text{C}_{\text{tuck-in}}$ bond lengths of 2.453(3) Å. The U1–C14 distance of 2.569(4) Å in **6** is similar to the Cp*–methyl group “tuck-in” U–C distances, but longer than the SiMe_3 -substituted “tuck-in” U–C distances, due to the more strained geometry of the molecule. As shown in Table 2, coordination of THF to the metal center alters the overall geometry of the molecule: both uranium–centroid distances increase, as do each of the U1–ring C(Cp*) bond lengths. The U1–C14/C33 bond lengthens significantly, and the Ct1–U1–Ct2 angle decreases as the coordination sphere widens to allow THF binding. In **6**, the “tuck-in” methylene group lies symmetrically between the ⁱPr groups attached to the COT ring, whereas in **6**·THF the THF molecule lies in this position instead, with the “tuck-in” group to one side.

Carbon Dioxide Insertion into U–C Alkyl Bonds. The alkyl U–C σ bond in **2–4** will readily insert CO_2 to form carboxylate products with the $\text{-O}_2\text{CR}$ ligand bound in a κ^2 fashion to the metal center (Scheme 3), a reaction conveniently

Scheme 3. Insertion of CO_2 into U–C_{alkyl} Bonds To Form κ^2 -Carboxylate Complexes

monitored by ^{13}C NMR using $^{13}\text{CO}_2$. No reaction was observed between **5** and CO_2 , presumably due to the large steric bulk of the $\text{-CH}(\text{TMS})_2$ ligand blocking access to the uranium center. Upon exposure of either 1 equiv or an excess (3–10 fold) of CO_2 to a hydrocarbon solution of alkyls **2–4**, an immediate color change from orange to deep red occurred, indicating formation of the carboxylates $[\text{U}(\text{COT}^{\text{TIPS}2})\text{Cp}^*(\kappa^2\text{-O}_2\text{CR})]$ ($\text{R} = \text{Me}$ (**7**), CH_2Ph (**8**), CH_2TMS (**9**)).

Carboxylates **7** and **8** have been crystallographically characterized, and the structures are shown in Figures 6 and 7, respectively. Attempts to collect X-ray diffraction data from numerous samples of **9** have only yielded poor-quality data, which would not refine sufficiently. However, connectivity could still be established, and **9** does contain an $\kappa^2\text{-O}_2\text{CCH}_2\text{TMS}$ ligand as anticipated (see the Supporting Information for a partially refined structure of **9**). Both **7** and

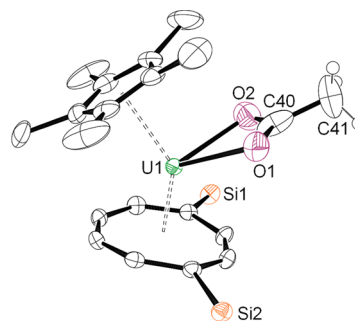


Figure 6. Molecular structure of **7** with thermal ellipsoids at the 50% probability level. Non-alkyl ligand hydrogen atoms and ⁱPr groups are omitted for clarity. Selected bond lengths (Å) and angles (deg): U1–O1 = 2.409(5), U1–O2 = 2.408(5); O1–C40–O2 = 120.4(8).

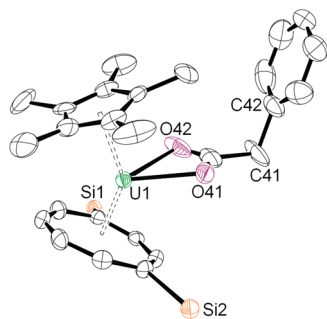


Figure 7. Molecular structure of one of the two crystallographically independent molecules of **8** in the asymmetric unit, with thermal ellipsoids at the 50% probability level. Hydrogen atoms and 'Pr groups are omitted for clarity. Selected bond lengths (Å) and angles (deg): U1–O41 = 2.405(5), U1–O42 = 2.423(5); O41–C41–O42 = 118.7(8).

8 are structurally similar, featuring terminal bidentate carboxylate ligands with near-identical U–O_{carboxylate} and O–C–O bond lengths and angles. In **7**, the acetate moiety is symmetrical with identical U–O_{acetate} bond lengths within standard error, whereas the U–O_{carboxylate} bonds in **8** vary marginally from 2.405(5) to 2.424(5) Å, which may be an effect of the location of the attached benzyl group positioned between the 'Pr groups to avoid steric crowding.

As the “tuck-in” complex **6** is essentially a tethered alkyl, it also reacts with CO₂ to form an insertion product. After exposure to 1 equiv (or an excess) of CO₂ to a *d*₈-toluene solution of **6**, the brown solution became orange in color and deposited a large amount of red precipitate. Recrystallization of the red solid from either THF or hot benzene yielded red crystals of the dimeric CO₂ insertion product [$\{U(COT^{TIPS2})-(\eta^5-\eta^1-C_3Me_4H_2-\mu^1-\mu^1-O_2C)\}_2$] (**10**; Figure 8).

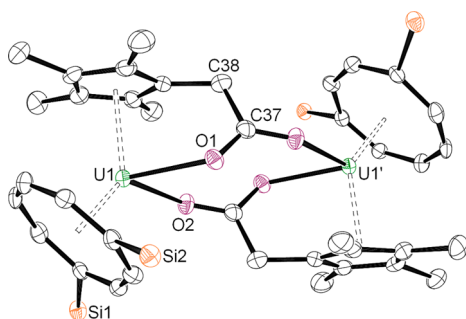


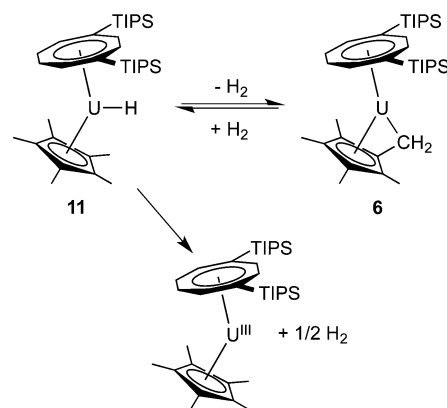
Figure 8. Molecular structure of **10** with thermal ellipsoids at the 50% probability level. Hydrogen atoms, 'Pr groups, and a cocrystallized molecule of benzene are omitted for clarity. Selected bond lengths (Å) and angles (deg): U1–O1 = 2.405(3), U1–O2 = 2.404(3); O1–C37–O2 = 122.8(5).

Three other U(IV) bidentate terminal acetate complexes have been structurally characterized, and only one is mononuclear. Domingos et al. reported the X-ray crystal structure of U(Tp*)(OAc)₃, a tris-acetato complex formed by the reaction of the parent trichloride complex with NaO₂CMe.⁴² The six U–O_{acetate} bond lengths range between 2.406(12) and 2.439(11) Å, generally greater than in **7**, with more acute O–C–O angles (118.2(8)–120.0(6) °), presumably due to greater steric crowding around the metal center from the three acetate ligands. The other acetate complexes are both tetranuclear and contain Cp ligands, featuring both

bridging and terminal acetate ligands; however, in both cases the terminal acetates also interact weakly with another U atom. Brianese et al.⁴³ report the U–O_{acetate} distances in their acetate cluster as 2.24(1) and 2.69(1) Å, the differing lengths being an effect of the weak interaction with a second uranium center, with an O–C–O angle of 119(1)°, similar to the angle in **7**. In the tetrakis-Cp uranium acetate dioxide complex described by Rebizant et al.⁴⁴ the terminal acetate ligands contain more symmetrical U–O_{acetate} bond lengths of between 2.50(1) and 2.57(1) Å but smaller O–C–O angles of 116(2) and 117(2)° in comparison to **7** and the other reported acetate complexes, again likely due to effects of the weak interaction with a second uranium center. No other U(IV) terminal phenyl carboxylate complexes have been structurally characterized; however, a U(III) phenyl carboxylate, (Tp*)₂U(κ²-O₂CCH₂Ph), has been synthesized by Bart et al. via the insertion of CO₂ into the U–C bond of the parent alkyl complex, (Tp*)₂U(CH₂Ph).²⁴ The structure of this phenyl carboxylate is, like that of **8**, terminal and bidentate, with near-identical U–O_{carboxylate} bond lengths of 2.490(7) and 2.494(7) Å and an O–C–O angle of 119.9(9)°. **8** has an almost identical O–C–O angle; however, the U–O_{carboxylate} distances are notably shorter, owing to the differing ionic radii of U(III) and U(IV). While **10** differs from the reported carboxylates, as it has a bridging –O₂C moiety which is “tethered” to the Cp* ring, the U1–O1 and U1–O2 bond lengths in **10** are comparable to the U–O_{carboxylate} lengths in **7** and **8**. The O1–C37–O2 angle of 122.8(5)° in **10** is short in comparison with the O–C–O angles in the bridging acetate ligands contained in the tetranuclear acetate compounds described above, which range from 122(2) to 125(1)° in the acetate cluster and from 124(2) to 128(2)° in the tetrakis-Cp uranium acetate, due to the close proximity of the two U centers in **10** enforced by the “tethered” ligands.

Hydride Complex: Synthesis and Reactivity. It was hoped that the alkyls **2–6** would undergo σ-bond metathesis with hydrogen to form a hydride complex with the elimination of free alkane, or, in the case of **6** + H₂, re-forming the Cp* ring (Scheme 4). Indeed, exposure of a hydrocarbon solution of any

Scheme 4. Decomposition Routes of **11**



of the alkyls **2–6** to 1 equiv or an excess (3–10 equiv) of H₂ resulted in a red solution which, by ¹H NMR spectroscopy, contained a single new product featuring the COT^{TIPS2} and Cp* ligands with no other identifiable features other than the presence of free alkane eliminated after hydrogenolysis. This product is reasoned to be the hydride complex [U(COT^{TIPS2})-Cp*H] (**11**). Over a period of 24 h the “tuck-in” complex **6** is

also observed in solution; this increases in proportion relative to **11** over a further week, and resonances corresponding to the trivalent mixed-sandwich complex $[\text{U}^{\text{III}}(\text{COT}^{\text{TIPS}_2})\text{Cp}^*]$ also appear and slowly increase in intensity. Removal of the reaction mixture headspace so that no excess H_2 is present results in an increase in proportion of **6** and $[\text{U}^{\text{III}}(\text{COT}^{\text{TIPS}_2})\text{Cp}^*]$ relative to the hydride **11**; removal of all volatiles results in the complete decomposition of **11** into a mixture of **6** and $[\text{U}^{\text{III}}(\text{COT}^{\text{TIPS}_2})\text{Cp}^*]$. It is proposed that the hydride **11** and the “tuck-in” **6** exist in equilibrium and that **11** will also lose H_2 to form the trivalent species $[\text{U}^{\text{III}}(\text{COT}^{\text{TIPS}_2})\text{Cp}^*]$ when not under a hydrogen headspace (Scheme 4), in a fashion similar to that reported for $[\text{UCp}^*_2\text{H}_2]$, which also readily loses H_2 to form a U(III) complex.²⁵

As a result of this limited stability it has not been possible to analyze **11** by mass spectrometry, elemental analysis, or infrared spectroscopy using standard techniques. In situ IR spectroscopy using a React IR system, featuring an IR probe inside a gastight IR cell that can be attached to a Toepler pump, was employed to follow the reaction of the benzyl alkyl **3** and H_2 . However, no new vibrational band corresponding to a hydride ligand (expected to occur at ca. 1400 cm^{-1})⁴⁵ was observed during the course of the reaction due to strong ligand resonances masking the area of interest. In a further attempt to confirm the existence of the hydride ligand in **11**, the reactions of the alkyls **2–6** with D_2 were carried out in order to locate the resultant deuteride ligand resonance using ^2H NMR spectroscopy. However, these reactions all resulted in a complex mixture of partially deuterated species. As **11** and the “tuck-in” complex **6** are in equilibrium, H/D exchange into the Cp^* ring Me groups can occur and was indeed observed. ^2H NMR spectroscopic studies on the reaction of the benzyl alkyl **3** and an excess of D_2 (ca. 3 equiv) followed over the course of 2 weeks showed increasingly intense and numerous resonances at shifts corresponding not only to deuterium in the Cp^* -Me groups of **11**, **6**, and the U(III) complex $[\text{U}^{\text{III}}(\text{COT}^{\text{TIPS}_2})\text{Cp}^*]$ (see Scheme 4) but also to the $^i\text{Pr-CH}_3$ groups of all three species present. Although no evidence has yet been seen for the existence of a stable “tuck-in” complex formed by activation of a COT-TIPS group, it is possible that deuterium incorporation into the $^i\text{Pr-CH}_3$ groups occurs via a transient “ ^iPr tuck-in”, whose reversible formation is too rapid to be observed on the NMR time scale. In any event, no resonance assignable to a deuteride ligand was observed within a window of ± 600 ppm throughout these deuterium studies. It is likely that the signal is extremely broadened due to contact shift effects caused by the paramagnetic uranium center.

Despite the tendency of **11** to lose H_2 , it was possible to collect X-ray diffraction data for two samples of **11** formed under different reaction conditions: one via the reaction of a concentrated pentane solution of **3** and 1 bar of H_2 and the other from the reaction of solid **3** and 1 bar of H_2 . In both cases, a small number of red crystals were formed; these were extracted from the reaction vessels and rapidly mounted under a cryostream for X-ray diffraction studies. Refinement of the data collected resulted in two structures, both monoclinic, with one in the $P2_1/m$ space group (**11A**, Figure 9) and the other in space group Cc (**11B**, Figure 10) with two crystallographically distinct molecules in the asymmetric unit (see Table 3 for selected bond lengths and angles).

In **11B**, one molecule contains a persistent Q peak $1.04(2)\text{ \AA}$ from uranium center U2 that could be assigned as a hydrogen atom. Inspection of the bond lengths and angles of the two

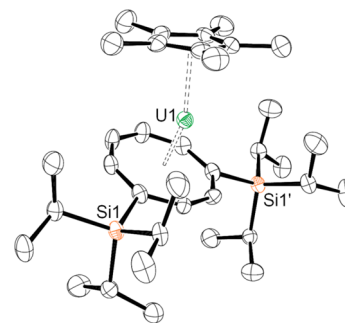


Figure 9. Molecular structure of **11A** with thermal ellipsoids at the 50% probability level. Hydrogen atoms are omitted for clarity.

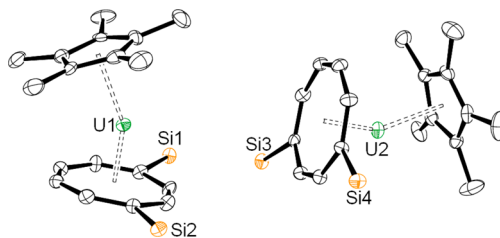


Figure 10. Molecular structure of **11B**, showing two crystallographically independent molecules in the asymmetric unit (thermal ellipsoids at the 50% probability level). Hydrogen atoms and ^iPr groups are omitted for clarity. $\text{U1–U2} = 11.167\text{ \AA}$.

Table 3. Selected Bond Distances (Å) and Angles (deg) for Structures **11A** and **11B**^a

	11A	11B (U1)	11B (U2)
U–Ct1	1.9182(6)	1.917(4)	1.917(2)
U–Ct2	2.4945(6)	2.471(4)	2.464(3)
Ct1–U–Ct2	150.20(3)	152.14(10)	152.4(2)

^aCt1 is defined as the COT ring centroid, and Ct2 is defined as the Cp^* ring centroid.

structures reveals that **11A** and **11B** differ marginally; while the Ct1–U1 and Ct2–U1 distances are marginally longer, the Ct1–U1–Ct2 angle is 2° smaller. In comparison to the other crystallographically characterized U(IV) $\text{COT}^{\text{TIPS}_2}/\text{Cp}^*$ complexes within this work, the U–Ct1 distances of **11A** and **11B**, although among the shortest, lie within the expected range ($1.0966(3)$ – $1.9991(4)\text{ \AA}$), as do the Ct2–U distances (range $2.33464(3)$ – $2.5211(2)\text{ \AA}$), consistent with **11** also being a U(IV) complex. The Ct1–U1–Ct2 angle is greater in **11A** and **11B** than in the other U(IV) complexes reported herein, presumably due to the small steric bulk of the hydride ligand in comparison to the alkyl and carboxylate ligands, which force a more acute Ct1–U–Ct2 angle.

By analogy to the formation of the κ^2 -carboxylates by CO_2 insertion into an alkyl U–C bond, CO_2 was added to the hydride complex **11** (formed in situ) and resulted in formation of the κ^2 -formate complex $[\text{U}(\text{COT}^{\text{TIPS}_2})\text{Cp}^*(\kappa^2\text{-O}_2\text{CH})]$ (**12**), thus also providing additional evidence for the hydride ligand in **11**. The hydrogen atom attached to the formate group can be observed in the ^1H NMR spectrum at δ 8.6 ppm, and an IR stretch at 1558 cm^{-1} assigned to the formate group rapidly appears after the addition of $^{12}\text{CO}_2$ to a methylcyclohexane solution of the hydride **11** in the React IR apparatus. The proton-coupled ^{13}C NMR spectrum of **12** synthesized with $^{13}\text{CO}_2$ shows a doublet with $J_{\text{CH}} = 210\text{ Hz}$ at -20.1 ppm , with

the peak at δ 8.6 ppm, due to the formate hydrogen, in the ^1H NMR spectrum split into a doublet with the same coupling constant.

Recrystallization of **12** from pentane at -35 °C afforded a red crystalline solid suitable for X-ray diffraction studies; the molecular structure (Figure 11) confirms a monomeric, κ^2 -

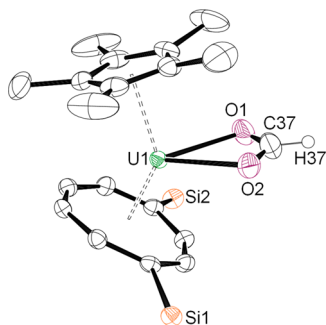


Figure 11. Molecular structure of **12** with thermal ellipsoids at the 50% probability level. ^iPr groups and COT and Cp ligand based hydrogen atoms are omitted for clarity. Selected bond lengths (Å) and angles (deg): U1–O1 = 2.451(3), U1–O2 = 2.455(3); O1–C37–O2 = 122.2(5).

formate complex. Only two other examples of crystallographically characterized U(IV) formate complexes are present in the literature, as reported by Takao et al. in 2009.⁴⁶ Both complexes are hexanuclear, containing bridging—not terminal—formate ligands, and are formed from the addition of formic acid to an aqueous U(IV) solution. The U–O_{formate} bond distances in the two complexes range from 2.396 to 2.495 Å, and the bridging formate O–C–O angles range from 123.16 to 135.85°; as expected, the O1–C37–O2 angle in **12** is more acute than in the bridging formate moieties, while the U1–O_{formate} bond distances lie in the middle of the reported range. In comparison to the carboxylate complexes reported in this work, the formate complex has longer U–O distances and a larger O1–C37–O2 angle than **7** or **8**; however, the overall geometries of the three complexes **7**, **8**, and **12** are very similar.

CONCLUSION

A series of new mixed-sandwich uranium(IV) alkyl complexes have been synthesized, and their reactivity toward CO₂ and H₂ has been investigated. Particularly noteworthy is the synthesis of a monomeric hydride complex and the insertion of CO₂ therein to form the first crystallographically characterized uranium(IV) bidentate formate complex.

EXPERIMENTAL SECTION

General Information. All manipulations involving air- or moisture-sensitive materials were performed under an inert atmosphere of argon using standard Schlenk techniques or in an MBraun N₂- or Ar-filled glovebox. Solvents were dried over appropriate drying agents (NaK₃, pentane and Et₂O; K, THF; Na, toluene) before distilling under N₂ and degassing before use. Solvents were stored over K mirrors, with the exception of THF, which was stored over activated 4 Å molecular sieves. Deuterated solvents were dried over K, vacuum-distilled and freeze–pump–thawed before storage under N₂. NMR spectra were recorded on a Varian VNMR 400 MHz spectrometer at 303 K, with ^1H NMR spectra run at 399.5 MHz and ^{13}C NMR spectra run at 100.5 MHz. Chemical shifts are quoted in parts per million and are referenced internally to residual protic solvent shifts (^1H) or deuterated solvent shifts (^{13}C). EI-MS was performed by Dr. A. K. Abdul-Sada at the University of Sussex using a VG Autospec Fisions

instrument (EI at 70 eV). IR spectra were recorded as Nujol mulls on a Perkin-Elmer Spectrum One FTIR instrument or using a ReactIR system attached to a Toepler pump. Elemental analyses were performed by Mikroanalytisches Labor Pascher or the University of Bristol Microanalysis Service. The compounds [U^{III}(COT^{TIPS2})Cp*-(THF)],³¹ KCH₂Ph,⁴⁷ LiCH₂TMS,⁴⁸ and KCH(TMS)₂⁴⁹ were prepared according to published procedures.

[U(COT^{TIPS2})Cp*Cl] (1). An excess of $^i\text{BuCl}$ (210 μL , 1.90 mmol) was added via microsyringe to a stirred pentane solution (100 mL) of [U^{III}(COT^{TIPS2})Cp*-(THF)] (1.56 g, 1.80 mmol), resulting in an immediate color change from dark brown to red. Volatiles were removed under reduced pressure, yielding **1** as a red-brown powder (1.34 g, 90%). Recrystallization from a saturated pentane or THF solution afforded red crystals of **1**. ^1H NMR (C₆D₆): δ 80.28 (br s, 2H, COT-H), 10.15 (s, 15H, C₅Me₅), –7.44 (m, 6H, $^i\text{Pr-CH}$), –7.73 (d, $J_{\text{HH}} = 5.4$ Hz, 18H, $^i\text{Pr-CH}_3$), –8.69 (d, $J_{\text{HH}} = 5.4$ Hz, 18H, COT $^i\text{Pr-CH}_3$), –84.70 (br s, 2H, COT-H), –103.65 (br s, 2H, COT-H). Anal. Calcd for C₃₆H₆₃Si₂UCl: C, 52.41; H, 7.64. Found: C, 52.44; H, 7.78.

[U(COT^{TIPS2})Cp*Me] (2). MeLi (1.82 mmol, 0.334 M solution in Et₂O) was added dropwise to a solution of **1** (1000 mg, 1.21 mmol) in 40 mL of Et₂O pre-cooled to -78 °C. After it was stirred for 1 h, the resultant orange solution was dried under reduced pressure, extracted in pentane, and filtered via filter cannula to remove residual white solids. Removal of volatiles under reduced pressure yielded **2** as an orange-red powder (729 mg, 75%). ^1H NMR (C₆D₆): δ 52.79 (br s, 3H, Me), 14.85 (br s, 2H, COT-H), 0.93 (s, 15H, C₅Me₅), –4.44 (br s, 2H, COT-H), –7.46 (d, $J_{\text{HH}} = 7.4$ Hz, 18H, $^i\text{Pr-CH}_3$), –11.27 (d, $J_{\text{HH}} = 5.4$ Hz, 18H, $^i\text{Pr-CH}_3$), –12.40 (m, 6H, $^i\text{Pr-CH}$), –69.11 (br s, 2H, COT-H). Anal. Calcd. for C₃₇H₆₆Si₂U: C, 55.19; H, 8.26. Found: C, 54.45; H, 8.24. MS (EI)⁺: m/z 789 (M⁺ – CH₃). X-ray-quality crystals of **2** were obtained by recrystallization from a saturated Et₂O solution at -30 °C.

[U(COT^{TIPS2})Cp*(CH₂Ph)] (3). KCH₂Ph (190 mg, 1.46 mmol) was added as a THF solution (30 mL) dropwise to a red solution of **1** (997 mg, 1.21 mmol in 40 mL THF) pre-cooled to -30 °C. Stirring at -30 °C for 1 h resulted in a brown solution; volatiles were removed under reduced pressure, and extraction in pentane and storage of the brown solution at -20 °C yielded **3** as dark red X-ray-quality crystals (500 mg, 47%). ^1H NMR (C₆D₆): δ 17.64 (br, s, 2H, COT-H), 10.45 (t, $J_{\text{HH}} = 7.3$ Hz, 2H, $m\text{-C}_6\text{H}_5$), 7.76 (d, $J_{\text{HH}} = 7.7$ Hz, 2H, $o\text{-C}_6\text{H}_5$), 6.96 (br, s, 2H, CH₂-Ph), 3.75 (s, 15H, C₅Me₅), 1.62 (t, $J_{\text{HH}} = 7.3$ Hz, 1H, $p\text{-C}_6\text{H}_5$), –8.09 (d, $J_{\text{HH}} = 7.2$ Hz, 18H, $^i\text{Pr-CH}_3$), –10.00 (d, $J_{\text{HH}} = 7.3$ Hz, 18H, $^i\text{Pr-CH}_3$), –11.44 (br, s, 2H, COT-H), –11.87 (m, 6H, $^i\text{Pr-CH}$), –76.80 (br, s, 2H, COT-H). Anal. Calcd for C₄₃H₇₀Si₂U: C, 58.60; H, 8.00. Found: C, 58.62; H, 7.94. MS (EI)⁺: m/z 789 (M⁺ – CH₂Ph).

[U(COT^{TIPS2})Cp*(CH₂TMS)] (4). LiCH₂TMS (14 mg, 0.14 mmol) in Et₂O (10 mL) was added as a white slurry to a solution of **1** (99 mg, 0.12 mmol) pre-cooled to -40 °C. After it was stirred for 1 h, the resultant red-orange solution was filtered via filter cannula to remove white solids and the solvent volume concentrated to ca. 4 mL. Storage of the solution at -50 °C overnight afforded red rodlike crystals of **4** of suitable quality for X-ray studies (41 mg, 39%). ^1H NMR (C₆D₆): δ 8.49 (s, 9H, SiMe₃), 1.80 (s, 15H, C₅Me₅), –8.83 (d, $J_{\text{HH}} = 6.9$ Hz, 18H, $^i\text{Pr-CH}_3$), –9.12 (d, $J_{\text{HH}} = 6.9$ Hz, 18H, $^i\text{Pr-CH}_3$), –11.51 (m, 6H, $^i\text{Pr-CH}$); additional resonances at δ 66.83 (br s, 2H), 11.10 (br s, 2H), –4.81 (br s, 2H), and –66.00 (br s, 2H) were attributed to COT-H and CH₂TMS protons but could not be definitively assigned. MS (EI)⁺: m/z 833 (M⁺ – Me₃). Anal. Calcd for C₄₃H₇₀Si₂U: C, 54.76; H, 8.50. Found: C, 54.24; H, 7.91.

[U(COT^{TIPS2})Cp*(CH(TMS)₂)] (5). KCH(TMS)₂ (47 mg, 0.24 mmol) in pentane (30 mL) was added as a white slurry to a red solution of **1** (200 mg, 0.24 mmol) as a pentane/THF (30 mL/5 mL) solution pre-cooled to -78 °C. After it was stirred for 12 h, the brown solution was filtered via filter cannula and volatiles were removed under reduced pressure, giving **5** as a brown powder: crude yield 40%. ^1H NMR (C₆D₆): δ 74.22 (br s, 1H, CH(TMS)₂), 8.17 (br s, 2H, COT-H), –6.67 (s, 15H, C₅Me₅), –2.18 (d, $J_{\text{HH}} = 7.4$ Hz, 18H, $^i\text{Pr-CH}_3$), –3.45 (d, $J_{\text{HH}} = 7.6$ Hz, 18H, $^i\text{Pr-CH}_3$), –5.10 (br s, 2H, COT-

H), -5.74 (m, 6H, $^1\text{Pr-CH}$), -12.10 (s, 18H, $\text{CH}\{\text{SiMe}_3\}_2$), -52.48 (br s, 2H, COT-H). MS (EI)⁺: m/z 789 ($\text{M}^+ - \text{CH}\{\text{SiMe}_3\}_2$). X-ray-quality crystals were grown from a saturated pentane solution at -35 °C. Thermal instability precluded meaningful microanalysis.

[U(COT^{TIPS2})($\eta^5\text{-}\eta^1\text{-C}_5\text{Me}_4\text{CH}_2$)] (6). A toluene solution (50 mL) of **2** (400 mg, 0.50 mmol) in a greaseless-joint ampule was heated at 70 °C in an oil bath for 24 h, during which time the solution changed color from red to brown. Filtration away from the small amount of white solids via filter cannula and removal of all volatiles under reduced pressure yielded **6** as a brown powder (274 mg, crude yield 70%). ^1H NMR (C_6D_6): δ 57.83 (br s, 2H, $\text{C}_5\text{Me}_4\text{CH}_2$), 25.43 (s, 6H, C_5Me), -1.26 (m, 6H, $^1\text{Pr-CH}_3$), -1.90 (d, $J_{\text{HH}} = 7.4$ Hz, 18H, $^1\text{Pr-CH}_3$), -3.88 (d, $J_{\text{HH}} = 7.2$ Hz, 18H, $^1\text{Pr-CH}_3$), -39.77 (s, 6H, C_5Me), -70.09 (br s, 2H, COT-H), -76.41 (br s, 2H, COT-H), -85.86 (br s, 2H, COT-H). MS (EI)⁺: m/z 788 (M^+). Small amounts of ligand degradation products, which proved impossible to completely separate from **6** despite repeated recrystallizations, precluded satisfactory microanalysis despite repeated attempts.

[U(COT^{TIPS2})Cp*($\kappa^2\text{-O}_2\text{CCH}_3$)] (7). A toluene solution (5 mL) of **2** (40 mg, 0.050 mmol) was cooled to -78 °C and exposed to 1.5 equiv of CO_2 (0.075 mmol) via Toepler pump; upon warming the solution changed color to a more vivid red. Concentration of the solution to 1 mL and slow cooling to -35 °C afforded red X-ray-quality crystals of **7** (28 mg, 66%). Alternatively, using ^{13}C in the method above yields the labeled product $^{13}\text{C-7}$. ^1H NMR (C_6D_6) δ 5.80 (s, 15H, C_5Me_5), 4.24 (d, 3H, Me), -2.26 (br s, 2H, COT-H), -4.61 (d, $J = 7.4$ Hz, 18H, $^1\text{Pr-CH}_3$), -5.76 (d, $J = 5.4$ Hz, 18H, $^1\text{Pr-CH}_3$), -6.66 (m, 6H, $^1\text{Pr-CH}$), -21.71 (br s, 2H, COT-H), -52.44 (br s, 2H, COT-H). $^{13}\text{C}\{^1\text{H}\}$ NMR (C_6D_6 , selected data): δ 32.4 (s, $\text{O}_2^{13}\text{C-Me}$). IR (Nujol, cm^{-1}): 1501 w, 1225 m, 1068 w, 1028 s, 1016 s, 993 w, 933 m, 882 s, 767 s, 680 m, 669 s, 637 s, 528 m. Anal. Calcd for $\text{C}_{38}\text{H}_{66}\text{Si}_2\text{O}_2\text{U}$: C, 53.75; H, 7.83. Found: C, 53.27; H, 7.77. MS (EI)⁺: m/z 849 (M^+).

[U(COT^{TIPS2})Cp*($\kappa^2\text{-O}_2\text{CCH}_2\text{Ph}$)] (8). A pentane solution (5 mL) of **3** (49 mg, 0.056 mmol) was exposed to 1 bar of CO_2 at ambient temperature, resulting in an immediate color change from brown to red. Stirring overnight yielded a more vivid red solution containing some pink solids. Filtration of the solution via filter cannula and concentration to ca. 2 mL and slow cooling to -35 °C afforded **8** as X-ray-quality red crystals (24 mg, 46% yield). Alternatively, exposing a d_6 -benzene solution of **3** to 1 equiv of ^{13}C via Toepler pump afforded the labeled product $^{13}\text{C-8}$. ^1H NMR (C_6D_6): δ 7.01 (t, 1H, $p\text{-C}_6\text{H}_5$), 6.73 (d, 2H, $o\text{-C}_6\text{H}_5$), 6.04 (s, 15H, C_5Me_5), 4.90 (br s, 2H, $\text{CH}_2\text{-Ph}$), 0.81 (br s, 2H, COT-H), -4.82 (d, 18H, $^1\text{Pr-CH}_3$), -5.61 (br s, 18H, $^1\text{Pr-CH}_3$), -6.93 (m, 6H, $^1\text{Pr-CH}$), -24.25 (br s, 2H, COT-H), -54.01 (br s, 2H, COT-H); resonance attributable to $m\text{-C}_6\text{H}_5$ overlapped with solvent residue at 7.1 ppm. $^{13}\text{C}\{^1\text{H}\}$ NMR (C_6D_6 , selected data): δ 21.6 (s, $\text{O}_2^{13}\text{C-CH}_2\text{Ph}$). IR (Nujol, cm^{-1}): 1506 w, 1418 w, 1261 w, 1020 m, 882 m, 789 w, 757 m, 669 m, 640 m, 581 m. Anal. Calcd for $\text{C}_{44}\text{H}_{70}\text{Si}_2\text{O}_2\text{U}$: C, 57.11; H, 7.63. Found: C, 56.23; H, 7.77. The low percentage of C is often found with organouranium complexes and is attributed to incomplete combustion.⁵⁰ MS (EI)⁺: m/z 924 (M^+), 789 ($\text{M}^+ - \text{O}_2\text{CCH}_2\text{Ph}$).

[U(COT^{TIPS2})Cp*($\kappa^2\text{-O}_2\text{CCH}_2\text{TMS}$)] (9). A pentane (5 mL) solution of **4** (36 mg, 0.042 mmol) was frozen and exposed to 1.5 equiv of CO_2 via Toepler pump. When it was warmed to ambient temperature, the solution turned dark red and spontaneously deposited **9** as a red powder. Slow evaporation of the pentane solution yielded further powdery material (65 mg, 55%). Repeating the reaction with ^{13}C afforded the labeled product $^{13}\text{C-9}$. ^1H NMR (C_6D_6): δ 10.54 (br s, 2H, CH_2TMS), 5.25 (s, 15H, C_5Me_5), 0.31 (s, 9H, SiMe_3), -5.01 (d, $J = 7.2$ Hz, 18H, $^1\text{Pr-CH}_3$), -6.09 (d, $J = 7.2$ Hz, 18H, $^1\text{Pr-CH}_3$), -7.23 (br s, 2H, COT-H), -7.58 (m, 6H, $^1\text{Pr-CH}$), -13.01 (br s, 2H, COT-H), -50.83 (br s, 2H, COT-H). $^{13}\text{C}\{^1\text{H}\}$ NMR (C_6D_6 , selected data): δ 57.4 (s, $\text{O}_2^{13}\text{C-CH}_2\text{TMS}$). IR (Nujol, cm^{-1}): 1504 w, 1234 m, 1021 m, 920 m, 667 m, 640 m, 540 m. MS (EI)⁺: m/z 920 (M^+), 785 ($\text{M}^+ - \text{Cp}^*$). Small amounts of ligand degradation products, which proved impossible to completely separate from **9** despite repeated recrystallizations (and coupled with the limited stability of **9** in solution), precluded satisfactory microanalysis despite repeated attempts.

[[U(COT^{TIPS2})($\eta^5\text{-}\eta^1\text{-C}_5\text{Me}_4\text{CH}_2\text{-}\mu^1\text{-}\mu^1\text{-O}_2^{13}\text{C}$)] (10). A d_8 -toluene solution of **6** (20 mg, 0.023 mmol) in a J. Young NMR tube was cooled to -78 °C and then exposed to ca. 3 equiv (0.07 mmol) of $^{13}\text{CO}_2$ via Toepler pump, resulting in an orange solution and red precipitate upon warming to ambient temperature. Removal of volatiles under reduced pressure afforded red solids; recrystallization from a saturated THF solution yielded X-ray-quality crystals of **10**. Performing the reaction in d_6 -benzene and heating the solution to 70 °C for 1 h yielded X-ray-quality crystals of **10** upon cooling to ambient temperature. ^1H NMR ($d_8\text{-THF}$): δ 49.44 (br s, 2H, $\text{C}_5\text{Me}_4\text{CH}_2$), 49.18 (br s, 2H, $\text{C}_5\text{Me}_4\text{CH}_2$), -21.61 (br s, 2H, COT-H), -15.44 (br s, 2H, COT-H), -4.80 (s, 6H, C_5Me), -0.47 (m, 6H, $^1\text{Pr-CH}$), -0.12 (s, 6H, C_5Me), -0.21 (s, 18H, $^1\text{Pr-CH}_3$), -1.95 (s, 18H, $^1\text{Pr-CH}_3$), -3.49 (s, 18H, $^1\text{Pr-CH}_3$), -4.18 (s, 18H, $^1\text{Pr-CH}_3$), -6.70 (m, 6H, $^1\text{Pr-CH}$), -10.76 (br s, 6H, C_5Me), -11.37 (br s, 6H, C_5Me), -55.49 (br s, 2H, COT-H), -59.51 (br s, 2H, COT-H), -76.02 (br s, 2H, COT-H), -80.25 (br s, 2H, COT-H). $^{13}\text{C}\{^1\text{H}\}$ NMR ($d_8\text{-toluene}$): 60.37 (bound $^{13}\text{CO}_2$). IR (Nujol, cm^{-1}): 3232 w, 2277 s, 1611 m, 1542 s, 1457 m, 1372 m, 1262 w, 1079 w, 1014 m, 880 m, 807 w, 673 m, 640 m, 575 w, 490 m, 458 s. MS (EI)⁺: m/z 834 ($\text{M}^+ - \text{U}\{\text{COT}^{\text{TIPS}2}\}\text{-C}_5\text{Me}_4\text{CH}_2\text{O}_2^{13}\text{C}$). Anal. Calcd for $\text{C}_{74}\text{H}_{124}\text{Si}_4\text{O}_4\text{U}_2$: C, 53.34; H, 7.50. Found: C, 52.69; H, 7.26.

[U(COT^{TIPS2})Cp*H] (11). *Method A.* A pentane solution (0.5 mL) of **3** in a greaseless-joint ampule was frozen and exposed to an excess of H_2 (ca. 0.76 mmol) via Toepler pump. After the mixture was warmed to room temperature, a color change from brown to red occurred. While still under a headspace of H_2 , cooling the solution to -30 °C yielded a small quantity of red-brown crystals of **11A** suitable for X-ray diffraction studies.

Method B. A crystalline sample of **3** (114 mg, 0.129 mmol) in a greaseless-joint ampule was stirred vigorously to produce a finely ground brown powder which was cooled to -78 °C before being exposed to 1 bar of H_2 . After the mixture was stirred for 45 min at -78 °C, a small amount of dark red crystals of **11B** were observed, suitable for X-ray studies.

Method C. A d_6 -benzene solution of any alkyl **2-6** in a J. Young NMR tube exposed to ca. 3 equiv of H_2 resulted in a red solution, identified as >90% conversion to **11** as determined by ^1H NMR spectroscopy. ^1H NMR (C_6D_6): δ 36.97 (br s, 2H, COT-H), -2.42 (s, 15H, C_5Me_5), -7.66 (d, $J_{\text{HH}} = 4.9$ Hz, 18H, $^1\text{Pr-CH}_3$), -9.73 (br s, 24H, $^1\text{Pr-CH}_3$ and $^1\text{Pr-CH}$ overlapped), -36.08 (br s, 2H, COT-H), -83.64 (br s, 2H, COT-H); resonance attributable to U-H could not be located. Further analysis and recording of isolated yields were not possible due to instability of the complex.

[U(COT^{TIPS2})Cp*($\kappa^2\text{-O}_2\text{CH}$)] (12). A pentane (3 mL) solution of **3** (175 mg, 0.217 mmol) in a high-pressure ampule was frozen before being exposed to 1 bar of H_2 , forming **11** in situ upon warming to ambient temperature with stirring over 1 h. The red solution was cooled to -78 °C, and the ampule headspace evacuated and then pressurized with 0.8 bar of CO_2 . When the solution was warmed, the color deepened and red crystalline **12** formed spontaneously within the ampule; the solids were isolated, and the mother liquor was cooled to -30 °C to yield X-ray-quality crystals (combined yield 60 mg, 33%). Performing the reaction as a d_6 -benzene solution in a J. Young NMR tube with ^{13}C afforded the labeled product $^{13}\text{C-12}$. ^1H NMR (C_6D_6): δ_{H} 13.82 (br s, 2H, COT-H), 8.58 (d, $J_{\text{HH}} = 210$ Hz, 1H, $\text{O}_2^{13}\text{C-H}$), 7.53 (s, 15H, C_5Me_5), -4.61 (d, $J_{\text{HH}} = 7.3$ Hz, 18H, $^1\text{Pr-CH}_3$), -4.91 (d, $J_{\text{HH}} = 7.3$ Hz, 18H, $^1\text{Pr-CH}_3$), -5.67 (m, 6H, $^1\text{Pr-CH}$), -40.80 (br s, 2H, COT-H), -59.24 (br s, 2H, COT-H). $^1\text{H}\{^{13}\text{C}\}$ NMR (C_6D_6 , selected data): δ 8.55 (br s, 1H, $\text{O}_2^{13}\text{C-H}$). $^{13}\text{C}\{^1\text{H}\}$ NMR (C_6D_6 , selected data): δ_{C} -19.97 (br s, O_2^{13}CH). ^{13}C NMR (C_6D_6 , selected data): δ_{C} -20.05 (d, $J_{\text{CH}} = 210.4$ Hz, O_2^{13}CH). Data for $^{13}\text{C-12}$ are as follows. MS (EI)⁺: m/z 835 (M^+), 700 ($\text{M}^+ - \text{Cp}^*$). IR (cm^{-1} , React IR in methylcyclohexane, selected data): 1558 s. Anal. Calcd for $\text{C}_{37}\text{H}_{64}\text{Si}_2\text{O}_2\text{U}$: C, 53.27; H, 7.72. Found: C, 54.16; H, 7.77.

X-ray Crystallographic Studies. All data sets were collected on a Bruker-Nonius Kappa CCD area detector diffractometer with a sealed-tube source (Mo $\text{K}\alpha$) and an Oxford Cryosystems low-temperature device, operating in ω scanning mode with ψ and ω scans to fill the Ewald sphere. The programs used for control and integration were

Collect,⁵¹ Scalepack, and Denzo.⁵² Absorption corrections were based on equivalent reflections using SADABS.⁵³ The crystals were mounted on a glass fiber with silicon grease, from dried vacuum oil kept over 4 Å sieves in a MBraun glovebox under Ar. All solutions and refinements were performed using the WinGX package⁵⁴ and all software packages within. All non-hydrogen atoms were refined using anisotropic thermal parameters, and hydrogens were added using a riding model. Crystal structure and refinement data are given in Tables S1–S3 of the Supporting Information.

■ ASSOCIATED CONTENT

● Supporting Information

Tables S1–S3 and CIF files giving crystal structure and refinement data for **2–6**, **6-THF**, **7**, **8**, **10**, **11A,B**, and **12** and a figure giving the not fully refined molecular structure of **9**. This material is available free of charge via the Internet at <http://pubs.acs.org>.

■ AUTHOR INFORMATION

Corresponding Author

*E-mail for F.G.N.C.: f.g.cloke@sussex.ac.uk.

Notes

The authors declare no competing financial interests.

Biography



Geoff Cloke went to Balliol College, Oxford, U.K., as an undergraduate, and it was his Part II year there with Malcolm Green that stimulated his longstanding interests in metal vapor synthesis and sandwich complexes. He stayed on in Malcolm Green's group as a D.Phil. student and was then awarded a Ramsay Memorial Research Fellowship at Balliol College in 1979. In 1981 he spent a year as a Postdoctoral Fellow with Dick Schrock at MIT and then in 1983 moved to Sussex, initially as an EPSRC Advanced Fellow, where he was awarded a New Blood Lectureship in 1984. He was promoted to Reader in 1991 and a Chair in 1995 and is currently Head of Chemistry at Sussex. During his early years at Sussex, his research focused on applying the metal vapor technique to the synthesis of early-transition-metal and f-element compounds in novel oxidation states and culminated in the isolation of the first lanthanide complexes in oxidation state 0. Subsequently he expanded his research interests to include the design of new polyfunctional amide ligands for early-transition-metal-mediated olefin polymerization and dinitrogen cleavage, the development of silylated pentalene ligands for organometallic chemistry, and synthetic and mechanistic studies on catalytic C–X bond formation by palladium N-heterocyclic carbene complexes. His current research focuses on the reductive coupling of CO and activation of CO₂ and other small molecules by uranium(III) and uranium(IV) mixed-sandwich complexes. In addition to the 2012 Sir Geoffrey Wilkinson Prize, he is a past recipient of the Royal Society of

Chemistry's Sir Edward Frankland Fellowship (1988), Corday-Morgan Medal (1990), and Tilden Lectureship (1998). He was elected a Fellow of the Royal Society in 2007.

■ ACKNOWLEDGMENTS

We thank the European Research Council (F.G.N.C.) and The University of Sussex (J.A.H.) for financial support. Thanks go to Dr. A. S. P. Frey (University of Sussex) for assistance with crystallography and to Dr. Alaa Abdul-Sada (University of Sussex) for mass spectrometry.

■ REFERENCES

- (1) Gebala, A. E.; Tsutsui, M. *J. Am. Chem. Soc.* **1972**, *95*, 91.
- (2) Brandi, G.; Brunelli, M.; Lugli, G.; Mazzei, A. *Inorg. Chim. Acta* **1973**, *7*, 319.
- (3) Marks, T. J.; Seyam, A. M. *J. Am. Chem. Soc.* **1972**, *91*, 6545.
- (4) Marks, T. J.; Seyam, A. M.; Kolb, J. R. *J. Am. Chem. Soc.* **1973**, *95*, 5529.
- (5) Simpson, S. J.; Turner, H. W.; Andersen, R. A. *J. Am. Chem. Soc.* **1979**, *101*, 7728.
- (6) Turner, H. W.; Andersen, R. A.; Zalkin, A.; Templeton, D. H. *Inorg. Chem.* **1979**, *18*, 1221.
- (7) Fagan, P. J.; Manriquez, J. M.; Marks, T. J.; Day, C. S.; Vollmer, S. H.; Day, V. W. *Organometallics* **1982**, *1*, 170.
- (8) Di Bella, S.; Lanza, G.; Fragala, I. L.; Marks, T. J. *Organometallics* **1996**, *15*, 205.
- (9) Kiplinger, J. L.; Morris, D. E.; Scott, B. L.; Burns, C. J. *Organometallics* **2002**, *21*, 5978.
- (10) Evans, W. J.; Kozimor, S. A.; Hillman, W. R.; Ziller, J. W. *Organometallics* **2005**, *24*, 4676.
- (11) Evans, W. J.; Takase, M. K.; Ziller, J. W.; Rheingold, A. L. *Organometallics* **2009**, *28*, 5802.
- (12) Duttera, M. R.; Fagan, P. J.; Marks, T. J.; Day, V. W. *J. Am. Chem. Soc.* **1982**, *103*, 865.
- (13) Jantunen, K. C.; Haftbaradaran, F.; Katz, M. J.; Batchelor, R. J.; Schatte, G.; Leznof, D. B. *Dalton Trans.* **2005**, *2005*, 3083.
- (14) Monreal, M. J.; Diaconescu, P. L. *Organometallics* **2008**, *27*, 1702.
- (15) Hayes, C. E.; Leznof, D. B. *Organometallics* **2010**, *29*, 767.
- (16) Mora, E.; Maria, L.; Biswas, B.; Camp, C.; C, S. I.; Pécaut, J.; Cruz, A.; Carretas, J. M.; Marçalo, J.; Mazzanti, M. *Organometallics* **2013**, *32*, 1409.
- (17) Andreychuk, N. R.; Ilango, S.; Vidjayacoumar, B.; Emslie, D. J. H.; Jenkins, H. A. *Organometallics* **2013**, *32*, 1466.
- (18) Domingos, Â.; Marques, N.; Pires de Matos, A.; Santos, I. C.; Silva, M. *Organometallics* **1994**, *13*, 654.
- (19) Matson, E. M.; Fanwick, P. E.; Bart, S. C. *Organometallics* **2011**, *30*, 5753.
- (20) Sonnenberger, D. C.; Mintz, E. A.; Marks, T. J. *J. Am. Chem. Soc.* **1984**, *106*, 3484.
- (21) Moloy, K. G.; Marks, T. J. *Inorg. Chim. Acta* **1985**, *110*, 127.
- (22) Evans, W. J.; Siladke, N. A.; Ziller, J. W. *C. R. Chim.* **2010**, *13*, 775.
- (23) Evans, W. J.; Walensky, J. R.; Ziller, J. W. *Organometallics* **2010**, *29*, 945.
- (24) Matson, E. M.; Forrest, W. P.; Fanwick, P. E.; Bart, S. C. *J. Am. Chem. Soc.* **2011**, *133*, 4948.
- (25) Fagan, P. J.; Manriquez, J. M.; Maatta, E. A.; Seyam, A. M.; Marks, T. J. *J. Am. Chem. Soc.* **1981**, *103*, 6650.
- (26) Berthet, J. C.; Le Maréchal, J. F.; Ephritikhine, M. *J. Chem. Soc., Chem. Commun.* **1991**, 360.
- (27) Berthet, J. C.; Le Maréchal, J. F.; Lance, M.; Nierlich, M.; Vigner, J.; Ephritikhine, M. *J. Chem. Soc., Dalton Trans.* **1992**, 1573.
- (28) Evans, W. J.; Miller, K. A.; Kozimor, S. A.; Ziller, J. W.; Dipasquale, A. G.; Rheingold, A. L. *Organometallics* **2007**, *26*, 3568.
- (29) Simpson, S. J.; Turner, H. W.; Andersen, R. A. *Inorg. Chem.* **1981**, *20*, 2991.

- (30) Berthet, J. C.; Ephritikhine, M. *New J. Chem.* **1992**, *16*, 767.
- (31) Summerscales, O. T.; Cloke, F. G. N.; Hitchcock, P. B.; Green, J. C.; Hazari, N. *Science* **2006**, *311*, 829.
- (32) Frey, A. S. P.; Cloke, F. G. N.; Coles, M. P.; Maron, L.; Davin, T. *Angew. Chem.* **2011**, *123*, 7013.
- (33) Takase, M. K.; Siladke, N. A.; Ziller, J. W.; Evans, W. J. *Organometallics* **2011**, *30*, 458.
- (34) Finke, R. G.; Hirose, Y.; Gaughan, G. J. *Chem. Soc., Chem. Commun.* **1981**, 232.
- (35) Simpson, S. J.; Andersen, R. A. *J. Am. Chem. Soc.* **1981**, *103*, 4063.
- (36) Evans, W. J.; Miller, K. A.; Dipasquale, A. G.; Rheingold, A. L.; Stewart, T. J.; Bau, R. *Angew. Chem., Int. Ed.* **2008**, *47*, 5075.
- (37) Evans, W. J.; Siladke, N. A.; Ziller, J. W. *Chem. Eur. J.* **2009**, *16*, 769.
- (38) Gardner, B. M.; McMaster, J.; Lewis, W.; Blake, A. J.; Liddle, S. T. *J. Am. Chem. Soc.* **2009**, *131*, 10388.
- (39) Montalvo, E.; Ziller, J. W.; Dipasquale, A. G.; Rheingold, A. L.; Evans, W. J. *Organometallics* **2010**, *29*, 2104.
- (40) Montalvo, E.; Miller, K. A.; Ziller, J. W.; Evans, W. J. *Organometallics* **2010**, *29*, 4159.
- (41) Evans, W. J.; Siladke, N. A.; Ziller, J. W. *Chem. Eur. J.* **2010**, *16*, 796.
- (42) Domingos, Â.; Marçalo, J.; Marques, N.; De Matos, A. P. *Polyhedron* **1992**, *11*, 501.
- (43) Brianese, N.; Casellato, U.; Ossola, F.; Porchia, M.; Rosseto, G.; Zanella, P. J. *Organomet. Chem.* **1989**, *365*, 223.
- (44) Rebizant, J.; Spirlet, M. R.; Apostolidis, C. *Acta Crystallogr., Sect. C: Cryst. Struct. Commun* **1992**, *48*, 452.
- (45) Ephritikhine, M. *Chem. Rev.* **1997**, 2193.
- (46) Takao, S.; Takao, K.; Kraus, W.; Emmerling, F.; Scheinost, A. C.; Bernhard, G.; Hennig, C. *Eur. J. Inorg. Chem.* **2009**, 4771.
- (47) Schlosser, M.; Hartman, J. *Angew. Chem., Int. Ed.* **1973**, *12*, 508.
- (48) Wiberg, N.; Wagner, G. *Chem. Ber.* **1986**, *119*, 1455.
- (49) Avent, A. G.; Cloke, F. G. N.; Elvidge, B. R.; Hitchcock, P. B. *Dalton Trans.* **2004**, *7*, 1083.
- (50) Siladke, N. A.; Ziller, J. W.; Evans, W. J. *Z. Anorg. Allg. Chem.* **2010**, *636*, 2347.
- (51) *Collect*; Bruker-AXS, Madison, WI, 1997–2004.
- (52) Otwinowski, Z.; Minor, W. *SCALEPACK and DENZO. Methods Enzymol.* **1997**, *276*, 307.
- (53) Sheldrick, G. M. *SADABS V2008/1*; University of Göttingen, Göttingen, Germany.
- (54) Farrugia, L. J. *J. Appl. Crystallogr.* **1999**, *32*, 83.



Cite this: DOI: 10.1039/c4dt02362e

Mixed sandwich thorium complexes incorporating bis(tri-isopropylsilyl)cyclooctatetraenyl and pentamethylcyclopentadienyl ligands: synthesis, structure and reactivity†

Zoë E. Button, Jessica A. Higgins, Markéta Suvova, F. Geoffrey N. Cloke* and S. Mark Roe

The Th(IV) mixed-sandwich halide complexes Th(COT^{TIPS2})Cp*X (where COT^{TIPS2} = 1,4-{SiⁱPr₃}₂C₈H₆, X = Cl, I) have been synthesised, and structurally characterised. When Th(COT^{TIPS2})Cp*I is reduced *in situ* in the presence of CO₂, a mixture of dimeric carboxylate and oxalate complexes {Th(COT^{TIPS2})Cp*}₂(μ-κ¹:κ²-CO₃) and {Th(COT^{TIPS2})Cp*}₂(μ-κ²:κ²-C₂O₄) are formed, possibly via a transient Th(III) species. Th(COT^{TIPS2})Cp*Cl is readily alkylated to yield the benzyl complex Th(COT^{TIPS2})Cp*CH₂Ph, which reacts with CO₂ to form a carboxylate and with H₂ to form a hydride; the latter inserts CO₂, giving the bridging formate complex {Th(COT^{TIPS2})Cp*}(μ-κ¹:κ¹-O₂CH)₂.

Received 4th August 2014,
Accepted 20th October 2014

DOI: 10.1039/c4dt02362e

www.rsc.org/dalton

Introduction

The activation of small molecules by uranium(III) complexes is currently an area of considerable interest, and we and others have reported a number of novel reductive transformations of, for example, CO, CO₂ and N₂ by molecular U(III) compounds.¹ Extension of this reduction chemistry to thorium is potentially of considerable interest, especially in view of the Th(IV)/Th(III) redox couple which is expected to be considerably more negative than that of uranium. However, unlike uranium, access to the trivalent oxidation state of thorium is not straightforward. Indeed, only a handful of unambiguously characterised Th(III) complexes have been reported in the literature: Th(Cp'')₃ (where Cp'' = C₅H₃{SiMe₃}₂, C₅H₃{SiMe₂tBu}₂), [Th(COT'')]₂[K(DME)]₂ (where COT'' = 1,4-{SiⁱBuMe₂}₂C₈H₆), and ThCp*₂(ⁱPrNC(Me)NⁱPr).^{2–5} It was envisaged that the mixed-sandwich ligand system consisting of dianionic COT^{TIPS2} (where COT^{TIPS2} = 1,4-{SiⁱPr₃}₂C₈H₆) and monoanionic Cp* ligands may provide sufficient steric and electronic stabilisation to isolate a Th(III) compound, which would be expected to display high reactivity towards CO or CO₂ in a manner similar to the analogous trivalent uranium system U(COT^{TIPS2})-

Cp*.^{6,7} Alternatively, the *in situ* reduction of a mixed sandwich Th(IV) halide precursor in the presence of a small molecule may produce a transient Th(III) intermediate, which could induce reductive transformations.

In addition to the reduction chemistry, the reactivity of Th–C and Th–H bonds in thorium(IV) systems towards small molecules such as CO₂ is also of interest. This was first reported by Marks and Moloy in 1985, who demonstrated the ability of Th(Cp*)₂(Me)₂ to insert 2 equivalents of CO₂ to form a bis-acetate, Th(Cp*)₂(OAc)₂, and that Th(Cp*)₂(OCH^tBu₂)(H) will insert 1 equivalent of CO₂ to yield a formate complex, Th(Cp*)₂(OCH^tBu₂)(κ²-O₂CH).⁸ Subsequently, a number of Th(IV) alkyl complexes have been synthesised, both in metallocene^{9–16} and non-metallocene^{17–20} ligand frameworks, and a small number of these have shown insertion reactivity towards CO₂.^{20–22} Th(IV) hydride complexes have also been synthesised, mainly supported by cyclopentadienyl-based ligands, and containing both bridging and terminal hydride ligands, however their CO₂ insertion chemistry has not been extensively explored.^{10,13–16,23–29} Alkyl and hydride compounds of the mixed-sandwich thorium system containing an unsubstituted COT ring and a Cp* ligand have been described by Sattelberger *et al.*; the crystal structure of Th(COT)Cp*(CH{TMS})₂ was reported, along with some evidence for the formation of an oligomeric hydride, [Th(COT)Cp*H]_x.¹⁴ It was anticipated that the increased solubility and greater steric shielding provided by use of the silyl-substituted COT^{TIPS2} ligand might allow the stabilisation and structural characterisation of such a hydride complex.

In this paper we describe the synthesis and characterisation of two Th(IV) halide complexes, Th(COT^{TIPS2})Cp*X (where

Department of Chemistry, School of Life Sciences, University of Sussex, Brighton, BN1 9QJ, UK. E-mail: f.g.cloke@sussex.ac.uk

† Electronic supplementary information (ESI) available: Crystallographic data collection details for compounds 1–6 and 8, along with the unrefined molecular structure of 6, and cyclic voltammograms of 1 and 2 are given in the ESI. CCDC 1008139–1008144 for compounds 1–5 and 8. For ESI and crystallographic data in CIF or other electronic format see DOI: 10.1039/c4dt02362e

X = Cl, I), attempted reduction of the latter, and the formation of dimeric carbonate and oxalate complexes, $\{\text{Th}(\text{COT}^{\text{TIPS}2})\text{Cp}^*\}_2(\mu\text{-}\kappa^1:\kappa^2\text{-CO}_3)$ and $\{\text{Th}(\text{COT}^{\text{TIPS}2})\text{Cp}^*\}_2(\mu\text{-}\kappa^2:\kappa^2\text{-C}_2\text{O}_4)$, from the *in situ* reduction of the iodide with NaK_3 under an atmosphere of CO_2 . Furthermore, we also present the synthesis of a Th(IV) alkyl and a hydride complex, and the results of their reactivity towards CO_2 , and a comparison with the related U(IV) chemistry using the same mixed-sandwich ligand system.³⁰

Results and discussion

Synthesis and characterisation of halide complexes

The thorium mixed-sandwich chloride complex, $\text{Th}(\text{COT}^{\text{TIPS}2})\text{Cp}^*\text{Cl}$ (**1**), was prepared from the reaction of ThCl_4 and $\text{MgClCp}^*(\text{THF})(\text{PhMe})_{0.5}$, forming the intermediate $\text{ThCp}^*\text{Cl}_3(\text{THF})_2$ without isolation, followed by the addition of $\text{K}_2(\text{COT}^{\text{TIPS}2})$ to yield **1** as light yellow crystals after workup. A sub-stoichiometric quantity of $\text{K}_2(\text{COT}^{\text{TIPS}2})$ was used to inhibit the very favourable formation of the ‘thorocene’ complex, $\text{Th}(\text{COT}^{\text{TIPS}2})_2$. The related iodide complex, $\text{Th}(\text{COT}^{\text{TIPS}2})\text{Cp}^*\text{I}$ (**2**), can be synthesised by stirring a toluene solution of **1** with an excess of TMSI for three days. After removal of volatiles, **2** can be isolated as light yellow crystals from toluene, slow-cooled to -35°C . Attempts to synthesise **2** *via* the analogous mono- Cp^* iodide complex, $\text{ThCp}^*\text{I}_3(\text{THF})_x$, from $\text{ThI}_4(\text{THF})_4$ and $\text{MgClCp}(\text{THF})(\text{PhMe})_{0.5}$ and subsequent reaction with $\text{K}_2(\text{COT}^{\text{TIPS}2})$ were unsuccessful due to the apparent instability of $\text{ThCp}^*\text{I}_3(\text{THF})_x$.

Both **1** and **2** were characterised by mass spectrometry, displaying the anticipated M^+ parent ions at $m/z = 818$ and 910 respectively. The ^1H and $^{13}\text{C}\{^1\text{H}\}$ NMR data are consistent with the expected η^5 - and η^8 -coordination of the Cp^* and $\text{COT}^{\text{TIPS}2}$ ligands, and the elemental analyses returned the expected values. The molecular structures of **1** and **2** are shown in Fig. 1 and 2, and geometric parameters are summarised in Table 1. Both **1** and **2** crystallise in the triclinic $P\bar{1}$ space group, containing two independent molecules in the unit cell, and are structurally similar; the Th–halide bond distance in **2** is, as

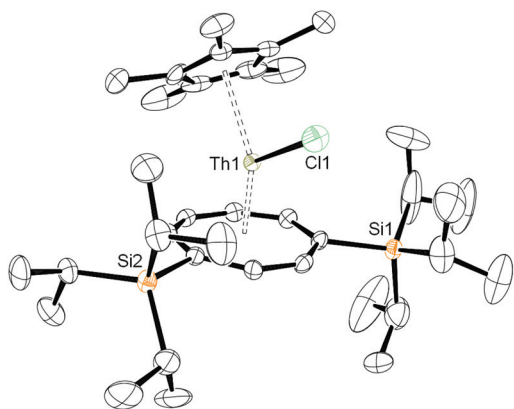


Fig. 1 Molecular structure of **1** with thermal ellipsoids at the 50% probability level. Hydrogen atoms omitted for clarity.

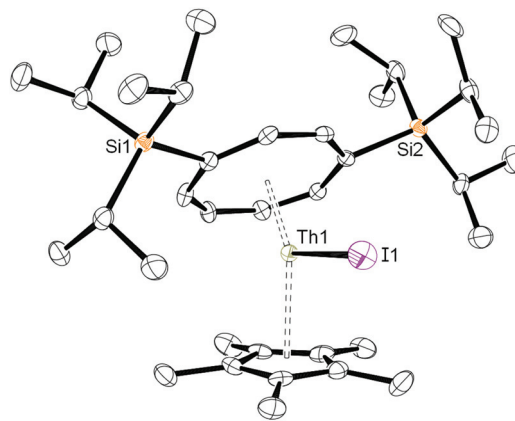


Fig. 2 Molecular structure of **2** with thermal ellipsoids at the 50% probability level. Hydrogen atoms omitted for clarity.

Table 1 Selected bond distances (Å) and angles ($^\circ$) for **1** and **2**. Ct1 is the Th–COT centroid, Ct2 is the Th– Cp^* centroid, X is the halide ligand

	1	2
Th–X	2.6865(16)	3.1104(5)
Th–Ct1	1.9846(3)	1.980(18)
Th–Ct2	2.5292(3)	2.530(7)
Ct1–Th–Ct2	140.531(15)	140.2(4)

anticipated, longer than in **1** (2.6865(16) v. 3.1104(5) Å), and the Ct1–Th1–Ct2 angle in **2** is marginally smaller than in **1**, due to the larger size of the iodide ligand. The Th–X (where X = Cl, I) bond distances in **1** and **2** are consistent with those previously reported for other terminal thorium halide complexes (averages: 2.70(6) Å for Th–Cl, 3.09(9) Å for Th–I).³¹

Attempted synthesis of Th(III) mixed-sandwich complexes and *in situ* reductive reactions with small molecules

Since the synthesis of a Th(III) mixed sandwich complex was one of the principle aims of this work, reaction of both halides **1** and **2** with reducing agents was investigated. Initial cyclic voltammetry studies showed irreversible reduction waves for **1** and **2** at -3.33 and -3.32 V (with respect to the ferrocene/ferrocenium couple), respectively, presumably corresponding to a one-electron reduction of the metal centre (see ESI† for voltammograms and full details). Shortly after this event was detected, decomposition of the thorium complexes ensued, apparent from diminishing current response over successive cycles and from deposition of material on the working electrode surface, and eventual discolouration of the solution after many cycles. Attempted chemical reduction of **1** or **2** with KC_8 resulted in no reaction, even after sonication; reacting **1** or **2** with NaK_3 yielded the substituted ‘thorocene’ $\text{Th}(\text{COT}^{\text{TIPS}2})_2$ and a dark precipitate, presumably thorium metal, both at ambient and elevated temperatures. Thus it would appear that any Th(III) mixed sandwich species disproportionates to Th(IV) and ‘Th(0)’.

In view of the above results, *in situ* reactions of toluene solutions of **1** or **2** with NaK₃ under an atmosphere of either ¹³CO or ¹³CO₂ were performed. The chloride **1** showed no reactivity towards either gas, while **2** did not react with ¹³CO, instead yielding Th(COT^{TIPSP2})₂ and elemental thorium after 14 days. However stirring **2** with an excess of ¹³CO₂ and NaK₃ for a period of 12 days resulted in the appearance of two new resonances, at δ 167 and 172 ppm, in the ¹³C{¹H} NMR spectrum of a reaction aliquot. Workup and selective crystallisation yielded two new dinuclear thorium species: a Th(IV) carbonate (**3**), and a Th(IV) oxalate (**4**) in low yields (12 and 2% respectively), the molecular structures of which are shown in Fig. 3 and 4.

The carbonate **3** crystallises in the triclinic space group *P* $\bar{1}$, containing half of the dimeric structure in the asymmetric unit, with the carbonate moiety bound in an κ¹:κ² fashion to two thorium centres, modelled in this structure as a 50:50 mixture of superimposed κ¹:κ² and κ²:κ¹ moieties, similar to the U(IV) carbonate previously reported in this

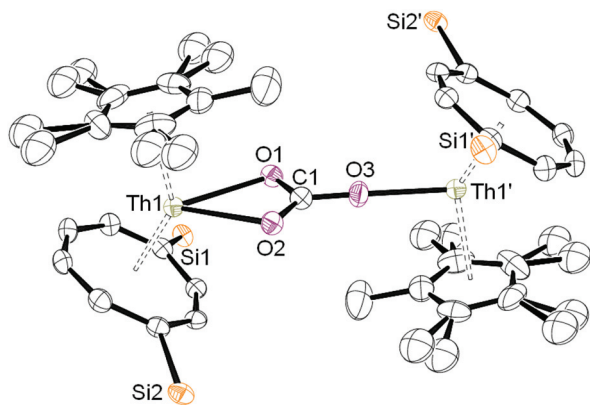


Fig. 3 Molecular structure of **3** with thermal ellipsoids at the 50% probability level. Carbonate core shown is one of two overlapping positions – for alternative views of the structure, see ESI.† Hydrogen atoms and ⁱPr groups omitted for clarity.

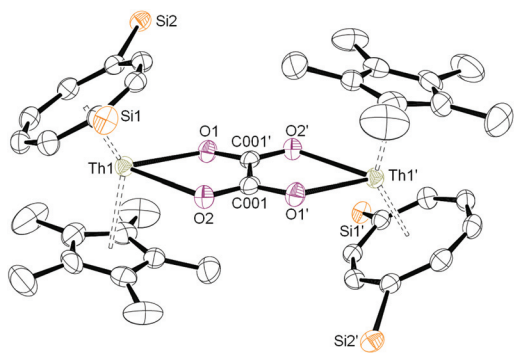


Fig. 4 Molecular structure of **4** with thermal ellipsoids at the 50% probability level. Hydrogen atoms, ⁱPr groups and co-crystallising molecule of toluene omitted for clarity. Th1–O1 = 2.473(2) Å, Th1–O2 = 2.475(3) Å, O1–C001 = 1.264(4) Å, O2–C001 = 1.260(4) Å, C001–C001' = 1.518(7) Å.

mixed-sandwich system (for more detail, see ESI†).⁷ As a result of this superimposition, metrical parameters describing the carbonate unit cannot be reliably reported, however, the rest of the structure can be accurately described. The oxalate **4** also crystallises in *P* $\bar{1}$ with half the molecule in the asymmetric unit, and does not contain disorder around the central oxalate moiety. The Th1–O1 and Th1–O2 bond distances are virtually identical (2.473(2) and 2.475(3) Å respectively), as are the O1–C001 and O2–C001 bond distances (1.264(4) and 1.260(4) Å respectively). The bond between C001 and C001' (symmetry generated) is single in nature, at 1.518(7) Å. There are no other Th(IV) oxalates supported by metallocene frameworks reported in the literature, however, several inorganic thorium oxalates have been reported containing bridging oxalate moieties as part of larger structural frameworks, *i.e.* Th(C₂O₄)₂(H₂O)₂·2H₂O.^{32–36} The Th–O_{oxalate} bond distances in **4** lie just outside the lower range of those found in the latter (2.481(2)–2.578(7) Å), whilst the O–C_{oxalate} bond distances in **4** are above the upper range of those found in the inorganic oxalates (1.242(3)–1.261(4) Å). The difference in oxalate bond distances in **4** as compared to those in the purely inorganic oxalates is likely due to the supporting ligands: the oxophilic thorium centre in **4** is only bound to soft carbocyclic ligands, rather than to other, hard oxygen donors. The C–C_{oxalate} bond distance in **4** is, however, comparable to those in the other inorganic oxalate structures (range 1.50(2)–1.545(7) Å). The Th–centroid bond distances for both Th–Ct1 and Th–Ct2 (COT^{TIPSP2} centroid and Cp* centroid respectively) in **3** and **4** are greater than in the halides **1** and **2**: the bridging nature of the former structures, together with the bidentate bonding mode of the oxalate and carbonate ligands, introduces steric repulsion between the COT^{TIPSP2} and Cp* ligands, in contrast to the monomeric η¹-coordinated halide ligands in **1** and **2**. The Ct1–Th–Ct2 angles are similarly smaller in **3** and **4** than in **1** and **2** (Table 2).

The formation of **3** and **4** could be ascribed to the reduction of CO₂ by a transient Th(III) species generated by the reaction of **2** with NaK₃, but which rapidly disproportionates in the absence of CO₂. However, other pathways cannot be excluded: for example, alkali metals alone will reduce CO₂ to oxalate and carbonate salts,³⁷ so it is possible that **3** and **4** result from a transmetallation reaction between sodium/potassium carbonate and oxalate and the iodo-complex **2**. However two factors mitigate against the latter pathway: (i) the reaction to form **3** and **4** does not occur with the chloro-complex **1** which would be expected to undergo such a transmetallation reaction with equal facility; (ii) attempts at recreating the transmetallation reaction by treatment of a toluene solution of **2** with a mixture

Table 2 Selected bond distances (Å) and angles (°) for **3** and **4**. Ct1 is the Th–COT centroid, Ct2 is the Th–Cp* centroid, X is the halide ligand

	3	4
Th–Ct1	2.0226(9)	2.02932(17)
Th–Ct2	2.5388(11)	2.54142(17)
Ct1–Th–Ct2	138.88(3)	139.402(7)

of excess Na_2CO_3 and K_2CO_3 or excess of $\text{Na}_2\text{C}_2\text{O}_4$ for an extended period (11 days) failed to produce either 3 or 4.

Synthesis and reactivity of Th(IV) alkyl and hydride complexes

The previously reported U(IV) mixed-sandwich alkyls, $\text{U}(\text{COT}^{\text{TIPS}_2})\text{Cp}^*(\text{R})$ (where $\text{R} = \text{CH}_3, \text{CH}_2\text{Ph}, \text{CH}_2\text{TMS}, \text{CH}(\text{TMS})_2$), and hydride, $\text{U}(\text{COT}^{\text{TIPS}_2})\text{Cp}^*(\text{H})$, are reactive towards CO_2 and will undergo insertion reactions to form the corresponding monomeric carboxylate and formate products, $\text{U}(\text{COT}^{\text{TIPS}_2})\text{Cp}^*(\kappa^2\text{-O}_2\text{CR})$ (where $\text{R} = \text{CH}_3, \text{CH}_2\text{Ph}, \text{CH}_2\text{TMS}, \text{H}$).³⁰ The thorium benzyl alkyl, $\text{Th}(\text{COT}^{\text{TIPS}_2})\text{Cp}^*(\text{CH}_2\text{Ph})$ (5), was synthesised *via* salt metathesis between 1 and KCH_2Ph , yielding yellow crystalline 5 in a 60% yield. The molecular structure of 5 (Fig. 5) shows the benzyl ligand in the expected η^1 -coordination mode. In comparison to the uranium analogue, the metal-centroid and metal- CH_2Ph bond distances are longer in 5, in accordance with the larger ionic radius of Th(IV) *vs.* U(IV) (Table 3). In comparison to other Th(IV) benzyl complexes, the Th-C bond length is greater than any previously reported (range: 2.53(2)–5.581(19) Å),³¹ likely due to the steric demands imposed by the bulky TIPS groups on the COT ring. Unlike its uranium analogue, 5 appears to be stable in solution and in the solid state at ambient temperature. No evidence has been seen for the existence of a ‘tucked-in’ species – formed *via* activation of a Cp* methyl group and loss of toluene – as occurs in the uranium system.

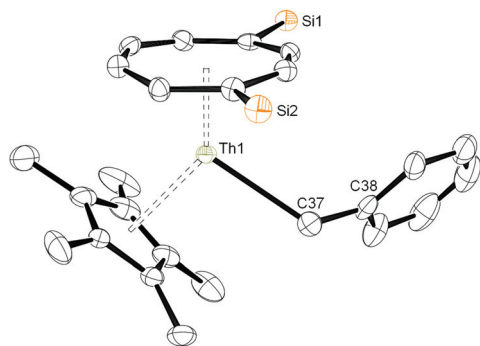


Fig. 5 Molecular structure of one crystallographically independent molecule of 5 in the asymmetric unit, with thermal ellipsoids at the 50% probability level. Hydrogen atoms and ^1Pr groups omitted for clarity.

Table 3 Bond distances (Å) and angles (°) in 5 ($\text{An} = \text{Th}$) and in $\text{U}(\text{COT}^{\text{TIPS}_2})\text{Cp}^*\text{CH}_2\text{Ph}$ ($\text{An} = \text{U}$). Ct1 is the COT-ring centroid, Ct2 is the Cp*-ring centroid. Two values quoted for each compound equate to the two crystallographically independent molecules in the asymmetric units

	An = Th	An = U
An–Ct1(Ct3)	2.0025(14)	1.9297(3)
	2.0056(14)	1.9304(3)
An–Ct2(Ct4)	2.538(2)	2.4899(3)
	2.539(2)	2.4836(3)
Ct1(Ct3)–An–Ct2(Ct4)	138.13(6)	137.217(13)
	137.07(7)	137.977(13)
An–C37(C87)	2.597(5)	2.532(4)
	2.598(4)	2.543(4)

Exposure of 5 to either 1 equivalent or 1 bar of CO_2 yields the expected κ^2 phenyl carboxylate complex, $\text{Th}(\text{COT}^{\text{TIPS}_2})\text{Cp}^*(\kappa^2\text{-O}_2\text{C-CH}_2\text{Ph})$ (6). Performing the reaction with 1 equivalent of $^{13}\text{CO}_2$ affords the corresponding labelled product, ^{13}C -6, and results in a prominent resonance at δ 188 ppm in the $^{13}\text{C}\{^1\text{H}\}$ NMR spectrum assigned to the inserted ^{13}C -labelled carboxylate carbon. This is in agreement with data reported by Mora *et al.* for a related Th(IV) carboxylate complex which includes a ^{13}C NMR resonance at δ 190.3 ppm assigned to the carboxylate carbon.²⁰ The ^1H NMR spectrum of ^{13}C -6 contains a doublet at 3.3 ppm ($J_{\text{CH}} = 7.6$ Hz) of integration 2H corresponding to the two $\text{O}_2^{13}\text{C-CH}_2\text{Ph}$ protons, which weakly couple to the ^{13}C atom. IR spectroscopic analysis of ^{13}C -6 shows stretching frequencies at 1536 and 1383 cm^{-1} , corresponding to C–O asymmetric and symmetric stretches respectively. The mass spectrum of 6 shows the expected parent ion at $m/z = 919$, and the $\text{M}^+ - \text{Cp}^*$ fragment at $m/z = 785$. Whilst X-ray diffraction data was collected from several crystalline samples of 6, the data could not be sufficiently refined: persistent electron density positioned above the COT-ring, and attributed to twinning in the crystal samples that could not be modelled, prevented satisfactory refinement of the data. However, connectivity could be established and the phenyl carboxylate ligand is bound κ^2 to the metal centre, and the structure is virtually identical to that of the uranium analogue (see ESI† for the unrefined structure).

With the alkyl complex 5 in hand, the synthesis of a hydride complex was explored. Exposure of a d_6 -benzene or pentane solution of 5 to 1 bar of H_2 resulted in a colour change from bright yellow to paler yellow over the course of several hours. The addition of 1 equivalent of H_2 yields the same colour change over a period of 48 hours, during which time some decomposition occurs, with free ligand and a small quantity of $\text{Th}(\text{COT}^{\text{TIPS}_2})_2$ observed by ^1H NMR spectroscopy. The ^1H NMR spectrum of the product of the reaction between 5 and 1 bar of H_2 exhibits resonances attributable to free CH_3Ph , and a new resonance at 23.3 ppm of integration 1H relative to the other ligand signals, corresponding to a hydride ligand. Previously reported examples of Th(IV) metallocene hydride complexes reveal that ^1H NMR spectroscopic shifts of the hydride ligands are at notably low-field ppm values (between 17.1–20.5 ppm, Table 4). The IR spectrum of the reaction mixture contained intense vibrational bands at 1260, 1089, and 802 cm^{-1} , typical for bridging rather than terminal hydride complexes, as determined by comparison with previously reported Th(IV) hydride IR data (Table 4). It is hence proposed that, unlike the U(IV) analogue, the Th(IV) mixed-sandwich hydride is bridging, not terminal, in structure, giving $\{\text{Th}(\text{COT}^{\text{TIPS}_2})\text{Cp}^*\text{H}\}_2$ (7, Fig. 6). As previously noted, the larger ionic radius of Th(IV) *vs.* U(IV) is presumably responsible for this difference in structure.

Despite our best efforts, the isolation of 7 as a pure crystalline material has not been successful, hence elemental analysis has not been possible. Mass spectral analysis does not show the expected parent ion for a bridging hydride, however, an ion at $m/z = 784$ is observed, corresponding to the fragment

Table 4 IR spectroscopic data and ^1H NMR spectroscopic shifts of hydride ligands in reported Th(IV) hydride metallocene complexes (where available). IR data in cm^{-1} , ^1H NMR data in ppm^a

Complex	IR data	^1H NMR data	Ref.
$\{\text{Cp}^*_2\text{Th}(\text{H})\text{Cl}\}_2(\text{b})$	1229, 1152, 829, 672	19.0	24
$\{\text{Cp}^*_2\text{Th}(\text{H})\text{Me}\}_2(\text{b})$		18.6	27
$\{\text{Me}_2\text{Si}(\text{Cp}^{\text{Me}4})_2\text{ThH}_2\}_2(\text{b})$	1285, 1155, 654, 481	18.36	13
$\{\text{Cp}^*\text{Th}(\text{O}-2,6\text{-}^t\text{Bu}-\text{C}_6\text{H}_3)_2\}_3(\text{b})$		18.54	16
$\{(\text{COT})\text{Cp}^*\text{Th}(\text{H})\}_x(\text{b})$	1147		14
$\{\text{Th}(\text{O}-2,6\text{-}^t\text{Bu}-\text{C}_6\text{H}_3)_2\}_3(\text{b})$	1336, 975, 795	20.54	15
$\{\text{Cp}^*_2\text{Th}(\text{H}_2)\}(\text{b/t})$	1404, 1370 (t) 1215, 1114, 844, 650 (b)	19.2	24
$\text{Cp}^*_2\text{Th}(\text{H})(\text{OTf})(\text{t})$		20.0	27
$\text{Cp}^*_2\text{Th}(\text{H})(\text{OSiMe}_2^t\text{Bu})(\text{t})$		18.1	27
$\text{Cp}^*_2\text{Th}(\text{H})(\text{OCMe}_3)(\text{t})$	1359	17.4	24
$\text{Cp}^*_2\text{Th}(\text{H})(\text{OCH}^t\text{Bu}_2)(\text{t})$		18.0	28
$\text{Cp}^*_2\text{Th}(\text{H})(\text{O}-2,6\text{-}^t\text{Bu}-\text{C}_6\text{H}_3)(\text{t})$	1365	19.1	28
$\text{Cp}^*_2\text{Th}(\text{H})(1\text{S-endo-bornoxide})(\text{t})$	1348	17.7	29
$(\text{C}_5\text{Me}_4\text{SiMe}_3)_3\text{Th}(\text{H})(\text{t})$	1460	12.94	25
$(\text{C}_9\text{H}_6\text{SiMe}_3)_3\text{Th}(\text{H})(\text{t})$	1485	14.73	25
$(\text{N}(\text{TMS})_2)_3\text{ThH}(\text{t})$	1480	0.63	17

^a (b) denotes bridging hydride ligand, (t) denotes terminal hydride ligand, (b/t) denotes both bridging and terminal hydride ligands.

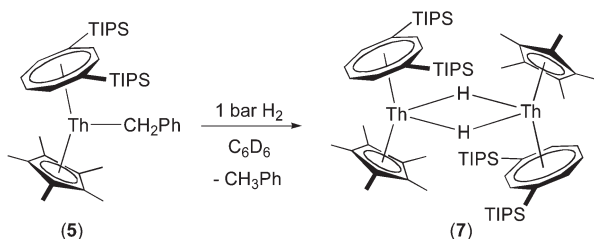


Fig. 6 Formation of proposed bridging hydride complex, **7**, from the reaction of **5** with 1 bar of H_2 .

$\text{ThCOT}^{\text{TIPS}2}\text{Cp}^*$, along with an ion at $m/z = 1065$, indicating the fragmentation and rearrangement product, $\text{Th}(\text{COT}^{\text{TIPS}2})_2$. **7** appears to be noticeably more stable than the uranium analogue, $\text{U}(\text{COT}^{\text{TIPS}2})\text{Cp}^*(\text{H})$ and does not decompose to any significant extent to either a trivalent mixed-sandwich product or to a ‘tucked-in’ product when subjected to reduced pressure. The lack of ready access to the Th(III) oxidation state may explain this observation, potentially also implying that the ubiquitous ‘tucked-in’ product in the uranium system, $\text{U}(\text{COT}^{\text{TIPS}2})(\eta^5\text{-}\eta^1\text{-C}_5\text{Me}_4\text{CH}_2)$, may be formed *via* a U(III) intermediate, hence its absence in the Th(IV) reaction mixtures. This same marked contrast in stability of a Th(IV) hydride in comparison to the U(IV) analogue was also noted by Marks *et al.* in their studies on the actinide hydrides, $\{\text{AnCp}^*_2\text{H}_2\}_2$.²⁴

Further evidence for the formulation and hydride bridging conformation of **7** arises from reaction of the latter with CO_2 . Upon the addition of 1 equivalent of $^{13}\text{CO}_2$ to a frozen d_6 -benzene solution of **7**, a colour change to deeper yellow occurs whilst warming to ambient temperature. ^1H NMR

spectroscopic analysis of the reaction mixture shows the formation of a single new product **8** and the disappearance of the hydride resonance at 23.4 ppm; the $^{13}\text{C}\{^1\text{H}\}$ NMR spectrum contains an intense singlet resonance at 177.2 ppm. The ^1H coupled ^{13}C NMR spectrum of **8** exhibits a doublet at 177.2 ppm with $J_{\text{CH}} = 211$ Hz which correlates to a doublet in the ^1H NMR spectrum at 9.0 ppm ($J_{\text{CH}} = 211$ Hz), consistent with the a single proton attached to the inserted ^{13}C atom. IR spectroscopic data shows a vibration at 1543 cm^{-1} , assigned to a formate ligand.

X-ray diffraction quality crystals of **8** were grown from a saturated toluene solution cooled to $-35\text{ }^\circ\text{C}$, revealing the structure to be the bridging formate complex, $\{\text{Th}(\text{COT}^{\text{TIPS}2})\text{Cp}^*(\mu\text{-}\kappa^1\text{-O}_2\text{-}^{13}\text{CH})\}_2$ (Fig. 7). This supports the proposition that the parent hydride complex, **7**, is also bridging in nature. The dimeric structure of **8** is in contrast to that of the monomeric U(IV) formate complex, $\text{U}(\text{COT}^{\text{TIPS}2})\text{Cp}^*(\kappa^2\text{-O}_2\text{CH})$, again due to the larger ionic radius of Th(IV) vs. U(IV) (Table 5).

Only two other crystallographically characterised Th(IV) formate complexes have been reported, both of which are hexanuclear: neutral $\text{Th}_6(\text{OH})_4\text{O}_4(\text{H}_2\text{O})_6(\text{HCO}_2)_{12}\cdot n\text{H}_2\text{O}$, and $[\text{Th}_6(\mu_3\text{-O})_4(\mu_3\text{-OH})_4(\text{HCOO})_{12}(\text{H}_2\text{O})_6]\text{Na}_3(\text{ClO}_4)_{3.5}(\text{H}_2\text{O})_{5.5}(\text{H}_3\text{O})_{0.5}$.^{38,39} In each structure, the formate moieties bridge between two Th centres, as in **8**, but the Th atoms are also bound to either ($\mu_3\text{-O}$) or ($\mu_3\text{-OH}$) bridges, which dictate the overall geometry of

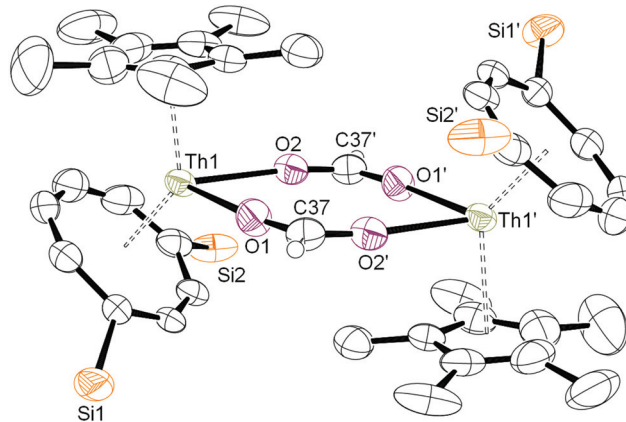


Fig. 7 Molecular structure of **8** with thermal ellipsoids at the 50% probability level.

Table 5 Selected bond distances (Å) and angles ($^\circ$) for **8**

Metric	Value
Th1–O1	2.408(5)
Th1–O2	2.394(4)
O1–C37	1.240(8)
O2–C37	1.231(7)
Th1–O1–C37	169.7(4)
Th1–O2–C37	166.9(5)
O1–C37–O2	126.8(6)
O1–Th1–O2	75.88(16)
Ct1–Th	2.045(3)
Ct2–Th	2.557(4)
Ct1–Th–Ct2	135.15(12)

the cluster. The Th–O_{formate} bond lengths in the former complex range from 2.478(14)–2.523(16) Å, and in the latter from 2.463–2.543 Å, both significantly longer than in **8**. The O–C–O angles of the bridging formate moieties range from 124(2)–129.3(2)° in both structures, comparable to the O₁–C₃₇–O₂ angle of 126.6(6)° found in **8**. In comparison to the two other dimeric Th(IV) mixed-sandwich structures reported in this work, **3** and **4**, the Ct1–Th and Ct2–Th distances of 2.045(3) and 2.557(4) Å in **8** are marginally longer, and the Ct1–Th–Ct2 angle of 135.15(12)° is also greater.

Conclusions

Attempts to prepare a stable Th(III) mixed sandwich complex of the type 'ThCOT^{TIPS2}Cp*' by reduction of Th(IV) halide precursors have been unsuccessful, although such a species may be implicated in reductions carried out under a CO₂ atmosphere which result in dimeric thorium carbonate and oxalate products. Synthesis of the benzyl derivative Th(COT^{TIPS2})Cp*CH₂Ph proceeds straightforwardly, and the former reacts readily with hydrogen to yield a hydride complex and hence a formate derivative *via* insertion of CO₂ into the Th–H bond. However, in contrast to the U(IV) chemistry reported for this mixed-sandwich system, the larger ionic radius of Th(IV) compared to U(IV) results in dimeric structures for both the hydride and formate complexes. In addition, no evidence has been seen for the existence of a 'tucked-in' Th(IV) complex, Th(COT^{TIPS2})(η^5 : η^1 -C₅Me₄CH₂), formed *via* the activation of a Cp* methyl group, a commonly observed degradation pathway for alkyls and hydrides in the U(IV) system.

Experimental

General experimental details

Air-sensitive compound manipulations were carried out under an inert atmosphere of N₂ or Ar using standard Schlenk techniques or in an MBraun glove box (N₂ or Ar, <1 ppm H₂O and <1 ppm O₂). Solvents were pre-dried over sodium wire (with the exception of DCM which was not pre-dried) before heating at reflux over the appropriate drying agent (NaK₃: pentane, Et₂O; K: THF, 1,4-dioxane; Na: toluene; CaH₂: DCM). Dried solvents were degassed and stored in potassium-mirrored ampoules after collection, with the exception of THF, which was stored in an ampoule containing flame-dried 4 Å molecular sieves. Deuterated NMR solvents were purchased from GOSS Scientific Ltd. and purified by heating at reflux over the appropriate drying agent, vacuum transferred into ampoules and stored under nitrogen prior to use. NMR spectroscopic analysis was performed using a Varian VNMR 400 spectrometer: ¹H NMR was run at 399.5 MHz, ¹³C NMR at 100.5 MHz. Chemical shifts are quoted in parts per million and are internally referenced to residual protic solvent (¹H) or deuterated solvent shifts (¹³C). EI-MS was performed by Dr A. K. Abdul-Sada at the University of Sussex using a VG Autospec Fissions

instrument (EI at 70 eV). IR spectra were recorded using NaCl plates on a Perkin-Elmer Spectrum One FTIR machine. Elemental analyses were performed by Mr Des Davis at the University of Bristol. All XRD data sets were collected on a Bruker-Nonius Kappa CCD area detector diffractometer with a sealed tube source (Mo or Cu α) and an Oxford Cryosystems low temperature device, operating in ω scanning mode with ψ and ω scans to fill the Ewald sphere. Structures were either determined using Olex2,⁴⁰ solved with the Superflip structure solution program using Charge Flipping⁴¹ and refined with ShelXL refinement program,⁴² or solved using the WinGX package and all software within.⁴³ CCDC 1008139–1008144 contain the supplementary crystallographic data for compounds **1–5** and **8**. ThCl₃Cp*(THF)_x,⁴⁴ KCH₂Ph,⁴⁵ and K₂(COT^{TIPS2})⁶ were prepared using standard literature procedures. ¹³CO₂ (99%) was supplied by EuroIsotop and used as supplied. Gas transfer was *via* Toepler pump. Electrochemical studies (cyclic voltammetry) were carried in dry THF containing 0.1 M [NⁿBu₄][PF₆] as the supporting electrolyte using a BASi Epsilon-EC potentiostat under computer control, performed by A. Kilpatrick of the University of Sussex. Cyclic voltammetry experiments were performed using a three-electrode configuration with a glassy carbon disc having an area of 7.0 mm² as the working electrode, a platinum wire as the counter electrode and a silver wire as the pseudoreference electrode. The Ag wire pseudoreference electrode was calibrated to the ferrocene/ferrocenium couple in THF, relative to which all of the standard potentials are reported. Ferrocene (*ca.* 3 mg) was added to a 0.1 M solution of electrolyte in THF (5 cm³) containing the dissolved metal complexes (5–8 mM).

Synthesis of Th(COT^{TIPS2})Cp*Cl (**1**)

A stirred solution of ThCp*Cl₃(THF)₂ (492 mg, 0.797 mmol in 20 cm³ of THF) was cooled to –78 °C, and to this was added a THF solution of K₂COT^{TIPS2} (355 mg, 0.717 mmol, 0.9 eq.) dropwise over 20 minutes. The resulting off-white suspension was allowed to stir for a further 18 hours whilst warming to ambient temperature, during which time it became light yellow with white solids. Removal of volatiles gave yellow viscous solids, and extraction with pentane followed by filtration gave a yellow solution which, when slow-cooled to –50 °C, yielded yellow prisms of **1** suitable for X-ray diffraction studies. Yield = 382 mg (0.466 mmol), 59% w.r.t. ThCp*Cl₃(THF)₂. ¹H NMR (C₆D₆, 399.5 MHz): δ _H 7.12 (s, 2H, COT-H), 6.70 (m, 2H, COT-H), 6.41 (m, 2H, COT-H), 1.95 (s, 15H, Cp*), 1.59 (septet, *J*_{HH} = 7.5 Hz, 6H, ¹Pr-CH), 1.32 (d, *J*_{HH} = 7.6 Hz, 18H, ¹Pr-CH₃), 1.22 (d, *J*_{HH} = 7.5 Hz, 18H, ¹Pr-CH₃). ¹³C{¹H} NMR (C₆D₆, 100.5 MHz, 303 K): δ _C 127.6 (Cp-CCH₃), 113.5 (COT-CH), 107.6 (COT-CH), 107.1 (COT-CSi), 105.0 (COT-CH), 20.1 (¹Pr-CH₃), 19.7 (¹Pr-CH₃), 12.8 (¹Pr-CH), 11.8 (Cp-CH₃). MS (E)⁺: *m/z* 818 (M⁺, 95%), 775 (M⁺, ¹Pr, 33%), 683 (M⁺ – Cp*, 100%). Anal. Found: C, 53.00; H, 8.00. C₃₆H₆₃Si₂ClTh requires C, 52.76; H 7.75%.

Synthesis of Th(COT^{TIPS2})Cp*1 (2)

An excess of trimethylsilyliodide (552 mg, 2.76 mmol) was added to a stirred toluene solution of **1** (420 mg, 0.513 mmol) at ambient temperature. After stirring for three days, all volatiles were removed from the yellow solution under reduced pressure, giving light yellow solids. Extraction in toluene (*ca.* 5 cm³) and slow-cooling to -35 °C yielded light yellow prisms of **2** in good yield, suitable for X-ray diffraction studies. Yield = 277 mg (0.304 mmol), 59% w.r.t. **1**. ¹H NMR (C₆D₆, 399.5 MHz, 303 K): δ_H 7.18 (s, 2H, COT-H), 6.70 (m, 2H, COT-H), 6.38 (m, 2H, COT-H), 2.00 (s, 15H, Cp*), 1.62 (septet, *J*_{HH} = 7.6 Hz, 6H, ¹Pr-CH), 1.33 (d, *J*_{HH} = 7.5 Hz, 18H, ¹Pr-CH₃), 1.24 (d, *J*_{HH} = 7.5 Hz, 18H, ¹Pr-CH₃). ¹³C{¹H} NMR (C₆D₆, 100.5 MHz, 303 K): δ_C 128.8 (Cp-CCH₃), 114.4 (COT-CH), 109.0 (COT-CSi), 107.6 (COT-CH), 104.7 (COT-CH), 20.3 (¹Pr-CH₃), 20.2 (¹Pr-CH₃), 13.0 (¹Pr-CH), 12.7 (Cp-CH₃). MS (EI)⁺: *m/z* 910 (M⁺, 13%), 867 (M⁺, ¹Pr, 10%), 157 (Si¹Pr₃, 100%). Anal. Found: C, 47.64; H, 6.87. C₃₆H₆₃Si₂ITh requires C, 47.46; H 6.97%.

Synthesis of {Th(COT^{TIPS2})Cp*}₂(μ-κ¹:κ²-CO₃) (3)

To a pale yellow solution of **2** (0.090 g, 0.0989 mmol) in toluene (1 cm³) was added an excess of NaK₃; the mixture was cooled to -78 °C and ¹³CO₂ (3 eq.) was added. This mixture was allowed to stir for 16 days before filtration. Storage at -35 °C yielded pale yellow rectangular crystals of **3** in poor yield that were suitable for X-ray diffraction analysis. Yield = 0.010 g (0.00615 mmol), 12% w.r.t. **2**. ¹H NMR (C₇D₈, 399.5 MHz, 303 K): δ_H 6.73 (m, 4H, COT-H), 6.53 (m, 2H, COT-H), 2.01 (s, 15H, Cp*), 1.62 (septet, *J*_{HH} = 7.45 Hz, 6H, ¹Pr-CH), 1.32 (d, *J*_{HH} = 7.38 Hz, 18H, ¹Pr-CH₃), 1.24 (d, *J*_{HH} = 7.75 Hz, 18H, ¹Pr-CH₃). ¹³C{¹H} NMR (C₇D₈, 100.5 MHz, 303 K): δ_C 177.5 (Cp-CCH₃), 167.8 (CO₃), 111.1 (COT-CH), 108.2 (COT-CH), 106.5 (COT-CH), 105.5 (COT-CH), 20.7 (¹Pr-CH₃), 20.5 (¹Pr-CH₃), 13.5 (¹Pr-CH), 11.9 (Cp-CH₃). MS (EI)⁺: *m/z* 1494 (M⁺ - Cp*, 1%), 1449 (M⁺ - Cp*, ¹Pr, 2%), 784 (*Th(COT^{TIPS2})-Cp*, 100%). Anal. Found: C 47.05, H 6.56. C₇₃H₁₂₆O₃Si₄Th₂ requires C 46.9, H 6.74%.

Synthesis of {Th(COT^{TIPS2})Cp*}₂(μ-κ²:κ²-C₂O₄) (4)

To a pale yellow solution of **2** (0.100 g, 0.110 mmol) in toluene (1 cm³) was added an excess of NaK₃; the mixture was cooled to -78 °C and ¹³CO₂ (5 eq.) was added. This mixture was allowed to stir for 5 days before filtration. Storage at -35 °C yielded pale yellow rectangular crystals of **4** in poor yield that were suitable for X-ray diffraction analysis. Yield = 0.002 g (0.00122 mmol), 2% w.r.t. **2**. ¹H NMR (C₆D₆, 399.5 MHz, 303 K): δ_H 6.82 (m, 2H, COT-H), 6.70 (m, 4H, COT-H), 1.99 (s, 15H, Cp*), 1.63 (septet, *J*_{HH} = 7.59 Hz, 6H, ¹Pr-CH), 1.31 (d, *J*_{HH} = 7.51 Hz, 18H, ¹Pr-CH₃), 1.28 (d, *J*_{HH} = 7.51 Hz, 18H, ¹Pr-CH₃). ¹³C{¹H} NMR (C₆D₆, 125.72 MHz, 303 K): δ_C 172.1 (C₂O₄), 128.4 (CpCCH₃), 109.9 (COT-CH), 105.3 (COT-CH), 105.2 (COT-CH), 20.1 (¹Pr-CH₃), 19.8 (¹Pr-CH₃), 12.9 (¹Pr-CH), 11.7 (Cp-CH₃). MS (EI)⁺: *m/z* 1657 (M⁺, 1%), 1552 (M⁺ - Cp*, 1%).

Synthesis of Th(COT^{TIPS2})Cp*CH₂Ph (5)

KCH₂Ph (9 mg, 0.072 mmol) and **1** (60 mg, 0.072 mmol) were dissolved in 10 cm³ of toluene and stirred for 12 hours, during which time the solution changed colour from light yellow to a darker yellow. Removal of volatiles under reduced pressure and subsequent extraction and filtration in pentane afforded a yellow solution, from which yellow crystals of X-ray diffraction quality were isolated upon slow-cooling to -20 °C. Yield: 38 mg (0.043 mmol), 60% w.r.t. **1**. ¹H NMR (C₆D₆, 399.5 MHz, 303 K): δ_H 7.30 (t, *J*_{HH} = 7.6 Hz, 2H, *meta*-C₆H₅), 7.02 (s, 2H, COT-H), 7.01 (s, 2H, *ortho*-C₆H₅), 6.75 (t, *J*_{HH} = 7.5 Hz, *para*-C₆H₅), 6.63 (m, 2H, COT-H), 6.28 (m, 2H, COT-H), 1.90 (s, 15H, Cp*), 1.45 (septet, *J*_{HH} = 7.4 Hz, 6H, ¹Pr-CH), 1.27 (d, *J*_{HH} = 7.4 Hz, 18H, ¹Pr-CH₃), 1.21 (d, *J*_{HH} = 7.4 Hz, 18H, ¹Pr-CH₃), 1.13 (s, 2H, C₆H₅CH₂). ¹³C{¹H} NMR (C₆D₆, 100.5 MHz, 303 K): δ_C 128.4 (Cp-CCH₃), 127.7 (Ph-CH), 126.5 (Ph-CH), 124.8 (Ph-CH), 113.3 (COT-CH), 110.4 (COT-CH), 107.9 (COT-CSi), 104.4 (COT-CH), 95.6 (C₆H₅CH₂), 20.4 (¹Pr-CH₃), 20.3 (¹Pr-CH₃), 13.0 (¹Pr-CH), 11.8 (Cp-CH₃). Ph-C could not be definitively assigned. MS (EI)⁺: *m/z* 783 (M⁺, -CH₂Ph, 12%), 157 (Si¹Pr₃, 100%). Anal. Found: C, 59.41; H, 8.25. C₄₃H₇₀Si₂Th requires C, 59.01; H 8.06%.

Synthesis of Th(COT^{TIPS2})Cp*(κ²-O₂¹³C-CH₂Ph) (1³-6)

A C₆D₆ solution of **5** (12.6 mg, 0.014 mmol) was cooled to -78 °C, the ampoule headspace degassed, and a slight excess (0.024 mmol) of ¹³CO₂ was delivered *via* Toepler pump. Upon warming to ambient temperature, a colour change to pale yellow was observed. Removal of volatiles under reduced pressure and extraction of the resulting yellow solids into pentane, followed by slow-cooling to -35 °C yielded pale yellow crystals of **1³-6**. Yield: 10.3 mg (0.011 mmol) 80% w.r.t. **5**. ¹H NMR (C₆D₆, 399.5 MHz, 303 K) δ_H 7.25–7.00 (overlapping signals, 5H, aromatic protons), 6.81 (m, 2H, COT-H), 6.57 (m, 2H, COT-H), 3.36 (d, *J*_{CH} = 7.6 Hz, 2H, CH₂-C₆H₅), 1.82 (s, 15H, Cp*), 1.61 (septet, *J*_{HH} = 7.5 Hz, 6H, ¹Pr-CH), 1.28 (d, *J*_{HH} = 7.4 Hz, 18H, ¹Pr-CH₃), 1.25 (d, *J*_{HH} = 7.5 Hz, 18H, ¹Pr-CH₃). ¹³C{¹H} NMR (C₆D₆, 100.5 MHz, 303 K): δ_C 188.2 (O₂¹³C), 130.4 (d, *J*_{CC} = 1.9 Hz, CH₂C₆H₅), 128.9 (C₆H₅), 128.7 (Cp-CCH₃), 127.5 (C₆H₅), 125.1 (C₆H₅), 111.0 (COT-CH), 107.6 (COT-CSi), 106.2 (COT-CH), 105.8 (COT-CH), 20.2 (¹Pr-CH₃), 19.8 (¹Pr-CH₃), 12.9 (¹Pr-CH), 11.6 (¹Pr-CH). MS (EI)⁺: *m/z* 918 (M⁺, 15%), 783 (M⁺ - Cp*, 90%). IR (NaCl plates, cm⁻¹) 2942 s, 2864 s, 2342 w, 1536 br, 1462 m, 1383 m, 1260 w, 1015 w, 927 w, 881 m, 799 w. Anal. Found: C, 57.80; H, 7.80. (C₄₃H₇₀Si₂O₂Th requires C, 57.54; H 7.67%.

Synthesis of {Th(COT^{TIPS2})Cp*H}_x (where x = 1 or 2) (7)

A C₆D₆ solution of **5** (10.7 mg, 0.012 mmol) was frozen, the headspace evacuated, and 1 bar of H₂ was added to the J Young NMR tube. The reaction mixture was thawed, and a colour change to pale yellow was observed after 12 hours. Extraction into a variety of solvents (pentane, ether, TMS₂O) only yielded a viscous yellow-orange oil in all cases. Yield as determined by ¹H NMR spectroscopy: >90%. Crude isolated

yield: ca. 7 mg (0.009 mmol), 75% w.r.t. 5. ^1H NMR (C_6D_6 , 399.5 MHz, 303 K): δ_{H} 23.4 (s, 1H, Th-H) 7.14 (s, 2H, COT-H), 6.70 (m, 2H, COT-H), 6.37 (m, 2H, COT-H), 2.02 (s, 15H, Cp*), 1.59 (septet, $J_{\text{HH}} = 7.5$ Hz, 6H, $^1\text{Pr-CH}$), 1.31 (d, $J_{\text{HH}} = 7.5$ Hz, 18H, $^1\text{Pr-CH}_3$), 1.26 (d, $J_{\text{HH}} = 7.4$ Hz, 18H, $^1\text{Pr-CH}_3$). Resonances attributed to CH_3Ph were also observed at 7.11–7.00 ppm, and at 2.11 ppm. $^{13}\text{C}\{^1\text{H}\}$ NMR (C_6D_6 , 100.5 MHz, 303 K): δ_{C} 125.7 (Cp-CCH₃), 112.6 (COT-CH), 108.8 (COT-CSi), 105.3 (COT-CH), 20.0 ($^1\text{Pr-CH}_3$), 19.8 ($^1\text{Pr-CH}_3$), 12.7 ($^1\text{Pr-CH}$), 11.6 (Cp-CH₃). IR (NaCl plates, cm^{-1}) 2943 s, 2865 s, 1463 m, 1383 w, 1218 br, 1260 s, 1089 br s, 1030 s, 931 w, 882 s, 803 s, 758w, 624 s, 669 s.

Synthesis of $\{\text{Th}(\text{COT}^{\text{TIPS}_2})\text{Cp}^*(\mu\text{-}\kappa^1\text{:}\kappa^1\text{-O}_2\text{ }^{13}\text{CH})\}_2$ (**13-8**)

The *in situ* reaction of a C_6D_6 solution of 5 (21 mg, 0.024 mmol) and H_2 was performed in a J Young NMR tube and left for 12 hours to form the hydride, 7. Once frozen, the vessel headspace was evacuated and 1 equivalent of $^{13}\text{CO}_2$ (0.024 mmol) was added *via* Toepler pump. A colour change to bright yellow was observed upon thawing and warming to ambient temperature. Removal of volatiles under reduced pressure and extraction in toluene, followed by slow-cooling to -35 °C yielded off-white crystals of **13-8**. Yield: 14 mg (0.017 mmol), 71% w.r.t. 5. ^1H NMR (C_6D_6 , 399.5 MHz, 303 K) δ_{H} 9.02 (d, $J_{\text{CH}} = 211$ Hz, 1H, $\text{O}_2\text{ }^{13}\text{C-H}$), 6.91 (2H, COT-H), 6.76 (m, 2H, COT-H), 6.57 (m, 2H, COT-H), 1.84 (s, 15H, Cp*), 1.63 (septet, $J_{\text{HH}} = 7.4$ Hz, 6H, $^1\text{Pr-CH}$), 1.29 (d, $J_{\text{HH}} = 7.4$ Hz, 18H, $^1\text{Pr-CH}_3$), 1.24 (d, $J_{\text{HH}} = 7.5$ Hz, 18H, $^1\text{Pr-CH}_3$). $^1\text{H}\{^{13}\text{C}\}$ NMR (C_6D_6 , 399.5 MHz, 303 K, selected data) δ_{H} 9.02 (s, 1H, $\text{O}_2\text{ }^{13}\text{CH}$). $^{13}\text{C}\{^1\text{H}\}$ NMR (C_6D_6 , 100.5 MHz, 303 K): δ_{C} 177.2 ($\text{O}_2\text{ }^{13}\text{CH}$), 124.8 (Cp*-CCH₃), 110.7 (COT-CH), 108.1 (COT-CH), 107.0 (COT-CSi), 19.8 ($^1\text{Pr-CH}_3$), 12.5 ($^1\text{Pr-CH}_3$), 12.5 ($^1\text{Pr-CH}$), 11.3 ($^1\text{Pr-CH}$). ^{13}C NMR (C_6D_6 , 100.5 MHz, 303 K, selected data) δ_{C} 177.2 (d, $J_{\text{CH}} = 211$ Hz, $\text{O}_2\text{ }^{13}\text{CH}$). MS (EI)⁺: m/z 830 ('Th(COT^{TIPS}₂)Cp*(O₂¹³CH)', 10%), 694, ('Th(COT^{TIPS}₂) (O₂¹³CH)', 60%), 667, ('Th(COT^{TIPS}₂)(F)', 100%), the F is the result of abstraction from the mass spectrometer calibrant. IR (NaCl plates, cm^{-1}) 3583 w, 2943 s, 2865 s, 1543 br m, 1494 m, 1462 s, 1380 s, 1350 m, 1252 w, 1032 m, 1070 m, 1015 m, 930 w, 882 s, 752 m, 670 s. Anal. Found: C, 53.80; H, 7.81. (^{13}C)₂C₇₂H₁₂₈Si₄O₄Th requires C, 53.65; H 7.77%.

Acknowledgements

We thank the European Research Council for financial support of this work and Dr G. J. Tizzard (NCS Southampton) for assistance with X-ray crystallography.

Notes and references

- H. S. La Pierre and K. Meyer, *Prog. Inorg. Chem.*, 2014, **58**, 303–416.
- P. C. Blake, M. F. Lappert, J. L. Atwood and H. Zhang, *J. Chem. Soc., Chem. Commun.*, 1986, **15**, 1148.
- J. S. Parry, F. G. N. Cloke, S. J. Coles and M. B. Hursthouse, *J. Am. Chem. Soc.*, 1999, **121**, 6867.
- P. C. Blake, N. M. Edelstein, P. B. Hitchcock, W. K. Kot, M. F. Lappert, G. V. Shalimoff and S. Tian, *J. Organomet. Chem.*, 2001, **636**, 124.
- J. R. Walensky, R. L. Martin, J. W. Ziller and W. J. Evans, *Inorg. Chem.*, 2010, **49**, 10007.
- O. T. Summerscales, F. G. N. Cloke, P. B. Hitchcock, J. C. Green and N. Hazari, *Science*, 2006, **311**, 829.
- O. T. Summerscales, A. S. P. Frey, F. G. N. Cloke and P. B. Hitchcock, *Chem. Commun.*, 2009, 198.
- K. G. Moloy and T. J. Marks, *Inorg. Chem. Acta*, 1985, **110**, 127.
- T. J. Marks and W. A. Wachter, *J. Am. Chem. Soc.*, 1976, **98**, 703.
- J. M. Manriquez, P. J. Fagan and T. J. Marks, *J. Am. Chem. Soc.*, 1978, **100**, 3939.
- E. A. Mintz, K. G. Moloy, T. J. Marks and V. W. Day, *J. Am. Chem. Soc.*, 1982, **104**, 4692.
- P. C. Blake, M. F. Lappert, R. G. Taylor, J. L. Atwood and H. Zhang, *Inorg. Chem. Acta*, 1987, **139**, 13.
- C. A. Fendrick, L. D. Schertz, V. W. Day and T. J. Marks, *Organometallics*, 1988, **7**, 1828.
- T. M. Gilbert, R. R. Ryan and A. P. Sattelberger, *Organometallics*, 1989, **8**, 857.
- D. L. Clark, S. K. Grumbine, B. L. Scott and J. G. Watkin, *Organometallics*, 1996, **15**, 949.
- R. J. Butcher, D. L. Clark, S. K. Grumbine, B. L. Scott and J. G. Watkin, *Organometallics*, 1996, **15**, 1488.
- H. W. Turner, R. A. Andersen, A. Zalkin and D. H. Templeton, *Inorg. Chem.*, 1979, **18**, 1221.
- K. C. Jantunen, R. J. Batchelor and D. B. Leznoff, *Organometallics*, 2004, **23**, 2186.
- C. A. Cruz, D. J. H. Emslie, L. E. Harrington and J. F. Britten, *Organometallics*, 2008, **27**, 15; C. A. Cruz, D. J. H. Emslie, C. M. Robertson, L. E. Harrington, H. A. Jenkins and J. F. Britten, *Organometallics*, 2008, **28**, 1891; C. A. Cruz, D. J. H. Emslie, H. A. Jenkins and J. F. Britten, *Dalton Trans.*, 2010, **39**, 6626.
- E. Mora, L. Maria, B. Biswas, C. Camp, I. C. Santos, J. Pécaut, A. Cruz, J. M. Carretas, J. Marçalo and M. Mazzanti, *Organometallics*, 2013, **32**, 1409.
- D. C. Sonnenberger, E. A. Mintz and T. J. Marks, *J. Am. Chem. Soc.*, 1984, **106**, 3484.
- I. Korobkov and S. Gambarotta, *Organometallics*, 2004, **23**, 2003.
- H. W. Turner, S. J. Simpson and R. A. Andersen, *J. Am. Chem. Soc.*, 1979, **101**, 2782.
- P. J. Fagan, J. M. Manriquez, E. A. Maatta, A. M. Seyam and T. J. Marks, *J. Am. Chem. Soc.*, 1981, **103**, 6650.
- X. Jemine, J. Goffart, M. Ephritikhine and J. Fuger, *J. Organomet. Chem.*, 1993, **448**, 95.
- M. Ephritikhine, *Chem. Rev.*, 1997, **97**, 2193.
- Z. Lin and T. J. Marks, *J. Am. Chem. Soc.*, 1987, **109**, 7979.
- K. G. Moloy and T. J. Marks, *J. Am. Chem. Soc.*, 1984, **106**, 7051.

- 29 Z. Lin and T. J. Marks, *J. Am. Chem. Soc.*, 1990, **112**, 5515.
- 30 J. A. Higgins, F. G. N. Cloke and S. M. Roe, *Organometallics*, 2013, **32**, 5244.
- 31 *CSD Search*, May 2014; D. A. Fletcher, R. F. McMeeking and D. Parkin, *J. Chem. Inf. Comput. Sci.*, 1996, **36**, 746.
- 32 K. Ziegelgruber, K. Knope, M. Frisch and C. Cahill, *J. Solid State Chem.*, 2008, **181**, 373.
- 33 P. Ramaswamy, R. Prabhu and S. Natarajan, *Inorg. Chem.*, 2010, **49**, 7927.
- 34 N. Clavier, N. Hingant, M. Rivenet, S. Obbade, N. Dacheux, N. Barré and F. Abraham, *Inorg. Chem.*, 2010, **49**, 1921.
- 35 G. Andreev, N. Budantseva, A. Fedoseev and P. Moisy, *Inorg. Chem.*, 2011, **50**, 11481.
- 36 P. Thuéry, *Inorg. Chem.*, 2011, **50**, 1898.
- 37 F. A. Henglein and H. Sontheimer, *Z. fuer Anorg. und Allg. Chemie*, 1951, **267**, 181.
- 38 S. Takao, K. Takao, W. Kraus, F. Emmerling, A. C. Scheinost, G. Bernhard and C. Hennig, *Eur. J. Inorg. Chem.*, 2009, **32**, 4771.
- 39 K. E. Knope, R. E. Wilson, M. Vasiliu, D. A. Dixon and L. Soderholm, *Inorg. Chem.*, 2011, **50**, 9696.
- 40 O. V. Dolomanov, L. J. Bourhis, R. J. Gildea, J. A. K. Howard and H. Puschmann, *J. Appl. Crystallogr.*, 2009, **42**, 339.
- 41 L. Palatinus and G. Chapuis, *J. Appl. Crystallogr.*, 2007, **40**, 786; L. Palatinus and A. van der Lee, *J. Appl. Crystallogr.*, 2008, **41**, 975; L. Palatinus, S. J. Prathapa and S. van Smaalen, *J. Appl. Crystallogr.*, 2012, **45**, 575.
- 42 G. M. Sheldrick, *Acta Crystallogr., Sect. A: Fundam. Crystallogr.*, 2008, **64**, 112.
- 43 L. J. Farrugia, *J. Appl. Crystallogr.*, 1999, **32**, 82.
- 44 K. W. Bagnell, A. Beheshti, F. Heatley and A. C. Tempest, *J. Less-Common Met.*, 1979, **64**, 267; E. A. Mintz, K. G. Moloy, T. J. Marks and V. W. Day, *J. Am. Chem. Soc.*, 1982, **104**, 4692.
- 45 M. Schlosser and J. Hartman, *Angew. Chem., Int. Ed. Engl.*, 1973, **12**, 508.